19th Edition

HERVEX

ISSN 1454 - 8003

# PROCEEDINGS OF INTERNATIONAL SALON OF HYDRAULICS, PNEUMATICS, TOOLS, SEALING ELEMENTS, FINE MECHANICS, SPECIFIC ELECTRONIC EQUIPMENT & MECHATRONICS

# HERVEX 2011

www.hervex.eu

Noiembrie 2011
Editia a XIX-a

November 2011
19th Edition

# SALONUL INTERNATIONAL
# INTERNATIONAL SALON

# HERVEX 2011

**Hidraulica ; Pneumatica ; Elemente de etansare**
**Mecanica fina ; Scule ; Mecatronica**
**Dispozitive si echipamente electronice specifice**

**Hydraulics ; Pneumatics ; Sealing systems**
**Fine mechanics ; Tools ; Mecatronics**
**Dedicated electronic devices and equipment**

| SIMPOZION | EXPOZITIE | BROKERAJ |
|---|---|---|
| SIMPOSYUM | EXHIBITION | BROKERAGE |

CALIMANESTI - CACIULATA, 9 - 11 NOIEMBRIE 2011
CALIMANESTI - CACIULATA, 9 - 11 NOVEMBER 2011

# HERVEX 2011

| ORGANIZATORI | ORGANIZERS |
| --- | --- |
| CAMERA DE COMERT SI INDUSTRIE VALCEA, ROMANIA | CHAMBER OF COMMERCE AND INDUSTRY VALCEA, ROMANIA |
| INSTITUTUL DE CERCETARI PENTRU HIDRAULICA SI PNEUMATICA BUCURESTI, ROMANIA | HYDRAULICS AND PNEUMATICS RESEARCH INSTITUTE BUCHAREST, ROMANIA |
| UNIVERSITATEA POLITEHNICA BUCURESTI, ROMANIA | "POLITEHNICA" UNIVERSITY OF BUCHAREST, ROMANIA |
| UNIVERSITATEA TEHNICA "GH. ASACHI"DIN IASI, ROMANIA | "GHEORGHE ASACHI" TECHNICAL UNIVERSITY OF IASI, ROMANIA |
| INSTITUTUL PIA AACHEN - GERMANIA | PIA INSTITUTE, AACHEN, GERMANY |
| UNIVERSITATEA DIN WROCLAW, POLONIA | WROCLAW UNIVERSITY OF TECHNOLOGY, POLAND. |

**Conferinta desfasurata sub patronajul**
- CETOP
- Ministerul Educației, Cercetării şi Inovării

**Conference held under the patronage of**
- CETOP
- Romanian Ministry of Education, Research and Innovation

**COMMITTEE OF HONOR**

Etienne PIOT - President of CETOP

Henryk CHROSTOWSKI - Wroclaw University of Technology, POLAND

Giorgio BERETTA - President of ASSOFLUID, ITALY

Valentin CISMARU - CCI Valcea

Petrin DRUMEA - INOE 2000 IHP Bucharest

Elmar DORGELOH- University of Aachen

Heinrich THEISSEN - IFAS - Aachen, Germany

**Published by** - Hydraulics and Pneumatics Research Institute, Bucharest, Romania
- Chamber of Commerce and Industry Valcea, Romania
with the support of the National Professional Association of Hydraulics and Pneumatics - "FLUIDAS"

**Editat de** - Institutul de Cercetari pentru Hidraulica si Pneumatica din Bucuresti
- Camera de Comert si Industrie Valcea, Romania
cu sprijinul Asociatiei Nationale Profesionale de Hidraulica si Pneumatica din Romania - "FLUIDAS"

# SPONSORS

SC Hydramold SRL
700050 Iasi, str. D. Mangeron nr. 49

---

Parker Hannifin Romania
Bucuresti, Bd. Ferdinand nr.27, Sector 2

---

SC ROMFLUID SA
Str. Cutitul de Argint nr. 14, sector 4 ,
Bucuresti, Romania

---

SC Fast Eco SA
Str.Fabricii, nr.47,
Bucuresti, Romania

# COMMITTEES

## *HONORARY COMMITTEE*

Etienne PIOT – President of European Fluid Power Committee - CETOP
John SAVAGE – Vice President CETOP – Education / BFPA Chairman Education and Training, England
Henryk CHROSTOWSKI - Wroclaw University of Technology, POLAND
Humbertus MURRENHOFF - Institute for Fluid Power Drives and Controls at Aachen University -, GERMANY

## *ORGANIZING COMMITTEE*

### *COORDINATED BY*

Eng. Gheorghe RIZOIU - General Manager of Chamber of Commerce and Industry Valcea, Romania
Dr. Ing. Corneliu CRISTESCU - Hydraulics and Pneumatics Research Institute in Bucharest, Romania
Assoc.Prof. PhD.Eng. Erol MURAD - "POLITEHNICA" University of Bucharest, Romania

### *MEMBERS*

PhD.Eng. Mohamed HAJJAM – University of Poitiers - IUT Angouléme France
Eng. Peter ABPLANALP - BIBUS -Switzerland
Prof. PhD.Eng. Nicolae ALEXANDRESCU - "POLITEHNICA" University of Bucharest, Romania
Eng. Ionel ANDREI - Romanian Ministry of Education, Research and Innovation
Eng. Radu ALEXANDRU - FESTO S.R.L.
Prof. PhD.Eng. Victor BALASOIU - "POLITEHNICA" University of Timisoara, Romania
Prof. PhD.Eng. Valeriu BANU - S.M.C. Romania
PhD.Eng. Zygmunt DOMAGALA – Wroclaw University of Technology, POLAND
PhD.Eng. Krzysztof KEDZIA - Wroclaw University of Technology, POLAND
Prof. PhD.Eng. Guido BELFORTE - "POLITEHNICA" University of Torino, Italy
PhD.Eng. Amadio BOLTZANI - ASSOFLUID – Italy
PhD.Eng. Gabriela MATACHE - Hydraulics and Pneumatics Research Institute in Bucharest, Romania
Eng. Marius BURLANESCU - S.C. HERVIL Ramnicu Valcea, Romania

Prof. PhD.Eng. Doru CALARASU - Technical University “Gheorghe Asachi”- Iasi, Romania

Eng. Ioan CAMPEAN - S.C. HIDROSIB S.A. Sibiu, Romania

Assoc.Prof. PhD.Eng. Constantin CHIRITA - Technical University “Gheorghe Asachi”- Iasi, Romania

PhD.Eng. Tudor CRACIUNOIU - S.C. ICTCM S.A. Bucharest, Romania

PhD.Eng. Corneliu CRISTESCU - Hydraulics and Pneumatics Research Institute in Bucharest, Romania

Eng. Mircea DANCIU - PARKER HANNIFIN Corporation Romania

Prof. PhD.Eng. Gheorghe GHEORGHE - General Manager - National Institute of Research and Development in Mechatronics and Measurement Technique (INCDMTM), Bucharest, Romania

Prof. PhD.Eng. Vasile JAVGUREANU - Technical University of Chisinau Moldova

PhD.Eng. Ioan LEPADATU - Hydraulics and Pneumatics Research Institute in Bucharest, Romania

Eng. Leopold LUPUSANSCHI- S.C. CEROB S.R.L. Bucharest, Romania

Prof. PhD.Eng. Pavel MACH – Technical University of Praga, Czech

PhD.Eng. Daniel MARIN- S.C. General Fluid S.A. Bucharest, Romania

Eng. Eduard MILEA - S.C. PROCONS S.R.L. Bucharest, Romania

PhD.Eng. Adrian MIREA – SC ROMFLUID SA, Bucharest, Romania

Eng. Ioan MOLDOVEANU - Festo S.R.L.,Bucharest, Romania

PhD.Eng. Andrei Drumea - “POLITEHNICA” University of Bucharest, Romania

Prof. PhD.Eng. Erol MURAD - “POLITEHNICA” University of Bucharest, Romania

Prof. PhD.Eng. Johann NICOLICI - Technical University of Viena, Austria

Eng. Cristian Sen - SUSZI - INDUSTRIAL SRL Constanta, Romania

Prof. PhD.Eng. Petru PATRUT - Technical University of Civil Engineering of Bucharest, Romania

PhD.Eng. Ion PIRNA - General Manager - National Institute Of Research - Development for Machines and Installations Designed to Agriculture and Food Industry – INMA, Bucharest- Romania

PhD.Eng. Mircea PRICOP- S.C. HESPER S.A. Bucharest- Romania

Eng. Petru BREAZ - HIDRAULICA U.M. PLOPENI – Plopeni, Romania

Prof. PhD.Eng. Liviu VAIDA - Technical University of Cluj, Romania

Prof. PhD.Eng. Nicolae VASILIU - “POLITEHNICA” University of Bucharest, Romania

Eng. Nicolae TASU - HANSA FLEX Romania

Prof. PhD.Eng. Kallita WLODZIMIERZ – Faculty of Rezjow – Poland

***EXECUTIVE COMMITTEE***

Eng. Valentin CISMARU - President of Chamber of Commerce and Industry Valcea, Romania

PhD.Eng. Petrin DRUMEA – Manager - Hydraulics and Pneumatics Research Institute in Bucharest, Romania

Assoc.Prof. PhD.Eng. Constantin CHIRITA - Technical University "Gheorghe Asachi"- Iasi, Romania

Eng. Mircea DANCIU - PARKER HANNIFIN Corporation Romania

Prof. PhD.Eng. Gheorghe GHEORGHE General Manager - National Institute of Research and Development in Mechatronics and Measurement Technique (INCDMTM), Bucharest, Romania

Prof. PhD.Eng. Alexandru MARIN – "POLITEHNICA" University of Bucharest, Romania

Assoc.Prof. PhD.Eng. Erol MURAD - "POLITEHNICA" University of Bucharest, Romania

PhD.Eng. Adrian MIREA - ROMFLUID Bucharest, Romania

Eng. Gheorghe RIZOIU - General Manager of Chamber of Commerce and Industry Valcea, Romania

PhD.Eng. Corneliu CRISTESCU - Hydraulics and Pneumatics Research Institute in Bucharest, Romania

***SECRETARY***

Valentin MIROIU - Hydraulics and Pneumatics Research Institute in Bucharest, Romania

PhD.Eng. Iulian DUTU - Hydraulics and Pneumatics Research Institute in Bucharest, Romania

Alexandru Ciuca - Chamber of Commerce and Industry Valcea, Romania

***EXCHIBITION ORGANIZING COMMITTEE***

Alexandru Ciuca - Chamber of Commerce and Industry Valcea, Romania

PhD.Eng. Ioan LEPADATU - Hydraulics and Pneumatics Research Institute in Bucharest, Romania

***SPECIALIZED REVIEWER COMMITTEE***

PhD.Eng. Heinrich Theissen - Institute for Fluid Power Drives and Controls, Aachen University - Germania

Prof. PhD.Eng. Mircea BARGLAZAN - "POLITEHNICA" University of Timisoara, Romania

Prof. PhD.Eng. Guido BELFORTE - "POLITEHNICA" University of Torino, Italy

PhD.Eng. Petrin DRUMEA - Manager - Hydraulics and Pneumatics Research Institute in Bucharest, Romania

Prof. PhD.Eng. Nicolae ALEXANDRESCU - Politehnica University of Bucharest, Romania

Prof. PhD.Eng. Paul SVASTA - Politehnica"POLITEHNICA" of Bucharest, Romania

Assoc.Prof. PhD.Eng. Constantin CHIRITA - Technical University "Gheorghe Asachi"- Iasi, Romania
PhD.Eng. Mohamed HAJJAM - University of Poitiers - IUT Angouléme France
Prof. PhD.Eng. Vasile JAVGUREANU - Technical University of Chisinau Moldova
Prof. PhD.Eng. Pavel MACH - Technical University of Praga, Czech
Prof. PhD.Eng. Johann NICOLICS - Technical University of Viena, Austria

***EDITORIAL STAFF***

Chief Editor - PhD. Eng. Gabriela MATACHE - Hydraulics and Pneumatics Research Institute in Bucharest, Romania

Executive editors - Ana-Maria POPESCU - Hydraulics and Pneumatics Research Institute in Bucharest, Romania

- Valentin MIROIU - Hydraulics and Pneumatics Research Institute in Bucharest, Romania

***MANAGER OF PUBLICATION***

PhD.Eng. Petrin DRUMEA - Manager - Hydraulics and Pneumatics Research Institute in Bucharest, Romania

# CONTENTS

## SCIENTIFIC PAPERS PRESENTED BY STUDENTS, MSc. STUDENTS, PhD. STUDENTS

## HUMAN RESOURCES DEVELOPMENT IN FLUID POWER

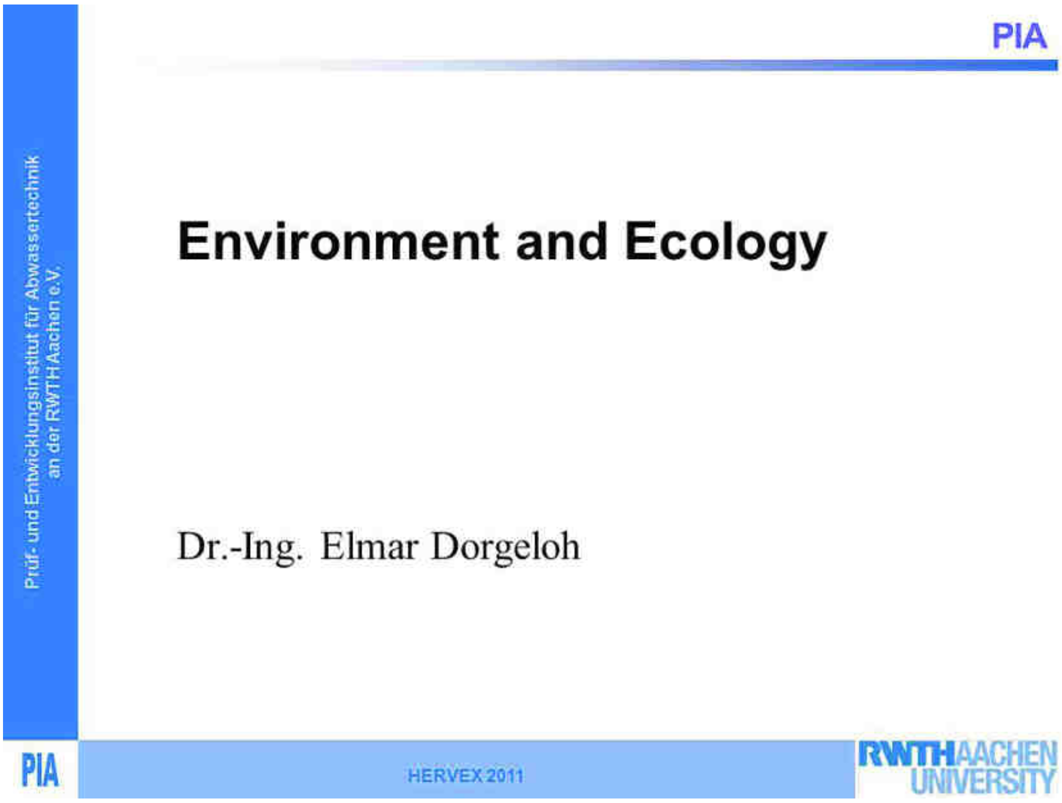

PIA
Environment and Ecology
Dr.-Ing. Elmar Dorgeloh
Prüf- und Entwicklungsinstitut für Abwassertechnik
an der RWTH Aachen e.V.
PIA
HERVEX 2011
RWTH AACHEN
UNIVERSITY


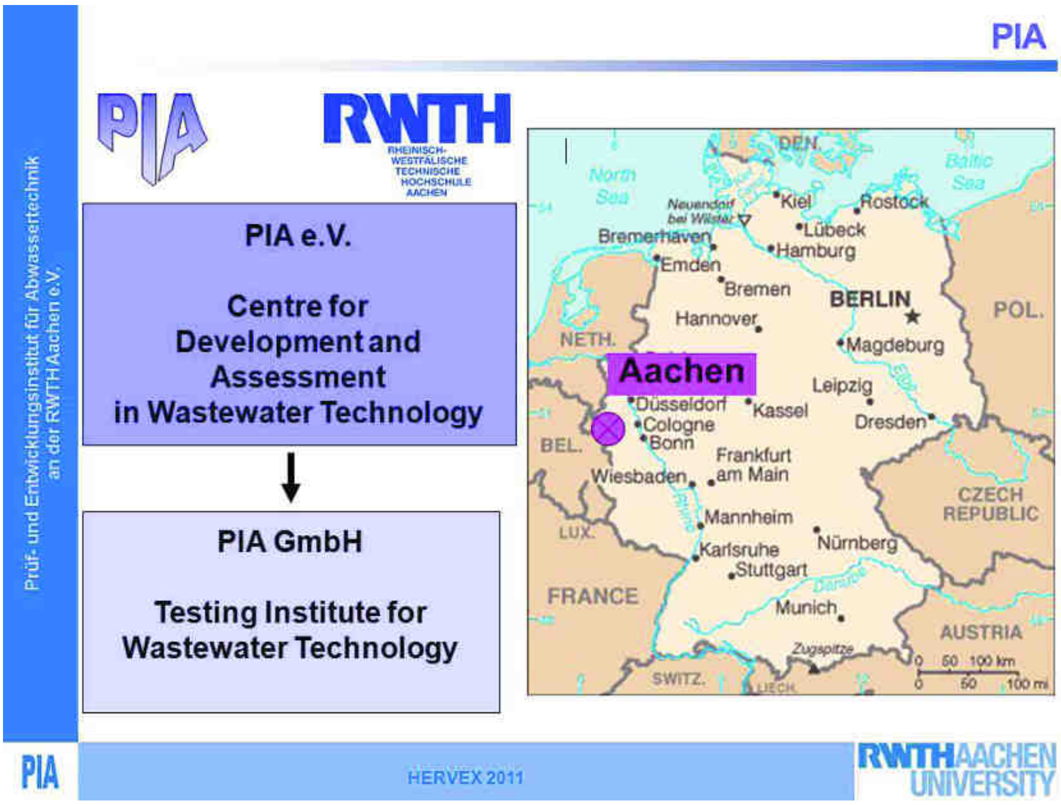

PIA
PIA
RWTH
RHEINISCH-
WESTFÄLISCHE
TECHNISCHE
HOCHSCHULE
AACHEN
PIA e.V.
Centre for
Development and
Assessment
in Wastewater Technology
PIA GmbH
Testing Institute for
Wastewater Technology
DEN.
North
Sea
Baltic
Sea
Neuendorf
bei Wilster
Kiel
Rostock
Lübeck
Bremerhaven
Hamburg
Emden
Bremen
BERLIN
POL.
Hannover
NETH.
Magdeburg
Aachen
Leipzig
Düsseldorf
Kassel
Cologne
Dresden
Bonn
BEL.
Frankfurt
am Main
Wiesbaden
CZECH
REPUBLIC
LUX.
Mannheim
Karlsruhe
Nürnberg
Stuttgart
FRANCE
Munich
AUSTRIA
Zugspitze
SWITZ.
LIECH.
0 50 100 km
0 50 100 mi
Prüf- und Entwicklungsinstitut für Abwassertechnik
an der RWTH Aachen e.V.
PIA
HERVEX 2011
RWTH AACHEN
UNIVERSITY

ISSN 1454 - 8003
Proceedings of 2011 International Salon of Hydraulics and Pneumatics - HERVEX
*9 – 11 November, Calimanesti-Caciulata, Romania*

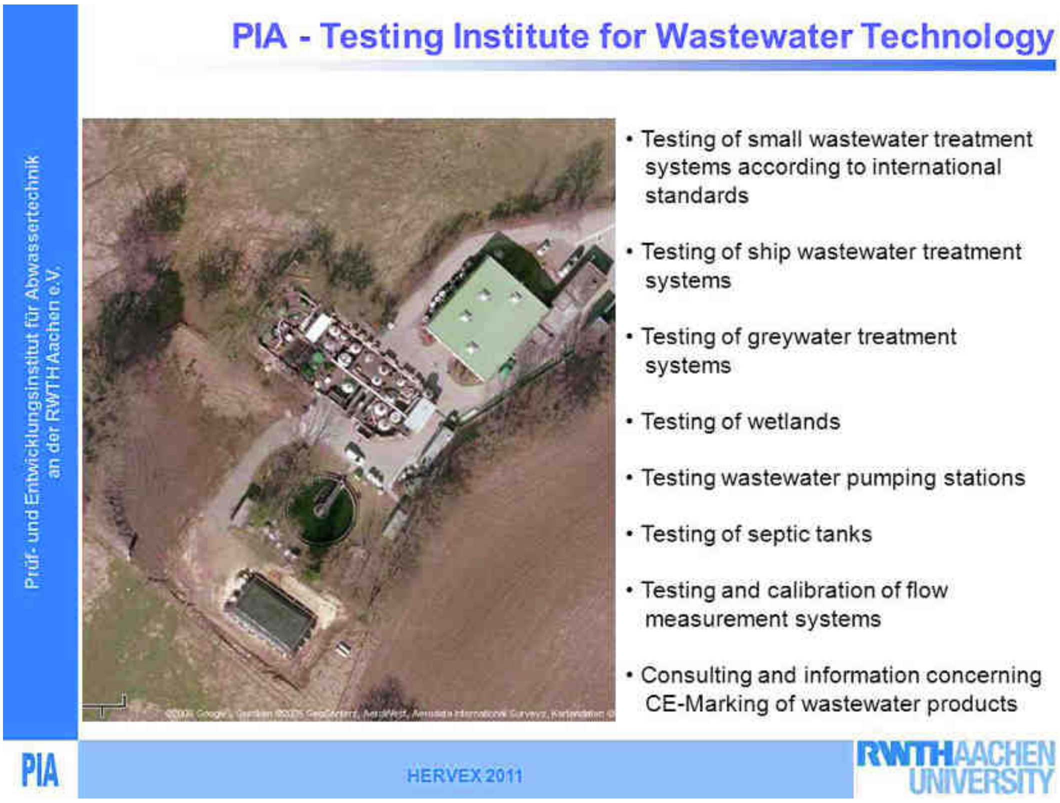


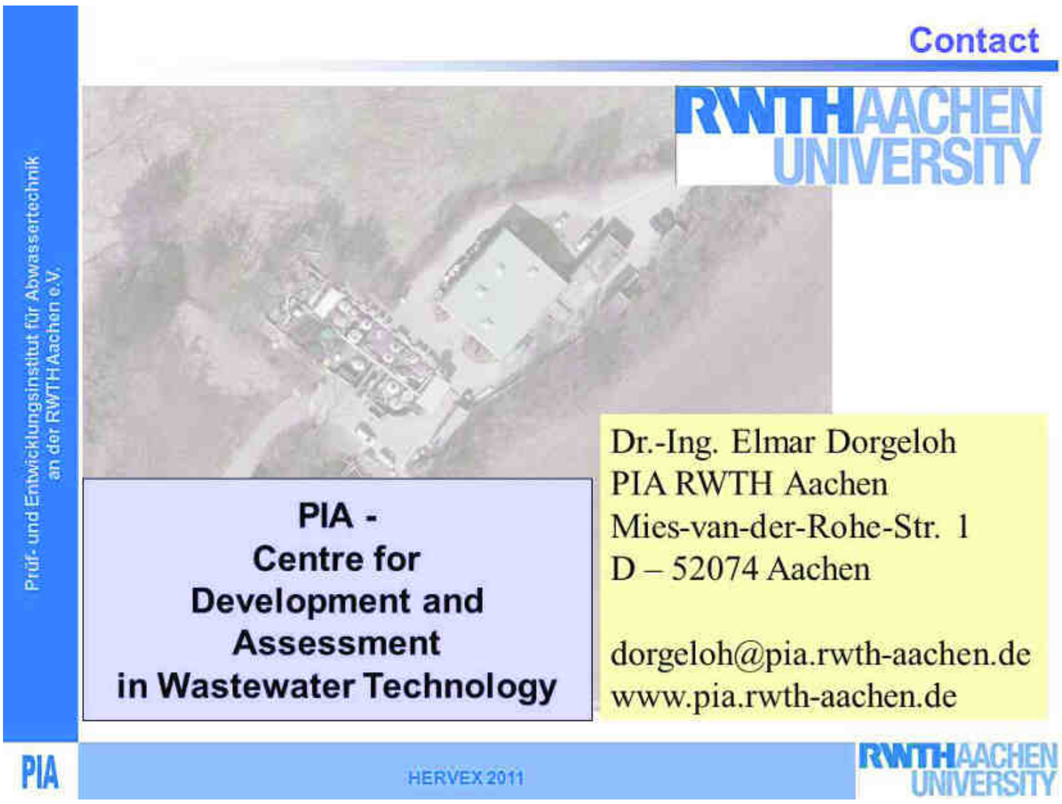

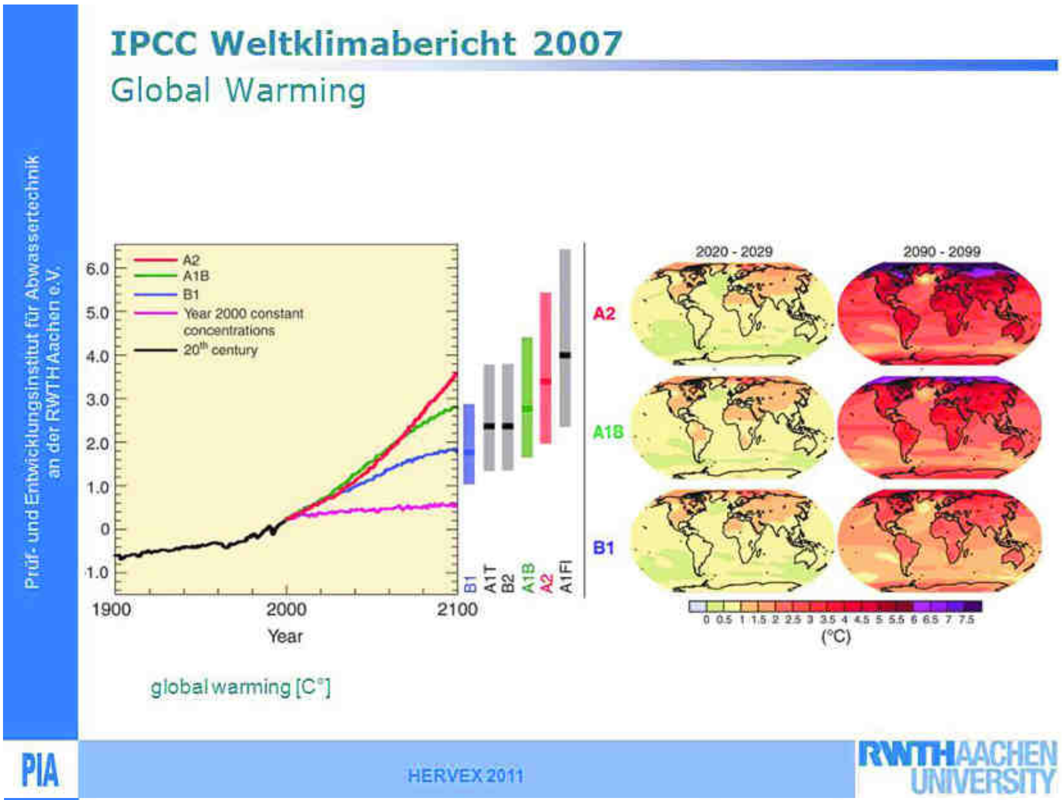

IPCC Weltklimabericht 2007
Global Warming
Prüf- und Entwicklungsinstitut für Abwassertechnik an der RWTH Aachen e.V.
A2
A1B
B1
Year 2000 constant concentrations
20th century
6.0
5.0
4.0
3.0
2.0
1.0
0
-1.0
1900
2000
2100
Year
B1
A1T
B2
A1B
A2
A1FI
2020 - 2029
2090 - 2099
A2
A1B
B1
0 0.5 1 1.5 2 2.5 3 3.5 4 4.5 5 5.5 6 6.5 7 7.5
(°C)
global warming [C°]
PIA
HERVEX 2011
RWTH AACHEN UNIVERSITY


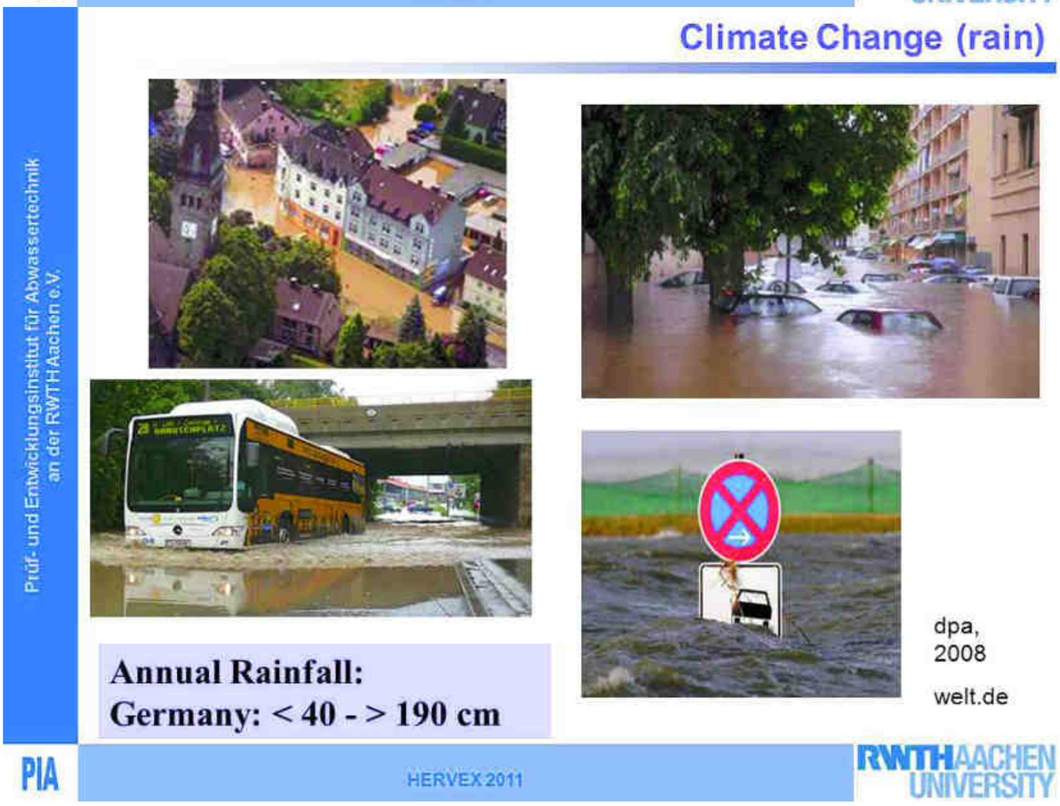

Climate Change (rain)
Prüf- und Entwicklungsinstitut für Abwassertechnik an der RWTH Aachen e.V.
Annual Rainfall:
Germany: < 40 - > 190 cm
dpa,
2008
welt.de
PIA
HERVEX 2011
RWTH AACHEN UNIVERSITY


Basic Conditions: Water level
Google earth
Prüf- und Entwicklungsinstitut für Abwassertechnik an der RWTH Aachen e.V.
PIA
HERVEX 2011
RWTH AACHEN UNIVERSITY

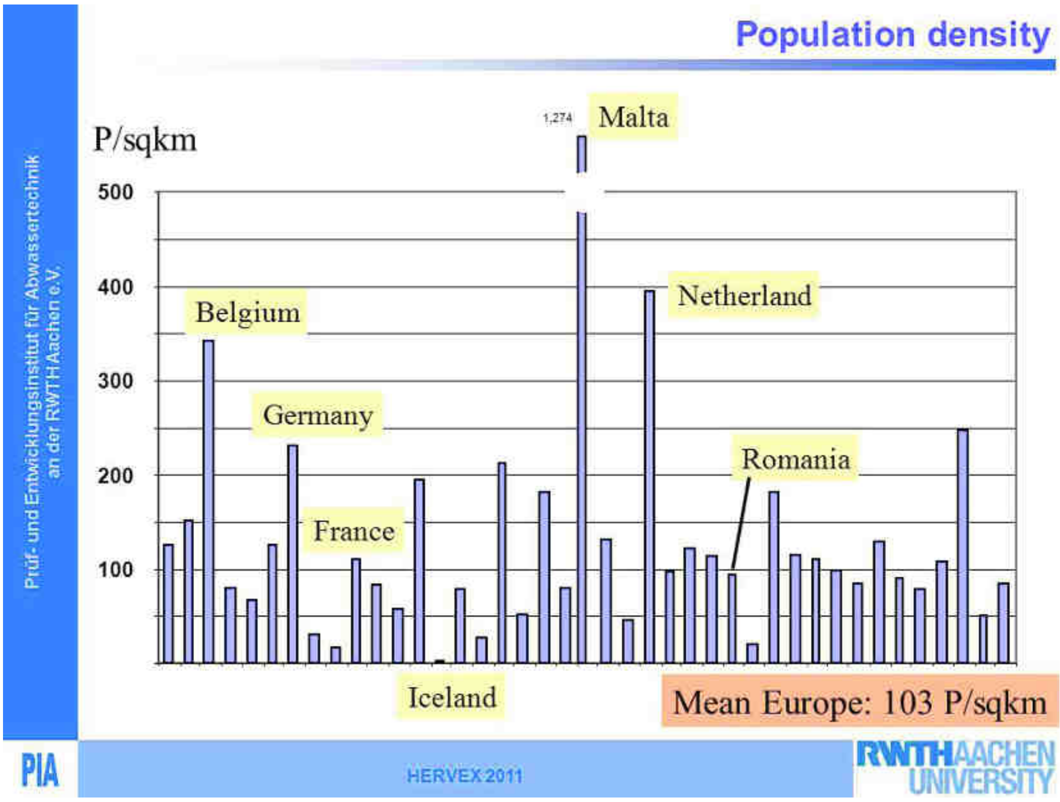
Population density
P/sqkm
500
400
300
200
100
1,274
Malta
Belgium
Netherland
Germany
Romania
France
Iceland
Mean Europe: 103 P/sqkm
Prüf- und Entwicklungsinstitut für Abwassertechnik an der RWTH Aachen e.V.
PIA
HERVEX 2011
RWTH AACHEN UNIVERSITY

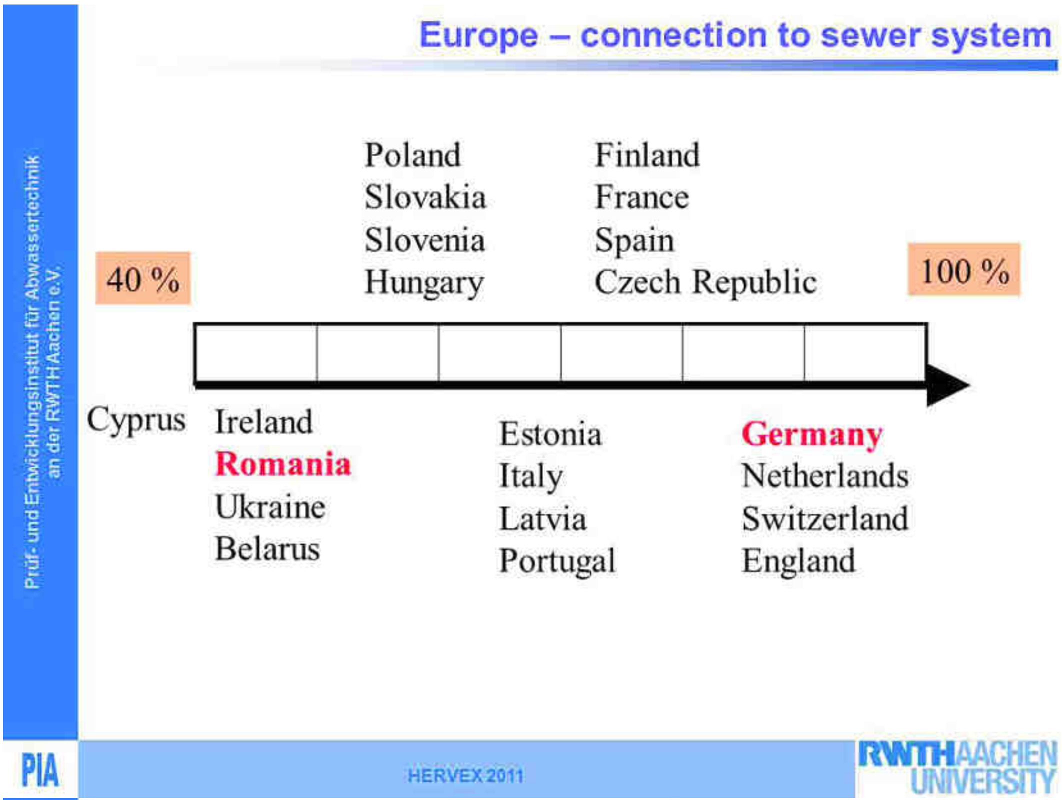
Europe – connection to sewer system
40 %
Poland
Slovakia
Slovenia
Hungary
Finland
France
Spain
Czech Republic
100 %
Cyprus
Ireland
Romania
Ukraine
Belarus
Estonia
Italy
Latvia
Portugal
Germany
Netherlands
Switzerland
England
Prüf- und Entwicklungsinstitut für Abwassertechnik an der RWTH Aachen e.V.
PIA
HERVEX 2011
RWTH AACHEN UNIVERSITY

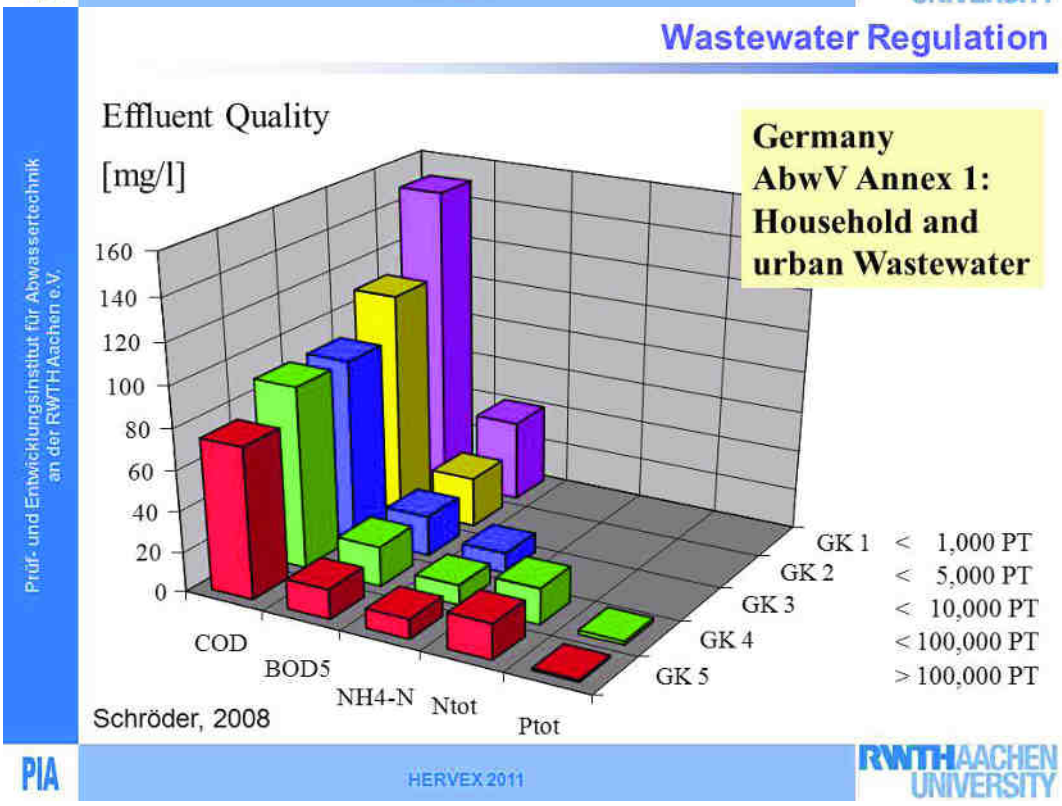
Wastewater Regulation
Effluent Quality
[mg/l]
Germany
AbwV Annex 1:
Household and
urban Wastewater
160
140
120
100
80
60
40
20
0
COD
BOD5
NH4-N
Ntot
Ptot
GK 1 < 1,000 PT
GK 2 < 5,000 PT
GK 3 < 10,000 PT
GK 4 < 100,000 PT
GK 5 > 100,000 PT
Schröder, 2008
Prüf- und Entwicklungsinstitut für Abwassertechnik an der RWTH Aachen e.V.
PIA
HERVEX 2011
RWTH AACHEN UNIVERSITY


Wastewater Treatment Systems
Aerated sludge reactor
Fixed film reactor
Moving bed reactor
SBR
Trickling filter
Membrane bioreactor
Constructed wetland
Tank
Reactor
Machine
Construction products
Prüf- und Entwicklungsinstitut für Abwassertechnik an der RWTH Aachen e.V.
PIA
HERVEX 2011
RWTH AACHEN UNIVERSITY


SWTS: Materials
Concrete
Steel
GRP
PE
HDPE
Prüf- und Entwicklungsinstitut für Abwassertechnik an der RWTH Aachen e.V.
PIA
HERVEX 2011
RWTH AACHEN UNIVERSITY

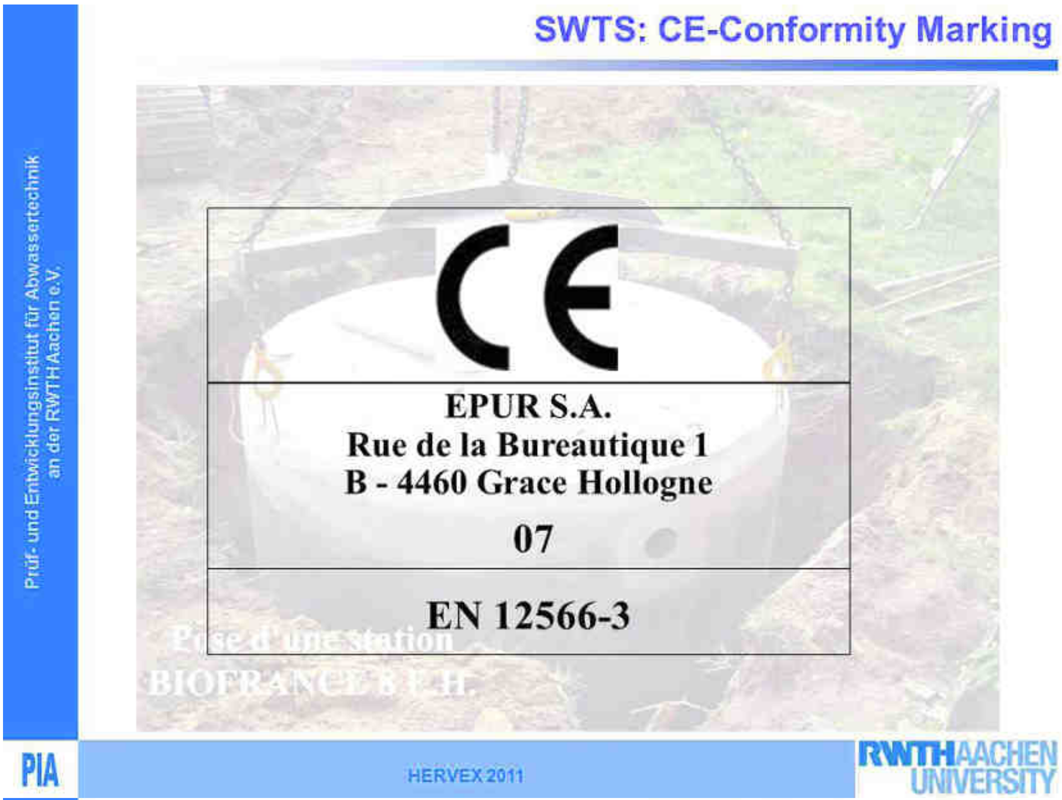
SWTS: CE-Conformity Marking
CE
EPUR S.A.
Rue de la Bureautique 1
B - 4460 Grace Hollogne
07
EN 12566-3
Pose d'une station
BIOFRANCE B.E.H.
Prüf- und Entwicklungsinstitut für Abwassertechnik an der RWTH Aachen e.V.
PIA
HERVEX 2011
RWTH AACHEN UNIVERSITY

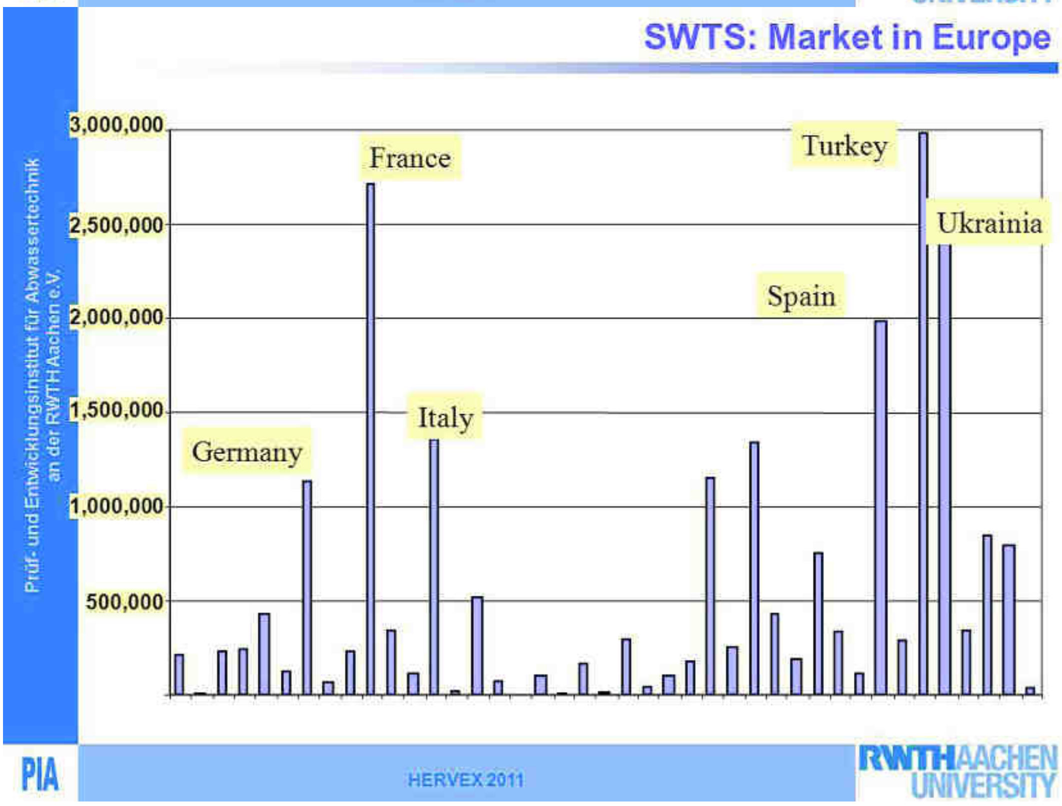
SWTS: Market in Europe
3,000,000
2,500,000
2,000,000
1,500,000
1,000,000
500,000
Germany
France
Italy
Spain
Turkey
Ukrainia
Prüf- und Entwicklungsinstitut für Abwassertechnik an der RWTH Aachen e.V.
PIA
HERVEX 2011
RWTH AACHEN UNIVERSITY

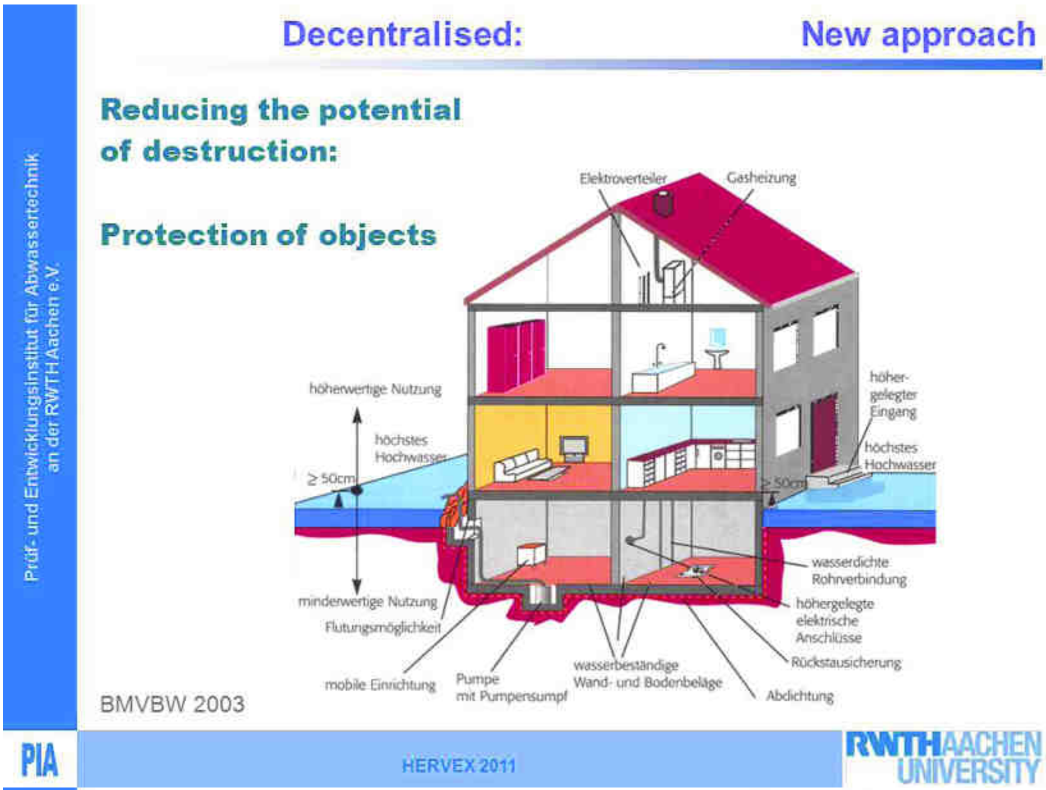
Decentralised:
New approach
Reducing the potential of destruction:
Protection of objects
Elektroverteiler
Gasheizung
höherwertige Nutzung
höchstes Hochwasser
≥ 50cm
höher-gelegter Eingang
höchstes Hochwasser
≥ 50cm
wasserdichte Rohrverbindung
höhergelegte elektrische Anschlüsse
Rückstausicherung
minderwertige Nutzung
Flutungsmöglichkeit
mobile Einrichtung
Pumpe mit Pumpensumpf
wasserbeständige Wand- und Bodenbeläge
Abdichtung
BMVBW 2003
Prüf- und Entwicklungsinstitut für Abwassertechnik an der RWTH Aachen e.V.
PIA
HERVEX 2011
RWTHAACHEN UNIVERSITY

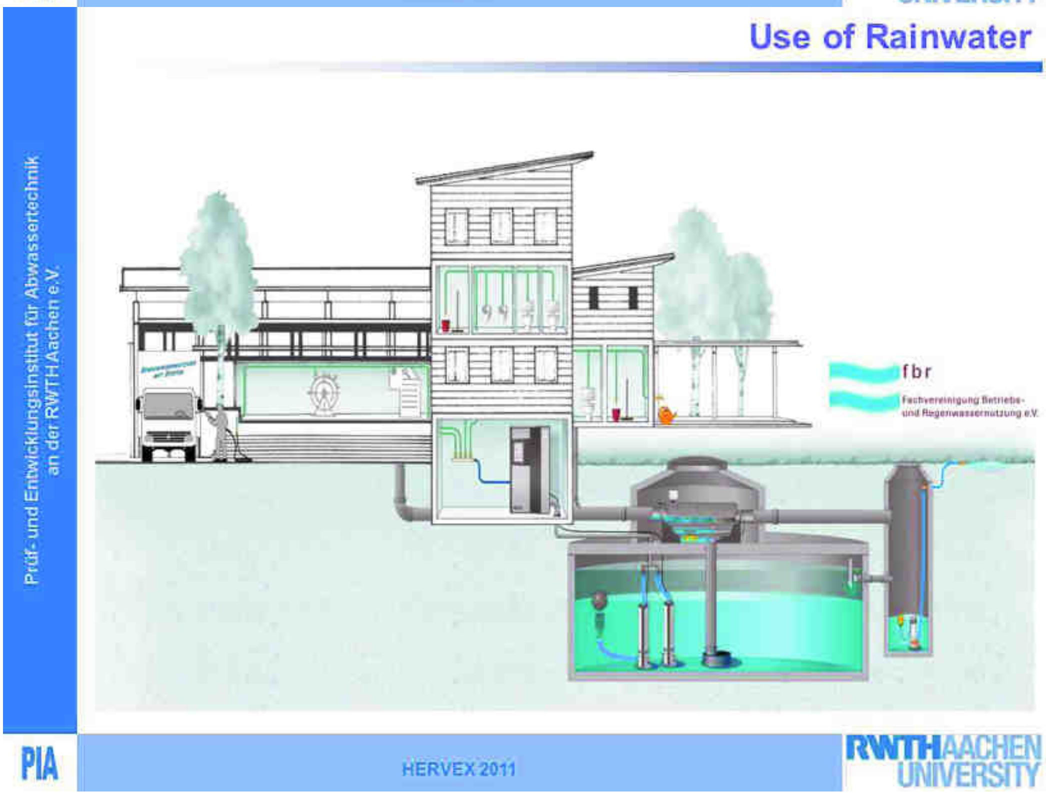
Use of Rainwater
fbr
Fachvereinigung Betriebs- und Regenwassernutzung e.V.
Prüf- und Entwicklungsinstitut für Abwassertechnik an der RWTH Aachen e.V.
PIA
HERVEX 2011
RWTHAACHEN UNIVERSITY

**ISSN 1454 - 8003**
**Proceedings of 2011 International Salon of Hydraulics and Pneumatics - HERVEX**
*9 – 11 November, Calimanesti-Caciulata, Romania*

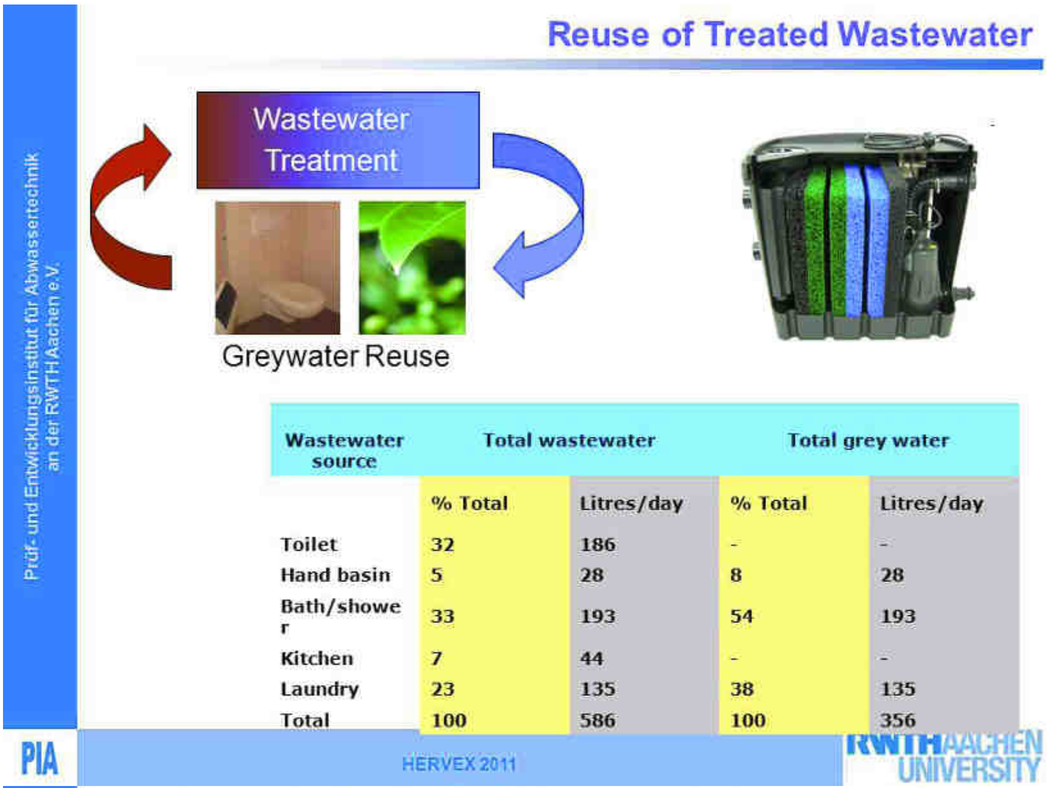


| Wastewater source | Total wastewater | | Total grey water | |
|---|---|---|---|---|
| | % Total | Litres/day | % Total | Litres/day |
| Toilet | 32 | 186 | - | - |
| Hand basin | 5 | 28 | 8 | 28 |
| Bath/showe r | 33 | 193 | 54 | 193 |
| Kitchen | 7 | 44 | - | - |
| Laundry | 23 | 135 | 38 | 135 |
| Total | 100 | 586 | 100 | 356 |

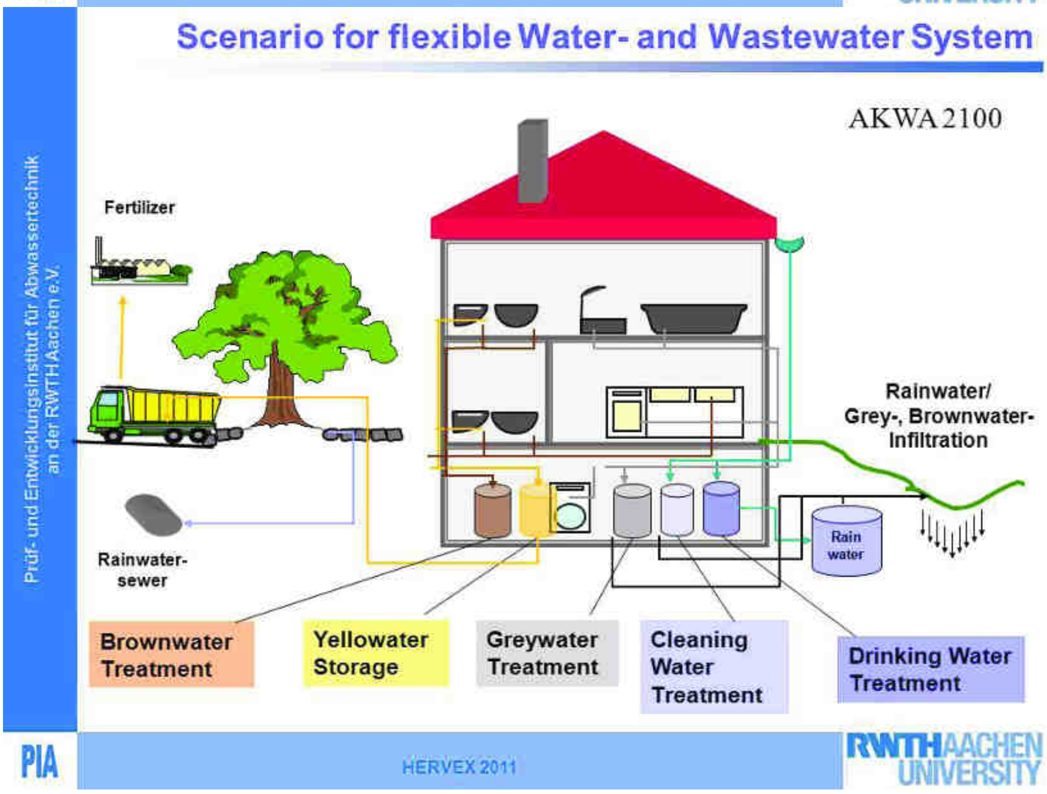

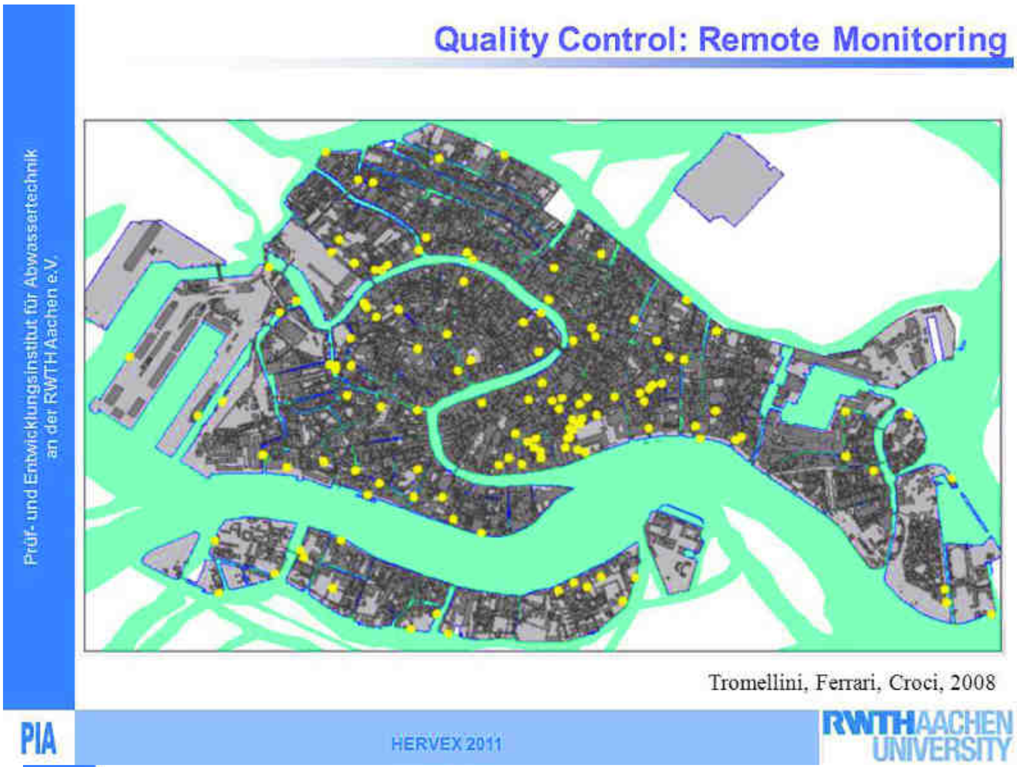
Quality Control: Remote Monitoring
Prüf- und Entwicklungsinstitut für Abwassertechnik an der RWTH Aachen e.V.
Tromellini, Ferrari, Croci, 2008
PIA
HERVEX 2011
RWTHAACHEN UNIVERSITY

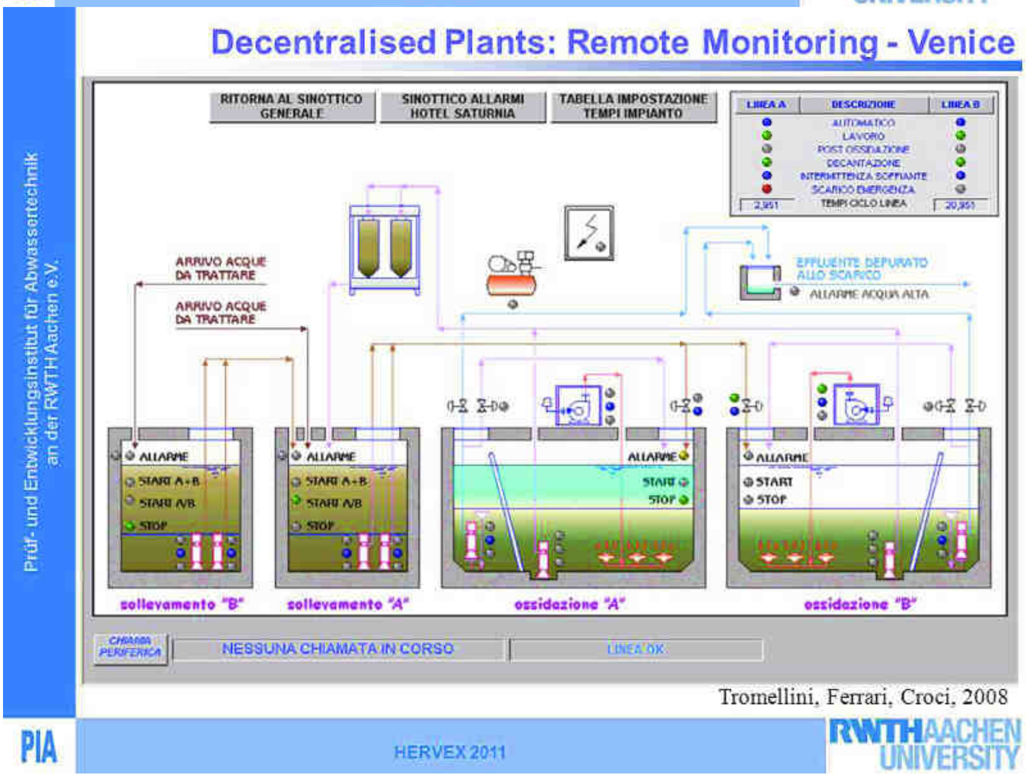
Decentralised Plants: Remote Monitoring - Venice
Prüf- und Entwicklungsinstitut für Abwassertechnik an der RWTH Aachen e.V.
RITORNA AL SINOTTICO GENERALE
SINOTTICO ALLARMI HOTEL SATURNIA
TABELLA IMPOSTAZIONE TEMPI IMPIANTO
LINEA A
DESCRIZIONE
LINEA B
AUTOMATICO
LAVORO
POST OSSIDAZIONE
DECANTAZIONE
INTERMITTENZA SOFFIANTE
SCARICO EMERGENZA
TEMPI CICLO LINEA
ARRIVO ACQUE DA TRATTARE
ARRIVO ACQUE DA TRATTARE
EFFLUENTE DEPURATO ALLO SCARICO
ALLARME ACQUA ALTA
ALLARME
START A+B
START A/B
STOP
ALLARME
START
STOP
sollevamento "B"
sollevamento "A"
ossidazione "A"
ossidazione "B"
CHIAMA PERIFERICA
NESSUNA CHIAMATA IN CORSO
LINEA OK
Tromellini, Ferrari, Croci, 2008
PIA
HERVEX 2011
RWTHAACHEN UNIVERSITY


Air Blowers for a Grit chamber
source: Pumpen + Pneumatik Service Danielis GmbH
Prüf- und Entwicklungsinstitut für Abwassertechnik an der RWTH Aachen e.V.
PIA
HERVEX 2011
RWTH AACHEN UNIVERSITY


Aeration Tank, WWTP Heilbronn
www.wilo.de
Prüf- und Entwicklungsinstitut für Abwassertechnik an der RWTH Aachen e.V.
PIA
HERVEX 2011
RWTH AACHEN UNIVERSITY


Aeration Tank WWTP
source: Markus Zimmermann-Dürkop
Prüf- und Entwicklungsinstitut für Abwassertechnik
an der RWTH Aachen e.V.
PIA
HERVEX 2011
RWTH AACHEN UNIVERSITY


Gate Valves
Source: Passavant
Prüf- und Entwicklungsinstitut für Abwassertechnik
an der RWTH Aachen e.V.
PIA
HERVEX 2011
RWTH AACHEN UNIVERSITY

ISSN 1454 - 8003
Proceedings of 2011 International Salon of Hydraulics and Pneumatics - HERVEX
*9 – 11 November, Calimanesti-Caciulata, Romania*

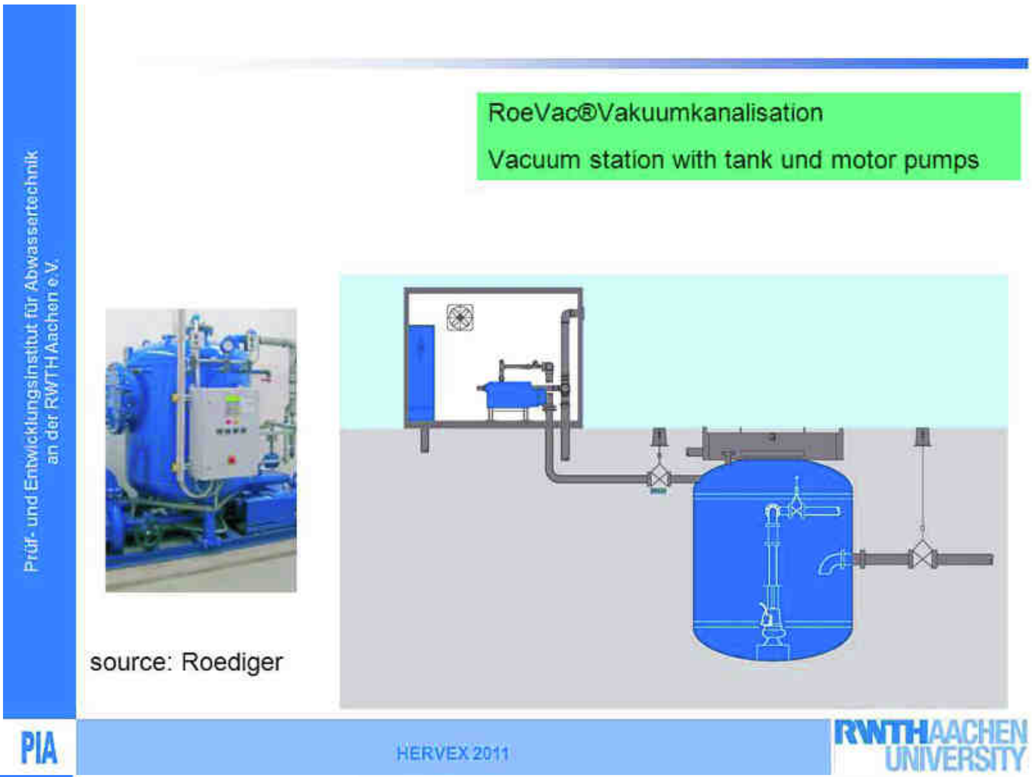


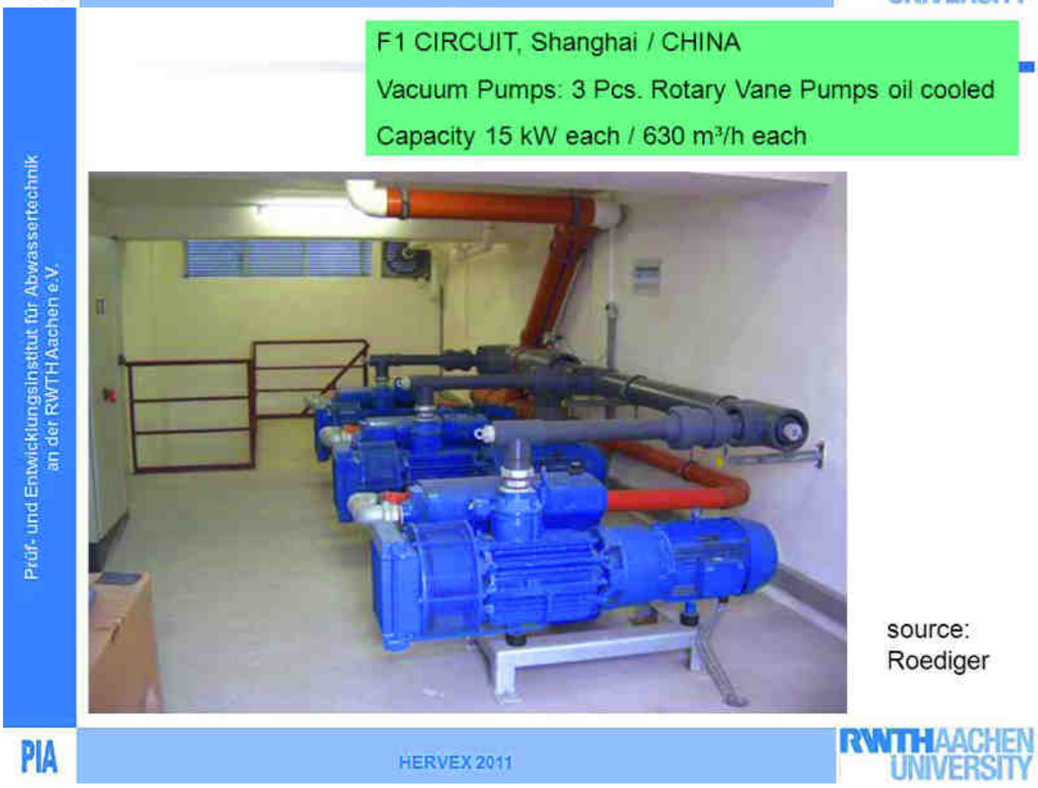

ISSN 1454 - 8003
**Proceedings of 2011 International Salon of Hydraulics and Pneumatics - HERVEX**
*9 – 11 November, Calimanesti-Caciulata, Romania*

# APPLYING FICK'S LAW IN MODELING ATMOSPHERIC DIFFUSION OF ASH PARTICLES DISPERSED IN CRAIOVA BY A POWER PLANT FURNACE

**Gabriel VLADUT[1], Monica MATEESCU[2], Liana Simona SBIRNA[2] and Sebastian SBIRNA[3]**

[1] IPA CIFATT Craiova, office@ipacv.ro

[2] Faculty of Chemistry, University of Craiova, monica.daniela.mateescu@gmail.com, simona.sbirna@gmail.com

[3] Craiova Regional Environment Protection Agency, s.sbirna@gmail.com

***Abstract:*** *A three-dimensional diffusion model based on Fick's law has been developed for modeling the distribution of ash particles originating from burning fossil fuels in one of the three power plants that affect Craiova as elevated pollution point sources, in order to predict the average concentration of the dangerous particulates with a diameter less than 10 μm (referred to as $PM_{10}$) at various distances from the selected power plant furnace.*

***Keywords****: power plant, furnace, Fick's law, monitoring air quality, $PM_{10}$, wind velocity, Craiova*

## 1. Introduction

Monitoring air quality is a major environmental risk to health and it is estimated to cause approximately two million premature deaths worldwide per year. Exposure to air pollutants is largely beyond the control of individuals and requires action by public authorities at national, regional and even international level.

## 2. What does PM10 stand for?

Particulate matter (PM10) is a dangerous urban pollutant. It is a complex mixture of particles of various origin and chemical composition, smaller than 10 μm in aerodynamic diameter, usually consisting of smoke and dust from industrial processes, incineration of refuse, heat and power generation, road traffic, construction, agriculture, as well as plant pollen and other natural sources.
PM10 is considered a serious air pollution problem in urban agglomerations, because of its detrimental impact on human health and living standards.
The European Union has established air quality standards for PM10, in order to improve the quality of ambient air. The former Directive 30/1999, as well as the later Directive 50/2008 state that since January 1$^{st}$ 2005 the daily average values of PM10 concentration may not exceed 50 μg/m$^3$ more than 35 days a year and the annual average value of PM10 concentration may not exceed 40 μg/m$^3$.

## 3. Craiova – important city of Romania

Craiova is Romania's sixth largest city and capital of Dolj County. It is situated near the east bank of the Jiu river in the middle of Oltenia region at an average altitude of 100 m and it the most important city of Oltenia. It is situated at 44°20′00″ North latitude and 23°49′00″ East longitude.
Specific relief is mainly plain. To the North a slight influence of the hills is observed, whereas to the South it exhibits meadow characteristics.
According to the last Romanian census, from 2002, there were 302 600 people living within the city of Craiova, making it the sixth most populous city in Romania. It is a longstanding political center, located at quite equal distances from the Southern Carpathians (North) and the Danube River (South).
As far as air quality is concerned, the ash dumps from three power plants affect Craiova, namely CET I (Isalnita), CET II (Simnic) and CET Turceni from Gorj county.

## 4. Monitoring PM10 in Craiova

Within Craiova urban area, the air quality is continuously monitored. The concentration of different air pollutants is recorded by five modern monitoring station provided by the European Community, denoted as DJ1, DJ2, …, DJ5 (DJ is the abbreviation for Dolj county, whose capital city is Craiova). The results recorded by these stations are validated and processed by experts from the Craiova Regional Environment Protection Agency. $PM_{10}$ concentration is recorded by four of these stations.
As an example, figure 1 presents a graphic showing the variation of this parameter during the year 2010 recorded by DJ1. We may observe that, sometimes, values over 50 μg/m$^3$ were recorded.

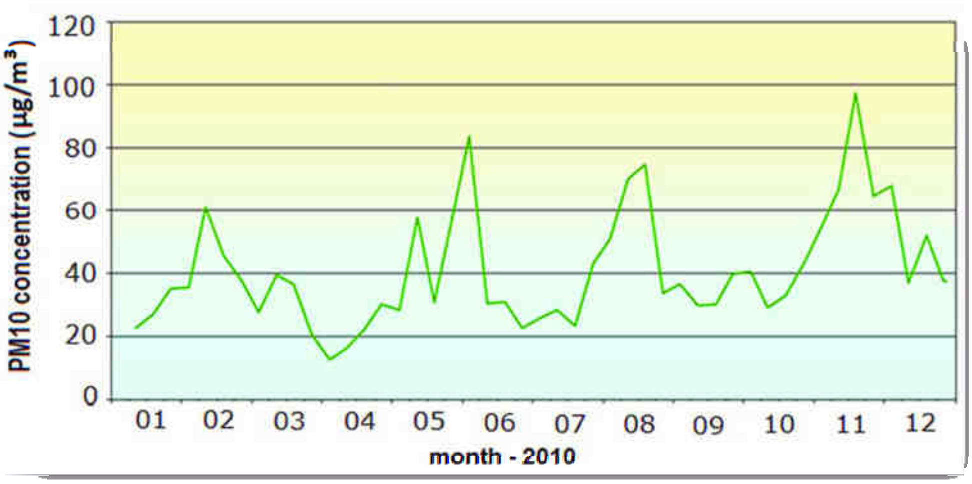


Figure 1. $PM_{10}$ concentration - data recorded at DJ1 station in 2010

In order to verify the results of our theoretical study, we shall present – in figure 2 – a graphic relating $PM_{10}$ concentration to the wind velocity. The atmospheric dynamism is a particular one: DJ4 station is located in the Jiu Valley corridor, being affected by air streams orientated from NW towards SE.

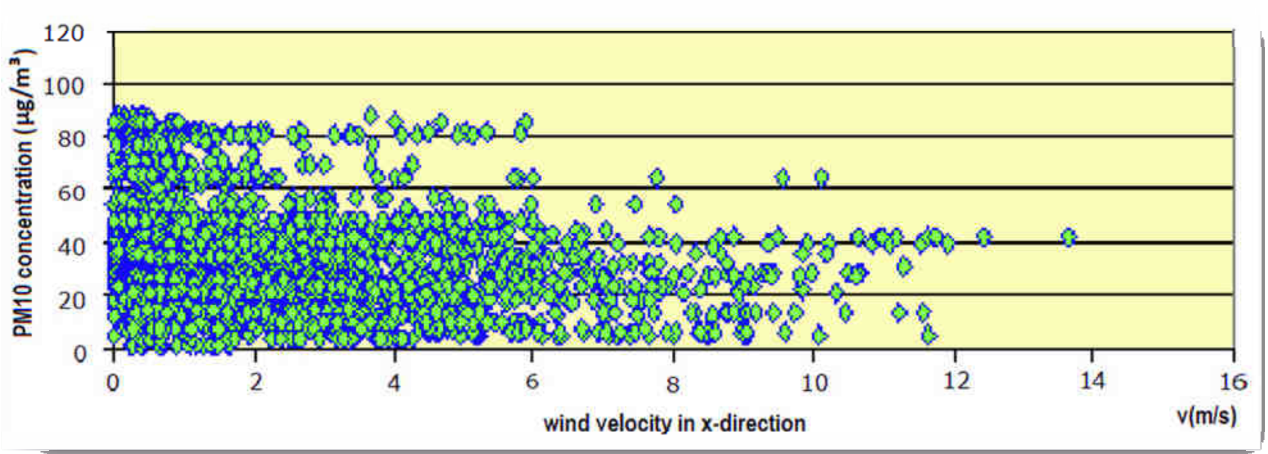

Figure 2. Correlation between $PM_{10}$ concentration measured at DJ1 and wind velocity in x direction, measured at DJ4

## 5. Mathematical model

Validated values of different parameters provided by the Craiova Regional Environment Protection Agency were used as input data, as well as meteorological parameters, mainly wind direction and wind velocity (the low average value of the wind velocity indicates a poor capacity of carrying away the dangerous particulate matter).
A tridimensional diffusion model has been developed for computing the concentration of $PM_{10}$ originated from a furnace of CET II (Simnic) – a particular point source that continuously disperses particles into the air.
The model is based on a partial differential equation which is constructed by using Fick's law. Under these circumstances, consideration of variable wind speed and variable dispersion coefficients is only possible by applying limiting assumptions.
In this diffusion model, variation of $PM_{10}$ concentration with distance obeys a log-normal correlation near the source, as shown in figure 3. Unfortunately, no analytical method for solving diffusion equations considers the log-normal profile of wind velocity.

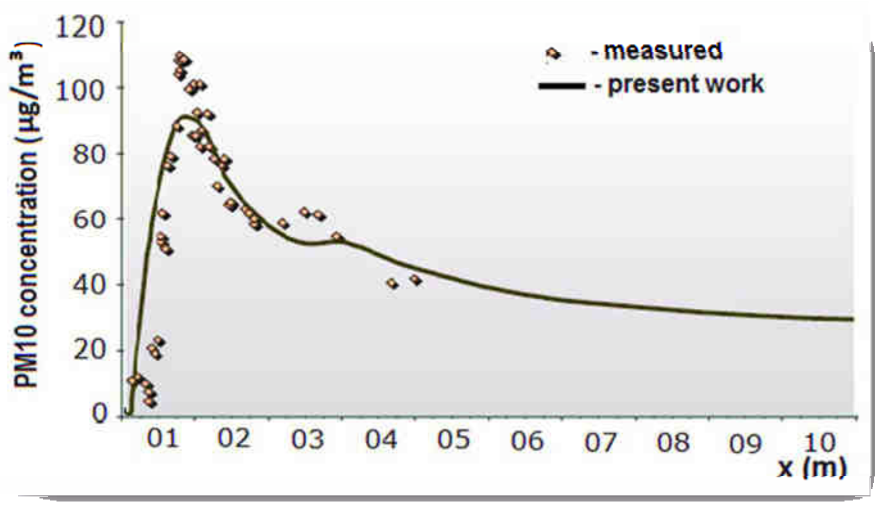


Figure 3. Log-normal variation of PM10 concentration measured on *x* direction

Thus, numerical solution methods including better and more complete atmospheric parameters within the model should be used (high-speed computers make a numerical method the best and most appropriate method for solving diffusion equations).
Any chemical reaction of the pollutants may be ignored in this analysis, but settling on the earth has to be considered.
Pollutants move horizontally in the wind direction (this direction is denoted as *x,* while X stands for the distance corresponding to the point at which a particle is carried away from the source).
$PM_{10}$ particles from the furnace power plant diffuse into the atmosphere in the y and z directions, chosen so that (*x*, *y*, *z*) represents a cartesian coordinate system. With increasing distance from the source, dispersion profile changes. Diffusion in wind direction is ignored.
Boundary conditions must be taken into account: particle concentration is considered zero before point source; particles settle on the ground with terminal velocity V; particle diffusion in the

vertical *z* direction is ignored beyond the mixing height; particle penetration in the horizontal *y* direction is ignored after a certain distance, which may be calculated knowing the wind velocity.
The continuity equation for particles – taking diffusion into account – may be represented as:

$$v\frac{\partial[PM10]}{\partial x}-\frac{\partial}{\partial y}\left(D_y\frac{\partial[PM10]}{\partial y}\right)-\frac{\partial}{\partial z}\left(D_z\frac{\partial[PM10]}{\partial z}\right)=0$$

*v* being the wind velocity in *x* direction, [PM10] – the ambient particle concentration, $D_y$ and $D_z$ – the dispersion coefficients in *y* and *z* directions.
It shows that, in computing the continuity equation for predicting particle concentration, wind velocity and PM10 dispersion coefficients must be known.
"The finite volume method", incorporating the Powerlaw scheme [1] and a stretched grid in the *x* direction was employed to obtain the numerical solution of the continuity equation for particles.
To identify the dispersion coefficients and wind profile, the surface roughness and wind speed in the mixing height must first be determined.

### 6. Results and discussions

Since determining the surface roughness is difficult, in this study the surface roughness parameter is considered to be 0.05 m (based on local topographical conditions).
Regarding atmospheric stability, the particle diffusion domain in the *y* direction is reached at about 2000 m.
For all the results presented, the height of the mixing layer is 250 m, whereas the height of the surface layer is 80 m.
Thus, with *dy*=20 m and *dz*=10 m, there are 100 elements in the *y* and *z* directions, respectively.
Generally, each section will involve 25×100 cells (i.e., 2500 cells). The domain of particle dispersion in the *x* direction is 10000 m.
To reduce the time required for calculation, the sizes of *dx* will be diverse, i.e., in a point situated close to the ash dump, where rapid changes of concentration occur, values of *dx* will be lower, while in a point situated far away from it they will be higher.
Instead of directly solving the continuity equation, the atmosphere is considered to be divided into small elements. A mass conservation equation is written for each element [2].
A small volume of fluid, with dx, dy and dz dimension, is considerate as unit cell [3], which is located in point (a, b, c).
$PM_{10}$ concentrations are supposed to be known in points (a-1,b,c), (a+1,b,c), (a,b-1,c), (a,b+1,c), (a,b,c-1), (a,b,c+1), but the concentration is supposed to be unknown in (a, b, c). Thus, a mass conservation equation for a fluid element in point (a, b, c) may be written in order to determine it:

$$v_a dydz[PM10]_{a-1.b.c} - v_a dydz[PM10]_{a.b.c} =$$
$$= \frac{(D_y)_a dxdz}{dy}[PM10]_{a.b.c} + \frac{(D_z)_{a-1/2} dxdy}{dz}[PM10]_{a.b.c} + \frac{(D_z)_{a+1/2} dxdy}{dz}[PM10]_{a.b.c} - \frac{(D_y)_a dxdz}{dy}[PM10]_{a.b-1.c} +$$
$$\frac{(D_y)_a dxdz}{dy}[PM10]_{a.b+1.c} - \frac{(D_z)_{a-1/2} dxdy}{dz}[PM10]_{a.b.c-1} - \frac{(D_z)_{a+1/2} dxdy}{dz}[PM10]_{a.b.c+1}$$

which may be rewritten as:

$[PM10]_{a.b.c}$ =*A/B*

where:

$$A = v_a dydz[PM10]_{a-1.b.c} + \frac{(D_y)_a dxdz}{dy}[PM10]_{a.b-1.c} + \frac{(D_y)_a dxdz}{dy}[PM10]_{a.b+1.c} + \frac{(D_z)_{a-1/2} dxdy}{dz}[PM10]_{a.b.c-1} +$$

$$\frac{(D_z)_{a+1/2} dxdy}{dz}[PM10]_{a.b.c+1}$$

whereas

$$B = v_a dydz + \frac{(D_y)_a dxdz}{dy} + \frac{(D_z)_{a-1/2} dxdy}{dz} + \frac{(D_z)_{a+1/2} dxdy}{dz}$$

For the elements near the ground, diffusion toward the ground is not considered. Instead, it is assumed that pollutants settle on the ground with terminal velocity.
On the other hand,

$$\frac{\partial}{\partial z}\left(D_z \frac{\partial[PM10]}{\partial z}\right) = V\frac{\partial[PM10]}{\partial z}$$

*V* being the particle terminal velocity [4]:

$$V = \frac{\rho d^2 g}{18\eta}$$

where $\rho$ is the particle density (kg·m$^{-3}$), $d$ is the particle diameter (m), $g$ is the gravity acceleration (m·s$^{-2}$) and $\eta$ stands for the viscosity (kg·m$^{-1}$·s$^{-1}$).

**7. Graphic representation of the ash particles diffusion**

To obtain the concentration profile in the ground surface layer to be more clearly understood, a reliable graphical representaton is required. It is shown in figure 4.

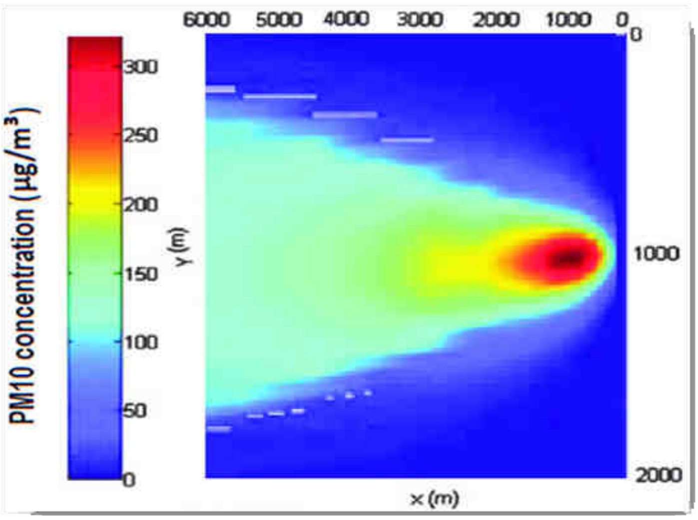


Figure 4. The concentration profile
in the ground surface layer

A code of colors has been used for designating the concentration values of $PM_{10}$ ($\mu g/m^3$) – as one might see on the right side of each figure – and they are both given in the cartesian coordinates ($x$, $y$, $z$) - $x$ and $y$ representing the distances from the power plant furnace ($x$ is the wind velocity main direction, whereas $z$ represents the concentration of the particulate matter). The figure (which seems to be bidimensional) shows the "map" seen from "above", i.e. from a point that is situated on the $z$ axis [5].

## 8. Conclusion

The study has shown that it is necessary to monitor the air quality, especially the concentration of those pollutants that may cause major health injury.
A comparisson between practical and theoretical data is useful in predicting the air pollution, so that measures can be taken to diminish it.
The paper proposed a theoretical manner to simulate the way the urban air may be afected by a pollution source, such as a power plant furnace (CET II – Simnic was selected for the present work).
It has been shown that $PM_{10}$ daily average in the ambiental air of Craiova city at distances between 0.31 and 1.44 km from the power plant furnace is often higher than the European Union thershold of 50 $\mu g/m^3$ (which may not be exceeded more than 35 times a year).
Therefore, urgent measures for reducing air pollution have to be taken in Craiova, as well as in other developed cities in Romania, for our country to get the exoneration from the European Union, as far as air pollution is concerned and, of course, for us to improve our own life quality.
As far as the model itself is concerned, the good agreement between the theoretical results and the measured data shows that this model can be a powerful tool in predicting $PM_{10}$ concentrations.

## REFERENCES

[2] (Example for a Proceedings/ journal paper – Arial, 10pt, Regular) T.C.Popescu, A.Drumea and I.Dutu, "Numerical simulation and experimental identification of the laser controlled modular system purposefully created for equipping the terrace leveling installations", ISSE-2008, Budapest, Hungary; 7-11 May, 2008, " Proceedings - Reliability and Life-time Prediction", ISBN: 978-963-06-4915-5; pp.336-341
[1] V.S. Patankar, "Numerical heat transfer and fluid flow," New York: McGraw Hill Book Company, 1980.
[2] D.M. Moreira, M.T. Vilhena, D. Buske and T. Tirabassi, "The GILTT solution of the advection – diffusion equation for an inhomogeneous and nonstationary PBL," Atmospheric Environment, vol. 40, pp. 3186-3194, 2006.
[3] S. Baroutian, A. Mohebbi and A. Soltani Goharrizi, "Measuring and modeling particulate dispersion: A case study of Kerman Cement Plant," J. Hazardous Materials, vol. 136, pp. 468-474, 2006.
[4] V. Guttal and C. Jayaprakash, "Spatial variance and spatial skewness: leading indicators of regime shifts in spatial ecological systems," Theor. Ecol., vol. 11, pp. 450–460, 2009.
[5] G. Vladut, M.D. Mateescu, L.S. Sbirna and S. Sbirna, "Mathematical model proposed for simulating the influence on air quality of the three ash dumps that affect Craiova, Romania" 14th International Conference on System Theory and Control (SINTESIS 14), Sinaia, 17-19 octombrie 2010, http://ace.ucv.ro/sintes14/

ISSN 1454 - 8003
Proceedings of 2011 International Salon of Hydraulics and Pneumatics - HERVEX
*9 – 11 November, Calimanesti-Caciulata, Romania*

# TECHNICAL EQUIPMENT FOR SOIL WORKING IN NARROW STRIPS, SOWING HOEING PLANTS, FERTILIZING AND DISTRIBUTING GRANULAR INSECTICIDES

**Eugen MARIN[1], Ion PIRNA[2], Cristian SORICĂ[3]**

[1] INMA Bucharest, emarin@inma.ro

[2] INMA Bucharest, pirna@inma.ro

[3] INMA Bucharest, sorica@inma.ro

***Abstract***: *In this paper are presented the experimental researches, which were performed at the establishment of corn crop, with a technical equipment for soil working in strips, sowing, fertilizing and distributing micro granular insecticides in aggregate with 140 HP tractor on wheels, New Holland T6070 type, for determining the working qualitative indicators and energy indicators and in aggregate with 150 HP wheeled tractor., Lamborghini 1506 type, for determining operating indicators. The results obtained from experimental investigations have assured the constructive validation for the working bodies of the technical equipment proposed within innovative technology for sowing hoeing plants in sustainable system. By using this technology it was assured the conservation or amelioration of soil characteristics and the maintaining of its structure by reducing the compaction due to the reduction of number of works performed.*

***Keywords:*** *soil, strips, sowing, hoeing plants, fertilizing, insecticides*

## 1. Introduction

Continuing intensification of agriculture will aggravate the negative effects on the environment through degradation of its various components: soil, atmosphere, surface and depth water etc., affecting the development and promotion of sustainable economy and a healthy society [1]. It results the need to find alternative for soil working and plant cultivation to minimize the depreciation of the soil and allow the performance of quality works on time and with minimum energy consumption, respectively low production costs and high profits. One of these alternatives is sustainable agriculture which aims to enhance agricultural production by optimizing the use of agricultural resources and helping to reduce lands widespread degradation through integrated management of available soil, waters and biological resources combined with external raw material. Mechanized work is replaced by the biological soil mixing, microorganisms in the soil, roots and soil fauna being designed to work and balance the soil nutrients. Soil fertility (nutrients and water) is controlled by managing the soil covering, crop rotation and weed control [7]. Technical equipment presented in this paper in a modulated construction is designed to allow, by simple mounting or dismounting of some assemblies, to be used independently in one passing for preparing, working and loosening the soil in an area called "narrow strip" and in another passing for hoeing plants sowing (seed by seed sowing for maize , sunflower, etc.) concomitantly with applying chemical fertilizers and insecticides or simultaneously applying the products above when the soil working in "narrow strips", sowing of hoeing plants, fertilizing, granular insecticides distribution, incorporation into soil, the covering and light compaction are achieved in a single passage, reducing significantly the soil compaction, energy consumption, labour cost, etc.

## 2. Materials and method

For performing the experimental researches in laboratory-field conditions, in order to determine the working qualitative indicators and energy indicators, was used a NEW HOLLAND T6070 tractor, as existing equipment within INMA Bucharest, which has the following main technical characteristics: overall dimensions (length x width x height ), mm: 5347x2230x3040; tractor mass, kg: 10000; wheelbase, mm: 2734; track at the front / rear axle, mm: 2030/2030; engine power: 141 HP [5]. Technical equipment for soil working in narrow strips, sowing, fertilizing and distributing granular insecticides (Fig. 1a) consists of an equipment for working the soil in narrow strips 1 (Fig. 1b) and a sowing machine for sowing hoeing plants concomitantly with fertilization and distribution of granular insecticides 2 (fig. 1b). On the frame of equipment 1 (Fig. 1b) are mounted the following components: a coupling bar, a left support wheel, a right support wheel and four sections for working the soil in narrow strips.


**a.** **b.**

**Fig. 1.** *Technical equipment for soil working in narrow strips, sowing, fertilizing and distributing granular insecticides (a - rear right side view, b - left side view)*

The section for soil working in narrow strips (Fig. 2) consists of two notched discs 1, mounted inclined in the form of "V" pointing toward the direction of advance, a straight notched disc 2, a knife with reversible chisel 3 and two spherical notched discs 4, mounted in the form of "V" pointing toward backwards with the possibility of adjusting the tilting angle. The two notched discs mounted tilted 1 perform the stripping of stubble or superficial layer the soil creating a strip wide of 20 centimeters cleared of plant debris. In this way, without having to increase the amount of herbicides used, are destroyed even the already emerged weeds and the emergence of others is delayed. This fact eliminates the danger of plants' suffocation with weeds, before they be vigorous enough to defend themselves or to be able to perform mechanical maintenance work. Under the weight of the soil working section the straight notched disc 2 enters the soil until the settled working depth (2...20 cm). It performs the vertical cutting of the soil and the cutting of plant debris, to facilitate the knife with reversible chisel 3 to enter the soil. During work, the knife with reversible chisel 3 performs one penetration movement and one translation movement or displacement which leads to the creation of a ditch filled with loose soil, which is gathered in narrow strips (width 20 cm) by two spherical notched discs 4 behind it.

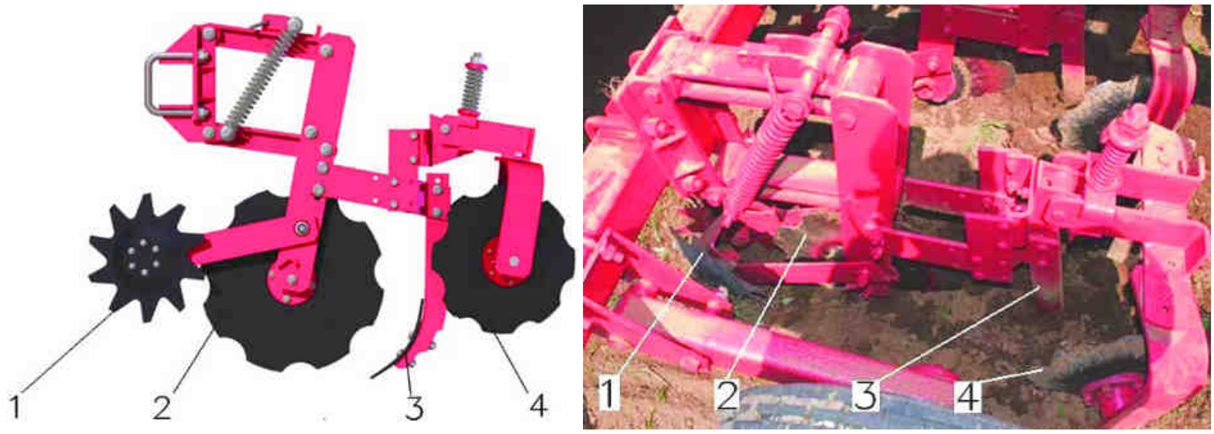


**Fig. 2.** *Module for soil working in narrow strips*

The constant maintaining of the working depth (Fig. 3) is performed using the two tension springs mounted on the deformable parallelogram and the compression spring 2 mounted on the mounting bracket of the two spherical notched discs.


**Fig. 3.** *The constant maintaining of the working depth*

The sections for sowing (fig.4) are mounted on the sowing machine frame bar2 (fig. 1b) through a system of articulated bars and a plate fixed with two clamps. A section for sowing is composed of a seed hopper 1, a pneumatic distribution device 2, a double disc coulter 3 and a compaction wheel 4. The constant maintaining of the working depth is performed using the a tension spring 5 mounted on the deformable parallelogram.

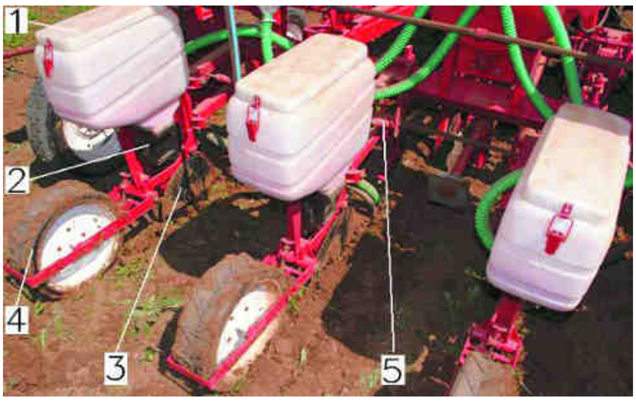


**Fig. 4.** *Sowing module*

The pneumatic distribution device (fig. 5), is made of two housings between which is rotating the interchangeable sowing disc. The sowing discs 1 are made of steel and are provided with holes for distributing the seeds. Depending on the seeds variety, the holes of sowing discs have the diameter between 2.5...5.5 mm. The discs are easily changed without using any tool. In order to eliminate losses of seeds and vacuum between the vacuum chamber 2 and the disc, a sealing gasket 3 is provided.

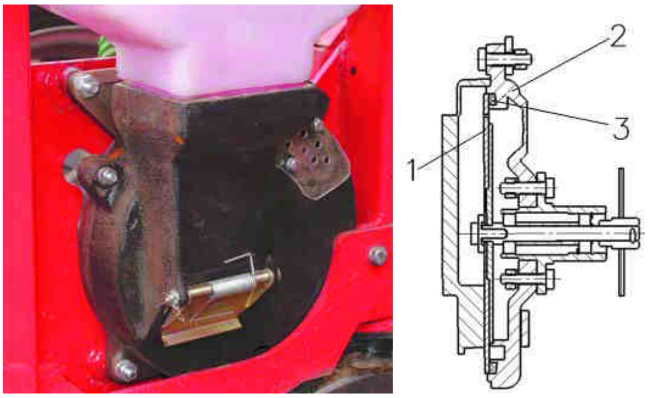


**Fig. 5.** *Pneumatic distribution device*

The main technical characteristics of the technical equipment are presented in table 1.

Table1

| Characteristic | UM | Value |
|---|---|---|
| Number of section for soil working | pcs | 4 |
| Distance between the sections for soil working | mm | 700 |
| Number of sowing sections | pcs | 4 |
| Number of sowing coulters | pcs | 4 |
| Distance between the rows sown | cm | 12.5 |
| Sowing depth | cm | 2...12 |
| Working width | m | 2.8 |
| Mass | kg | 1383 |

For manufacturing the technical equipment for soil working in narrow strips, sowing hoeing plants, fertilizing and distributing granular insecticides, were used solutions subjected to patent application no. A1637 / 10.11.2009 [6]. The main advantages of the new chosen solutions are: they ensure the access, facilitate and reduce the time needed for the mounting and dismounting of the coupling bars between the technical equipment for soil working and the sowing machine and as well as for technical interventions at components level..

The tests of technical equipment in laboratory-field conditions, for the determination of working qualitative indicators and energy indicators, were performed on the experimental fields of INMA Bucharest in accordance with a specific procedure for testing and requirements of SR 13238 [9] and STAS ISO 7256/1-92 [10].

The equipment used for determining the soil characteristics of the experimental field:
- Electronic digital cone penetrometer FIELDSCOUT SC 900;
- Capacitive soil humidity measuring device FIELDSCOUT TDR 300;
- Navigation device Garmin GPSMAP 60 CSx.

Equipment used for determining the working qualitative indicators:
- Mechanical timer;
- Electronic balance METTLER PM 6000;
- Portable scale RW10P;

- Electronic tachometer.

Equipment used for determining the energy and exploitation indicators:

- Frame with strain gauge marks;
- Amplification and data acquisition system MGCplus type.

The frame with strain gauge marks (fig. 6) is made of three frames (central 1 and side 2,3) and five adjustable supports with elastic rings 4 that can be mounted through fasteners in three positions, allowing its coupling both, to three-point linkages 3, 3N, 4, 4N category according to ISO 730:2009 [8] of the tractors, and coupling devices of agricultural machines within respective categories


**Fig. 6**. *The frame with strain gauge marks, coupled to three-point linkages 3 category according to ISO 730:2009 of the tractor*

There were determined the following qualitative indicators:

- *The depth for soil work* was determined by measuring the distance between the surface of the uncultivated field and the bottom of the furrow left by the working body.
- *The soil working width* of technical equipment was determined in 5 different places and for three working speeds (small, average and maximum), by measuring with tape the distance from each marking pole to furrow wall, making the difference with the previous passing.
- *The seeds incorporating depth* represents the distance measured from soil level, resulted following the sowing till the depth at which the seeds are. Measurements have been performed according to method ”in green”, namely after the plants arising, on all the rows, after a three-displacement passing, 3 times in 3 different areas of the plot(at the ends and in the middle).

For determining the traction force of technical equipment coupled by three-point suspension mechanism to tractor the tensometer method has been used [2] through the intermediate of a modern strain measuring instrument comprising a data amplifying and acquisition of MGCplus type, with 16 analogous input channels and 16 digital output channels and an amplifying module of ML 455 HBM type. In order to register the data acquired directly from a computer a soft CATMAN, specialized in data acquisition and processing has been used. The supplying power source of MGCplus was a battery of lead accumulators of 12 V voltage. CATMAN soft specialized in data acquiring and processing has allowed to filter the signals received from transducers and determine their minimum, average and maximum values.

The traction power $P_{tr}$ was calculated on basis of aggregate displacement speed $v_l$ and traction force $F_{tr}$ previously determined by means of relation [3], [4]:

$$P_{tr} = \frac{F_{tr} \times v_l}{270}, \text{ CP} \qquad (1)$$

where $F_{tr}$ is measured in N and $v_l$ in km/h.

**3. Results**

The graphical representation of average working depth and variation index for three working speeds are shown in figure 7.

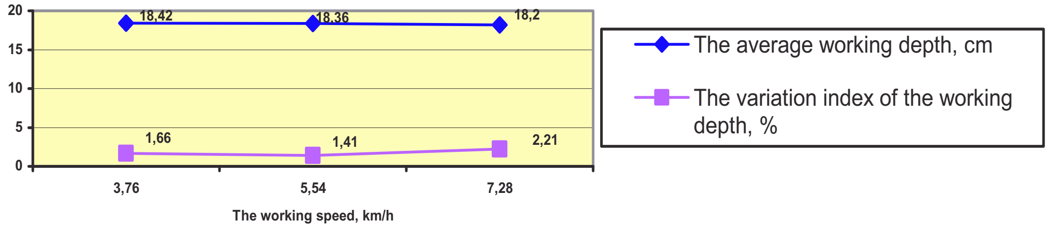


**Fig. 7.** *Graphical representation of soil average working depth*

Graphical representation of soil average working width and variation index for three working speeds are shown in figure 8.

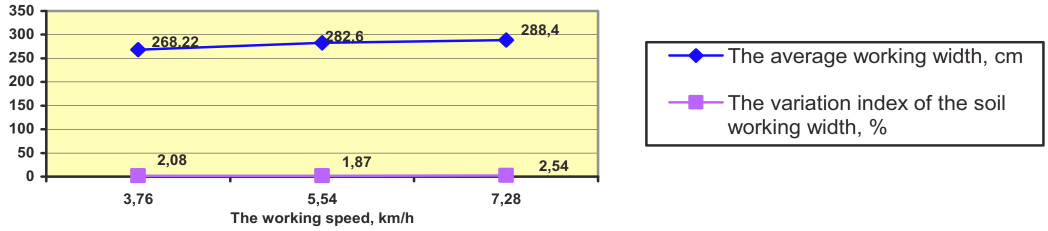


**Fig. 8.** *Graphical representation of soil average working width*

The graphical representation of variation of average incorporating depth of corn seeds and variation coefficient of incorporating depth depending on working speed on row 1 are presented in figure 9.

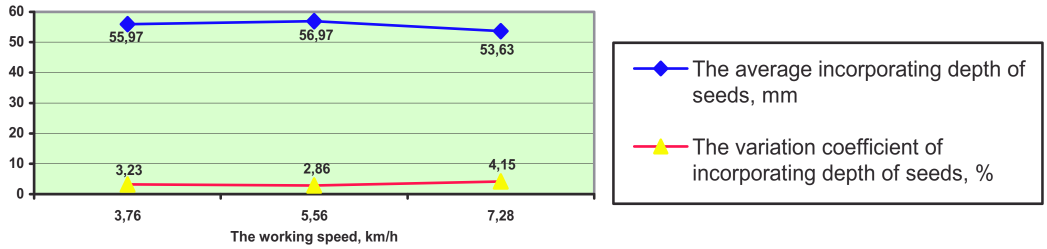


**Fig. 9.** *Graphical representation of variation of average incorporating depth and variation coefficient according to working speed for row 1*

The graphical representation of variation of average incorporating depth of corn seeds and variation coefficient of incorporating depth depending on working speed on row 2 are shown in figure 10.

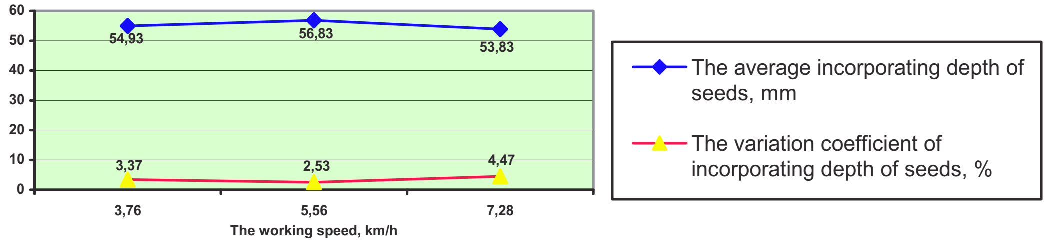


**Fig. 10.** *Graphical representation of average depth and variation coefficient according to working speed on row 2*

The graphical representation of variation of average incorporating depth of corn seeds and variation coefficient of incorporating depth depending on working speed on row 3 are shown in figure 11.

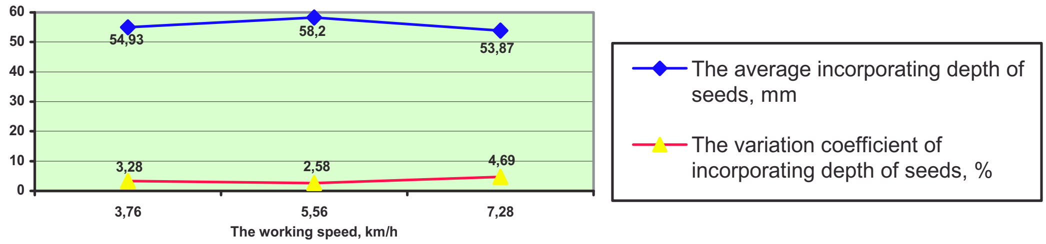


**Fig. 11.** *Graphical representation of average depth and variation coefficient according to working speed on row 3*

The graphical representation of variation of average incorporating depth of corn seeds and variation coefficient of incorporating depth depending on working speed on row 4 are shown in figure 12.

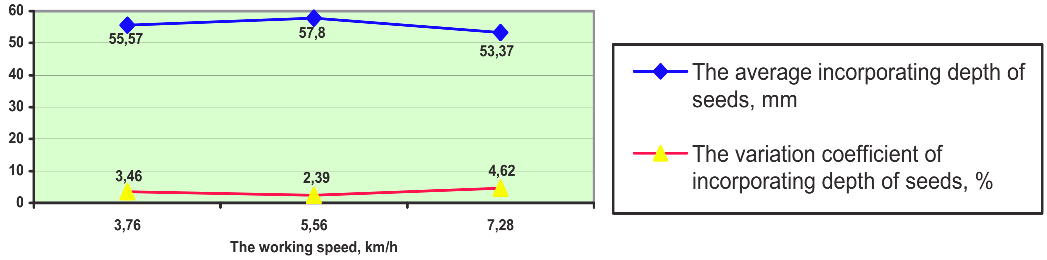


**Fig. 12.** *Graphical representation of average depth and variation coefficient according to working speed on row 4*

In figure 13 is graphically shown the variation of indexes determined for three speed stages of aggregate tractor.

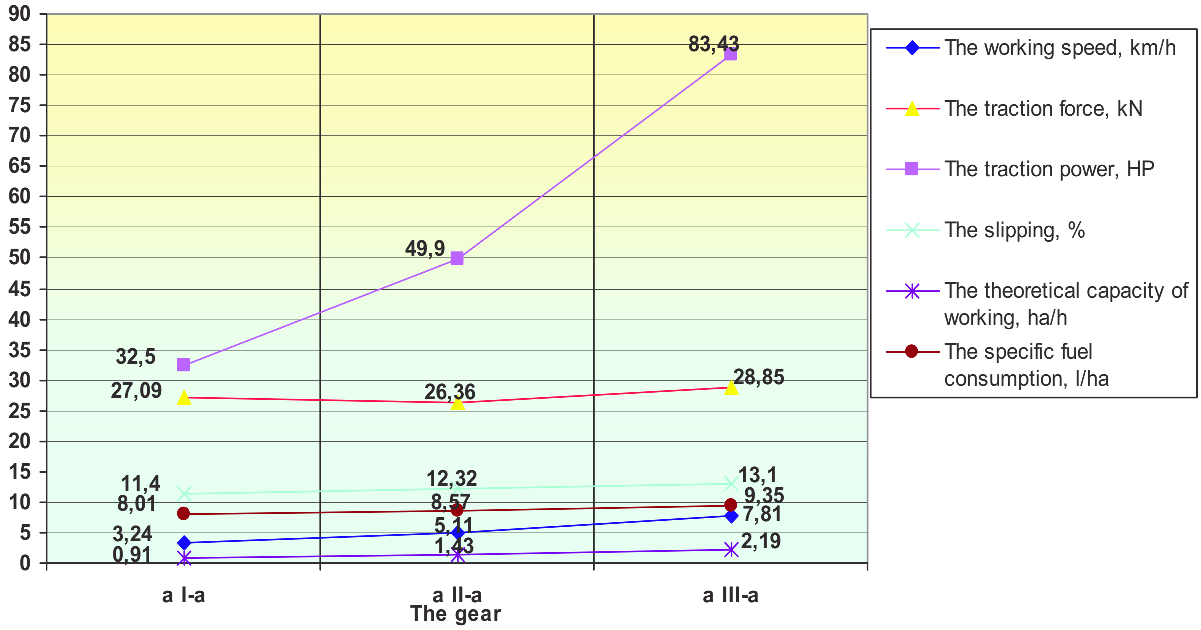


**Fig. 14.** *Graphical representation of variation of indexes determined for three speed stages*

**Results obtained during the tests performed in operating conditions of technical equipment,** working in aggregate with Lamborghini R1506 tractor on the agricultural field of ICDB Baloteşti, when sowing and fertilizing corn for silage, on a surface of 80 ha, in non prepared field, by applying the soil innovative working technology and setting crops by a single passing and weeds control technology with herbicides are shown in table 2.

Table 2

| **Specification** | **MU** | **Date at wich timing was performed** | | | | |
|---|---|---|---|---|---|---|
| | | **Day 1** | **Day 2** | **Day 3** | **Day 4** | **Day 5** |
| Crop sown | - | corn | corn | corn | corn | corn |
| Average displacement speed | km/h | 5.52 | 5.48 | 5.56 | 5.58 | 5.46 |
| Surface sown | ha | 10.2 | 9.8 | 10.4 | 10.6 | 9.6 |
| Real working time, $T_1$ | min | 342 | 331 | 344 | 348 | 326 |
| Time for turns at plot ends, $T_{21}$ | min | 16 | 17 | 15 | 18 | 19 |
| Time for seeds and fertilizers supplying, $T_{23}$ | min | 12 | 14 | 11 | 10 | 12 |
| Time for technical maintenance of equipment $T_{31}$ | min | 6 | 8 | 4 | 7 | 8 |
| Time for remedying the technological faults, $T_{41}$ | min | - | 4 | 3 | - | 5 |
| Time for remedying the technological faults, $T_{42}$ | min | 10 | 6 | - | 12 | - |
| Time of shift, $T_{07}$ | min | 420 | 411 | 417 | 431 | 409 |
| Working hourly capacity at real time, $W_{ef}$ | ha/h | 1.78 | 1.77 | 1.81 | 1.82 | 1.76 |
| Capacity of working per hour at shift time $W_{07}$ | ha/h | 1.46 | 1.43 | 1.49 | 1.48 | 1.40 |
| Coefficient of technological safety, $K_{41}$ | - | 0.98 | 0.97 | 0.97 | 0.98 | 0.99 |
| Coefficient of technological safety , $K_{42}$ | - | 0.92 | 0.90 | 0.91 | 0..95 | 0.90 |
| Coefficient of reliability, $K_4$ | - | 0.90 | 0.87 | 0.89 | 0.93 | 0.88 |

| Specification | MU | Date at wich timing was performed | | | | |
|---|---|---|---|---|---|---|
| | | Day 1 | Day 2 | Day 3 | Day 4 | Day 5 |
| Coefficient of using the shift time, $K_{07}$ | - | 0.75 | 0.74 | 0.76 | 0.76 | 0.79 |
| Consumption of fuel per ha | l/ha | 8.9 | 9.0 | 8.8 | 8.9 | 9.2 |

Aspect during the exploitation indexes determination-shown in figure 14.

**Fig. 14.** *Aspect during the exploitation indexes determination*

**4. Conclusions**

After the experimental tests performed with technical equipment at corn crop setting the following have resulted:
- The technical equipment was conceived on basis of innovating elements, representing the object of a patent demand;
- Values of working qualitative indexes were calculated using the algorithms of processing the theoretical and experimental data;
- In operating terms, the technical equipment has achieved working qualitative indexes which are in compliance with agrotechnical requirements for sowing hoeing plants, stipulated in standard in force. This fact is shown by the suitable uniformity of seeds incorporating into the soil for all three working speeds, (minimum speed- 3.23 km/h, average speed-5.56 km/h and maximum speed 7.28 km/h), with bigger values for working speed of 5.56 km/h.
- On the whole tests running period performed on 80 ha, in operating conditions, the technical equipment in aggregate with tractor Lamborghini R1506 had a good behaviour, achieving an average working capacity per hour at real working time of 1.78 ha/h appropriate to average working speed of 5.52 km/h and an average fuel consumption per ha of 8.96 l/ha;
- The experimental researches have allowed to validate the technical and technological solutions tackled when technical equipment parts were designed.

**REFERENCES**

[1]. Arshad M. A., „Preparing the soil and soil quality: Methods of preparing the soil for a sustainable agriculture and high quality environment in different agro-ecosystems", Vol. 53, Issue 1, Journal: Researches regarding the soil and its works, ISSN: 0167-1987, pg. 1-2, Printed ELSEVIER, November,1999
[2]. Constantinescu I., "Measuring the mechanical values by means of gauge measuring system", Technical Publishing House, Bucharest, 1989
[3]. Popescu S., Năstăsoiu S., Tane N., „Considerations on power consumption of agricultural machines driven by tractor PTO,", Vol. I, Bulletin CIT, pg. 221-226, Braşov, 1988

[4]. Tecuşan N., Ionescu E., „Tractors and motor cars”, Didactic and Pedagogic Publishing House, Bucharest, 1982
[5]. http://agriculture.newholland.com/uk/en/Products/Tractors, 2011
[6] http://pub.osim.ro/publication-server/pdf-document?PN=RO126262%20RO%20126262&iDocId=996&iepatch=.pdf, 2011
[7] http://soco.jrc.ec.europa.eu, 2009
[8]. ***ISO 730:2009: Agricultural wheeled tractors -- Rear-mounted three-point linkage -- Categories 1N, 1, 2N, 2, 3N, 3, 4N and 4, International Organization for Standardization, 2009
[9]. ***SR 13238-1:1994 – Agricultural Machines. Sowing machines seeds by seeds (Precision sowing machines). Technical quality conditions, Classifying index D 53, ASRO, 1994
[10]. ***STAS ISO 7256/1-92: Sowing tools. Testing methods. Part 1: Sowing machines seeds by seeds (Precision sowing), Classifying index D 53, ASRO, January 1992.

**ISSN 1454 - 8003**
**Proceedings of 2011 International Salon of Hydraulics and Pneumatics - HERVEX**
*9 – 11 November, Calimanesti-Caciulata, Romania*

# INFLUENȚA UTILIZĂRII ENERGIILOR REGENERABILE ASUPRA EFICIENȚEI ENERGETICE A CULTURII DE VIȚĂ DE VIE

**Haraga Georgeta, Murad Erol**

Universitatea POLITEHNICA din Bucureşti
g_haraga@yahoo.com ; erolmurad@yahoo.com

***Rezumat***

*Se analizează structura şi modul de realizare a unui bilanț energetic pentru cultura de viță de vie din care reiese o valoare energetică ridicată a unui subprodus secundar: corzile de viță tăiate anual.*

*Se aplică conceptul de eficiență energetică în locul noțiunii de randament, care este greşit utilizat încă în analizele efectuate pentru evaluăriile energetice ale culturilor agricole.*

*Se constată ca cu biomasa constituită din corzile de viță tăiate de pe un hectar se poate asigura irigarea anuală a acestuia, lucrare care ar necesita circa 420 litri de motorină.*

*Utilizarea biomasei produsă local, a corzilor de viță, pentru alimentarea cu energie a instalațiilor de irigare, conduce la mărirea substanțială a eficienței energetice a culturii de viță de vie prin reducerea apreciabilă a valorii energiilor de intrare în sistemul analizat. De asemenea se obține şi o creştere a producției medii neafectată de modificările climatice.*

***Cuvinte cheie:*** *bilanț energetic, eficiență energetică, biomasă, corzi de viță*

## 1. Introducere

Una din cerințele dezvoltării durabile a agriculturii, constă în utilizarea rațională şi ecologică a tuturor resurselor de energie regenerabile pentru reducerea emisiei de $CO_2$. În acest context utilizarea corzilor de viță de vie reprezintă o valoroasă sursă de energie regenerabilă, care se poate utiliza local, contribuind şi la creşterea nivelului de independență energetică a fermelor agricole. [4, 5, 16]

În lucrare se analizează eficiența energetică a culturii de viță de vie pentru două tehnologii:

- tehnologie utilizată actual;
- tehnologie modificată cu irigare realizată cu energie din biomasa rezultată ca produs secundar.

La Catedra de Sisteme Biotehnice din UPB s-a conceput un model şi un program pentru calculul bilanțurilor şi eficienței energetice pentru culturile de struguri pentru vinificație şi de masă.

Se constată că eficiența energetică a crescut substanțial în cazul aplicării tehnologiei modificate care are un nivel mai ridicat de independență energetică, obținută prin utilizarea corzilor de viță pentru producerea de energie prin gazeificare termo-chimică. Concomitent se reduce cu circa 930 kg/ha.an emisia de $CO_2$ ca urmare a neutilizării motorinei necesare pentru un irigarea unui hectar de vie.

## 2. Bilanțul energetic în viticultură

Bilanțul energetic general al unei culturi agricole în general şi al unei culturi de viță de vie în special are forma generală:

$$BEG = OE - IE \tag{1}$$

unde: BEG este bilanțul energetic general [GJ/ha]

OE – totalul energiilor de ieşire din sistem [GJ/ha]

IE – totalul energiilor de intrare în sistem [GJ/ha]

În abordarea structurii bilanțului energetic din această lucrare se utilizează o evidențiere a structurii energiilor de ieşire din sistem, în concordanță cu cerințele dezvoltării durabile, pentru a se pune în evidență posibilitățile de utilizare cât mai complete a tuturor energiilor de ieşire din sistem. Divizarea s-a făcut în:

OEP - totalul energiilor de ieşire principale, determinate de destinația produsului principal al culturii – strugurii;

OES - totalul energiilor de ieşire secundare, ale subproduselor culturii de viță de vie, utilizabile în alte destinații.

$$OE = OEP + OES \tag{2}$$

Ca urmare, bilanțul energetic total se poate diviza în două componente:

$$BEG = BEP + BES \tag{3}$$

unde: BEP este bilanțul energetic primar [GJ/ha]

BES - bilanțul energetic secundar [GJ/ha]

Pentru punerea în valoare a produselor secundare se mai consumă energie pentru preprocesarea acestora. Ca urmare este necesar să se descompună totalul energiilor de intrare în: energie de intrare primară IEP [GJ/ha] şi în energie de intrare secundară IES [GJ/ha]. Ca urmare rezultă că:

$$IE = IEP + IES \tag{4}$$

IEP - totalul energiilor de intrare principale, necesare pentru obținerea produsului principal al culturii – strugurii;

IES - totalul energiilor de intrare secundare, necesare pentru valorificarea subproduselor culturii de viță de vie.

Bilanțul energetic primar se defineşte ca diferența dintre totalul energiilor de ieşire principale, OEP, pentru care este realizată cultura, şi totalul energiilor de intrare în sistem, IE:

$$BEP = OEP - IEP \tag{5}$$

Bilanțul energetic secundar se defineşte ca fiind totalul energiilor de ieşire secundare, ale subproduselor culturii de viță de vie, utilizabile cu alte destinații:

$$BES = OES - IES \tag{6}$$

## 3. Intrările de energie în sistem

Totalul intrărilor de energie principale IEP în sistem, cultura de viță de vie, se poate defalca în două componente în funcție de modul de participare la realizarea produsului final:

$$IEP = IEPA + IEPP \tag{7}$$

IEPA - Energie de intrare principală activă [GJ/ha];

IEPP - Energie de intrare principală pasivă [GJ/ha].

Energiile de intrare principale active sunt definite ca fiind cele care sunt introduse în procesul de producție agricolă al unei culturi. Ele se pot defalca în energie de intrare activă directă – IEAD; şi energie de intrare activă indirectă – IEAI:

$$IEPA = IEPAD + IEPAI \tag{8}$$

Energia de intrare principală activă directă, **IEPAD**, este formată din din suma energiile înglobate în:

1. Energie umană – EUM = IEPAD;
2. Energie animală – EAN = IEPAD;
3. Energie combustibili – ECB = IEPAD;
4. Energie electrică – EEL = IEPAD;
5. Energie termică – ETR = IEPAD;
6. Energie solară – ESOL= IEPAD;

7. Energie pentru irigație – EIR = IEPAD;

Energia de intrare principală activă indirectă, IEPAI, este formată din suma energiilor înglobate în:

1. Tratamente chimice – ETCH = IEPAI[2];
2. Ingraşăminte – EING = IEPAI;
3. Amendamente – EAMD = IEPAI;

Energia de intrare principală pasivă – IEPP - este definită ca fiind suma energiilor care s-au folosit pentru realizarea maşinilor, instalațiilor şi a celorlate utilități care sunt utilizate pentru realizarea a mai multor culturi, fiind consumate treptat.

Energia de intrare principală pasivă, IEPP, este formată din suma energiile înglobate în:

1. Maşini agricole şi tractoare – EMAT = IEPP;
2. Construcții – ECON = IEPP;
3. Infințare cultură – EIC = IEPP;
4. Mijloace fixe – EMFX = IEPP;

## 4. Ieşiri energetice din sistem

### 4.1 Aspecte generale

Energiile de ieşire din sistem (OET) pentru cultura viței de vie, se clasifică în două mari categorii: primare OEP şi secundare - OES:

$$OET = OEP + OES \tag{9}$$

În cazul studiat, pentru cultura viței de vie, energiile de ieşire primare diferă în funcție de destinația masei de struguri recoltați: de masă (OEPM) sau pentru vinificație (OEPV). Astfel, se vor calcula două tipuri de totaluri de energie de ieşire pentru cele două destinații finale: OETM şi OETV.

Energia de ieşire primară este suma energiilor corespunzătoare substanțelor din struguri, digerabile de om, sau a celor din vinul care rezultă din producția de struguri.

Energia de ieşire secundară (OES) este suma energiilor disponibile pentru diferite utilizări, ale subproduselor culturii de viță de vie (OESM), sau a viticulturii (OESV). Aici pot fi incluse nu doar produsele secundare rămase în urma procesului de producere a vinului, ci şi materiale rezultate pe parcursul anului (corzi şi lăstari tăiați, material vegetal ierbos etc.).

$$OETM = OEPM + OESM \tag{10}$$

$$OETV = OEPV + OESV \tag{11}$$

### 4.2 Energiile de ieşire primare

Ieşirile de energie primară pentru cultura viței de vie sunt cele cuprinse în masa de struguri recoltată. Se ia în considerare numai masa uscată a strugurilor:

- masa uscată {în medie}: 0,190 kg.mu/kg. struguri;
- proteină brută digestibilă: 0,020 kg/kg. struguri;
- energie specifică masă uscată: $E_{mus}$=22,69 MJ/kg.mu = 6,3 kWh/kg.mu;
- energie ieşire specifică struguri: $OEP_s \approx$ 4,30 MJ/kg.struguri = 1,20 kWh/kg.struguri.

### 4.3 Energiile de ieşire secundare

La un hectar de cultură normal de viță de vie sunt 4000-5000 butuci care la tăiere produc 0,5-1 kg biomasă/butuc cu umiditatea realtivă în domeniul 30..40%, cu o media de 35%; deci între 2000-4000 kg.cv/an. Aceste valori pot varia relativ mult în funcție de condițiile de sol şi climaterice ale anului viticol. [2, 3, 17,18]

Masa uscată ($_{us}$) a corzilor are o puterea calorifică inferioară $PCI_{mu}$ (medie) de:

$$PCI_{us} \approx 18\ MJ / kg._{us} \tag{12}$$

La utilizare corzile au o umiditate relativă medie de 15%, valoare optimă pentru depozitare, ardere sau gazeificare termo-chimică, iar puterea calorifică inferioară $PCI_{cv}$ utilizabilă este:

$$PCI_{cv} \approx 15\ MJ/kg._{um} \quad (13)$$

Luând în considerare că masa medie de corzi de viță umede recoltată este de $M_{cvs} \approx 3000$ kg/ha, rezultă că masa uscată disponibilă energetic este $M_{mus}$=1950 $kg._{cvus}$. Această masă reprezintă un potențialul energetic anual de: $EP_{cvs} \approx$ 35.000 MJ/ha.an = 9700 kWh/ha.an

Considerând că randamentul minim de utilizare a energiei termice potențiale a corzilor de viță este de în medie $\eta_{ef}$ = 80% rezultă că de pe un hectar de vie se poate obține o energie termică utilă medie $EU_{cvs} \approx$ 24.500 MJ/ha.an = 6800 kWh/ha.an,ceea ce corespunde unui consum echivalent de 880 kg. motorină sau a 765 litri motorină.

Înlocuirea combustibililor clasici, de tip motorină, duce la reducerea emisiei de $CO_2$ cu 74,1 $t_{CO2}$/TJ. [11]

Rezultă că utilizarea energiei regenerabile din biomasa de corzi de viță recoltată de pe un hectar de vie duce la reducerea emisiei de $CO_2$ cu 2,03 $t_{CO2}$/ha.an.

La nivel național, luând în calcul o suprafață de minim 100.000 ha de vie în producție, rezultă un potențial energetic în biomasa formată din corzile de viță tăiate de: $EP_{cv} \approx$ 3500 TJ/an = 970 TWh/an, care corespunde unui consum anual de motorină de 615.000 t/an; precum şi cu reducerea emisiei de $CO_2$ cu 168.000 $t_{CO2}$/an; valori impresionante chiar şi la nivel național.

### 4.4 Irigarea cu energie din corzile de viță

Pentru irigarea unui hectar de vie pentru a se reduce, parțial sau total, necesarul de energii de intrare pentru irigare se poate utiliza ca sursa de energie primară biomasa formată din corzile de viță taiate, pentru alimentarea unui motopompe utilizate irigarea viei. Motopompa necesară pentru irigarea unei vii este alimentată cu gaz combustibil, denumit gazgen, produs de un gazogenerator termo-chimic alimentat cu tocătura de corzi de viță rezultate din tăierea anuală a viei.

Gazeificarea combustibililor omogeni se face cu un randament mediu de 70%, rezultând că prin gazeificare se poate obține gaz combustibil cu o energie de circa 6825 kWH/ha. Randamentul total al motorului termic alimentat cu gazgen este în medie de 25% iar al pompelor uzuale este de 60%. Rezultă că se poate obține o energie hidraulică utilă de 3685 MJ/ha cu care se poate pompa 1230 $m^3$ apă la 30 m înălțime.

Considerând că necesarul anual mediu de irigare, este de circa 1000 $m^3$.apa/ha, rezultă că din biomasa provenită din corzile de viță taiate de pe un hectar se poate asigura toată energia necesară pentru irigarea acestuia.

Dacă se realizează norma de irigare cu o motopompă alimentată cu motorină consumul anual este în medie de 425 litri şi se emit anual în mediu circa 930 $kg._{CO_2}$/ha.

## 5. Eficiența energetică

În aceasta lucrare se introduce şi se foloseşte **conceptul de eficiență energetică** în locul celui de randament energetic utilizat încă în literatura de specialitate agricolă. În bilanțul energetic se iau în considerare valorile energiilor de intrare controlate direct de producător, fără a se introduce şi energia solară convertită de procesele de fotosinteză în masă vegetală. Acest mod de abordare corespunde nivelului de certitudine în evaluarea valorilor energiilor care participă direct la realizarea producției agricole. Randamentul energetic al unui sistem care utilizează energie reprezintă raportul dintre enegia ce s-a concretizat într-un produs şi energia consumată pentru producerea acestuia. Conform principiului echilibrului energetic totdeauna randamentul este subunitar. Eficiența energetică se referea la modalitatea în care s-a utilizat o energie pentru a se obține un produs cu alt conținut de energie în cadrul unor procese neadiabate, în care mai intervin şi alte surse de energie. Ca urmare eficiența energetică poate fi subunitară sau supraunitară în funcție de sistemul analizat. Se subliniază acest aspect pentru că sistemele de producție agricole sunt utilizatoare de energie introdusă de om precum şi de energie din mediul natural.

Eficiența energetică generală – EFEN - a unei culturi agricole, în general, şi a culturi de viță de vie în special, se defineşte ca raportul dintre totalul energiilor OE obținute la ieşirea sistemului raportată la suma energiilor IE introduse la intrarea în sistem:

$$EFEN = \frac{OE}{IE} \tag{14}$$

Stiind că energia de ieşire toală este formată din energia de ieşire primară plus cea secundară, rezultă că şi eficiența energetică a unei culturi de viță de vie se poate descompune în două componente: eficiența energetică primară – EFENP şi eficiența energetică secundară - EFENS:

$$EFEN = EFENP + EFENS \tag{15}$$

Eficiența energetică primară a unei culturi de viță de vie este :

$$EFENP = \frac{OEP}{IEP} \tag{16}$$

Eficiența energetică secundară a unei culturi de viță de vie este :

$$EFENS = \frac{OES}{IES} \tag{17}$$

Din punct de vedere strict energetic relația (17) este corectă. Dar obiectivul urmărit este de a se realiza o procedură de selectare a tehnologiilor posibile, având ca criteriu principal bilanțul energetic şi eficiența energetică. Produsul principal al culturii de viță de vie, strugurii, sunt cu destinație alimentară: struguri de masă şi vinuri. Din cultura de viță de vie rezultă şi alte produse secundare cu valoare energetică efectivă mare, dar nu în domeniul alimentației umane, ca de exemplu corzile de viță de vie tăite care au o mare valoare energetică în domeniul producerii de energie termică.

În cazul general, al culturilor agricole, eficiența energetică generală este supraunitară, fiind cea mai mare la cultura de porumb EFEN≥8,5 şi cea mai mică la vița de vie.

## 6. Rezultate

Pentru calculul eficienței energetice s-a utilizat un software-ul dezvoltat special în acest scop, în care s-au introdus datele corespunzătoare operațiunii de irigare.

S-au introdus în programul de calcul al bilanțului energetic şi a eficienței energetice date corespunzătoare celor două tipuri de tehnologii. In figura 1 este prezentată un rezultat al programului de calcul.

Pentru o validare obiectivă a programului de calcul s-au utilizat date înregistrate în anii 2002 - 2004 la Stațiunea de cercetare viticolă Bujoru. In tabelele 1 şi 2 sunt prezentate rezultatele calculului eficienței energetice primare [EP], a eficienței energetice secundare [ES] şi a celei totale [ET], precum şi a bilanțului anual de $CO_2$ în t.$CO_2$/ha pentru culturi neirigate şi irigate.

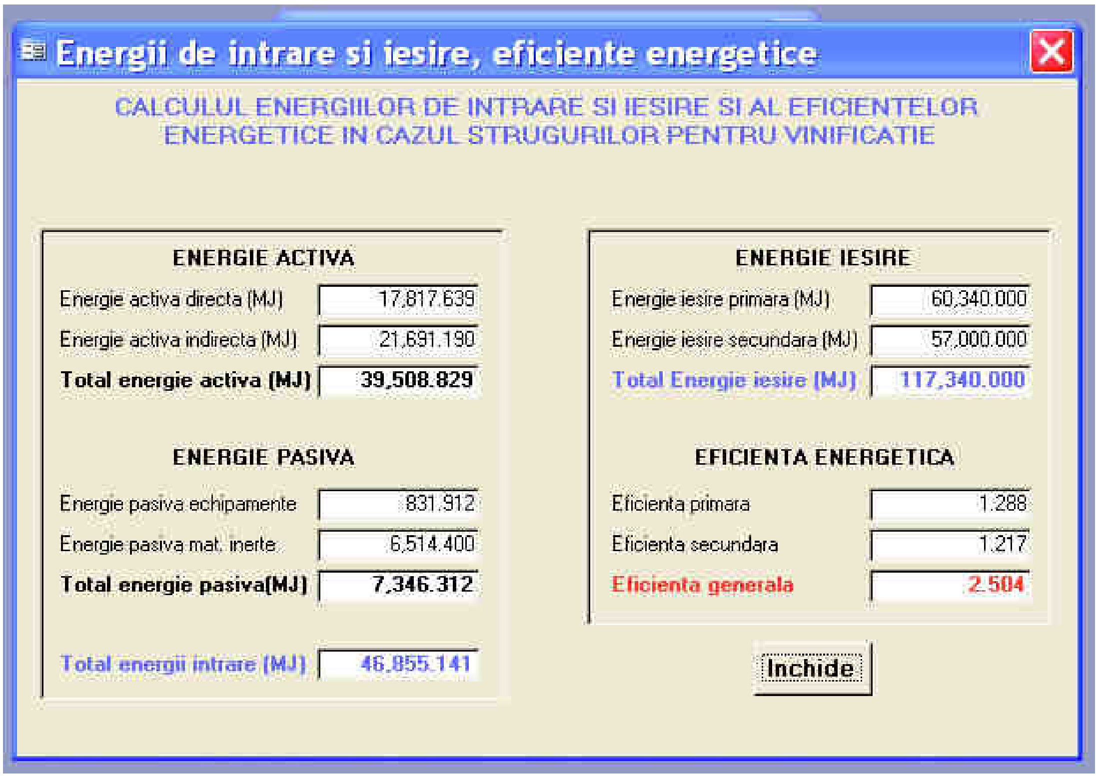


Fig. 1 Afişarea rezultatelor programului de calcul a eficienție energetice

Tabelul 1

| Anul | Cultură neirigantă | | | | | | |
|---|---|---|---|---|---|---|---|
| | EP | ES | | ET | | t.$CO_2$/ha | |
| | | uzual | en.reg | uzual | en.reg | uzual | en.reg |
| 2002 | 1.077 | 0 | 0.932 | 1.077 | 2.009 | 0 | -2.87 |
| 2003 | 1.062 | 0 | 1.109 | 1.062 | 2.171 | 0 | -2.98 |
| 2004 | 1.082 | 0 | 0.98 | 1.082 | 2.062 | 0 | -3.14 |

Tabelul 2

| Anul | Cultură irigantă | | | | | | |
|---|---|---|---|---|---|---|---|
| | EP | ES | | ET | | t.$CO_2$/ha | |
| | | uzual | en.reg | uzual | en.reg | uzual | en.reg |
| 2002 | 1.262 | 0 | 0.927 | 1.262 | 2.189 | 0.93 | -2.87 |
| 2003 | 1.236 | 0 | 1.048 | 1.236 | 2.284 | 0.93 | -2.98 |
| 2004 | 1.409 | 0 | 1.103 | 1.409 | 2.512 | 0.93 | -3.14 |

La culturile neirigate se constată că eficiența energetică primară variază relativ puțin în timp deoarece vița de vie este o cultură cu o mare rezistență la deficit hidric. Utilizarea corzilor de viță ca sursă de energie regenerabilă dublează valoarea eficienței energetice totale. Deoarece nu s-a consumat motorină pentru irigare s-a luat ca bază de comparație un bilanț anual nul de $CO_2$.

La culturile irigate se constată că eficienţă energetică primară creşte în medie cu 21% şi eficienţa energetică totală în medie cu 12%, din care aportul corzilor de viţă este de 6%. Se constată deci că irigarea produce o creştere nesemnificativă a masei de corzi de viţă tăiate.

**Concluzii**

În acesta lucrare se introduce şi se foloseste *conceptul de eficienţă energetică* a culturior agricole în locul celui de *randament energetic* utilizat încă în literatura de specialitate. Acest mod de abordare corespunde nivelului de certitudine în evaluarea valorilor energiilor care participă direct la realizarea producţiei agricole.

S-a constatat că introducerea în calculul eficienţei energetice totale a valorii energetice utile a subproduselor valorificate pentru a se produce energie regenerabilă duce la concluzia că eficienţa utilizării energiei solare de către culturile agricole este mult mai bine valorificată.

În cultura de viţă de vie principalul subprodus cu valore energetică ridicată este biomasa de corzi de viţă tăiate, care în medie este de circa 3000 kg/ha. Aceasta are o energie potenţială de circa 35 GJ/ha, putând fi utilizată ca combustibil atât pentru producerea de energie termică, cât şi pentru energie mecanică şi electrică.

Utilizarea utilizarea corzilor de viţă ca sursă de energie duce la creşterea eficienţei energetice totale cu 100%. Irigarea cu energie regenerabilă conduce şi aceasta la o creştere cu încă 12 % a eficienţei energetice totale.

Este de remarcat că utilizarea corzilor de viţă ca sursă de energie regenerabilă pentru irigare poate reduce emisia anuală de $CO_2$ în medie cu 930 kg./ha.

Modelul dezvoltat şi algoritmul complex de calcul pentru eficienţa energetică, reprezintă un instrument de lucru extrem de puternic pentru realizarea unui produs software complex destinat conducerii optimale a procesului de producţie a viţei de vie, precum şi pentru lucrările de cercetare viitoare.

**Mulţumiri.**

Această lucrare a fost realizată în cadrul proiectului de cercetare GLOBALCLIM finanţat de ANCS în cadrul Programului Naţional de Cercetare Dezvoltare II 2007-2011

**BIBLIOGRAFIE**

[1]. Douglas G. Tiffany**,** *Agricultural Energy: Understanding Usage - Anticipating Policy*, D*irections*, College of Agriculture, Food, & Environ. Sciences University of Minnesota, 2002

[2]**.** Gruia Romulus**,** *Managementul Eco-Fermelor*, Ed.: Ceres, Bucuresti, 2006

[3]. Jinescu Valeriu, *ENERGONICA*, Ed. Semne, Bucureşti 1997[4]. Maican E., Murad E., Haraga G., Biris St.S., *Utilizarea potentialului energetic al culturilor viticole pentru reducerea efectelor schimbărilor climatice*, Conference - Alternative Renewable Energy Business Opportunities, Camera de Comert si Industrie Ramnicu Valcea, 1-2 iulie 2010

[5]. Murad Erol, *Producerea de energie prin gazeificarea resurselor regenerabile de biomasă agricolă,* INMATEH- 2002, România, Bucureşti, mai 2002

[6]. Murad E., *Model for optimal control of biomass gasification*, Conference MACHINE-BUILDING AND TECHNOSPHERE OF THE XXI CENTURY, Sevastopol , 12-17 septembrie, 2005

[7]. Murad E., Haraga G., Biris St.S., Sima C., *Module energetice TLUD pentru biomasa*, Conference - Alternative Renewable Energy Business Opportunities, Camera de Comert si Industrie Ramnicu Valcea, 1-2 iulie 2010

[8]. Romanelli T.L., Milan M**.,** *Energy balance methodology and modeling of suplplementary forage production*, Advance in energy Studies, iunie, 2004

[9]. Samsom R.A., Stamler S.B., Going *Green for Lees: Cost-Effective alternative Energy Sources*, C.C Howe Institut COMMENTARY, feb. 2009

[10]. Teşu Ion, Baghinschi Vasile, *Energia şi agricultura*, Ed. Ceres, Bucureşti 1984

[11]. * * * O.M. Mediu nr. 1175 din 31.10.2006 - *Ghid privind monitorizarea şi raportarea emisiilor de gaze cu efect de ser*

**ISSN 1454 - 8003**
**Proceedings of 2011 International Salon of Hydraulics and Pneumatics - HERVEX**
*9 – 11 November, Calimanesti-Caciulata, Romania*

# BIOCHAR- ECONOMICALLY AND ECOLOGICALLY EFFICIENT TECHNOLOGY FOR CARBON FIXING

Murad Erol, Culamet Aylin, Zamfiroiu Georgiana
POLITEHNICA University of Bucharest
erolmurad@yahoo.com

**Abstract**

The project is centered on the analysis of reducing the atmospheric concentrations of carbon dioxide. The charcoal - called biochar - obtained using the TLUD energy units for biomass gasification can be incorporated into the soil and therefore increase its productive potential. Currently, this process is known as Terra-Preta and is one of the few technologies that is relatively inexpensive, widely applicable, and quickly scalable.

The analysis of the TLUD biomass gasification process shows that by controlling the amount of the specific air flow for gasification and combustion can ensure both heat energy and the reduction of the CO2. The experiments were conducted using a simulated program for the gasification of chopped vine ropes thus obtaining a negative CO2 balance (-0,35..0) CO2 kg/kg.bm and (-0,1..0) CO2kg/kWh.

**Keywords:** biomass, gasification, biochar, terra-preta

## 1. Introduction

One of the problems concerning the energy production is the reduction of the atmospheric $CO_2$ emissions. The usage of the renewable energy types such as aeolian/wind and sun energy, or photovoltaic energy produces a slightly positive balance of specific $CO_2$ emission ($CO_2$kg./kWh) due to the large amount of carbon dioxide released during the production and maintenance of the equipment.

Using the biomass as an energy source requires a null $CO_2$ balance, but in the actual $CO_2$ balance is slightly positive because of the amount of carbon dioxide required for the maintenance of the fire and gasification equipment.

In well-defined modes of operation the gasification of biomass leads to a by-product, charcoal which once stored in agricultural soils leads to carbon sequestration and therefore to negative $CO_2$ balances for carbon dioxide emissions.

One of the requirements concerning the sustainable development of the agriculture is the rational and ecological use of all the renewable energy resources for decreased $CO_2$ emissions. Thus, utilizing by-products as biomass with energy value contributes to both lower $CO_2$ emissions and an increased productive potential of the agricultural areas. This type of technology is known as Terra-Preta and is the basis of large scale research. [15,16]

The biochar is obtained through biomass gasification using TLUD energy units, with high reliability and stability. [6, 15]

One of the main characteristics of TLUD energy units is the low concentrations of CO and $PM_{2,5}$ lost during the pyrolysis, which is an ecological advantage. [6]

## 2. TLUD energy unit

The fixed bed gasification process, TLUD (Top-Lit-Up-Draft) can be used in order to produce energy/heat and biochar from biomass if it is coupled directly to a burner. [6, 12]. Figure 1 shows the operational chart of the TLUD unit.

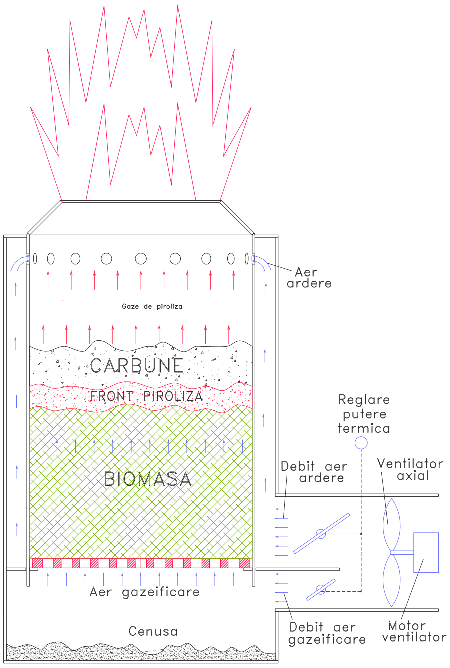


Fig. 1. TLUD operational chart

The necessary air flows for gasification $D_{ag}$ and burning $D_{ar}$ are generated by a high speed axial fan powered by an electrical engine with continuous current.

The fast pyrolysis process is caused by the heat flow from the carbon oxidation front and tar combustion. The flaming pyrolysis front descents continuously consuming the biomass from the reactor. The fast pyrolysis process produces gas, tar and biochar. The tars going through the flaming carbon front are cracked while the carbon dioxide from the pyrolysis gases goes through the carbon front and reduces a part of the biochar resulting CO. [3,13]

The fuel gas flow $D_{gas}$ from the burner is mixed with the air combustion flow $D_{ar}$ and is introduce into the combustion chamber from the top of the reactor. Its high turbulence causes the gas mixture to burn with open flame in the upper part of the combustion chamber.

The thermal power is adjusted through the CAG flap by varying the $D_{ag}$ type flow or by modifying the fan speed. Figure 2 shows the flow chart of the TLUD energy unit.

Outputs are:

- The biochar mass, BC ($kg_{ch}/kg_{bm}$),
- The thermal power $P_{th}$ ($kW_{th}$),
- The $CO_2$ emission ($kg_{CO2}/kg_{bm}$).

Inputs are:

- The air flow $D_a = D_{ag} + D_{ar}$ (kg.air/s),
- The biomass consumption $C_{bm}$ (kg.bm/s).

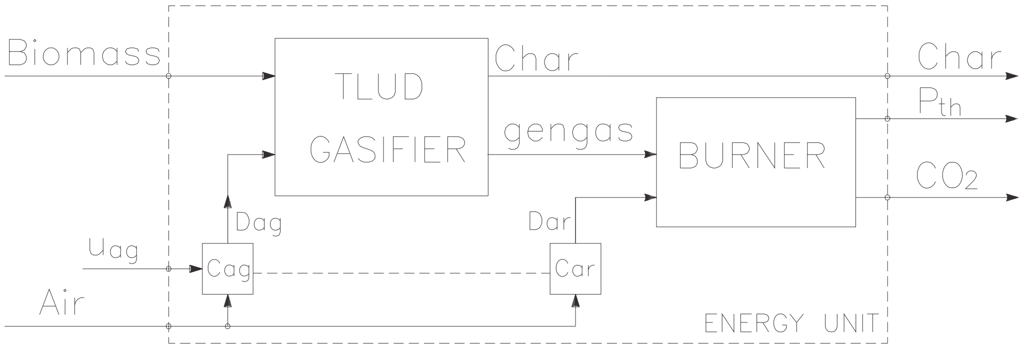


Fig.2 The flow chart of the TLUD energy unit

## 3. The analysis of the gasification process

The air weight rate $D_{ag}$ (kg.air/s) is the dominant characteristic of the gasification process. In order to analyze the gasification process in the reactor the specific value of the air weight rate $D_{ags}$ (kg.$_{air}$/m$^2$s) and of the biomass $C_{bms}$ (kg$_{bm}$/m$^2$s) are taken into consideration:

$$D_{ags} = \frac{D_{ag}}{S_R} \tag{1}$$

$$C_{bms} = \frac{C_{bm}}{S_R} \tag{2}$$

In which: $S_R$ is the area of the reactors section (m$^2$)

The temperature of the flaming pyrolysis front $T_{fp}$ (K) is determined by $D_{ags}$ [1, 9, 10, 13]:

$$T_{fp} = CT_0 + CT_1 \cdot D_{ags} + CT_2 \cdot D_{ags}^{\ 2} \tag{3}$$

Equation (3) shows that $T_{fp}$ front temperature has a non-linear variation dependent on $D_{ags.}$ This type of temperature also determines the value of the transferred heat flow during the pyrolysis and therefore of the specific consumed weight rate of the biomass, $C_{bms}$.

One of the characteristics of the gasification process the air-fuel ratio AF (kg$_{air}$/kg$_{bm}$), which is the ratio between $D_{ags}$ and $C_{bms,}$ the specific weight rate used during gasification.

One of the main characteristics of the gasification process is the equivalence ratio, ER, which is the ratio between AF and the stoichiometric air weight rate $D_{ast}$ (kg$_{air}$/kg$_{bm}$) used for biomass burn-out [6]:

$$ER = \frac{AF}{D_{ast}} \tag{4}$$

Experimental research for the biomass gasification in fixed bed shows that at lower values of the ER part of the carbon from the biomass is not reduced and therefore it is turned to carbonized residue, currently called biochar. [1, 3, 11, 13, 14]

Because of the strong influence of the biomass's relative humidity $\varphi_{bm}$ on the amount of biochar the researchers proposed an empiric model for biochar production estimation, BC.

$$BC = (CH_0 + CH_1 \cdot ER + CH_2 \cdot ER^2) \cdot (CH_3 + CH_4 \cdot \varphi_{bm} + CH_5 \cdot \varphi_{bm}{}^2) \tag{5}$$

By taking into consideration the amount of carbon CC ($kg_C/kg_{bm.db}$) from the biomass, the unconverted carbon UCC ($kg_{ch}/kg_C$) was determined [2,4,5]

$$UCC = \frac{BC}{(1-\varphi_{bm}) \cdot CC} \tag{6}$$

During the biochar production, the specific potential energy $P_{ths}$ ($MJ/kg_{bm}$) of the gas from the gasification process is lower that the inferior caloric power $LHV_{bm}$ of the biomass [2, 4, 5]:

$$P_{ths} = LHVbm - BC \cdot LHVC \tag{7}$$

Or

$$P_{ths} = (1-\varphi_{bm}) \cdot (VC \cdot LHVvol + FC \cdot LHVC - BC \cdot LHVC \tag{8}$$

Where: $LHV_{bm}$ the inferior caloric power of the biomass ($MJ/kg_{bm}$),
- $LHV_c$ carbon inferior caloric power ($MJ/kg_c$),
- $LHV_{vol}$ the inferior caloric power of the volatile gases ($MJ/kg_{vol}$).

At the burner's output the carbon dioxide flow $D_{CO2}$ ($kg_{CO2}/kg_{bm}$):

$$D_{CO2} = \frac{kmol\, CO_2}{kmol\, C}(1-UCC) \cdot CC \tag{9}$$

Much lower than when biochar is not produced.

## 4. $CO_2$ emission balances

The heat production of this process should have a neutral balance of $CO_2$, because the amount of the discharged carbon into the environment is the same one as the one the plants use during photosynthesis. When during the gasification process biochar is formed the CO2 balance [$B_{CO2}$ ($kg_{co2}/kg_{bm}$)] becomes negative.

$$B_{CO2} = 0 - \frac{kmol\ CO_2}{kmol\ C} \cdot BC \tag{10}$$

Where: kmol $CO_2$ = 44; kmol C = 12.

It could also be ecologically iteresting to determine the specific $CO_2$emission for the amount of heat produced, $BE_{CO2}$ ($kg._{CO2}/kWh_{th}$):

$$BE_{CO2} = \frac{B_{CO2}}{P_{ths}} \tag{11}$$

## 5. Results

The simulation program and model for biochar production process has been developed in order to determine the importance of biochar sequestration into the soil for reducing $CO_2$ atmospherical emissions. The experiments involve using chopped grape wine biomass. [7,8]. The results of the experiments are shown in fig. 3 and 4.

The 3rd image consists in the variation of the measures which determine the gasification process and biochar production dependent on the values of the specific gasification flow, $D_{ags}$, $T_{fp}$, $C_{bms}$, ER, BC and $P_{ths}$.

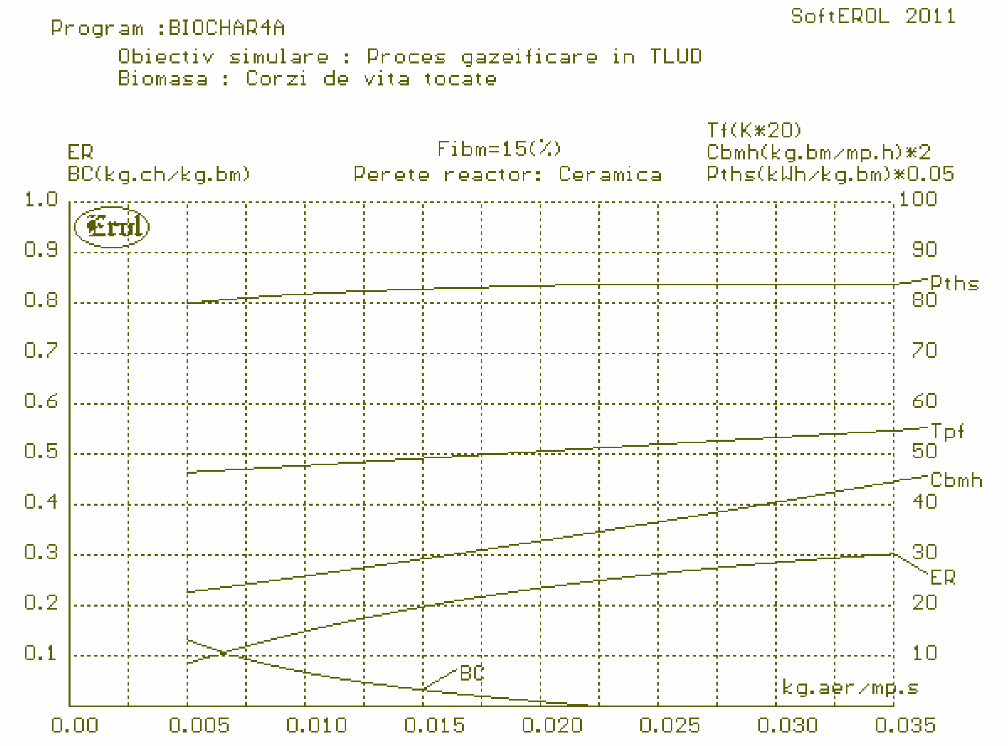


Fig. 3 TLUD gasification process

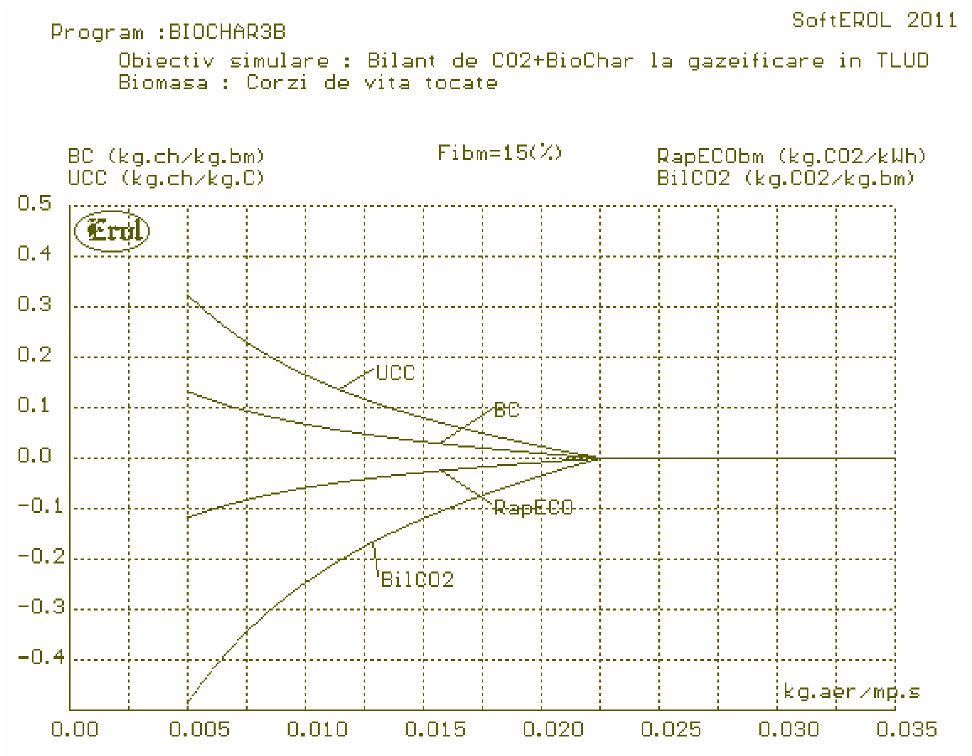


Fig.4. Biochar and $CO_2$ balances for TLUD

The biochar's shares decreases with the increase of the $D_{ags}$ flow, because of the increase of the flaming pyrolysis front's temperature $T_{fp}$, which accelerates the carbon reduction. Therefore, at values hiher than 0,023 $kg_{air}/m^2s$ there is no residual charcoal produced. This type of practice functions at about 1050 K $T_{pf}$ temperature (787 °C).

Flaming pyrolysis front $T_{pf}$ temperatures which are over 750 °C may appear only when the wall of the reactor is sealed or made of ceramic material with high thermal resistance. In order to control the biochar production the reactor should be metalic so that the trasfered temperature could be monitorised nd kept below 650°C.

Figure 4 describes the functioning regimes in which biochar is produced, when BC>0, the $CO_2$ balance dependent on biomass consumption $BilCO_{2bm}$ is negative in the -0,4...0 $kg_{.CO2}/kg_{.bm}$ domain while when dependent on thermal energy, $RapCO_{2bm}$, is negative in the -0,1..0 $kg_{.CO2}/kWh_{th}$ domain.

Example given: the $CO_2$ balance from burning diesel oil is +0.274 $kg_{.CO2}/kWh_{th}$.

## Conclusions

An environmentally and economically efficient way to reduce the atmospheric $CO_2$ concentrations is the biochar soil sequestration. Biochar is a type of charcoal created by pyrolysis of biomass during gasification while also producing energy.

By using biochar for the agricultural soil it can improve soil quality and increase its fertility and productive capacity. Thus, by incorporating the biochar into the soil the CO2 emission balances become negative. The $CO_2$ emissions are dependent on the amount of gasified biomass and produced thermal energy.

The TLUD energy unit can ensure a controlled biochar production due to its constructive solutions (metallic wall for the reactor) and to less intense pyrolysis regimes, in which case the specific biomass consumption is lower than 70 $kg._{bm}/.m^2h$.

The operating regime is controlled by the air flow variation for gasification which simplifies the automatic control system of the installation.

Using the TLUD energy units for biochar and thermal energy production is economically advantageous: the installation costs and exploitation costs are lower than those of other types of gasification or pyrolysis procedures.

The simulation program offers sufficient information in order to study the production of biochar in TLUD energy units. The conducted experiments as well as the program itself could be perfected and therefore improve the biomass energy production both ecologically and economically.

## Bibliography

[1]. Bellais Michel, Modelling of the pyrolysis of large wood particles, Doctoral Thesis, Department of Chemical Engineering and Technology KTH - Royal Institute of Technology, Stockholm, Sweden 2007
[2]. Demirbaş A., Calculation of higher heating values of biomass fuels, FUEL, Vol. 76, Issue 5, 1997
[3] Di Blasi Colomba, Kinetic modeling of biomass gasification and combustion, THERMALNET, INTELLIGENT ENERGY EUROPE
[4]. Erol M., Haykiri-Acma H., Küçükbayrak S., Calorific value estimation of biomass from their proximate analyses data, Renewable Energy, Vol.35, Issue 1, ian. 2010
[5]. Jenkins B., Ebeling J., Thermochemical proprieties of biomass fuel, CALIFORNIA AGRICULTURE, May-June 1985, pag. 14..16
[6]. Mukunda H. s., ş.a, 2010. Gasifier stoves – science, technology and field outreach, CURRENT SCIENCE, vol. 98, no. 5, 10 march 2010
[7]. Murad E., Optimisation of biomass gasification load regime, Conferința Internațională ENERGIE – MEDIU CIEM 2005, UPB, Bucureşti oct. 2005
[8]. Murad E., Seiculescu M., Sima C., Haraga G., Utilizarea potențialului energetic al corzilor de viță, Conferința de Comunicari Stiintifice, INCVV Valea Călugărească, 10 iunie 2010
[9]. Porteiro J., Patino D., Moran J., Granada E., Study of a Fixed-Bed Biomass Combustor: Influential Parameters on Ignition Front, Energy Fuels 2010, 24, 3890–3897
[10]. Porteiro J., Patiño D., Collazo J., Granada E., Moran J., Miguez J.L., Experimental analysis of the ignition front propagation of several biomass fuels in a fixed-bed combustor, Fuel 89 (2010) 26–35
[11]. Reed T.B., Das A., Handbook of Biomass Downdraft Gasifier Engine Systems, U.S Department of Energy, Colorado, 1988
[12]. T. B. Reed, R. Walt, S. Ellis, A. Das, S. Deutch, Superficial velocity - the key to downdraft gasification, Presented at 4th Biomass Conference of the Americas; Oakland, CA, 8/29/99
[13]. Saastamoinen J.J., Taipale R., Horttanainen M., Sarkomaa P., Propagation of the Ignition Front in Beds of Wood Particles, COMBUSTION AND FLAME 123:214–226 (2000), Elsevier Science
[14]. H. Zhou, A.D. Jensen, P. Glarborg, P.A. Jensen, A. Kavaliauskas, Numerical modeling of straw combustion in a fixed bed, Fuel 84 (2005) 389–403
[15] * * * Biochar Soil Management, Departament of Crop and Soil Science, Cornell University
[16] * * * Terra Preta, Wikipedia

ISSN 1454 - 8003
Proceedings of 2011 International Salon of Hydraulics and Pneumatics - HERVEX
*9 – 11 November, Calimanesti-Caciulata, Romania*

# COMPLEX SYSTEM FOR ASSESSMENT OF PHYSICAL AND MECHANICAL CHARACTERISTICS OF SOILS

**Cristian SORICĂ [1], Eugen MARIN [2], Florean RUS[3]**

[1] INMA Bucharest, sorica@inma.ro

[2] INMA Bucharest, emarin@inma.ro

[3] Transylvania University of Brasov, florus@unitbv.ro

***Abstract:*** *Compaction of agricultural land is a form of soil degradation, being an unwanted accompanying phenomenon that occurs during the execution of agricultural works, the phenomenon being unavoidable, but which can be kept under control through proper management of the agricultural holding. On agricultural lands with compacted soils, the soil works, both the basic ones but also those of maintenance, are performed with high energy consumption, with high wear of working bodies and in qualitative terms are inappropriate. Under these conditions appears naturally the need to monitor the state of soil compaction. In this paper is presented a complex system for assessing the physical and mechanical characteristics of soils designed to the works in agriculture for mapping and assessment of soil compaction caused by repeated transitions of agricultural machinery and by the agro-technical works performed.*

***Keywords****: assessment system, physical and mechanical characteristics, soil compaction*

## 1. Introduction

The soil is the main means of agricultural production, the actions of agricultural machinery working bodies on its aiming finally to obtain material goods. As a biological medium in which occur complexes processes and transformations, the soil acts directly and influence on the plants development. The production capacity of the soil is dependent on its fertility, characterizing the soil's ability to provide to the plants continuous and abundant quantities of water needs, air and nutrients. In the same time, the soil should be a favorable environment for plant root growth and root system support, so that they are well fixed, without any danger of being uprooted as a result of violent action of meteorological factors. Agricultural practice of the last 30...40 years is characterized by the execution of agricultural works under conditions of increased moisture of soil, of execution of multiple and high intensity operations on the soil, of changes the share of perennial crops in favor of annual crops, of the use of some equipment with big mass etc.

## 2. Aspects concerning the influence of tillage on the soil physical and mechanical characteristics

Modern agriculture, intensive, of high productivity involves the use of high capacity equipment, exercising significant strain on the soil. Insufficient knowledge of how the the soil responds to such increased stresses may have negative consequences, manifested by processes of degradation, even of destruction of its production capacity.

The soil works, besides the direct and unusual effects, beneficial within the technologies of plant cultivation, induce in the soil and lasting remanent effects, acting on the physical and physico-mechanical properties of the soil, amending them.

As a result of soil compaction changes the pore dimensions and their distribution and orientation in soil mass, the soil structure is degraded or totally destroyed, the aero-hydric regime becomes deficient and the activity of aerobic microorganisms is slowed down or eliminated. By modifying the taxonomic structure of microorganisms, decreases the content of humus and nutrients and the development and penetration of plant roots in the soil mass is hampered. The direct consequence of porosity changes are also chemical changes that occur in soil due to the intensification of chemical processes (hydrolysis, dissolution, carbonation, oxidation etc.) that changes the nutrient regime in soil.

The soil compaction prevents the rapid drainage of water from precipitation or irrigation. On sloping land, compacted soils and poorly drained emphasizes the tendency of surface drainage on land surface and thereby increase the risk of hydraulic erosion.

The biological activity in the tamping soil reaches minimum rates, highlighted of very slow decomposition of plant debris embedded in the the soil and by the poor root and plant waist development.

Working of the soil processes are among the most energy intensive processes and labor force, and lead, by the way of actual execution, to high pollution of the atmosphere, generally come from burning of fuels or from leakage of fuels and oils. On the other hand, these processes are accompanied by intense wear not only of the soil processing machines (especially of their active working bodies), but also of tractors working in the aggregate with such machines. These processes, still produce a negative phenomenon, extremely dangerous, given the impossibility of total and immediate removal of its, namely the soil compaction.

## 3. Measures taken to improve the negative effects of tillage processes

Taking into account the negative phenomena accompanying the process of the the soil processes, were made during the last decades many researches which, if not eliminate, even improves the degradation processes of the environment.

Among the ways approached until now in order to improve the negative effects of soil working processes, can be enumerate: route optimization for processing soil aggregates (for example in Şandru and collab., 1982), reducing the number of soil works (especially the deep plowing, which still remain necessary at a number of years, depending on soil quality), lower the weight of aggregates, development of culture technologies with minimum works, design and manufacture of tractors with better working performance.

International regulations on environmental protection and in particular of the soil impose severe conditions on constructive solutions concerning the mass and tires for machinery and agricultural tractors, and implementation of an appropriate management in the execution of agricultural works.

To assess the physical condition of the soil at a time, to determine the correlation between the state of compactness of the soil with the resistance to the execution of agricultural works or at the development of crop plant root as well as the development of crop plants roots, is used the technical procedure that simultaneously measure soil resistance at penetration with a standard metal body and the depth of penetration.

Depending on the mode of transmission of standard conical body strength, the penetrometers are grouped into two categories: statical and dynamical.

In the case of *statical penetrometers* the standard conical body is introduced in the soil with a standard speed (about 1 cm/s), for which reason the speed must be followed strictly during the performance of the measurements. The penetration resistance value of a particular soil type is characterized by the penetration index (cone index), noted with CI, expressed in units of pressure.

In the case of *dynamic penetrometers*, the penetration in soil of the standard conical body occurs following the impulse produced by the fall of a metal part with role of ram, from a height that is kept constant through a limiter adjustable as position. The ram slid on the penetrometer rod and in the fall strikes an anvil (stopper) rigidly mounted on the penetrometer rod, after impact the conical body, disposed on top of rod, penetrating the soil on a certain depth.

The interest in assessing the lands status by measurements with the penetrometer is the result of quick obtaining of information. Penetrometer is often used to determine the soil density, of the state of compactness, assessment of load bearing capacity for foundations or for wheel tractors and agricultural machinery and resistance opposed at performing of mechanical works.

The soil resistance values are important to the classification of land and the soil penetration resistance profile together with the depth is needed at quantification of the degree of soil compaction. Also contribute to the delivery of a common characterization system of soil properties of which might be possible to determine the number of passes of agricultural machinery in order to forecast the performance to traction (Wismer & Luth, 1974; Brixius, 1987; ASAE, 2000b).

## 4. Preoccupations concerning monitoring and control of soil compaction of agricultural land

***Worldwide***, countries like USA, Canada, Germany, UK and Netherlands, with high potential for research, promote sustainable policy to control the soil compaction of agricultural land by agricultural machinery and tractors, being realised penetrometers which ensure simultaneous and the measurement of soil moisture.

The use of penetrometers as devices to determine the soil penetration resistance was taken into consideration by researchers in the last forty years. One of the problems in measuring compaction and other soil characteristics is the absence of a method rapid and accurate to achieve the of the measurements. The two problems at using of most penetrometers for soil are laborious process of manually push the cone into the soil and registration of individual readings obtained at specified intervals. Another problem encountered at the manually operated penetrometers is the difficulty of obtaining of a constant speed of penetration when the cone is pushed into the soil. Different types of penetrometers and the effect of various factors on the resistance to penetration were studied by researchers.

The soil resistance measurement using cone penetrometer is an empirical method fast and cheap, widely used for monitoring and evaluation of the soil compaction (Pagliai and collab., 2000; Castrignanò and collab., 2002a). Bengough and Mullins (1990) assumed that the soil resistance measured by a penetrometer is equal to the pressure encountered by roots during growth. Other authors (Bennie,1991; Bathke and collab., 1992) have verified that the root elongation stopped where penetrometer resistance values ranging from 0.8 to 5 MPa. Consequently, readings up to 5 MPa can be considered as an indication of compacted the soil, preventing the root growth and adversely affect the crop. In the past were used the manually penetrometers. The accuracy of the measurements is closely related to the ability to push the penetrometer probe into the tested soil layer at a constant speed, even if it is almost impossible. Most of the times, data collection for the entire area required to achieve geo-referenced maps of the soil compaction consumes a long time, is costly and often inconvenient.

One approach is to achieve the interpolated maps for the values of penetrometer strength cone measured at different times, using geostatistical techniques and then comparing the maps to detect persistence or changes in spatial patterns along the time (Goovaerts and Chiang, 1993; Castrignanò and collab., 2002a).

Measurements made using electronic penetrometer, combined with geostatistical advanced methods, can provide to farmers informations concerning the compacted areas and depth of compaction, in order to apply recovery measures only in those areas and therefore minimizing the cost.

***Internal***, in a research project carried out on the national research programs, the partners: Transylvania University of Brasov, INMA Bucharest, USAMV Cluj and USAMV Iasi, have designed a ***complex system for assessing the physical and mechanical characteristics of the soil***.

The design was done in Solidworks, specialized software for modeling three-dimensional parts, subassemblies and assemblies. It was intended that within the design activities to obtain parts and subassemblies easy to achieve practically, removable and with easy maintenance. To the achievement of complex system for assessing physical and mechanical characteristics of the soil were used technical solutions which have been subject applied for a patent application number A2011/00868, filed with OSIM on 09/05/2011.

The complex system (fig. 1) consists of: self-propelled tracked module EFCO TN5600H with elastic crawler; electronic penetrometer with digital display Eijkelkamp Penetrologger for determining in situ the soil penetration resistance, endowed with humidity sensor and GPS receiver; actuating device of the penetrometer; coupling system to the crawler module and control position of the penetrometer actuator in longitudinal and transversal plane; hydraulic group consisting of electric motor, pump and oil tank; electric generator that provides the necessary operating voltage of 220 V to the hydraulic group and hydraulic installation of the system required for driving the mechanisms during the work. The system provides good uniformity of penetration speed, up to 2 m/s according to the instructions for using the digital penetrometer. Also, the hydraulic installation is designed so that it interrupt acting the double action hydraulic cylinder when the downforce reach values higher than 1000 N, according to the user manual of the digital penetrometer.

The system realises data acquisition regarding the push pressure exerted on the penetrometer rod, local humidity and GPS coordinates of sample points. The data collected is stored in the memory of electronic penetrometer with digital display following to be downloaded and further processed in order to calculate the force of resistance to penetration and achievement the maps concerning the state of soil compaction. The maps to be realised will highlight the characteristics of spatial variability of agricultural the soil, offering information necessary for the application of an efficient management of agricultural works.

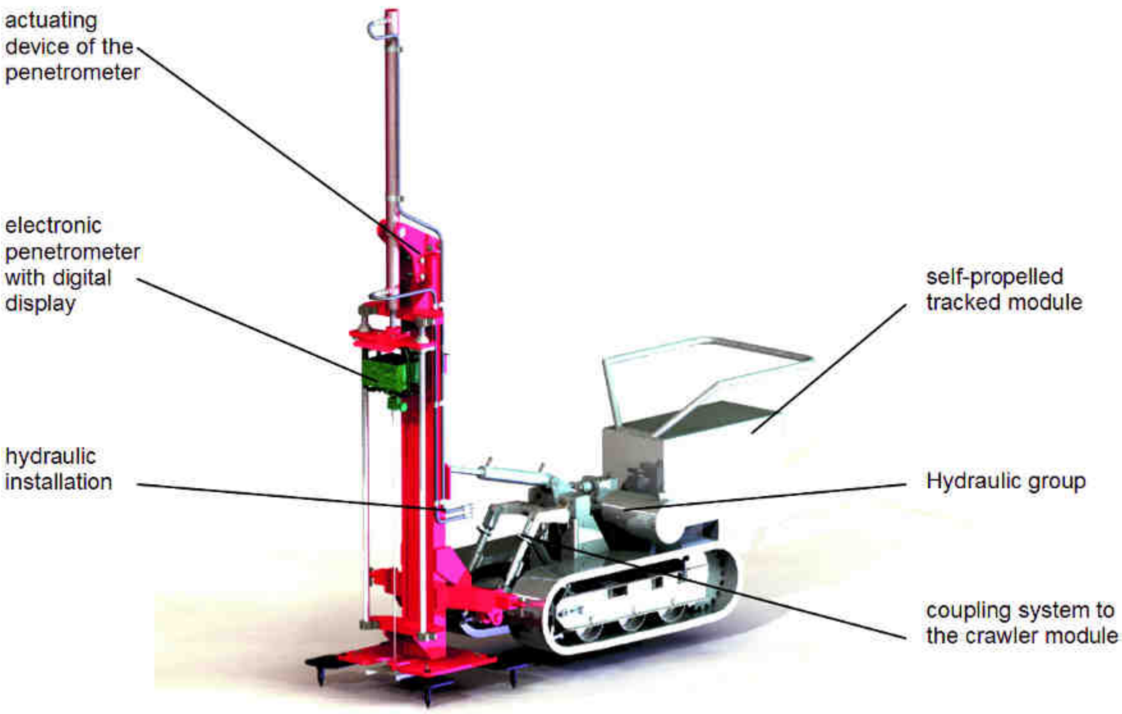


Fig. 1. Complex system for assessing physical and mechanical characteristics of the soil

***Self-propelled module with elastic crawler*** (fig. 2) support other equipment in the composition of the complex system and provide easy movement on the any type of terrain. The crawler module, acquired from Italian company EFCO, was adapted for the needs of the project by removing the bucket, designing of a coupling system of the actuating device of penetrometer to the self-propelled module and designing the mounting system of the other equipment of the system composition.

The technical characteristics are presented below:
- Kerb weight: 200...250 kg;
- Useful mass: 550 kg;
- Ground clearance: 100 mm;
- Engine type: 4-stroke gasoline;
- Engine power: 4 kW;
- Gearbox: 6 speed (4 forward + 2 backward)
- Steering radius: 700 mm;
- Caterpillar: Length / contact width: 600/180 mm;


Fig. 2. Self-propelled module with elastic crawler

***The electronic penetrometer with digital display Eijkelkamp Penetrologger*** (fig. 3) is used to determine in situ the soil penetration resistance, measuring the force of resistance to penetration up to a depth of 80 cm. Data is stored in internal memory and can later be downloaded and processed. It also stores the GPS position of the sample and local humidity.

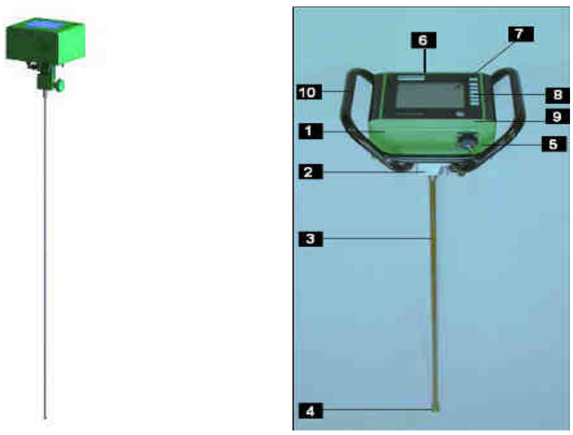


Fig. 3. Electronic penetrometer with digital display
*1. Housing; 2. Impact absorber; 3. Rod; 4. Con; 5. Communication port; 6. GPS antenna; 7. LCD display; 8. Control Panel; 9. Level; 10. Electrically insulated handles*

The technical characteristics are presented below:
- Memry: 1 500 măsurători;
- Maximum penetration force: 1000 N;
- Measuring total length of the rod: 97 cm (except the cone);
- Recording depth: 80 cm;
- GPS accuracy: <2,5 m CEP (Circular Error Probable);

***The actuator of penetrometer*** (fig. 4) consists of a welded metal frame, a double-acting hydraulic cylinder through which is transmitted the downforce to the electronic penetrometer, two slyders with linear ball bearings guiding the penetrometer and at the bottom has four plates provided with spurs for a better anchoring into the soil.

Fig. 4. Actuating device of the penetrometer

The system described above is in the phase of the experimental model, following that after this step to proceed with the experiment under laboratory and exploitation conditions.

## 5. Conclusions

Compaction of agricultural land is a form of soil degradation, being an unwanted accompanying phenomenon that occurs during the execution of agricultural works, the phenomenon being impossible to avoid, but which can be kept under control through an adequate management of the agricultural holding.

The soil resistance values are important to the classification of the land and the soil penetration resistance profile together with the depth is needed at quantification of the degree of soil compaction. The measurements performed using the electronic penetrometer, combined with advanced geostatistical methods, can provide to the farmers informations concerning the compacted areas and depth of compaction, in order to apply recovery measures only in those areas and, therefore, minimizing the cost.

## REFERENCES

[1] Carrara, M., Castrignanò, A., Comparetti, A., Febo, P., Orlando, S. *„Mapping of penetrometer resistance in relation to tractor traffic using multivariate geostatistics”*, Geoderma 142 (2007) 294–307;
[2] Dumitru, E. and collab. *„Residual effects of agricultural practices on the soil physical condition"*, Ed Risoprint, Cluj-Napoca, 1999;
[3] Guş, P. and collab. "*Research on the impact of tillage systems on the the soil porosity and structure*", International Symposium "Minimum Soil Systems Works" Cluj-Napoca, 21-22 oct. 1999;
[4] Molnar, A., Ros, V. "*The current state of research on soil compaction by tractors and agricultural machinery*", Referring I-st to doctoral, Technical University of Cluj-Napoca, 2002.

**ISSN 1454 - 8003**
**Proceedings of 2011 International Salon of Hydraulics and Pneumatics - HERVEX**
*9 – 11 November, Calimanesti-Caciulata, Romania*

# METODE DE OBTINERE A ENERGIEI REGENERABILE

**Iosif Ferenti[1], Dan Opruta[2]**

[1] Technical University of Cluj-Napoca, Department of Mechanical Engineering, e-mail: Iosif.Ferenti@termo.utcluj.ro

[2] Technical University of Cluj-Napoca, Department of Mechanical Engineering, e-mail: Dan.Opruța@termo.utcluj.ro

***Abstract:*** *Articolul prezinta o analiza a stadiului actual al sistemelor de recuperare a energiei cinetice in faza de franare a autovehiculelor rutiere. De asemenea, utilizarea energiei obtinute pentru fazele de demarare. Aceasta energie poate fi si de natura electrica si poate fi utlizizata la incarcarea unur acumulatori sau direct la alimentarea sistemelor auxiliare care folosesc curentul electric la autovehicul.*

***Keywords****: KERS, franare regenerative, schema bloc, autovehicule rutiere,combustibili fosili, sisteme hibride, CVT, MGU, HVB, KCU*

## 1. Introducere

Franarea regenerativa presupune recuperarea partiala a energiei cinetice a vehiculului si stocarea acesteia sub diverse forme (incarcarea unui accumulator sau a unui rezervor cu gaz sau lichid sub presiune) pentru ca ulterior sa poata fi folosita aceasta energie.

Avantajul este ca recupereaza energia care altfel ar fi fost pierduta, iar dezavantajul este ca are costul ridicat si faptul ca trebuie sa existe un motor secundar pe vehicul care sa preia energia produsa prin regenerare.

Din estimari se apreciaza ca resursele combustibililor fosili sunt limitate, iar numarul de autovehicule este intr-o continua crestere.Un alt aspect care trebuie luat in calcul este poluarea care are legatura directa cu numarul de autovehicule care circula pe drumurile publice.

Preocuparea inginerului contructor de autovehicule moderde este aceea de a proiecta autovehiculul cu poluare redusa si cu un consum de combustibil redus

O mare contributie adusa sistemelor de recuperare a energiei cinetice o are motorsportul. Federatia Internationala de Automobilism a promovat aceasta idée si a introdus in F1 incepand cu anul 2009 in regulamente posibilitatea folosirii sistemului KERS (Kinetic Energy Recovery Sistems) si de asemenea limitand puterea obtinuta de pana la 60 Kw, iar pilotul nu trebuie sa foloseasca mai mult de 400 Kj pe durata unui tur de pista. [1]

FIA reglementeaza puterea obtinuta ca limita superioara, deci posibilitatea obtinerii de puteri mai mari exista.

Una dintre solutiile radicale pentru a reduce substantial consumul de combustibili si a reduce emisiile poluante, este de a schimba modul de propulsie prin implementarea sistemelor de propulsie hibride, considerate ca tehnologie a viitorului.

Ca si sisteme de actionare pentru a reda energia recuperate avem: hidromecanice (hidrostatice, hidrodinamice), electromecanice de current continuu sau alternativ, sistemul hybrid termo-electric si sistemul hybrid termo-hidraulic.

## 2. Prezentarea sistemelor recuperative

Sistemul KERS a fost implementat de catre FIA in anul 2009 in Formula 1, fiind un system care are ca sis cop stocarea energiei cinetice produsa pe perioada de franare si eliberarea acesteia pe perioadele de accelerare si demarare, energie care este stocata intr-un rezervor (accumulator sau volanta).

Cand a fost conceput sistemul, inginerii au avut de ales intre doua abordari diferite. Prima consta intr-o volanta realizata din fibre de carbon, legata de diferentialul autovehiculuilui printr-o transmisie CVT (Continuous Variable Transimission). Sistemul stocheaza energia mecanica, ofera o capacitate mare de stocare si are avantajul de a functiona independent de cutia de viteze. Totusi pentru a putea fi folosit in modul cat mai eficient, este nevoie de cateva actuatoare puternice si voluminoase, si desigur de mult spatiu. A doua abordare a fost cea care se bazeaza pep e un motor electric care incarca acumulatorii pe toata perioada de franare si ofera cuplu pe accelerare.

Sistemul care foloseste motorul electric consta din tri componente principale:

- un motor electric (MGU: Motor Generator Unit) situat intre rezervorul de combustibil si motor, legat direct la vibrochenul motorului, pentru a oferi putere suplimentara
- acumulatori LI-ion de ultima generatie (HVB: High Voltage Battery Pack) capabili de a stoca si a elibera energia cu rapiditate
- o unitate de control (KCU: KERS Control Unit) ce controleaza comportamentul MGU cand stocheaza si elibereaza energie, aceasta fiind legata de unitatea standard de control al motorului

Constructorul suedez de autovehicule foloseste un system KERS, montat pe axa spate a autovehiculului, fiind dezvoltata o transmisie special creata, iar dimensiunile volantei a scazut pana la 6 Kg si diametrul acesteia pana la 20 cm, aceasta ajungand la o turatie de pana la 60000 rpm, oferind aproximativ 80 CP [1] [3]

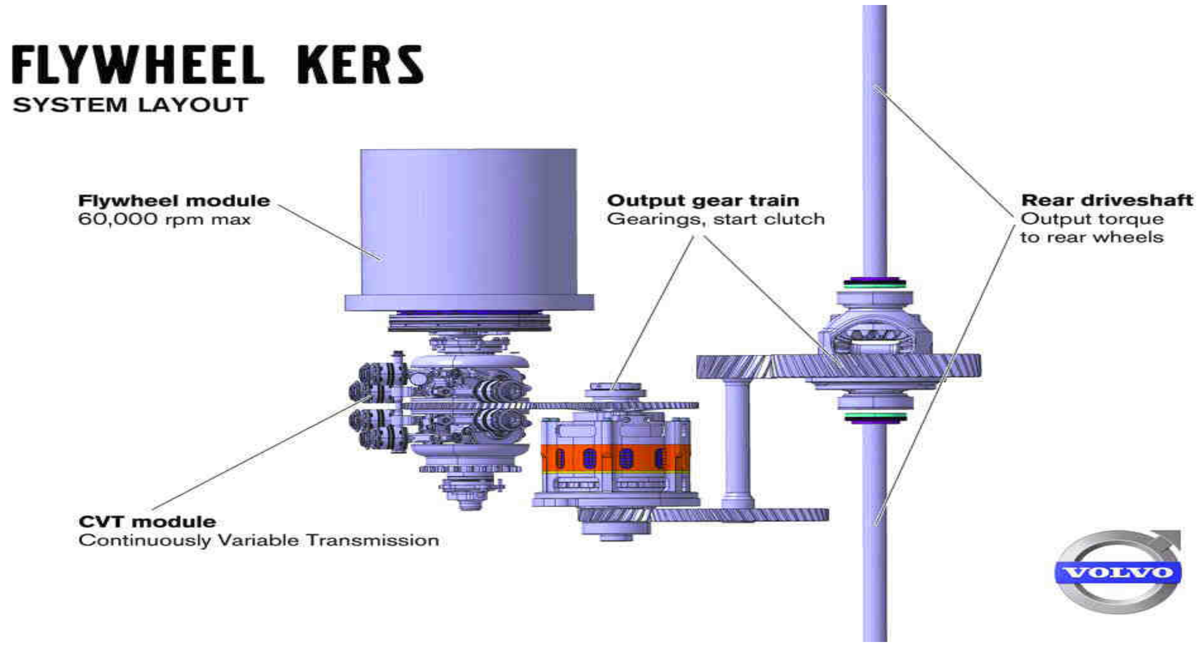


Fig 1 Schema de principiu al sistemului KERS

**ISSN 1454 - 8003**
**Proceedings of 2011 International Salon of Hydraulics and Pneumatics - HERVEX**
*9 – 11 November, Calimanesti-Caciulata, Romania*

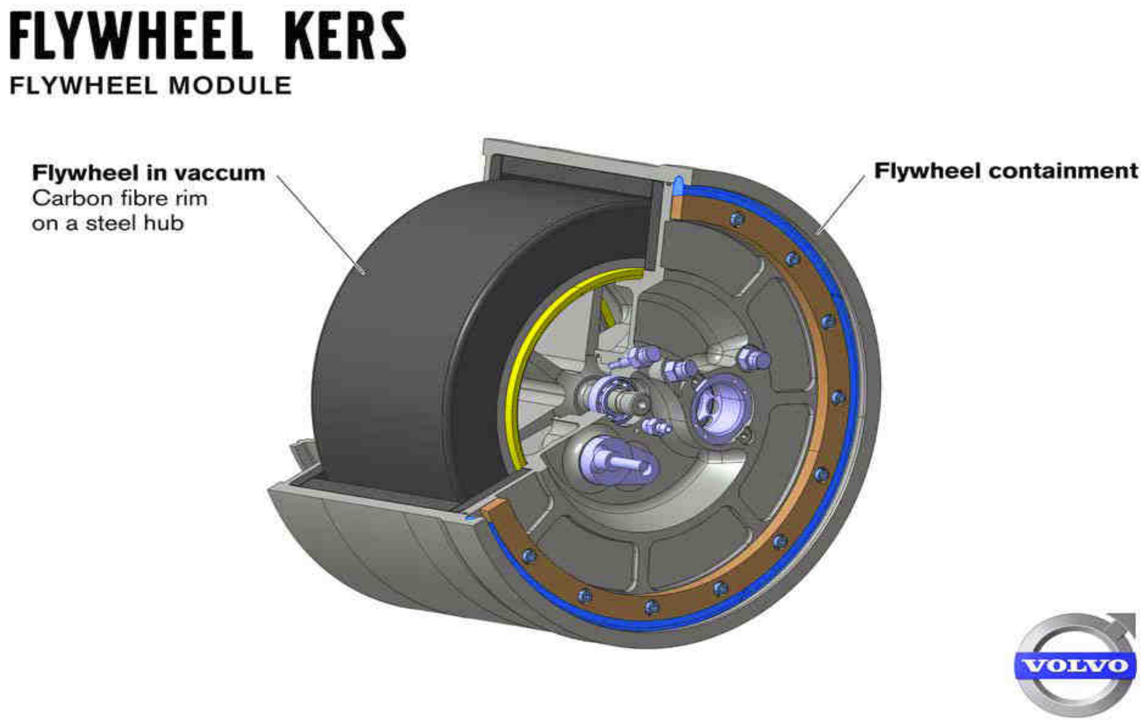


Fig 2. Volanta din fibre de carbon

**Sistem de recuperare a energiei termo-hidraulic**

In cadrul proiectului derulat cu ajutorul **INOE 2000-IHP**, impreuna cu partenerii INCDMF Bucuresti, INMA Bucuresti, Universitatea POLITEHNICA Bucuresti si ROMFLUID Bucuresti, au realizat un sistem de recuperare a energiei termo-hidraulic, acesta fiind montat pe un autoturism ARO 243 D. Solutia de principiu adoptata fiind una de recuperare hidraulica a energiei de franare cu stocare hidropneumatica si recuperare/redare hidrostatica. Mai jos se poate observa modelul conceptual de catre cercetatorii romani si schema bloc al acestuia.[2]

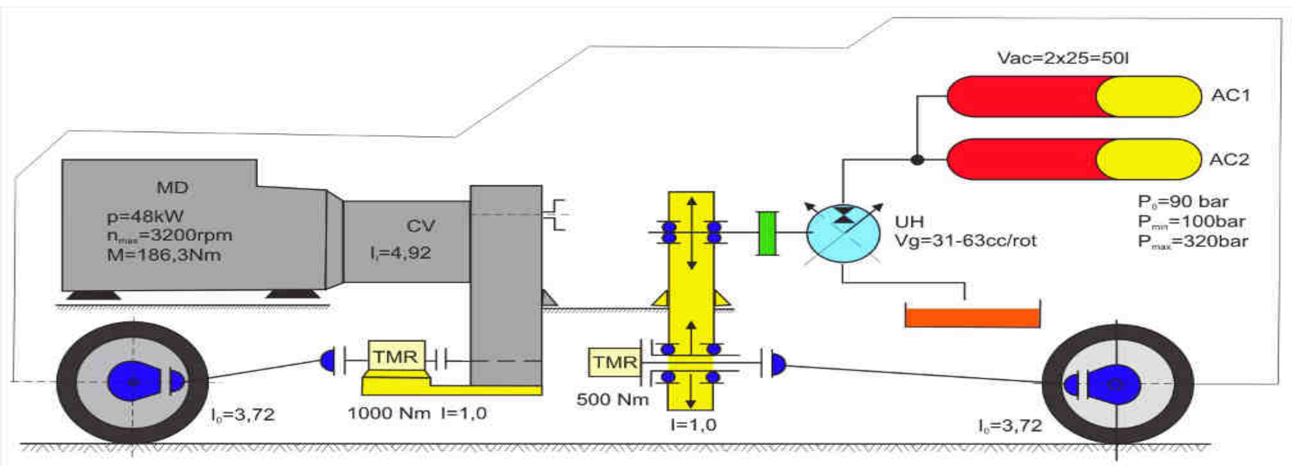


Fig.3 Model conceptual termo-hidraulic de propulsie

**Franare cu recuperare de energie**

Dacă din diverse cauze viteza de rotație a unui motor de curent continuu (cu excitație derivație) depăşeşte viteza de mers în gol ideal $n_0 = \frac{U_A}{k_e \cdot \Phi_0}$, tensiunea electromotoare indusă devine mai mare decât tensiunea de alimentare a indusului $U_A$, iar sensul curentului prin indus se schimbă:

$$I_A = \frac{U_A - k_e \cdot n \cdot \Phi_0}{R_A} < 0 \quad (1)$$

Deoarece sensul fluxului magnetic inductor rămâne neschimbat se va schimba şi sensul momentului cuplului electromagnetic ($M = k_M \cdot \phi_0 \cdot I_A$)

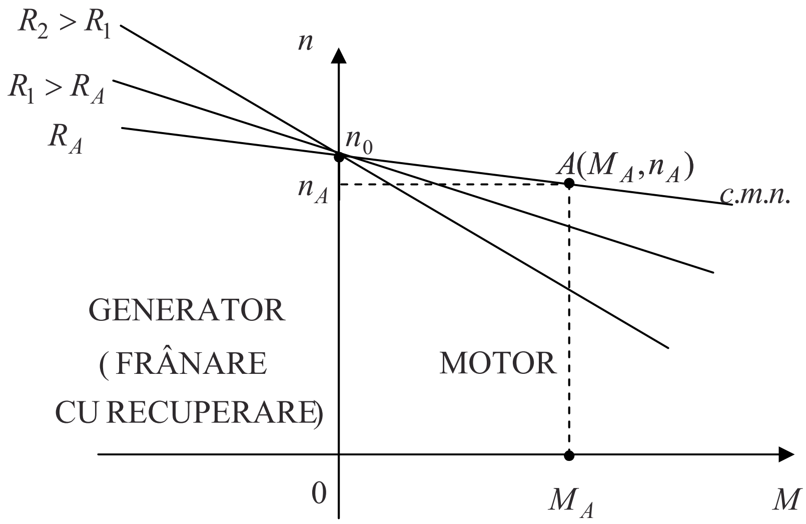


Fig.4. Caracteristicile mecanice de franare cu recuperare de energie

care devine astfel un cuplu de frânare. Maşina trece în regim de generator debitând în rețeaua de alimentare putere electrică. Frânarea cu recuperare de energie se poate realiza pornind de pe caracteristica mecanică naturală (c.m.n) sau de pe caracteristici mecanice artificiale reostatice, date de modelul:

$$n = n_0 - \frac{(R_A + R_f) \cdot M}{k_e k_M \Phi_0^2} = n_0 + \frac{(R_A + R_f) \cdot M_f}{k_e k_M \Phi_0^2} \tag{2}$$

unde: $M_f = -M$ reprezintă momentul cuplului de frânare.

Caracteristicile mecanice ale maşinii de curent continuu cu excitație derivație în regim de frânare cu recuperare de energie sunt prezentate în fig. 4.28.

Frânarea cu recuperare de energie este întâlnită frecvent în practică în cazul mecanismelor de ridicat şi a vehiculelor cu tracțiune electrică, în coborâre. Este cea mai economică metodă de frânare, dar prezintă dezavantajul că se poate aplica numai la viteze mai mari decât $n_0$ .

Prin urmare, prin această metodă nu se poate opri mecanismul de lucru, putându-se limita doar viteza acestuia.

Domeniul de frânare prin recuperare se poate extinde prin alimentarea maşinii de la o sursă de tensiune variabilă, obținându-se astfel diferite viteze de mers în gol ideal.

**Recuperare de energie din caldura reziduala**

Pe principiul schimbatoarelor de caldura apare sistemul Heat2Power, care peopune soluții pentru economia de combustibil şi reducerea de emisii de CO2 la motoarele cu ardere interna prin utilizarea căldurii reziduale de eşapament. Această economie de combustibil este accesibil pentru motoarele care rulează pe benzină, diesel, biocombustibili, hidrogen sau orice alt tip de combustibil.[6]

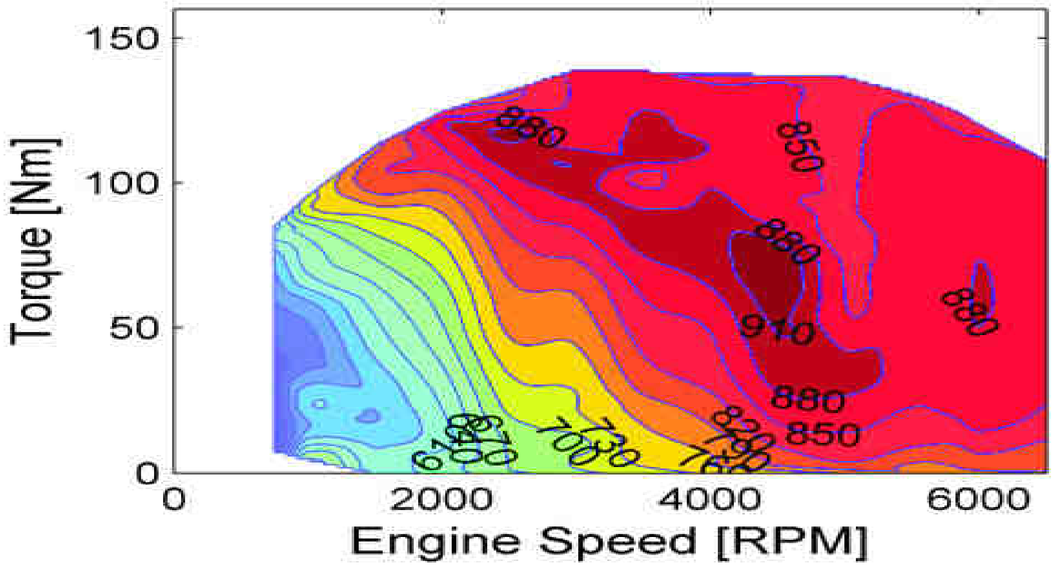


Fig.5. Variatia temperaturii in functie de turatie si incarcare

Sistemul Heat2Power se bazează pe utilizarea de unul sau mai multe butelii de regenerare a căldurii reziduale. Aceste butelii poat fi în înlocuirea sursei de ardere în interiorul unui motor existent sau ca un modul add-on, care este conectat la motor prin intermediul unui set de viteze sau o curea de transmisie. De asemenea, este posibil să nu existe nici o legatura mecanica intre motorul cu combustie şi unitatea de regenerare în cazul în care puterea de la unitatea de regenerare este scos electric. În general, pentru a scaderea pretului de instalare şi de dezvoltare recomandăm producătorii de echipament original de a folosi un sistem de add-on. În acest fel motorul original rămâne practic neschimbat.[6]

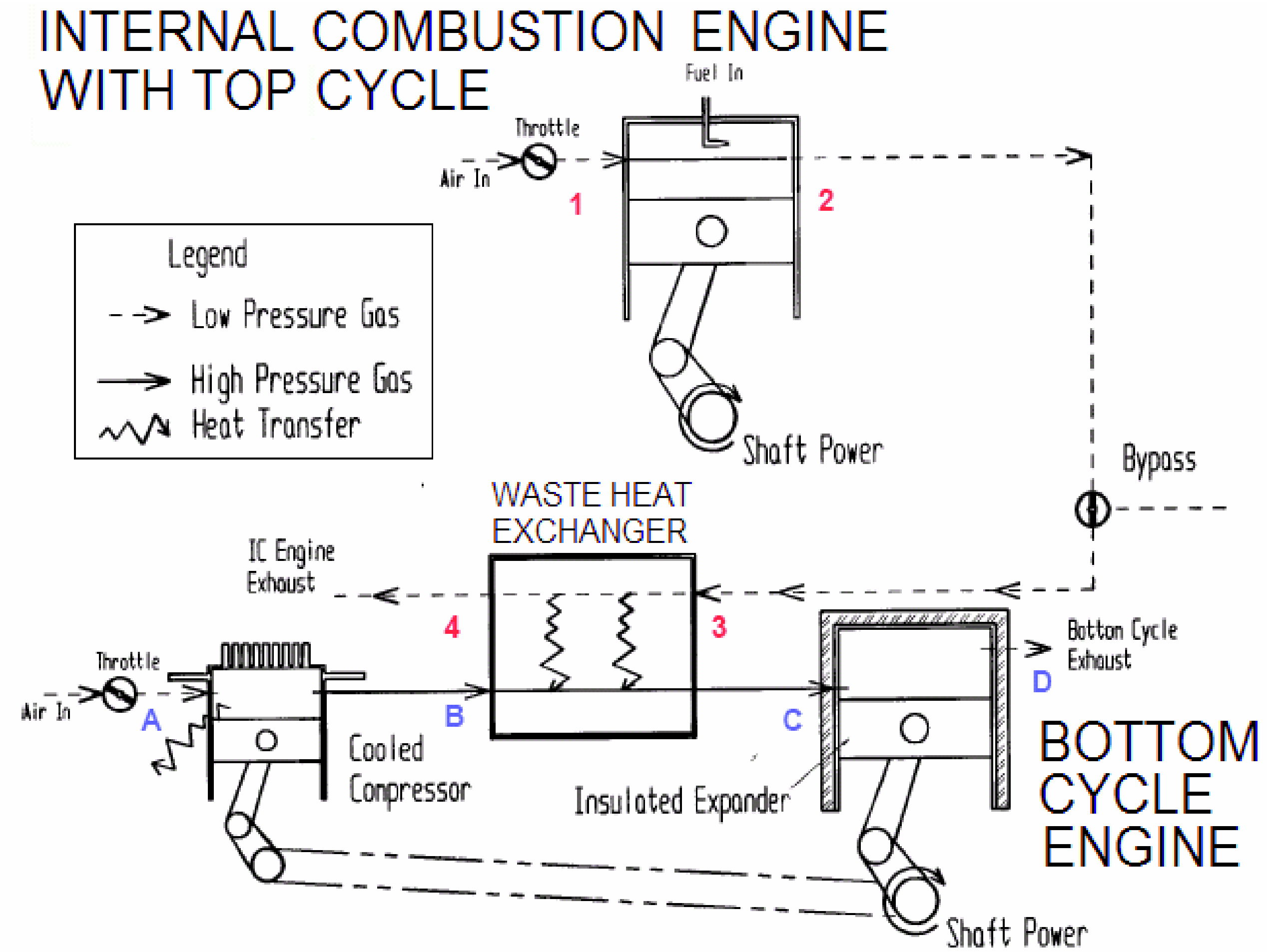


Fig.6. Schema de principiu al sistemului de regenerare a caldurii reziduale

In figura de mai sus s-a prezentat schematic sistemul de recuperare a energiei reziduale si utilizarea acesteia .

Pentru a tine pas cerintelor impuse de legislatia in vigoare cu referire la protectia mediului, motoarele moderne alimentate cu motorina beneficiaza de un sistem EGR, care functioneaza dupa principiul diminuarii emisiilor de NOx recirculând gazele de eşapament prin admisie pentru a scădea temperatura de ardere (gazele de eşapament iau locul oxigenului) [3]

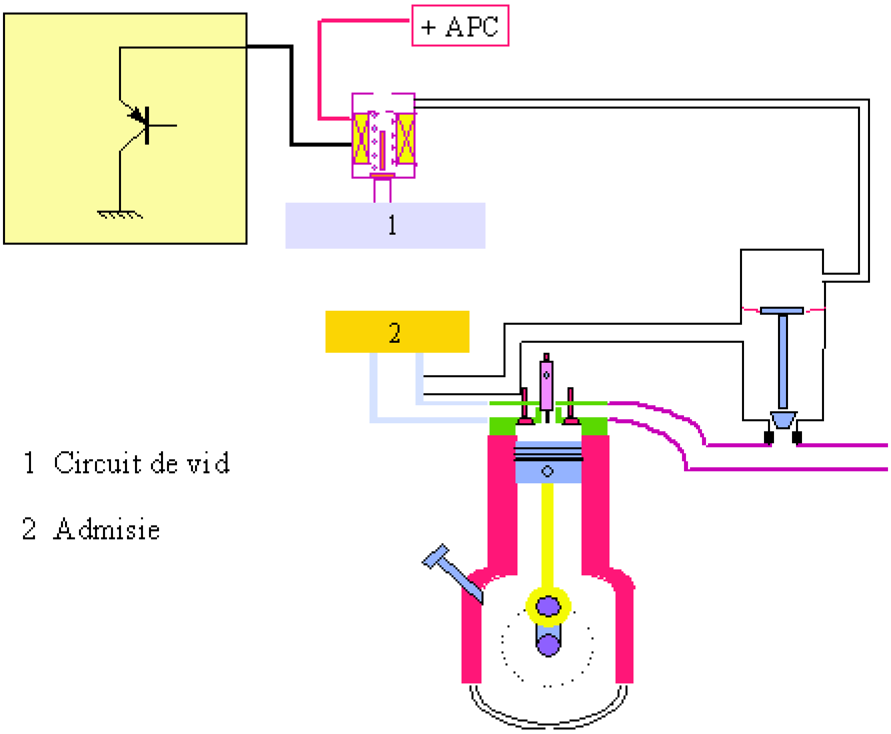


Fig.7 Schema de principiu al sistemului de recirculare EGR

**3. Concluzii**

Din cele prezentate mai sus putem concluziona urmatoarele :

- constructorii consacrati de automobile se indreapta din ce in ce mai mult spre **automobilul putin poluant** implementand pe acesta sisteme hibride de propulsie
- se poate observa ca inclusive in motorsport unde pana nu de mult nu se tinea cont de poluarea mediului acum sunt direct implicati in dezvoltarea si utilizarea sistemelor recuperatoare de energie cinetica
- in scopul de a eficientizarii energetice a automobilelor rezulta din cele de mai sus ca se poate implementa pe autovehiculele rutiere **sisteme de recuperare a energiei de franare** si utilizarea acesteia in fazele de **demarare/accelerare**
- solutiile tehnice ne indruma usor pentru a gasi componentele necesare realizarii unor astfel de sisteme, chiar si pe piata noastra
- exista posibilitatea regenerarii caldurii reziduale iar prin acest proces scade consumul de carburant si scad si emisiile $CO_2$
- o parte din gazele arse pot fi reciclate si combinate cu amestecul carburant

**REFERINTE**

[1] A. Atkins, J. Hey, D. Boggs, “Novel Flyweel Systems For Applications Requiring High Power Density” Ricardo Van Buren Township, Michigan, 48111
[2] Sistem mecatronic de recuperare a energiei de franare la autovehicule grele pentru eficientizarea energetica a acestora; Contract CEEX nr. XIC06/03.10.2005
[3] Auto Test – Revista editata de Registrul Auto Roman
[4] Professional Motorsport World Magazine November 2007
[5] Race Engine Tehnology – ‘The communications hub of the racing powertrain world’ ISSUE 046
[6] www.heat2power.net

ISSN 1454 - 8003
**Proceedings of 2011 International Salon of Hydraulics and Pneumatics - HERVEX**
*9 – 11 November, Calimanesti-Caciulata, Romania*

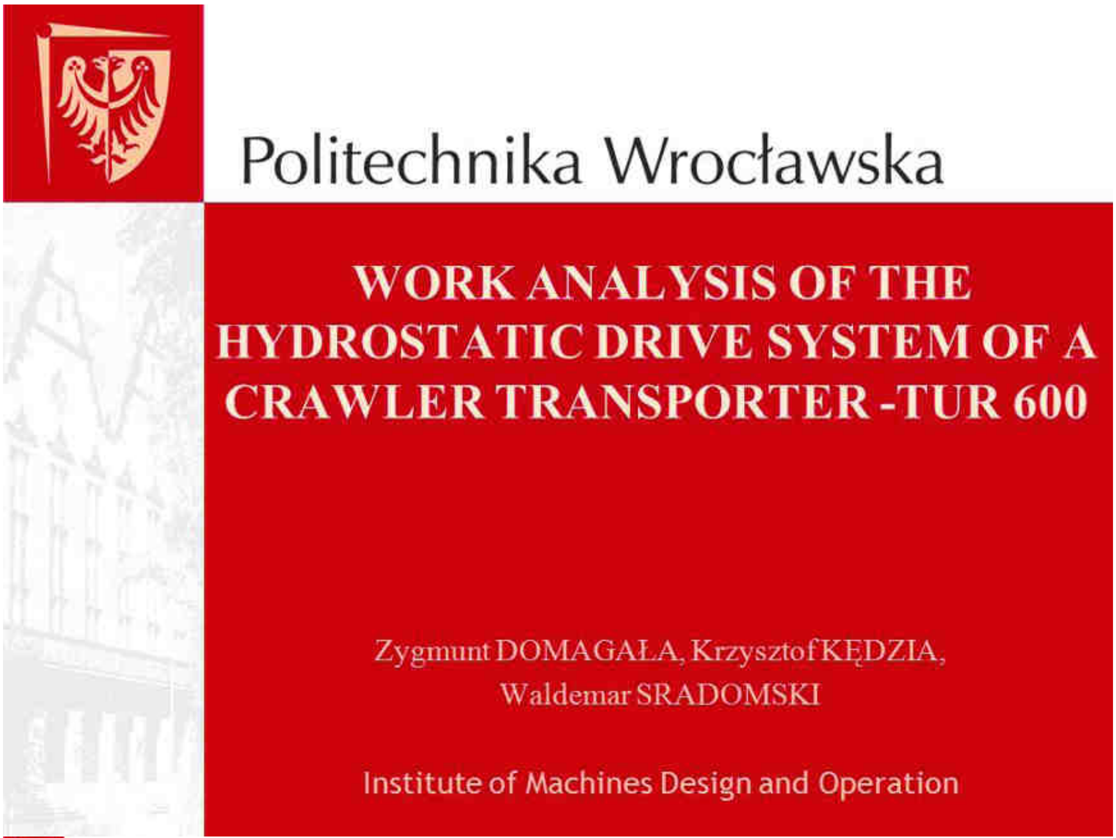


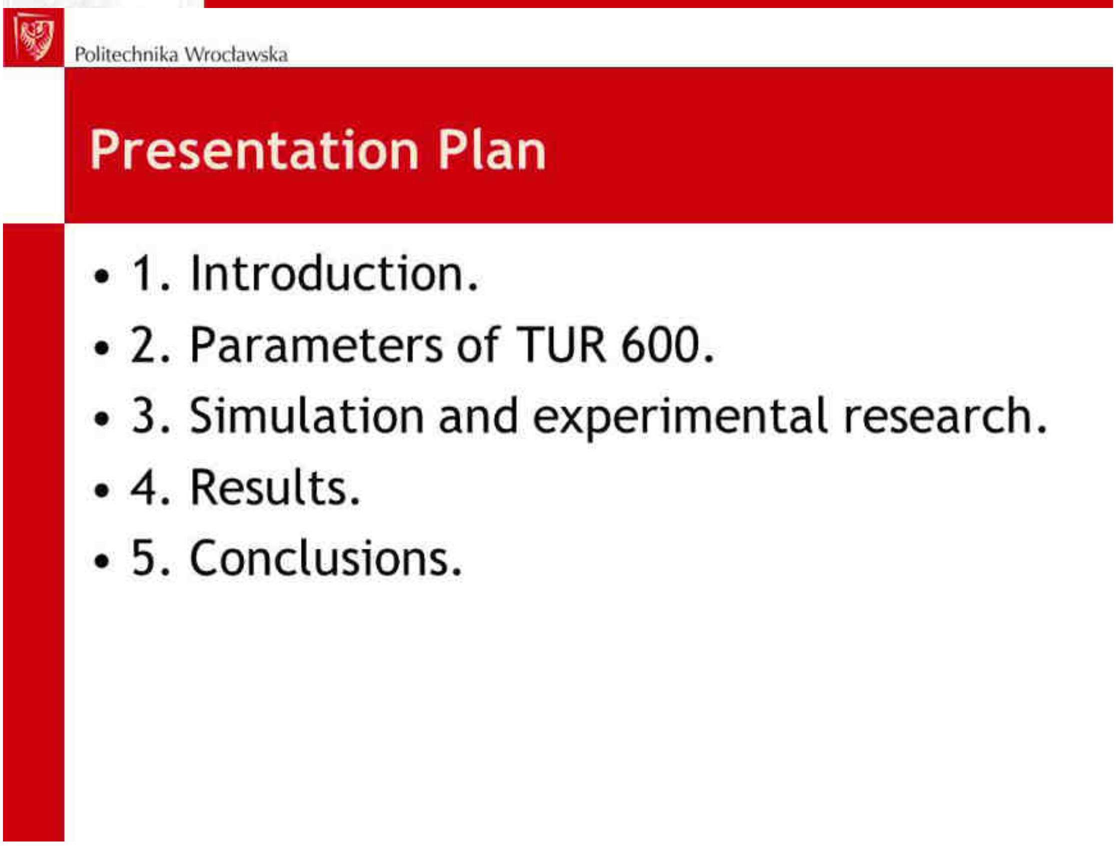

ISSN 1454 - 8003
Proceedings of 2011 International Salon of Hydraulics and Pneumatics - HERVEX
*9 – 11 November, Calimanesti-Caciulata, Romania*

Politechnika Wrocławska

# TUR - 600

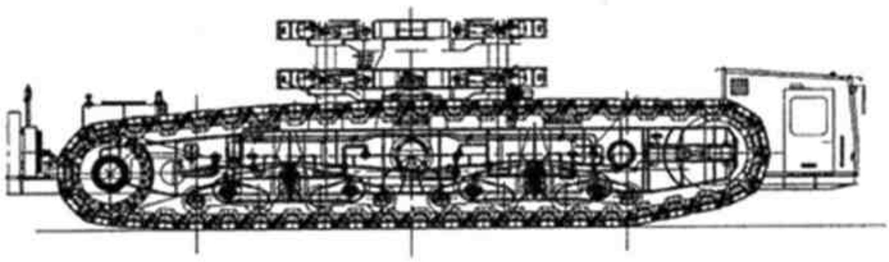

Fig. 1. Crawler transporter type TUR 600

Politechnika Wrocławska

# Technical data of TUR 600

Transporter TUR 600 should move with three speeds:

| | |
|---|---|
| maneuvering | -1 - 5 m / min, |
| transportation | -1.5 - 8 m / min, |
| without load | -1.5 - 16 m / min, |

Politechnika Wrocławska

## Additional requirments

Transporter should move on the ground :

- allowable slope of 1:10 terrain (inclination 10%),
- and must have the ability to transport cargo with mass 600T (600mg).

Politechnika Wrocławska

## Schema of hydraulic drive system

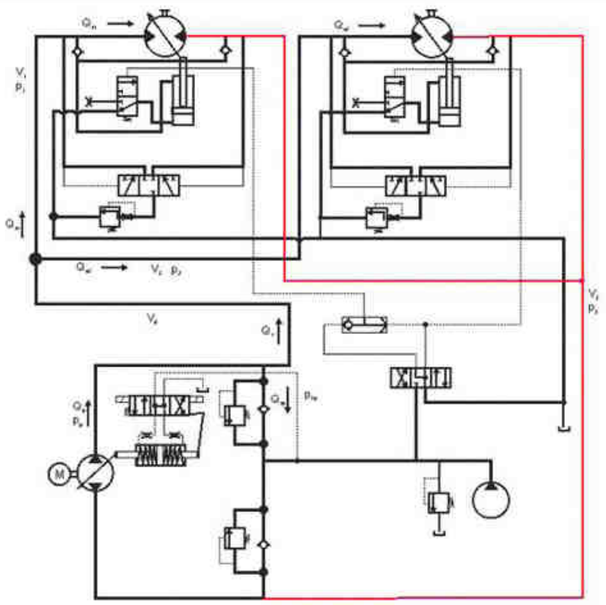

Fig. 2. Schematic of the hydraulic drive system

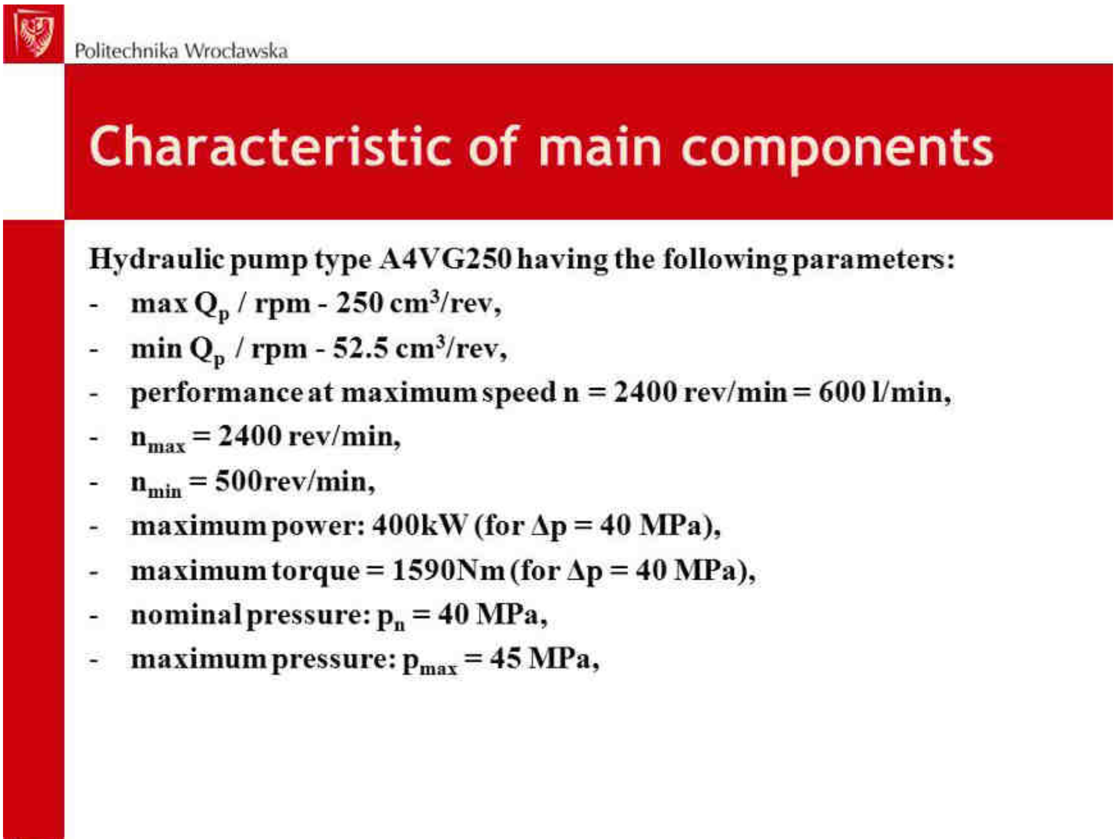
Politechnika Wrocławska
Characteristic of main components
Hydraulic pump type A4VG250 having the following parameters:
- max $Q_p$ / rpm - 250 $cm^3$/rev,
- min $Q_p$ / rpm - 52.5 $cm^3$/rev,
- performance at maximum speed n = 2400 rev/min = 600 l/min,
- $n_{max}$ = 2400 rev/min,
- $n_{min}$ = 500rev/min,
- maximum power: 400kW (for $\Delta p$ = 40 MPa),
- maximum torque = 1590Nm (for $\Delta p$ = 40 MPa),
- nominal pressure: $p_n$ = 40 MPa,
- maximum pressure: $p_{max}$ = 45 MPa,

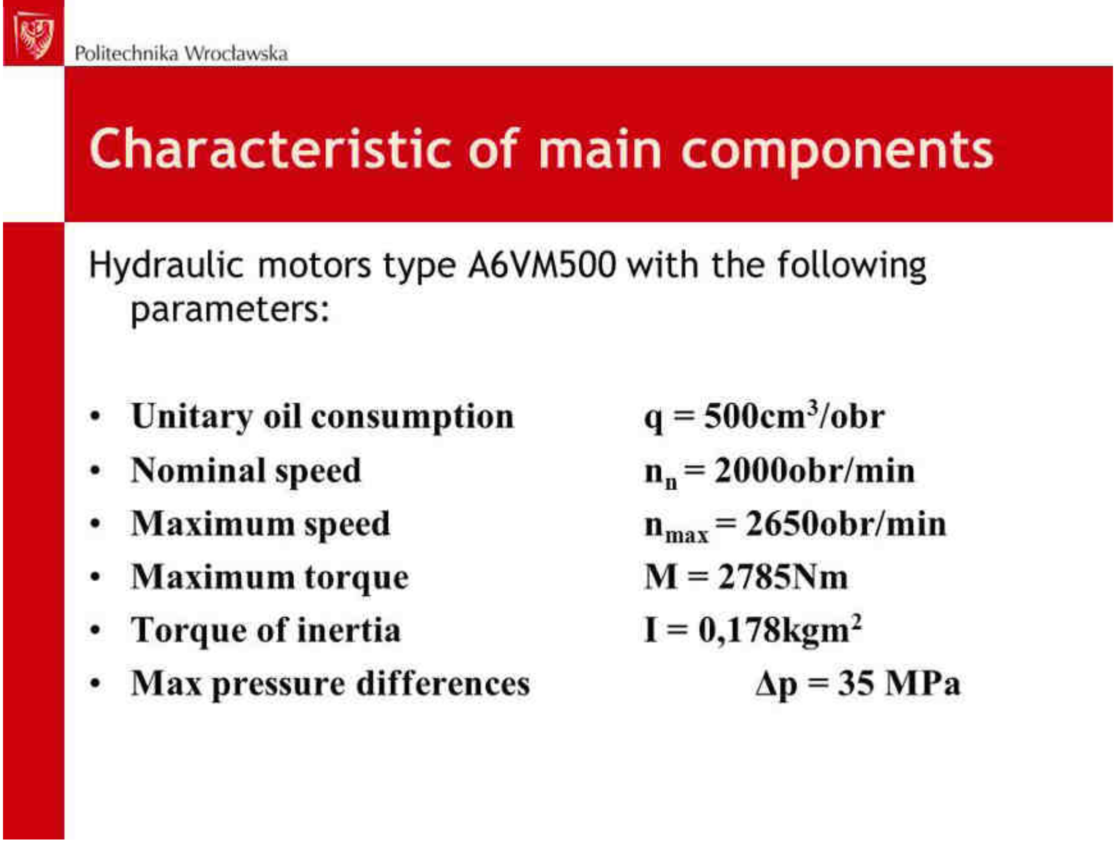
Politechnika Wrocławska
Characteristic of main components
Hydraulic motors type A6VM500 with the following parameters:
• Unitary oil consumption q = 500$cm^3$/obr
• Nominal speed $n_n$ = 2000obr/min
• Maximum speed $n_{max}$ = 2650obr/min
• Maximum torque M = 2785Nm
• Torque of inertia I = 0,178$kgm^2$
• Max pressure differences $\Delta p$ = 35 MPa

Politechnika Wrocławska

## TUR - 600


Fig.3. TUR 600 during the movement with the load (about 300T).

Politechnika Wrocławska

## TUR - 600

Fig. 4. Real viev of TUR 600 transporter without a load.

ISSN 1454 - 8003
**Proceedings of 2011 International Salon of Hydraulics and Pneumatics - HERVEX**
*9 – 11 November, Calimanesti-Caciulata, Romania*

Politechnika Wrocławska

## Distribution of measurement points

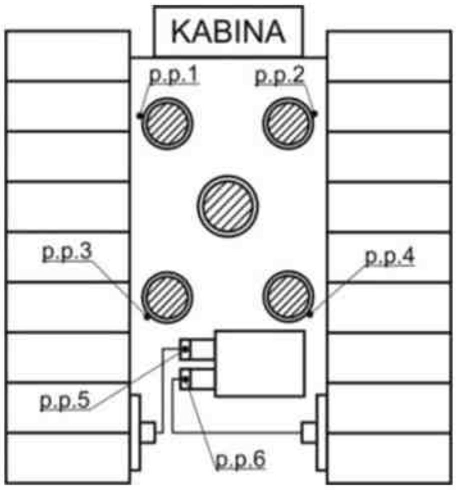


Fig. 5. Location of pressure measurement points in the lift and drive system

Politechnika Wrocławska

## Measurement system

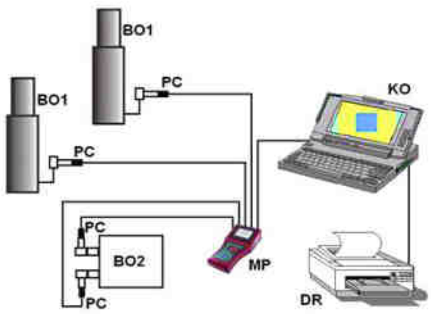


Fig. 6. Schema of measurement system

BO1 – cylinders of the platform lift system,
BO2 – hydraulic pump of drive system,
PC – pressure transducer type PR15,
MP – integrated measurement system HYDROTECHNIK 5060,
KO – computer,
DR – printer.

Politechnika Wrocławska

## An example of fixing of the pressure transducer

Fig. 7. Measurement point no 5 from fig. 5.

Politechnika Wrocławska

## Experimental tests results

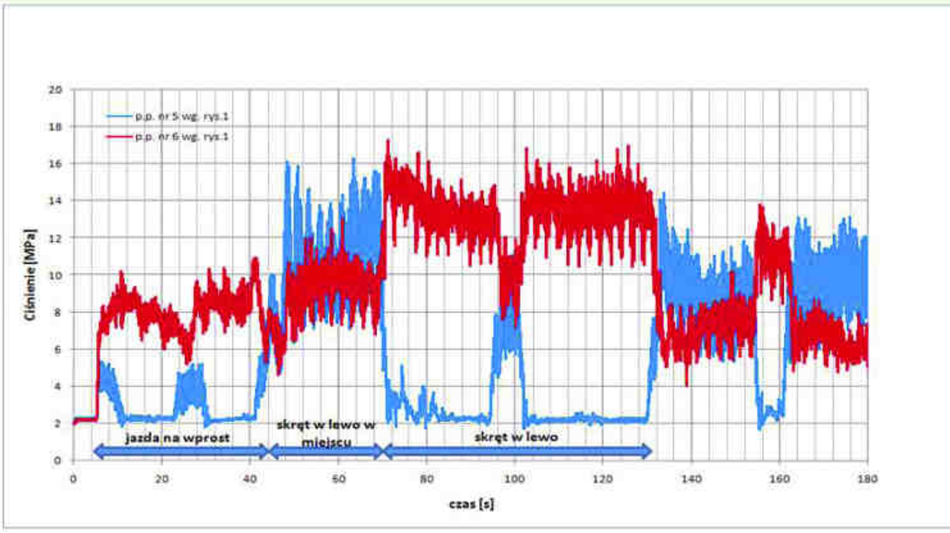


Fig. 8. An example of pressure values recorded in the hydrostatic drive system of TUR 600 during operating measurements

Politechnika Wrocławska

## Simulation research results

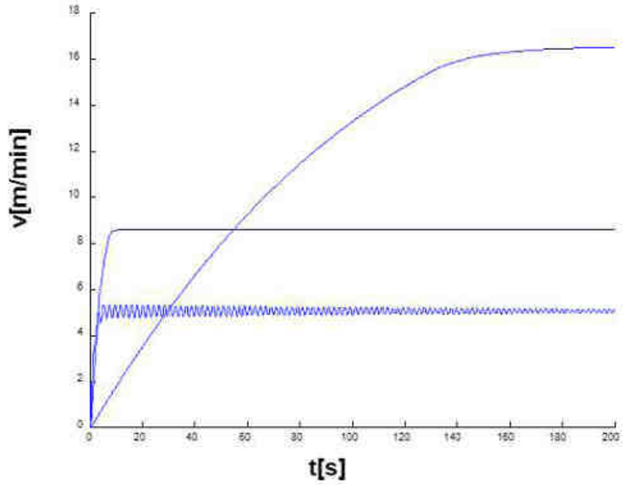


Fig. 9. Speed of the transporter for load 246T for 3 speed levels

Politechnika Wrocławska

## Simulation research results

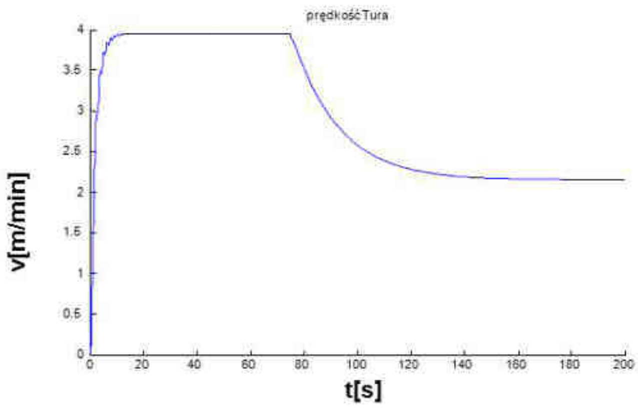


Fig. 10. Speed of Tur 600 with load of 600T, flat terrain, riding into the wind, the most difficult terrain.

Politechnika Wrocławska

# Conclusion

1. In terms of the functional diagram the hydraulic drive is designed properly.
2. Comparative analysis of simulation and experimental results of measurements showed that there were no grounds to reject mathematical models and simulation.
3. Unloaded TUR 600 can move with 3 speeds: maneuver, operational and without load.
4. Transporter TUR 600 with max load do not pass given assumption. Transporter is unable to move.

5. BUT….

Politechnika Wrocławska

# Simulation results

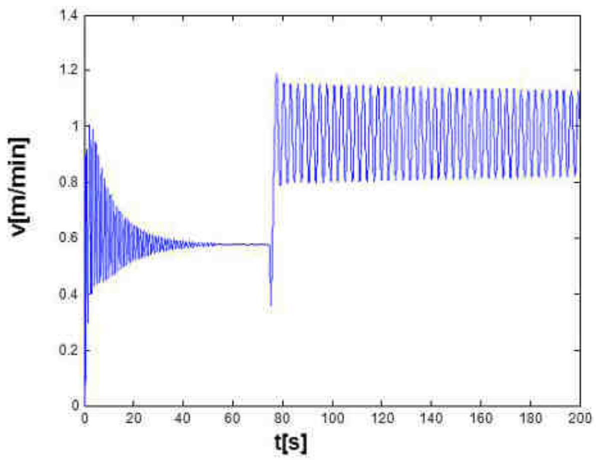


Fig. 11. Speed of Tur 600 for load torque 2264 Nm.

**ISSN 1454 - 8003**

**Proceedings of 2011 International Salon of Hydraulics and Pneumatics - HERVEX**

*9 – 11 November, Calimanesti-Caciulata, Romania*

# NUMERICAL STUDY OF PTFE-LIP SEALS WITH SPIRAL GROOVES

*Aurelian FATU, Mohamed HAJJAM*
*Pprime Institute, CNRS – University of Poitiers - ENSMA UPR 3346*
*Mechanical Engineering, Structures and Complex Systems Department, Poitiers, France*

In order to overtake the limitation of elastomeric lip seals at high ambient temperatures and high rotational speeds, the so-called PTFE lip seals with spiral grooves are being more and more met in the industrial applications. Unfortunately, very few experimental and no numerical studies have been dedicated to the understanding of this king of seal.

In this paper, a numerical model capable to predict the behaviour of PTFE lip seal is presented. The model combines an analytical approach of the fluid flow in the seal grooves with a numerical solution of the elastohydrodynamic contact between the seal pads and the shaft. To illustrate the approach, the liquid filled area of the seal and the friction torque are predicted for different rotational speed.

## 1 INTRODUCTION

At high ambient temperatures and high shaft speeds, PTFE sleeve type seals with spiral grooves often replace the classical elastomeric lip seals. Comparing with the elastomeric lip seals, the PTFE lip seal has different lip geometry: the return flow principle of the so-called screw seals ("visco-seal" or "wind-back seal") is adopted and a spiral groove is created in the contact zone between the seal and the shaft. In this seal the flank of a thread forms the slanted barrier and diverts the circumferential shear flow induced by the rotating shaft. This way the leakage is guided back toward the sealed space.

The precise function mode of the dynamic seal mechanism of PTFE-lip seals with spiral grooves is not yet known enough. In the authors' knowledge, there are not numerical models capable to evaluate the sealing performances in terms of leakage and friction. Only the experimental investigations proposed by Bauer & Hass (1, 2) seem to try an exact analysis of this type of sealing systems. However, many numerical studies have been published on elastomeric lip seals in recent decades. Generally, the computation of the film thickness and pressure distribution in the contact for this kind of seals is based on the theory of (elasto)hydrodynamic (E)HL lubrication represented by the Reynolds equation.

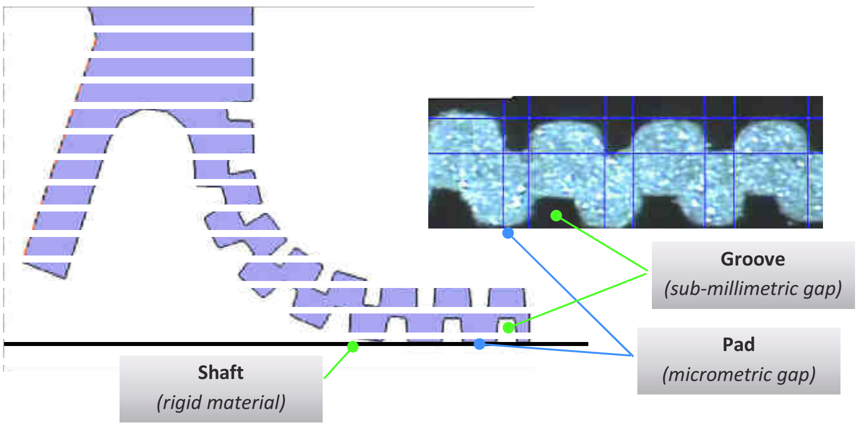


**Figure 1: PTFE-lip seals with spiral grooves**

In the particular case of lip seals with spiral grooves, the Reynolds equation can only be used to described the contact between the pads and the shaft. Between the pads (in the grooves), the fluid flow is governed by the Navier-Stokes equation (*see figure 1*). In fact, the spiral groove lip seals combines the functional principle of the classical lip seals with the functional principle of the visco-seal.

In this paper, the back-pumping behaviour is evaluated from analytical models developed to understand and predict the behaviour of visco-seals. The results show that when the shaft is rotating, the oil penetration in the seal convolutions is practically nil, which is in concordance with the experimental results presented by Bauer and Haas (1, 2). Therefore, the friction force is predicted by solving the Reynolds equation in the contact zones between the pads and the shaft

## 2 BACK-PUMPING AND ACTIVE SEAL LENGTH

A series of studies have been dedicated to the understanding and modelling of visco-seal. The work of Boon & Tal (3) is maybe the most comprehensive and detailed analysis available on the subject. Lately, an essential contribution has been made by Passera (4) and McGrew & McHugh (5). All this authors proposed analytical solutions to find the optimum sealing performances of the analysed visco-seal. Boon & Tall (3) considered a laminar flow through a rectangular groove. Passera (4) proposed an optimisation of the groove cross section geometry and McGrew & McHugh (5) investigated turbulent operation conditions.

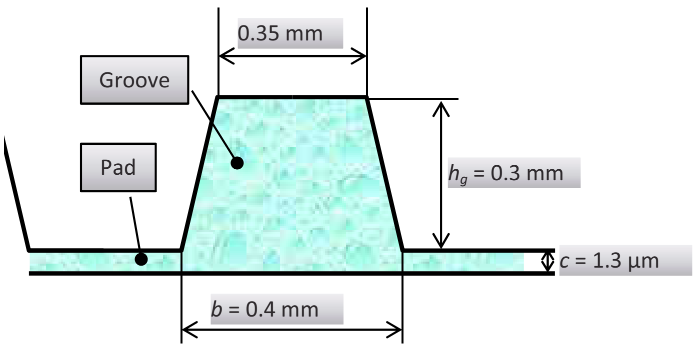


**Figure 2: Cross section of the PTFE lip seal groove**

Figure 2 shows a schematic representation of the PTFE lip seal groove. The axial groove width *b* is 0.4 mm; the groove depth $h_g$ is 0.3 mm; the clearance (*film thickness under the pad*) *c* is considered equal to 2 µm (*the value has been approximated by the EHD model described in the next section*). The helix period is 0.8 mm and the groove section is rectangular. The shaft diameter is 85 mm and fluid pressure in the sealed space is 0.01 MPa.

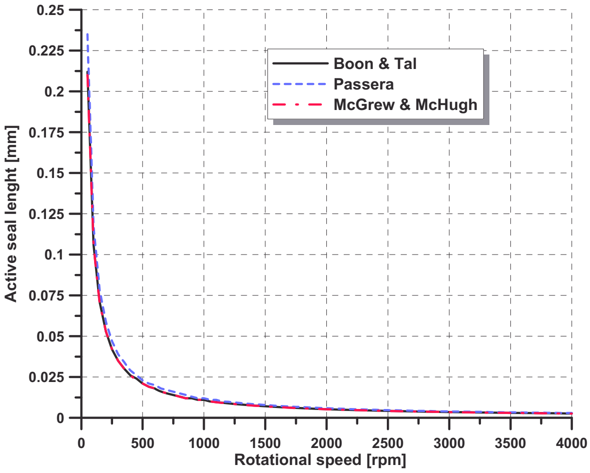


**Figure 3: Predicted active seal length as a function of the rotational speed**

Figure 3 shows the so-called active seal length (the liquid filled area of the seal) as a function of the rotational speed, predicted by three different analytical models. It can be observed that, even for low rotational speed, the active seal length is very small. This means that the groove is almost completely free of fluid. This result has been confirmed by the experimental investigation proposed in reference (1). Consequently, as a first approximation, the pressure into the groove is considered to be very close to the atmospheric pressure.

## 3 LUBRICATION EQUATIONS

Under the pads, the usual assumption of lubrication theory can be applied. Therefore, if a laminar flow with inertial effects neglected is considered, the Reynolds equation in the incompressible case can be solved.

A general form of Reynolds equation, that takes into account the active but also the non-active (cavitated) film zones has been previously described and used by the authors' to predict the elastohydrodynmic behaviour of elastomeric lip seals (6, 7). However, for a better understanding of the present paper, a brief description is given next.

We considered the following hypothesis: the pad is perfectly elastic, the shaft is perfectly smooth and rigid and the shaft eccentricity in the seal is nil (no whipping). The steady state Reynolds equation is:

$$\frac{\partial}{\partial x'}\left(\frac{\rho h^3}{12\mu}\frac{\partial p}{\partial x'}\right)+\frac{\partial}{\partial y'}\left(\frac{\rho h^3}{12\mu}\frac{\partial p}{\partial y'}\right)=\frac{U}{2}\frac{\partial \rho h}{\partial x'} \quad (1)$$

where *p* is the hydrodynamic pressure, *h* is the film thickness, *U* is the linear speed and *μ* is the oil viscosity.

ISSN 1454 - 8003
**Proceedings of 2011 International Salon of Hydraulics and Pneumatics - HERVEX**
*9 – 11 November, Calimanesti-Caciulata, Romania*

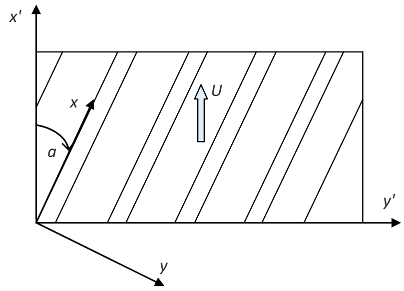


**Figure 4: Developed geometry of the seal**

In the case of the PTFE lip seal, equation 1 is solved in the helix coordinate system:

$$\frac{\partial}{\partial x}\left(\frac{\rho h^3}{12\mu}\frac{\partial p}{\partial x}\right)+\frac{\partial}{\partial y}\left(\frac{\rho h^3}{12\mu}\frac{\partial p}{\partial y}\right)=\frac{U}{2}\left(\frac{\partial \rho h}{\partial x}\cos(\alpha)-\frac{\partial \rho h}{\partial y}\sin(\alpha)\right) \qquad (2)$$

where $\alpha$ is the helix angle (*see figure 4*). According to the same development presented in reference (6) and (7), the general form of Reynolds equation is solved on both active and non-active films zones:

$$F\frac{\partial}{\partial x}\left(h^3\frac{\partial D}{\partial x}\right)+F\frac{\partial}{\partial y}\left(h^3\frac{\partial D}{\partial y}\right)=6\mu U\left[\left(\frac{\partial h}{\partial x}\cos(\alpha)-\frac{\partial h}{\partial y}\sin(\alpha)\right)+(1-F)\left(\frac{\partial D}{\partial x}\cos(\alpha)-\frac{\partial D}{\partial y}\sin(\alpha)\right)\right] \qquad (3)$$

where $D$ is a universal variable and $F$ a cavitation index:

- in the full film zone: $\begin{cases} D = p, \quad D \geq 0 \\ F = 1 \end{cases}$

- in the cavitated zone: $\begin{cases} D = r - h, \quad D < 0 \\ F = 0 \end{cases}$

where $r = \frac{\rho h}{\rho_0}$ is the so-called replenishment variable, $\rho$ represents the density of the lubricant-gas mixture and $\rho_0$ is the density of the lubricant. The equation is coupled, through an elasticity (compliance) matrix, to the elastic behaviour of the seal.

The finite element method is used to solve the previous equation. For each node of the film, the compatibility between the sign of $D$ and the assumed state of the film must be checked. The boundary conditions are reduced to outside boundaries of the domain as the boundary conditions between active and non-active are natural (*see reference (4)*).

## 4 COMPUTATION OF THE STATIC CONTACT DISTRIBUTION

The first step in the theoretical analysis of PTFE lip seals is the evaluation of static dry pressure profile and contact length. This computation is made with commercial FE software. The FE model of the seal is presented in figure 5. The seal is meshed with axisymmetric stress elements. The shaft is usually made in more rigid material (typically steel) than the PTFE seal. Consequently, it is reasonable enough to consider the shaft as an analytical defined rigid element. Close to the contact zones, the seal is meshed with structured quadratic elements, usually used in treating contact problems. Figure 6 a) shows the static contact pressure distribution under the three pads in contact with the shaft. The gap between the pads and the shaft is plotted in figure 6 b). It can be clearly observed that the contact length under each pad is smaller than his initial width.

This result is the starting point of the EHL modelling. The integration of the contact pressure gives the initial radial force that must be balanced by the hydrodynamic pressure. The axial contact length defines the study domain length in *y* direction. The second length is chosen equal to the roughness periodicity in the radial direction. The compliance matrix is computed as a linear perturbation of the mounted seal.

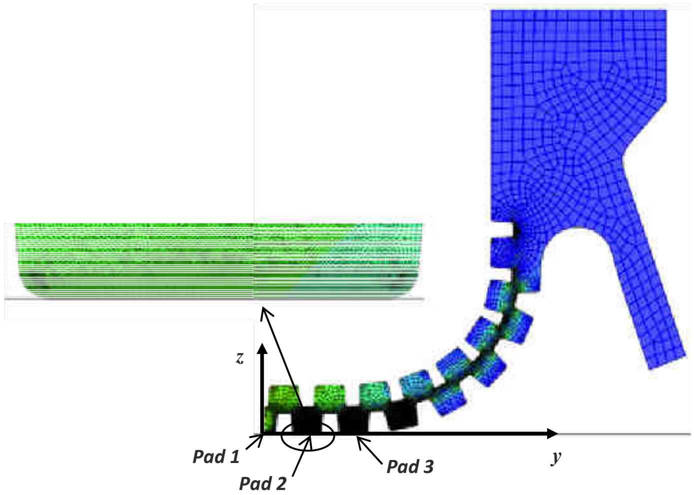


**Figure 5: FE model of the seal**

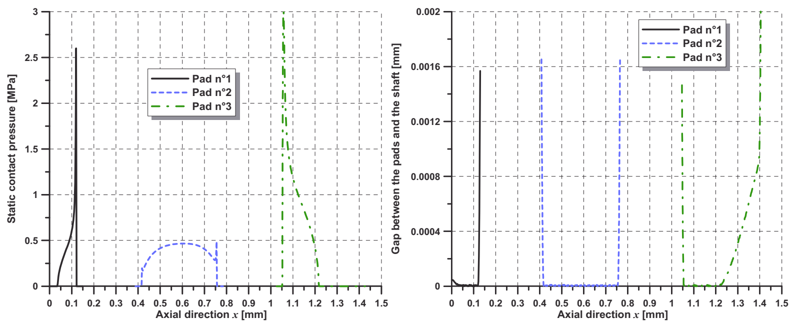


**Figure 6: Static contact pressure**

The film thickness in equation (3) depends on the hydrodynamic pressure but also on the surface microgeometry of the pad:

$$h(x,y) = f(x,y) + g(y) + h_0 + d_z \qquad (4)$$

where $h_0$ is the average film thickness, *g(y)* is the static gap between the seal and the shaft computed by the FE model (*figure 6 b)*) and *f(x,y)* is a mathematical function representing the surface microgeometry:

$$f(x,y) = \frac{A}{2}\cos(2\pi x)(1-\cos(2\pi Ny)) \tag{5}$$

where *A* is the roughness amplitude and *N* is the number of periods in *y* direction.

## 5 RESULTS

To illustrate the approach, several computations have been made for rotational speeds ranging from 1000 rpm up to 4000 rpm. The oil viscosity $\mu$ is equal to 0.04 Pa.s, the roughness amplitude *A* is 2 µm. The length of cell in the circumferential direction is 0.1 mm. Three different roughness periodicities has been investigated for the axial *x* direction: 0.14 mm (*N = 10*), 0.175 mm (*N = 8*) and 0.233 mm (*N* = 6).

Figure 7 shows the isometric views of the predicted film thickness and pressure field for 1000 rpm and *N = 8*. As the model is axisymmetric, the film pressure and thickness are periodic in the circumferential direction. It should be noted that the average profile of the film thickness is almost constant. Therefore, the lifting effect is only generated by the surface microgeometry.

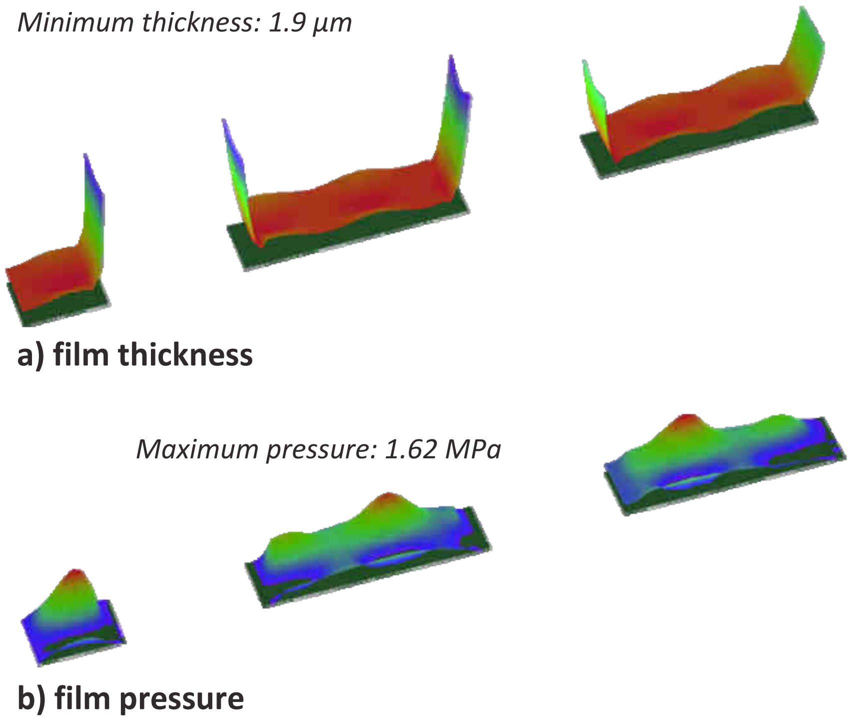


**Figure 7: a) Thickness of the lubricant film and b) distribution of the pressure predicted at 1000 rpm and *N* = 8**

Figure 8 shows the evolution of the friction torque versus the rotational speed. As expected, the friction torque increases linearly with the rotational frequency. However, it should be noted that the computations are made for a constant oil viscosity. Normally, the increase of the friction torque induces an increase of the contact temperature, which generally has non-negligible influence over the global seal functioning parameters. Also, it seems that the investigated different roughness periodicities have only a small influence over the predicted friction torque.

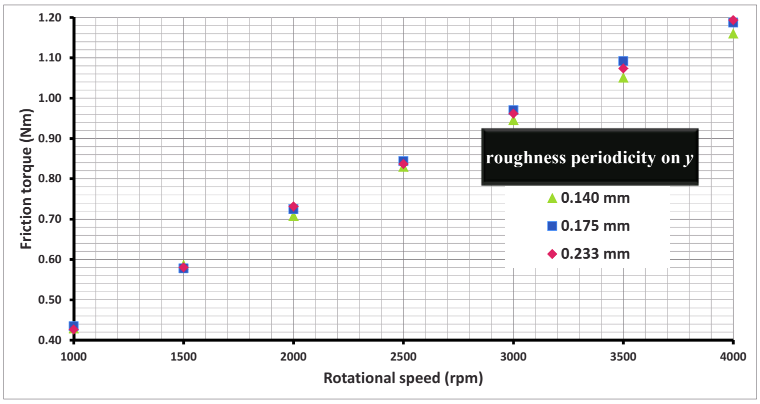


**Figure 8: Evolution of the predicted friction torque versus rotational speed**

## 6 CONCLUSION

In the authors' knowledge, this is the first time when a numerical model, capable to study the behaviour of PTFE lip seal with spiral grooves, is proposed. Starting from models developed to analyse the behaviour of so-called visco-seal systems, the presented model is capable to predict the liquid filled area of the seal. A very simple analysis shows that the groove is almost completely free of fluid, result that has been confirmed by the experimental investigation proposed by Bauer and Haas (1, 2). Therefore, the flow under the pads is treated by solving a mass conservation generalised Reynolds equation, coupled, through the elasticity matrix, to the elastic behaviour of the seal. It has been shown that the lifting force is essentially generated by the variation of the seal surface microgeometry. The friction torque has been calculated and it has been proved that, in isothermal conditions, the friction linearly increases with the rotational frequency.

## REFERENCES

(1) Bauer, F., Hass, W. ,2005, “A new approach to analyze the hydrodynamic flow in sealing aids-PTFE- lip seals with spiral grooves”, 60 th. STLE Annual Meeting, Las Vegas. USA.

(2) Bauer, F., Hass W., 2005, “PTFE lip seals with spiral groove – the penetration behaviour, hydrodynamic flow and back pumping mechanisms” BHR Group Fluid sealing 18.

(3) Boon E. F, Tal S. E., 1959, “Hydrodynamishe dichtung fur rotierend wellen”, Chemie-ingenieur-technik, Vol. 31, num. 3, pp:202-212.

(4) Passera W., 1971, "Concentric-running screw viscosity seals in laminar flow – 1.Therory", 5th International Conference on Fluid Sealing, Paper B5, pp: 58-88, Waewick, Coventry, England.

(5) McGrew, J. M., McHugh, J. D., 1965, "Analysis and test of screw seal in laminar and turbulent operation", J. of Basic Engineering, pp: 153-162.

(6) Hajjam M., Bonneau D., 2007, "A Transient Finite Element Cavitation Algorithm With Application to Radial Lip Seals", Tribol. Int. 40, pp.1258-1269

(7) Maoui. A., Hajjam. M., Bonneau. D., 2008, "Effect of 3D Lip Deformations on Elastohydrodynamic Lip Seals Behaviour", Tribology International, Vol. 41, Issues 9-10, pp. 901-907

**ISSN 1454 - 8003**
**Proceedings of 2011 International Salon of Hydraulics and Pneumatics - HERVEX**
*9 – 11 November, Calimanesti-Caciulata, Romania*

# TECHNICAL EQUIPMENT HYDRAULICALLY OPERATED FOR TREE CROWN SHAPING

**Dr.eng. Gheorghe IVAN[1], Dr.eng. Emil VOICU[1], eng. Ionela GHINIA[1]**

[1] INMA Bucharest, geoivan2006@yahoo.com

***Abstract**: The current technology for intensive and super intensive plantations of shrubs and fruit trees maintenance requires a lot of manual labor. The article presents a hydraulic equipment for the tree crown shapping from a new maintenance technologies of these plantations in order to achieve the technological spaces necessary for the maintenance equipment. This type of equipment is done internationally, but the one presented in the article is more efficient, especially due to the hydraulic installation made in collaboration with INOE 2000-IHP Bucharest.*

**Keywords**: equipment, hydraulic, plantation maintenance

## Introduction

According to the Ministry of Agriculture, the area covered with orchards in Romania in 2010 was 124,000 hectares, being properly maintained only 78,000 hectares, from which 35,000 hectares plum, and 31,000 hectares apple. Orchards are at least 80% aged, start-up area being of around 350 hectares per year, to a necessary minimum of two thousand hectares per year. Depending on the cultivation systems, orchards of our country are classified into three big groups: traditional orchards, intensive and super intensive orchards.

Traditional orchards are characterized by a variety of types in terms of planting distance, slope, surface size and culture system. In general, planting distances for this type of orchard is between 6 and 12 meters between rows and between 5 and 9 meters between trees per row, depending on the specie and culture system. Tree crown is free directed and is larger than the other types of plantations. In terms of mechanization, these plantations creates difficulties because most of them are located on slopes. There are plantations in which the undirected form of the crown prevent the passage of aggregates.

Intensive orchards provide high yields of fruit and good conditions for the mechanical maintenance execution. These plantations are located on plain ground or with small slopes and irrigation possibilities. Planting density depends on the culture of fruit growing, the distance between rows being 2.5 to 6 meters, and the distance between trees per row of 0.5 to 5.5 meters, according to table 1:

Table 1

| fruit growing culture | distance between rows (m) | row distance (m) |
|---|---|---|
| apple tree | 2.5…6 | 0.8…5 |
| pear tree | 3.5…5 | 1.5…4.5 |
| plum tree | 5…6 | 3.5…4.5 |
| apricot tree | 5…6 | 3.5…5.5 |
| peach tree | 4.5…5.5 | 3…4 |
| cherry tree | 5…7 | 4…5.5 |
| cherry tree | 4…6 | 2…4.5 |
| gooseberry | 2.8…3 | 1…1.2 |
| raspberry | 2.5 | 0.5 |
| blackberry | 2.5 | 1.5…1.8 |
| hazelnut tree | 4…5 | 3…3.5 |

Generally, intensive orchard trees have directed crown by flattening to the row direction or palisade to the row direction with trellis support system.

Super intensive orchards are high density and productivity orchards, located exclusively on plain land. They are characterized by small trees, directed with or without a support system, with valuable varieties with quick input bearing. Planting distances to these orchards are between 2.5 and 3.5m between rows and between 1.5 and 2m between rows tree. These plantations provide good conditions for mechanization by extending mechanization even some works to other types of without mechanization plantations, for example: harvesting fruit, trimming, etc..

A common feature of all types of orchards is the work of trimming the crown trees and harvesting fruit that requires a large amount of manual labor. Internationally this shortcoming is eliminated, the maintenance technology of these plantations is based on the use of machinery and efficients.

### 1. EFCP equipment

The new maintenance technology of fruit tree plantations demands the execution of a technical hydraulic equipment EFCP for the trees crown shapping, which execute the technological space necessary to the plantations maintenance with a high productivity, increase quality of work and will greatly reduce costs. The novelty and originality of the EFCP equipment are:

- trimming crown vertically and horizontally simultaneously;
- constructive and functional simplicity;
- easy settings;
- technical solutions to reduce weight and cost.

EFCP equipment (Figure 1) is mounted on the tractor Goldoni STAR 3070 SL and includes the following parts:

1. vertical cutting machine;
2. Horizontal cutting machine;
3. vertical support;
4. horizontal support;
5. intermediate telescopic assembly;
6. hydraulic;
7. protective lock assembly cut.

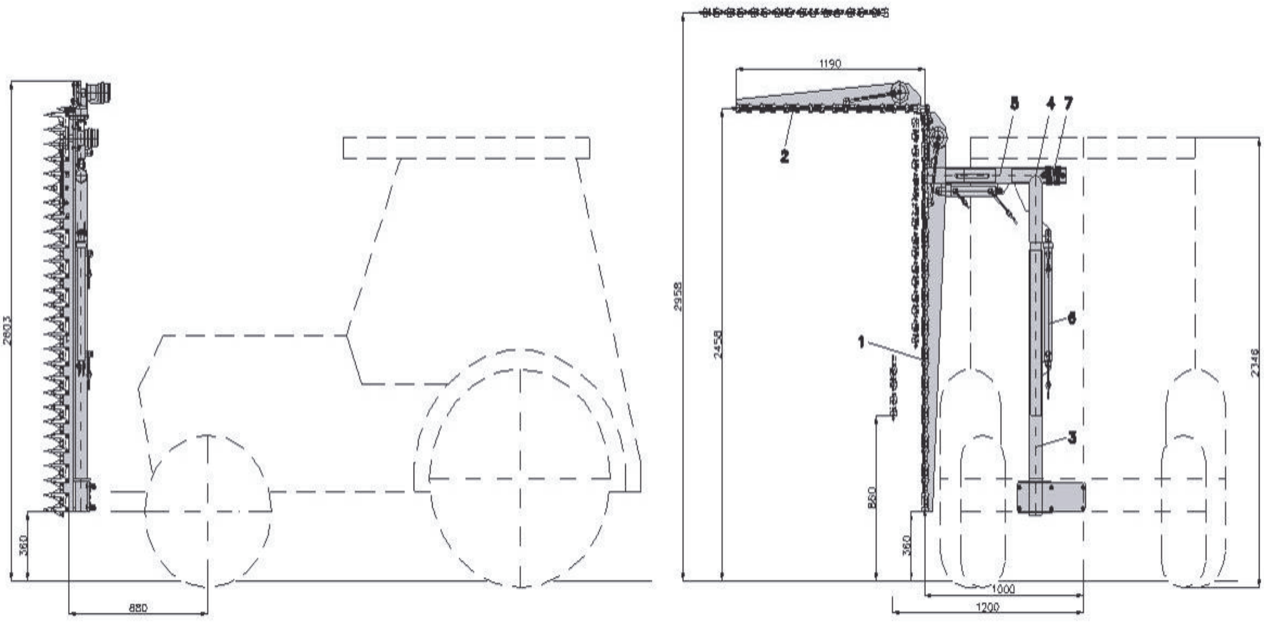


Fig.1 EFCP equipment for the tree crown shapping

The technical characteristics of Glodoni tractor:

- wheelbase: 1968mm;
- width min/max: 1340:1770 / 1547:1800cm;
- front wheels size: 280/70x16”;
- balloon width: 280mm;
- balloon height / balloon width: 70%;
- rim bead diameter: 16”;
- external diameter of the front wheels balloon:16”x25,4+2x0,7x280 = 798,4mm;
- rear wheels size: 380/70x24”;
- balloon width : 380mm;
- balloon height / balloon width: 70%;
- rim bead diameter: 24”;
- external diameter of the rear wheels balloon =24”x25,4+2x0,7x380 = 1141,6mm;
- tractor length / tractor cab height: 3348/2346mm.

Technical and functional characteristics of the EFCP equipment:

- number of cutting devices: 2;
- length of cutting device on the horizontal: 1190mm;
- length of cutting device on the vertical: 2100mm;
- maximum cutting height: 2958mm;
- cutting height adjustment: 500mm;
- adjustment of the equipment distance from the tractor: 200mm;
- speed of cutting machine: 520rot/min;
- overall dimensions: 3000x2400x450mm;
- mass of equipment: 150kg;

Functioning of the equipment consists in making of the following operations:

- adjusting by means of hydraulic installation of the revolving in horizontal position of the horizontal cutting device, of the vertical cutting device distance to the tractor and of the maximum cutting height;
- hydraulic engines start control acting cutting devices;
- adjustment of forward speed of the tractor to avoid cutting devices blocking;
- command to stop the tractor engines and hydraulic in case of blocking of cutting devices.

**2. Hydraulic installation of EFCP equipment**

Hydraulic installation of EFCP equipment provides performing the adjustments and commands required for the functioning of equipment.

2.1 Calculation memoir of hydraulic installation

Initial datas:

- length of the vertical cutting device: $l_1$ = 2,1m;
- length of horizontal cutting device: $l_2$ = 1,19m;
- estimated specific power consumed by the cutting device: P=4 CP/m;
- speed of cutting devices: n = 520rot/min;
- cutting devices stroke: s = 76,2mm;
- nominal pressure in the hydraulic installation of the tractor: $p_n$=160 kgf/cm$^2$;

Power consumption calculation by the vertical cutting device:

$$P_1 = P \times l_1 = 8{,}4CP \tag{1}$$

Power consumption calculation by the horizontal cutting device:

$$P_2 = P \times l_2 = 4{,}76CP \tag{2}$$

Resistant moment calculation on the vertical cutting device:

$$M_1 = 716{,}2\frac{P_1}{n} = 11{,}57daNm \tag{3}$$

Resistant moment calculation on the horizontal cutting device:

$$M_2 = 716,2\frac{P_2}{n} = 6,56\text{daNm} \tag{4}$$

Calculation of working pressure for hydraulic engines:

$$p_l = 0,8 \times p_{n.} = 0,8 \times 160\text{daN/cm}^2 = 128\text{daN/cm}^2 \tag{5}$$

Geometrical volume calculation of hydraulic engine MHR1 [1]:

$$V_{m1} = \frac{2\pi M_{r\,max1}}{(p_l - p_r)\eta_{mm}} = 63,6\text{cm}^3 \tag{6}$$

where $V_{m1}$ is the geometric volume of the hydraulic engine 1;
$M_{r\,rmax1}$ – maximum resistant moment, $M_{rmax1}$=$M_1$ = 11,57daNm;
$p_l$ – working pressure $p_l$ = 128daN/cm$^2$;
$p_r$ – pressure in the return $p_r$ = 1daN/cm$^2$;
$\eta_{mm}$ – mechanical yield of hydraulic engine, $\eta_{mm}$=0,9…0,95;

Geometrical volume calculation of hydraulic engine MHR2:

$$V_{m2} = \frac{2\pi M_{r\,max2.}}{(p_l - p_r)\eta_{mm}} = 31\text{cm}^3 \tag{7}$$

Geometrical volume calculation of hydraulic pump:

$$V_p = \frac{V_{m1} + V_{m2}}{\eta_{mp}} = 99,58\text{cm}^3 \tag{8}$$

where $V_p$ is the geometric volume of the hydraulic pump;
$\eta_{mp}$ – mechanical yield of hydraulic pump, $\eta_{mp}$=0,95;

Calculation of maximum oil flow rate introduced into the engine [1]:

$$Q_m = \frac{2\pi(M_{r\,max1} + M_{r\,max2})n}{(p_l - p_r)\eta_{mm}\eta_{mv}} = 60\ \text{l/min} \tag{9}$$

choose from the catalog Sauer-Danfoss [2]:
engine OMR 100 - for both cutting devices
geometric volume: 99,8cm$^3$;
maximum speed: 600rot/min ;
maximum moment: 24daNm ;
maximum power: 13kW;
maximum pressure drop: 175bar ;
maximum flowrate: 60l/min;

2.2 Composition and characteristics of hydraulic installation of EFCP equipment:

- oil tank of the Goldoni tractor;
- hydraulic pump of Goldoni tractor $Q_{max}$=38l/min, $P_{max}$=130bar;
- multiple distributor PVG32 – Lyra company;
- Radio Remote Control System TM70/1.13 – Lyra company;
- Receiver R70/13 – firma Lyra;
- vertical hydraulic cylinder C2S, stroke = 500mm, – Lyra company;
- horizontal hydraulic cylinder C2S, stroke=200mm, – Lyra company;
- tilting hydraulic cylinder C2S, stroke=70mm, – Lyra company;
- 2 hydraulic engines OMR100, $Q_{max}$=60l/min, $\Delta p_{max}$=140bar – Lyra company;
- track throttle G3/8”, Dn=10, $p_{max}$=350bar – Lyra company;
- vent filter for filling NBF403, G1 ½”, Fineţe 130μm – Lyra company;
- retour filter Pi50.016-075N+Pi 25 016 RN, G1 ¼”, Finesse 25μm, $Q_{max}$=160l/min – Lyra company;
- 2 antibumping valves HK FPMD70 ILP 12S20, G1/2”, Dn=16, $p_{work}$=80...280bar – Hansa flex company;
- taps, hoses, manometer, thermometer.

The hydraulic installation scheme of the EFCP equipment was performed in collaboration with INOE 2000-IHP Bucharest and is presented in Figure 2.

ISSN 1454 - 8003
**Proceedings of 2011 International Salon of Hydraulics and Pneumatics - HERVEX**
*9 – 11 November, Calimanesti-Caciulata, Romania*

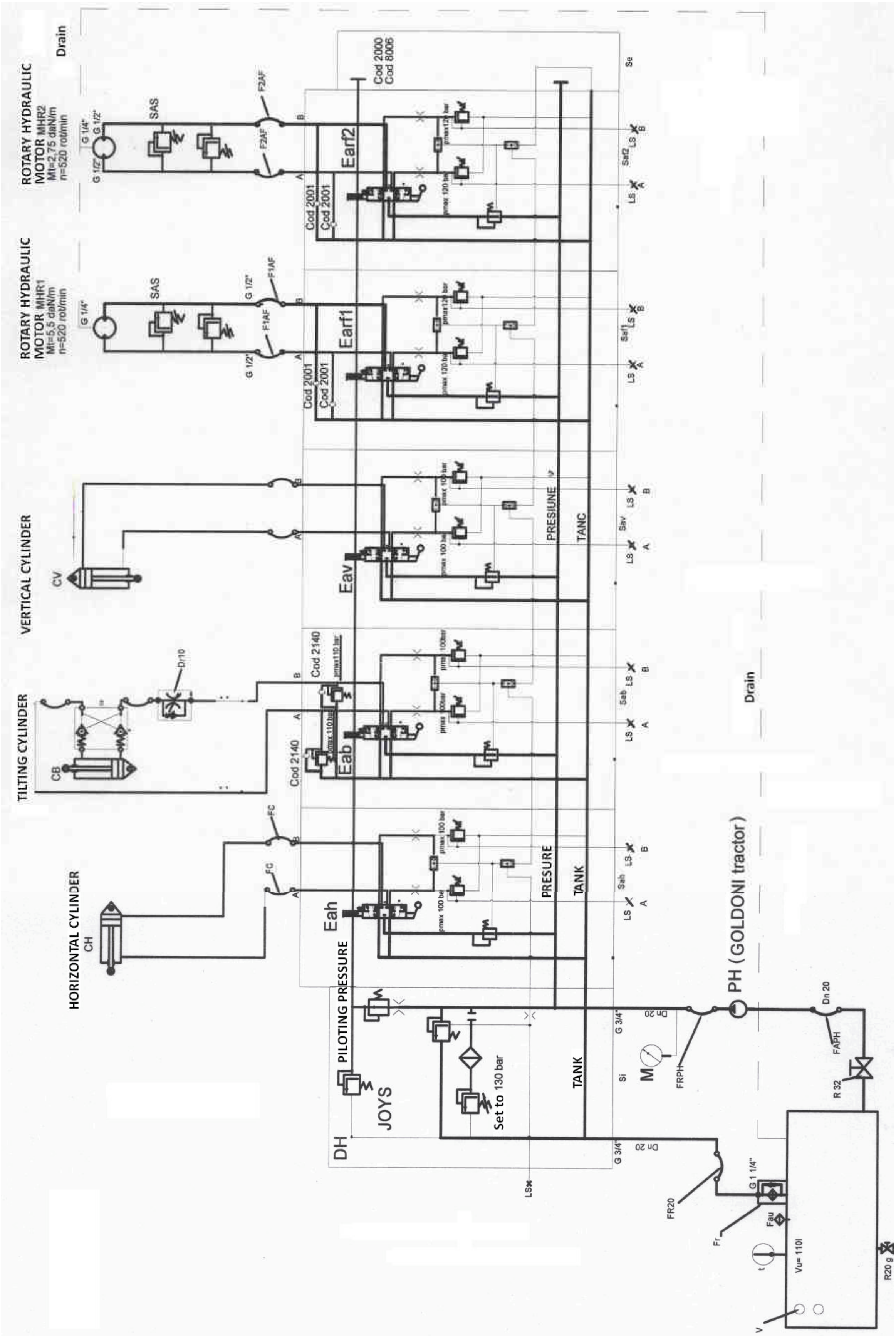


Fig.2 Hydraulic installation scheme of the EFCP equipment

Figure 3 presents Radio Remote Control System remote TM70/1.13.

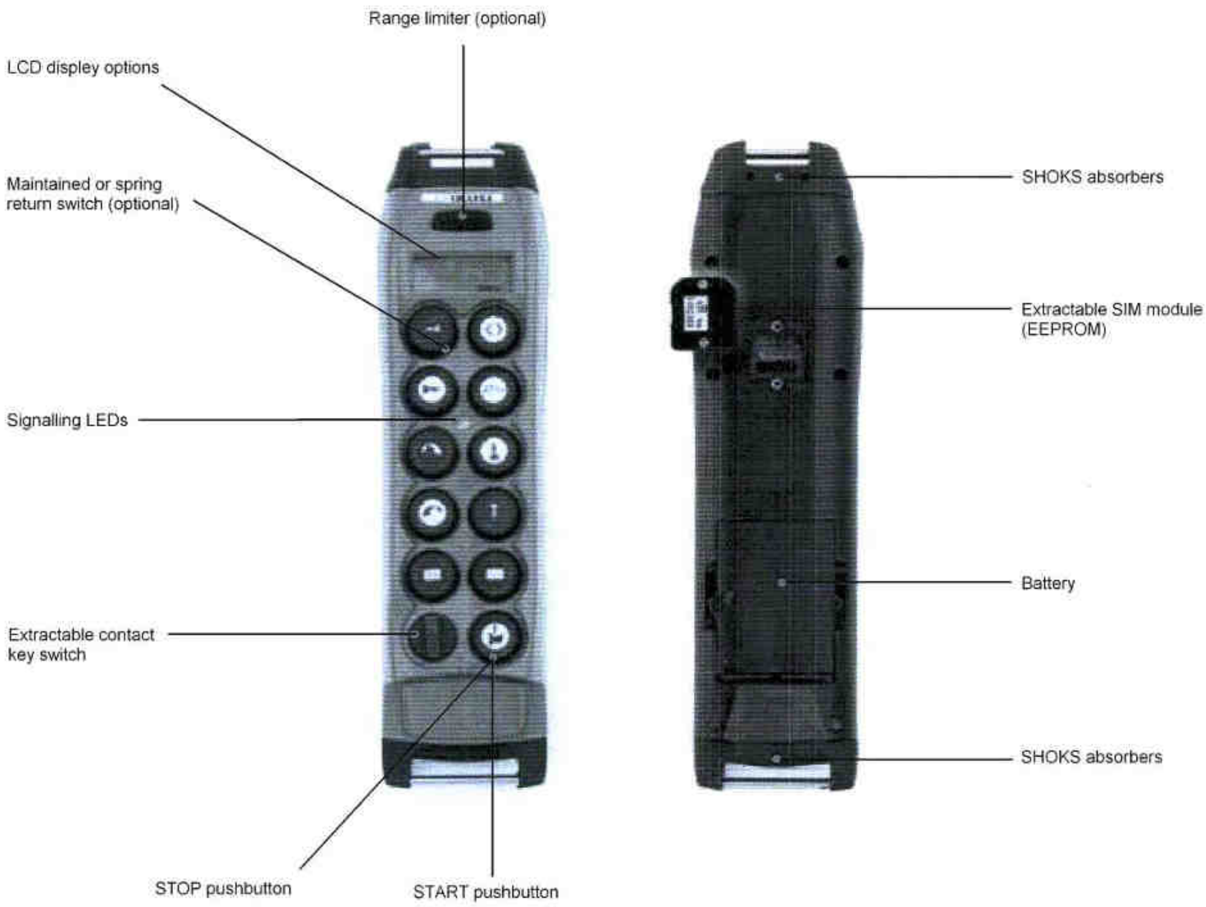


Fig.3 Radio Remote Control System TM70/1.13

## 3. Conclusions

Using the technical equipment hydraulically operated for crown shaping trees EFCP in the new maintenance technology of intensive and superintensive orchards will solve one of the real needs of Romanian Horticulture, and the production of the equipment in Romania will create new jobs and reduction the cost price.

## REFERENCES

[1] P.Babiciu, V.Scripnic, Al. Fratila, "Hydraulic systems of tractors and agricultural machinery" Ceres Publishing House, Bucharest, 1984 - pg.234…241;
[2] Sauer-Danfoss Catalogue, pg. 3…56;
[3] Leaflet Goldoni tractor, Lantec company.

**ISSN 1454 - 8003**
**Proceedings of 2011 International Salon of Hydraulics and Pneumatics - HERVEX**
*9 – 11 November, Calimanesti-Caciulata, Romania*

# EXPERIMENTAL RESEARCHES REGARDING THE DYNAMICS OF MOBILE AGRICULTURAL MACHINERY

Mihaela Florentina DAVID, Edmond MAICAN, Erol MURAD

*Rezumat: În această lucrare s-a verificat şi s-a corectat programul de modelare necesar studiului dinamicii agregatelor agricole mobile.*

*Abstract: In this paper is checked and is rectified the programmer of modeling necessary for the study of the dynamics of mobiles agricultural aggregate.*

**Keywords:** mobile agricultural aggregate, tractor, attachment, data acquisition sheet, experimental tests, time, velocities, accelerations.

## 1. Introduction

The main objective of experimental testing, constitute the checking and the rectification of the programmer of modeling from the study of the dynamics of mobiles agricultural aggregate.

The modeling of mobiles agricultural aggregate will be achieved considering the traction force that is necessary to displace the mobile agricultural aggregate is constant. In reality this traction force is variable because of the irregularity of the field. In time of the experimental testing is recorded the variation of traction force when the aggregate is moving. This variation will be approximate with a function that is a sinusoidal shape and in the programmer of modeling of the mobile agricultural aggregate are introduced the relations of calculation of the traction forces for three rates of travel of the aggregate.

It was checked if the experimental values of the steering wheel accelerations and of the driving wheel accelerations of the tractor correspond of the calculated values with the programmer of modeling.

From the rectified of the programmer of modeling of the dynamics of mobiles agricultural aggregate, for an considering aggregate, who are moved on the field with known parameters, will be determinates, for each velocity stage, the following parameters: the traction force, slipping coefficient, real velocity of move, time consumption and the effective specific fuel consumption, the accelerations and the oscillations amplitudes of the steering wheels and the driving wheels of the tractor.

## 2. The description of the experimental installation

For performed the experimental testing we used a mobile agricultural aggregate formed by U-650 M tractor and the agricultural attachment RPV – 2 (figure 1).

Fig. 1. The mobile agricultural aggregate used at the experimental testing

For measurement and recording the parameters who define the dynamic behaviors for the considered mobile agricultural aggregate we used the following equipment:

- 486 DX Professional Computer;
- Data acquisition sheet;
- Inductive accelerometer type B 12/200 (Hottinger);
- Draw bar for U – 650 M tractor;
- Fifth gear for establishing of predicted rate of movement of aggregate.

In figure 2 are presented the assembly of the accelerometers for recording of the acceleration of the steering wheel and the driving wheel of the tractor.

In figure 3 are presented the assembly of additional wheel for the determination of a predicted rate of movement of the tractor.

In figure 4 are presented the draw bar with measuring head of the traction force and the pressing force of the attachment, as well as the mount of the data acquisition system.

Fig. 2. The mount at the measuring head of the acceleration of the steering wheel and driving wheel of the tractor

Fig. 3. The mount at the additional wheel

Fig. 4. Draw bar with the force cells and the mount of the data acquisition system

### 3. The manner of the progress of the tests

The experimental tests are done in November 2006 on the field path with the following parameters:

- The amplitude of the dishevelment: 0,06 m;
- The length of the dishevelment: 0,039 m.

The predicted rates for the movement at the mobile agricultural aggregate were: 6, 54 km/h, 8, 95 km/h, 12, 32 km/h. The mobile agricultural aggregate it was started in one of the predicted rates who was mentioned and after the aggregate reached the stationary regime of working (after 15 – 20 seconds) it was done, for a 15 seconds length, the following recordings:

- The traction force;
- The pressing force of the tractor attachment;
- The acceleration of the front bridge of tractor;
- The acceleration of the back axel of tractor;
- The acceleration of the mass point of tractor;
- Number of rotations of steering wheel;
- Number of rotations of fifth gear.

The results obtained are presented in graphs and tables. For each rate of travel, for the mobile agricultural aggregate are done two successions of tests.

### 4. Processing and interpreting of the experimental tests

The recordings performed for determination of the real velocity of movement, of predicted rate and of the skidding of steering wheels of the tractor are presented in table 1.

*Table 1*

**The establishment of the predicted rate, of the real velocity and of the skidding on base of experimental tests of the mobile agricultural aggregate: U – 650 M tractor – RPV – 2 attachment**

| No. | N [rotations] | Ns [rotations] | Time [s] | Real velocity | | Predicted rate | | Skidding [%] |
|---|---|---|---|---|---|---|---|---|
| | | | | [m/s] | [km/h] | [m/s] | [km/h] | |
| 1. | 5.5 | 21.5 | 15 | 1.8 | 6.49 | 1.816 | 6.54 | 0.76 |
| 2. | 5.5 | 21.6 | 15 | 1.808 | 6.51 | 1.816 | 6.54 | 0.46 |
| 3. | 7.5 | 29.4 | 15 | 2.463 | 8.87 | 2.486 | 8.95 | 0.89 |
| 4. | 7.5 | 29.5 | 15 | 2.472 | 8.90 | 2.486 | 8.95 | 1.005 |
| 5. | 10.25 | 40.5 | 15 | 3.394 | 12.22 | 3.422 | 12.32 | 0.81 |
| 6. | 10.25 | 40.6 | 15 | 3.402 | 12.25 | 3.422 | 12.32 | 0.57 |

For each velocity stage was done two experimental tests on 15 seconds time. The tests were being performed after the mobile agricultural aggregate entered in the stationary regime of working. It was done the following recordings:

- Number of rotations of steering wheel (N);
- Number of rotations of fifth gear (Ns);
- The experimental test time: 15 seconds.

For each experimental test it was calculated the real velocity of movement with the relation:

$$v_r = \frac{2 \cdot \pi \cdot N \cdot r}{t} \qquad (1)$$

and the predicted rate of movement:

$$v_t = \frac{2 \cdot \pi \cdot N_s \cdot r_s}{t} \qquad (2)$$

where: $r$ - is the dynamic radius of the steering wheel;

$r_s$ - is the radius of the fifth gear;

$t$ - time of experimental test.

For the calculation of skidding of steering wheel of tractor it was used the relation:

$$\delta = \frac{v_t - v_r}{v_t} \cdot 100 \qquad [\%] \qquad (3)$$

From each of the six experimental tests are recorded the acceleration of the steering wheel, the acceleration for the driving wheel, the traction and the pressing force. For each of the six tests with 15 seconds time, are done 15000 recordings for each of the measurements amounts.

For a measuring fault of acceleration of 0, 65 and a degree of reliability of 90% were selected 76 values that are corresponded at the done tests at an interval of time of 0, 2 seconds. For the mobile agricultural aggregate velocity of 12,321 km/h are presented in figure 5 the variation of the pressing force of agricultural attachment on the coupling eyelet with the tractor and the variation of the traction force.

For the traction and pressing force on the coupling eyelet of the agricultural attachment, are followed to obtain some function that approximated the variation of these.

For the three predicted rates of movement of the mobile agricultural aggregate who was tested, are calculated the medium values, the amplitude, the period and the oscillatory pulsation of the traction force and the pressing force are presented in tables 2 and 3.

The mathematical relations who approximate the variation of traction force necessary to movement of mobile agricultural aggregate are:

$v = 6{,}54$ km/h $\quad F_t = 118.4 + 95.37 \cdot \sin(8.64 \cdot t)$ [daN] (4)

$v = 8{,}95$ km/h $\quad F_t = 162.8 + 145.12 \cdot \sin(9.67 \cdot t)$ [daN] (5)

$v = 12{,}32$ km/h $\quad F_t = 133.55 + 144.88 \cdot \sin(9.89 \cdot t)$ [daN] (6)

The calculation relations of the pressing force are:

$v = 6{,}54$ km/h $\quad F_a = 267.5 + 38.45 \cdot \sin(9.04 \cdot t)$ [daN] (7)

$v = 8{,}95$ km/h $\quad F_a = 246.15 + 55.2 \cdot \sin(9.82 \cdot t)$ [daN] (8)

$v = 12{,}32$ km/h $\quad F_a = 232.55 + 80.68 \cdot \sin(10.06 \cdot t)$ [daN] (9)

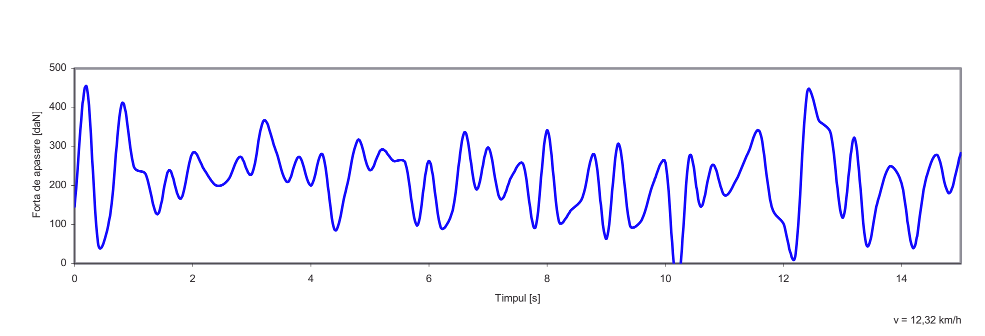


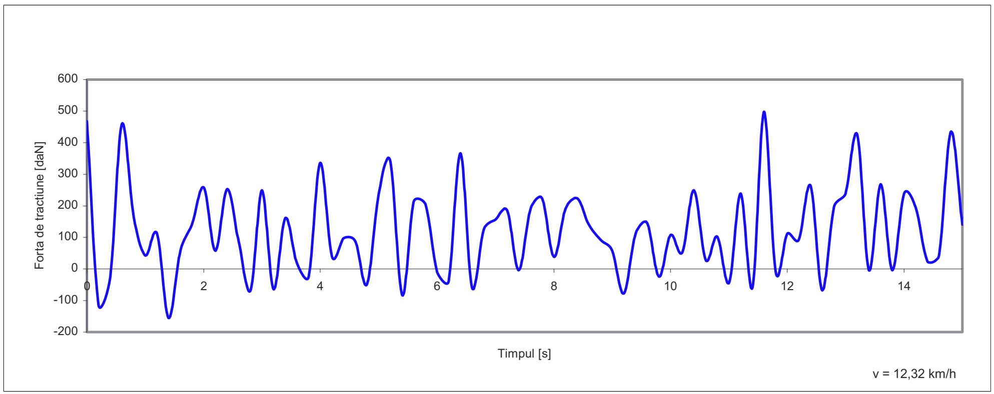


Fig. 5. The variation of the pressing force of the RPV – 2 attachment on the coupling eyelet and the tractio force for $v = 12{,}32$ km/h

The calculations of the traction and pressing force on the coupling eyelet are introduced in modelling programme of the dynamic mobile agricultural aggregate.

With the modelling programme of an mobile agricultural aggregate, particularized for RPV 2 attachment, are calculated the acceleration of steering wheel and the acceleration of the driving wheel for the three predicted rates of movement.

*Table 2*

**The parameters of the traction force determinate on base of experimental dates**

| Velocity[km/h] | Average [dan] | σ [daN] | Amplitude [daN] | Period [s] | ω [rad/s] |
|---|---|---|---|---|---|
| 6.54 | 102.1 | 142.1 | 88.827 | 0.764 | 8.224 |
| | 134.7 | 189.5 | 101.928 | 0.694 | 9.053 |
| 8.95 | 141.5 | 208 | 153.188 | 0.708 | 8.87 |
| | 181.1 | 254.6 | 137.066 | 0.6 | 10.47 |
| 12.32 | 119.7 | 197 | 144.472 | 0.682 | 9.213 |
| | 147.4 | 240.9 | 145.303 | 0.594 | 10.577 |

*Table 3*

**The parameters of the pressing force determinate on base of experimental dates**

| Velocity [km/h] | Average [dan] | σ [daN] | Amplitude [daN] | Period [s] | ω [rad/s] |
|---|---|---|---|---|---|
| 6.54 | 263.4 | 266.5 | 36.534 | 0.724 | 8.678 |

| | | | | | |
|---|---|---|---|---|---|
| | 271.6 | 275.9 | 40.371 | 0.668 | 9.406 |
| 8.95 | 257.3 | 269.4 | 60.676 | 0.644 | 9.756 |
| | 235 | 243.8 | 49.737 | 0.636 | 9.88 |
| 12.32 | 207.1 | 223.9 | 80.539 | 0.658 | 9.549 |
| | 258 | 277.1 | 80.829 | 0.594 | 10.577 |

In table 4 are presented the amplitudes of steering wheel and of driving wheel experimental determinate and calculated with the modeling programmer of mobile agricultural aggregate.

*Table 4*

**The experimental and calculated acceleration of the steering wheel and of the driving wheel of a tractor**

| Velocity [km/h] | Acceleration of steering wheel [m/s$^2$] | | | Acceleration of driving wheel [m/s$^2$] | | |
|---|---|---|---|---|---|---|
| | Exp. | Calculated | Error [%] | Exp. | Calculated | Error[%] |
| 6.54 | 3.874 | 3.39 | 12.5 | 2.05 | 1.96 | 4.4 |
| 8.95 | 4.213 | 4.56 | -8.23 | 2.055 | 2.73 | -32.8 |
| 12.32 | 4.761 | 4.4 | 7.58 | 2.257 | 2.55 | -13 |

The real medium velocity of movement of the mobile agricultural aggregate and the medium coefficient of backlash, experimental and calculate determinate with the modeling programmer are presented in table 5

*Table 5*

**The real medium velocity and the medium coefficient of backslash**

| Predicted rate [km/h] | Medium real velocity [km/h] | | | Medium backlash coefficient [%] | | |
|---|---|---|---|---|---|---|
| | Exp. | Calculated | Error[%] | Exp. | Calculated | Error[%] |
| 6.54 | 6.5 | 6.47 | 0.46 | 0.61 | 0.5 | 18 |
| 8.95 | 8.885 | 8.81 | 0.84 | 0.947 | 0.9 | 4.9 |
| 12.32 | 12.235 | 12.25 | -0.122 | 0.69 | 0.65 | 5.8 |

## 5. Conclusion

At least of the experimental tests of the mobile agricultural aggregate are done the following conclusion:

- The recording of the variation of the traction force and of the pressing force of the agricultural attachment on the coupling eyelet permitted determination of relations who permit the calculation of these for each moving velocity of aggregate;
- Frequency of the traction and pressing force oscillation are 1,3–1,68Hz
- The programmer who permit the calculation of the dynamic parameters of the mobile agricultural aggregate corrected with the mathematic expressions of the traction and pressing force determinate from the experimental tests, permit the calculation of the real velocity, the backlash of the driving wheel, the accelerations of the steering wheel and driving wheel;
- The miscalculations of the accelerations of the steering wheel are in 7,58-12,5% limits, and the miscalculations of the accelerations of the driving wheel are in 4,4-13%;
- The miscalculations of the movement at the real velocity of the mobile agricultural aggregate are smallest for 1% given at the medium values experimental determinates and the miscalculations of the backlash coefficient given at the experimental determinates medium value is in 4,9-18% limits;
- Are estimated that the values obtain with the modeling programmer of the mobile agricultural aggregate for the oscillations amplitude of the steering wheel, and driving wheel are very close of the experimental values;
- The modeling programmer permits the determination of time consumption and the effective specific fuel consumption for can appreciated the economic of using at the mobile agricultural aggregate;

- The modeling programmer of the mobile agricultural aggregate, particularized for a special tractor and an agricultural machine at the movement for a custom field, will be use when the movement at the aggregate is done for other type of field. In this way are determinate the dynamics and economics parameters of the aggregate without be necessary the performance of other tests.

BIBLIOGRAPHY

[1]. *Păunescu I., Manole C.*, Tractoare şi automobile, Universitatea Politehnica din Bucureşti, 1993;
[2]. *Păunescu I., David L.,* Bazele cercetării experimentale a sistemelor biotehnice, Editura Printech, Bucureşti, 1999;
[3]. *Rădoi M., Deciu E.*, Mecanică, Editura Didactică şi Pedagogică, Bucureşti, 1981;
[4]. *Simion F.P., Decolon C.,Tarna D., Dinu I., Simion M.D.,* Introducere în studiul dinamicii sistemelor, Editura Matrix Rom, 2002;
[5]. *Simion F.P., Decolon C., Ion C.,* Elasticité des solides, Editura Matrix Rom, 2002;
[6]. *Voinea R., Voiculescu D., Simion F.P.*, Introducere în mecanica solidului cu aplicații în inginerie, Editura Academiei Române, Bucureşti, 1989;
[7]. *Voinea R., Decolon C., Simion F.P., Simion G., Nedelcu C.,* Introduction a la mécanique des milieux continus élastique, Editura Academiei Române, Bucureşti, 1997;
[8]. *Zeveleanu C., Bratu P.,* Vibrații neliniare, Editura Impuls, Bucureşti, 2001

**ISSN 1454 - 8003**
**Proceedings of 2011 International Salon of Hydraulics and Pneumatics - HERVEX**
*9 – 11 November, Calimanesti-Caciulata, Romania*

# A CONSTRUCTIONAL AND FUNCTIONAL IMPROVEMENT IN HYDRAULIC ROTARY PERCUSSIVE DRILL

**Claudia KOZMA[1], Liviu VAIDA[2]**

[1] Technical University of Cluj Napoca, Caudia.Kozma@termo.utcluj.ro

[2] Liviu.Vaida@termo.utcluj.ro

***Abstract:*** *Function principles of hydraulic hammer drill and hydraulic rotary percussive drill are analysed. Hydraulic schemes for these drills are conceived. A performance improvement for hydraulic rotary percussive drill is revealed.*

***Keywords****: Hydraulic rock drills, hydraulic breaker, hydraulic hammer drill, percussive, hydraulic scheme, function principle*

## 1. Introduction

The drill equipment that is used to realise holes, to drill water well, boreholes, for tunnelling, drilling and blasting, in the construction industry for drilling in rocks, breaking pavement and concrete, represents the whole aggregates, devices, tools, used in this manner. In drilling, force aggregates are represented by motors, drill turbines, electric down hole motor, hydro-percussive and pneumo-percussive mechanisms etc. [1].
Equipments with hydraulic transmission have oil to serve for transmitting motion from the driving motor (thermic or electric) [1] to an actuator or cylinder.
Complex hydraulic systems, specific to machine driving and general equipment driving and also to mining machine driving, are formed by simple hydraulic systems, each of them being destined to solve a functional task, a task which the hydraulic driving has to fulfill. These tasks refer to consecutive or concomitant activity assurance required for hydraulic motors, to assure a required movement for actuator etc.
The used hydraulic systems can be classified, accounting their command method, as systems with manual command and systems with automatic command. [2]
Hydraulic systems of mining machines with manual command that use force cylinders with simple action, are utilized to actuate loader's mechanisms, digging machine's mechanisms, mechanisms for drill devices and other mining equipments [2].
Hydraulic systems with automatic command and reciprocating movement of hydraulic motors are utilized to actuate the mechanisms of different mining machines to obtain alternating linear motion or alternating rotary motion of actuators [2].

## 2. Function principle for hydraulic breaker and rock drill

A representation for the working principle of the hydraulic system used by [4] is shown in Figure 1. It represents a hydraulic breaker. This demolition equipment realizes percussion on rock or on different hardness complex structure, like concrete and asphalt.

The problem solved by this patent is minimizing impact shock. The system includes two sources of hydraulic pressure, two pumps 3 and 4. The pumps provide consecutively liquid fluid to each chamber of the hydraulic cylinder 9. One pump helps to move the piston to a sense and the other pump helps to move the piston in the other sense of direction. Thus, the pump 3 supplies hydraulic energy for the piston during work stroke and the pump 4 supplies hydraulic energy during return stroke. The used control valve 5 realizes selectively the communication of the sources 3 and 4 with the hydraulic cylinder in with the piston moves. By selecting the supply from the source 3, fluid is sent to the hydraulic cylinder 9. Fluid acts on the piston work surfaces and drives the piston until it strikes the used work tool. It is created an impact shock and transmitted to the rock. A hydraulic accumulator 7 is included between the distributor 5 and the hydraulic cylinder 9 to absorb excess hydraulic energy from the hydraulic pressure source 3. During the work stroke, the control valve 5 assures also the closed position of the control valve 6 by the driving of the fluid upon its sleeve. To start the return stroke of the percussive piston, the control valve 5 commutes and isolates the pump 3 from its passages. In this position the control valve 5 allows the passage of the fluid from the hydraulic pressure source 4 to the chamber C2 of the hydraulic cylinder 9. By supplying from the pump 4, it determines the commutation of the control valve 6. Now, the fluid can pass from the source 4 to an accumulator 8 and to the chamber C2 of the hydraulic cylinder 9. The hydraulic accumulator 8 absorbs excess hydraulic energy from the pump 4. The minimization of impact shock at the end of the return stroke is realized by damping. There is a damping chamber with damping fluid in which the velocity of the piston during the return stroke is reduced. Consequently, the severity of impact shock decreases. Movement of the piston during the work stroke creates a partial vacuum in the damping chamber and the damping fluid is advanced from the reservoir 10 and through the check valve 11 and the throttling valve 12. The check valve 11 also prevents damping fluids from being advanced to the reservoir 10 during the return stroke. The rod piston has at the end a shoulder with the surface named damping surface and during the return stroke the damping surface compress the damping fluid accumulated in the damping chamber. The damping fluid may be either in a liquid state, a gaseous state, or a mixture of the liquid and the gaseous states. The piston urges the damping fluid through the check valve 13. Force of the spring keep the check valve 13 closed during the work stroke. In the next paragraphs it is described the working principle of two patented structure of hydraulic rotary percussive hammer drills mounted on the drill rig's carrier to a better understanding of used command elements.

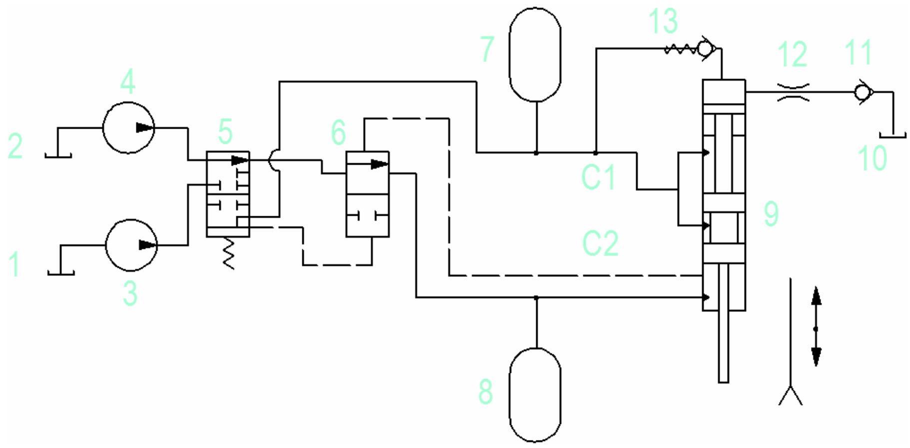


Fig. 1 Hydraulic scheme for [4] where: 1, 2 – reservoir; 3, 4 – hydraulic pump; 5, 6 – control valve; 7, 8 – hydraulic accumulator; 9 – hydraulic cylinder; 10 – sump; 11 – check valve; 12 – throttling valve.

The patent [5] presents a hydraulic rotary percussive drill. The work principle of this equipment is represented in figure 2. The components of this hydraulic rotary percussive perforator are the body of the hydraulic drifter, the percussive piston mounted in a cylinder, a hydraulic distributor, a check valve and a hydraulic diaphragm type accumulator. The percussive piston delimits in the cylinder 7 two annular chambers, C1 and C2, and an intermediate chamber. The one way valve 4 is a control valve that in the position allowing the supply of the percussive mechanism assures the communication of the hydraulic accumulator with the chamber C1 through the control valve 6. The control valve 4 is a common valve and frequently used valve in the construction of hydraulic rock drills. The chamber 7 communicates through the control valve 6 alternatively with the tank T or with the high pressure pipe (the inlet pipe) coming from the pump 2. The control valve 6 is actuated by the piston movements. The control valve 4 comprises a lateral connection allowing the connection of the inlet pipe to the return pipe, to a tank T. In this case only the rotary mechanism works. The rotary motor 3 is mounted in the inlet pipe, supplied directly from the hydraulic pressure source 2. When the inlet fluid flow becomes greater than a predetermined value, the created pressure is thus sufficient to move the non-return valve 4 against the force of its spring, thus compressing the spring. The valve 4 commutes and, thus closes-off the direct passage to the return pipe but it opens the passage to the accumulator 5 and allows the passage of the inlet fluid to the chamber C1. Thus, the piston begins the return stroke and the accumulator 5 stores the hydraulic fluid under pressure. To notice that the pump 2 supplies the rotary motor 3 on the one hand and the percussion device on the other hand, these two systems mounted "in series" operating simultaneously. When the supplied fluid flow remains less than the predetermined value, the one way valve 4 cannot be moved against its force spring and remains in a position such that the percussion mechanism is blocked. The percussion mechanism and the rotation mechanism work „in series” permitting the work tool (the drill pipe and the bit) to rotate without necessitating to start the percussion mechanism and by varying the inlet rate of flow.

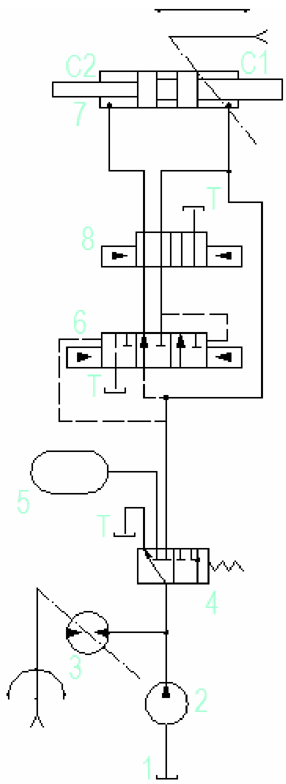

Fig. 2 Hydraulic scheme for [5] where: 1 – reservoir; 2 – hydraulic pump; 3 – hydraulic motor; 4 – one-way valve; 5 – hydraulic accumulator ; 6 – hydraulic distributor; 7 – hydraulic cylinder; 8 – control valve; T – tank.

During the return stroke the piston determines the command of the hydraulic distributor 6 by uncovering certain orifices, named control orifices, through which fluid under pressure passes and acts on the sleeve of the distributor to commute it. Now the chamber C2 is under pressure and supplied from the pump 2 while the chamber C1 is under pressure too. These control orifices helps also to control, to adjust, the piston stroke and can be partially or completely obstructed. The pressure in the chamber C2 is higher than the pressure in chamber C1 owing to its large work area causing the piston to do the work stroke. During the work stroke piston strikes the work tool and uncovers the control orifices and connecting them to the return pipe. Thus, the control valve 6 is restored to its initial position in which it connects the chamber C2 to the return pipe. The same cycle is repeated according to the supplied pressure.
Naturally, it is always possible to rotate the tool by a mechanism which is completely independent of the percussion mechanism, which also has the advantage of allowing great operating flexibility, but necessitates two separate pumps and supply circuits, problem solved by this patent [5]. This solution is less expensive and more reliable. The control valve 8 is conceived to show the functional principle of the cylinder 7. So that the valve 8 indicates that fluid passes through the control pipe commanding the valve 6 during the work stroke and during the return stroke fluid from the command pipe is drained to tank.

**ISSN 1454 - 8003**
**Proceedings of 2011 International Salon of Hydraulics and Pneumatics - HERVEX**
*9 – 11 November, Calimanesti-Caciulata, Romania*

It has already been considered to mount the percussion mechanism and the rotary mechanism "in series" hydraulically in [6], which makes it possible to have a single pump and also to simplify the hydraulic circuits but the rotation has been made completely dependent on the percussion.

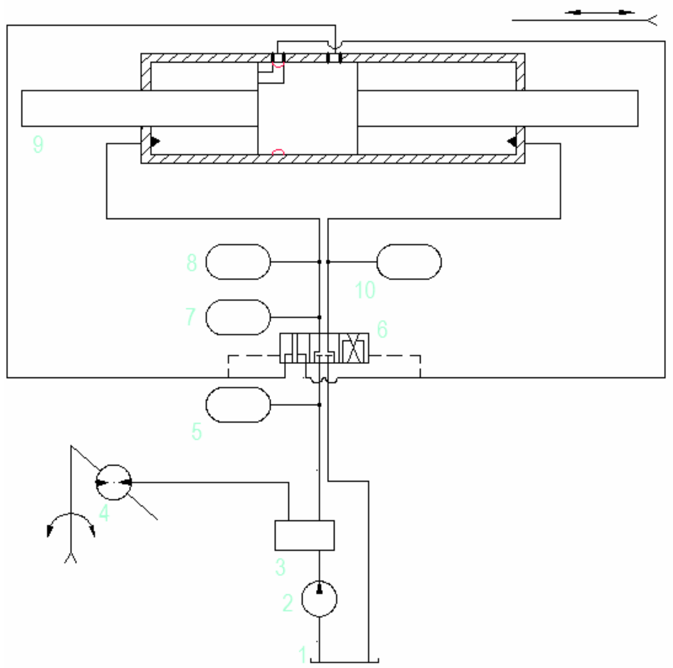


Fig. 3 Hydraulic scheme for [7] where: 1 – sump; 2 – positive displacement pump; 3 – control valve; 4 – hydraulic motor; 5, 7, 8, 10 – accumulators; 6 – control valve; 9 – hydraulic cylinder.

The patent [7] with the hydraulic scheme presented in figure 3, describes a hydraulic rotary percussive dril. The percussive mechanism can be used for a crusher, a ram or a percussive drill. The perforator comprises a body in which it is included a striker piston sliding in a cilinder, four hydraulic accumulators, a 6/3 distributor, a pin and a rotation mechanism. The piston has a cylindrical rod with two piston portion shaped as a series of coaxial cylinders of differing diameters. Thus, it is improved the centering in the cylinder and counteracted oblique load of the piston if such load should occur.

The circuit is supplied by a hydraulic pressure source 2. How the supplied fluid from the pump 2 acts the rotation mechanism and the percussion mechanism it is not described. Consequently, the work positions of the valve 3 are not revealed.

The hydraulic control valve 6 is utilized to assure turning and returning of the hydralic fluid to the cylinder's chambers. The command of the valve 6 is realized hydraulically by piston motion. Hereby, by uncovering a certain orifice during the work stroke the valve 6 is commuted to a position and by uncovering another orifice during the return stroke the valve 6 is commuted to the other work position. These two orifices realize the communication through two pipes of the piston's chambers and the valve 6. Fluid acts on the end surfaces of the sleeve and the control valve is moved to a position. One of this orifices represents in fact five branches that open in the cylinder 9. The pin can be set into various positions so as to block one or several of these branches. Consequently the percussion energy per blow can be varied.

The flow which is necessary to provide the reciprocatory movement of the piston varies periodically with the velocity of the piston and the position of the control valve 6. The periodical variation of the flow is compensated, by means of hydraulic fluid accumulators.

The accumulators used here are with spring-loaded piston and are gas pressure loaded accumulators. The type of these accumulators are used for large volume and large rate of flow and the force applied to the piston, thus storing energy, is created by the spring. The accumulator 5 is permanently connected to the supply pipe so as to receive the hydraulic fluid that is supplied when the valve 6 by commuting positions blocks the supply pipe for a short moment. When the piston reaches the speed that corresponds to the supplied flow, the accumulators 8 and 10 start to supply pressurized hydraulic fluid accordingly to the piston stroke and thus increases the speed of the piston. The distance of the piston travel can not be substantially increased because of the high braking pressure in the accumulator 7.

According to the patent [7], the accumulators 7 and 8 can be replaced by a two-stage accumulator.

## 3. Improvement in the construction of percussive drill

The reciprocating motion and impact of the piston in a hammer drill actuates significant oil pressure oscillation in hydraulic system. The peak pressure variation can double the mean value in some case. Usually accumulators are used to damp the pressure pulsation but they can not effectively solve the pressure oscillation and cavitations problems. The patent [8] implements floating pistons in hydraulic rock drills, or hydraulic hammer breakers, or fluid down-to-hole hammers to damp the pulsation, to prevent cavitations and to assist the forwarding and the returning movement of the striker piston. The floating pistons connect via ports the chambers from the hammer body and balance the pressure difference when pressure pulsation happens in the chambers. The device will be potential to increase the efficiency and impact power of the hammers.

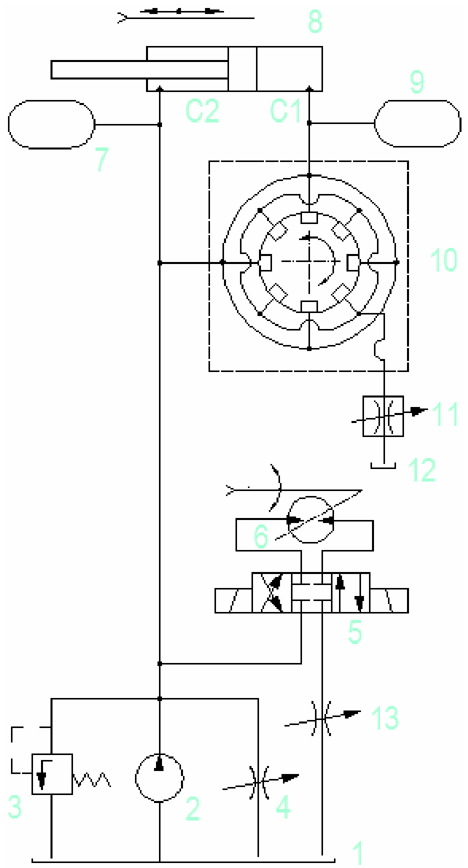

Fig. 4 Hydraulic scheme for [9] where: 1 – reservoir; 2 – hydraulic pump; 3 – pressure safety valve; 4, 13 – variable throttling valve; 5 – directional control valve; 6 – hydraulic motor; 7, 9 – hydraulic accumulator; 8 – hydraulic cylinder; 10 – hydraulic rotary valve; 11 – variable throttling valve; 12 – tank.

The hydraulic scheme from the figure 4 reveals, idem, a compact hydraulic rock drill structure with rotary and percussive mechanisms. The purpose of this perforator is to improve its performances by reducing at minimum the hydraulic parasite capacities – long communications between the hydraulic cylinder and its command element – and to continuously generate adjustable vibrations. As it can be seen in figure 4, frequency is limited just by the supplied fluid flow. The supply with hydraulic fluid provides the positive displacement pump 2. The linear hydraulic motor 8 is actuated by a hydraulic rotary valve 10. The impact piston has one rod on a side and on the other side has a bore realized in which the rotary actuator 10 is inserted. On the piston annular area eight longitudinal channels are maded. The disposition of these is so as to consequently realize by four channels the communications of the chamber C1 with the inlet pipe and with the tank.

During the activity of the rotary valve 10, chamber C2 is continuously supplied by the hydraulic source 2. Different piston areas induces different work pressures. The supply of chamber C2 simultaneously and the area difference cause the piston impact stroke. The motor that drives the rotary valve 10 is not shown in the figure 4, afterwards remaining to choose a hydraulic, electric or electrohydraulic drive motor. The accumulators 7 and 9 absorb the hydraulic shocks generated by the piston movements and thus increase the speed of the piston. The purpose of the relief valve 3 is to protect the system from pressure exceeding the design pressure by more that a fixed predetermined safe value. The spring operated valve 3 discharges the excess of the fluid automatically and is designed to re-close and prevent further flow of fluid after normal pressure conditions of service have been restored. The discharging velocity and also the piston velocity, in this case, can be adjusted by the variable throttling valve 4. The hydraulic distributor 5 is with four ways and three positions and controlled by solenoid. In the midstroke position there is no flow through the valve and consequently the rotary motor is not actuated. The other positions provide the rotary movements of the motor in both sides. The rotation is transmitted forward to the work tool or to the drill rod through couplings.

The percussive force depends on oil pressure and piston size. Impact energy depends on piston velocity which determined by rate of flow that supplies the hydraulic cylinder 8. Due to the exponential decrease of the amplitude of motion it is reduced the maximum fluid flow required to provide a vibratory movement caracterized by a constant acceleration. When using a pressure source with constant flow, the acceleration can be increased at higher frequencies by using a flow reserve from source 2. It explains the performance increase simultaneously with the increase of impact frequency.
The system presented in figure 4 reveals a solution for reducing inertial mass by minimizing hydraulic parasite capacities and by its compact construction. Double stroke frequency is limitted only by the supplied fluid flow and by the driving frequency of the hydraulic rotational distributor 10. Theoretically, the system develops superior energy density of hydraulic oil and allows the obtainig of superior performances under high dynamic conditions.
Definition of high frequency varies concordantly with rock type. As early as the mid070s, hydraulic rock drills worked in tunnelling at impact frequencies of between 100 and 200 Hz. The design principle made possible the successful use of those rock drills only in soft rock. Up to 1985, hydraulic rock drills used in hard rock succeeded to work with an impact frequency of 50 Hz. [10]

## 4. Conclusions

Hydrostatic transmissions, because of their important properties of transmitting the motion from the distance, provide easiest kinematic and structural scheme and they are easy to realize and diversify. High feed velocity can be obtained only by certainly knowing the bore and core drill technology. [3]

In any equipment, devices can be grouped in driving equipment – drill motors, drill aggregates – transmission, pulley, rotary and percussive devices, manipulation equipment, fluid circulation equipment. [3]

To understand the command of hydraulic rock drill it must figure out the rotation and percussion working, know elements that stop and run hydraulic cylinder, the element used to adjust the piston stroke, the element that determines the rock drill to operate at a predetermined pressure, predetermined frequency, predetermined velocity and energy. Regarding to rotary motion, to understand the command it must figure out which are the elements running and stopping the rotary movement, elements commanding rotation sens and speed.

The increase of penetration rate by increasing the frequency can be obtained by the improved drill. Impact frequency can go beyond the value 102 Hz (succeeded by some ATLAS COPCO drills). [11]

## REFERENCES

[1] I. Petrescu, “Foraje şi lucrări miniere”, Babeş-Bolyai University of Cluj-Napoca, 1981
[2] V. Rădulescu, “Acționări hidraulice şi pneumatice în foraj - extracție”, Technical Publishing House, Bucharest, 1984
[3] I. Costin, “Instalații pentru foraj de mică adâncime”, Technical Publishing House, Bucharest, 1972
[4] W.M. Barden, “Hydraulic hammer assembly having low vibration characteristics”, Patent No: 5944120, 1999
[5] R.J. Perraud, “Rotary percussion hydraulic drilling machine“, Patent Number(s): 4291771, 1981
[6] R. Montabert, “Rock drill“, Patent Number(s): US 3822752, 1974
[7] G.V.R. Romell, A.T. Eklof, “Hydraulic fluid actuated percussion tool“, Patent Number(s): US 3741072, 1973
[8] N. Dongmin “Floating piston _ an oil pressure oscillation damping device for rock drilling and breaking hammers“, Patent Number(s): US 2008/0230248 A1, 2008
[9] L. Vaida, C. Kozma, “Hydraulic mechanical vibration generator”, in course of being patented in Romania
[10] http://www.miningandconstruction.com/Portals/0/DynamicForms_Uploads/Technically%20speaking%20-%20The%20development%20of%20COP%203038%20%203-04_11-25-2009%201-16-04%20PM.pdf
[11] http://www.atlascopco.ro/rous/products/navigationbyproduct/index.aspx#1401245

**ISSN 1454 - 8003**
**Proceedings of 2011 International Salon of Hydraulics and Pneumatics - HERVEX**
*9 – 11 November, Calimanesti-Caciulata, Romania*

# HYDRAULIC ACTUATION UNITS

**Mihai AVRAM[1], Despina DUMINICĂ[2]**

[1] POLITEHNICA University of Bucharest, mavram02@yahoo.com

[2] despina_duminica@yahoo.com

***Abstract:*** *The paper presents the hardware structure of open loop and feedback hydraulic actuation units. An example of feedback positioning unit, developed by the authors at the Mechatronics Dept. of the "Politehnica" University of Bucharest, is also depicted.*

***Keywords****: hydraulic actuation units, open loop actuation unit, feedback actuation unit*

## 1. Introduction

A hydraulic actuation unit represents an assembly consisting of a hydraulic motor (linear, oscillating or rotary), one or more proportional equipments (in most cases, a flow control equipment) and an "electronic amplifier". From the construction point of view, the unit presents a compact structure. The proportional equipment is usually mounted on the fixed side of the motor and in many cases the mechanical structure integrates the control electronics.

The characteristic feature of hydraulic actuation units is that they are conceived as automated control units. Accordingly, their structure includes a number of sensors for various mechanical magnitudes (position, speed, pressure, temperature, flow). Such units are also known as "proportional hydraulic axes".

In most cases, the units have to achieve rigorous positioning of the load only in certain points of the working stroke, involving also a strict control of the load displacement speed. There are also situations when it is important to develop programmable forces / torques.

A distinction has to be made between the applications where the load has to be positioned in a finite number of points on the working stroke and the applications requiring positioning in every point of the stroke. In the first case, a discrete positioning unit is required, while in the second case it is necessary to use a continuous positioning unit. The following versions of hydraulic actuation units can be found in practical situations:

- open loop positioning units;
- units featuring automated control of load position;
- units featuring automated control of load speed;
- units featuring automated force/torque control.

## 2. Open loop positioning units

Figure 1 presents the principle scheme of an open loop actuation unit. Such a unit features, besides the hydraulic motor *MH*, a flow control proportional equipment *ERP* and the electronic control system *SCE*. The proportional equipment *ERP* modifies the flow rate according to the electric control signal received from the electronic control system *SCE*, whose role is to convert the input value $x_i$ in electric signals $i_1$ and $i_2$ needed in order to supply the converters included in the structure of the proportional hydraulic equipment.

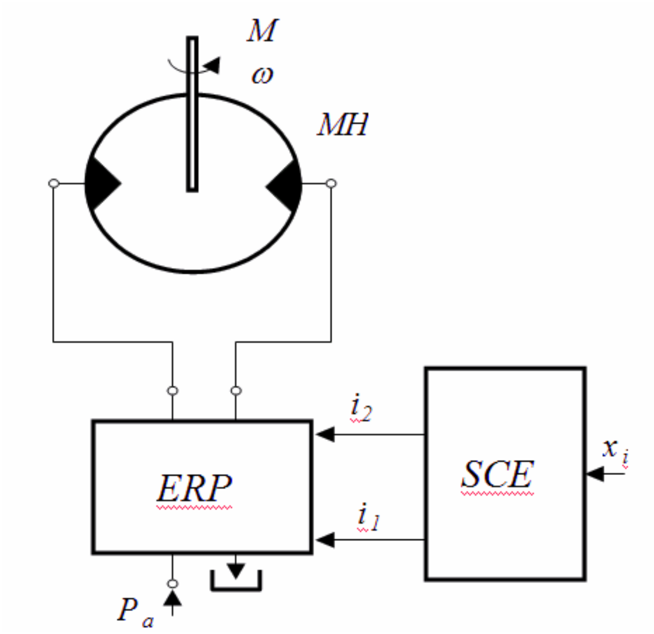


*Fig.1 Principle scheme of an open loop actuation unit*

A flow rate proportional to the input will be obtained, leading to a certain speed of the driven load. The stop in the desired point can be controlled in function of the time or of the run. At this moment, the electronic control system will set to zero its output signal and the valve will move to the preferred position (the closed center one).

The advantage of such units consists of the simple electronic control system and of the rigorous load positioning, under certain conditions. Such units present a simplified structure, without the position sensor. Their use is limited to the applications free of perturbations (load variation, feed pressure variation, variation of working fluid temperature, uncontrolled leakage etc.).

The accuracy of the system depends on various factors, mostly of the type of control used. There are two alternatives:

- units with time-dependent braking;
- units with stroke-dependent braking.

➢ *Case of the time-dependent braking*

It is supposed that the load has to be positioned in the point *A* (fig. 2). This means that the stop command has to be given sooner, in the position $y_{STOP}$. Knowing the working speed $\dot{y}_r$ and the deceleration *a*, the displacement of the mobile assembly of the motor from the moment of the STOP command to its stopping can be computed:

$$y_f = \dot{y}_r^2 / (2 \cdot a) \tag{1}$$

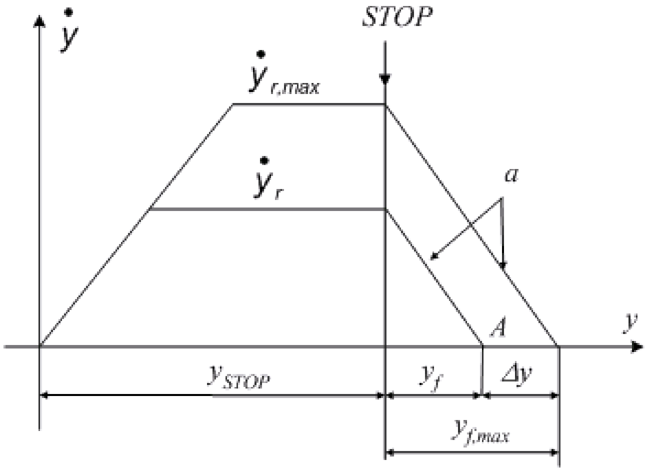


*Fig.2 Giving the STOP command*

Modifying the working speed causes the corresponding modification of $y_f$. The positioning error can be defined as follows:

$$\Delta y = \left[1 - \left(\frac{\dot{y}_r}{\dot{y}_{r,\max}}\right)^2\right] \cdot 100\% \qquad (2)$$

where $\dot{y}_{r,\max}$ represents the maximum speed that can be achieved during working regime.

If, for instance, a speed of $\dot{y}_r = 0.2\dot{y}_{r,\max}$ is imposed for the working regime, the positioning error will be: $\Delta y = 96\%$, value not accepted for a great number of applications. This problem is often forgotten when it is necessary to displace the load to a certain position with different speeds.

There are a number of ways for solving it:

a. two-step braking

In this case (fig. 3) the stop command is given in the point $y = y_{STOP,2}$. Because the stopping succeeds always with the same speed, positioning accuracy is very good.

b. variable slope braking

In this case the slope of the control signal in the braking stage is modified together with the speed, as shown in figure 4. The braking duration unfortunately increases in this case. On the other hand the precise control of the ramp must be mastered, reason for which the method is less used.

c. variable braking start time

In this case the start moment of the braking depends on the value of the speed in functioning, as shown in figure 5.

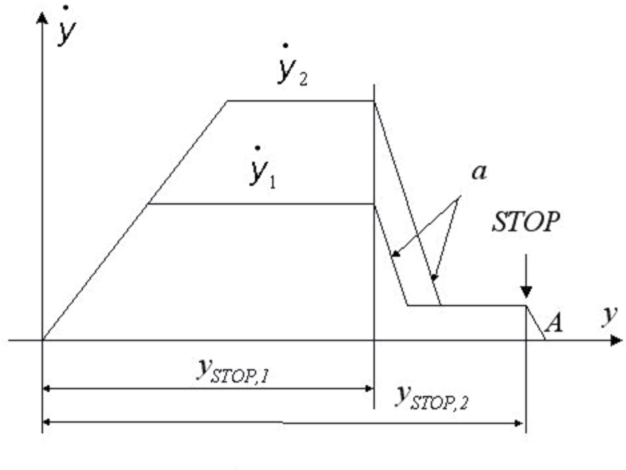


*Fig.3 Two-step braking*

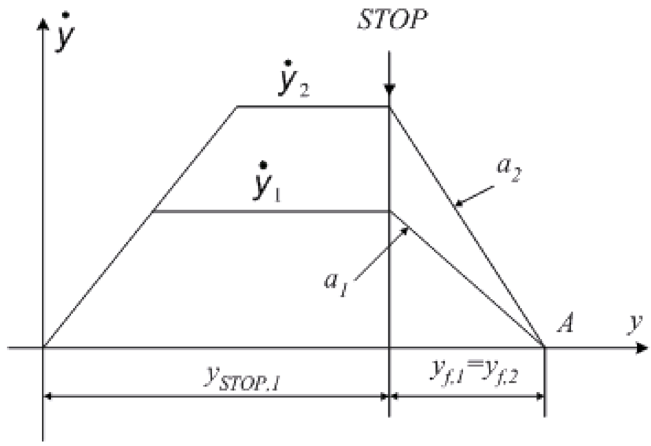


*Fig.4 Variable slope braking*

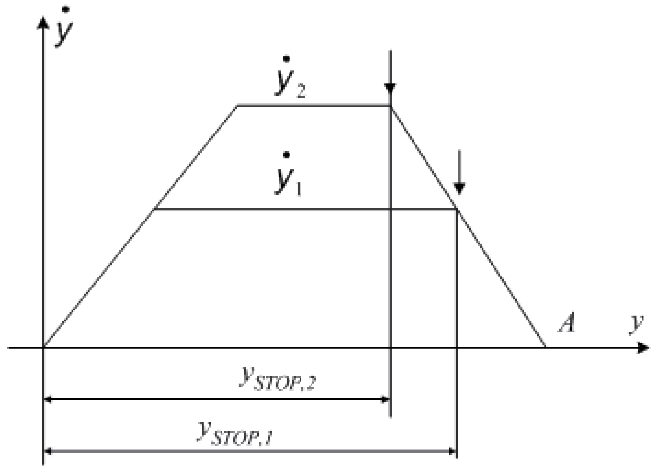


*Fig.5 Variable braking start time*

- *Case of the stroke dependent braking*

This case is shown in figure 6. The braking start time is in function of the desired stroke. This way, the braking is independent of the slope of the control signal in the deceleration stage.

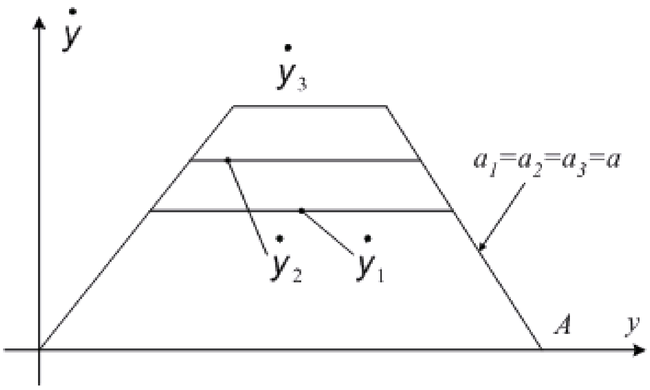


*Fig.6 Stroke dependent braking*

The method requires including an “analogue initiator” in the electric control system. This module outputs a tension dependent of the distance to a metal part (cam *C*, as shown in figure 7). Accordingly, as the cam *C* closes to the “initiator” *I*, the output signal progressively decreases together with the distance $s_x$, tending to 0V when $s_x = s_0$. The output signal is applied to an “amplifier” conceived especially for such an application, as shown in figure 8.

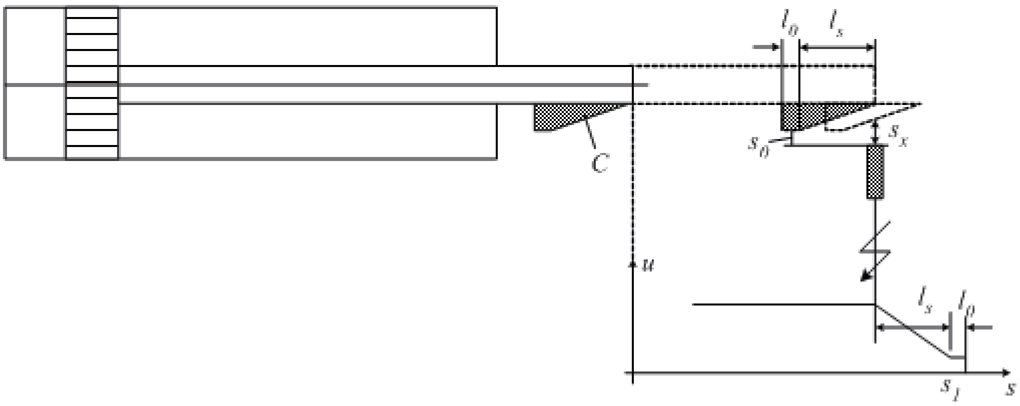


*Fig.7 Including an analogue initiator in the electric control system*

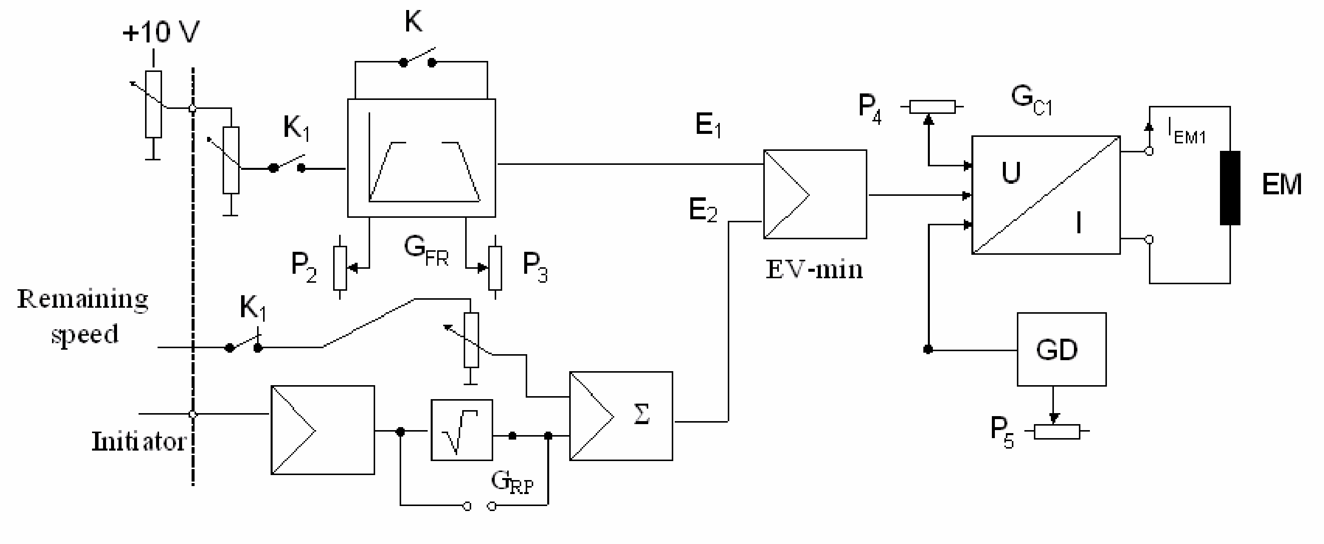


*Fig.8 Principle scheme of the electronic control system*

### 3. Feedback positioning units

Considering the loop nature, these units can be classified as mechanical position feedback units or electrical position feedback units.

The principle scheme of an electrical position feedback unit is presented in figure 9.

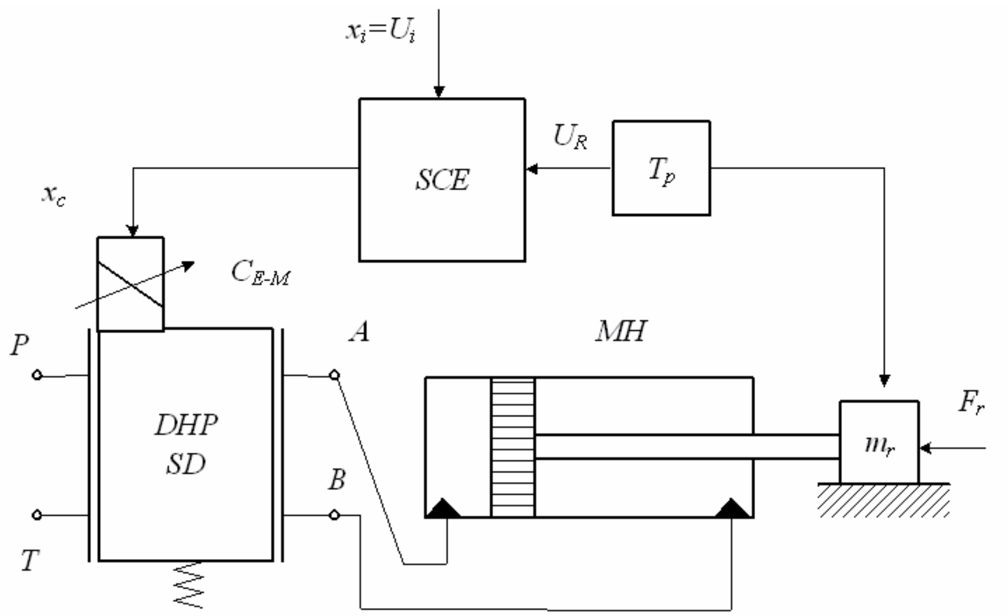


*Fig.9 Principle scheme of an electrical position feedback unit*

**ISSN 1454 - 8003**
**Proceedings of 2011 International Salon of Hydraulics and Pneumatics - HERVEX**
*9 – 11 November, Calimanesti-Caciulata, Romania*

A proportional direction control valve *DHP* or a servo valve *SD* allows the control of the supply flow rate and of the corresponding discharge flow rate in the two chambers of the hydraulic linear motor *MH*. The two flow rates depend on the control signal $x_c$. The displacement of the mobile unit together with the driven load appears if the working pressures in the two chambers of the motor reach the required values. A position sensor *Tp* determines the load position. The electronic control system *SCE* compares its signal $U_R$ to the programmed signal $U_i$. Control signal $x_c$ becomes zero when the actual and the programmed displacement coincide, leading to the cancellation of the control flow in the motor chambers. The distribution equipment must have very good static and dynamic performances. The presented system uses a single feedback or at the most two (when a supplementary local feedback is used at the $C_{E\text{-}M}$ converter level).

Figure 10 presents the structure of such a positioning unit. Figure 11 presents a picture of the unit developed in the frame of the Laboratory of Robotics, Actuation and Automated Positioning Systems from the Department of Mechatronics and Precision Mechanics, POLITEHNICA University of Bucharest.

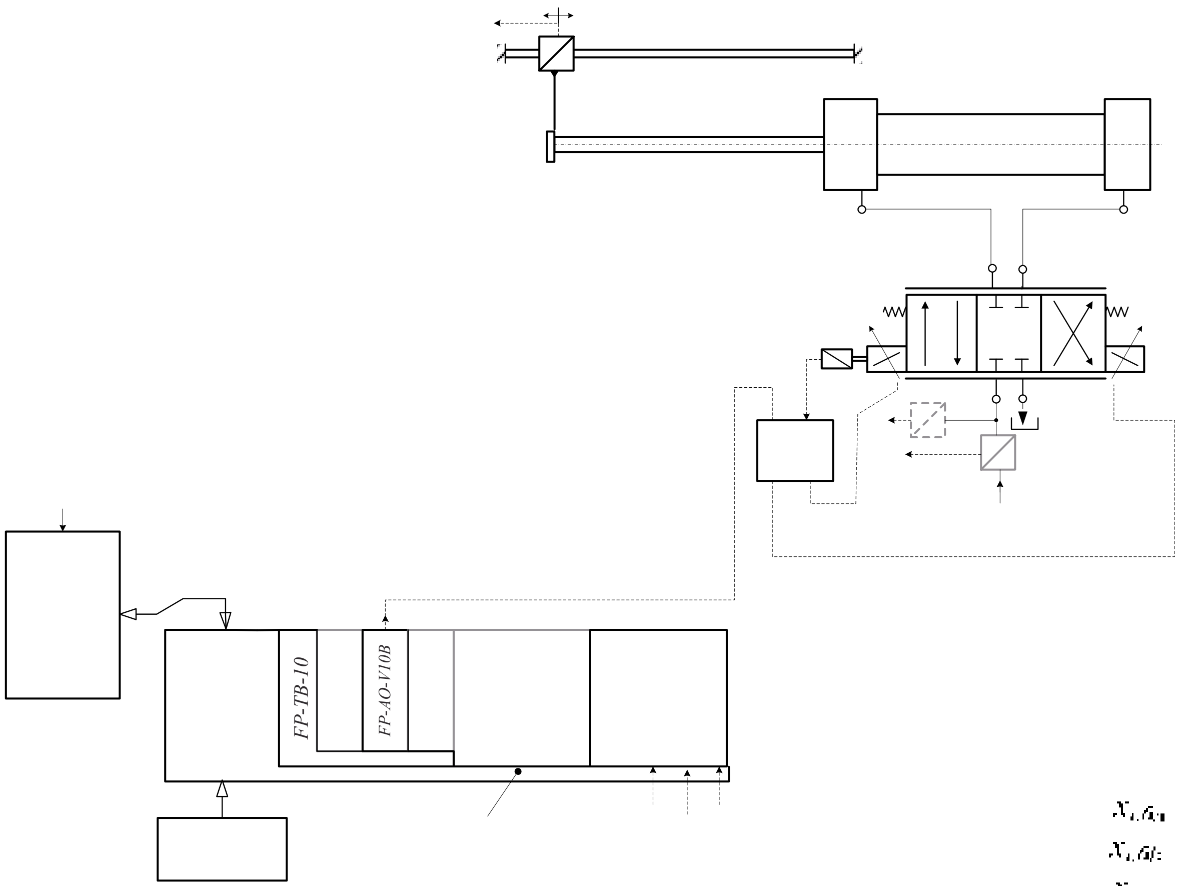


*Fig.10 Structure of an electrical position feedback unit*

The following equipments can be identified:

- proportional direction control valve *DHP*;
- electronic amplifier $AE_{DHP}$ that serves the proportional direction control valve ;

- linear hydraulic motor $MH_{RE}$;
- position sensor $T_{poz,1}$;
- FieldPoint I/O modular system *FP* that connects the personal computer with the electronic amplifier and the position sensor;
- direct current supply unit that feeds the FieldPoint system;
- personal computer *PC*.

*Fig.11 Electrical position feedback unit*

Using a modular I/O system in the structure of the positioning unit offers a wide range of advantages, the most important being the following ones:

- simplified acquisition and control system;
- connection of the transducers to the PC via an industrial network, in this case RS-232;
- saving in signal wiring, by replacing long signal wires with a single low-cost network cable;
- easy functioning and maintenance;
- easy programming;
- adjustable configuration in order to comply with the requirements of the application;
- possibility of later mounting of other transducers using I/O modules;
- reduced installation duration;

- avoidance of noise corruption problems that occur when using long-distance analog signal wiring;
- rugged modular solution, designed to operate in the harsh environments of industrial applications;
- very good performance.

The easy installation, configuration and maintenance of FieldPoint systems, as well as the check of their correct functioning requires the use of FieldPoint Explorer software, developed by National Instruments in order to work together with the FieldPoint hardware.

## 4. Conclusions

The positioning units used in applications that require accurate actuation (industrial robots, CNC, shooting devices) are automated control units able to achieve the rigorous positioning of the load. The paper performs a comparative analysis of open loop positioning units and feedback positioning units, as well as the hardware structure of an electrical position feedback unit. The main advantage of the proposed solution consists of the possibility of later mounting of other sensors: for speed, flow, pressure etc.

The information gathered from the system allows the software compensation of positioning errors. It is therefore possible to compare the performances obtained by a classical structure positioning unit (consisting of proportional direction control valve, hydraulic motor, position sensor, electronic control system) and a mechatronic unit. In the second case, supplementary sensors appear, as well as dedicated correction algorithms.

## REFERENCES

[1] M. Avram, D. Duminică, C. Udrea, V. Gheorghe, "Hydronics and Pneutronics – Applications" (in Romanian), Universitary Publishing House, Bucharest, Romania, 2008.
[2] M. Avram, “Hydraulic and Pneumatic Actuation – Classical and Mechatronic Equipment and Systems” (in Romanian), Universitary Publishing House, Bucharest, Romania, 2005.
[3] M. Avram, N. Alexandrescu, D. Duminică, Şt. Țuineag, „FieldPoint Modular I/O System Part I: General Presentation” (in Romanian), Proc. 11th Annu. Conf. on Hydraulics HERVEX, ISSN 1454-8003, Călimăneşti, Romania, 2003, pp. 53-58.

**ISSN 1454 - 8003**
**Proceedings of 2011 International Salon of Hydraulics and Pneumatics - HERVEX**
*9 – 11 November, Calimanesti-Caciulata, Romania*

# HYDRAULIC DRIVES FOR ASPHALT POURING EQUIPMENT

Victor Balasoiu, Ilare Bordeasu

Timisoara "Politehnica" University, Hydraulic Machinery Department,
Bulev Mihai Viteazul, No. 1, 300222, Timisoara, Romania
Adresa e-mail: balasoiu@mec.upt.ro; balasoiu89@yahoo.com;ilarica@mec.upt.ro
Telefon: 004.0256.403680; 004.0356426950; 0726760207; Fax 004.0256.403682

**Abstract:** The present paper is concerned with the problems occurring in the design and manufacturing of the mobile equipments destined for asphalt pouring. The continuous development of the civil engineering works implies a new conception of the equipments used in this branch of industrial activity. That is why, the range of the devices used in civil engineering works utilizing hydraulic actuators became in our days very large, this category of equipments becoming one of the principal users of hydraulic driving systems. After presenting some principles aspects of driving equipments for mobile devices there are presented various types of hydrostatic actuators used in mobile equipments. Analyzing the specific design problems, we insisted upon the computation of the hydraulic diagram putting in evidence some examples of hydrostatic traction in close circuit with integral hydrostatic transformation.
The main advantages of the hydraulic driving systems are: the stability of the moving velocity, rapid adjustment or inversion of the movement and the possibility to standardize both the elements and the whole system. These advantages determined the rapid extension of the hydraulic drive systems in the civil engineering plants.

**Key words:** Hydraulic driving systems, Hydrostatic actuator, Civil engineering plant, Asphalt pouring equipments.

## 1. Introduction

The continuous development of the civil engineering works implies a new conception of the equipments used in this branch of industrial activity. The introduction and the development of hydraulic actuators for the majority of the civil engineering plants, represented a qualitative jump for the improvement of these devices. The introduction of hydraulic driving for the discussed equipments must take into consideration the following characteristics:

- the dimensions and the weight must be cut to a minimum to find room in the limited dimensions of the vehicle and to maintain a reduced fuel consumption;
- the driving possibilities for pump (or pumps) are limited;
- the hydraulic installation is subjected to severe conditions from the ergonomic and maneuvering points of view as a result of both the reduced room and the multiple tasks of the driver, most of them requiring great manual dexterity;
- between the pumping, distribution and adjusting elements and those for execution, often exist relative movements and that circumstance implies the use of flexible pipes;
- the access for the repair work and correct maintenance are sometimes inauspicious and in the same time the equipment is running in an unfavorable environment (dust, mud, rain and great temperature variations); supplementary, sometime the personnel does not have adequate qualifications for the maintenance of hydraulic equipments.

Despite of those adversities, in the building of the mobile equipments there are in use a great number of hydraulic devices from both points of view as nomenclature and as manufacturing volume.

**2 The hydraulic transmission in the manufacturing of the equipments for asphalt pouring**

The object of the driving system is the hydraulic transmission, which consist invariably from two basic components (fig. 1): the volumetric pump 1, which transform the mechanical energy taken from the driver 2, in hydraulic energy, preponderantly potential energy (pressure) and the hydrostatic motor, which reconvert the hydraulic energy into a mechanical one but with modified parameters; this energy that is afterwards transmitted to the working mechanism 4.
Although the driving systems are con-fronted with a great variety of conditions (various technological processes, different environments and stresses) there are a lot of unique features the most important being:

- the system running is based on the same power processes;

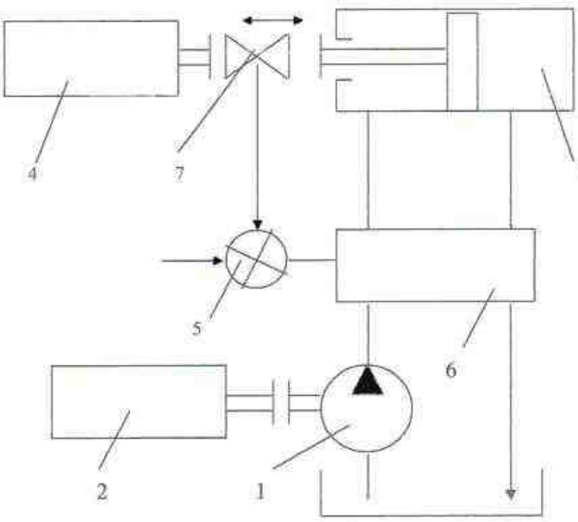

Fig. 1. The diagram of a hydraulic driving system

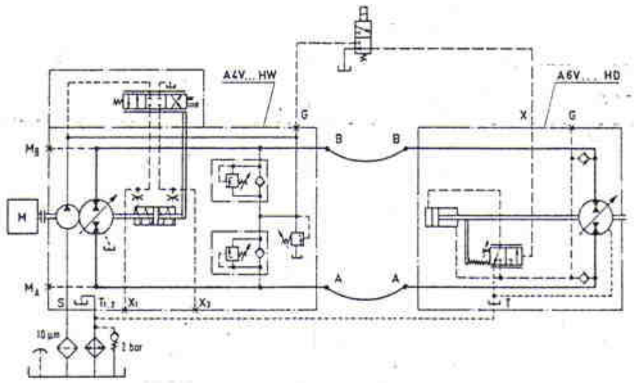

Fig. 2. The principle hydraulic diagram in close circuit

- the flow between the pump and the motor is the same; but from this point of view this systems can be divided into two great groups: with open circuit (for which the liquid is under the atmospheric pressure at the level of the oil tank) and with close circuit (for which the energy level is exchanged between the pump and the motor in a circuit without contact to the atmosphere).
For the following discussions the chosen hydraulic diagram is presented in fig. 2.
The transmission is equipped with a pump A4VG having axial pistons and inclined disks as well as a motor A6V with axial pistons and an inclined block both produced by the German business house REXROTH. The system has a mixed transmission, the primary adjustment being continuous through changing the inclination of the disk and the secondary adjustment being realized in steps, through tipping the pistons block, in two positions.
The primary adjustment is localized at the primary unit. Simply by changing the geometric volume of the primary unit (the pump) and maintaining the other parameters, there are obtained various working regimes. The secondary adjustment is localized at the level of the rotating motor and is realized by modifying the pressure. Different working positions of the units with axial pistons, respectively the modifications their geometric volumes are obtained with the help of hydraulic *servo-flow* control valves. The protection of the mechanical elements is assured through the pressure valves included in the pump. The principal pump adjustment cylinder, in the absence of the driving pressure, maintain the pump disk –through back springs- at the angle zero, so that the pump does not deliver liquid.

In the moment of distributor commutation the cylinder tilt the disk in the commanded direction, determining a value different from zero of the geometric volume, and the pump deliver oil in the commanded direction. The motor, in the supplying moment has the maximum geometric volume and begin to rotate with the normal speed.
The presented drive system can operate both as motor and brake. For a system in close circuit the braking operation is realized in counter-flow. That means a superposition of two flows:

-the flow given by the motor, running as pump, from the beginning of the braking;

-the flow absorbed or delivered by the pump working either as motor or pump.

It is to observe three running regimes of the pump:

a. Running as a motor and maintaining the delivery direction, permitting the adjustment of the geometric volume from the maximum value to zero. The reverse flow can be considered as negative and assures a moderate braking similarly to those of the motor brake for common motor vehicle.

b. The inactive regime, with “zero” reverse flow (zero geometric volume). The pump does not deliver liquid and assure an abrupt brake closing the flow delivered by the motor, and provoking the opening of the pressure valve for the branch under pressure.

**c. The pumping regime, with changing the delivery direction and permitting the adjustment of the geometric regime from zero to the maximum value. The counter flow is considered “positive” and assures a violent brake provoking overpressures controlled by the shock valves. 3. Diagram of hydraulic traction, in close circuit, with integral hydrostatic transformations. Typical examples.**

*3.1. Diagram with manual adjustment of the velocity, without automatic limitation of the consumed (fig.3)*

The system is characterized through the manual command of the pump discharge adjustment. The command can be executed both direct, as is presented in fig. 3a and with hydraulic assistance as in fig. 3b. The moving direction of the vehicle is achieved directly by the pump adjustment device. The maximum level of the consumed power is not supervised by the hydraulic system at overloads, so there is possible the sudden shutdown of the thermal motor.

*3.2. The diagram with manual adjustment of the velocity and with automatic limitation of the consumed power, through the “sliding” under load of thermal motor (fig.4*)

In such a diagram the moving direction of the vehicle is selected with the directional control valve 4, with an electric command. The adjustment of the movement velocity is done by acting manual (or with a pedal) the device 3. The limitation of the consumed power till to the value momentary developed by the thermal motor is realized in this way: with the increase of the traction load, the rotation speed of the motor 1 decreases, producing the decrease of the command pump 2 discharge; this reduction has as effect –when the valve of the device 3 is maintained in the same position- the reduction of the command pressure of the pump adjusting device and implicitly the decrease of the main pump discharge.

*3.3. The diagram with manual adjustment of the velocity and with automatic limitation of the consumed power, through “sliding” under load of thermal motor (fig.5).*

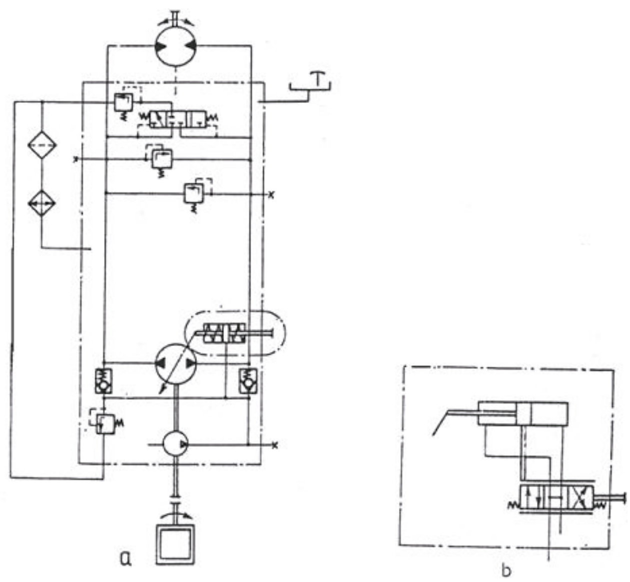


Fig. 3

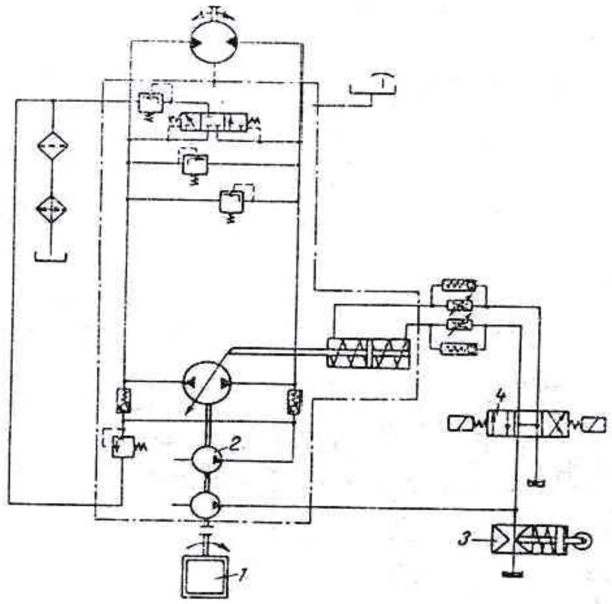


Fig. 4

For the selection of the movement direction, both the automatic adjustment of the velocity and the limitation of the consumed power is realized through devices similarly to those in fig. 4. From the presented device with valve the system in fig. 5a differs only through the elements for the manual adjustment of the velocity. The system in fig. 5.b is provided with the same device but having hydraulic piston, which annihilate the command pressure, and in the same time the flow capacity of the main pump, in the moments when the traction load exceeds the values established by the spring adjustment.

The system in fig.5.c annihilate the advance movement through the increase of the load upon an auxiliary device, hydraulic actuated by a supplementary pump driven by same thermal motor.

*3.4. The diagram with manual adjustment of the velocity and the automatic limitation of the consumed power through a power valve (fig.6).*

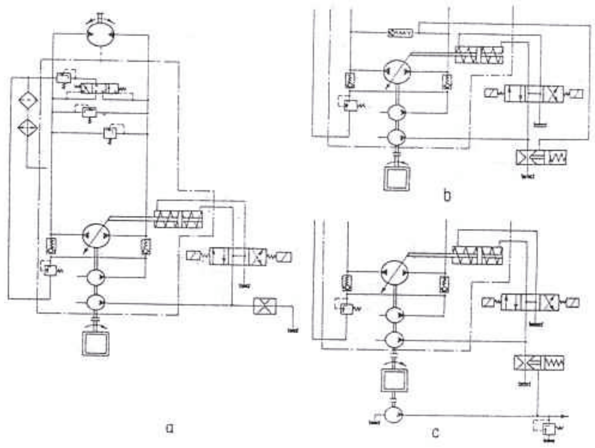


Fig.5

The tilting angle, respective the main pump 2 discharge is controlled by three variable elements: the rotational speed "n" of the thermal motor 1, automatically adjusted by the device 6; the working pressure "p" acting upon the surface "s" of the power limiting device 4 and the command pressure "$p_c$" acting upon the surface "S" of the command device 5.

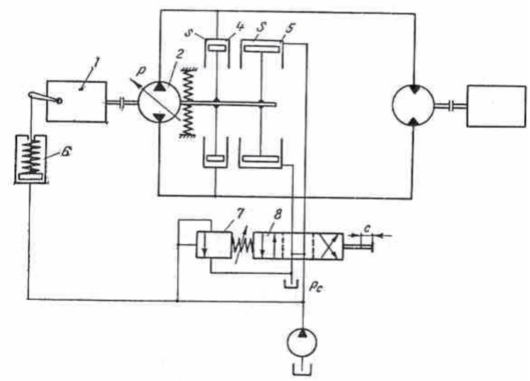

Fig. 6

As a consequence the flow capacity “Q” varies with the mentioned elements:

$$Q=K_1n(p_sS-p_S) \qquad (1.1)$$

$$P=K_2Qp=K_1K_2n(p_cS-p_S) \qquad (1.2)$$

From the presented relations it can be seen that -in principle- the consumed power “P” can be maintained constant, for a constant command pressure „$p_c$”. This pressure, which selects the maximum advance velocity, is manually commanded with the help of the flow control valve 8. At the neutral position of the flow control valve $p_c$=0 the vehicle is at rest. With the increase of the stroke “c” of the spool valve 8, in one or the other direction, increases also the tension in the spring, of the valve 7, respective the command pressure „$p_c$” and implicit the flow capacity „Q”.

*3.5. Diagram with manual adjustment of the velocity, automatic limitation of the consumed power through the power valve and with mechanic command of the thermal motor rotational speed (fig.7)*

The command section, which creates the command pressure “$p_c$”, is identical to that of the precedent case. Because the pump adjusting device needs an increased pressure, it is provided the circuit „$p_a$”. The command applied upon the actuating flow control valve 1 is simultaneously transmitted, on a mechanic way, at the hand lever or the pedal for the acceleration of the thermal motor.

The limitation of the consumed power is realized with the help of the power valve 3. When the pressure „p” on the working circuit overcame the value anterior adjusted with the spring of the valve 3 (respective the value that coupled at the pump maximum flow capacity attains the level of the installed power) the valve 3 opens, less or more, provoking the decrease of the command pressure „$p_c$” and simultaneously the valve 3 opens more or less provoking the decrease of the command pressure, the decrease of the flow capacity and in this way the vehicle velocity.

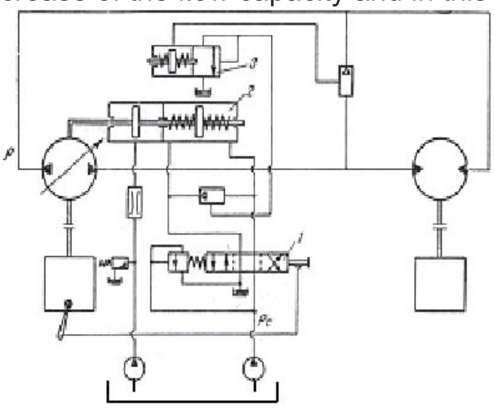

Fig. 7

*3.6. Diagram with manual adjustment of the velocity, automatic limitation of the consumed power through the power valve and with hydraulic command of the thermal motor rotational speed (fig.8)*

The diagram is identical with the precedent one, with a small difference, namely the device for the motor acceleration is hydraulic actuated with the help of a flow control valve 2, supplementary to those for the command of the principal pump flow capacity (flow control valve 1).

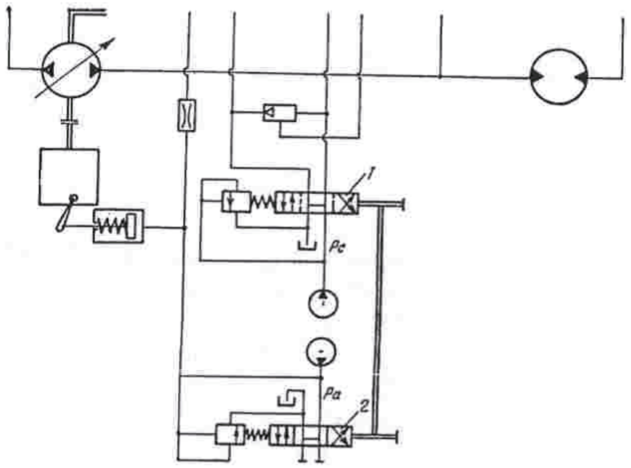


Fig. 8

It is to be mentioned that the circuit for the command of acceleration cannot be the same with those for „$p_c$" because an overloading „$p_c$" will be reduced automatically as a result of the intervention of the power valve so the rotation velocity will be also simultaneously reduced.

## 4. Conclusions

1. The majority of the hydrostatic traction systems included in the working devices are realized in close circuit, from strategic reasons, specific to the building of mobile devices (reduced weights and volumes).

2. Introducing hydraulic adjustable pumps and motors in the diagram (fig.2) has favorable effects concerning the elastic adaptation of the traction characteristics (force and velocity) to the terrain conditions, the thermal motor (frequently of Diesel type) remaining at a stable running point.

3. Supplementary, the system presented in fig.2 offer the possibility of continuous adjustment of the motor regime with the help of a servo commanded pump.

4. In accordance with the considered equipment, it is possible to adopt one of the presented transmission or a combination of two or more variants (fig.3... 8).

5. Pursuing the equipment evolution it can be concluded that the mechanical transmission is gradually replaced by the hydraulic transmissions, because the later present the following advantages:

- Continuous adjustment without shocks, for the whole range of rotational velocities and torques.
- High torque at the beginning of motion.
- Safe working at normal parameters to positive and negative slopes.
- Simple handling without the necessity of great efforts from the driver.
- Great efficiency and reliability.
- Easy maintenance.

In order to assure the basic functions, the presented hydraulic systems, besides the fundamental elements, are provided with some supplementary devices necessary for specific adjustments.

As a general conclusion it must be said that a severe procedure in the use of the hydraulic transmission devices must be compulsory respected.

**Bibliografie**

[1] Bălăşoiu V., - Echipamente hidraulice de actionare, fundamente teoretice, fiabilitate, Editura Eurostampa, Timisoara, 2001.
[2] Bălăşoiu V., Cristian I., Bordeaşu Il – Echipamente şi sisteme hidraulice de acționare şi utomatizare, Maşini Volumice, Vol I, Editura Orizonturi Universitare Timişoara, 2007
[3]Bălăşoiu V., Cristian I., Bordeaşu Il – Echipamente şi sisteme hidraulice de acționare şi automatizare, Aparatura hidraulica, Vol II, Editura Orizonturi Universitare Timişoara, 2008,
[4]Bălăşoiu V.,- Cercetari teoretice si experimentale asupra sistemelor electrohidraulice tip servovalva-cilindru-sarcina, pentru module de roboti industriali, Teza de doctorat, Institutul Politehnic Timisoara, 1987.
[5] Călăraşu D., - Reglarea secundara a sistemelor de actionare hidrostatica in regim de presiune cvasiconstanta, Editura MEDIATECH, 1999,
[6] Cristian I., - Servosisteme electrohidraulice analogice, Editura Universitatii Transilvania, Brasov, 2003,
[7] Esnault Fr., Beneteau P.,- Hydrostatique 1, Hydrostatique, Transmision de puissance, Cours et applications, Ed. Ellipses, 1997, Paris,
[8] Murvay P. – Cercetari privind comportarea transmisiilor hidrostatice pentru sistemele de propulsie in sistem de franare, Teza de doctorat, Universitatea Politehnica din Timisoara, 1998
[9] Oprean A. - Actionari si automatizari hidraulice, Sisteme mecano - pneumo - electrohidraulice, Editura Tehnica, Bucuresti1 1983.
[10] Pătruț P., Nicolae I., - Actionari hidraulice si automatizari, Teorie, aparate, sisteme automate si aplicatii industriale, Editura “Nausicaa” Bucuresti, 1998.
[11] Vasiliu N., Vasiliu Dana., - Actionari hidraulice si pneumatice, Vol. 1, Editura Tehnica, Bucuresti, 2005. ***
[12]- Hydraulik Komponent.,MANNESMANN REXROTH, Lohr am Main, 1989.
[13] *** - Components for Hydraulic Proportional and Servo Systems Electronics and accessories., MANNESMANN REXROTH. Lohr am Main. 1984.
[14] Vasiliu N., Catana Il., - Transmisii hidraulice si electrohidraulice, Reglarea masinilor hidraulice volumice, Vol II, Editura Tehnica, Bucuresti. 1997.
[15] *** - Hydraulik Trainer , MANNESMAN REXROTH, Lohr am Main, 1986.
[16] *** - Der Hydraulik Trainer, Band 2, Proportional -und Servoventil Technik, Mannesmann, REXROTH, GmbH, 1986

**ISSN 1454 - 8003**
**Proceedings of 2011 International Salon of Hydraulics and Pneumatics - HERVEX**
*9 – 11 November, Calimanesti-Caciulata, Romania*

# IMPROVING QUALITY OF LIFE THE ATHLETE AND PEOPLE WITH LIMBS AMPUTATED. SYSTEM SENSORY UPPER LIMB PROSTHESES

Jean FIRICĂ
University of Craiova, firicajean@yahoo.com

***Abstract***
*The production of prostheses we need sensory and actuator systems similar to human anatomy. Characteristics have important influences on the aesthetics of microprocessors computing products. Digital techniques are commonly used in signal processing. Pressure sensors of transmit sensitive skin objects. Microprocessor signals contribute to hand movements. It exists in the system of alternative prostheses and implant electrode.*

***Keywords:*** *processor, sensors, prosthetic, actuators, systems*

In manufacture of prostheses are necessary sensory and actuator systems integration and faithful reproduction of human anatomical systems. These sensors form a first interface between the physical and system devices, and the second interface includes actuators that convert electrical signals into physical phenomena. Current characteristics of microprocessors have significant impact on computational aesthetics localized products. The latest generations of products that use microprocessors to control functionality is becoming more extensive and is capable of performing. Most processors operate on voltage input for receiving information. In addition to these features of microprocessors we can use enough sensors in various practical applications. Sensors have the advantage that the output electrical signal has the same properties as electrical devices and convert signals or stimuli into electrical output signals. For active sensors, we need an external source of excitation, and those liabilities shall require such information. Classification of sensors is achieved by physical property measurement, and among the best known of them mention the force, temperature, pressure, motion, etc.

Sensors that measure different properties can have the same type of electrical signal output. Thermal detector resistive strain sensor as is variable resistance circuits are located in similar points. Many active and passive sensors have low output, minor changes in voltage, current or resistance and need a proper conditioning before analogue or digital signal changes. For this reason, we have a range of circuits called signal conditioning circuits. Amplification, galvanic isolation, and impedance level transformation, filtering and conditioning are important functions of the applied signal possible. Circuit depends on the nature and performance of electric signal without keeping in mind the form of conditioning. Apply the sensor to output parameters (sensitivity, threshold voltage, impedance, power, dispersion, while constantly running) make the difference between substandard and successful application of the device, especially when we need high accuracy and low level measurements. When the sensor output signal we recorded stimuli nonlinear analogue linearization techniques interfere with their correct measurements. With a powerful converter software and will achieve more efficient and accurate linearization stimuli and will eliminate manual calibration. At present, the output signal processing and sensor data collection, process control and measurement shall be carried out with new digital techniques. When using A / D conversion and microcontroller programmability on the sensor will use one or more sensors with auto calibration and applications we use 8-bit microcontrollers for good speed and power. Basics of intelligent sensors are integrated circuits, multiplexers performance converters, memories, microcontrollers etc. They are intelligent sensory data acquisition systems on a single chip. The quantitative measurements are often used sensors and the detection using qualitative measurements, which involves the selection of sensor and determine the application. Because the sensors have different measurements, the quantitative determination we determine what we intend to measure and sensor operating environment. Many times, the sizes measuring system records errors due to environmental influence. Sometimes, the response to external factors is higher than the ground measurements. The application process is very important to evaluate external factors and to estimate their impact on measurement systems. In addition to temperature, pressure and vibration, external factors include the type of mounting the sensor, electromagnetic effects, changing environmental parameters. The choice of sensor application will take account of possible errors due to high registration and rapid changes in temperature and measurement uncertainties. With measurements, we follow to obtain a minimum of uncertainty, we analyze the use of measurements, we take account of changes in uncertainty and we'll see if the signal received from the sensors is covered by noise during signal recording. Modern systems of records obtained more accurate data than the sensor used to measure quantities. But as these systems work only on the basis of compatible sensors and a calibrated system. We propose that high-performance sensors to meet some of the following characteristics: have a good dynamic transfer function and a good resolution, sensitivity, accuracy etc. The sensors have limited time to time changes in physical signal and a decay time which is the time of the gradual change of physical output signal to the baseline and opposite these times correspond to high frequencies and low cut. Physical sensor electronic component has an important role in overall device performance and may limit the applicability and scope.

Continuous pressure sensor matrix is studied to give a sense equivalent inorganic sensory systems of the skin and pressure sensitivity. The matrix is made of organic or plastic material applied to an area flexible transistors and whereby the dense matrix can be achieved on large areas. It was developed a prototype sensor that working leather and wrapped in a very small diameter and is composed of a matrix of 32x32 film with organic sensors and a density of 16 sensors per square centimetres, although we have nearly 1500 fingertip sensor per square centimetres. The sensors the rubber of pressure prototype of a layer containing graphite particles that directs electricity and electrical resistance changes at different pressures. Because organic transistors are large and slow, are increasingly using silicon transistors in electronic components. We believe that as this type of leather factory and used in robotics and prosthetics, to produce and organic transistors. As we know, prosthetic systems have mechanisms for sensory feedback loop physiological and movement joints shall be based on relevant signals and systems using mioelectrice intercepted. Any motor activity develops mioelectrice or exciter signals. Horny muscle motor actions will produce voltage changes associated with the nervous system and are intercepted by sensors on muscle length. The signals are read and verify the microprocessor calculates the signal strength and articulation with the upper limb prosthetic systems in the wrist and elbow. Prototypes that take environmental information exchange could influence the prosthesis and can transmit the body by stimulating methods. Stimulus leads prosthetic system interpreted movement and muscle contraction strength amputation change to achieve the desired end. Mioelectric signal potential drive or motor are electric impulse that causes muscle contractions of the human body, especially in skeletal muscle because it controls voluntary movements. Signal frequency range up to 300 Hz mioelectrice and tension between 10 μV - 1 mV. To detect signals mioelectrice, introducing electrodes under the skin. Positioning the two electrodes depends on the voltage and the third is inserted in the neutral zone whose signal is used to cancel interference. Differential amplifier voltage processes and offer a higher voltage and current good enough to control electromechanical or electronic devices. Signal will cause the operation of a computer and use the voluntary movements of small amplitude. The user will have to arm mioelctric produce a signal strong EMG recording, amplification and separation of muscle contractions. By separating the contraction of a muscle contraction and relaxation understand the antagonist muscle. At a simultaneous contraction of the muscles controller receives signals on and off while driving. Using electrodes with high selectivity and smart chips can make a difference in proportion. These devices have satisfactory performance, but the complexity of use, reliability, control, and aesthetics and allow users to determine their independence the new prosthesis. These implants have electrodes implanted alternative and winding around a nerve or muscle to read the information transmitted by radio frequency or other techniques. Spatial filtering technologies are based on all signs point detected by electrodes placed evenly. Using modern filtration through concentric circular electrodes selectively transmit a response. Signal detection is based on the total signal detected by different monopolar electrodes and concentric system has a non-periodic transfer function and unchanged for rotation. The analysis of recorded signals we see a circular electrodes increased spatial selectivity than conventional systems. It was confirmed and noted that the system consists of a single concentric ring and a punctual electrode has a high capacity compared to the matrix consists of nine electrodes. Concentric systems have the advantage of simple procedures and tracking system is due to insensitivity to muscle fibre orientation, increased spatial selectivity and low complexity of electronic circuit dependent.

**ISSN 1454 - 8003**
**Proceedings of 2011 International Salon of Hydraulics and Pneumatics - HERVEX**
*9 – 11 November, Calimanesti-Caciulata, Romania*

Annexes :

| | |
|---|---|
| <br>The forearm prosthesis with passive function mioelectric pro with passive supination. | <br>The ante-arm prosthesis functional passive. |
| <br>The ante-arm prosthesis driven by the cable. | <br>The ante-arm prosthesis functional mioelctric with pro-active supination. |
| <br>The ante-arm prosthesis functional simple. | 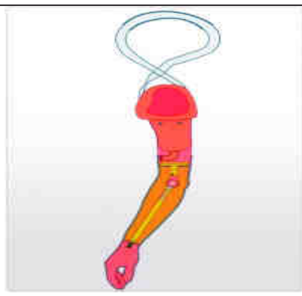<br>The prosthetic arm powered and passive functional. |
| 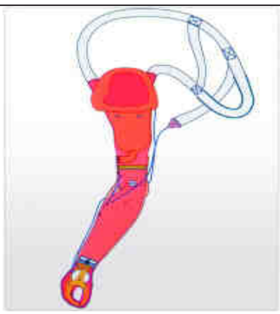<br>The functional prosthetic arm and operated by cable. | <br>The functional prosthetic arm mioelctric with the elbow joint with mechanical locking |

**Références:**

Abul-Haj, C.J., Hogan N., *Functional assessment of control systems for cybernetic elbow prostheses.* IEEE Trans Biomed Eng, 1990
Alstrom, C., Herberts, P., Korner, L., *Experience with Swedish multifunctional prosthetic hands controlled by pattern recognition of multiple myoelectric signals*. Int Orthop, 1981
Berceanu, C., Tarniță, D., *A new fabrication method for a computer controlled artificial hand with electric actuators*, International Journal of Modern Manufacturing Technologies I.J.ModTech), Vol. I, 2009
Carlson, L., Radocy, R., Marshall, P., D., *Spectron 12 cable for upper-limb prostheses*. J Prosthet Orthot, 1991
Clippinger, F., *A sensory feedback system for an upper-limb amputation prosthesis*. Bull Prosthet Res, 1974
Crowder, R.,M., *Local actuation of multijointed robotic fingers.* IEE Conference Publication, 1991
Erb, R., A.,*Cosmetic covers for upper and lower extremity prostheses*. Progress reports, J Rehabil Res Dev, 1990
Fillon, Mike, *The New Bionic Man.* Popular Mechanics 176, 1999
Firică, Jean, *Models using pneumatic artificial muscles human muscle system for active movement of the human body,* International Salon of Hydraulics and Pneumatics, HERVEX, 2010
Firică, J., *Dicționar sportiv român-englez.* Ed. Sitech, Craiova, 2006
Gruver, W., A., *Intelligent robotics in manufacturing, service and rehabilitation : an overview* . IEEE Trans Indust Electron, 1994
Iberall, T., Sukhatme, G.S., Beattie, D., Bekey, G.A., *On the development of EMG control for a prosthesis using a robotic hand*. Proceedings of the 1994 IEEE International Conference on Robotics and Automation, 1994
Kaneko, K., Harada, K., Kanehiro, F., *Development of Multi-fingered Hand for Life-size Humanoid Robots*, Proceedings of the IEEE International Conference on Robotics and Automation, Roma, Italy, 2007
Kargov, A., Asfour, T., Pylatiuk, C., Oberle, R., Klosek, H., Schulz, S., Regenstein, K., Bretthauer, G., *Development of an Anthropomorphic Hand for a Mobile Assistive Robot,* 2005
Kelly, M.F., Parker, P.A., Scott, R.N., *The application of neural networks to myoelectric signal analysis*: A preliminary study. IEEE Trans Biomed Eng, 1990
Lyman,J. Freedy,A., Solomonow, M., *Studies toward a practical computer-aided arm prosthesis system*. Bull Prosthet Res, 1974
Meek,S., Jacobsen, S.C., Straight, R., *Development of advanced body-powered prosthetic arms.* Progress reports, J Rehabil Res Dev, 1990
Michael, J.,W., *Upper limb powered components and controls: current concepts* . Clin Prosthet Orthot, 1968
Nader, N., *The artificial substitution of missing hands with myoelectrical prostheses*. Clin Orthop, 1990
Reswick, J.B., Vodovnik, L., *External power in prosthetics and orthotics, an overview* . Artif Limbs, 1967
Sartori,A., Simoni, A., Maloberti, F., Torelli, G., *A 2-D photosensor array with integrated charge amplifier* . Sensors and actuators, 1995
Scott, R.N., Brittain, R.H., Caldwell, R.R., et al : *Myoelectric control systems-Progress report No. 17*. UNB Bio-Eng Inst Res Rep, 1980
Shannon, G., F., *A myoelectrically controlled prosthesis with sensory feedback*. Med Biol Eng Comput , 1979
Simoni, A, Sartori, A., Maloberti, F., Torelli, G., Plevridis, S., *Motion detection with an intelligent optical sensor with on chip analog memory .* Proceedings ESSCIRC, 1994
Starețu, I., *Sisteme de prehensiune*, Editura Lux Libris, Braşov, 1996
Stein, R.B., Charles, D., Hoffer, J.A., et al (1980): *New approaches for the control of powered prostheses: Particularly by high-level arm amputees*. Bull Prosthet Res
Uellendahl, Jack E., *Upper Extremity Myoelectric Prosthetics*. Physical Medicine and Rehabilitation Clinics of North America, 2000

ISSN 1454 - 8003
Proceedings of 2011 International Salon of Hydraulics and Pneumatics - HERVEX
*9 – 11 November, Calimanesti-Caciulata, Romania*

# DETERMINATION OF EXERGY LOSS FOR DIESEL ENGINE

**ZORIN BERCEA[1] and LIVIU VAIDA[2]**

[1] *Technical University of Cluj Napoca,Faculty of Mechanics,Dpt.of Mecanical Engineering,Cluj-Napoca,România*
*e-mail*: Vasile.Bercea@termo.utcluj.ro;
[2] *e-mail*: Liviu.Vaida@termo.utcluj.ro

***Abstract.*** *Nowadays there exists a worldwide effort focused on the reduction of environmental pollution correlated with the specific fuel consumption of the Diesel engines in parallel with the determination of technical solutions for the increase of the overall efficiency of these motors. Within this framework, the authors determine the percentage of exergy loss with respect to the useful mechanical work generated by the motor. This paper analyzes the energy and exergy balance for Diesel motors proposing a case study on such an engine on a testing stand. In addition a comparison is made by evaluating the main heat and exergy losses with the thermal flux equivalent to the produced mechanical work, measured on the crankshaft. A theoretical study is achieved, aiming to determine the overall efficiency increase for these motors, by saving the lost exergy and converting it into useful mechanical work.*

***Key words:*** *Diesel motor, energy balance, exergy balance, efficiency, exergy recovery.*

## 1. Introduction

The paper theme integrates in the field of mechanical engineering and focuses on the improvement of one of the most important, present and acute problem, namely energy, with focus on fuels. The internal combustion engine transform the chemical energy of fuel through their combustion, in useful mechanical work at the crankshaft, with a series of losses, which represent the percentage of the generated energy obtained by fuel burning which does not reach the crankshaft [1,2]. The analysis of the state-of-the-art researches in the field of efficiency increase for internal combustion engines, show that no matter how performant an engine is, functioning with different fuels, it has a relatively low efficiency (35 – 40%) and large heat losses [1,2], polluting the environment with exhaust gasses, thermal and phonic emissions. The paper makes an analysis of energy and exergy balance for engines with compression combustion, named from this point on Diesel, the name of their inventor. The paper will determine the percentage of exergy loss during functioning through the lubricant, the cooling liquid and exhaust gasses, which represents also the maximum percentage of energy that can be recovered and transformed into useful mechanical work.

The case study is achieved on e Volkswagen industrial engine, model: VW TDI ® 1,9 AVM. This Diesel engine has four inclined cylinders in line, water cooling system, direct injection with turbine for the exhaust gasses and turbo compressor, cooler for the compressed air introduced in the combustion chamber, exhaust gasses recirculation and a complete electronic management system, which makes it highly performant, as shown in its specifications [8].

## 2. The energy balance for Diesel motors

### 2.1. Classical Diesel motors

The transformation of the chemical energy of the fuel by its combustion into useful mechanical work on the crankshaft, is subjected to a series of losses. Figure 1 illustrates the basic scheme of energy flux for a Diesel engine [1,5].

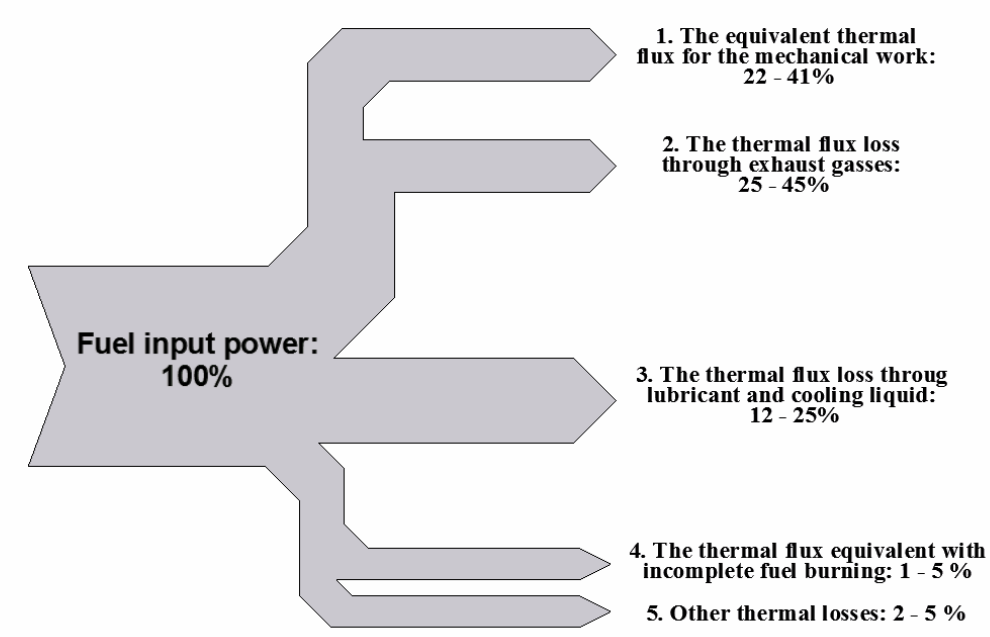


Fig. 1. The basic energy flux within a Diesel motor [1,5]

The energy balance for a Diesel engine is given by equation (1) [1,5,6]:

$$Q = Q_c + Q_r + Q_g + Q_{înc} + Q_{rez} \text{ [W]} \tag{1}$$

where: $Q$ – is the thermal flux available through fuel combustion;
$Q_c$ – the equivalent thermal flux for the mechanical work;
$Q_r$ – the thermal flux loss through lubricant and cooling liquid;
$Q_g$ – thermal flux loss through exhaust gasses;
$Q_{înc}$ – thermal flux equivalent with incomplete fuel burning;
$Q_{rez}$ – residual term (other thermal losses).

In order to make a percentual analysis, the terms of the energy balance with respect to the available thermal flux resulted by the combustion of the fuel Q, presented in equation (1), are multipled by 100/Q:

$$Q*100/Q = Q_c *100/Q+Q_r*100/Q+Q_g*100/Q+Q_{înc} *100/Q+Q_{rez} *100/Q \text{ [\%]} \tag{2}$$

The following notations are introduced:
- The term Q*100/Q is denoted with „q", representing the available thermal flux resulted by the fuel combustion, having a value of 100%;
- The terms $Q_c$*100/Q; $Q_r$*100/Q; $Q_g$*100/Q; $Q_{înc}$*100/Q; $Q_{rez}$ *100/Q with: $q_c$, $q_r$, $q_g$, $q_{înc}$, $q_{rez}$, representing the percentual values of the energy balance terms.

Thus, it results:

$$q = q_c + q_r + q_g + q_{înc} + q_{rez} = 100 \text{ [\%]} \tag{3}$$

Table 1 presents the percentual values of the energy balance terms for classical Diesel motors [1,5]:

**Table 1.**

Percentual values of the energy balance terms:

| Motor type | q [%] | $q_c$ [%] | $q_r$ [%] | $q_g$ [%] | $q_{înc}$ [%] | $q_{rez}$ [%] |
|---|---|---|---|---|---|---|
| Diesel | 100 | 22-41 | 12-25 | 25-45 | 1-5 | 2-5 |

The thermal balance shows the values of heat losses, pointing out the areas where improvements need to be done in order to increase the performances of the motor [1,5,6]. In table 1, the term $q_r$ includes also the heat losses by cooling the oil lubricant. In the following section an analysis will be achieved on the thermal flux losses through the oil lucricant and the cooling liquid, namely $q_r$ and also through the exhaust gasses, namely $q_g$. Making a comparison between these added heat loss fluxes ($q_r$+$q_g$) and the equivalent thermal flux of the useful mechanical work on the crankshaft, $q_c$, based in the data from table 1, results:

$$(4) \qquad (q_r + q_g)/q_c = (37\div70)/(22\div41) = (0{,}90 \div 1{,}70) \quad [-]$$

Conclusion 1. The heat losses cumulated by the cooling liquid, oil lubricant and exhaust gasses and comparable in size or even bigger with the thermal flux of the useful mechanical work on the engine crankshaft.

**2.2.** Case study: Diesel engine VW TDI® 1,9 AVM

In this section are presented the results of some experimental laboratory measurements on an industrial Diesel engine turbo supercharged, manufactured by VOLKSWAGEN AG. GERMANY, model TDI® 1,9 AVM, with an effective power of 63 kW attained at 3100 rot/min and a specific fuel consumption (with maximum efficiency) of 0,207 kg/kWh, at a speed of 1740 rot/min.

The engine is mounted on a test bench manufactured by WEINLICH STEUERUNGEN, model MP 80/6000, equipped with dynamometer grip. The measurements where performed in the laboratory of thermal engines of the Faculty of Mechanical Engineering within the Technical University of Cluj-Napoca. Their main objective is the determination of the real functioning efficiency of the analyzed motor for different functioning regimes.

The notations and measurements units used in the paper by the authors are presented as follows [1,5,6]: $n_m$ - cranckshat speed [rot/min];

- m – the fuel weight (Diesel) consumed in the time τ [g];
- $\tau$ – the time interval for one measurement [s];
- $P_e$ - the effective power on the [kW];
- $M_e$ – effective torque [N*m];
- $C_h$ – hourly fuel consumption [kg/h];
- $c_e$ – speficic fuel consumption [kg/kwh].

The measurements were performed for different functionsing regimes of the engine, by varying the following parameters: $n_m$ [rot/min]; m [g]; τ [s]; $P_e$ [kW]; $M_e$ [N*m] (indicated by the electronic equipment of the testing bench):

The following equations are used [1,5,6]:

$$(5) \qquad C_h = 3{,}6\,\frac{m}{\tau} \quad [kg/h],$$

$$(6) \qquad c_e = \frac{C_h}{P_e} \quad [kg/kWh]$$

(7) $$\eta_{ef} = \frac{3600}{c_e Q_i} \quad [-]$$

The following parameters have been calculated:
- hourly consumption $C_h$ [kg/h], using equation (5);
- specific fuel consumption $c_e$ [kg/kWh], using equation (6);
- the efficiency $\eta_{ef}$ [-], using equation (7).

The inferior caloric value of Diesel fuel, $Q_i$, is 41800 kJ/kg [1,5].

Based on equation (7), the maximum efficiency that can be obtained for the Diesel engine VW TDI® 1,9 AVM is:

(8) $$\eta_{ef\,\max} = \frac{3600}{c_e Q_i} = \frac{3600}{0{,}207 * 41800} = 0{,}416 \ [-].$$

The results of the expermental measurements performed by the authors, analysing the motor functiong of the testing bench are presented in Table2:

**Table 2**
Experimental results

| Nr. crt. | $n_m$ [rot/min] | m [g] | τ [s] | $C_h$ [kg/h] | $P_e$ [kw ] | $M_e$: [N*m] | $C_e$ [Kg/kwh] | $\eta_{ef}$ calculated | Observations |
|---|---|---|---|---|---|---|---|---|---|
| 1 | 1100 | 9,20 | 60 | 0,552 | 0,5 | 3 | | | No load |
| 2 | 1250 | 12,00 | 60 | 0,72 | 0,5 | 3 | | | No load |
| 3 | 1340 | 13,00 | 60 | 0,78 | 0,5 | 3 | | | No load |
| 4 | 1470 | 14,00 | 60 | 0,84 | 0,5 | 3 | | | No load |
| 5 | 1520 | 15,00 | 60 | 0,9 | 0,5 | 3 | | | No load |
| 6 | 1620 | 15,50 | 60 | 0,93 | 0,5 | 3 | | | No load |
| 7 | 1000 | 36,70 | 30 | 4,404 | 15 | 150 | 0,29 | 0,29 | Load, error |
| 8 | 1100 | 37,00 | 30 | 4,44 | 20 | 150 | 0,22 | 0,39 | Load, accepted |
| 9 | 1270 | 37,20 | 30 | 4,464 | 20,3 | 150 | 0,22 | 0,39 | Load, accepted |
| 10 | 1000 | 33,00 | 30 | 3,96 | 15,9 | 141 | 0,25 | 0,35 | Load, accepted |

Conclusion 2. The energetic efficiency of the tested engies for different functioning regimes and speeds, are somewhat smaller that 0.4, and confirm the data supplied by the producer.

## 3. Exergy loss determination for Diesel

### 3.1. Exergy balance

The heat losses by cooling the oil lubricant, the cooling liquid and the exhaust gasses are mainly produced by the irreversibility of the motor cycle and only a percentage of this energy can be used as heat source in a motor cycle transforming it into useful mechanical work. This percentage that can be used for the conversion as heat source, is called exergy. In the following paragraphs is determined the exergy percentage resulted from the heat losses by engine cooling and exhaust gasses.

Based on [7], the heat exergy given by any source $(E_Q)_{12}$ is:

(9) $$(E_Q)_{12} = Q_{12} - T_0 \int_1^2 \frac{dQ}{T} = \int_1^2 \left(1 - \frac{T_0}{T}\right) dQ \qquad [J];$$

where: $Q_{12}$ represents the heat quantity given by the heat source, of, in this case, the heat losses that can be recovered without affecting the functioning of the motor;

(10) $$\left(1 - \frac{T_0}{T}\right) = \theta_e \qquad [-]$$

where: $\theta_e$ represents the exergy temperature factor corresponding to the efficiency of the Carnot cycle where the cold source has the environment temperature, $T_o$, while the heat source, the temperature T (which can vary).

Using (9), the exergy expression can be written as:

$$(11) \qquad (E_Q)_{12} = \int_1^2 \theta_e \, dQ = \theta_{em} Q_{12} \qquad [J];$$

where: $\theta_{em}$ represents the average temperature $T_m$ exergy factor when the heat release takes place in the thermodynamic process of exergy transformation in useful mechanical work. [7].

The exergy withhold by the recovered heat losses for the motor $E_Q$ can be transformed in useful mechanical work $E_u$ based on the second principle, with the losses $E_p$, based on equation (12), which is the exergy balance equation [7]:

$$(12) \qquad E_Q = E_u + E_p \qquad [J],$$

Where: $E_Q$ – exergy consumption (recovered exergy) [J];
$E_u$ – useful exergy (transformed recovered exergy) [J];
$E_p$ – exergy loss during transformation [J].

The diagram in figure 3 represents schematically, the exergy balance of a thermal engine [7].

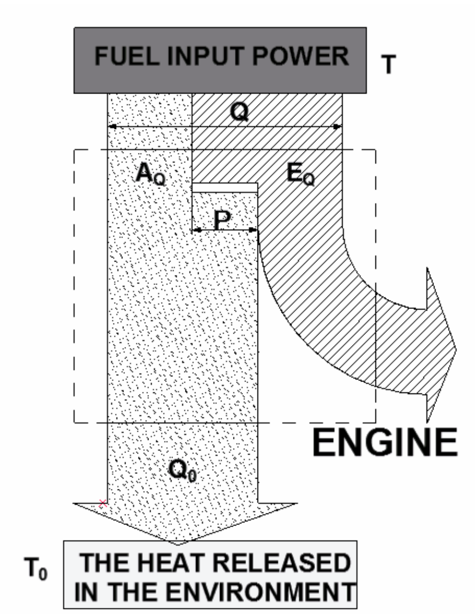


Fig. 3. The exergy balance of a thermal engine

$A_Q$ represents the anergy heat $Q_{12}$, while $Q_0$ the heat released in the environment [7].

The exergy efficiency, shows the amount of the exergy consumed within a process which is found as useful exergy (ex: useful mechanical work).

The exergy efficiency is calculated with the formula (13), [7]:

$$(13) \qquad \eta_{ex} = \frac{E_u}{E_Q} = \frac{E_Q - E_P}{E_Q} = 1 - \frac{E_P}{E_Q} \qquad [-]$$

For the equation expressing the exergy balance and the diagram from figure 3 results that for determining the exergy loss due to the heat losses of the engine is necessary to conduct an analysis upon these heat losses, as presented in the next section.

**3.2.** The exergy loss due to the engine cooling liquid and the lubrication oil

In the studied literature [8], the heat losses through the liquid based cooling system $Q_{r\ lichid}$ of a Diesel engine turbo supercharged, measured in laboratory conditions, represents aproximatively 15% of the available thermal flux which results following the transformation of the chemical energy resulted during the fuel combustion into heat Q, while the heat losses through the lubricant cooling system represent aproximatively 5%. It results:

$$(14) \quad Q_r = Q_{r\ lichid} + Q_{r\ ulei} = (15+5)*Q/100 = 20\% * Q \qquad [W];$$

Using the tables 1 and 2 it can be established the thermal flux equivalent to the useful mechanical work $Q_c$ with respect to the thermal flux resulted through the fuel combustion Q:

$$(15) \quad Q_c = 40\%\ Q \quad [W]$$

From the equations (14) and (15) results that the cummulated flux of heat losses through the cooling liquid and respectively through the cooling of the lubricant, with respect to the thermal flux of the useful mechanical work, $Q_c$ represents:

$$(16) \quad Q_r = 50\%\ Q_c \quad [W]$$

In order to determine the exergy percentage out of this heat losses, one has to calculate the exergy factor $\theta_{rm}$ of the average temperature $T_m$ at which the heat is released in the termodynamicprocess of exergy transformation into useful mechanical work [7]. For this purpose the ambient temperature, $T_0$ is determined (the average air temperature where the heat is evacuated into, which is considered in this case study to be 288 $^oK$ (15 $^oC$)) and the average temperature of the heat source (these temperatures, for both the cooling lequid and the lucricant are almost simular, and for this case study are considered to be 363 $^oK$ (90 $^oC$)).

Using the equation (10) $\theta_{rm}$ can be calculated:

$$(17) \quad \theta_{rm} = 1 - T_0/T = 1 - 288/363 = 1 - 0{,}793 = 0{,}207 \qquad [-];$$

For the calculus the of the exergy of the flux of the heat losses (cumulated) by the cooling liquid and lubricant cooling, with respect to the thermal flux equivalent to the useful mechanical work $Q_c$, the equations (11) and (15) are used:

$$(18) \quad E_{Qr} = \theta_{rm}\ Q_r = 0{,}207\ Q_r = 0{,}207 * 0{,}5\ Q_c = 0{,}103 * Q_c = 10{,}35\%\ Q_c \qquad [W];$$

Conclusion 3. The exergy $E_{Qr}$ contained within the flux of cumulated heat losses for the cooling liquid and the lubricant cooling $Q_r$, represents 10,35% of the thermal flux equivalent to the useful mechanical work $Q_c$.

**3.3.** The exergy loss through the exhaust gasses for a Diesel engine

The temperature of the exhaust gasses, at the exit point from the engine is of aproximatively 350 $^oC$ [1,5,6], confirmed also by laboratory experiments (after 10 minutes of engine running).

The literature [8], shows that the losses flux of the heat released into the atmosphere by the exhaust gasses of the Diesel engine, $Q_g$ , represents 25% of the available thermal flux resulted during the transformation of the fuel chemical energy, by combustion, into heat, Q:

$$(19) \quad Q_g = 25\%\ Q \quad [W],$$

Using the equations (15) and (19) one can determine the heat loss flux through the exhaust gasses for the motor $Q_g$,with respect to the thermal flux equivalent to the mechanical work $Q_c$:

$$(20) \quad Q_g = (25/100) * (100/40) * Q_c = 0{,}625\ Q_c = 62{,}5\%\ Q_c [W]$$

This equations shows that the heat losses flux through the exhasut gasses of a Diesel engine $Q_g$,represents 62.5% of the thermal flux equivalent to the mechanical work $Q_c$.

In order to determine the exergy from the herat flux lost through the exhasut gasses, the exergy temperature factor, $\theta_{gm}$, has to be determined.

$T_0$ [$^oK$] is the minimum temperature of the exhaust gasses released in the environment, in the termodynamic process of transformation of exergy into useful mechanical work (process in which the gasses are cooled) [7], in order to avoid condens.

For this calculus example, is considered $T_0$ [$^oK$] = 403 $^oK$ (130 $^oC$).

T [$^oK$] represents the temperature of the exhaust gasses when they exit the engine. Based on [1,5,6] results that T [$^oK$] is aproximatively 623 [$^oK$] (350 $^oC$).

Using the equation (10), the exergy temperature factor, $\theta_{gm}$, is calculated:

$$(21) \quad \theta_{gm} = 1 – T_0/T = 1 – 403/623 = 1 - 0{,}647 = 0{,}353 \quad [-].$$

By using the equations (11) and (20) is determined the exergy $E_{Qg}$ contained in the flux of heat losses through the exhaust gasses $Q_g$, with respect to the thermal flux equivalent to the useful mechanical work, $Q_c$:

$$(22) \quad E_{Qg} = \theta_{gm} Q_g = 0{,}353\ Q_g = 0{,}353 * 0{,}625\ Q_c = 0{,}22\ Q_c \quad [J].$$

Conclusion 4. The exergy $E_{Qg}$ contained in the flux of heat losses through the exhaust gasses $Q_g$, represents 22.06% of the thermal flux equivalent to the useful mechanical work, $Q_c$.

## 4. Conclusions

Conclusion 1. The heat losses cumulated by the cooling liquid, oil lubricant and exhaust gasses and comparable in size or even bigger with the thermal flux of the useful mechanical work on the engine crankshaft.

Conclusion 2. The energetic efficiency of the tested engies for different functioning regimes and speeds, are somewhat smaller that 0.4, and confirm the data supplied by the producer.

Conclusion 3. The exergy EQr contained within the flux of cumulated heat losses for the cooling liquid and the lubricant cooling Qr, represents 10,35% of the thermal flux equivalent to the useful mechanical work Qc.

Conclusion 4. The exergy EQg contained in the flux of heat losses through the exhaust gasses Qg, represents 22.06% of the thermal flux equivalent to the useful mechanical work, Qc.

Conclusion 5. The useful exergy, $E_Q$, resulted through the heat losses cumulated by the cooling liquid, lubrication oil and exhaust gasses, with respect the the equivalent thermal flux of the useful mechanical work $Q_c$ represents (10,35+22,06)% =32,41 %, justifying the need of determining innovative technical solutions for transforming this energy resource into useful mechanical work.

***Acknowledgements.*** This paper was supported by the project "Improvement of the doctoral studies quality in engineering science for development of the knowledge based society-QDOC" contract no. POSDRU/107/1.5/S/78534, project co-funded by the European Social Fund through the Sectorial Operational Program Human Resources 2007-2013.

## REFERENCES

[1] Băţagă N., Burnete N., Căzilă A., Rus I., Sopa S., Teberean I., *Motoare cu ardere internă*, Editura didactică şi pedagogică, Bucureşti, 1995, pp. 210-218.

[2] Bercea V. Z., *Bilan urile energetic i exergetic ale motoarelor cu aprindere prin comprimare,* Referat- Ma ini i Echipamente Termice, coala doctorală, UTCN, Cluj-Napoca, 2011.

[3] Bercea V. Z., *Utilizarea ciclului Kalina pentru cre terea randamentului global de func ionare a motoarelor cu ardere internă*, Sesiunea de comunicări ştiinţifice a studenţilor facultăţii de mecanică, Cluj-Napoca, 20 mai 2011.

[4] Bombarda P., Invernizzi Constante M, Pietra C., *Heat recovery from Diesel engines: a thermodynamic comparison between Kalina and ORC cycle*, Applied Thermal Engineering 30 (2010), pag. 212-219.

[5] Burne te N., s.a., *Motoare Diesel i biocombustibili pentru transportul urban*, Editura Mediamira, Cluj-Napoca, 2008.

[6] Grünwald B., *Teoria, calculul şi construcţia motoarelor pentru autovehicule rutiere*, Editura didactică şi pedagogică, Bucureşti, 1980.

[7] Popa B., Vintilă Constanţa, *Termotehnică şi maşini termice*, Editura didactică şi pedagogică Bucureşti, 1977.

[8] Radcenco V., *Termodinamică tehnică i ma ini termice – Procese ireversibile*, Editura didactică i pedagogică, Bucure ti, 1976.

[9] http://www.vw-industrial-engines.com - en_TDI_1-9-463-MB.pdf. Powersystems & Components. Volkswagen AG. D-38436 Wolfsburg. 2005.

**ISSN 1454 - 8003**
**Proceedings of 2011 International Salon of Hydraulics and Pneumatics - HERVEX**
*9 – 11 November, Calimanesti-Caciulata, Romania*

# ELABORATION OF MICRO-HYDROPOWER STATION FOR KINETIC ENERGY CONVERSION OF FLOWING WHATER

Ion BOSTAN, academician; Valeriu DULGHERU, Dr.Sc. PhD, prof.; Viorel BOSTAN

*Technical University of Moldova, 168, Ştefan cel Mare str., Chişinău, 2004, Republic of Moldova*

**Abstract:** Increased efficiency of elaborated micro-hydropower stations is achieved by an optimum position of the blades with hydrodynamic profile. The formulation used to compute the hydrodynamic forces is an inviscid –boundary layer model. Micro-hydropower station provides kinetic energy conversion of river water into mechanical or electrical energy without building barrages. Increased efficiency is provided by blades aerodynamic profile and their optimum position for efficient conversion of water kinetic energy. Two industrial prototypes are fabricated. The efficiency of the micro-hydro power stations as conversion systems of renewable energy sources kinetic energy of flowing rivers depends mostly on profiles of the hydrofoils used in the rotor's construction for interaction with fluid. The main goal of this paper consists in the elaboration of the modified hydrofoils, and based on them of the turbines with increased conversion efficiency. The following objectives were established: Elaboration of the transient computational models of the hydrodynamic turbine with 3 and 5 hydrofoils for extensive simulations in the framework of computational fluid dynamics (CFD) using software applications ICEM CFD, CFX, TurboGrid and ANSYS, that will allow a variation of the attack angle for each individual blade during a full rotor's revolution.

*Expected results:* Elaboration of the technical and technological documentations, manufacturing and testing of the hydrodynamic rotor for the micro-hydro power station.

**Key words:** *water wheel, hydrodynamic profile, micro-hydropower station.*

## 1. INTRODUCTION

The existence of water on the Earth has conditioned the emergence and development of life. From the times immemorial, man has chosen a place to live near rivers and lakes to meet their natural needs in water, but also for carrying out basic irrigation works. Floating or rowing led human thought by observation, to use water force and energy. Thus, the mechanical power of running water can be considered one of the oldest tools.

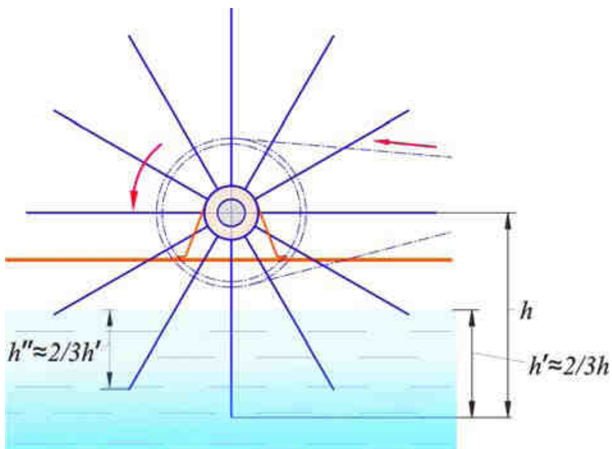

Figure 1: Conceptual diagram of the water wheel with rectilinear profile of blades

The means of water use and exploitation have evolved from a historical epoch to another, from one nation to another, in relation to the natural conditions, depending on the level of production relationships and forces. Thus, water energy uses has marked stages of development of the social systems from the primitive to modern society.

To avoid the construction of dams, the kinetic energy of rivers can be utilized by means of exploiting water stream turbines. This type of turbines is easily mounted, is simple in operation and maintenance cost is suitable. The 1m/s current velocity represents an energetic density of 500W/m²

of the crossing section, but only a part of this energy can be drawn off and converted into useful electrical or mechanical energy. This fact depends on the type of rotor and blades. Velocity is especially important as a double increase in the water velocity can result in an eight times rising of energetic density. Prut river has a section equivalent to 60 $m^2$ and an average velocity in explorable zones of (1 – 1,3) m/s, which is equivalent to an approximate theoretical energy of (30 – 65) kW. Taking into account the fact that the turbine can occupy only a portion of the river bed the generated energy might be much smaller. There are various conceptual solutions, but the issue of increasing the conversion efficiency of water kinetic energy is in the view of researchers. The analysis of constructive versions of floatable micro-hydro power stations previously examined did not satisfy at all from the point of view of conversion efficiency of water kinetic energy. In a classical hydraulic wheel horizontal axle (Fig. 1) [1] the maximum depth at which one of blades is sunk makes approximately 2/3 of the blade height *h*. Namely, only this area participates in the transformation of water kinetic energy into mechanical one. As well, the prior blade covers approximately *2/3* of the blade surface sunk utmost in the water *(h''≈ 2/3h')*. This fact reduces significantly the water stream pressure on the blade. The blade that comes next to the blade that sunk maximally into water is covered completely by it and practically does not participate in the conversion of water kinetic energy. Therefore, the efficiency of such hydraulic wheels is small.
The insistent searches of authors lead to the elaboration and patenting of some advanced technical solutions for floatable micro-hydro power stations, based on the hydrodynamic effect, generated by the hydrodynamic profile of blades, and their orientation at optimum hydrodynamic profile of the blades and the design of the orientation mechanism towards the water streams.

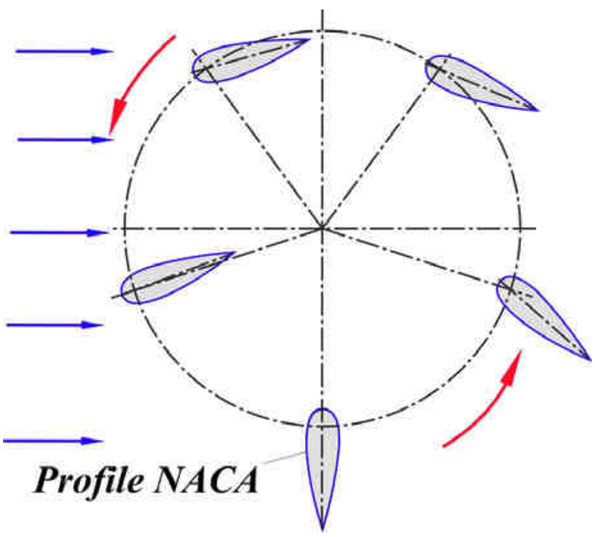

Figure 2: Conceptual diagram of the rotor with hydrodynamic profile of adjustable blades concerning the water streams.

## 2. CONCEPTUAL DIAGRAM OF THE MICRO HYDROPOWER PLANT WITH HYDRODYNAMIC ROTOR

The results of the carried out research by the authors concerning the water flow rate in the location selected for the micro-hydro power stations mounting, the geological prospecting of the river banks in the place of anchoring foundation mounting, the energetic needs of the consuming potential, represent initial data for the conceptual design of the micro-hydro power stations and its working element.
Aiming at an increase of the conversion coefficient of the water kinetic energy (Betz coefficient), a number of structural diagrams of floatable micro-hydro power plants have been designed and patented [2-7]. They comprise a rotor with pintle and vertical blades, and hydrodynamic profile in normal section. The blades are interconnected by an orientation mechanism towards the direction of the water streams. The motion of rotation of the rotor with pintle is multiplied by a mechanical transmission system and is transmitted to an electrical generator or to a hydraulic pump. The mentioned knots are fixed on a platform, mounted on floatable bodies. The platform is linked to the bank by a hinged metallic truss and by straining cables.
A very important aspect in the functional optimization of micro-hydro power plants is the selection of optimum hydrodynamic profile of the blades which allows increasing the conversion coefficient (Betz coefficient). Due to the hydrodynamic upward forces the increase in the conversion level is reached by means of ensuring the optimum position of the blade towards the water streams in various phases of rotor rotation by utilizing blades orientation mechanism. Thus, practically all blades (even those which

move opposite the water streams) participate simultaneously in the generation of summary torque moment. The blades which move along the water streams utilize both hydrodynamic forces and water pressure exercised on blade surfaces for the generation of the torque moment. The blades which move opposite the water streams utilize only hydrodynamic upward forces for the generation of the torque moment. Due to the fact that the relative velocity of the blades toward water streams at their motion opposite water streams is practically twice bigger, the hydrodynamic upward force is relatively big and the generated torque moment is measurable to the one generated by the water pressure. This effect forms the basis of all patented technical solutions.

The adopted technical solutions have resulted in an ample theoretical and experimental research carried out at the Centre for Renewable Energy Conversion Systems Design, Department of the Theory of Mechanisms and Machine Parts. To justify the constructive and functional parameters, supplementary digital modelling and simulation have been carried out by utilizing ANSYS CFX5.7 software. Subprograms developed by authors for the MathCAD, AutoDesk MotionInventor, etc. software, have been utilized, namely simulation of the interaction „*flow-blade*" of the floatable steadiness and also the optimization of blades hydrodynamic profile, with the purpose to increase the river water kinetic energy conversion efficiency for different velocities by using 3, 4 and 5 blade rotors. In the process of micro-hydro power plants design, the experience gained at research-design-manufacturing of the pilot plant was utilized.

The efficiency of micro-hydro power plant operation by private consumers for special purposes depend on the right selection of micro-hydro power plant constructive configuration and of the functional characteristics of the component aggregates participating in the process of flowing water kinetic energy conversion into useful energy. In order to satisfy the objectives and consumers demand for micro-hydro power plants, and also for the increase in the flowing water kinetic potential conversion efficiency in the certain zone of the river, the authors have designed various constructive and functional concepts based on modular assembling. The mentioned micro-hydro power plants, conceived as modular ones, allow the modification of destination and functional characteristics by replacing certain aggregates with other (generator, pump, blades with different hydrodynamic profile, 3-5 blades rotor).

Micro-hydro power plants have similar resistance structure as constructions calculated from the point of view of resistance and rigidity at dynamic demands. Floatability and maintenance of the perpendicularity of micro-hydro power plant rotor spindle for a variable river water level are ensured by technical solutions protected by patents [3-7]. The instant orientation mechanism of blades for a constant entering angle concerning the direction of the water flow represents Know-How and it is not described. The main working element on which the quantity of kinetic energy converted into useful energy depends is the blade with the hydro-dynamic profile NACA 0016, developed on the basis of the performed digital modelling. Two types of rotors with 3 and 5 blades have been designed for the mentioned micro-hydro power plants. The installed capacity of micro-hydro power plants with diameter $D = 4\ m$, water-submersed blade height $h = 1{,}4\ m$ and the length of the blade cord $l = 1{,}3\ m$ for water flowing velocity $V = 1...2\ m/s$ can be within $P = 2...19\ kW$.

***In micro hydro power plant*** (Fig. 3) [3] the turbine 1 comprises blades 2, executed with the hydrodynamic profile and mounted on the axles 3, fixed by their upper part on the extreme ends of the bars 4, with the possibility to rotate around their axles. The position of the blades 2 at angle α to the direction of water flow is ensured by the controlling mechanism 5. Platform 6 is consolidated additionally by a winch 7 fixed on the truss that is mounted unshiftable on the shore pillar 8. The turbine 1 and the blades 2 are placed in the river water flow. The floating bodies 9 and the hollow blades 2 themselves control the position of turbine 1 and blades 2 concerning the water level. The multi-blade rotor is connected cinematically and coaxially to the electric generator 11 by the multiplier 10. The winch 7 is used for turbine 1 maintenance which fact requires its removal from the water. The blade 2 is positioned under angle α towards the water flow; it changes depending on the blade position to the water flow direction.

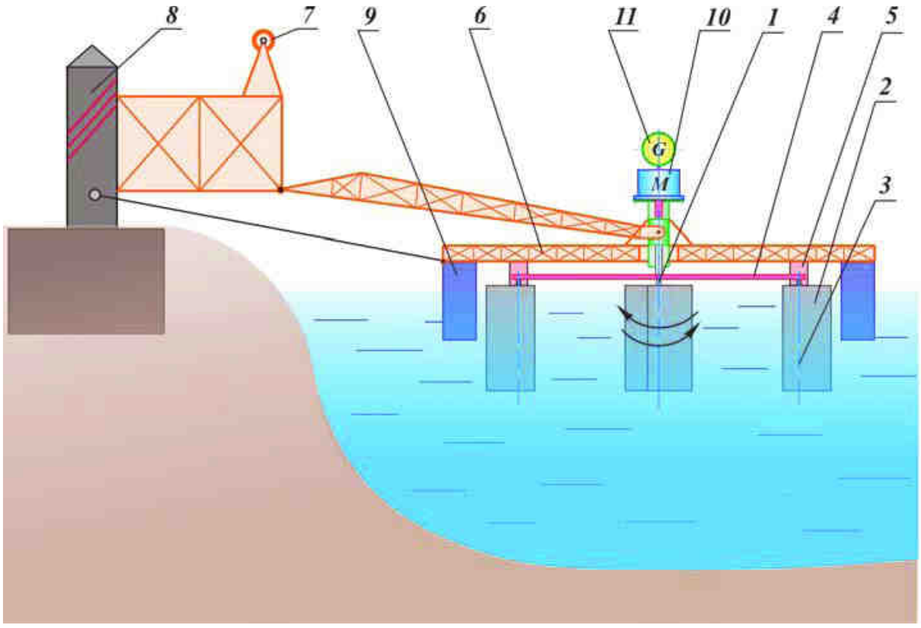

Figure 3: Floatable micro hydropower plant with blades orientation mechanism

The components of force *F*, acting on the blade, are determined from the relationships:

$$F_x = C_x \cdot \frac{\rho \cdot v^2}{2} \cdot S,$$

$$F_y = C_y \cdot \frac{\rho \cdot v^2}{2} \cdot S, \quad (1)$$

where: *ρ* is water density; *v* is the water flow linear velocity; *s* is the blade surface; $C_x$, $C_y$ are lift and drag (resistance) coefficients of the blade profile. Coefficients $C_x$ and $C_y$ depend on the blade entering angle **α** (the angle between the blade and the water flow direction) and on the profile shape. The angle is determined either experimentally or by numerical calculations. The torque developed by one blade is described by the equation:

$$M = F_\tau \cdot \frac{d}{2} = (\cos\gamma \cdot F_y - \sin\gamma \cdot F_x)\frac{d}{2}, \quad (2)$$

where $F_\tau$ is the projection of force *F* on the tangent drawn to the path of motion of the blade axis.
The summary torque includes the general component of the resistance force $F_h$. The torque moment generated by the turbine consists of the torques generated by each separate blade. Currently only one blade will not generate positive moment (it will generate a negative moment – the resistance one). Thus, the torque generated by the proposed turbine will be essentially bigger than the torque produced by the existing turbines for the same geometrical (blades dimensions) and kinematical parameters of water. The proposed micro hydro power plant allows the transformation of the water flow kinetic energy into mechanical or electrical energy with an increased utilization coefficient of water energy.

## 3. INDUSTRIAL PROTOTYPE OF MICRO-HYDRO POWER PLANT WITH HYDRODYNAMIC ROTOR

The micro-hydro power plant for river water kinetic energy conversion into electrical and mechanical energy (Fig. 4) [1,2] is poli-functional and can be utilized for street illumination, heating, water pumping for irrigation by weeping, for drainage of agricultural areas adjacent to rivers. The assembling of blades 1 with NACA 0016 profile in hydrodynamic rotor 2 and its mounting on the inlet shaft of the multiplier 3 are done in the same manner as for micro-hydro-power plant. The kinematics and constructive peculiarities of micro-hydro plant are the following: rotation motion of hydrodynamic rotor 2 with angular speed $\omega_1$, by means of multiplier 3 and of belt drive 4 having an effective multiplying coefficient $i = 212,8$, is being multiplied up to angular working speed of the generator with permanent magnets with small rotations 5:

$$\omega_3 = \omega_1 \cdot i_1 \cdot (s^{-1}).$$

Torque moment $T_3$, applied to rotor 5, is:

$$T_3 = \frac{T_1 \cdot \eta_1 \cdot \eta_2 \eta_r}{i}, (Nm),$$

where: $\eta_1$ is the mechanical efficiency of the multiplier ($\eta_1 = 0,9$);
$\eta_2$ - mechanical efficiency of the belt drive ($\eta_1 = 0,95$);
$\eta_r$ - mechanical efficiency of the hydrodynamic rotor bearings ($\eta_1 = 0,99$).

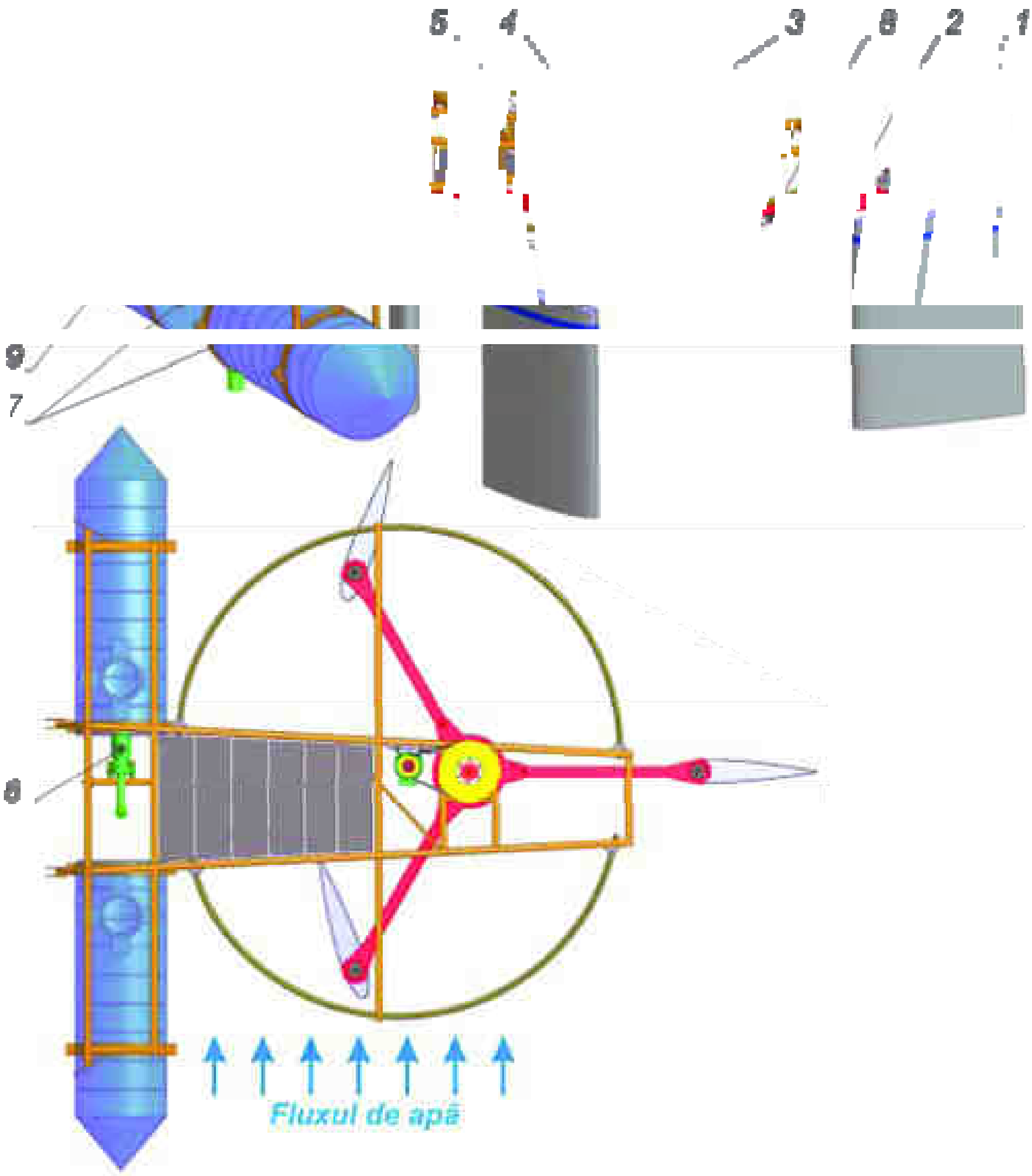


Figure 4: Micro-hydro power plant with hydrodynamic rotor river water kinetic energy conversion into electrical and mechanical energy (rotor diameter $D$ = *4m*, water-submersed blade height $h$ = *1,4m*, length of the blade cord $l$ =*1,3.*

*i* – effective multiplication coefficient equal to the composition of multiplying ratios of the planetary multiplier and of the belt drive.

The electric energy produced by the generator with permanent magnets 5 (fig. 4,5) can be utilized both for private consumer needs of power and for supplying electricity to impeller pump 6 (CH

400), for water pumping into irrigation systems by means of weeping or drainage of agricultural areas adjacent to the rivers (by relocation of the impeller pump 6). In the fig. 6 the dependence of the torque moment $T_1$ at hydrodinamic rotor shaft at one rotation is presented. In the case of electric energy production, the energy utilization efficiency with account of mechanical losses in the kinematics chain of the micro-hydro power plant and in the generator with permanent magnets makes up (at generator terminal)

$$\eta_\Sigma = \eta_1 \eta_2 \eta_r \eta_g = 0,9 \cdot 0,95 \cdot 0,99 \cdot 0,87 = 0,736,$$

and in case of water pumping (at the shaft of the pump):

$$\eta_\Sigma = \eta_1 \eta_2 \eta_r \eta_g \eta_{me} = 0,9 \cdot 0,95 \cdot 0,99 \cdot 0,87 \cdot 0,91 = 0,67,$$

where: $\eta_g$ is generator efficiency;

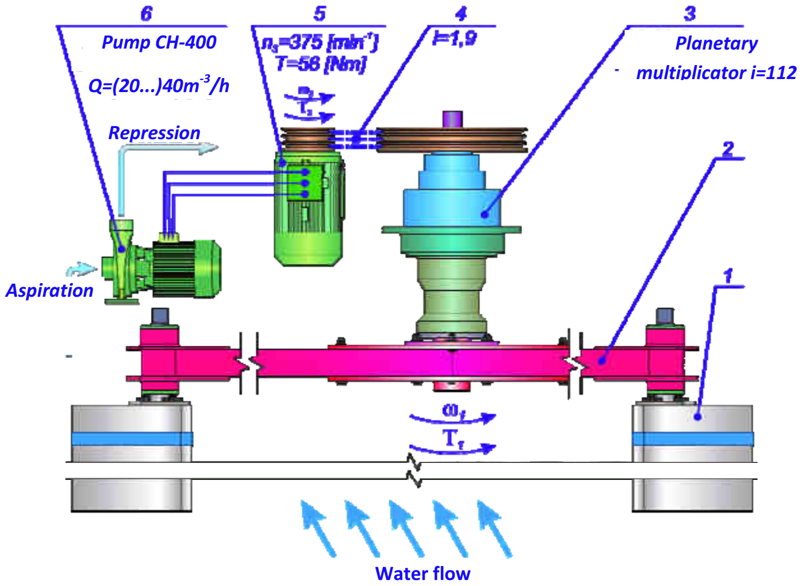


Figure 5: Micro-hydro power plant kinematics.

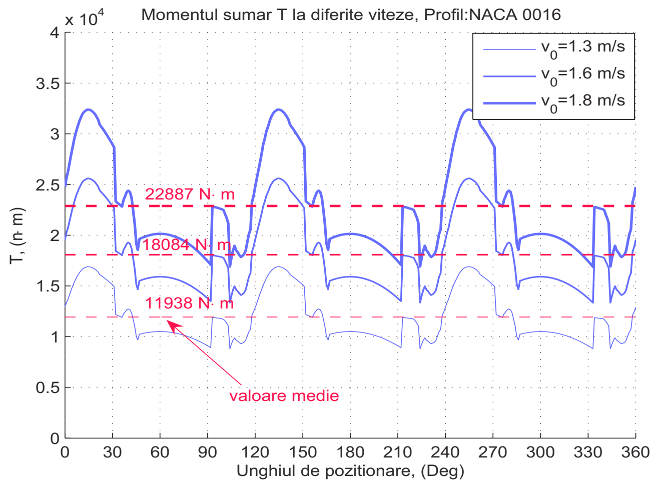


Figure 6. Torque moment $T_1$ at hydrodinamic rotor shaft with NACA 0016 profile blades.

$\eta_{me}$ – efficiency of the hydraulic pump of the electric motor.

On the basis of the conceptual diagram designed above, technical documentation was developed industrial prototype of micro-hydro power plant for river water kinetic energy conversion into electrical and mechanical energy was manufactured (fig. 7). Thus, micro-hydro power plant provides conversion of up to 73,6% and 67% of useful energy for electricity production and for water pumping from the energy potential of flowing water entrapped by the hydrodynamic rotor. Now, the industrial prototype of micro-hydro power plant is tested on the test area on the Prut river, c. Stoieneşti, Cantemir (fig. 8).

## CONCLUSIONS

In conclusion, we state that micro hydropower plants ensures the transformation of 70…86 % of the flowing water potential energy into useful electrical energy transmitted to the hydrodynamic rotor.

The basic advantages of micro-hydro power stations are as follows:

- small impact on the environment; it is not necessary to carry out civil constructions;
- the river does not change its natural course; the possibility to utilise local knowledge in order to produce floatable turbines;
- the possibility to mount a series of micro-hydro stations at small distances (approximately 30-50 m) because the influence of turbulence provoked by the adjacent installations can be excluded.

## REFERENCES

[1] Bostan I., Dulgheru V., Sobor Ion, Bostan V., Sochirean A., (2007), Systems for Renewable Energies Conversion: eolian, solar and hydraulic (in Romanian), Ed.: BonsOffices SRL, 592pp.

[2] Bostan I., Dulgheru V., Bostan V., Ciupercă R. (2009), Anthology of Inventions, vol. 3. Systems for Renewable Energies Conversion (in Romanian). Ed.: BonsOffices SRL, 458pp.

[3] Bostan I., Dulgheru V., Bostan V., Ciobanu O., Sochireanu A., (2006), Hydro-electric plant. Patent MD Nr. *2991*.

[4] Bostan I., Dulgheru V., Sochireanu A., Bostan V., Ciobanu O., Ciobanu R., (2006), Hydro-electric plant. Patent MD Nr. *2992*.

[5] Bostan I., Dulgheru V., Bostan V., Sochireanu A., Trifan N., (2006), Hydro turbine. Patent MD Nr. *2993*.

[6] Bostan I., Dulgheru V., Bostan V. Sochireanu A., Ciobanu O., Ciobanu R., Dicusară I., (2006), Hydro-electric plant. Patent MD Nr. 3104.

[7] Bostan I., Dulgheru V., Bostan V., Sochireanu A., Ciobanu O., Ciobanu R., (2009), Hydro-electric station. Patent MD Nr. *3845*.

ISSN 1454 - 8003
Proceedings of 2011 International Salon of Hydraulics and Pneumatics - HERVEX
*9 – 11 November, Calimanesti-Caciulata, Romania*

# SISTEME ELECTROHIDRAULICE DE CONTROL PENTRU SUSPENSIE AUTO
# ELECTROHYDRAULIC CONTROL SYSTEMS FOR AUTOMOTIVE SUSPENSION

Florin Nicanor Nicoara, Cristian Lucian Dobocan, Liviu Ioan Vaida
Universitatea Tehnica Cluj-Napoca, Dep, de Inginerie Mecanica, e-mail:
Florin.Nicoara@termo.utcluj.ro ; Lucian.Dobocan@termo.utcluj.ro ; Liviu.Vaida@termo.utcluj.ro

**Abstract:**
The complexity of the guiding – suspension systems of the passenger cars makes it very difficult to handle the error in the case of simultaneous achievement of the entire model (full-vehicle model). In this situation, partial models can be tested, for the wheel or axle suspension: quarter car model (independent wheel suspension): half car model (independent axle suspension, dependent axle suspension). In these terms, the paper presents the study of the vertical oscillations of the car body in dynamic with shock regime, which consists in the sudden release of the car to fall on the ground from a given height.

Cuvinte cheie: axe electrohidraulice, suspensie auto

1. Introducere
Modelul dinamic al sistemului de ghidare - suspensie utilizat la autovehicule este deosebit de complex, incluzând elemente cinematice (caroserie, punte, portfuzete, bare de ghidare s.a.), elemente elastice și de amortizare (arcuri, tampoane, pneuri, amortizoare ș.a.) și legături compliante (flexiblocuri). Practic, abordarea unui astfel de model, cu multe grade de libertate, este foarte dificilă, situație în care de preferat este să se construiască / testeze, pentru început, modele parțiale (simplificate), segmentate pe roțile sau punțile autovehiculului. Pentru a fi cu adevărat utile, modelele parțiale trebuie să corespundă, evident, ca și comportament dinamic, cu modelul tot - vehicul.
Pe aceste premize, în lucrare se analizează comparativ cu modelul tot - vehicul o serie de modele parțiale (sfert, jumătate de autovehicul), având ca obiectiv evaluarea comportamentului dinamic al vehiculului în mișcare, considerând cu prioritate oscilațiile verticale ale caroseriei, factor determinant al comfortului.
O bară de suspensie, în configurația sa mai clasice şi convenționale (vezi Figura 1) este constituit de trei elemente principale:

• Un element elastic (de obicei o arcuri elicoidale), care oferă o forță proporțională şi vizavi de alungire suspendare; această parte transportă toate sarcina statică.
• Un element de amortizare (de obicei, un amortizor de socuri hidraulic), care ofera un disipativ orță proporțională şi vizavi de viteza de alungire; această parte oferă o neglijabilă vigoare la starea de echilibru, dar joacă un rol crucial în comportamentul dinamic al suspensiei.
• Unset de elemente mecanice care link-uri suspendată (suspendate),caroserie la nesuspendate masă. Aproximativ vorbind, este o suspensie mecanică filtrul low-pass, care atenuează efectele de perturbare (de exemplu, un profil de drum neregulate ale inimii) pe o variabilă de ieşire. Variabilă de mieşire este de obicei, atunci când organismul accelerare confortul este principalul obiectiv, atunci când deformarea cauciucului.

Fig.1 Schemă clasică de o suspensie roata-la-şasiu într-o maşină.

Scopul design-ul este rutier exploatație. Din Figura 2, este clar că aceste două obiective sunt oarecum contradictorii: Tuning şi proiectarea unei suspensie mecanică încearcă să găsească cel mai bun compromis între aceste două obiective. Acest critic comerț-off este agravată de faptul că o suspendare are o călătorie limitată; în cazul în care sfârşit-stop (bucsa) de o suspensie este atins, atât confortul şi rutier-depozit spectacole sunt deteriorat în mod dramatic, şi apariția de această situație trebuie să fie atent evitate.

Fig.2 Exemple de amortizoare controlate electronic de şoc semi-activ, cu ajutorul a trei tehnologii diferite. De la stânga la dreapta: solenoid valve electro amortizor (Sachs), Magnetorheological (Delphi) şi electroreologic amortizor (Fludicon).

Fig.3 Exemple de "full-colț" arhitecturi vehicul: Michelin Active Wheel © (stânga) şi Siemens VDO e Corner © (dreapta).

(Clasic) electrohidraulice (EH) tehnologie, pe baza electrovalve amplasate în interiorul sau în afara corpului principal al amortizor, acestea pot modifica raportul de amortizare prin modificarea dimensiunea de orificii.
• magnetorheological (MR) tehnologie, bazată pe lichide, care pot schimba lor vâscozitate atunci când sunt expuse la câmpuri magnetice.
• electroreologic (ER), tehnologie, bazată pe lichide, care pot schimba vâscozitatea atunci când sunt

ISSN 1454 - 8003
**Proceedings of 2011 International Salon of Hydraulics and Pneumatics - HERVEX**
*9 – 11 November, Calimanesti-Caciulata, Romania*

expuse la campuri electrice.
Toate aceste tehnologii sunt potrivite pentru aplicații de vehicule. Astfel de tehnologii sunt astăzi în concurență puternică pe baza de multe caracteristici şi parametri, cum ar fi: timpul de răspuns, gama de controlabilitate, stick-slip, gestionarea defect, fiabilitatea pe termen lung, costuri, greutate şi ambalare, cerințele de întreținere, de putere-electronica cerințele, etc Fiecare
Tehnologia are argumentele sale pro şi contra, şi nici una dintre ele oferă cele mai bune caracteristici peste toate aceste caracteristici.
Reprezentarea grafică a unui sistem de suspensie într-un vehicul este raportat în Figura 2.1, în cazul în care aşa-numitul sfert-model de masina este reprezentat (a se vedea de
exemplu, Isermann,2003). În trimestrul-car are drept scop de a descrie interacțiunile dintre sistemul de suspensie, anvelope şi într-un şasiu colțul unui singur vehicul.
După cum este evident din Figura 2.1, reprezentarea sfert de masini este format din patru simplificate elemente:
• Masa suspendat reprezentând şasiu.
• Masa nesuspendate, care cuprinde dispozitive cum ar fi masa roată, frâna de, grosime, etc
• anvelope, care este modelat ca un element elastic.

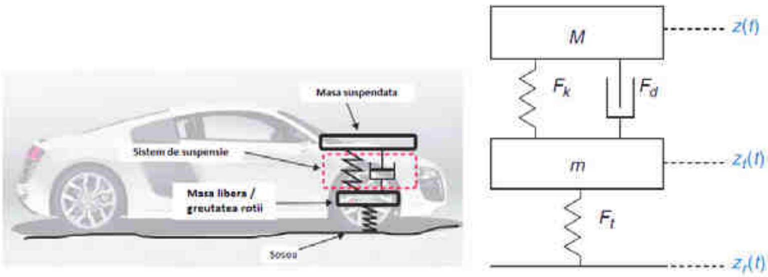


Fig. 4 Sfert-car reprezentare a unui sistem de suspensie într-un vehicul

Sistem de suspensie, care constă dintr-un element elastic şi un
element disipativ. Contribuțiile de elemente elastice şi disipative sunt presupuse a fi aditiv.
De echilibrare a forțelor implicate în sistemul de trimestrul-masina (cum este reprezentat în Figura 4), este posibil să se scrie următorul set de două ecuații de ordinul dinamice:

$$\begin{cases} M\ddot{z}(t) = F_k(t) + F_d(t) - Mg \\ m\ddot{z}_t(t) = -F_k(t) - F_d(t) + F_t(t) - mg \end{cases} \qquad (1)$$

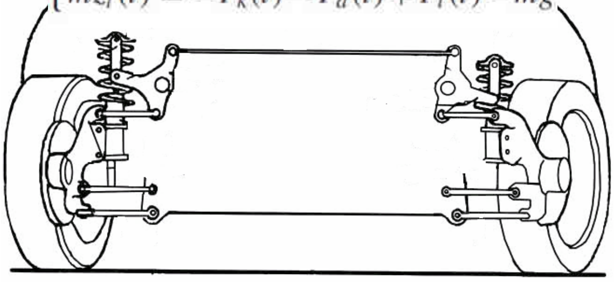

Fig.5 Sistem de suspensie, cu o legătură anti-ruliu compensatoare

**2. Concluzii**

Sistemul de suspensie este un mecanism ce face legătura intre roti şi caroseria maşinii, care transmite uniform fortele (greutatea) ce acționează asupra vehiculului către suprafața de rulare (sosea) şi, în acelaşi timp, îl izolează de fortele ce apar dinspre calea de rulare, îmbunătățind astfel

comfortul şi manevrabilitatea acestuia. Pentru asigurarea unui confort corespunzător , parametrii suspensiei trebuie să fie aleşi ținăndu-se seama de anumite condiții şi anume:
- frecvența oscilațiilor proprii pentru autoturisme să fie de 50-70 oscilații pe minut.
- rigiditatea elementelor elastice a suspensiei să fie pe cât posibil mai reduse pentru a rezulta frecvențe proprii mici.
- amortizarea oscilațiilor terbuie să fie suficientă astfel încât după o perioadă amplitudinile să se micşoreze de 3 până la 8 ori.
- indicele de bază al mersului lin al unui automobil este valoarea medie pătratică a accelerațiilor verticale măsurate în locuri caracteristice.

**MULȚUMIRI:** Această lucrare a fost realizată cu sprijinul acordat prin proiectul " QDOC - Creșterea calității studiilor doctorale în științe inginerești pentru sprijinirea dezvoltării societății bazate pe cunoaștere” contract nr. POSDRU/107/1.5/S/78534, proiect cofinanțat din Fondul Social European prin Programul Operațional Sectorial pentru Dezvoltarea Resurselor Umane 2007-2013.

**BIBLIOGRAFIE**

[1] D. Geoff Rideout , “Model complexity requirements in design of half car active suspensions controllers“
[2] Catalin Alexandru,” MODELARI DINAMICE PENTRU SISTEMUL DE GHIDARE - SUSPENSIEAL AUTOVEHICULELOR” Simpozionul național cu participare internaționalăPRoiectarea ASIstată de Calculator PRASIC 2002
[3] Jain, KK, Asthana RB. In:”Automobile Engineering”, London, Tata McGraw-Hill 2002: 293-294.
[4] Michele Ieluzzi, Patrizio Turco, Mauro Montiglio, “Development of a heavy truck semi-active suspension control“, Control Engineering Practice 14 (2006) 305–312
[5] Farzad Ahmadkhanlou., “Design, Modeling and Control of Magnetorheological Fluid-Based Force Feedback Dampers for Telerobotic Systems“, This research is based upon work supported by the National Science Foundation under Grant Number 0528395.
[6 www.carbibles.com

ISSN 1454 - 8003
**Proceedings of 2011 International Salon of Hydraulics and Pneumatics - HERVEX**
*9 – 11 November, Calimanesti-Caciulata, Romania*

# FLUID POWER FOR SUSTAINABILITY

**PhD. Eng. Heinrich THEISSEN**
Scientific Director of Institute for Fluid Power Drives and Controls – IFAS,
Aachen, Germany

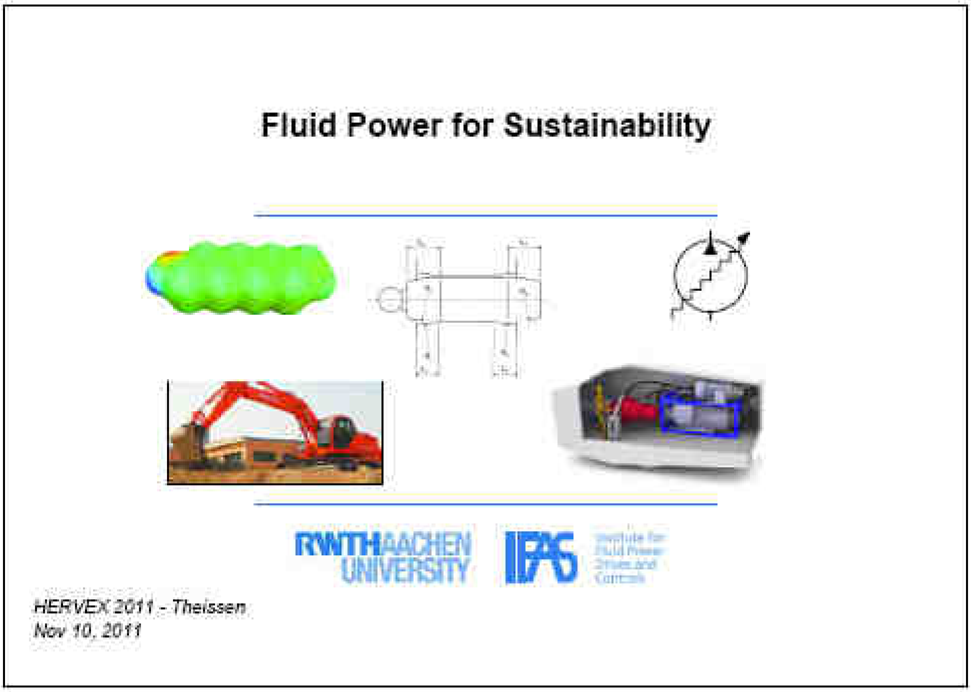


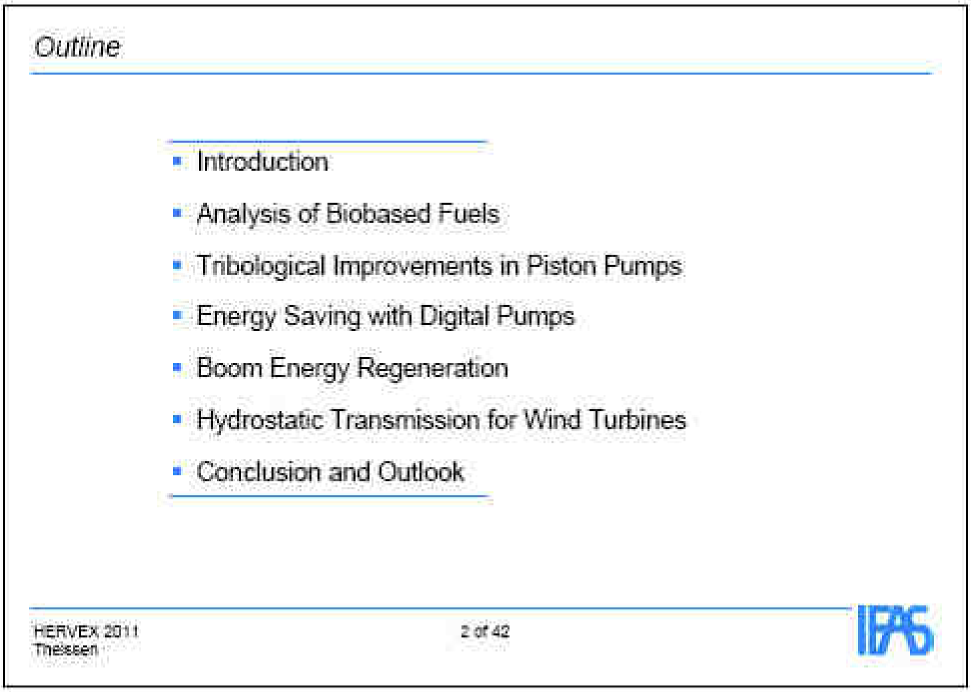

## *Introduction*

- Limited resources and growing emissions are leading to depletion, pollution and global warming, endangering our environment.
- On a planet with 7 billion people, sustainability should be priority #1.
- Some examples how fluid power can contribute to this #1 goal will be presented here:
  - New engine fuels from renewable feedstock
  - Minimizing wear and losses of hydrostatic displacement units
  - Digital pumps for improved efficiency
  - Excavator boom energy recuperation
  - Efficient and intelligent hydrostatic drives for wind turbines
- All examples are part of actual research activities.

HERVEX 2011
Theissen

3 of 42

## *Outline*

- Introduction
- Analysis of Biobased Fuels
- Tribological Improvements in Piston Pumps
- Energy Saving with Digital Pumps
- Boom Energy Regeneration
- Hydrostatic Transmission for Wind Turbines
- Conclusion and Outlook

HERVEX 2011
Theissen

4 of 42

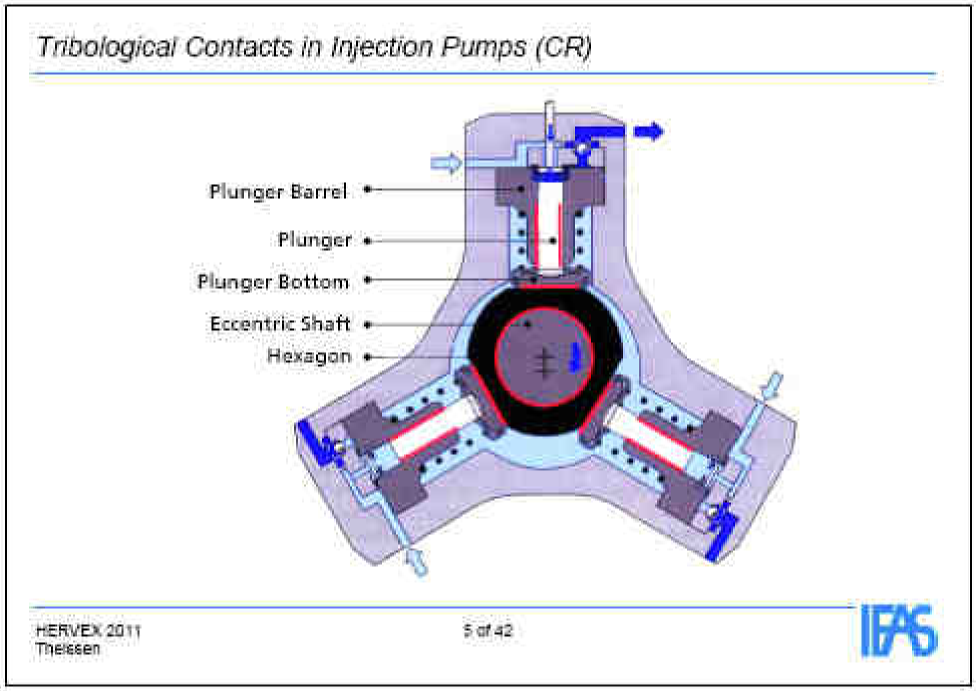
Tribological Contacts in Injection Pumps (CR)
Plunger Barrel
Plunger
Plunger Bottom
Eccentric Shaft
Hexagon
HERVEX 2011
Theissen
5 of 42
IFAS

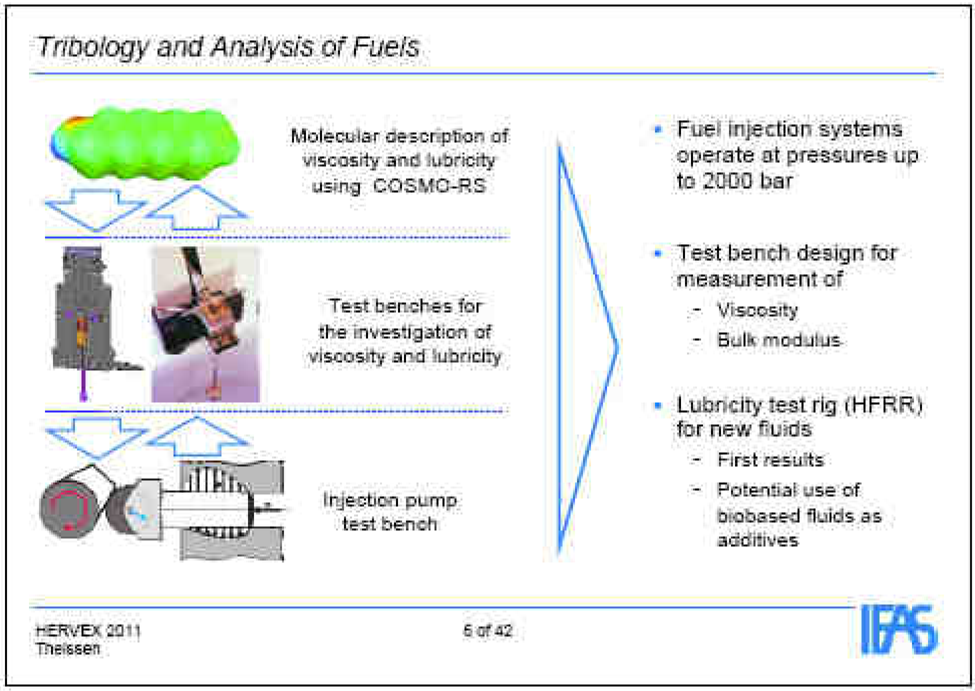
Tribology and Analysis of Fuels
Molecular description of viscosity and lubricity using COSMO-RS
Test benches for the investigation of viscosity and lubricity
Injection pump test bench
• Fuel injection systems operate at pressures up to 2000 bar
• Test bench design for measurement of
- Viscosity
- Bulk modulus
• Lubricity test rig (HFRR) for new fluids
- First results
- Potential use of biobased fluids as additives
HERVEX 2011
Theissen
6 of 42
IFAS

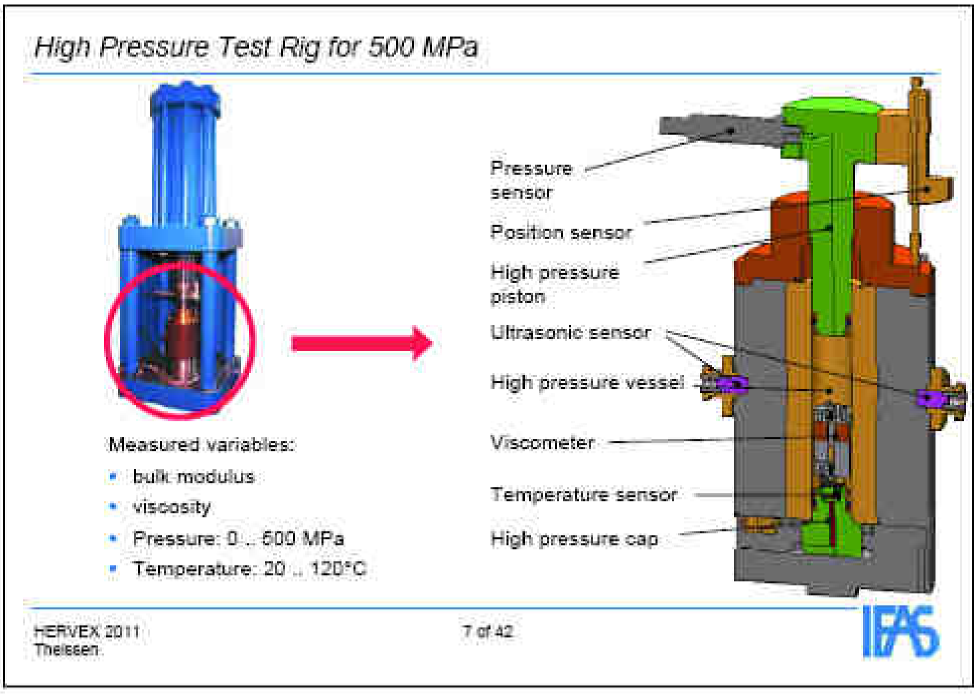
High Pressure Test Rig for 500 MPa
Pressure sensor
Position sensor
High pressure piston
Ultrasonic sensor
High pressure vessel
Viscometer
Temperature sensor
High pressure cap
Measured variables:
bulk modulus
viscosity
Pressure: 0 .. 500 MPa
Temperature: 20 .. 120°C
HERVEX 2011
Theissen
7 of 42
IFAS

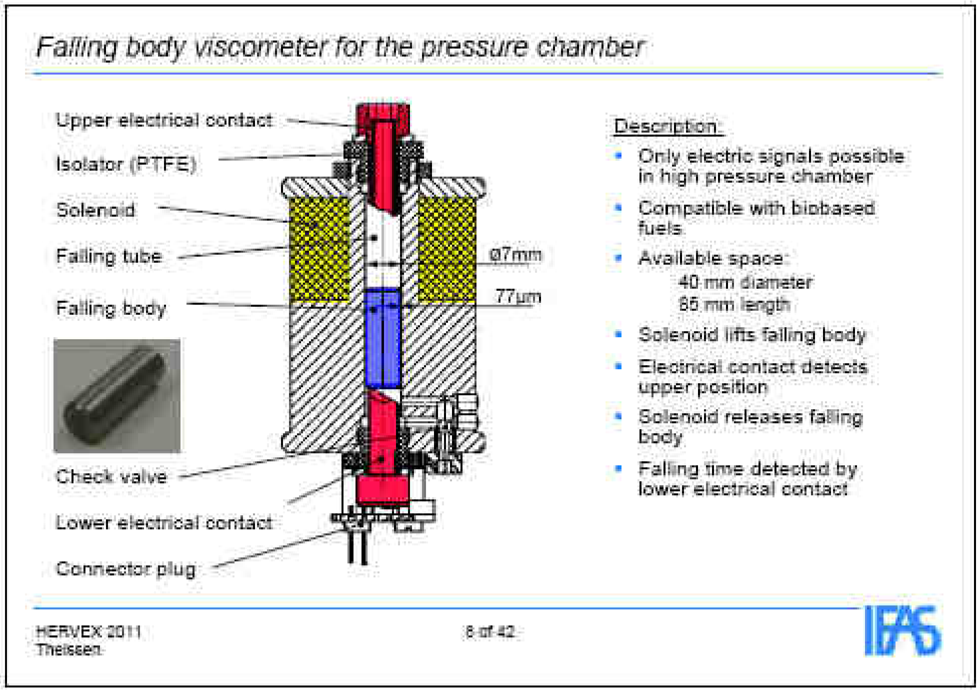
Falling body viscometer for the pressure chamber
Upper electrical contact
Isolator (PTFE)
Solenoid
Falling tube
Falling body
Check valve
Lower electrical contact
Connector plug
ø7mm
77µm
Description:
Only electric signals possible in high pressure chamber
Compatible with biobased fuels
Available space:
40 mm diameter
85 mm length
Solenoid lifts falling body
Electrical contact detects upper position
Solenoid releases falling body
Falling time detected by lower electrical contact
HERVEX 2011
Theissen
8 of 42
IFAS

*Results for viscosity of ethanol*

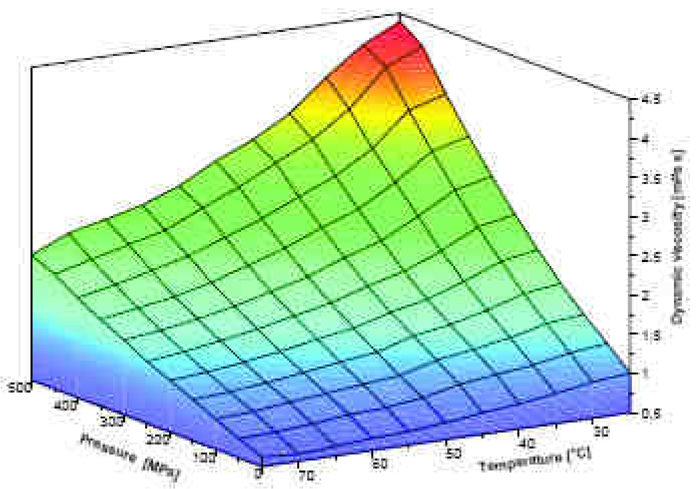


HERVEX 2011
Theissen

9 of 42

*Results for bulk modulus of bio-fuel candidates*

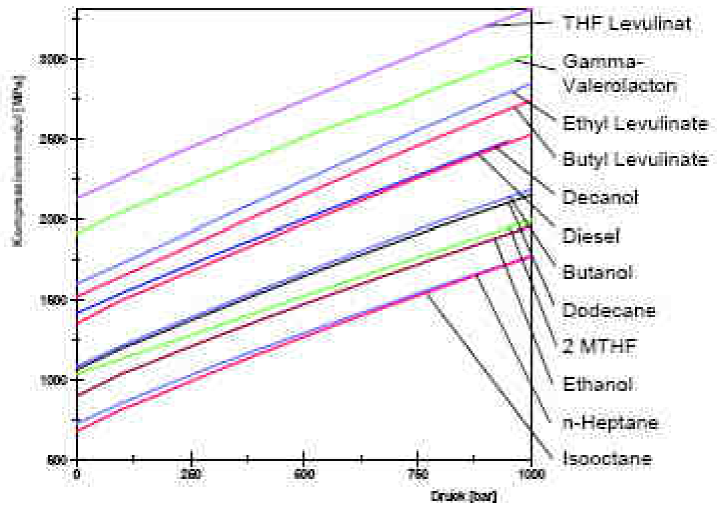


HERVEX 2011
Theissen

10 of 42

ISSN 1454 - 8003


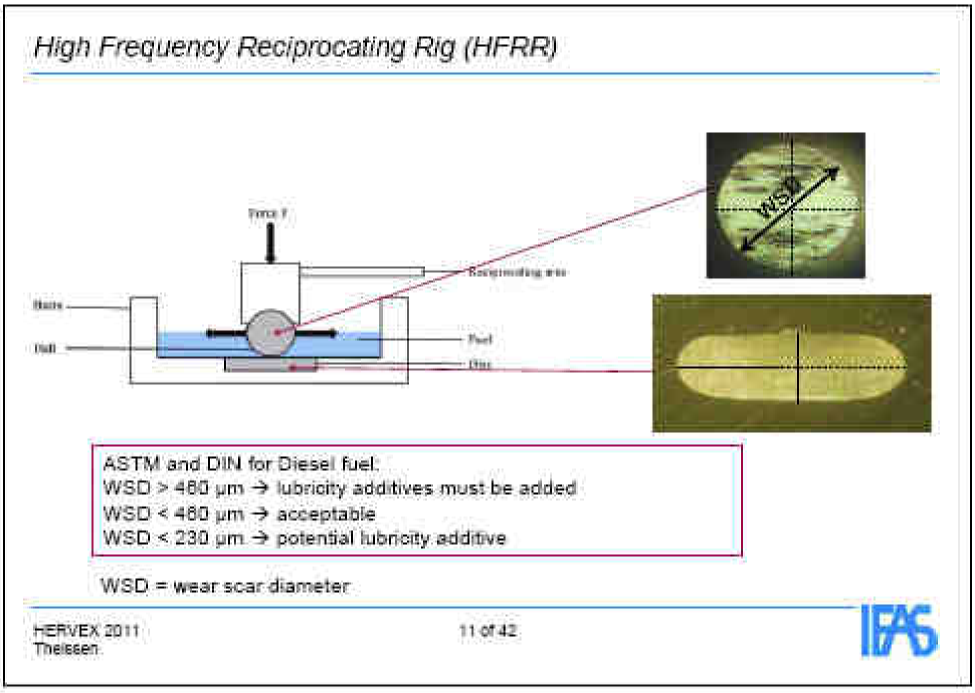


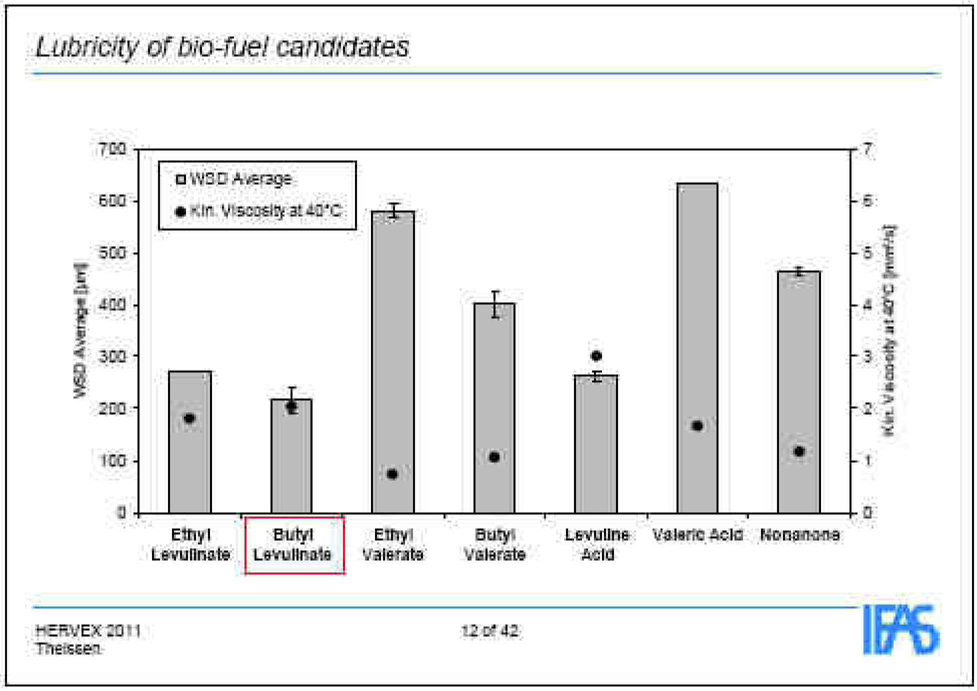

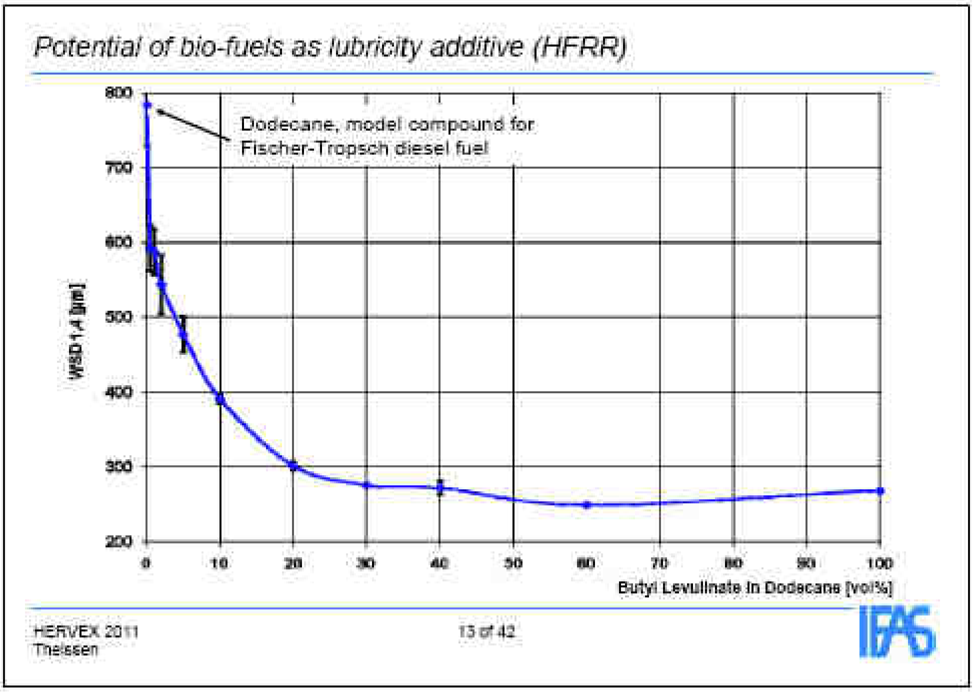
Potential of bio-fuels as lubricity additive (HFRR)
Dodecane, model compound for Fischer-Tropsch diesel fuel
WSD1.4 [µm]
800
700
600
500
400
300
200
0
10
20
30
40
50
60
70
80
90
100
Butyl Levulinate in Dodecane [vol%]
HERVEX 2011
Theissen
13 of 42

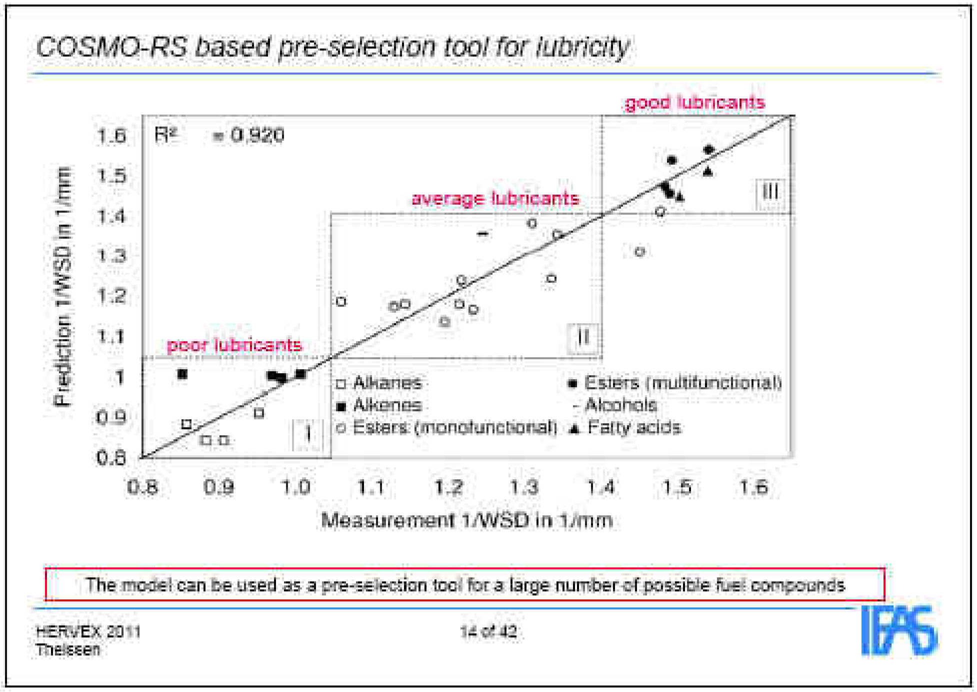
COSMO-RS based pre-selection tool for lubricity
good lubricants
average lubricants
poor lubricants
R² = 0.920
I
II
III
Prediction 1/WSD in 1/mm
Measurement 1/WSD in 1/mm
0.8
0.9
1.0
1.1
1.2
1.3
1.4
1.5
1.6
Alkanes
Alkenes
Esters (monofunctional)
Esters (multifunctional)
Alcohols
Fatty acids
The model can be used as a pre-selection tool for a large number of possible fuel compounds
HERVEX 2011
Theissen
14 of 42

*Outline*

- Introduction
- Analysis of Biobased Fuels
- Tribological Improvements in Piston Pumps
- Energy Saving with Digital Pumps
- Boom Energy Regeneration
- Hydrostatic Transmission for Wind Turbines
- Conclusion and Outlook

HERVEX 2011
Theissen

15 of 42

*Axial piston pump without copper alloys*

- Advantages:
  - Ageing of oil is slowed down
  - Environmental protection
  - Reduction of costs
  - Reduction of wear and extension of component life-time
  - ...
- Disadvantages:
  - No running-in phase no longer possible
  - Piston-cylinder contact must receive final contour before assembly
  - Pistons or cylinders should be coated to avoid seizure

HERVEX 2011
Theissen

16 of 42

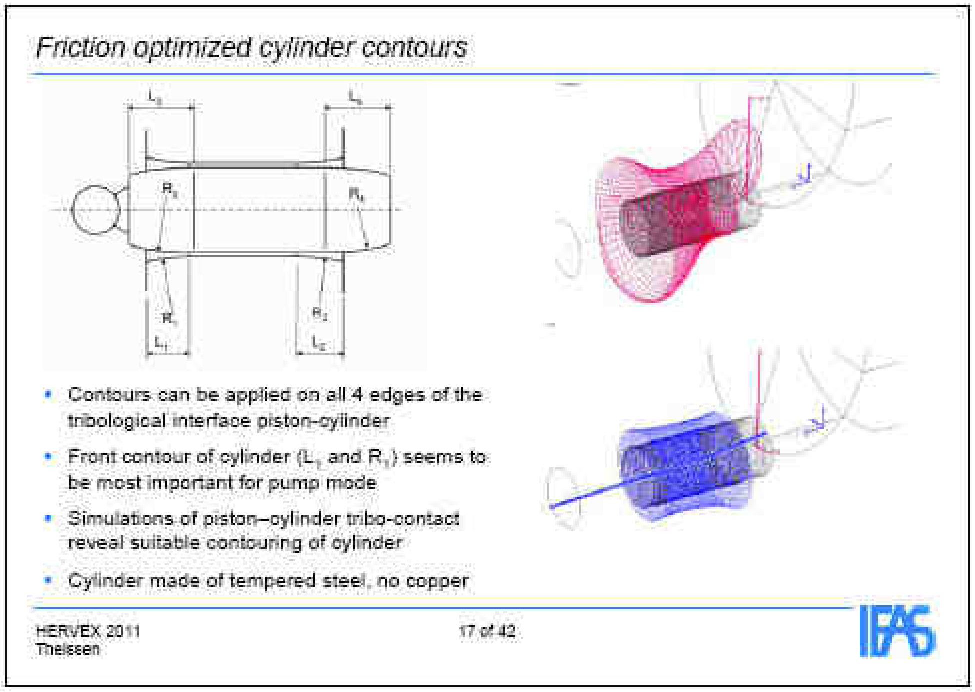
Friction optimized cylinder contours
L₁
L₄
R₃
R₄
R₁
R₂
L₁
L₂
• Contours can be applied on all 4 edges of the tribological interface piston-cylinder
• Front contour of cylinder (L₁ and R₁) seems to be most important for pump mode
• Simulations of piston–cylinder tribo-contact reveal suitable contouring of cylinder
• Cylinder made of tempered steel, no copper
HERVEX 2011
Theissen
17 of 42

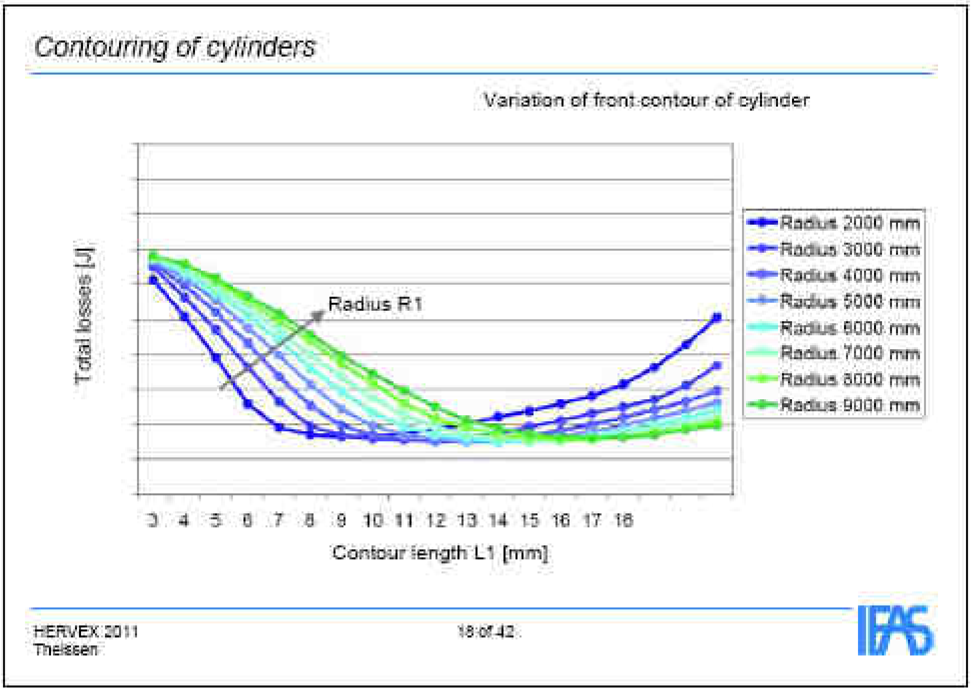
Contouring of cylinders
Variation of front contour of cylinder
Total losses [J]
Radius R1
3 4 5 6 7 8 9 10 11 12 13 14 15 16 17 18
Contour length L1 [mm]
Radius 2000 mm
Radius 3000 mm
Radius 4000 mm
Radius 5000 mm
Radius 6000 mm
Radius 7000 mm
Radius 8000 mm
Radius 9000 mm
HERVEX 2011
Theissen
18 of 42

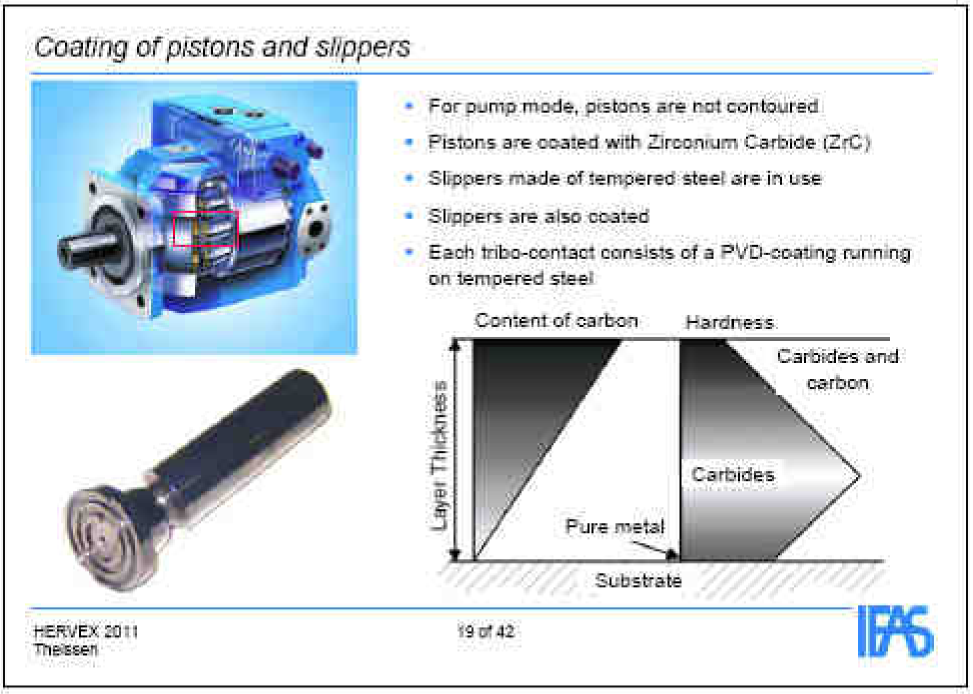
Coating of pistons and slippers
For pump mode, pistons are not contoured
Pistons are coated with Zirconium Carbide (ZrC)
Slippers made of tempered steel are in use
Slippers are also coated
Each tribo-contact consists of a PVD-coating running on tempered steel
Content of carbon
Hardness
Carbides and carbon
Layer Thickness
Carbides
Pure metal
Substrate
HERVEX 2011
Theissen
19 of 42

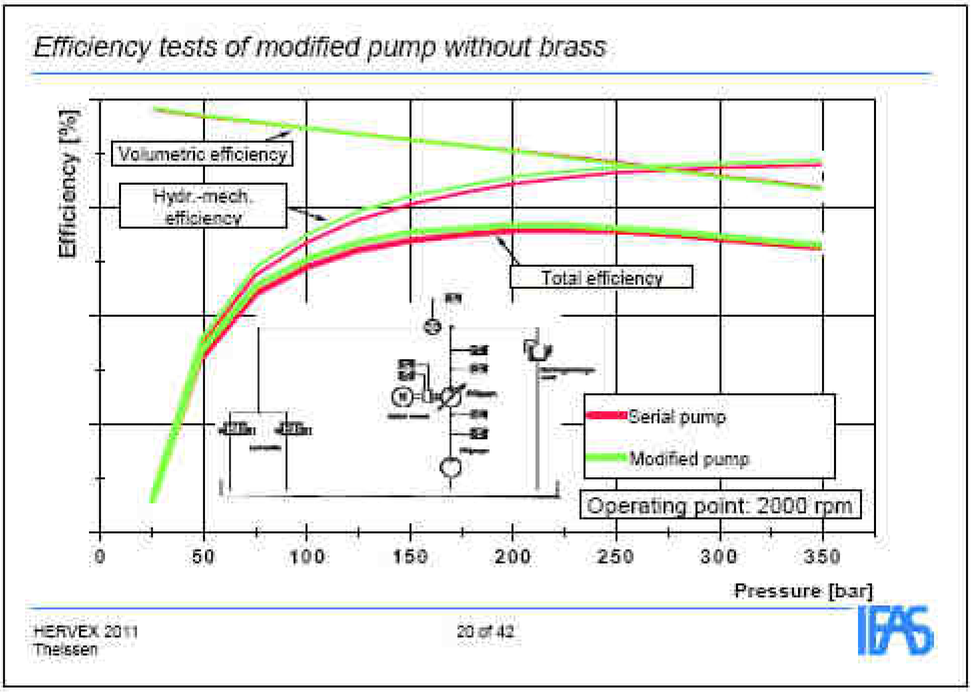
Efficiency tests of modified pump without brass
Efficiency [%]
Volumetric efficiency
Hydr.-mech. efficiency
Total efficiency
Serial pump
Modified pump
Operating point: 2000 rpm
0
50
100
150
200
250
300
350
Pressure [bar]
HERVEX 2011
Theissen
20 of 42

ISSN 1454 - 8003
Proceedings of 2011 International Salon of Hydraulics and Pneumatics - HERVEX
9 – 11 November, Calimanesti-Caciulata, Romania

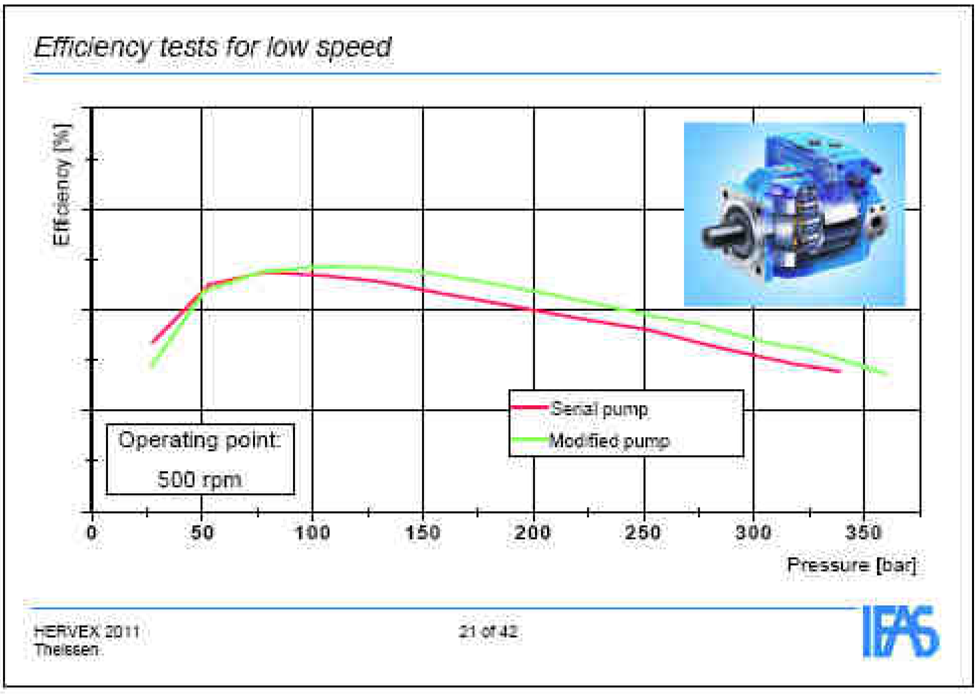


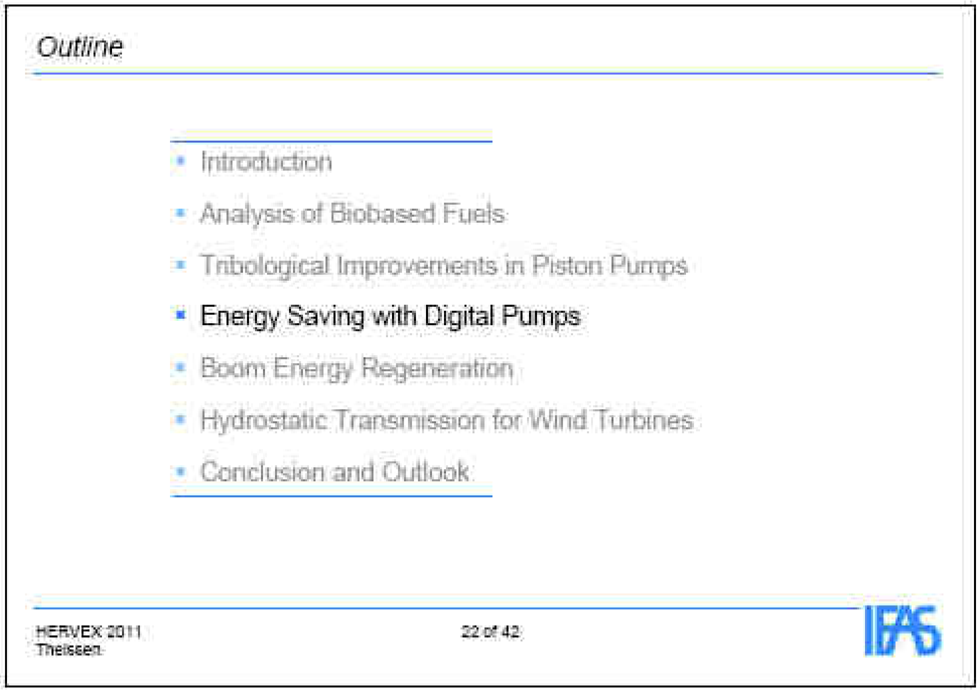

*Digital pumps*

Digital pump drives have been simulated

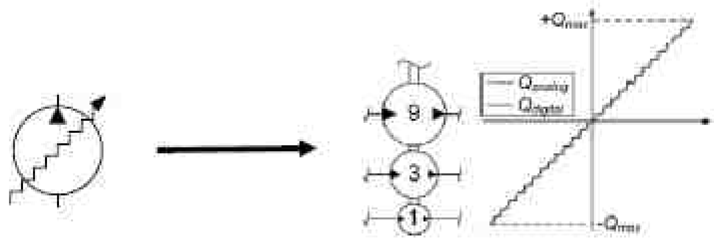


HERVEX 2011
Theissen

23 of 42

*Digital pump: pump mode, idle mode, and motor mode*

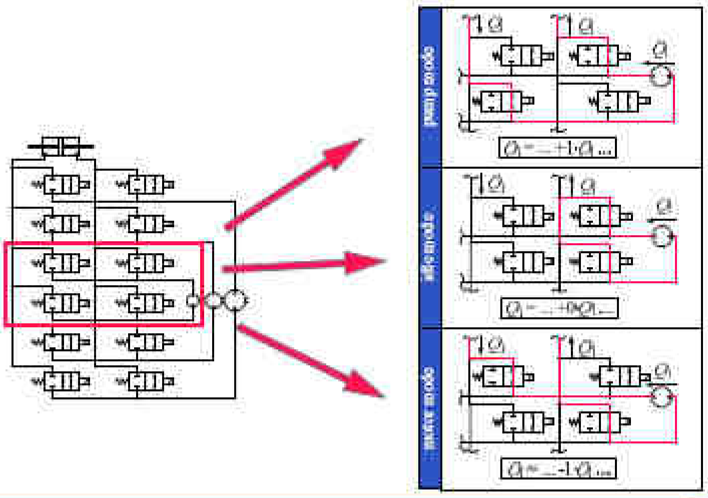

HERVEX 2011
Theissen

24 of 42

## *Binary vs. ternary gradation*

**Binary gradation**

- $2^k$ flow rates
- no motor mode

| 1 | 2 | 4 | Q |
|---|---|---|---|
| | | | 0 |
| + | | | 1 |
| | + | | 2 |
| + | + | + | 3 |
| | | + | 4 |
| + | | + | 5 |
| | + | + | 6 |
| + | + | + | 7 |

**Ternary gradation**

- $3^k$ flow rates
- motor mode necessary

| 1 | 3 | 9 | Q |
|---|---|---|---|
| | | | 0 |
| + | | | 1 |
| – | + | | 2 |
| | + | | 3 |
| + | + | | 4 |
| – | – | + | 5 |
| | – | + | 6 |
| + | – | + | 7 |
| – | | + | 8 |
| | | + | 9 |
| + | | + | 10 |
| – | + | + | 11 |
| | + | + | 12 |
| + | + | + | 13 |

k: number of parallel constant pumps

HERVEX 2011
Theissen

25 of 42

## *Basic closed circuit layouts A and B*

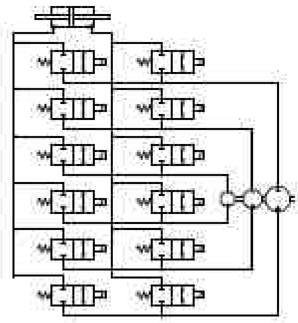

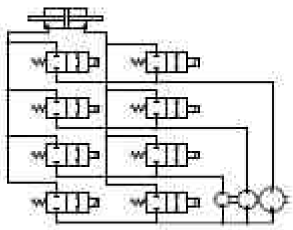

**System layout A:**

- binary and ternary
- motor, pump and idle modes
- $3^k$ pump states

**System layout B:**

- only binary
- pump and idle mode
- $2^k$ pump states

HERVEX 2011
Theissen

26 of 42

## Efficiency, binary vs. ternary

B

T

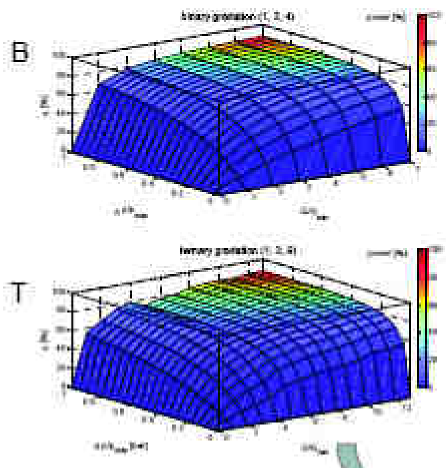

| 1 | 3 | 9 | Q |
|---|---|---|---|
| | | | 0 |
| + | | | 1 |
| - | + | | 2 |
| | + | | 3 |
| + | + | | 4 |
| - | - | + | 5 |
| | - | + | 6 |
| + | - | + | 7 |
| - | | + | 8 |
| | | + | 9 |
| + | | + | 10 |
| - | + | + | 11 |
| | + | + | 12 |
| + | + | + | 13 |


HERVEX 2011
Theissen

27 of 42

## System structure

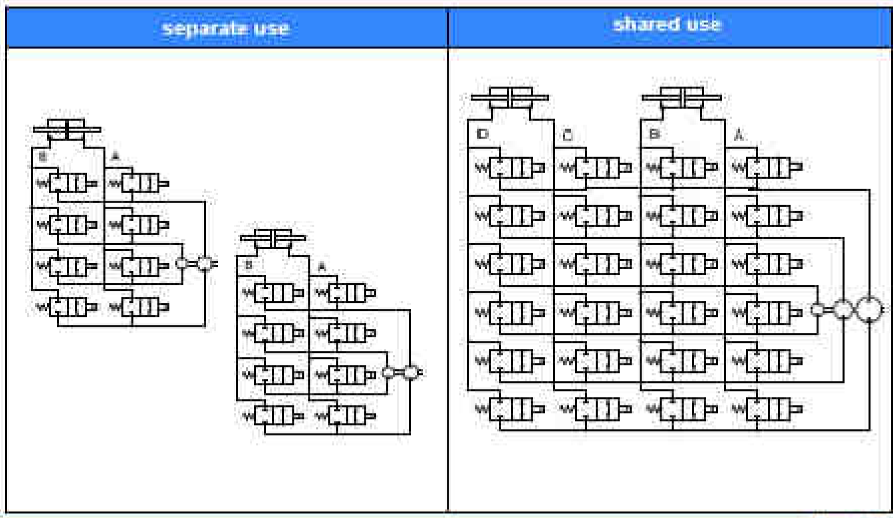


HERVEX 2011
Theissen

28 of 42

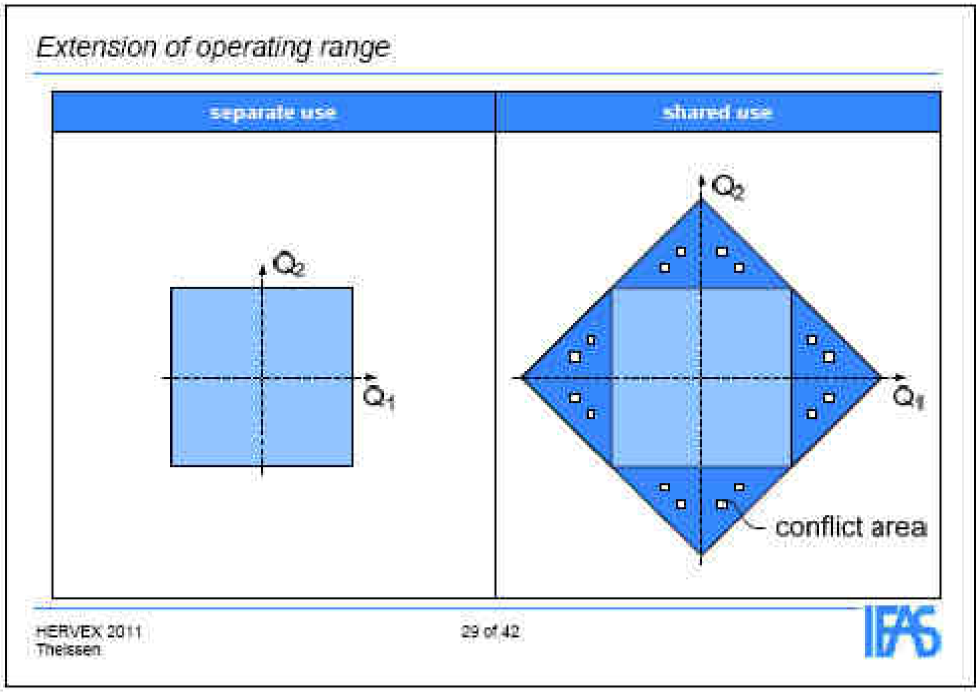
Extension of operating range
separate use
shared use
Q2
Q1
conflict area
HERVEX 2011
Theissen
29 of 42
IFAS

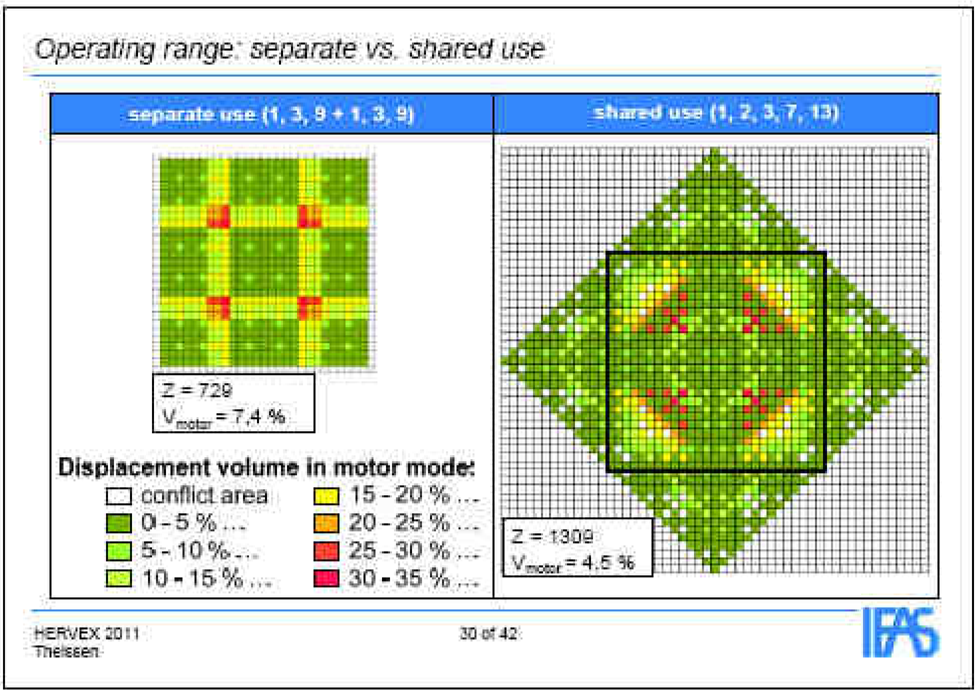
Operating range: separate vs. shared use
separate use (1, 3, 9 + 1, 3, 9)
shared use (1, 2, 3, 7, 13)
Z = 729
V motor = 7,4 %
Displacement volume in motor mode:
conflict area
0 - 5 % ...
5 - 10 % ...
10 - 15 % ...
15 - 20 % ...
20 - 25 % ...
25 - 30 % ...
30 - 35 % ...
Z = 1309
V motor = 4.5 %
HERVEX 2011
Theissen
30 of 42
IFAS

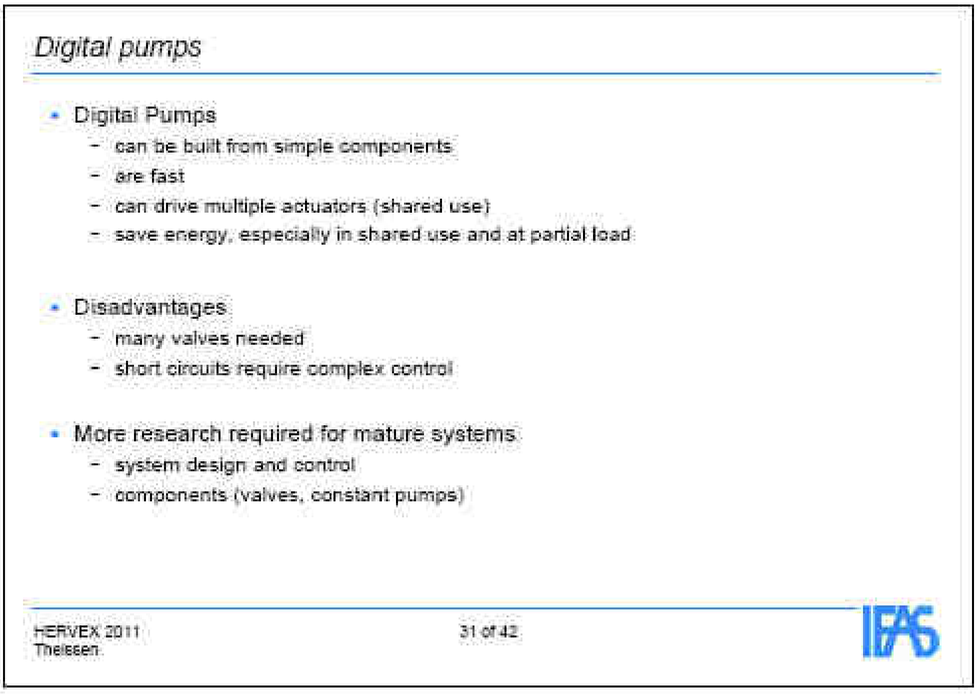
Digital pumps
Digital Pumps
can be built from simple components
are fast
can drive multiple actuators (shared use)
save energy, especially in shared use and at partial load
Disadvantages
many valves needed
short circuits require complex control
More research required for mature systems
system design and control
components (valves, constant pumps)
HERVEX 2011
Theissen
31 of 42
IFAS

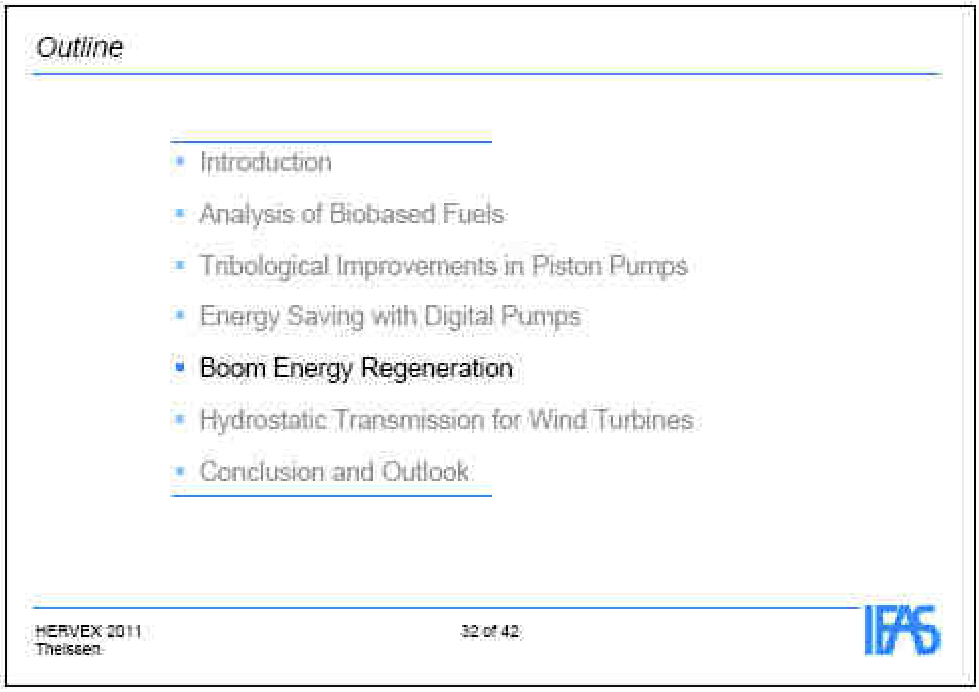
Outline
Introduction
Analysis of Biobased Fuels
Tribological Improvements in Piston Pumps
Energy Saving with Digital Pumps
Boom Energy Regeneration
Hydrostatic Transmission for Wind Turbines
Conclusion and Outlook
HERVEX 2011
Theissen
32 of 42
IFAS

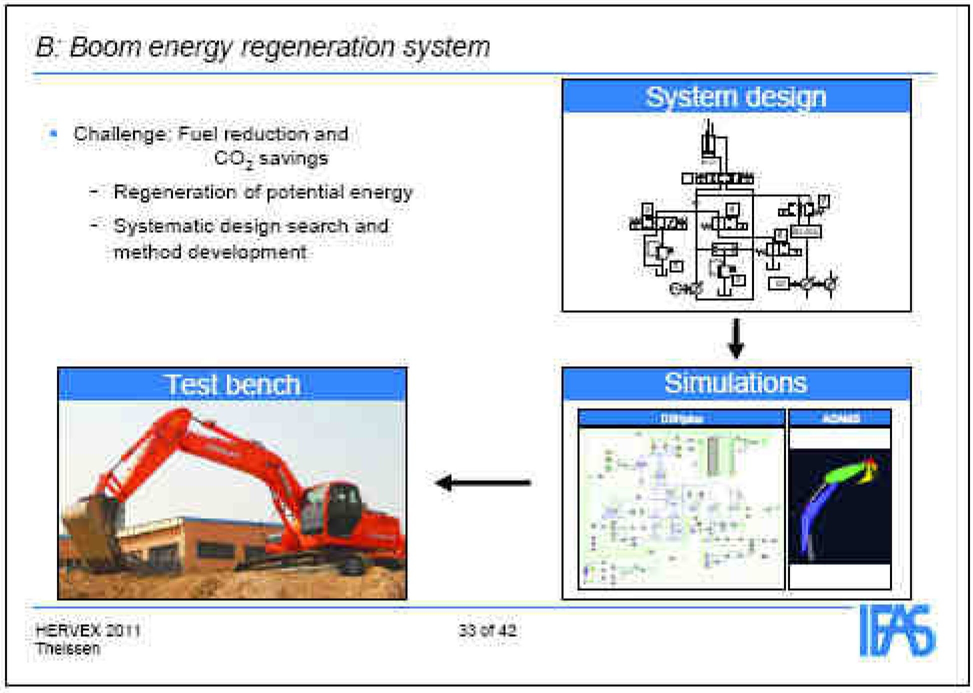
B: Boom energy regeneration system
Challenge: Fuel reduction and $CO_2$ savings
- Regeneration of potential energy
- Systematic design search and method development
System design
Simulations
Test bench
HERVEX 2011
Theissen
33 of 42
IFAS

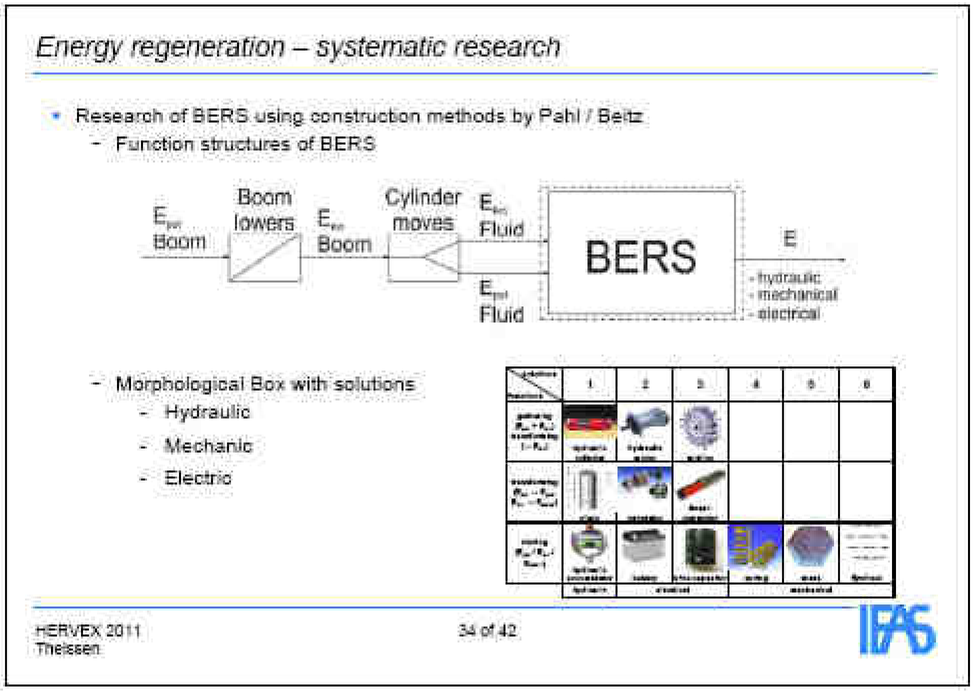
Energy regeneration – systematic research
Research of BERS using construction methods by Pahl / Beitz
- Function structures of BERS
$E_{pot}$ Boom
Boom lowers
$E_{kin}$ Boom
Cylinder moves
$E_{kin}$ Fluid
$E_{pot}$ Fluid
BERS
E
- hydraulic
- mechanical
- electrical
- Morphological Box with solutions
- Hydraulic
- Mechanic
- Electric
1
2
3
4
5
6
HERVEX 2011
Theissen
34 of 42
IFAS

## *Energy regeneration – system design*

- Development of different concepts for the Boom Energy Regeneration System
  - Hydraulic Systems
  - Mechanical Systems
  - Electrical Systems
  - Compound Systems

Exemplary systems

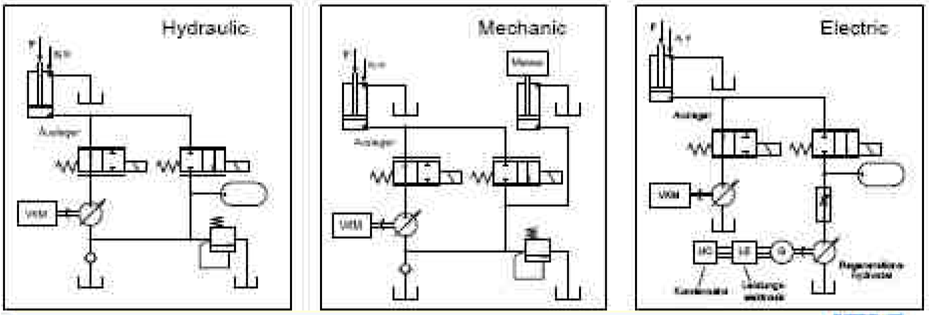


HERVEX 2011
Theissen

35 of 42

## *Energy regeneration – simulation results*

- New system has the same operating behaviour as the standard excavator
  ➔ operator does not feel any differences
- Increased efficiency compared to standard excavator for boom rising and lowering
  ➔ About 54 % of the potential energy of the boom can be regenerated

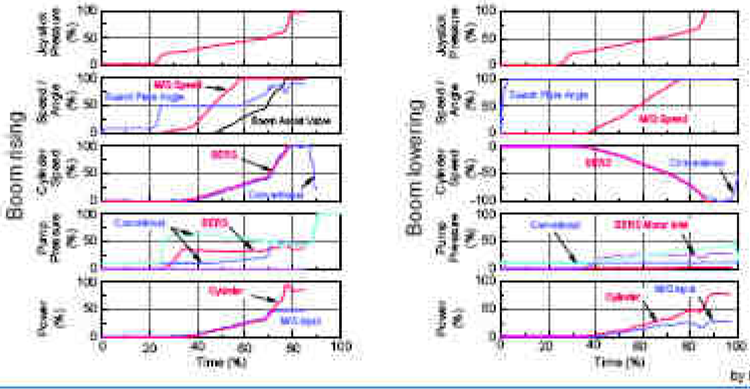


by Kang et al., Doosan

HERVEX 2011
Theissen

36 of 42

*Outline*

- Introduction
- Analysis of Biobased Fuels
- Tribological Improvements in Piston Pumps
- Energy Saving with Digital Pumps
- Boom Energy Regeneration
- Hydrostatic Transmission for Wind Turbines
- Conclusion and Outlook

HERVEX 2011
Theissen

37 of 42

*Test bench design*

**Challenges**

- Drive with high torque at low speed
- Applying dynamic loads
- Minimize installed electrical power

**Test bench layout**

- Hydrostatic power feed-back
- Generators replaced by electrical motors and axial piston pumps
- Turbine is simulated by radial piston motor
- Drive is controlled by variable displacement pumps

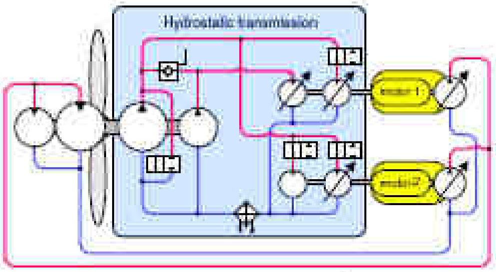


HERVEX 2011
Theissen

38 of 42

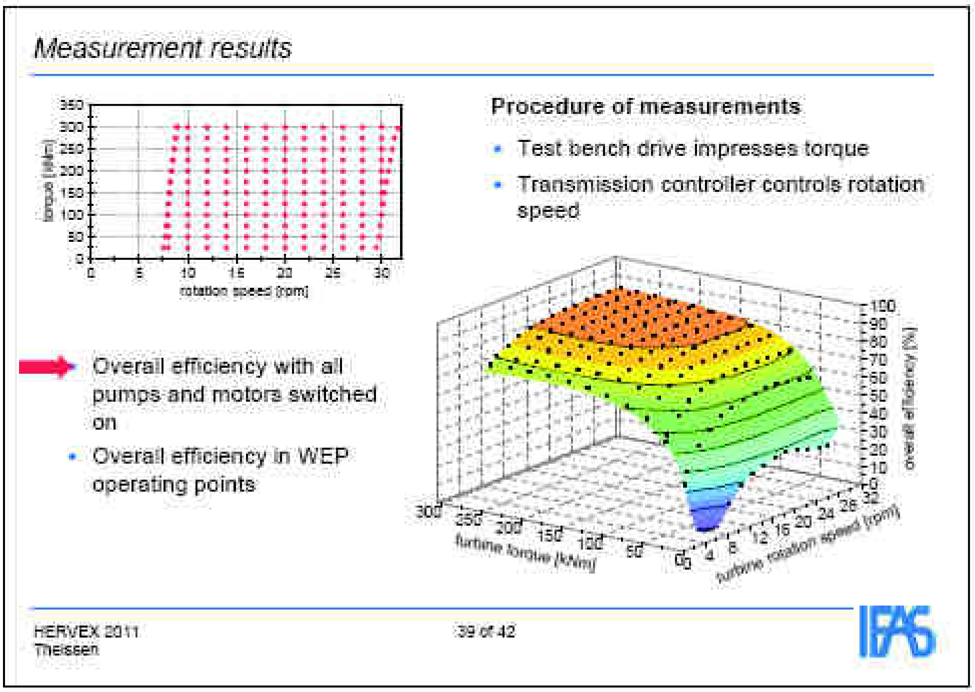
Measurement results
torque [kNm]
rotation speed [rpm]
Procedure of measurements
Test bench drive impresses torque
Transmission controller controls rotation speed
Overall efficiency with all pumps and motors switched on
Overall efficiency in WEP operating points
overall efficiency [%]
turbine torque [kNm]
turbine rotation speed [rpm]
HERVEX 2011
Theissen
39 of 42
IFAS

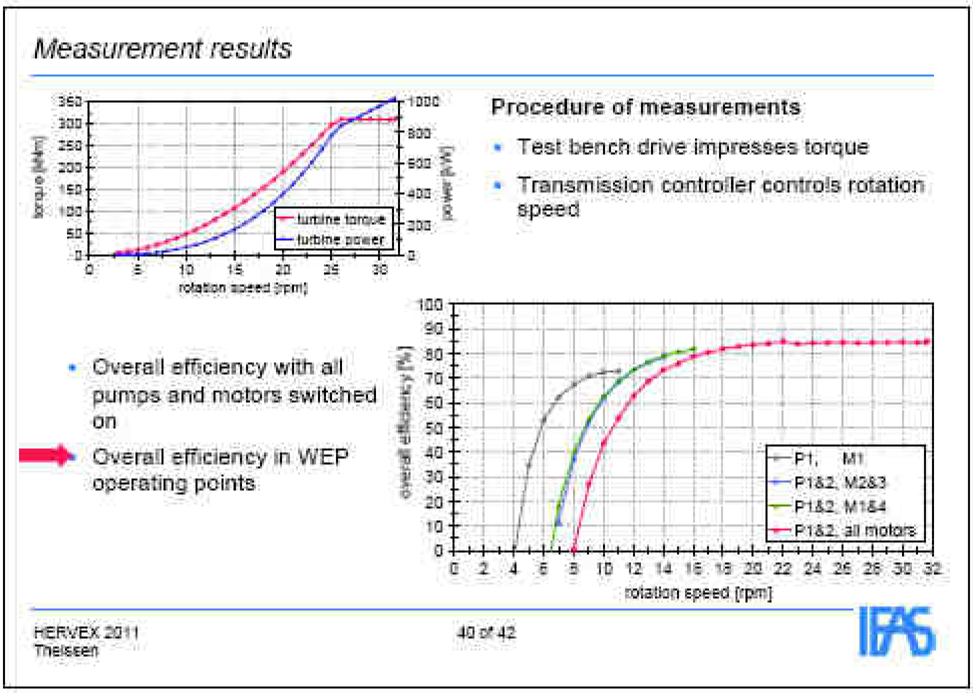
Measurement results
torque [kNm]
power [kW]
rotation speed [rpm]
turbine torque
turbine power
Procedure of measurements
Test bench drive impresses torque
Transmission controller controls rotation speed
Overall efficiency with all pumps and motors switched on
Overall efficiency in WEP operating points
overall efficiency [%]
rotation speed [rpm]
P1, M1
P1&2, M2&3
P1&2, M1&4
P1&2, all motors
HERVEX 2011
Theissen
40 of 42
IFAS

## *Outline*

- Introduction
- Analysis of Biobased Fuels
- Tribological Improvements in Piston Pumps
- Energy Saving with Digital Pumps
- Boom Energy Regeneration
- Hydrostatic Transmission for Wind Turbines
- Conclusion and Outlook

HERVEX 2011
Theissen

41 of 42

## *Conclusion and Outlook*

- Fluid power can contribute to save natural resources and increase efficiency
- Biobased fluids are suitable for energetic use and some even as additives
- Incremental innovations help existing piston pump designs to minimize losses
- Digital pumps in shared use offer energy saving potential
- System approach is important for the design of drive trains and work hydraulics including the combustion engine
- Important potential for fluid power drives with switchable units in wind turbines

---

- Advancing fluid power components and systems remains a rewarding challenge for the future towards the stated goals
- The innovation process for fluid power requires excellently educated engineers and scientists
- Satisfying these requirements by universities and companies will lay the foundation for continuing growth of our industry

HERVEX 2011
Theissen

42 of 42

**ISSN 1454 - 8003**
**Proceedings of 2011 International Salon of Hydraulics and Pneumatics - HERVEX**
*9 – 11 November, Calimanesti-Caciulata, Romania*

# SELECTION OF MATERIALS TO FABRICATE PRESSURE CONTROL VALVE COMPONENTS FOR WATER HYDRAULICS SYSTEMS APPLICATION - SELECTED ASPECTS

Andrzej Sobczyk*, Paweł Walczak**

**Dr Eng.,email:sobczyk@mech.pk.edu.pl,**MSc.Eng.,email:walczakp@mech.pk.edu.pl*
*Cracow University of Technology, Krakow, Poland*

**Key words: Water hydraulics, application, design, new materials and technology**

## 1. Introduction

Water hydraulics systems are relatively recent, dating back to 1978 in Great Britain where research work was undertaken to utilise seawater as a hydrostatic medium for power transmission systems and new designs of valves and hydraulic units were developed accordingly. In 1994 the Danish company Danfoss, a well-established manufacturer of oil hydraulics components, introduced a water hydraulic system technology utilising tap water allowing the application of high pressures and flow rates in hydraulic systems [10].

Presently water hydraulics systems are used by companies for several reasons:

- reduced risk of a fire,
- reduction of operating costs,
- replacement of conventional fluids in applications requiring large volumes of the working medium, to reduce costs,
- lower risk of contamination of products,
- environmental regulations;

Water is an easily available and commonly used medium, hence the acquisition costs are negligible in relation to traditional hydraulic media and are in fact independent of its market demand and supply level.

Costs involved in transport, storage and safe-keeping are also lower. The regulations currently in force in several countries have prompted the withdrawal of certain media, even biodegradable and non-toxic fluids, imposing additional fees upon the users and those fees will certainly increase in the future. Fluids with water admixtures are hardly flammable whilst pure water is inflammable – which reduces the costs of fire insurance. When tap water is used, there is no risk of the personnel being poisoned by oil vapours, water is safe for the eyes and the skin. In certain sectors of industry, the purity of manufactured products is a major concern. Contamination with oil precludes further processing of fabrics or wood (dyeing, lacquering), changes the colour of paper, leads to modification of chemical compounds in medicines, changes the taste of food. Contaminated products must not be admitted for sale, which involves considerable losses to manufacturers.

## 2. Water as a working medium

The use of water as the working medium poses new challenges for system designers (in comparison to oil hydraulics) and the following problems have to be addressed:

- internal and external leakages;
- erosion and corrosion;
- the maximal working temperature;
- development of microorganisms;
- hydraulic hammer effects in the system;
- lubrication of moving parts;

Meeting new requirements involves higher manufacturing costs of hydraulic system components, yet as they are becoming more widespread and the production volumes increase, the unit price will certainly go down.

Water has lower viscosity than oil and hence it is difficult to maintain the system tight-proof. Valves intended for water hydraulics have components tight-fitted, to reduce the leakages. For that very reasons, some parts are made from plastics and ceramic materials. Proper connections inside the valves ensure that the flow becomes less turbulent and proceeds at a lower speed (despite smaller viscosity of water and its greater specific gravity in relation to oil), which helps reduce the erosion of materials. Corrosion can be eliminated through the use of specific materials, such as stainless steel, brass, anodised aluminium, glass fibre, PVC and other plastics and as well as anti-corrosion coatings. Lubrication of moving parts in valves and pumps is a problem that can be solved by using special sealing materials (self-lubricating sealings), coatings or water admixtures. The working temperature range is restricted by the properties of water and materials from which valve components are made. The approximate working range is taken to be 2-50 $^{o}$C. The lower limit can be further decreased by adding admixtures that lower the freezing temperature. The growing bacteria in the tank can cause filters clogging and produce an unpleasant smell. We can battle against bacteria by the use of UV light or pasteurised water and by adding bactericides. To hinder bacteria from getting into water, the water tanks have to be properly sealed and air filters installed.

### 3. Properties of materials

The valve considered in the study is intended for use in a water hydraulic and oil hydraulic systems, so it has to be made of carefully selected materials. One has to bear in mind that treatment of corrosion-resistant steels required different technologies and tools than those used when working standard steels.

Generally, stainless steels are hard to treat. Their reduced machinability adds to their tendency to strain hardening, low thermal conductivity and high ductility. To make steel more workable, sulphur has to be added, in consequence leading to formation of magnesium sulphide inclusions producing short, brittle chips during treatment, smoother surfaces and reducing the tool wearing. Steels that are easier to treat due to the presence of non-metallic admixtures easily succumb to pitting corrosion so these should not be used in more aggressive environments (for example in seawater), besides, their ductility is impaired. Resistance to pitting corrosion increases with chromium, nickel and manganese contents in steel. These elements have a strong influence on stability of the austenite phase (Fig 1), improving the steel's resistance to corrosion. Several manufacturers world-wide produce workable stainless steels whose mechanical properties, weldability and corrosion resistance are the same as those displayed by their hard-to-treat counterparts, however the manufacturing technologies are all patented.

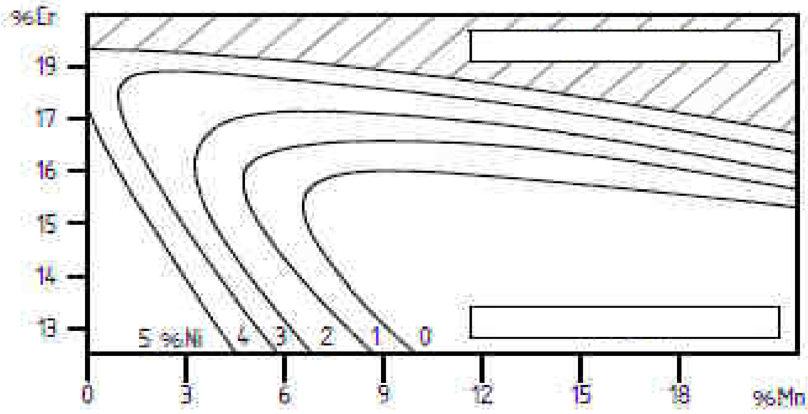


Fig 1. Stability of the austenite phase at 1075 $^{o}$C

## 4. Treatment procedures and tools

Tools for working stainless steels can be made from high-speed steels, brass carbides, sintered carbides, ceramet, ceramic materials. Depending on the steel grade, the cutting speed during the rough turning ranges from 100 to 800 m/min, the advance rate being 0.1- 0.3 mm per revolution. The cutting depth should not exceed 1.9 mm. Drills and reamers to be used when handling stainless steels are made from fast-speed steels. The drilling rate falls in the range 16-40 m/min, the advance rate being 0.07-0.3 mm per revolution. The mill cutting operations use inserts made from sintered carbides. The milling speed falls in the range 90-200 m/min for tools made from sintered carbides and 50-150 m/min for tools made from other materials. The respective advance rates are: 0.012 and 0.125 mm/revolution. When stainless steels are milled, larger cutting forces are produced, which necessitates the lowering of the treatment parameters or application of high-power mill cutters. Threading operations are very difficult when treating stainless steels (especially austenite steels), particularly when working holes with small diameter. During this operation chips are formed which may eventually damage the tool. To prevent that, three-or four-grooved threaders are used. The threading rate ranges from 5 to 30 m/min. Threading requires the use of lubricants and of chip-breaking tools. The threads are cut with knifes with sintered carbide inserts, using threading dies and flat dies fixed in the spindle.

The thread cutting rate ranges from 5 to 25 m/min. Grinding operations are performed with the use of abrasive discs containing corundum or carborundum particles, at the rate of 20-30 m/s. Stainless steels displaying the martensite structure can be subjected to thermal treatment and the hardness of heat-hardened steels depends on the carbon contents (Fig 2).

## 5. Materials

All components of the designed valve are made of corrosion-resistant materials or have a protective coating. Small elements requiring thermal treatment are made of steel grade 4H13, those not requiring thermal treatment are made of steel 0H18N9 and tin-coated steel A10X, the spring is made from wire SANDVIK 12R10. The properties of selected stainless steels are summarised in Table 2, those of the wire- in Table 3.

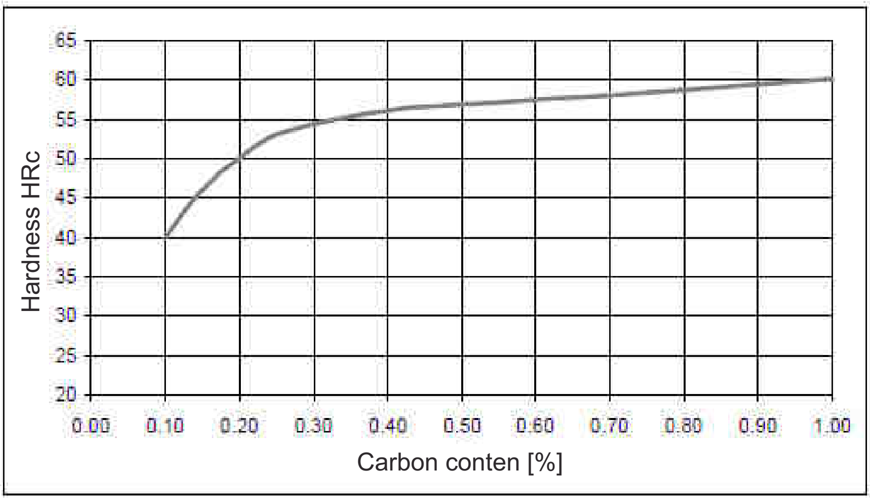


Fig 2. Carbon content vs hardness of corrosion-resistant, heat-treated marteniste steels

Table 2. Chemical composition and properties of corrosion-resistant steels [1]

| Designaction from Polish Standard | | 0H18N9 | 0H17N14M2 | 0H22N24M4TCu | 2H13 | 4H13 |
|---|---|---|---|---|---|---|
| Designaction from European Standard | | 1.4301 | 1.4404 | 1.4539 | 1.4021 | 1.4031 |
| | $C_{max}$ | 0,07 | 0,03 | 0,02 | 0,16 – 0,25 | 0,36 – 0,42 |
| | $Si_{max}$ | 1 | 1 | 0,7 | 1 | 1 |
| | $Mn_{max}$ | 2 | 2 | 2 | 1,5 | 1 |
| | $P_{max}$ | 0,045 | 0,045 | 0,03 | 0,04 | 0,04 |
| | $S_{max}$ | 0,015 | 0,015 | 0,01 | 0,015 | 0,015 |
| | Cr | 17 – 19 | 16,5 – 18,5 | 19 – 21 | 12 – 14 | 12,5 – 14,5 |
| | Ni | 8 – 10,5 | 10 – 13 | 24 – 26 | - | - |
| | Cu | - | - | 1,2 – 2 | - | - |
| | Mo | - | 2 – 2,5 | 4 – 5 | - | - |
| | $N_{max}$ | 0,11 | 0,11 | 0,15 | - | - |
| Hardness $HB_{max}$ | | 215 | 200 | 230 | 225 | 240 |
| $R_{m\ max}$ [MPa] | | 540 – 750 | 530 – 680 | 530 – 730 | 700 | 740 |
| $R_{e0,8\ max}$ [MPa] | | 230 | 240 | 240 | 345 | 345 |
| A5 [%] | | 45 | 40 | 35 | 15 | 15 |
| Resistance to corrosion in seawater in 20 °C | | Partial | Total | Total | Not resistant | Not resistant |
| Structure | | Austenite | Austenite | Austenite | Martensite | Martensite |
| Weldability | | Weldable | Weldable | Weldable | Hard-to-weld | Not weldable |
| Workability | | Easily workable | Easily workable | Hard-to-work | Hard-to-work | Hard-to-work |
| Thermal treatment | | Solution heat treatment 1000-1100 °C | Solution heat treatment 1020-1120 °C | Solution heat treatment 1020-1100 °C | quenching 980-1050 °C, tempering 660-770 °C | quenching 1000-1050 °C, tempering 100-300 °C |

Table 3. Properties of the wire used to make a spring 12R10

| Material | SANDVIK 12R10 | | | | | |
|---|---|---|---|---|---|---|
| Chemical composition [%] | C | Si | Mn | | Cr | Ni |
| | 0,08 | 0,6 | 1,2 | | 18 | 9 |
| Shear modulus G [MPa] | 70000 | | | | | |
| | Wire diameter [mm] | | | | | |
| Tensile strength $R_m$ [MPa] | 2,5 – 3,0 | | 3,0 – 3,5 | | 3,5 – 4,25 | |
| | 1600 – 1800 | | 1600 – 1800 | | 1550 - 1750 | |

The valve head is guided in the housing with the use of the PTFE tape, having a very low friction coefficient. The coefficients of static and operational friction are very similar, hence the scuffing and stick-slip effects will not occur. The valve is sealed with o-rings made from NBR80. These two materials can be well used in contact with mineral oils and water, in the specified range of working temperatures. Properties of the selected sealing material are summarised in Table 4.

Table 4.

| Name | Working temperature | Range of applications and properties |
|---|---|---|
| **NBR**<br><br>Elastomer<br>Nitrile butadiene rubber | From – 30<br>to + 110 °C | Special-purpose material, highly resistant to media used in hydraulics and pneumatics. Resistant to oil-based hydraulic fluids, oils and vegetable and animal fats, inflammable fluids (HFA, HFB, HFC), aliphatic hydrocarbons (propane, butane, gasoline), silicone oils and fats, water up to +80°C, air, bio-oils containing synthetic esters, vegetable oils, energising elements in hydraulic sealings |

## 6. Summing-up

Designing hydraulic components intended for water hydraulic systems is a most complex and cumbersome task, requiring an extensive expertise in the field of hydraulics and mechanics as well as wide engineering experience. Physical and chemical properties of water represent a major challenge, hence the need to carefully select the materials to fabricate valve housings and kinematic pairs in which metallic parts will not be cooperable for the lack of a lubricating film. In very few solutions now available worldwide, we find interlayers made from plastics, composite or ceramic materials. These solutions are the result of extensive research work and their chemical composition and manufacturing technologies are, naturally, protected from copying.

In the light of these consideration, own research work aimed to develop new materials to be used to fabricate the components of water hydraulics systems is fully merited. For example, the research program on sealing in cylinders reported in the work by W. Okularczyk and A. Sobczyk [8] summarises the testing done on sealing of the piston rod made from UHMPWE and guiding rings made from Kefloy 22. It is a composite material obtained by adding 23% of carbon and 2% of graphite to the polymer PTFE. Tests reveal that Kefloy displays better lubricating properties and is a better alternative to be used in the water environment than other sealing materials. It is recommended for applications in water hydraulic systems even though its resistance to abrasion is lower than in sealing made from UHMPWE.

## 7. Valve design objectives

The overflow valve to be design is an direct-action valve with a conical head. The valve can be used in pipe lines in the hydraulic systems, parallel to the pressure line. The operating parameters of the valve are summarised in Table 1.

Table 1. Valve parameters

| | |
|---|---|
| Working fluid | Water, hydraulic oil |
| Working temperature range | 2-50 $^{o}$C |
| Pressure settings | 3-20 MPa |
| Maximal flow rate | 60 l/min |

The 3-D view of fabricated overflow valve components are shown in Table 5. Details of design, modelling and tests results are described in paper

Table 5. Fabricated components of an overflow valve

| | | |
|---|---|---|
|  |  |  |
| Housing | Valve seat | Valve head |

| | | |
|---|---|---|
|  |  |  |
| Piston | Sealing elements | Spring |
|  | | |
| Complete overflow valve | | |

Developing the possibility of using water as a hydraulic system fluid, Cracow University of Technology Fluid Power Laboratory took place in EU project Called HYDROCOAT, in which the advanced technology of hydraulic components surface coating were tested in stand, as well as, simulated hydraulic drive and control systems.

The HYDRO-COAT project was financed by the European Union and belongs to the Seventh Framework Programme (grant agreement 232562). It started 1 October 2009 and finished 30 September 2011. Project developed the knowledge and the technology to produce a new range of “environmental friendly” machines for construction and mining sector using water as hydraulic fluid, addressing the technical barriers imposed by the use of water instead of oil by the introduction of a new knowledge in the flied to coatings and specific design of mechanical components for water hydraulics.

In this project materials with very low coefficient of friction, auto-lubricant proprieties and high wear resistance play a very critical role in the performance and life of water hydraulic components. HYDRO-COAT developed new knowledge on chemical and physical coating technology to integrate Diamond Like Carbon (DLC) Coating with innovative self-lubricant Columnar Nanostructured Coating (CNC).

The obtained results are promising as a method of making water resistive components of standard oil hydraulic elements as cylinder’s tubes and rods, pump pistons, valve poppet and/or spools, etc.

We hope that the author’s own experience in the field of water hydraulics summarised in referenced publications and the expertise gained by researchers from the Laboratory of Hydraulic Drives and

Control of the Cracow University of Technology should encourage the manufacturers and potential users of hydraulic systems to establish fruitful collaboration. As the applications are numerous and diverse, we hope to encourage research collaboration with other academic centres as well. Having the support in industry, we can start to develop our own offer of fluid power systems that would successfully compete with that of foreign manufacturers, to make it available to users in Poland at the time when more restrictive regulations are adopted in the field of environment protection work and occupational safety in operations using installations with hydraulic drives.

## 8. References

[1] Dobrzański L. A., *Metaloznawstwo z podstawami nauki o materiałach*, wydanie V, Wydawnictwa Naukowo-Techniczne, Warszawa 1999.
[2] Garbacik A., *Studium projektowania układów hydraulicznych*, Zakład Narodowy im. Ossolińskich, Krakow 1997.
[3] Schmitt A., *Vademecum hydrauliki. Informator i podręcznik hydrauliki,* G.L. Rexroth GmbH.
[4] Semeniuk E., Sobczyk A., Walczak P.: *„Wybrane problemy doboru materiałów na elementy zaworów układów siłowej hydrauliki wodnej”,* V Ogólnopolska Konferencja Naukowa “Nauka i Przemysł”, Krakow 2010.
[5] Semeniuk E., Sobczyk A., Walczak P., *Modelowanie i badania nowych konstrukcji elementów wysokociśnieniowej hydrauliki wodnej na przykładzie zaworu przelewowego,* XXII Konferencja Naukowa Problemy Rozwoju Maszyn Roboczych, Zakopane 2009.
[6] Stecki J.S., Garbacik A.*, Design and steady – state analysis of hydraulic control systems,* Fluid Power Net Publications, Krakow 2002.
[7] Stryczek S., *Napęd hydrostatyczny. Elementy i układy*, Wydawnictwa Naukowo-Techniczne, Warszawa 1984.
[8] Okularczyk W., Sobczyk A. *Experimental investigations of guide rings made of UHMWPE and PTFE composite in water hydraulic systems,* Proceedings of 5th FPNI PhD Symposium, Krakow 2008.
[9] Tasak E., Obróbka ubytkowa i spajanie, Wydawnictwa AGH, Krakow 2001.
[10] Trostmann E., *Water hydraulics control technology*, Marcel Dekker inc., New York 1996.
[11] www. Hydrocoat.eu

ISSN 1454 - 8003
Proceedings of 2011 International Salon of Hydraulics and Pneumatics - HERVEX
*9 – 11 November, Calimanesti-Caciulata, Romania*

# OPTIMISATION OF THE SPACE CONTROL TRAJECTORY WITH PROPER NEURAL NETWORK AND LABVIEW INSTRUMENTATION

**Adrian OLARU[1], Aurel OPREAN [1], Serban OLARU[2], Dan PAUNE[3]**

[1] Machines and Manufacturing Systems Dep. University Politehnica of Bucharest, UPB, Bucharest, Romania, olaru_robotics@yahoo.com

[2] Mechatronics Department, RomSYS Company, Bucharest, Romania, serban1978@yahoo.com

[3] General Manager, S.C.Metal Plast, Bucharest, Romania, danpaune@yahoo.com

***Abstract:*** *The paper shown one assisted method to construct simple and complex neural network and to simulate on-line them. By on-line simulation of some more important neural simple and complex networks is possible to know what will be the influences of all network parameters like the input data, weight, biases matrix, sensitive functions, closed loops and delay of time. There are shown some important neurons types, transfer functions, weights and biases of neurons, and some complex layers with different type of neurons. By using the proper virtual LabVIEW instrumentation in on-line work, were established some influences of the network parameters to the number of iterations before canceled the mean square error to the target. Numerical simulation used the proper teaching law and proper virtual instrumentation. In the optimization step of the research on used the minimization of the error function between the output and the target and the proper teaching low. The new network type bipolar sigmoid hyperbolic tangent neural network with time delay and recurrent links was established after assisted research of some known networks, by eliminate the deficiencies of them and was applied in to the solving of the inverse kinematics problem and optimize the space trajectory.*

***Keywords****: sensitive function, neuron, neural network, control system, direct and inverse kinematics, optimization of the space trajectory, virtual simulation, LabVIEW instrumentation*

## 1. Introduction

In many applications where were needed extreme precision, accuracy and stability of the way or of the guidance, the accuracy of taking the image, the accuracy to talk or to here, will be necessary to apply the neural networks.
A first wave of interest in neural networks was the introduction of simplified neurons by McCulloch and Pitts in 1943. These neurons were presented as models of biological neurons and as conceptual components for circuits that could perform computational tasks. Many other application of the neural networks has try to developing this field, most notably were Teuvo Kohonen, Stephen Grossberg, James Anderson and Kunihiko Fukushima [1…10].
Neural network are composed of simple elements operating in parallel, like a biological nervous systems. As in nature, the elements of the neural networks (neurons) are connected between them with the synapses what well balance the information. Thus, the decision will be taken after analyze of the sum of these information from the neurons after was applied the influences of each biases and sensitive functions. You can train a neural network to perform a particular function by adjusting the value of the connections (weights) between elements. Neural network have been trained to perform complex functions in various fields including pattern recognition, identification, classification, speech, vision and control systems. We consider neural network as an alternative computational scheme rather that anything else. The artificial neural networks which we described in this paper are all variation on parallel distributed processing (PDP) idea. An artificial network consists of a pool of simple processing units which communicate by sending signals to each other a large number of

weighted connections, number and sensitive functions what can be changed by using the LabVIEW optimization method shown in this paper. Typically, neural network are adjusted, or trained, so that a particular input leads to specific target output. The network is adjusted, based on comparison of the output and the target, until the network output matches the target. Typically, many such input/target pairs are needed to train a network.

## 2. The more important used sensitive functions

The sensitive functions are applied in each neuron types. In a dependence of the target, will be applied one or other of them. To know the action of them will be necessary to simulate them. The most important sensitive functions are presented in fig.1.[10]

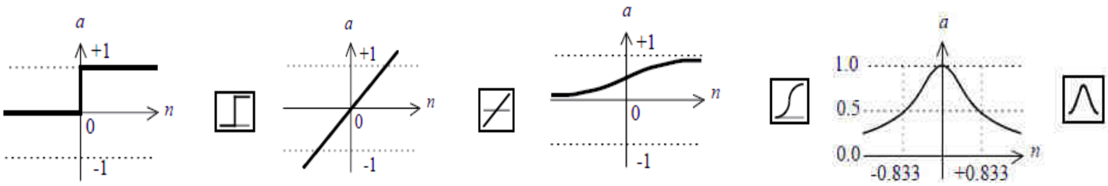

*Figure 1.* Sensitive functions: a) perceptron; b)linear; c) sigmoid unipolar; d) radial

Each of the used sensitive functions determines one general function of the neural layer, such a saturation to 1 of all positive values (fig.1a), the same output like a input (fig.1b), progressive convergence to the 1 or 0, if the inputs are positive or negative, Gauss variation to the 1 value, if the inputs are near 0 value, and s.o. By each type of the sensitive functions, the neurons or the layers involves them like a special filter, amplifier and with the influence of the biases matrix, what assures the translation of the function, can adjusting the field of the output.

## 3. Mathematical models of some important complex neural networks

The more important neural network and proper mathematical models used in the recognition the voice, the form, to optimize the guidance trajectory are presented in the figs.2-7[10].

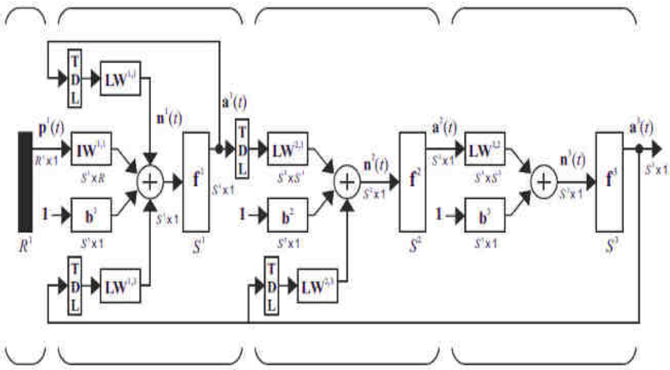

*Figure 2.* Layered Digital Dynamic Network (LDDN)

$$\begin{aligned}
a^1(t) &= f^1[IW^{1,1}p^1(t)+b^1+LW^{1,1}a^1(t-1)+LW^{1,3}a^3(t-1)] \\
a^2(t) &= f^2[LW^{2,1}a^1(t-1)+b^2+LW^{2,3}a^3(t-1)] \\
a^3(t) &= f^3[LW^{3,2}a^2+b^3]
\end{aligned} \tag{1}$$

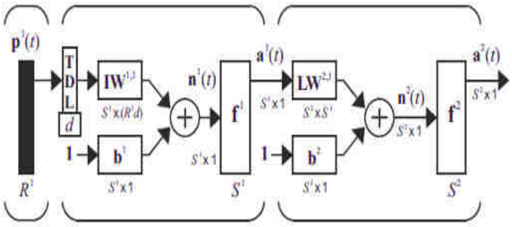


*Figure 3*. Focused Time-Delay Neural Network (FTDNN)

$$\begin{aligned} a^1(t) &= f^1[IW^{1,1}p(t-d+1)+b^1] \\ a^2(t) &= f^2[LW^{2,1}a^1(t)+b^2] \end{aligned} \quad (2)$$

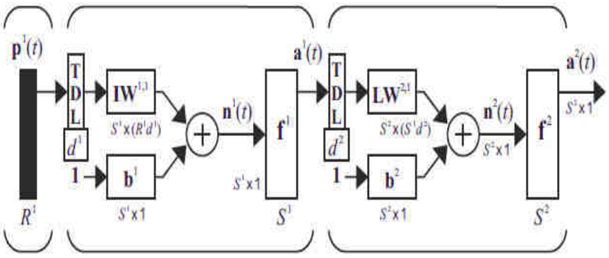


*Figure 4*. Distributed Time-Delay Neural Network (DTDNN)

$$\begin{aligned} a^1(t) &= f^1[IW^{1,1}p^1(t-d^1+1)+b^1] \\ a^2(t) &= f^2[LW^{2,1}a^1(t-d^2+1)+b^2] \end{aligned} \quad (3)$$

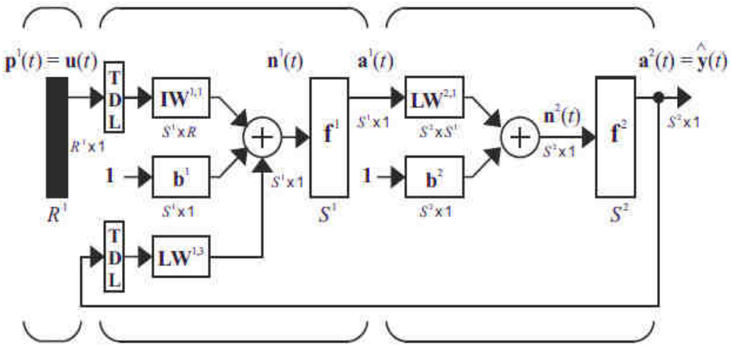


*Figure 5*. Nonlinear antiregresive with exogene inputs NARX

$$\begin{aligned} a^1(t) &= \frac{1}{1+e^{-[IW^{1,1}u(t-1)+b^1+LW^{1,3}a^2(t-1)]}} \\ a^2(t) &= \frac{1}{1+e^{-[LW^{2,1}a^1(t)+b^2]}} \end{aligned} \quad (4)$$

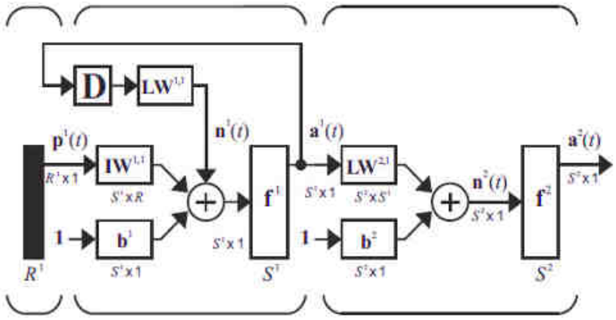

*Figure 6*. Layer-Recurrent Network (LRN)

$$a^1(t) = \frac{1}{1+e^{-[IW^{1,1}p^1(t)+b^1+LW^{1,2}a^1(t-1)]}} \quad (5)$$
$$a^2(t) = LW^{2,1}a^1(t)+b^2$$

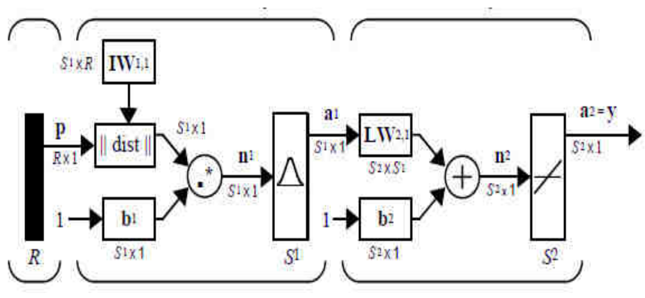

*Figure 7*. Radial base Neural Network

$$a^1 = \begin{cases} 1\forall\left|p^1 - IW^{1,1} + b^1\right| \neq 0 \\ 0\forall\left|p^1 - IW^{1,1} + b^1\right| = 0 \end{cases} \quad (6)$$
$$a^2 = LW^{2,1}a^1 + b^2$$

All proper mathematical models assures conditions for the simulation and optimization them with LabVIEW propre virtual instrumentation.

## 4. The numerical simulation of the neural networks

The numerical simulation of the neural network used one algorithm presented in [11, 12] what contents the elements specified in fig.8.

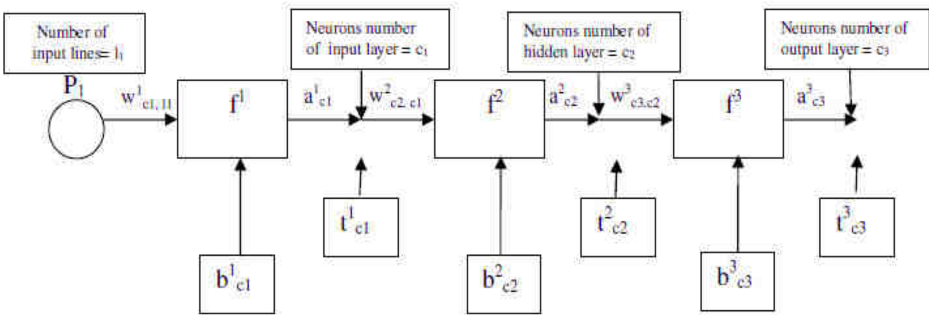


*Figure 8*. The neural network general schema with input LabVIEW data

The input data for the numerical simulation with LabVIEW will be: the number and data of the input vector, the number of neurons for each of the layers, the teaching gain, the sigmoid bipolar gain and the target output data. All matrixes of biases and weights were initialized at 0. To easily obtain the convergence was created one proper method of teaching law, what was applied in the paper. The base of the teaching law is to determine the error between the target and the output in each layer, by the transfer the target to each layer and adjust the error by teaching gain $v^i$. The mathematical equations are:

$$\begin{aligned} [w^{3,2}]_{new} &= [w^{3,2}{}_{old}] + ((t^3) - (a^3))\nu^3 \\ [w^{2,1}]_{new} &= [w^{2,1}{}_{old}] + ((t^2) - (a^2))\nu^2 \\ [w^{1,1}]_{new} &= [w^{1,1}{}_{old}] + ((t^1) - (a^1))\nu^1 \\ b^3_{new} &= b^3_{old} + ((t^3) - (a^3)) \end{aligned} \quad (11)$$

$$\begin{aligned} b^2_{new} &= b^2_{old} + ((t^2) - (a^2)) \\ b^1_{new} &= b^1_{old} + ((t^1) - (a^1)) \\ (t^2) &= [f^{-3}(t^3) - b^3]\left[w^{3,2}\right]^{-1} \\ (t^1) &= [f^{-2}(t^2) - b^2]\left[w^{2,1}\right]^{-1} \end{aligned}$$

$$\begin{aligned} f^{-3}(t^3) &= \ln(t^3) - \ln(1 - t^3) \\ f^{-3}(t^3) &= \ln[-(t^3 - 1) + \sqrt{(t^3)^2 - 6t^3 + 1}] - \ln(2t^3) \end{aligned}$$

where $t^i$ is the target and $a^i$ is the output of each layer, $f^i$ is the inverse sensitive function of each layer, $w^{-i,j}$ is the inverse weight matrix between the network layers. The numerical simulation of the neurons and networks was doing with the LabVIEW soft, version 8.2 from National Instruments. Icons and diagram of some of the virtual proper LabVIEW instruments designed specially for these investigations are shown in figs.9-11.

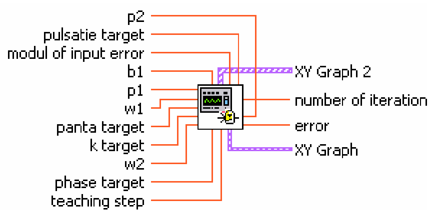


*Figure 9*. Icon of the virtual LabVIEW instrument for the assisted theoretical research of the simple linear neuron

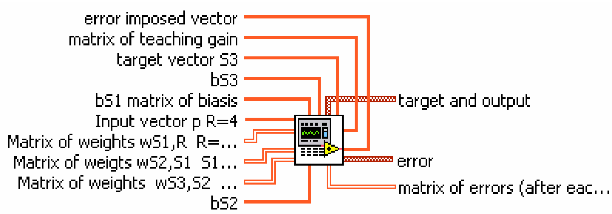


*Figure 10.* Icon of the virtual LabVIEW instrument for the assisted theoretical research of the linear neural network

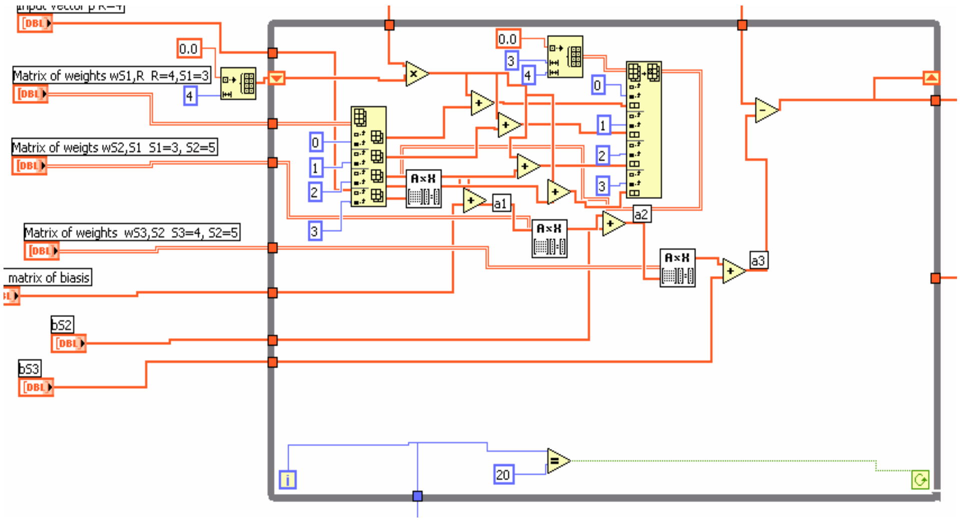


*Figure 11*. Part of the block diagram of the virtual LabVIEW instrument for the assisted theoretical research of the linear neural network

The simulation consisted in the simulation of the sensitive functions, some different neuron types, some simple layers and complex neural network. The assisted research was made to determine the error characteristics after each iteration and to trace the matrix target ***t*** in the same characteristics with the output ***a*** and compare them. All the virtual instruments worked on-line, to see easily what are the changes of the error or of the trace of the output, comparing with the target, when was changed the sigmoid bipolar gain, teaching gain ***v***, the inputs ***p***, the weights ***w***, and the bias ***b*** and the number of neurons in each of the layers. Some results of the assisted research of the different neurons types, the simple neural network and the complex neural network are shown in figs.12-18.

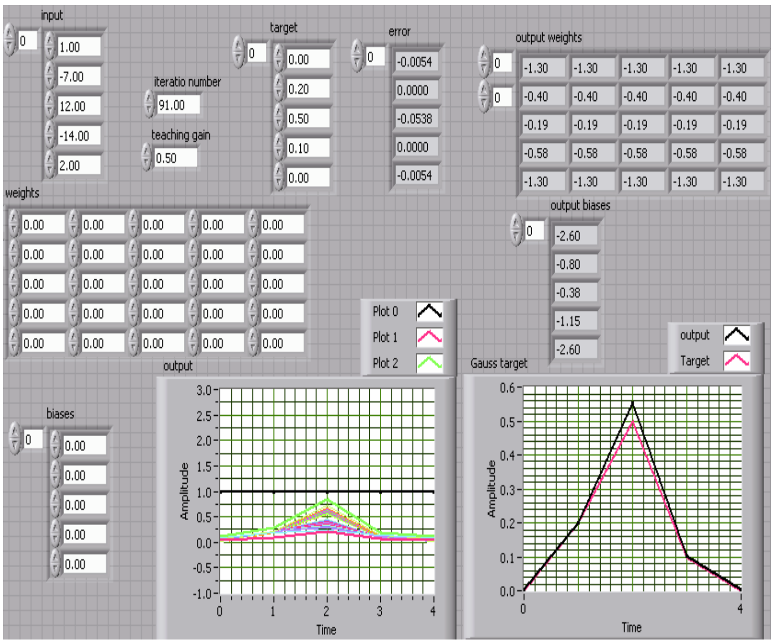


*Figure 12.* The results of the assisted research of the gauss network when the teaching law was 0.5

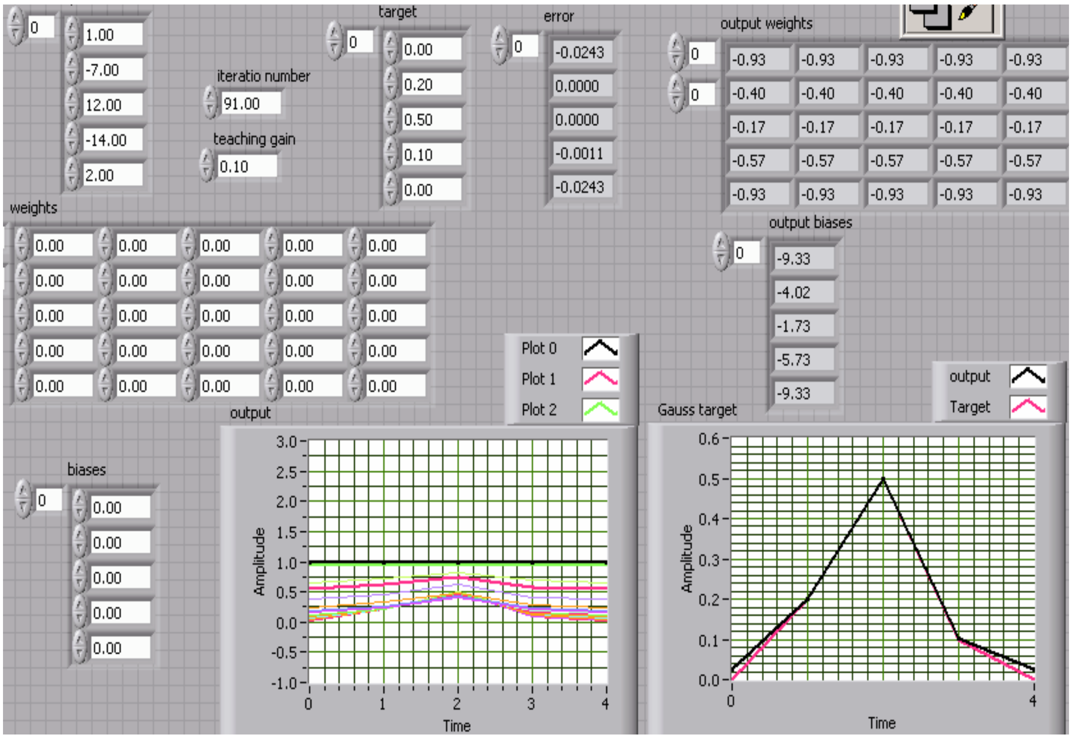


*Figure 13.* The results of the assisted research of the gaussnetwork when teaching law was 0.1

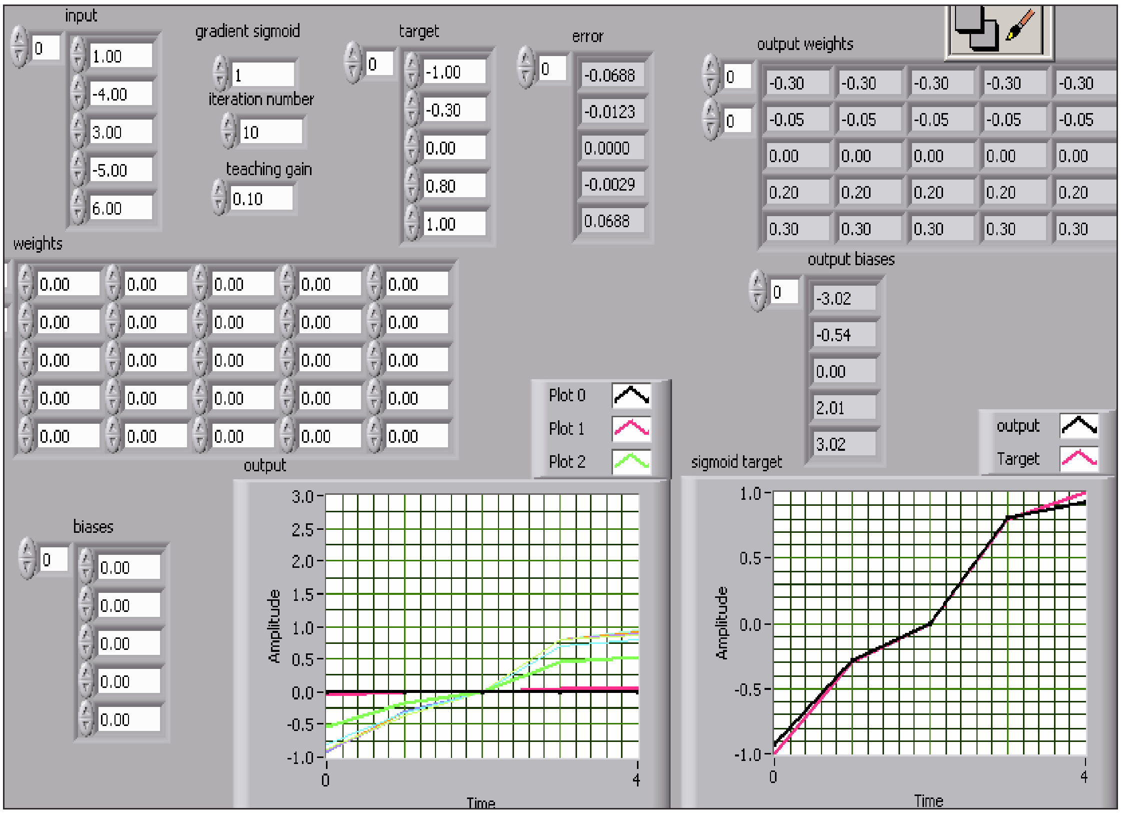


*Figure 14.* The results of the bipolar sigmoid neural network when the simoid gradient was 1, number of iterration 10, and teaching gain 0.1

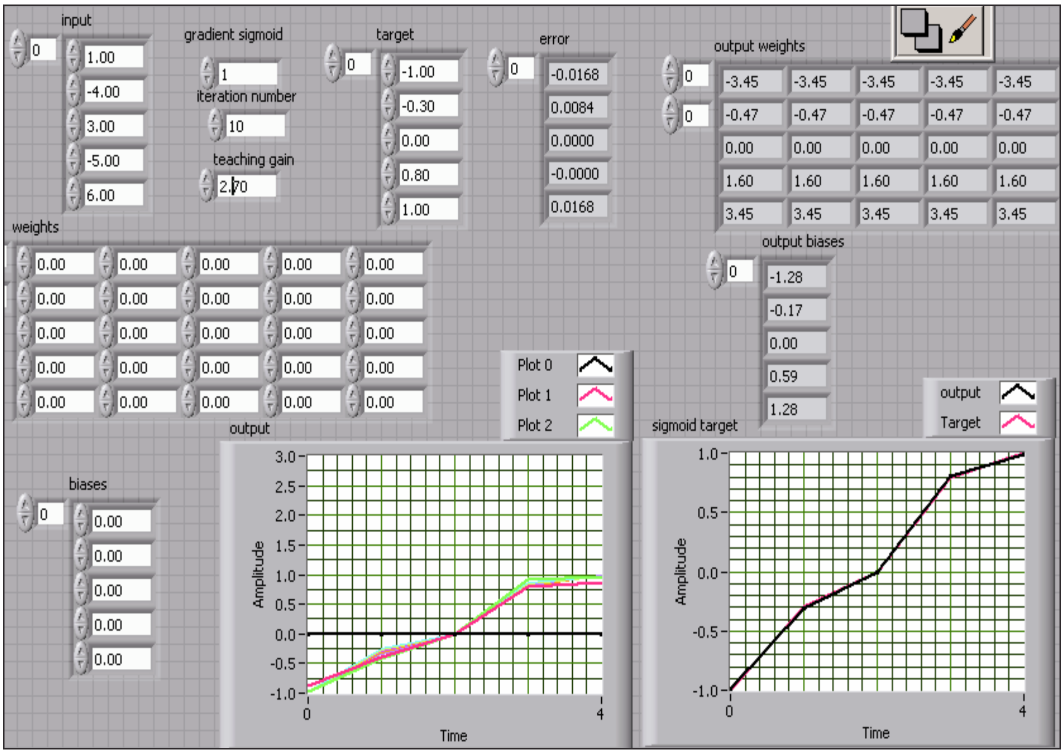


*Figure 15.* The results of the bipolar sigmoid neural network when the sigmoid gain was 3, iteration number 11, and teaching gain 0.1

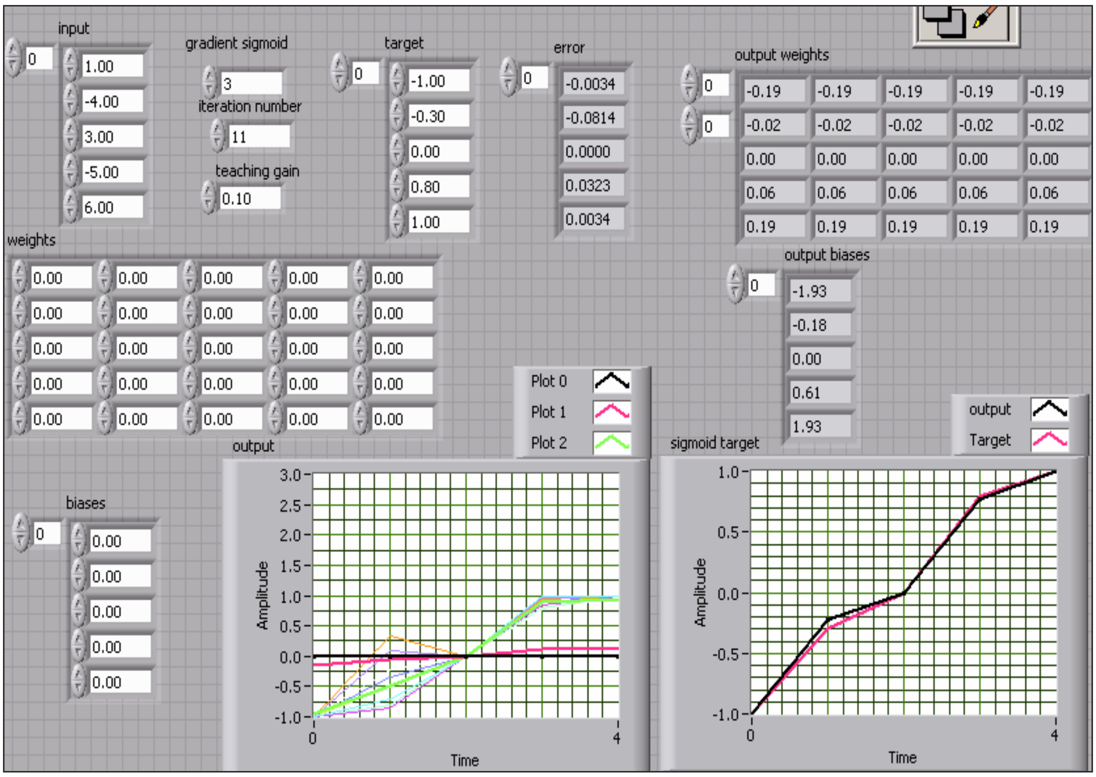


*Figure 16.*The results of the sigmoid bipolar neural network when the sig,oid graident was 1, number of iteration 10, and teaching gain 2.7

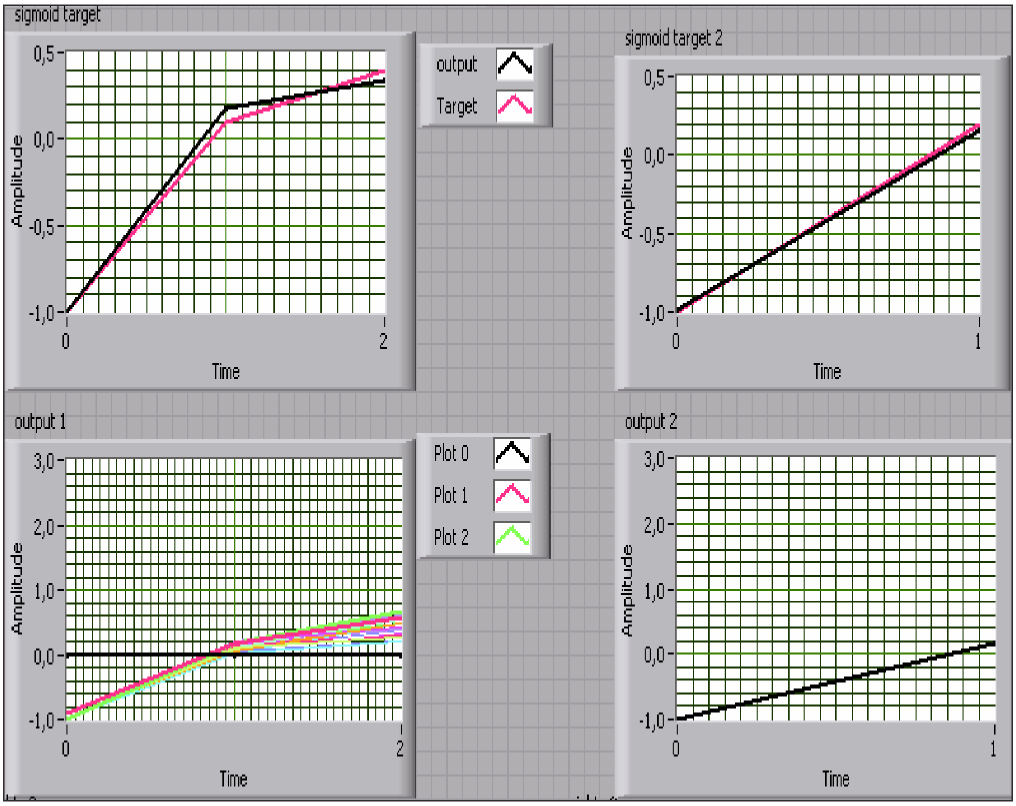


Figure 17. The results of the double bipolar sigmoid neural network when the sigmoid gain was 1, iteration number 17, and teaching gain 0.1

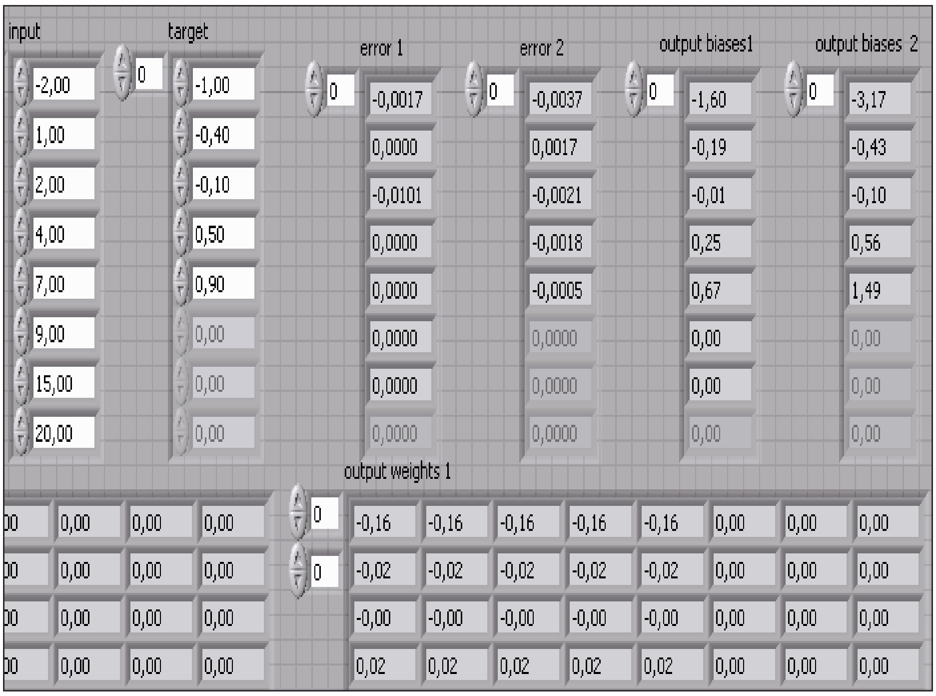


*Figure 18*. The front panel with the results of simulation of double sigmoid bipolar hyperbolic tangent neural network

All virtual instrumentation were used to simulate some more important neural network with the goal to establish one new form of the network with very quickly approach to the target and with minimum of the errors. After simulation of the neural network form the figs. 2-7 we can remark the followings: the time delay with the parameter *d* determines one general possibility to adjust the parameters, but it is necessary to respect the essential condition that *d* must be one odd number comparing with the next layer to assure the alternative oscillation near the target curve; in the network with many time-delay, the delay parameter $d^2$ must be odd number comparing with $d^1$; the closed loop with time-delay applied with one weight matrix can determine the instability of the network solution. To eliminate some of the deficiencies of the researched neural network, we were proposed one new structure of the neural network what will be analyzed in the paper. The proposed neural network was Bipolar Sigmoid Hyperbolic Tangent Neural Network with Time Delay and Recurrent Links (BSHTNN(TDRL)) the network what accept the teaching proposed low, by applied the inverse sensitive function.

## 5. Assisted research of the proper neural network (BSHTNN(TDRL))

Assisted research of new neural network contents the simulation of the proposal structure with the same input, output, target, number of the neurons in each layers and teaching gain data, but in different cases of the structure of the network. To compare in the same conditions we used the simulation in different cases for the same number of iteration and for the same input data, with the matrix for weights and biases initialized at first values to zero. The icon of the LabVIEW *VI* is shown in fig.20.
The researched cases of the neural network was: without time-delay; with the time- delay after output $a^1$(t); with the time- delay after output $a^1$(t) and $a^2$(t); with the time-delay after $a^1$(t) and one recurrent link between the output and the input vector. For the simulation was used one proper virtual LabVIEW instrument designed by use the neural network type BSHTNN(TDRL) fig.19.

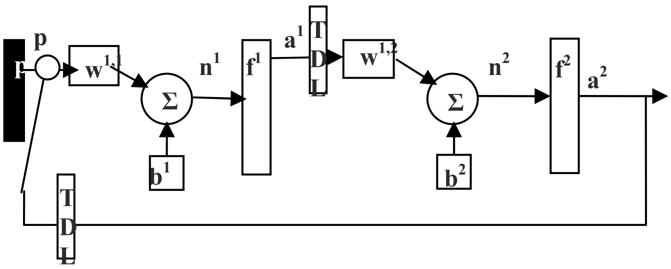


*Figure 19.* The block schema of the proposed new neural network type BSHTNN(TDRL)

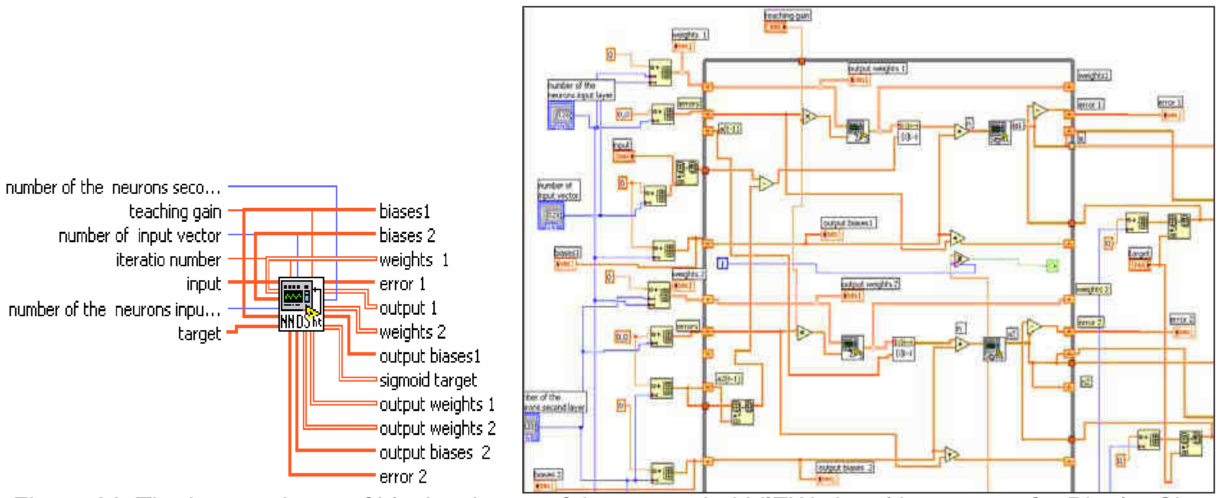


*Figure 20*. The icon and part of block schema of the proper LabVIEW virtual instrument for Bipolar Sigmoid Hyperbolic Tangent Neural Network with Time Delay and Recurrent Links (BSHTNN(TDRL))

The part of the complex virtual program of the proposed neural network is shown in figure 20. Mathematical model of the proposed neural network have the following form:

$$
\begin{aligned}
n^1(t) &= w^{1,1}p^1 + w^{1,2}a^2(t-1) + b^1 \\
a^1(t) &= \frac{a(1-e^{-n^1})}{1+e^{-n^1}} \\
n^2(t) &= w^{2,1}a^1(t-1) + b^2 \\
a^2(t) &= \frac{a(1-e^{-n^2})}{1+e^{-n^2}}
\end{aligned}
\qquad (12)
$$

where: $n^i$ is the input in each senzitive functions; $w^{i,j}$- weights matrices; $p$- input vector; $a^i$- output from each layer of the network; $a$- sigmoid bipolar hiperbolic tangent gain.

With this mathematical mmodel was designed one new proper virtual LabVIEW instrument for the assisted research of the neural network. Some results of the nnumerical simulation, byu changing some value or numeber of data from the network are presented in figs.21- 34.

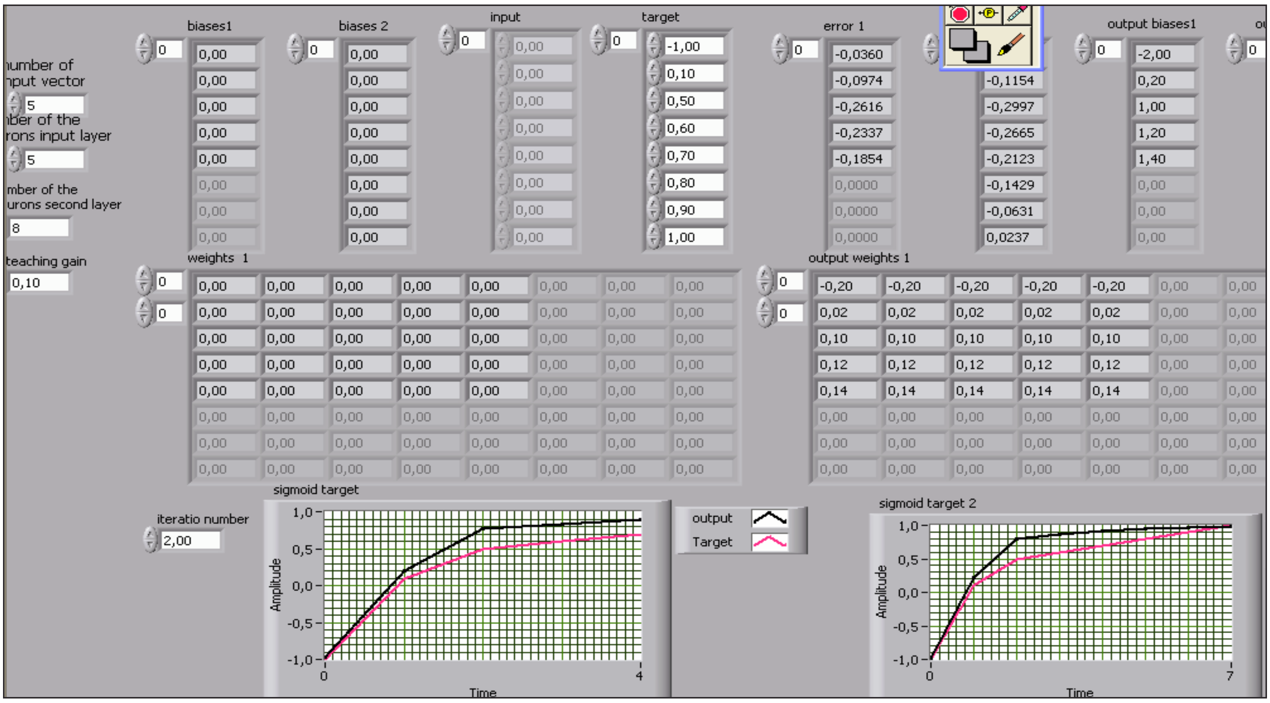


*Figure 21*. Bipolar Sigmoid Hiperbolic Tangent Neural Network with Time Delay and Recurrent Links with the input vector- 5, number of input layer neurons-5, number of output layer neurons- 8, teaching gain 0.1, sigmoid bipolar hiperbolic tangent gain 1 after two iterrations

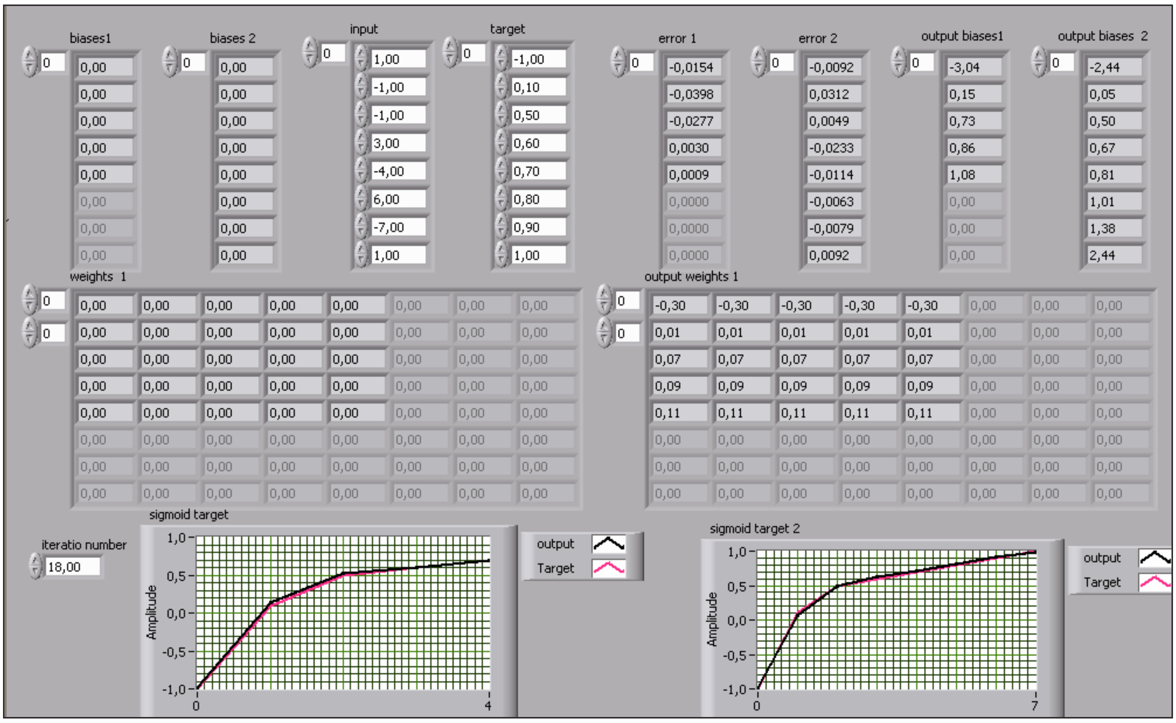


*Figure 22.* Bipolar Sigmoid Hiperbolic Tangent Neural Network with Time Delay and Recurrent Links with the input vector- 5, number of input layer neurons-5, number of output layer neurons- 8, teaching gain 0.1, sigmoid bipolar hiperbolic tangent gain 1 after 18 iterrations

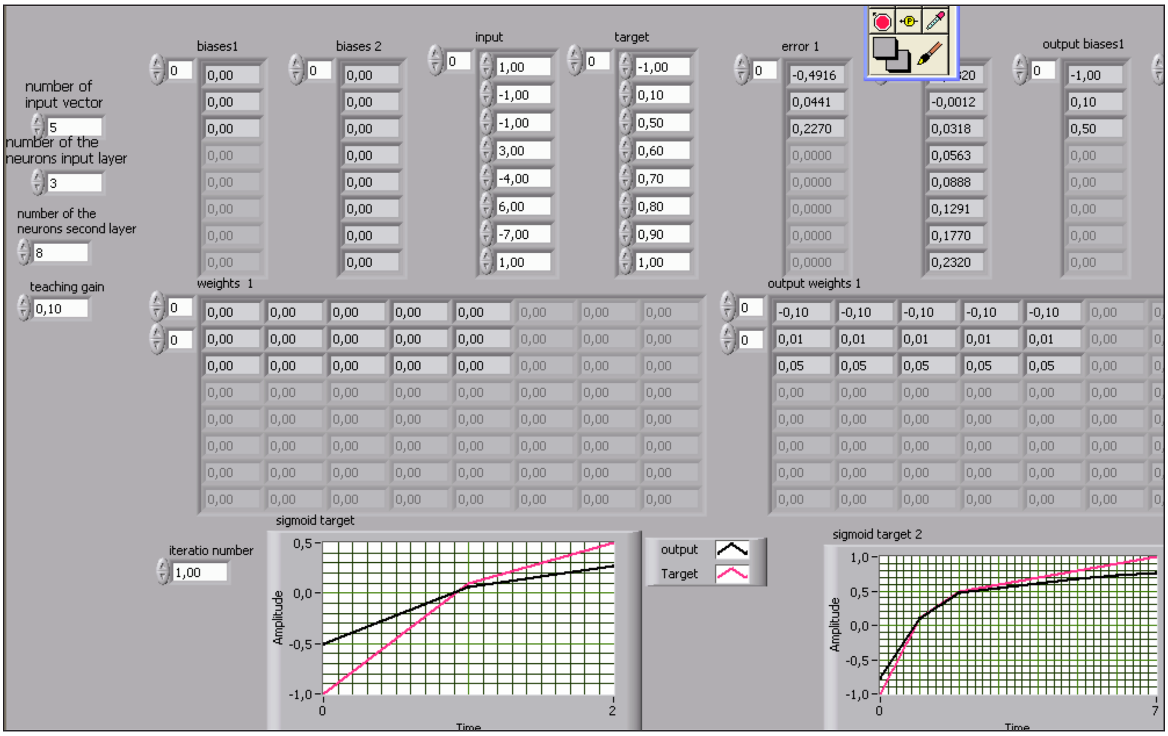


*Figure 23.* Bipolar Sigmoid Hiperbolic Tangent Neural Network with Time Delay and Recurrent Links with the input vector- 5, number of input layer neurons-3, number of output layer neurons- 8, teaching gain 0.1, sigmoid bipolar hiperbolic tangent gain 1 after two iterrations

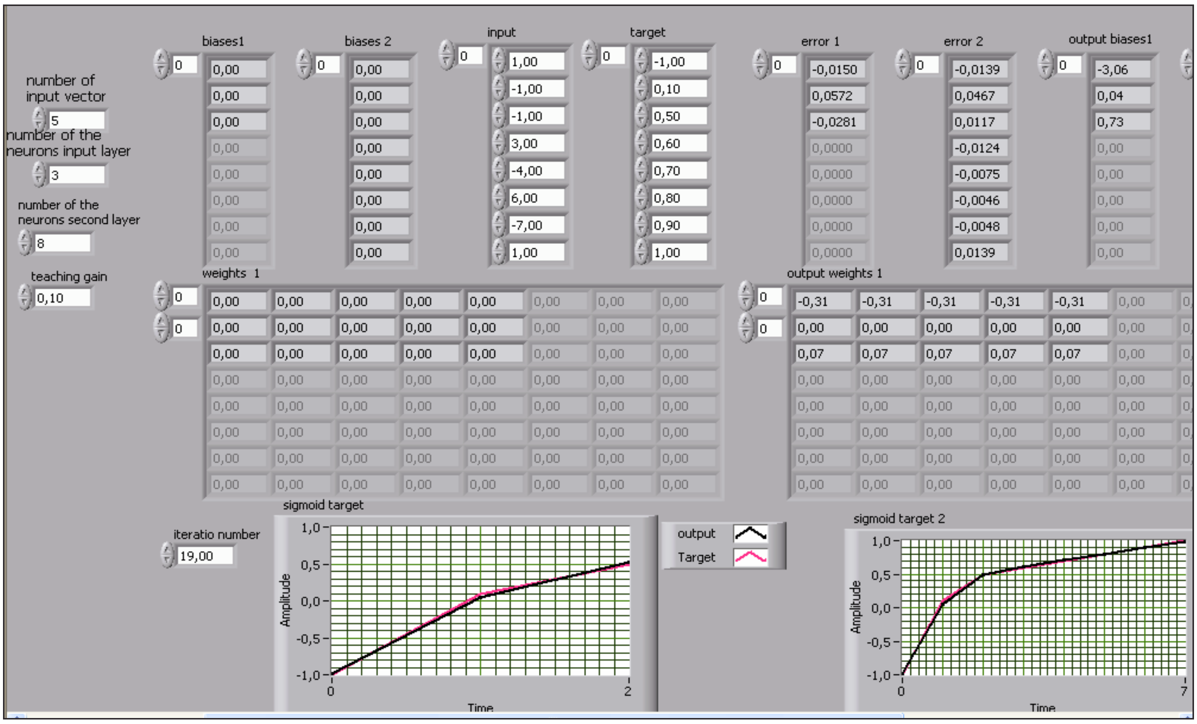


*Figure 24.* Bipolar Sigmoid Hiperbolic Tangent Neural Network with Time Delay and Recurrent Links with the input vector- 5, number of input layer neurons-3, number of output layer neurons- 8, teaching gain 0.1, sigmoid bipolar hiperbolic tangent gain 1 after 19 iterrations

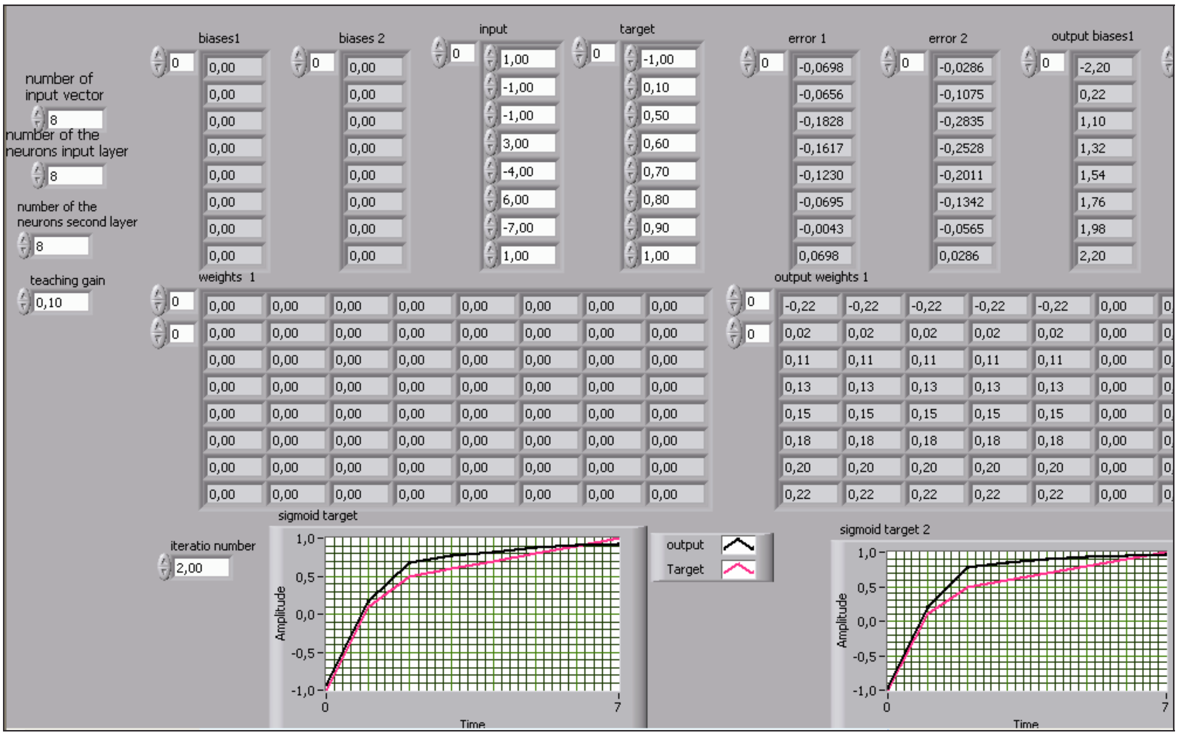


*Figure 25.* Bipolar Sigmoid Hiperbolic Tangent Neural Network with Time Delay and Recurrent Links with the input vector- 8, number of input layer neurons-8, number of output layer neurons- 8, teaching gain 0.1, sigmoid bipolar hiperbolic tangent gain 1 after two iterations

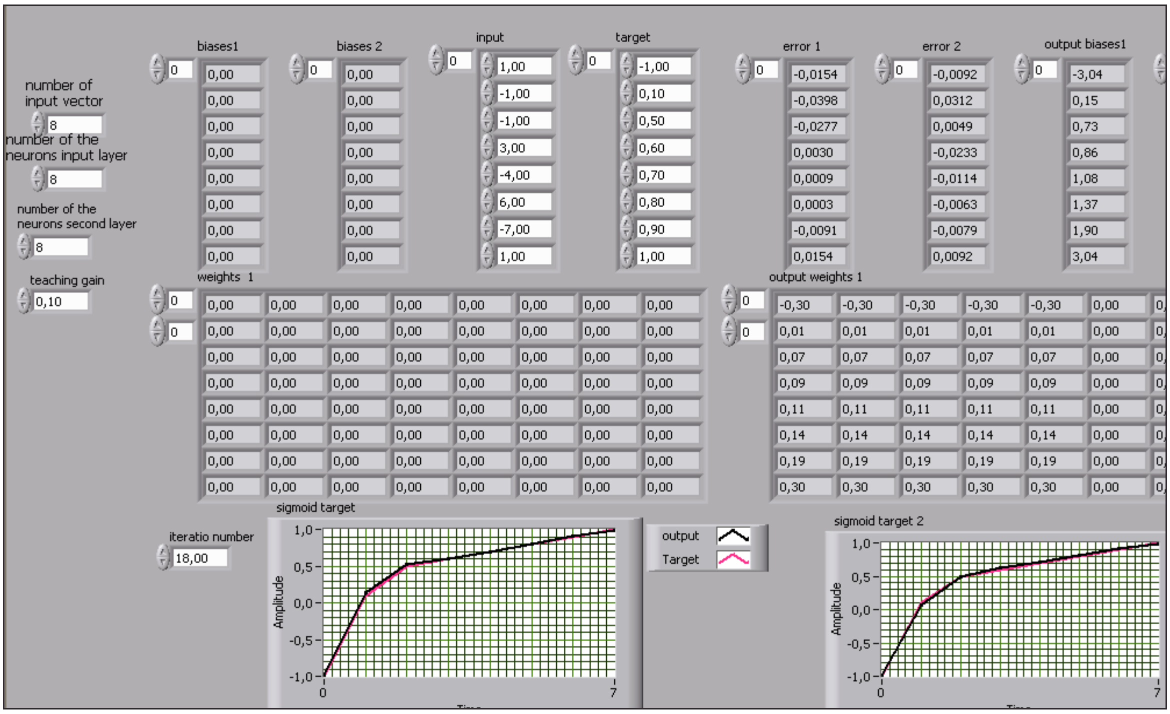


*Figure 26*. Bipolar Sigmoid Hiperbolic Tangent Neural Network with Time Delay and Recurrent Links with the input vector- 8, number of input layer neurons-8, number of output layer neurons- 8, teaching gain 0.1, sigmoid bipolar hiperbolic tangent gain 1 after 18 iterrations

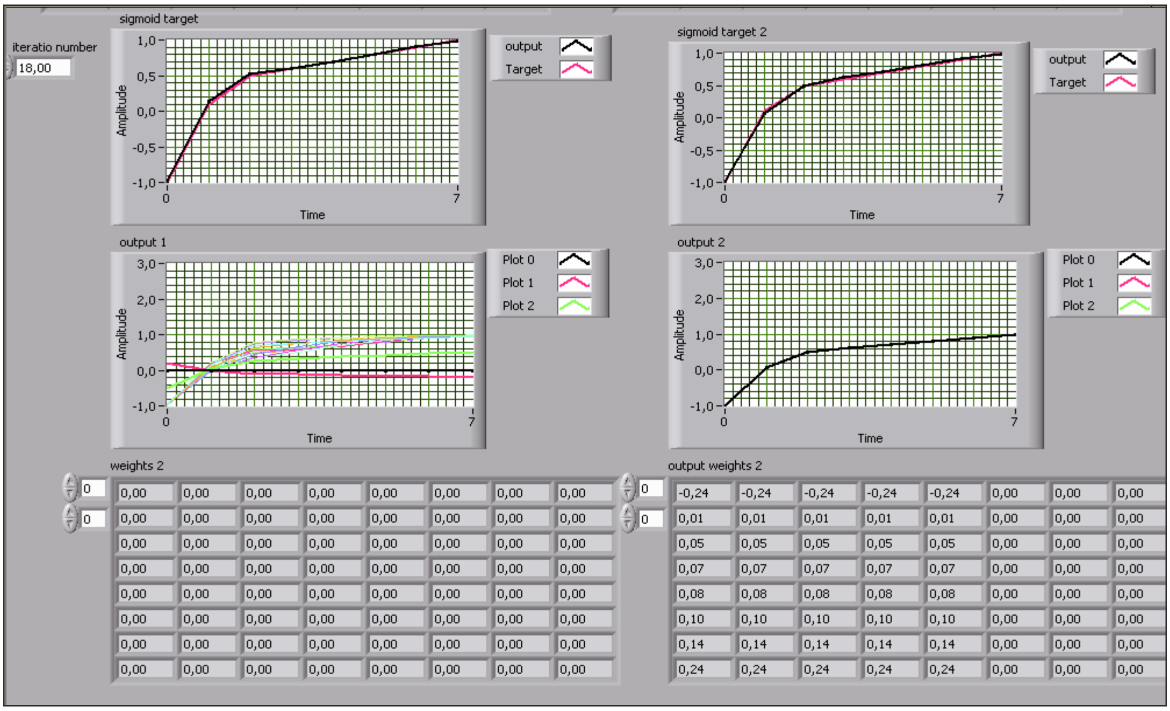


*Figure 27*. Bipolar Sigmoid Hiperbolic Tangent Neural Network with Time Delay and Recurrent Links with the input vector- 8, number of input layer neurons-8, number of output layer neurons- 8, teaching gain 0.1, sigmoid bipolar hiperbolic tangent gain 1 after 18 iterrations – intermediate results and weights matrices

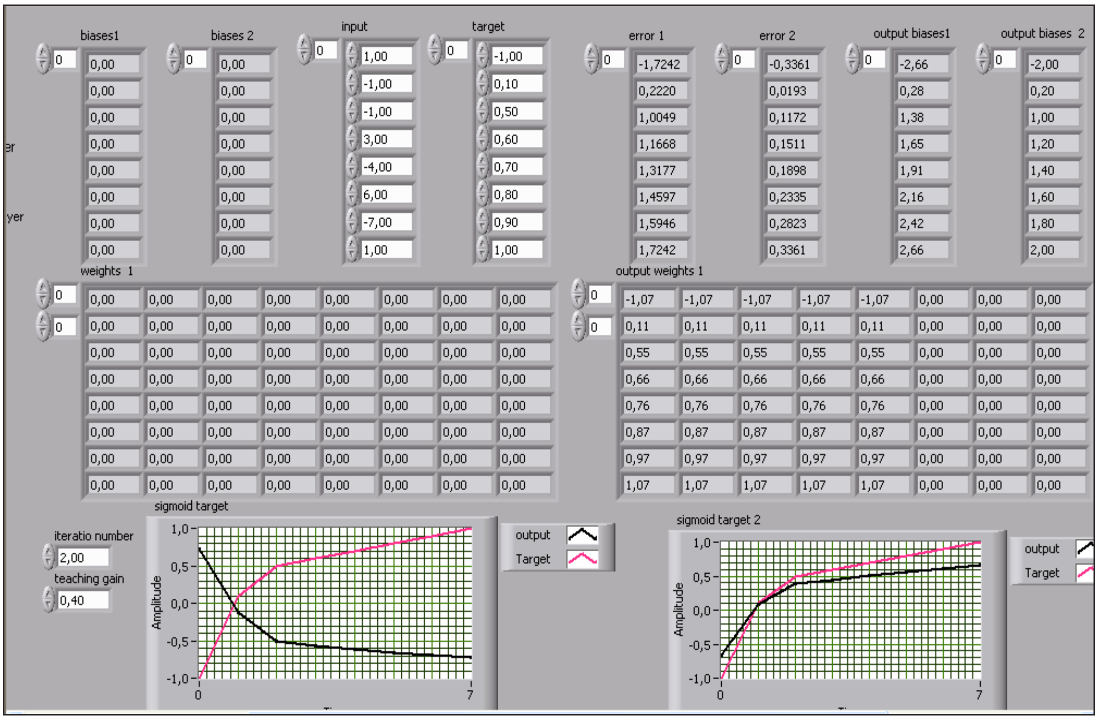


*Figure 28.* Bipolar Sigmoid Hiperbolic Tangent Neural Network with Time Delay and Recurrent Links with the input vector- 8, number of input layer neurons-8, number of output layer neurons- 8, teaching gain 0.4, sigmoid bipolar hiperbolic tangent gain 1 after two iterrations- error and weights matrices.

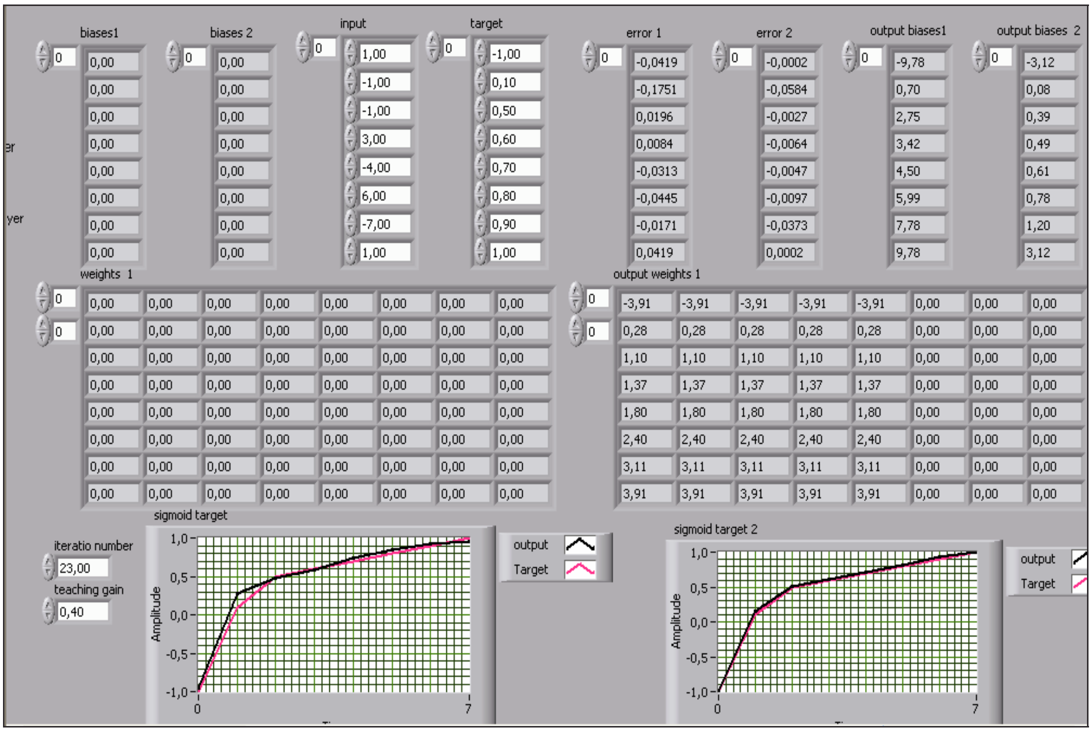


*Figure 29.* Bipolar Sigmoid Hiperbolic Tangent Neural Network with Time Delay and Recurrent Links with the input vector- 8, number of input layer neurons-8, number of output layer neurons- 8, teaching gain 0.4, sigmoid bipolar hiperbolic tangent gain 1 after 23 iterrations.

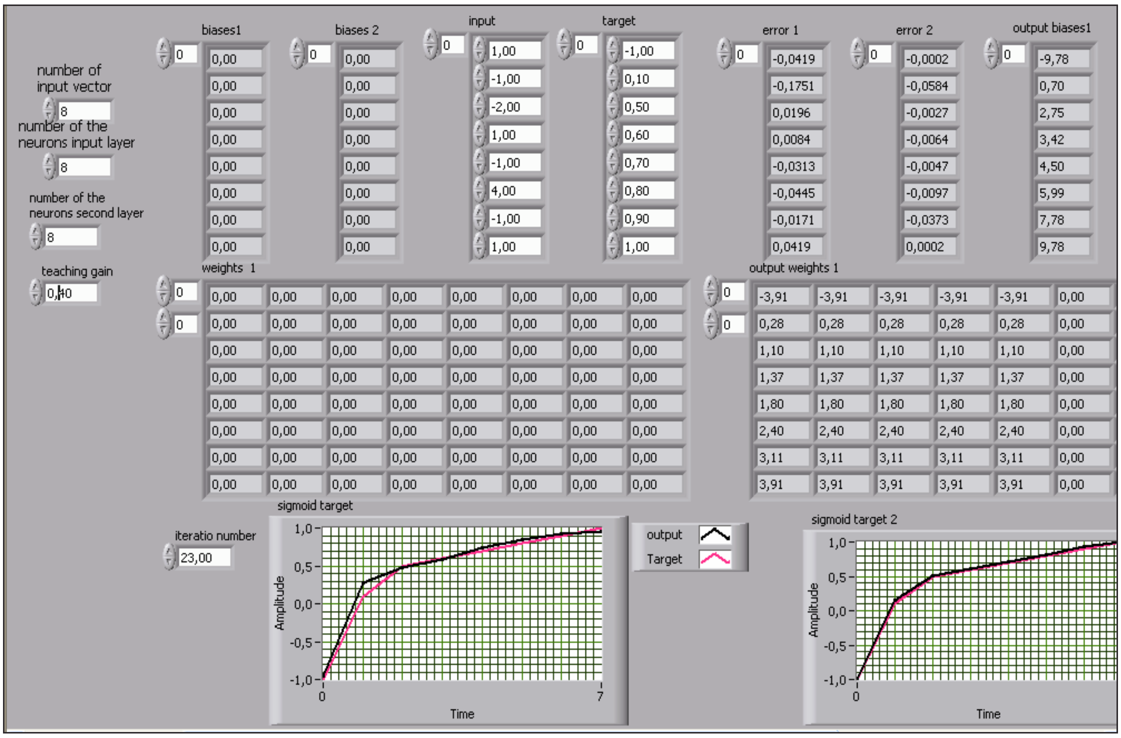


*Figure 30.* Bipolar Sigmoid Hiperbolic Tangent Neural Network with Time Delay and Recurrent Links with the input vector- 8, number of input layer neurons-8, number of output layer neurons- 8, teaching gain 0.3, sigmoid bipolar hiperbolic tangent gain 1 after 23 iterrations

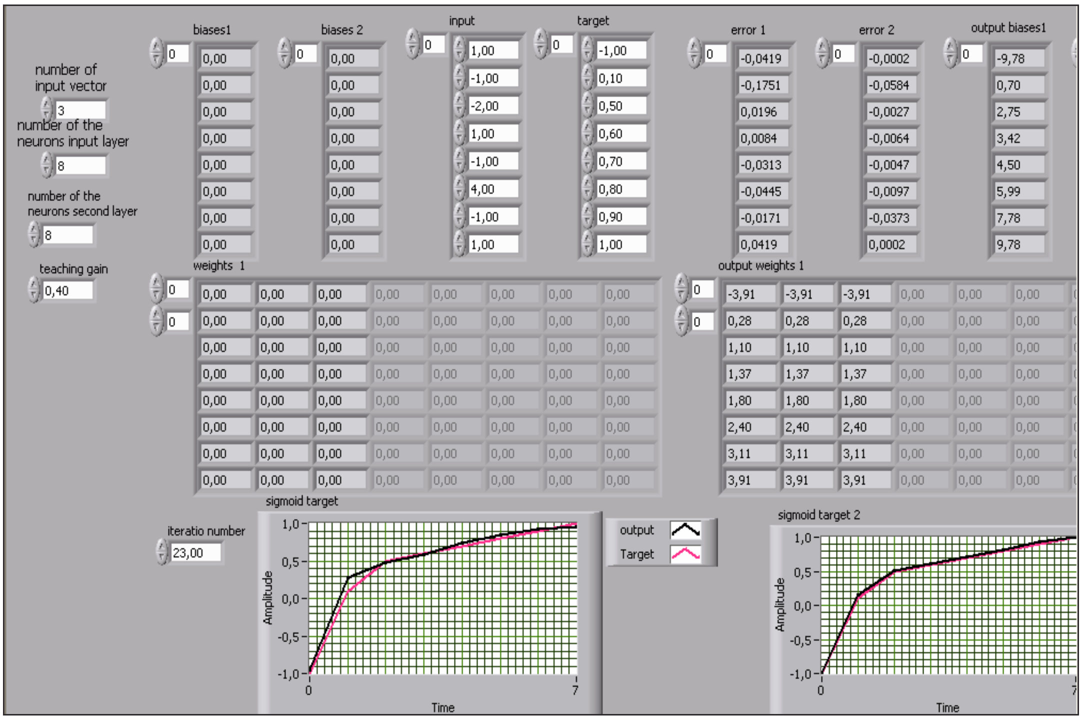


*Figure 31.* Bipolar Sigmoid Hiperbolic Tangent Neural Network with Time Delay and Recurrent Links with the input vector- 3, number of input layer neurons-8, number of output layer neurons- 8, teaching gain 0.4, sigmoid bipolar hiperbolic tangent gain 1 after 23 iterrations.

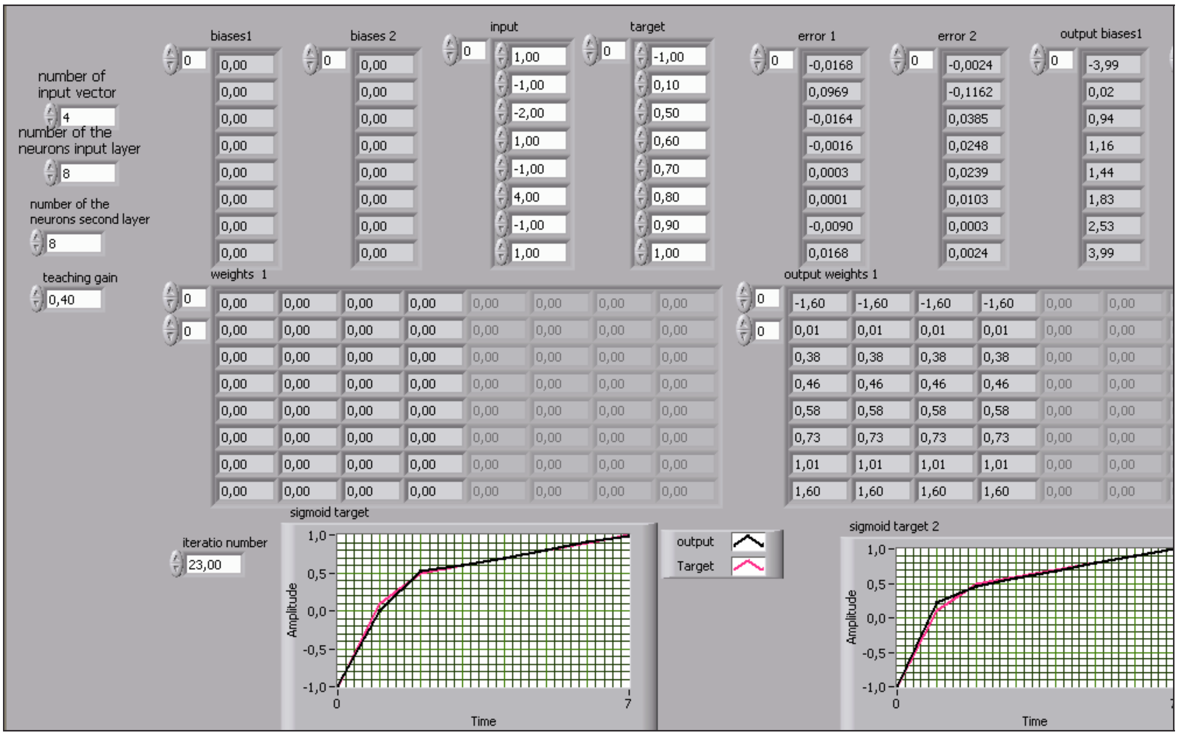


*Figure 32*. Bipolar Sigmoid Hiperbolic Tangent Neural Network with Time Delay and Recurrent Links with the input vector- 4, number of input layer neurons-8, number of output layer neurons- 8, teching gain 0.4, sigmoid bipolar hiperbolic tangent gain 1 after 23 iterrations

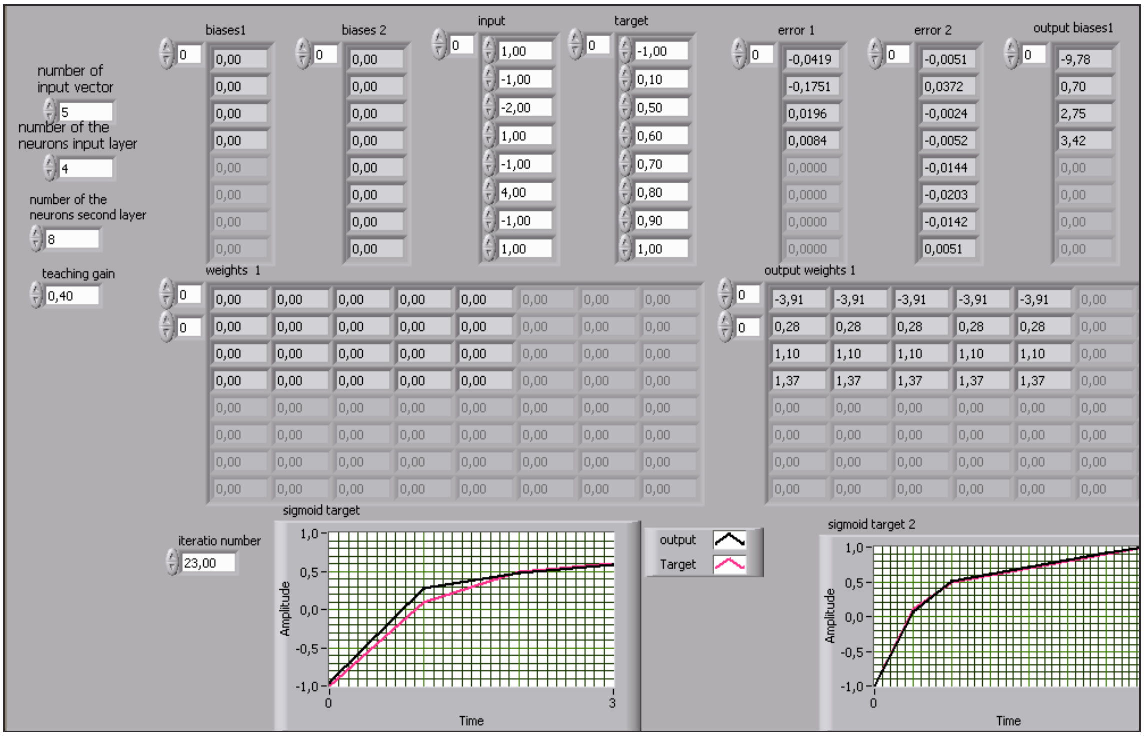


*Figure 33.* Bipolar Sigmoid Hiperbolic Tangent Neural Network with Time Delay and Recurrent Links with the input vector- 5, number of input layer neurons-4, number of output layer neurons- 8, teching gain 0.4, sigmoid bipolar hiperbolic tangent gain 1 after 23 iterrations

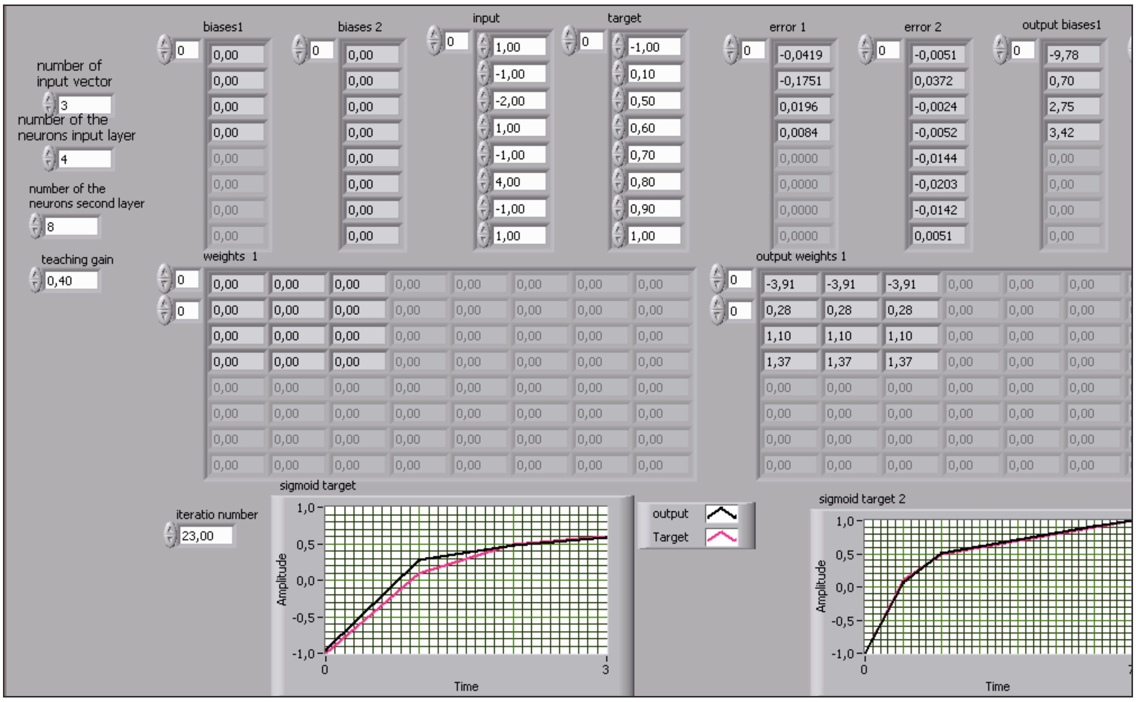


*Figure 34.* Bipolar Sigmoid Hiperbolic Tangent Neural Network with Time Delay and Recurrent Links with the input vector- 3, number of input layer neurons-4, number of output layer neurons- 8, teching gain 0.4, sigmoid bipolar hiperbolic tangent gain 1 after 23 iterrations- optimal result-all errors before 0.04

## 6. Optimization of the robots space trajectory by using inverse kinematics, proper neural network and LabVIEW simulation

The experimental research and the theoretical kinematics analysis is been realized using an arm type robot (Fig. 35) and some proper virtual LabVIEW instruments. The structural kinematical schema is shown in Fig.36. Using the recurrent matrix method were obtained all joints positions of the robot structure.

The recurrent general mathematical model contains the following matrix form:

$$(r)_i^0 = (r)_{i-1}^0 + [D]_{i-1}^0 (r)_i^{i-1} \quad (13)$$

with the notations: $(r)_i^0$ - the matrix form of the absolute position vector of the *i* joint; $(r)_{i-1}^0$ - the matrix form of the position vector of the *i*-1 joint; $(r)_i^{i-1}$ - the matrix form of the relative position vector from *i* to *i*-1 joint; $[D]_{i-1}^0$ coordinates transformation matrix from the *i*-1 joint to the base fixed frame [23], [24].

*Fig. 35* Arm type robot using in the theoretical and experimental research

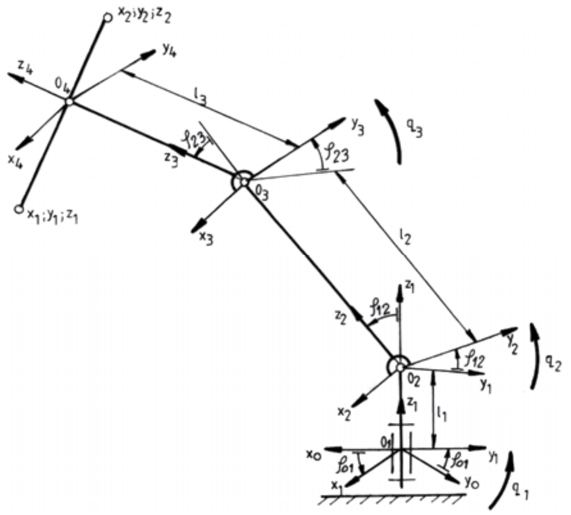

*Fig. 36* Kinematical-structural schema of the arm type robot

After applying the recurrent mathematical model to the presented robot structure, were been obtained the following position vectors of all robot's joints:

$$(r)_1^0 = \begin{pmatrix} 0 \\ 0 \\ l_1 \end{pmatrix}; (r)_2^0 = \begin{pmatrix} 0 \\ 0 \\ l_1 + l_2 \end{pmatrix}; (r)_3^0 = \begin{pmatrix} c_1 s_2 l_3 \\ s_1 s_2 l_3 \\ l_1 + l_2 + c_2 l_3 \end{pmatrix};$$
$$(r)_4^0 = \begin{pmatrix} c_1 s_2 l_3 + (c_1 c_2 s_3 + c_1 s_2 c_3) l_4 \\ s_1 s_2 l_3 + (s_1 c_2 s_3 + s_1 s_2 c_3) l_4 \\ l_1 + l_2 + c_2 l_3 + (-s_2 s_3 + c_2 c_3) l_4 \end{pmatrix} \quad (14)$$

where $l_i$ is the lengths of each robot modules; $c_i$, $s_i$ are known cosines and sinus functions of the relative angle and $q_i$ is the relative robot coordinates between *i* and *i*-1 robot bodies. The direct kinematics LabVIEW results are shown in Fig.37 for some values of internal coordinates.

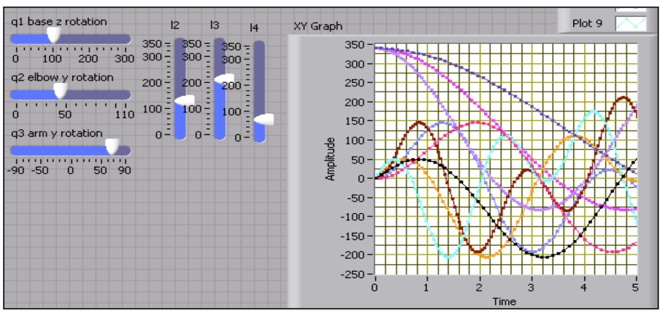


*Fig. 37* Variation of the absolute coordinates versus the internal variables $q_1$, $q_2$, $q_3$

**7. The research of the proper neural network to obtain the optimal results of the inverse kinematics**

To easily obtain the convergence to the target after solving the inverse kinematics problem was applied one proper neural network Bipolar Sigmoid Hyperbolic Tangent type with Time Delay and Recurrent Links and proper teaching law method [13-17]. The neural network had one 3-8-3-3

neuronal structure to assure the link with the real target and the input data. The base of the teaching law is to determine the error between the target and the output in each layer, by the transfer the target to each layer and adjust the errors by teaching gain $v^i$ and amplifier gain and adjust not only the weights and biases matrix but the target of the hidden layer. The mathematical model is here created by using the schema of the proposed neural network for solving the inverse kinematics problem and the proposed teaching laws given by the relations (15).
where $t^i$ is the target, $a^i$ is the output of each layer, $f^i$ is the inverse sensitive function of each layer, $w^{-i,j}$ is the inverse weight matrix between the network layers, $b^i$ is the biases matrices, noting that the old and the new indices are designed before and after applying correction. (15)

$$n_1 = [\underbrace{w^1}_{p_1} + \underbrace{tcg_1}_{p_2} \cdot \varepsilon_1](p - a_2(t - p_3 + 1)) + (b_1 + \varepsilon_1)$$

$$a_1 = \frac{p_4(1 - e^{-n_1})}{1 + e^{-n_1}}$$

$$\varepsilon_1 = t_1 - a_1$$

$$n_2 = [w^2 + \underbrace{tcg_2}_{p5} \cdot \varepsilon_2](a_1(t - p_6 + 1)) + (b_2 + \varepsilon_2)$$

$$a_2 = \frac{p_7(1 - e^{-n_2})}{1 + e^{-n_2}}$$

$$\varepsilon_2 = t_2 - a_2$$

$$q_i = p_8(a_2 - \varepsilon_f)$$

$$r_i = \begin{pmatrix} c_1 s_2 l_3 + (c_1 c_2 s_3 + c_1 s_2 c_3) l_4 \\ s_1 s_2 l_3 + (s_1 c_2 s_3 + s_1 s_2 c_3) l_4 \\ l_1 + l_2 + c_2 l_3 + (-s_2 s_3 + c_2 c_3) l_4 \end{pmatrix}$$

$$\varepsilon_{pos} = t_3 - r_i$$

$$n_3 = [w^3 + \underbrace{tcg_2}_{p_5} \cdot \varepsilon_{pos}](q_i) + (b_3 + \varepsilon_{pos})$$

$$a_3 = \frac{p_9(1 - e^{-n_3})}{1 + e^{-n_3}}$$

$$\varepsilon_f = t_2 - a_3$$

$$[w^{3,2}]_{new} = [w^{3,2}{}_{old}] + ((t^3) - (a^3))\nu^3$$

$$[w^{2,1}]_{new} = [w^{2,1}{}_{old}] + ((t^2) - (a^2))\nu^2$$

$$[w^{1,1}]_{new} = [w^{1,1}{}_{old}] + ((t^1) - (a^1))\nu^1$$

$$b^3_{new} = b^3_{old} + ((t^3) - (a^3))$$

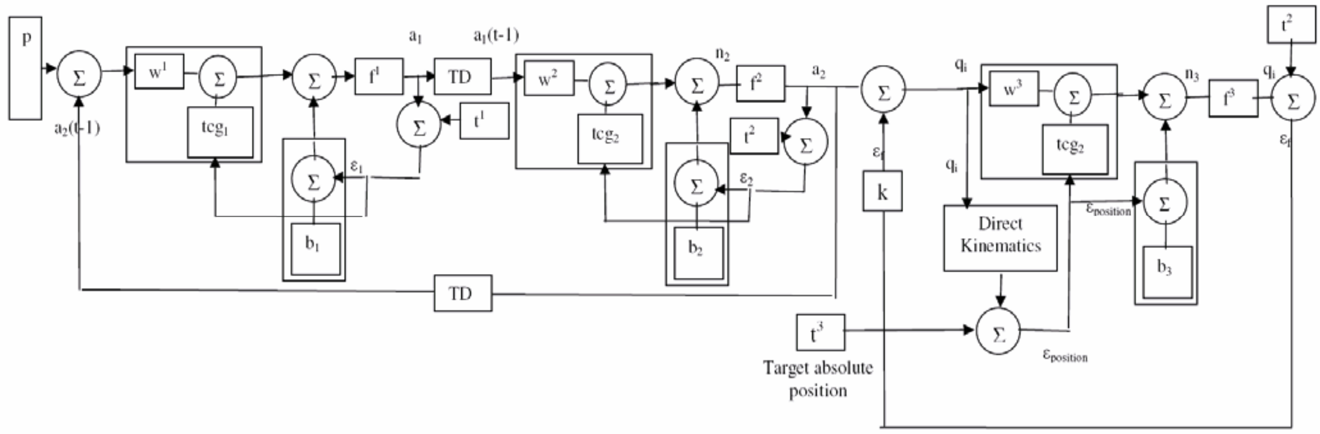


*Fig. 38* Complex schema of the proper neural network

After was applied the proposed neural network were obtained the errors between the target and the proposed end-effector space position more that 20%. To obtain the optimization of these errors was researched all influences of some more important parameters of the model to the errors.
Following parameters are researched [23]: $p_1$- the number of neurons; $p_2$ - the first teaching gain; $p_3$- step of the first time delay; $p_4$- the first sensitive function gain; $p_5$- the second teaching gain; $p_6$- the step of the second time delay; $p_7$- the second sensitive function gain; $p_8$- the magnify gain of the proportional error control; $p_9$- the third sensitive function gain and some more recurrent links, see the relations (15). The research in this paper shown the analyze of influences of some neural network modules to the space trajectory errors like: time delay, place of applying, different recurrent links and closed loops (see the table 1).

## 8. Optimization by applying the proper neural network and numerical simulation with LabVIEW

A numerical simulation of the network was doing with the LabVIEW soft, version 8.2 from National Instruments. The design of the virtual instruments was done by transpose the mathematical model of the direct kinematics and of the network with proposed teaching law (relations (15)) in the soft applications. The simulation consist in the determination of the error after each iteration and the trace of the matrix target ***t*** in the comparative characteristics with the output ***a*** and compare them. All the virtual instruments work on-line, to see easily what are the changes of the errors or of the output trace, comparing with the target, when was changed the sigmoid bipolar gain, teaching gain ***v***, the inputs ***p***, the weights ***w***, and the bias ***b***. Some results of the assisted research are shown in Fig.39 and Fig.40 and the synthesis of these results is shown in the Table 1.

*Table 1*

**Synthetic results of the assisted research of the neural network for solving inverse kinematics**

| | Type | Comp. NN | A mplif. gain | Teach. gain | Target | Obt. Pos. | Obt. $\varphi_i$ | Trg. hiddn | Iter. Nr. | Rel. err. |
|---|---|---|---|---|---|---|---|---|---|---|
| | **3-8-3-3** | **BSHTNN TDRL** | **52.01** | **0.189** | **20<br>17.3<br>-10** | **20.239<br>17.0259<br>30.0138** | **-37.718<br>-82.67<br>-78.435** | **-1<br>0.5<br>-0.6** | **42** | **1%** |
| | **3-7-3-3** | **BSHTNN** | 52.01 | 0.189 | -‘- | 12.30<br>29.32<br>24.23 | -38.23<br>-112<br>-85 | -1<br>0.5<br>-0.6 | **132** | 30% |
| | **3-8-3-3** | **BSHTNN TD** | 52.01 | 0.189 | -‘- | 15.1764<br>24.9820<br>27.3053 | 67.595<br>21.751<br>26.088 | -1<br>0.5<br>-0.6 | 132 | 20% |
| | 3-8-3-3 | **BSHTNN TD+TD** | 52.01 | 0.189 | -‘- | 19.8665<br>16.650<br>30.4646 | -38.759<br>-82.682<br>-78.515 | -1<br>0.5<br>-0.6 | 132 | 10% |
| | 3-8-3-3 | **BSHTNN TDRL** | **48** | 0.189 | -‘- | 19.397<br>15.835<br>31.193 | -34.894<br>-76.274<br>-72.448 | -1<br>0.5<br>-0.6 | 132 | 11% |
| | 3-8-3-3 | BSHTNN TDRL | 52.01 | 0.189 | -‘- | 16.686<br>13.741<br>33.656 | -45.40<br>22.213<br>26.253 | **-0.5<br>1<br>-0.6** | **42** | 14% |

## 9. Discussion on the assisted research results

The numerical simulation shown that one of the most important influences in the optimization of the output way to approach to the target are the teaching algorithm, gain, the number of iterations and the hidden target data. We observe that the small gain determine one sensitive and stable approach to the target and the big one determines one oscillation with different magnitude of the output, balanced to the target.

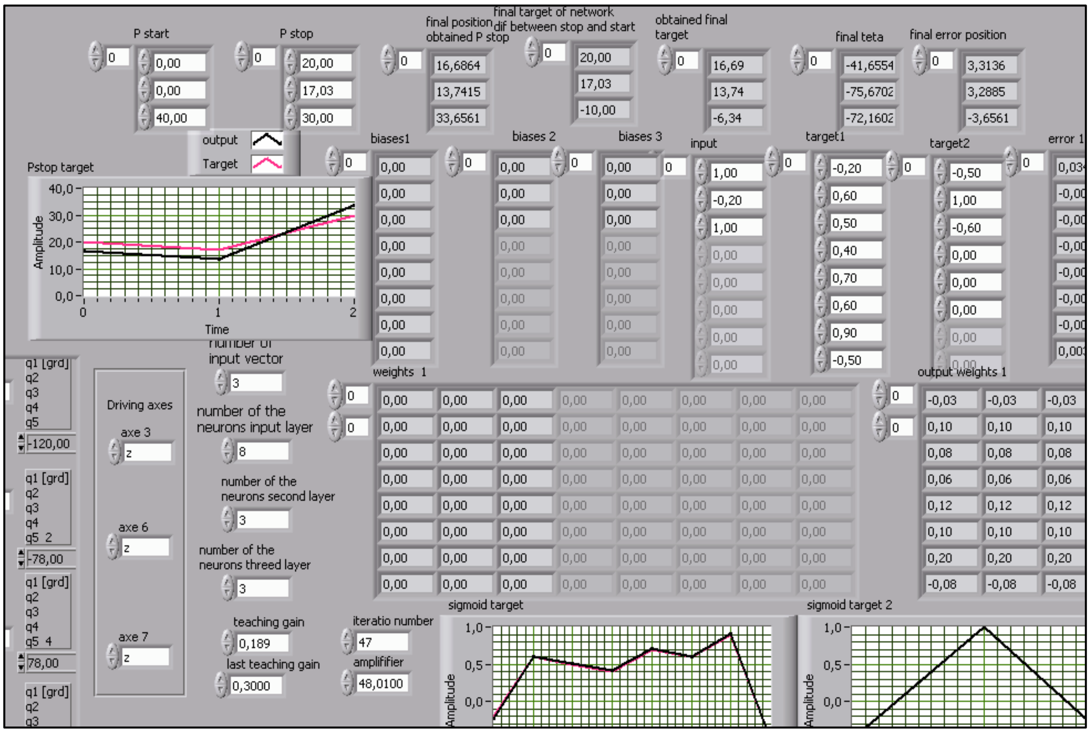


*Fig. 39* Results of the space position after applying the neural network type SBHTNN with TDRL

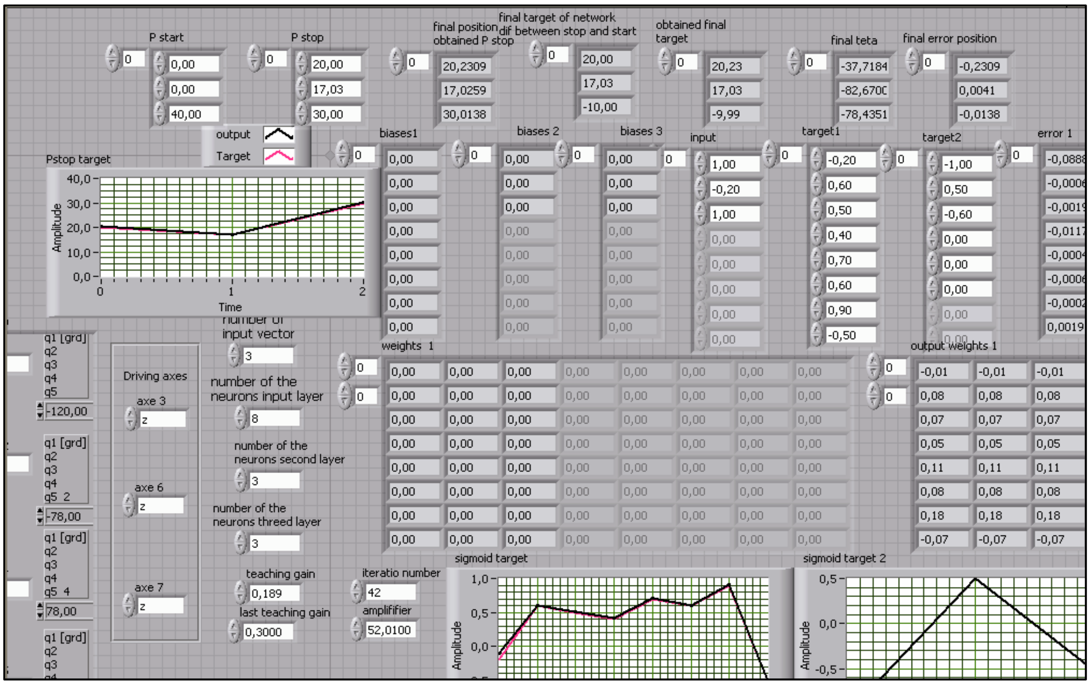


*Fig.40* Results of the space position after applying the neural network type SBHTNN with TDRL when the amplifier gain and the number of iteration were changed

After the assisted research of the sigmoid bipolar neural network parameters, relation (15), we could remark the followings: the complex obtained neural network schema assure the fast convergence of the iteration process and a very small error (1%); by input in the neural block schema of the TD decrease the relative errors from the 30% to 20%, respectively 10%; by using the time delay with different time step assure the decreasing of the errors from 30% to 10%; the changing of the number of the neurons in the first layer don't modify the values of the errors; the changing of the amplifier gain and the teaching gain assured the decreasing of the errors from 11% to 10% for the 132 iterations; a substantial decreasing of the errors and the decreasing of the number of iteration was obtained by on-line changing of the hidden layer target data, from 14% to 1% for 42 iterations; the change of the number of the neurons in the first layer don't change the errors; one big difference between the input profile and target data determines divergence; increasing the teaching gain over than one limit determines the instability.

## 10. Discussion and future work

The results of the weight matrix after obtain the minimum of the error function are shown in figs.21-34, after application one double sigmoid hyperbolic tangent bipolar neural network. We can see that after 113 number of iterations process was obtained the minimum output error, under the 0.002, for each point of the curve.

The numerical simulation shown that one of the most important influence in the optimization of the output way, to approach to the target is the teaching algorithm, gain, number of neurons in each layer, dependences between the number of the neurons, time delay and where will be applied, dependences between the time delay form each layers, recurrent links, sensitive function and the number of iterations. We observe that the small teaching gain, 0.1, determine one sensitive and stable approach to the target and one big teaching gain, for example 0.2 or 0.3, determine one bigger oscillation with different magnitude of the output, balanced near the target way. After the simulation of the double bipolar sigmoid hyperbolic tangent neural network we could remark the followings: the increase of the sigmoid bipolar gain determines minimization of the errors in the end of curve and increase errors in the middle of curve; one big difference between input and target data determines divergence (-9, or -10 with the target -0.4); increasing the teaching gain over than one limit determines instability (0.6 compare with 0.1). The time delay applied in each layers must alternate, if in one layer is applied one step of time delay, in the second must be applied two time delay steps. The number of neurons of the output layer must be double from the precedent.

By using the on-line work of the virtual LabVIEW instrumentation was possible to choose the optimal values of the weight and biases matrix to obtain one smaller errors and one fast approach after one small number of iterations.

The paper shown some of the more important neurons and neuron network types, proper mathematical models for them, how can teaching these networks and what are the results after numerical simulation with proper virtual LabVIEW instrumentation. All created virtual instruments work on-line and it is possible to see the influences of the input elements, weights, biases or of the number of the neurons in hidden layer or in the input data layer. It is possible to see on-line what is happened when was changed the target form of the curve, the components of some layers, the sensitive functions or the teaching gain. With this instrumentation we can choose the optimal form of the neural network concerning the type of the neurons in each layer, the neuron number and the biases, weights, input matrix and the teaching gain. The results and the created virtual LabVIEW instrumentation can be used in many other mechatronic guided applications, to perform the error between the target and the output and to obtain the short time of convergence.

The virtual proper LabVIEW instrumentation designed for these research activities open the way to the on-line optimization of the many other application what use the complex neural network.

Front panel of the virtual instrumentation work friendly, we can create easily all complex neural network for different application and we can choose on-line all network's parameters, like a biases and weights matrices, sensitive functions and number of neurons in each layer, teaching and sigmoid bipolar gains with the finally goal to obtain the minimum of the gradient error, with minimum number of iterations.

Showed algorithm, virtual instrumentation, proper mathematical models and the results, open the way to the optimal design of the complex neural network. In the future work will be analyzed other sensitive functions and the neural network by combined different types of these functions. The future work will be the application of the neural network to the optimal answer of the dynamic behavior with intelligent damper and proper intelligent vibration automation schema.

## 11. Conclusion

The paper was shown one assisted research of the more common neural networks and proposed one new neural network what introduce more rapidly convergence to the imposed target. With the proper mathematical model was possible to obtain one convergence without imposed input data, with small number of iterations and without teaching law based by teaching network with the input- target data pairs. The proposed mathematical model and the virtual proper LabVIEW instrumentation open the way to develop new generation of the intelligent systems and applied them in mechanical and aeronautical applications.

## REFERENCES

[1] Blelloch, G., & Rosenberg, C.R. "Network learning on the Connection Machine" Proc. of the Tenth International Joint Conference on Artificial Intelligence. Dunno, pp. 323-326, 1987.

[2] Cybenko, G. Approximation by superpositions of sigmoid function, Mathematics of Control, Signals, and Systems, vol. 2., pp.303–314, 1989

[3] Elman, J.L.Finding structure in time, Cognitive Science, 14, pp.179-211, 1990.

[4] Fukushima, K. Cognitron: A self- organizing multilayered neural network, Biological Cybernetics, 20, pp.121-136,1975.

[5] Hartman, E.J., Keeler, J.D.,&Kowalski, J.M. Layered neural network with Gaussian hidden units as universal approximations, Neural Computation, 2(2), pp.210-215, 1990.

[6] Hopfield, J.J. Neural networks and physical systems with emergent collective computational abilities, Proc.of the National Academy of Sciences, 81, pp.3088-3092, 1984.

[7] Lippmann, R.P. An introduction to computing with neural nets, IEEE Transactions on Acoustic, Speech, and Signal Processing, 2(4), pp.4-22, 1987.

[8] Minsky, M., & Papert, S. Perceptron: An Introduction to Computational Geometry, The MIT Press, 1969.

[9] Rosenblatt, F. Principle of Neurodynamics, New-York: Spartan Book.

[10] Dimith, H., Beale M.& Hagan M.: Neural Network Toolbox™ 6- User Guide, The MathWorks, Inc. 3 Apple Hill Drive Natick, MA 01760-2098, USA.

[11] Alsina, P.J., Gehlot, N.S., Direct and inverse kinematics of robot manipulator based on modular neural networks, ICARCV, IEEE, pp. 1743-7, Volume 3, 1994.

[12] Manseur, R., Keith, D., A fast algorithm for reverse kinematics analysis of robot manipulator, International Journal of Robotics Research, 7, 3, pp. 622 - 648, 1998

[13] Gorinevsky, D., Connoly, T., Comparations of some neural network and scattered data approximations: The inverse manipulator kinematic example, Neural Computation, 6, 3, pp. 521-542.

[14] Lee, L., Training feed forward neural networks: An algorithm givin improved generalization, Neural Networks, 10, 1, pp. 61-68, 1997.

[15] Schittenkopf, C., Deco, G., Brauner, W., Two strategies to avoid overfitting in feedforward networks, Neural Networks, 10, 3, pp. 505-516, 1997.

[16] Staicu, S., Modèle dynamique en robotique, UPB Scientific Bulletin, Series D: Mechanical Engineering, 61, 3-4, pp. 5-19, 1999.

[17] Staicu, S., Power requirement comparison in the 3-RPR planar parallel robot dynamics, Mechanism and Machine Theory, 44, 5, pp. 1045-1057, 2009.

[18] Olaru, A., Olaru S., Ciupitu, L., Assisted research of the neural network by bach propagation algorithm, OPTIROB 2010 International Conference, Calimanesti, Romania, The RPS Singapore Book, pp. 194-200, 2010.

[19] Olaru, A., Olaru, S., Paune D., Ghionea A., Assisted research of the neural network, OPTIROB 2010 International Conference, Calimanesti, Romania, The RPS Singapore Book, pp. 189-194, 2010.

[20] Olaru, A., Olaru, S., Assisted research of the neural network with LabVIEW instrumentation, IEEE ICMENS-2010 Proceedings, Changsha, China, pp. 1-8, 2010.

[21] Olaru, A., Oprean, A., Olaru, S., Paune, D., Optimization of the neural network by using the LabVIEW instrumentation, IEEE ICMERA 2010 Proceedings, ISBN 978-1-4244-8867-4, IEEE catalog number CFP1057L-ART, pp. 40-44, 2010.

[22] Olaru, A., Olaru, S., Paune, D., Assisted research dynamic neural network with time delay and recurrent links, IEEE ICMERA 2010 Proceedings, ISBN 978-1-4244-8867-4, IEEE catalog number CFP1057L-ART, pp. 284-288, 2010.

[23] Olaru, A., Olaru, S., Paune, D., Oprean, A. Assisted Research and Optimization of the proper Neural Network Solving the Inverse Kinematics Problem, IACSIT OPTIROB 2011 Proceedings, ISSN 2010-460X, ISBN 978-981-108-8906-7, pp.15-23, 2011.

**ISSN 1454 - 8003**
**Proceedings of 2011 International Salon of Hydraulics and Pneumatics - HERVEX**
*9 – 11 November, Calimanesti-Caciulata, Romania*

# STUDIUL DISTRUGERILOR GENERATE DE CAVITAȚIE OȚELULUI INOXIDABIL MARTENSITIC G-X5CrNi13.4

**Ilare BORDEAŞU, Adrian KARABENCIOV,**
**Alin Dan JURCHELA, Octavian Victor OANCĂ**

**Rezumat.** În lucrare se studiază mecanismul eroziunii prin cavitație a oțelului inoxidabil martensitic G-X5CrNi13.4 folosit în ulima perioadă la turnarea paletelor turbinelor bulb, de la Porțile de Fier II şi Kaplan, de La Porțile de Fier I. Pentru aceasta, se va utiliza difracția cu raze X, prin care se pun în evidență modificările structurale din stratul de suprafață rezultate prin eroziune cavitațională la 30 minute, respectiv 120 minute de atac cavitațional şi se vor face discuții, cu imagini micrografice, pe baza spectrelor de difracție din domeniul unghiular $2\theta\in(44^{0,}\ 56^{0})$. De asemenea, se vor analiza microreliefurile suprafețelor erodate cavitațional, pe baza replicilor obținute, la timpii caracteristici (30 minute si 120 minute de atac cavitațional), prin microscopie electronică cu transmisie, folosind microscopul TESLA BS 613. Totodată se va analiza şi evoluția microdurității în suprafața erodată cavitațional. Pentru realizarea obiectivelor menționate vor fi studiate 2 probe provenite din semifabricatul turnat al paletei, una din zona periferiei şi cealaltă din zona flanşei. Atacul cavitațional este realizat în aparatul vibrator magnetostrictiv cu tub de nichel al Laboratorului de Maşini Hidraulice din Timişoara.

**Cuvinte cheie :** eroziune, cavitație, otel, microstructura, deformații, microduritate, difracție.

## 1.Introducere

Eroziune cavitațională a materialelor constituie o permanentă preocupare a oamenilor de ştiința şi mai ales a producătorilor de echipamente hidromecanice, datorită modificărilor aduse geometriei organelor aflate în contact cu fluidul cavitant, cu implicație asupra performanțelor şi duratei de exploatare a echipamentului.

Găsirea unor soluții tehnologice, de creştere a duratei de viață a componentelor maşinilor ce funcționează în regim de cavitație, în special a turbinelor hidraulice, a obligat cercetătorii să-şi orienteze studiile spre analizarea materialelor atât din punct de vedere al rezistenței la distrugere cavitațională cât şi din punct de vedere al fenomenelor ce se produc în structura materialului prin atacul cavitațional. Această directie este impusă de multitudinea factorilor ce influențează eroziunea cavitațională: componenta structurală, constituția chimică, tehnologia de elaborare a semifabricatului, tratamentele termice, chimice şi mecanice, etc. Pe această linie, în cadrul lucrării se analizează deformarea, prin cavitație, a oțelului inoxidabil martensitic G-X5CrNi13.4 folosit în ultima perioadă la turnarea paletelor turbinelor bulb, de la Porțile de Fier II şi Kaplan, de La Porțile de Fier I. Pentru aceasta, s-a utilizat difracția cu raze X, prin care se pun în evidență modificările structurale din stratul de suprafață rezultate prin eroziune cavitațională la 30 minute, respectiv 120 minute de atac cavitațional şi se fac discuții, cu imagini micrografice, pe baza spectrelor de difracție din domeniul unghiular $2\theta\in(44^{0,}\ 56^{0})$. De asemenea, se analizează microreliefurile suprafețelor erodate cavitațional, pe baza replicilor obținute, la timpii caracteristici (30 minute si 120 minute de atac cavitațional), prin microscopie electronică cu transmisie, folosind microscopul TESLA BS 613. Totodată se analizează şi evoluția microdurității în suprafața erodată cavitațional. Pentru realizarea obiectivelor menționate sunt studiate 2 probe provenite din semifabricatul turnat al paletei, una din zona periferiei şi cealaltă din zona flanşei. Atacul cavitațional este realizat în aparatul vibrator magnetostrictiv cu tub de nichel al Laboratorului de Maşini Hidraulice din Timişoara.

**2. Materialul testat**

Materialul testat este oțelul inoxidabil martensitic GX5CrNi13.4 folosit în turnarea paletelor turbinelor bulb, de la CHE Porțile de Fier II şi Kaplan, de la CHE porțile de Fier I. Au fost supuse cavitației vibratorii două probe; provenite din semifabricatul turnat al unei palete; una din zona periferiei şi cealaltă din zona flanşei. Din aceleaşi zone s-au fabricat epruvete pentru încercări statice de tracțiune, respectiv probele pentru analize microscopice şi studierea deformării prin eroziune cavitațională.

Compoziția chimică, determinată în laboratorul de analize chimice de la U.C.M. REŞIȚA, este:

Proba P1, prelevata de la periferia paletei: C = 0,05%; Mn = 0,223%; Si = 0,442%; Cr = 12-14%; Ni=3,45 %; S = 0,023%; P=0,012%; Mo=0,35%; N=0,02%; Fe=rest

Proba P2, prelevata din zona flanşei: C = 0,05%; Mn = 0,223%; Si = 0,442%; Cr= 12-14%; Ni=3,5%; S = 0,023%; P= 0,012%; Mo=0,38%; N=0,02%; Fe=rest

Caracteristicile mecanice măsurate în laboratorul de Rezistență mecanică al Universității Politehnica din Timişoara sunt:

Proba P1: $R_m$ = 73 daN/mm$^2$, Duritatea măsurată prin metoda Vickers: 371 HV5/30; Alungirea 14,8%; Proba P2: $R_m$ = 74 daN/mm$^2$; Alungirea 14,9%; Duritatea măsurată prin metoda Vickers: 392 HV5/30. Diferența de duritate dintre probele P2 şi P1 se expilcă prin viteza de răcire mai mare a flanşei palei turbinei decât cea a vârfului (periferiei).

**3. Aparatura utilizată şi metodica de încercare**

Testele de eroziune cavitațională au fost realizate în aparatul vibrator magnetostrictiv (fig.1), aflat în dotarea Laboratorului de Maşini Hidraulice din Timişoara [1]

Menținerea constantă a temperaturii lichidului din vas se realizează cu o serpentină din cupru prin care circulă apa de răcire de la rețea.

Metoda de încercare este cea stabilită de normele ASTM G32-2010 [10], iar ca mediu cavitant s-a folosit apă dublu distilată la $20 \pm 1\ ^0$C.

Principalele carateristici ale aparatului sunt:

- distanța de imersare a probei: 3-5 mm;
- amplitudinea oscilațiilor: 47 $\mu$m;
- frecvența de oscilație: 7000 $\pm$ 3% Hz;

Durata totală a atacului cavitațional a fost de 150 minute, împărțită în douăsprezece perioade: câte una de 5 şi 10 minute si 8 de câte 15 minute fiecare. După fiecare perioadă de încercare probele au fost spălate în apă distilată, alcool şi acetonă, iar ulterior uscate în curent de aer şi cântărite cu o balanță analitică ce permite citirea a şase cifre semnificative.

Examinarea suprafețelor şi a microstructurii stratului degradate, în urma imploziei bulelor cavitaționale, s-a făcut prin microscopie electronică cu baleiaj.

**4. Analize şi încercări**

<u>*Analiza metalografică şi măsurarea durității.*</u>

Din mărcile GX5CrNi134 au fost confecționate probe cu diametrul de 14 mm, pentru încercarea la eroziune cavitațională.

Structurile metalografice, ale celor două probe, prezentate în figurile 2 şi 3 sunt de tip banito-martensitic.

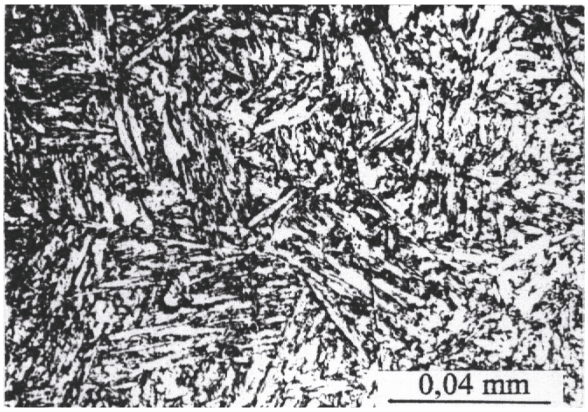


Fig.2 proba P1

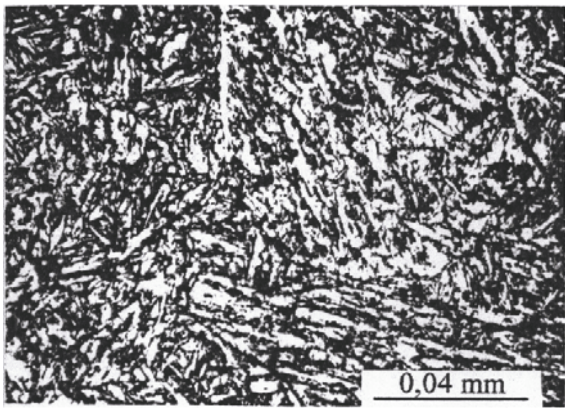


Fig.3 Proba P2

*Testul de eroziune prin cavitație*

Cele două probe au fost supuse procesului de eroziune cavitațională în instalație de cavitație magnetostrictivă, cu puterea de 500 W, în două etape de: $t_1$=30min şi $t_2$=120min.

Aspectul zonei de eroziune cavitațională este prezentat în tabelul 1, după 30 minute si respectiv 120 minute de atac cavitațional. Din examinarea acestor figuri se observă că în final zona cavitațională are aproximativ acelaşi diametru pentru ambele probele.

Tabelul 1 Aspecte ale zonelor erodate la diferiți timpi de atac cavitațional (vedere frontală)

| Proba | P1 | P2 |
|---|---|---|
| 30 minute de atac cavitațional |  |  |
| 120 minute de atac cavitațional | 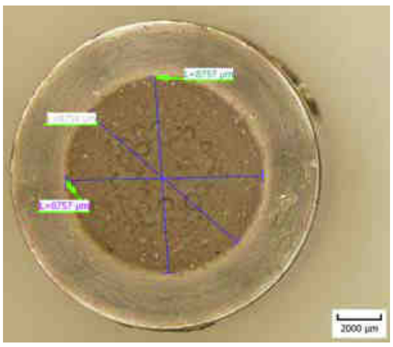 | 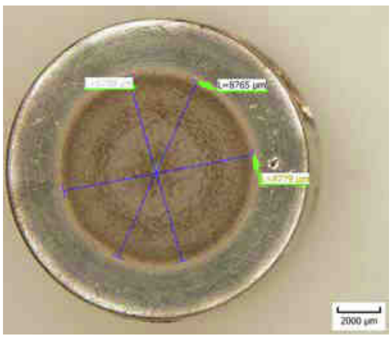 |

Aspectul reliefului zonei erodate cavitațional a fost examinat inițial pe bază de replici prin microscopie optică prin transmisie şi se prezintă în tabelul 2. Şi din examinarea acestor figuri se constată că probele P1 şi P2 sunt erodate aproximativ la fel.

Pentru a cunoaşte adâncimea de eroziune cavitațională finală probele au fost secționate longitudinal în lungul diametrului şi au fost lustruite. Astfel din tabelul 3 se constată că probele P1 şi P2 au fost erodate aproximativ la fel, pe adâncimi de până la 0,04 mm.

Tabelul 2 Aspecte ale reliefului zonelor erodate la diferiți timpi de atac cavitațional

| Proba | P1 | P2 |
|---|---|---|
| 30 minute de atac cavitațional | 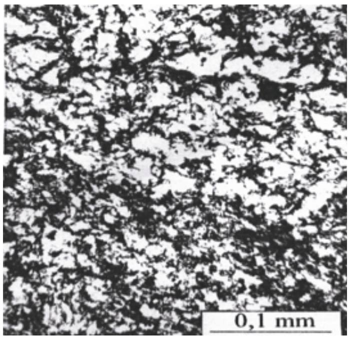  | 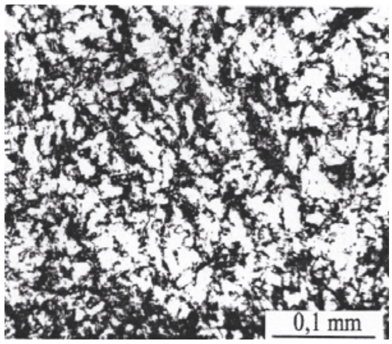  |

Tabelul 3 Aspecte ale reliefului zonelor erodate la diferiți timpi de atac cavitațional (secțiune axială)

| Proba | P1 | P2 |
|---|---|---|
| 120 minute de atac cavitațional | 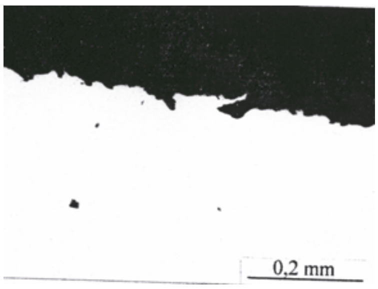  | 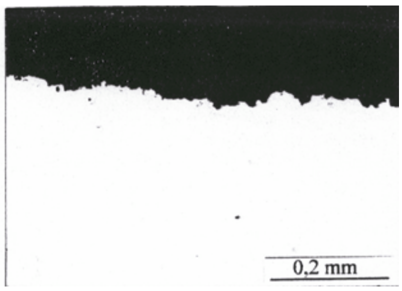  |

*Microrelieful suprafețelor erodate cavitațional*

Pentru cunoaşterea aspectului miroreliefului suprafețelor erodate prin cavitație au fost examitate replicile acestora, prin microscopie electronică prin transmisie cu ajutorul microscopului Tesla BS 613, după 30, respectiv 120 minute de atac (figura 4).

| | |
|---|---|
| 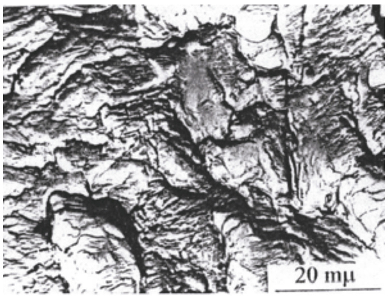  30 minute de atac cavitațional | 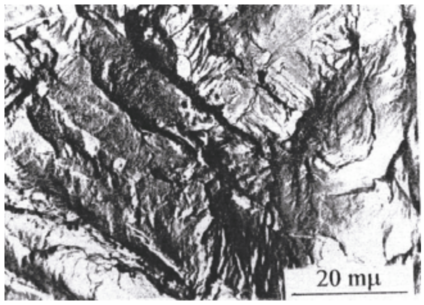  30 minute de atac cavitațional |
| 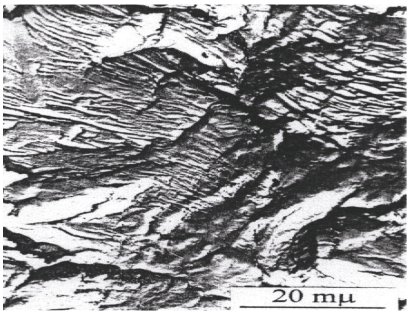  120 minute de atac cavitațional | 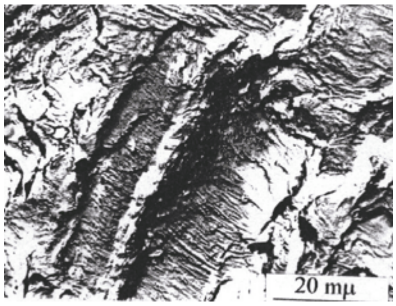  120 minute de atac cavitațional |
| Proba P1 | Proba P2 |

Fig.4

Microrelieful probelor erodate prin cavitație

Din examinarea probelor din figura 4, corelat cu aspectele din tabelul 3 se observă că în urma procesului de eroziune cavitațională microrelieful suprafețelor prezintă numeroase trepte de alunecare ale materialului, cu ruperi de grupuri de grăunți.

*Încercări de microduritate*

Au fost efectuate cu microdurimetrul PM3 cu scopul de a evidenția evoluția microduriății probelor de la suprafața erodată cavitațional spre miezul probelor. Pentru acesta, la finalul testului de eroziune, probele P1 si P2, au fost secționate longitudinal şi pregătite metalografic. Valorile de microduritate sunt prezentate în tabelul 5.

Tabelul 5

| Proba P2 | | Proba P1 | |
|---|---|---|---|
| d(μm) | $HV_{0,2}$ | d(μm) | $HV_{0,2}$ |
| 33 | 330 | 35 | 312 |
| 68 | 335 | 70 | 281 |
| 103 | 296 | 106 | 291 |
| 138 | 301 | 142 | 272 |
| 173 | 308 | 179 | 268 |
| 208 | 301 | 216 | 272 |

Din analiza datelor prezentate în tabelul 5 se observă că în cazul celor două probe, P2 şi P1, are loc o durificare a materialului în stratul marginal, care este plasat sub 0,04 μm față de suprafața probei. Astfel de durificări au fost sesizate şi în cercetările efectuate de către Knapp [3], Hammitt [1], Garcia [1], Steller [1], Franc ş.a [2]. Cum aceste durificări, în stratul marginal, nu sunt totuşi suficient de mari, rezultă că starea de tensiuni indusă de prin impactul dintre material şi undele de şoc, respectiv microjeturile, generate în timpul cavitației, nu este aşa de mare ca să conducă direct la fisurarea materialului, ci numai cu o deformare plastică, în prealabil.

## 5. Concluzii

Pe imaginile care evidențiază adâncimea de pătrundere a eroziunii cavitaționale, care este de până la 0,04 mm în cazul probelor P2 şi P1, nu se observă microfisuri din stratul marginal spre miezul probelor. De asemenea din măsurătorile de microduritate rezultă o durificare nesemnificativă a materialului probelor P2 şi P1. Lipsa fisurilor în stratul marginal se explică prin lipsa unei stării de tensiuni interne suficient de mare capabilă să le producă, creată de imploziile cavitaționale.

Detensionarea este atribuită încălzirii stratului superficial al probelor datorită procesului de generare al utrasunetelor şi în urma imploziilor cavitaționale. Examinările prin microscopie electronică a microreliefului suprafeței erodate, arată că porțiuni microscopice din această suprafață sunt supuse unor puternice procese de alunecare, în urma cărora sunt expulzate.

Astfel acest strat moale de la suprafață, cu grosimea maximă de 0,04 mm, este supus în mod continuu alunecării sub acțiunea imploziilor cavitaționale, iar de la suprafața probelor sunt expulzați, datorită alunecării puternice, mici grăunți microscopici. În acest mod cea mai mare parte din energia imploziilor este consumată în timpul procesului de alunecare, restul contribuind la încălzirea stratului superficial al probei.

**Recunoştiință**

**Lucrarea este finanțată din Grantul CNCSIS PN II: ID-34/2007: "Dezvoltarea de modele pentru evaluarea comportării materialelor la eroziunea prin cavitație"**

## BIBLIOGRAFIE

**[1] Bordeaşu, I**.,- *Eroziunea cavitațională asupra materialelor utilizate în construcția maşinilor hidraulice şi elicelor navale. Efecte de scară*, Teză de doctorat, Timişoara. 1997.
**[2] Frank, J., P., e.a**., -L*a cavitation, Mécanismes physiques et aspects industriels*, Presse Universitaires de Grenoble, 1995.
**[3] Knapp, R., T., Daily, J., W., Hammitt, F., G.,** -*Cavitation*. Mc.Graw-Hill, Book Company, H.Y. 1970.
**[4]** *** *Standard method of vibratory cavitation erosion test*, ASTM, Standard G32-2010.
**[5] *** GrantCNCSIS 154, Proiect TIP A, Tema 4, Contract nr. 32940/22.06.2004-** Studiul deformării şi fisurării produse prin eroziune cavitațională la oțelurile inoxidabile austenitice folosite la turnarea paletelor de turbină hidraulică, 2005

**ISSN 1454 - 8003**
**Proceedings of 2011 International Salon of Hydraulics and Pneumatics - HERVEX**
*9 – 11 November, Calimanesti-Caciulata, Romania*

# ABOUT HYDRODYNAMIC AND STEREO-MECHANIC DESIGN OF A DOUBLE-FLUX HYDRAULIC TURBINE

M. Bărglăzan, D.C. Stroiță

**Abstract:** This article presents the double-flux hydraulic turbine from two points of view, one is the optimization of turbine's hydrodynamics and the other is the strength of material analysis of the most stressed parts of the turbine, the runner and the wicket gate. In order two obtain the optimum running for a cross flow turbine it is necessary to study the all the parameters which interact in the design.
The BS 759 turbine parameters are presented through a software optimization program, used in order to establish the best correlation between the geometrical and running parameters.

## 1. Introduction

The design of hydraulic turbines is a compromise between the hydrodynamic interaction of the water stream with the runner and the resistance of the solid parts of the machines. This principle applied to cross-flow hydraulic turbines of double flux type permits to produce designs of best quality. Nowadays this procedure benefits of specialized soft for the hydrodynamic lay-out and the method of finite elements to verify the distribution of tensile stresses in the machines.

## 2. Hydrodynamic lay-out

For a hydropower plant with a double-flux hydraulic turbine the design data are:

- Turbines head $\mathbf{H_T = 40}$ [m]
- Rate of flow $\mathbf{Q = 1.8}$ [$m^3$ / s]

Following the lay-out procedure given in [1] and the soft programs from [2] it was possible to obtain the main dimensions and parameters of the machine.
First it was made a discussion about the main parameters of the double-flux hydraulic turbine. Especially the runner's speed of rotation and diameter was established by the data collected in Table 1.

Table 1

| Ht [m] | Q [m3/s] | Ps [kW] | pp [-] | n [rev / min] | $n_{s\ CP}$ [rev / min] | $D_1$ [m] |
|---|---|---|---|---|---|---|
| 40 | 1.8 | 564.854 | 5 | 600 | 165 | 0.422 |
| | | | 6 | 500 | 138 | 0.506 |
| | | | 7 | 428 | 118 | 0.590 |
| | | | 8 | 375 | 103 | 0.675 |
| | | | **9** | **333** | **91.8** | **0.759** |
| | | | 10 | 300 | 82.7 | 0.843 |
| | | | 11 | 272 | 75.1 | 0.928 |
| | | | 12 | 250 | 68.88 | 1.012 |
| | | | 13 | 230 | 63.58 | 1.096 |
| | | | 14 | 214 | 59.04 | 1.181 |

| | | | | | | |
|---|---|---|---|---|---|---|
| | | | 15 | 200 | 55.10 | 1.265 |
| | | | 16 | 187 | 51.66 | 1.349 |

From this table it was deduced the runner's speed of rotation of n = 333 [rev / min] and the diameter $D_1$ = 759 [mm].

Table 2

| | Values | Observations |
|---|---|---|
| $H_T$ [m] | **40** | Turbine's head |
| **n** [rev/min] | **333** | Speed of rotation |
| $k_{v1}$ [-] | **0.98** | Speed coefficient |
| $n_{11}$ [rev/min] | **40** | Double unitary speed |
| $\alpha_1$ [ $^0$ ] | **15.17343** | Absolute velocity entrance angle |
| $D_1$ [m] | **0.7597063** | Runner diameter |
| $v_1$ [m/s] | **27.44917** | Absolute velocity by entrance on the runner |
| $u_1$ [m/s] | **13.24612** | Peripheral velocity of the runner |
| $D_2$ [m] | **0.4719443** | Runner inner diameter |
| $D_2$ / $D_1$ [-] | **0.6212193** | Runner diameters ratio |
| $w_2$ / $w_1$ [-] | **0.7674842** | Relative velocities ratio |
| $n_s$ [rev/min] | **95.82016** | Specific speed |
| $\tau_a$ [MPa] | **24000000** | Admissible shear stress |
| $\beta_1$ [ $^0$ ] | **151.52494** | First entrance blade angle |
| $\beta_2$ [ $^0$ ] | **90** | First exit blade angle |
| $\beta_3$ [ $^0$ ] | **90** | Second entrance blade angle |
| $\beta_4$ [ $^0$ ] | **28.47506** | Second exit blade angle |
| $\eta_T$ [%] | **0.8733823** | Cross-flow hydraulic turbine maximum efficiency |
| $\eta_{had}$ [%] | **0.8946043** | Nozzle efficiency |
| $\eta_{hr}$ [%] | **0.8985676** | Runner efficiency |
| $\eta_{h1}$ [%] | **0.7637069** | Alternative formula for turbine efficiency |
| $\eta_{h2}$ [%] | **0.8579859** | Other formula for turbine efficiency |
| **z** [-] | **24** | Runner blades number |
| $\delta$ [mm] | **7.59063** | Blades thickness |
| $\alpha_2$ [rad] | **0.952392** | Absolute velocity exit angle |
| $w_2$ [m/s] | **11.5653** | Relative velocity by first exit |
| $u_2$ [m/s] | **8.228745** | Inner diameter peripheral velocity |
| $v_2$ [m/s] | **14.19396** | Absolute velocity by first exit |
| $\varepsilon$ [ rad ] | **1.904784** | Deviation angle |
| $P_s$ [kW] | **616.6704** | Hydraulic power of the turbine |
| **Q** [$m^3$/s] | **1.8** | Flow rate of the turbine |
| $b_r$ [m] | **0.8831724** | Runner width |
| **d** [m] | **0.1553983** | Shaft diameter |
| $s_0$ [m] | **0.07597063** | Nozzle breadth |
| $s_2$ [m] | **0.1469168** | Stream thickness between the first and second interaction |
| $\delta_1$ [mm] | **-0.01435607** | Distance between the stream and the runner shaft |
| $\delta_2$ [mm] | **0.02571224** | Distance between the stream and the inner diameter of the runner |
| $\rho_s$ [m] | **0.1326827** | Radius of runner blades |

| | | |
|---|---|---|
| **$\gamma$** $[^0]$ | **77.35959** | Blades angle at the radius center |
| **$\rho_{1p}$** [m] | **0.2707167** | Radius of the circle on which are disposed the blades radius centers |
| **$\rho_{1s}$** [m] | **0.2780525** | |
| **t** [mm] | **0.07087348** | Spacing distance at the runner diameter |
| **$H_{1r}$** [m] | **28.14387** | Runner head at the first interaction |
| **$H_{2r}$** [m] | **7.640306** | Runner head at the second interaction |
| **$H_r$** [m] | **35.7814** | Runner's head |
| **$\eta_r$** [ % ] | **0.8946043** | Runner hydraulic efficiency |
| **b** [m] | **0.8631724** | Nozzle's width |
| **$\rho_e$** [m] | **0.09942314** | Radius of the generator circle of the nozzle breadth walls |
| **$\delta_B$** $[^0]$ | **43.7804** | Angle at the runner axis covered by nozzle exit |
| **$l_s$** [m] | **0.1791454** | Length of the blades |
| **$w_m$** [m/s] | **13.3172** | Mean relative velocity in the first interaction with the runner |
| **T** [ s ] | **0.01345218** | Time spent of a fluid particle between the runner's blades |
| **S** [m] | **0.1781892** | Displacement of the runner periphery during particle flow through the blade channel |
| **$\gamma_1$** $[^0]$ | **26.87746** | Rotation angle at the runner center during the particle flow through the blade channel by the first interaction |
| $AOB$ $[^0]$ | **162.891** | The runner center angle between the inlet and outlet from the runner of the mean stream particle |
| **$\gamma_2$** $[^0]$ | **8.554504** | Rotation angle at the runner center during the particle flow through the blade channel by the second interaction |
| **$z_B$** [-] | **2.918693** | Number of runner blades covered by nozzle outlet |
| **$\varphi_{ext}$** $[^0]$ | **- 13.3357** | Deviation angle from the mean of the extreme exterior particle by the second interaction |
| **$\varphi_{int}$** $[^0]$ | **30.4447** | Deviation angle from the mean of the extreme interior particle by the second interaction |
| **$H_{av}$** [m] | **0.4798532** | Tail race level down from runner's axis |

Further all the important calculated dimensions of this turbine BS – 759 are given in Table 2.
Figure 1 explains some of the data given in table 2.

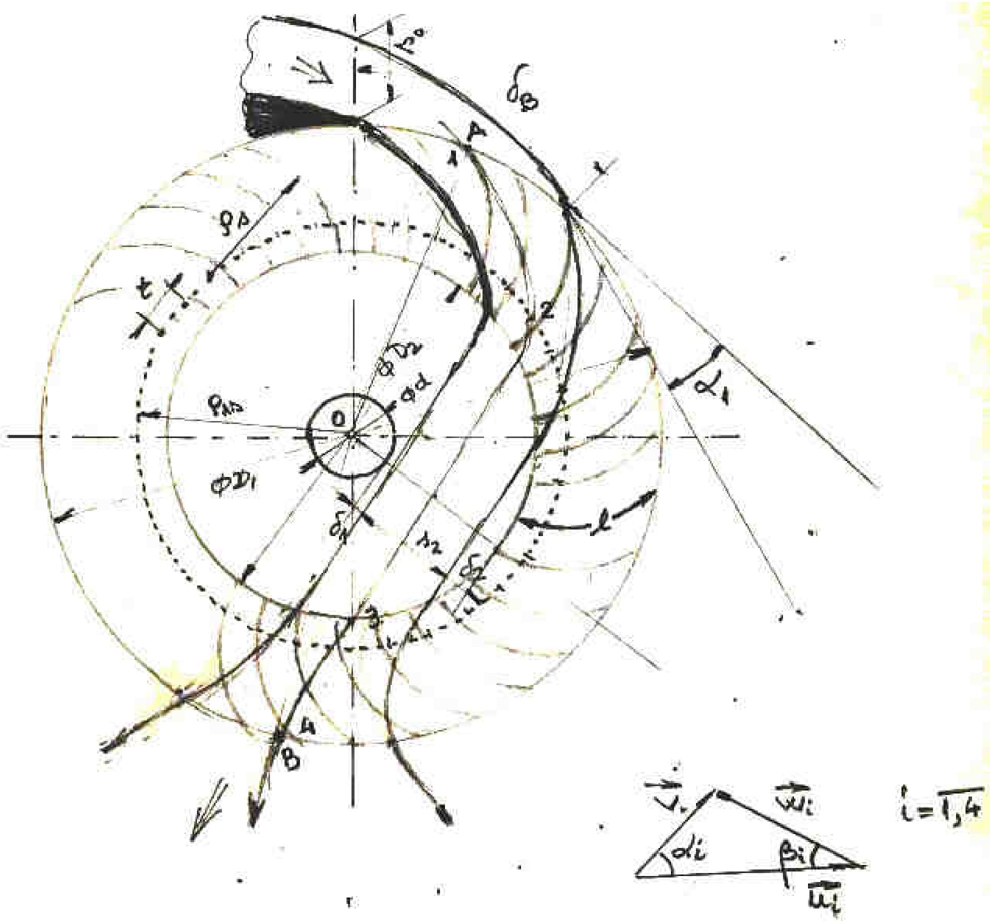

*Figure 1 Cross section through the double-flux runner.*

### 3. Strength of materials lay-out

The strength of materials lay-out was based on one-dimensional dimensioning and finite elements method verifying to the main parts of the machine namely, the runner and the wicket gate.
The software used for drawing is Solid Works and the analysis was made with ANSYS 11.0.

The geometry of the runner was generated, in accord with the hydrodynamic design, in Solid Works programs. The result of the modeling and simulation are presented in Fig. 2, Fig. 3 and Fig.4.
The simulation of the runner stresses are considered in the toughest situation: the runner is blocked and on it acts the whole force of the water jet (stream). The water acts on three blades as it is seen on Fig. 2.

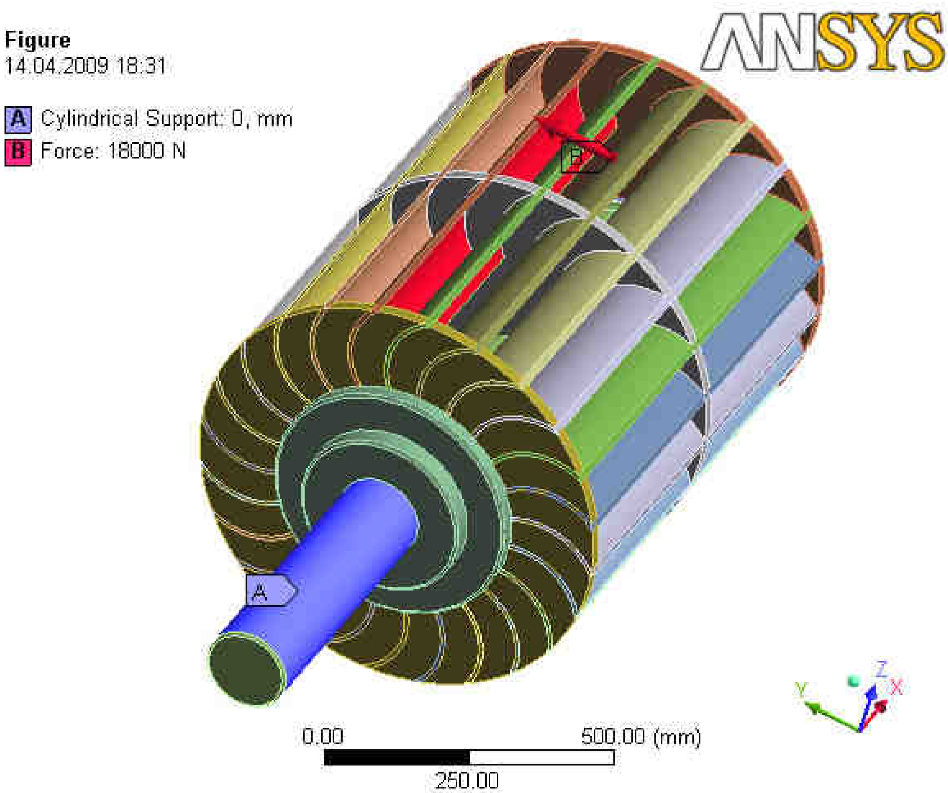


*Fig.2. The conditions for the simulation*

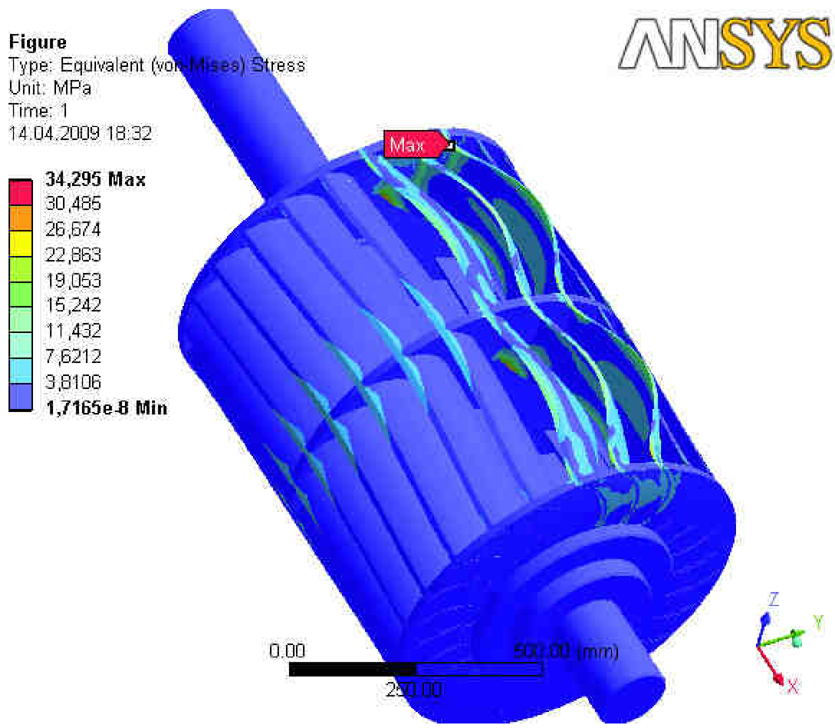

*Fig. 3. The equivalent Von Misses stresses in the BS – 759 double flux runner caused by the force of the water jet*

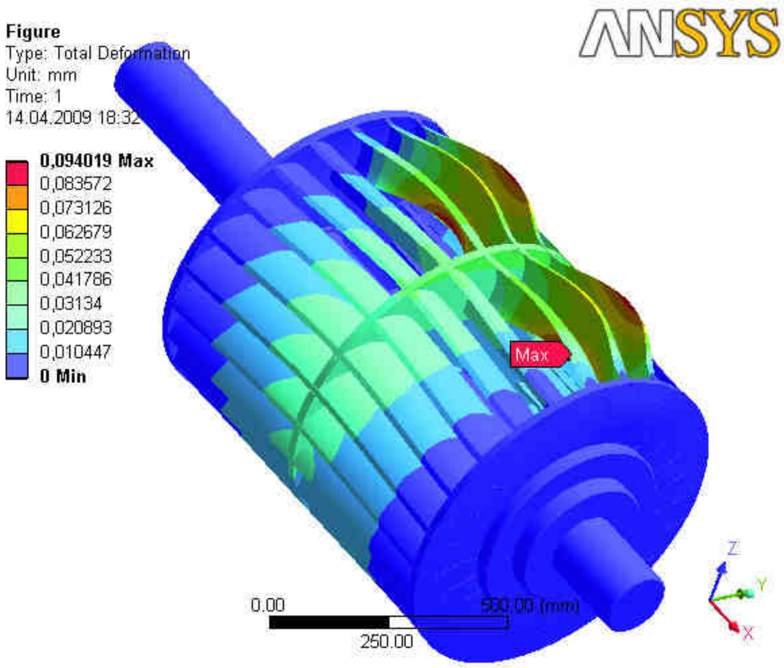


*Fig. 4 The total deformation of the runner caused by the water jet (stream) force*

The wicket gate is analyzed in two situations: closed, without and with water hammer effect.

Without water hammer the static pressure is p=0.4 MPa

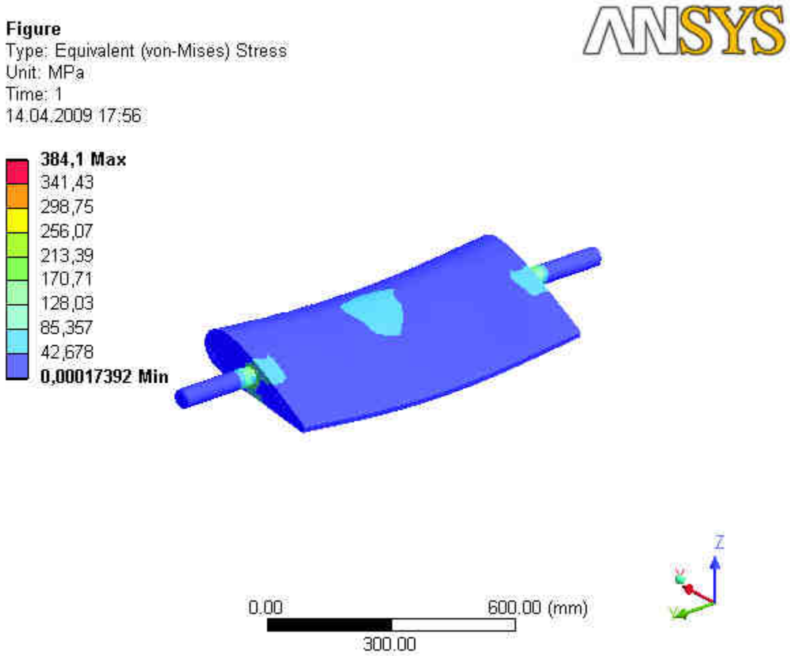


*Fig. 5 The von Misses stress diagram for the whole wicket gate for p=0.4 MPa*

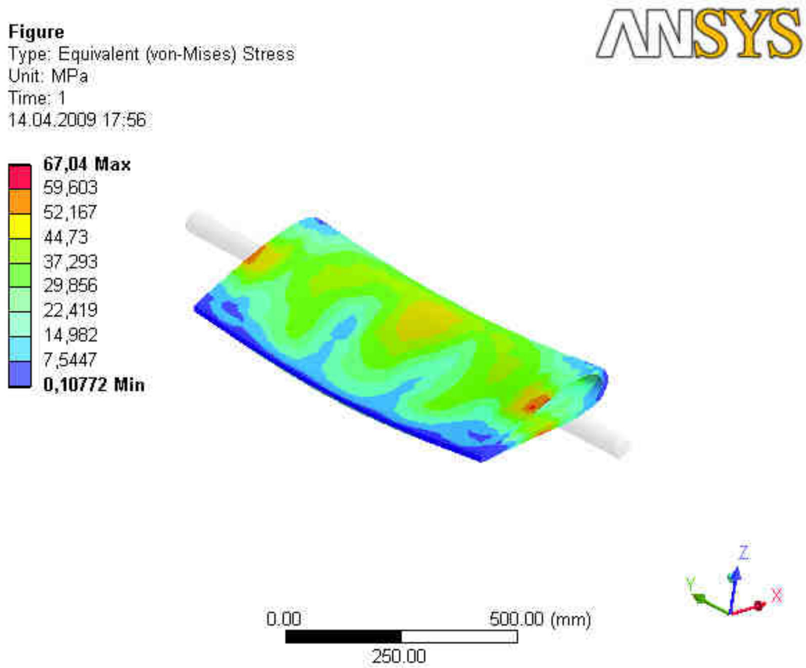


*Fig. 6 The von Misses stress diagram for the wicket gate coating for p=0.4 MPa*

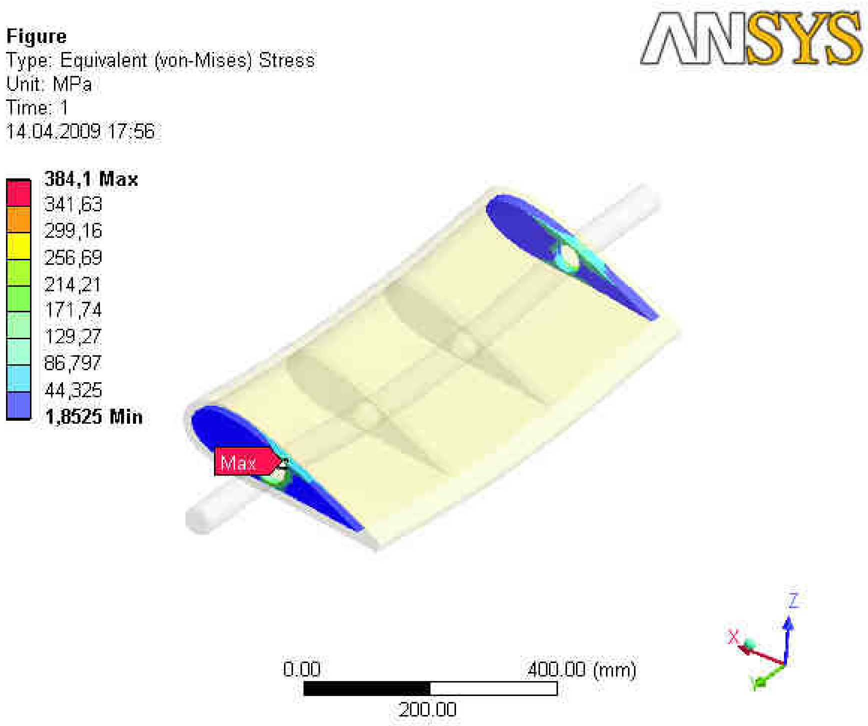


*Fig. 7 The von Misses stress diagram for the wicket gate frame work for p=0.4 MPa ( variant 1 ).*

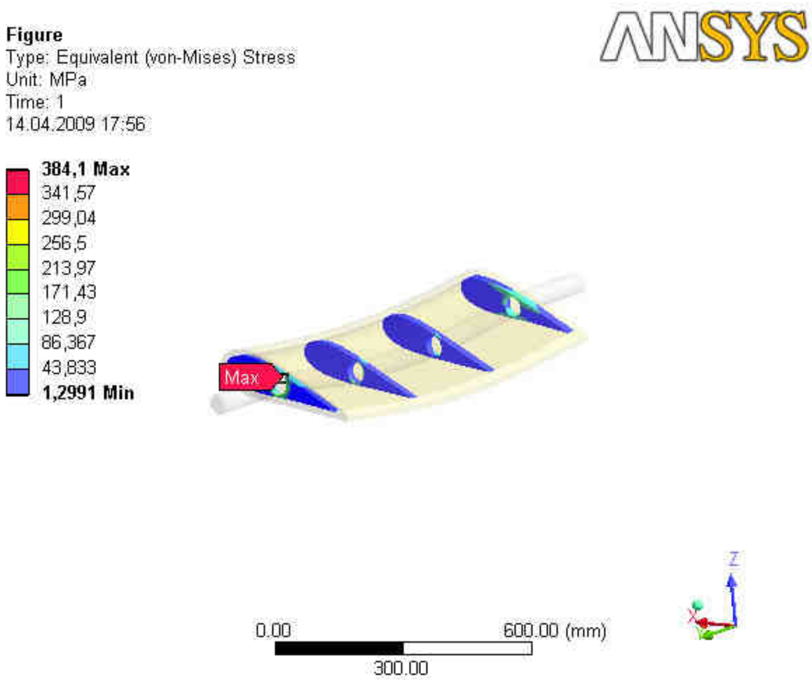

*Fig. 8 The von Misses stress diagram for the wicket gate framework for p=0.4 MPa ( variant 2 ).*

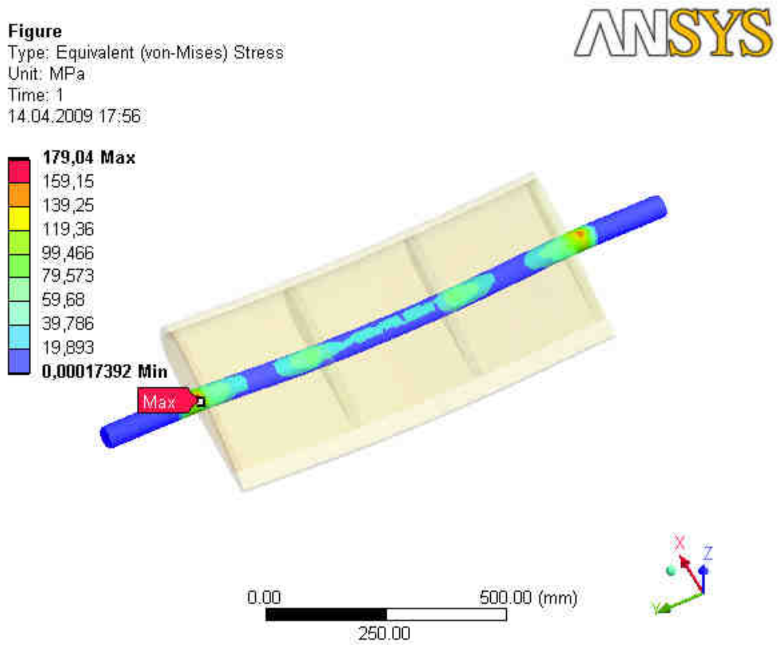


*Fig. 9 The von Misses stress diagram for the wicket gate shaft for p=0.4 MPa*

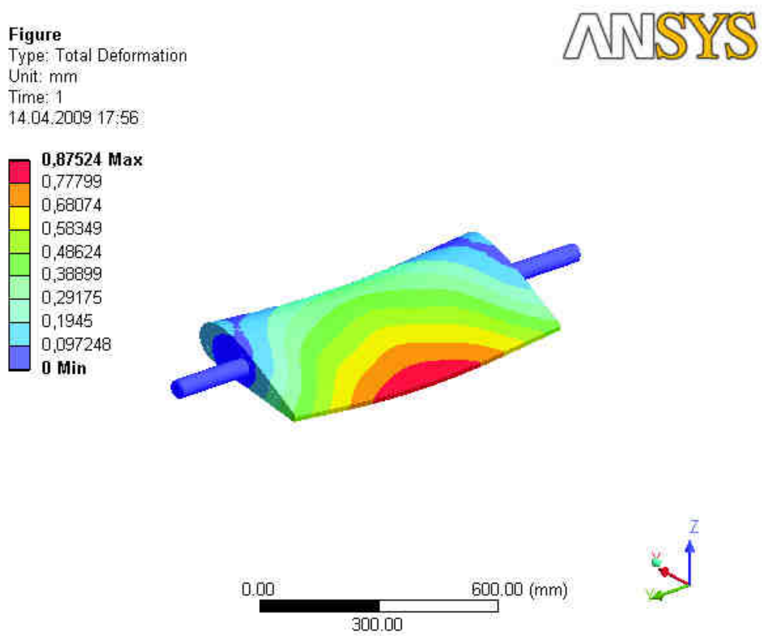

*Fig. 10 The total deformation of the whole wicket gate for p=0.4 MPa*

With water hammer the maximum pressure is p=0.8 MPa

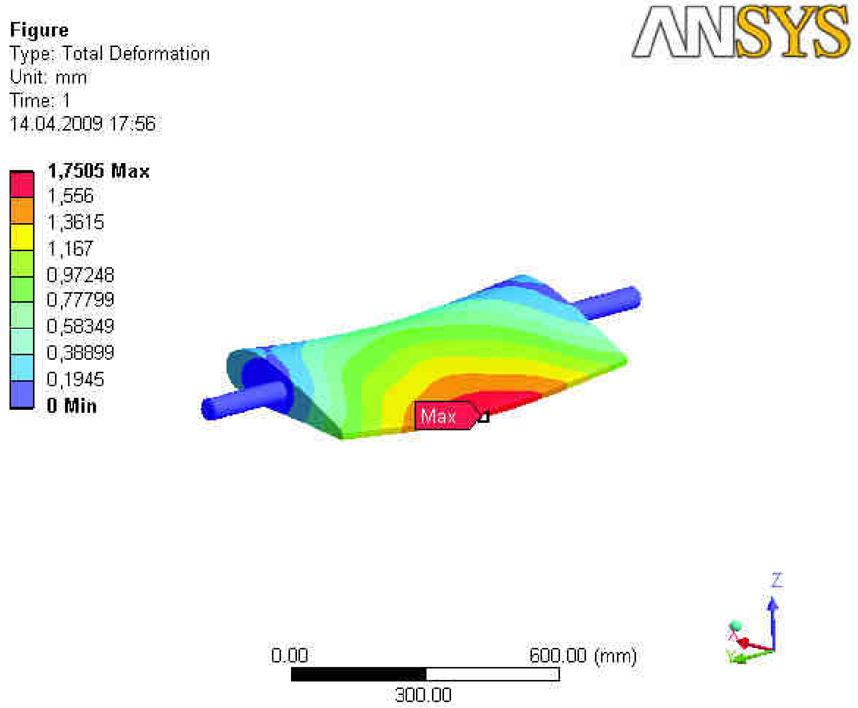


*Fig. 11 The total deformation of the whole wicket gate for p=0.8 MPa*

## 4. Conclusions

- Table1 offers a technique-economic optimized solution for the cross flow hydraulic turbine realizing a compromise between the specific speed domain, speed of rotation and runner diameter.
- Table 2 gives the main hydraulic parameters and geometric dimensions of the chose double flux machine.
- It was established the distribution of equivalent Von Misses stresses in the BS-759 cross flow runner caused by the force of the water jet.
- The total deformation of the runner under the water stream is represented
- The stresses with and without water hammer on the wicket gate are calculated and presented.
- The wicket gate deformation under the above mentioned conditions are figured in a color code.
- This article shows how the hydrodynamics of the double flux hydraulic turbine affects the strength of materials in the mainly parts of the turbine, runner and wicket gate.

## 5. References

[1] M. Bărglăzan, *Turbine hidraulice şi transmisii hidrodinamice*, Ed. Politehnica, Timişoara, 2000.

[2] M. Bărglăzan, *About Design Optimization of Cross-Flow Hydraulic Turbines*, Sci. Bul. "Politehnica" University of Timişoara, Fasc. 2 , 2005.

[3] D. C. Stroita, *Identificarea dinamică a turbinelor cu dublu flux*, Ed. Politehnica, Timişoara 2009.

[4] V. Obretenov, *Optimization of Cross-Flow Water Turbine*. The 26th Israel Conf. on. Mech. Eng. Technion City, Haifa, 1996.

**ISSN 1454 - 8003**
**Proceedings of 2011 International Salon of Hydraulics and Pneumatics - HERVEX**
*9 – 11 November, Calimanesti-Caciulata, Romania*

# ASUPRA CERINȚELOR TEHNOLOGICE SI FUNCȚIONALE IMPUSE APARATELOR VIBRATORII DESTINATE PRODUCERII CAVITAȚIEI

**Ilare BORDEAŞU, Octavian Victor OANCĂ, Alin Dan JURCHLEA, Adrian KARABENCIOV, Marcela Elena DIMIAN**

**Rezumat:** În lucrare sunt prezentate principalele condiții tehnico-funcționale ce trebuiesc realizate pentru ca aparatele vibratorii, utilizate în producerea cavitației, să respecte cerințele normelor internaționale ASTM G32-2010.

**Cuvinte cheie:** eroziunea cavitației, amplitudine, frecvență, traductoare, amplificatoare acustice, rezonanță

## 1. Introducere

Aparatele vibratorii utilizate în distrugerea materialelor prin eroziune cavitațională sunt sisteme deschise, acustice respectiv ultraacustice, care folosesc energia sonoră, respectiv ultrasonoră, pentru producerea de modificări în structura mediului prin care se propagă [1], [4], [6], [9].

Deşi procesul cavitațional este total diferit de cel din instalațiile industriale aparatele vibratorii sunt tot mai des folosite datorită următoarelor avantaje [1], [2], [10]: durata de încercare foarte mică, maxim 2 - 4 ore, spațiul ocupat foarte redus, permit utilizarea oricărui tip de lichid, au cea mai mare intensitate de distrugere, [2], [3], rezultatele obținute sunt acoperitoare pentru situațiile reale.

În cercetarea eroziunii cavitaționale a materialelor se utilizează următoarele două tipuri de aparate [1], [3]:

- magnetostrictive (cu transductoare feritice sau tuburi de nichel),
- piezoelectrice.

Calitatea bunei funcționări a acestor aparate depinde de asigurarea următoarelor condiții: amplitudine şi frecvență de lucru înalte, pierderi de căldură reduse, eficiență mare la transformarea energiei electrice în energie acustică.

În lucrare se prezintă condițiile funcționale de bază, factorii tehnologici şi acustici ce trebuiesc îndepliniți de către sistemul vibrator mecanic, pentru creearea condițiilor hidrodinamice necesare producerii eroziunii cavitaționale.

## 2. Condiții funcționale, tehnologice şi acustice

Elementul activ al aparatului este un transductor electromecanic care converteşte oscilațiile electrice produse de generatorul electric sau electronic în oscilații elastice. Aceste oscilații sunt transmise, concentrate şi localizate în mediu de prelucrare, prin intermediul transformatorului acustic.

Probele supuse atacului cavitațional pot fi staționare sau vibratorii (fixate de subansamblu transductor) [2].

În cazul probelor vibratorii montarea lor se face în punctul de amplificare maximă (capătul inferior al transformatorului acustic).

Eroziunea cavitațională are loc ca urmare a mişcării vibratorii pe verticală a transformatorului acustic care generează, periodic, un nor de bule cavitaționale. Prin surparea norului se nasc presiuni ridicate pe suprafața probei, producând ruperi de material. Pentru aceasta trebuiesc îndeplinite două condiții esențiale:

1. aparatul să funcționeze în regim de rezonanță, cu unde longitudinale plane, la amplitudini de vibrație A $\geq$ 8 $\mu$m [1], [3]. La aceste amplitudini cea mai mare parte din energia acustică este absorbită de material, restul disipându-se sub formă de caldură în mediul înconjurător [1].
2. norul de bule cavitaționale să adere pe suprafața probei. Această aderență este determinată de tensiunea superficială la interfețele lichid-solid- vapori şi interacțiunea mecanică dintre bule şi asperitățile suprafeței probei. Datorită aderenței fluidului, pe suprafața de atac a probei, în timpul oscilațiilor, la urcare, apare norul de bule cavitațional. La coborâre acest nor se surpă generând unde de şoc, microjeturi şi creşterea temperaturii pe suprafața probei. Prin acțiunea comună a celor trei factori are loc o distrugere rapidă a suprafeței, diferențiat de la un material la altul.

La aparatul vibrator cu tub de nichel nivelul amplitudinii este determinat de lungimea tubului, iar la cel cu transductor piezoceramic sau feritic este determinat de forma transformatorului acustic (conic, exponențial, cilindric în trepte, catenoidal, etc.) şi raportul secțiunilor intrare-ieşire [1], [4], [5], [6].

Indiferent de tipul aparatului vibrator calitatea legăturilor dintre părțile componente ale acestuia precum şi calitatea execuției pieselor componente ale sistemului mecanic vibrator au un rol decisiv asupra puterii de distrugere cavitațională a aparatului.

În figura 1 se prezintă schema principială a aparatului vibrator cu cristale piezoceramice T2, aflat în dotarea Laboratorului de Maşini Hidraulice din Timişoara şi construit cu respectarea prevederilor normelor ASTM G32-2010.

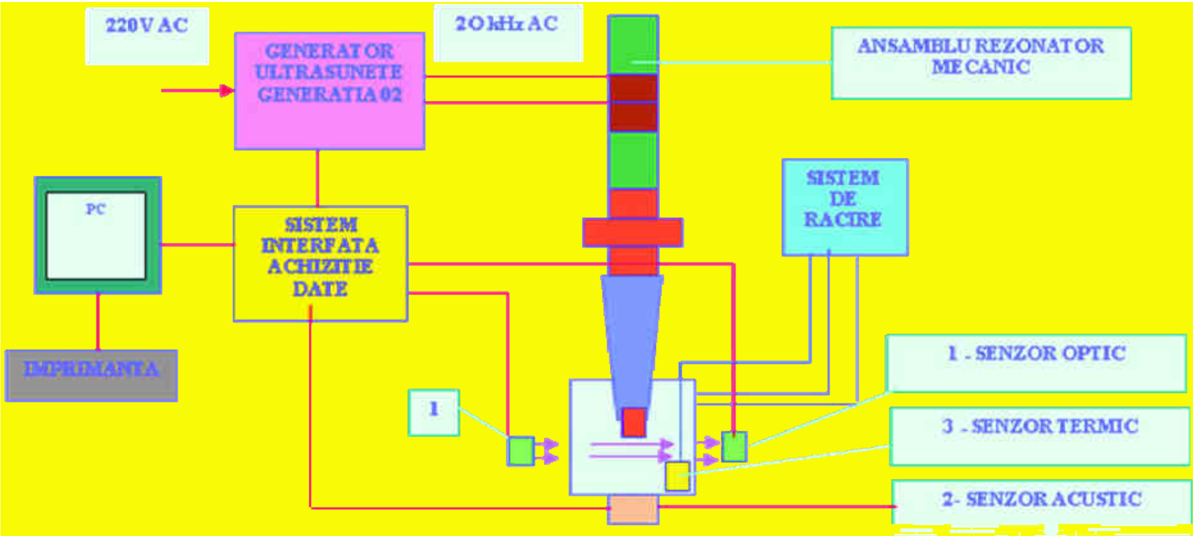


Fig, 1. Aparatul vibrator cu cristale piezoceramice T2
(schema principială)

Buna funcționare a aparatului vibrator cu ultrasunete depinde de respectarea condițiilor tehnologice şi a condițiilor acustice. Respectarea acestora asigură sistemului oscilator creearea regimului de vibrații enecesar transmiterii energiei ultrasonore de la transductor la mediu (proba solicitată la cavitație).

Condițiile tehnologice sunt determinate de:

**1.** precizia de calcul şi confecționare a elementelor blocului ultrasonic.

Realizările practice au demonstrat că dimensiunile pieselor calculate suferă modificări pe parcursul racordării blocului ultrasonic la frecvența de rezonanță produsă de generatorul electronic de ultrasunete [1], [3], [5]. Din acest motiv, în general, la lungimea finală a transformatorului acustic se adaugă 5-10 mm care se îndepărtează treptat, pe parcursul încercărilor de atingere a frecvenței de rezonanță. Procesul se numeşte ajustare la frecvența de rezonanță.

Pentru aparatul vibrator cu transductor piezoceramic sau feritic nivelul amplitudinii de vibrație, frecvența de rezonanță depind foarte mult de respectarea condițiilor geometrice, dimensionale şi calitatea suprafeței prelucrate. Astfel abaterile de la forma geometrică şi dimensională trebuie să fie în clasele 4 sau 5 de precizie, iar suprafețele de contact să fie plane (0,001/100). De asemenea se impune lepuirea sau superfinisarea tuturor suprafețelor (Ra = 0,025 - 0,04μm), pentru înlaturarea amorselor de fisuri.

**2.** Rezistența la uzură şi oboseală a materialelor utilizate în confecționarea blocului ultrasonic.

Materialele, care respectă condiția 2 şi se recomandă în realizarea transformatoarelor acustice sunt: oțelurile de scule, duraluminiu tip BSL5, aliajele pe bază de titan (90 %Ti, 6 %Al, 4 %V) şi pe bază de magneziu (93 %Mg, 6 %Al, 1 %Zn) [1], [6]. Pentru aparatele magnetostrictive în general se recomandă tuburile de nichel pur [7].

**3.** Rigiditatea sistemului.

**4.** Stabilitatea în funcționare a generatorului electronic de ultrasunete.

Menținerea constantă a frecvenței şi amplitudinii de vibrație, o durată cât mai mare de funcționare continuă, depinde de calitatea fabricației generatorului electric sau electronic de ultrasunete. De asemenea, în timp, piesele electrice şi electronice ale generatoarelor se încălzesc şi îşi modifică caracteristicile de funcționare, respectiv de vibrație. Din acest motiv toate aparatele vibratorii sunt prevăzute cu sisteme de ventilare a generatoarelor de vibrație, electronice sau electrice.

**5.** Calitatea îmbinării elementelor blocului ultrasonic (strângere puternică şi lipire perfectă).

La aparatele cu transductoare piezoceramice şi feritice, îmbinarea dintre transductor şi transformatorul acustic depinde de planeitatea şi rugozitatea suprafețelor de contact.

La aparatul vibrator magnetostrictiv cu tub de nichel, fig. 2, calitatea îmbinării este dată de strângerea în nodul de oscilație a tubului, după un cerc. Bucşa de care se fixează proba vibratorie în tubul de nichel, se recomandă a fi prinsă de tub prin lipire cu argint [7].

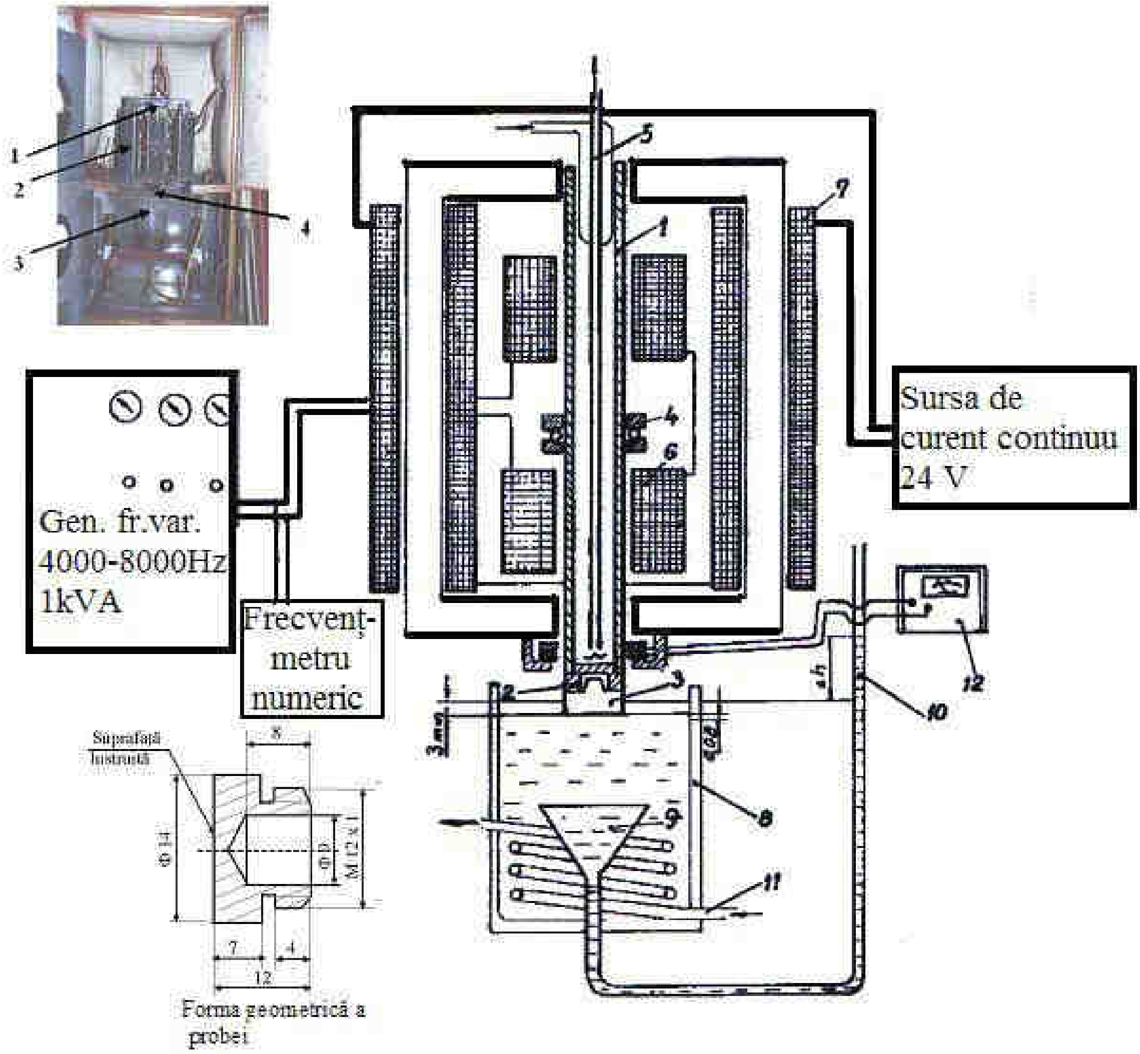


Fig.2 Aparatul vibrator magnetostrictiv cu tub de nichel T1-componenţă (realizator I. Potencz [23])
1- tub de nichel; 2 - piesa -fixare proba; 3 - proba; 4 - sistem inelar fixare tub nichel; 5 - sistem răcire tub nichel; 6 -bobine curent altenativ; 7 - bobine curent continuu; 8 - vas cu lichid de lucru; 9 - pâlnie captare unde sonice; 10 - piezometru; 11 - serpentina răcire; 12 - aparat electric (voltampermetru)

**6**. Calitatea suprafeţelor prelucrate (superfinisate) cu abateri strânse de formă şi poziţie (clasele 4 şi 5 de precizie)**.**

Condiţiile acustice ce trebuiesc îndeplinite de sistemul vibrator mecanic sunt:

**1.** pierderi minime de energie în transductor şi transformatorul acustic (realizabile prin precizia ridicată a prelucrării şi cuplarea perfectă a elementelor componente ale blocului ultrasonic). Reducerea pierderilor de energie depinde şi de modul de fixare sau rezemare a blocului ultrsonic. În general, rezemarea se face pe garnituri de cauciuc, iar locurile de fixare sunt noduri de oscilaţie (de deplasare));

2. concentrare maximă a energiei ultrasonore în suprafaţa supusă atacului cavitaţional (depinde foarte mult de repectarea condiţiilor de prelucrare dimensională şi geometrică a transformatorului acustic);
3. stabilitatea regimului de rezonanţă a sistemului oscilator în timp (depinde de fiabilitatea generatorului electronic de ultrasunete şi nivelul de răcire);
4. uniformitatea radiaţiei energiei acustice pe toată aria de utilizare (depinde de respectarea condiţiilor de coaxialitate între transductor şi transformatorul acustic şi de respectarea preciziei de prelucrare geometrică a transformatorului acustic);
5. adaptare optimă a sistemului vibrator mecanic (blocul ultrasonic) cu generatorul de oscilaţii electrice;

Respectarea acestor condiţii conduce la obţinerea valorilor optime ale principalilor parametrii de funcţionare (amplitudine şi frecvenţa de oscilaţie), respectiv la o fiabilitate sporită a aparatului vibrator.

## 3. Concluzii

Lucrarea prezintă condiţiile funcţionale de bază, factorii tehnologici şi acustici ce trebuiesc îndepliniţi de către aparatele vibratorii, pentru creearea condiţiilor hidrodinamice necesare producerii eroziunii cavitaţionale.

Creşterea duratei de funcţionare neîntreruptă şi pierderi minime de energie acustică se obţin când sistemul oscilator electro-mecanic lucrează în regim de rezonanţă şi depind în principal de:

- materialele din care sunt confecţionate elementele blocului ultrasonic,
- calitatea şi forma geometrică ale suprafeţelor elementelor blocului ultrasonic,
- fiabilitatea componentelor electronice din generatorul electronic de ultrasunete.

Reducerea pierderilor de energie este puternic influenţată de calitatea îmbinărilor dintre elementele blocului ultrasonic, care trebuie să asigure un cuplaj acustic bun, sigur şi o legătură fixă şi elastică. Din acest motiv suprafeţele de îmbinare trebuie să fie plane şi lepuite [3].

Reducerea pierderilor de energie depinde şi de modul de fixare sau rezemare a blocului ultrsonic. În general, rezemarea se face pe garnituri de cauciuc, iar locurile de fixare sunt noduri de oscilaţie (de deplasare).

Concentrarea energiei în focar (pe suprafaţa probei, supusă atacului cavitaţional) depinde de alegerea corespunzătoare a dimensiunilor de rezonanţă şi formei transformatorului acustic. Stabilitatea regimului de rezonanţă, al sistemului oscilator, se asigură prin: calculul corect şi alegerea corespunzatoare a dimensiunilor de rezonanţă a elementelor, stabilitatea variaţiei rezistenţei sarcinii şi funcţionării generatorului electronic de ultrasunete.

Materialele destinate construcţiei blocului ultrasonic trebuie să aibă o bună elasticitate, decrement scăzut de amortizare şi o mare rezistenţă la oboseală.

**RECUNOŞTIINŢĂ**

**Lucrarea este finanţată din Grantul CNCSIS PN II: ID-34/2007: "Dezvoltarea de modele pentru evaluarea comportării materialelor la eroziunea prin cavitaţie"**,
**Lucrarea a fost realizată cu sprijin parţial din grantul strategic POSDRU/88/1.5/S/50783 (2009) şi POSDRU/CPP107/DMI1.5/S/77265 (2010) cofinanţat din Fondul Social European "Investeşte în oameni", în cadrul Programului Operaţional Sectorial Dezvoltare Resurse Umane 2007-2013".**

## Bibliografie

1. **Amza. Gh., si altii** - Sisteme ultraacustice, Editura Tehnica, Bucuresti 1988.
2. **Anton I., -** Cavitatia, Vol I, Editura Academiei RSR, Bucuresti, 1984.

3. **Bordeasu I**.,- Eroziunea cavtațională asupra materialelor utilizate in constructia masinilor hidraulice si elicelor navale. Efecte de scara, teza de doctorat, Timisoara, 1997
4. **Crawford A E.,** - Tehnique de ultrasons, Dunod, Paris, 1959.
5. **Esminger D**., - Ultrasonics the lov and high intensity applications, New York, 1975.
6. **Ghersghel D. A. s. a.** - Aparate cu ultrasunete, Editura Tehnica, Bucuresti, 1984.
7. **Hrelescu M.,** - Cercetări asupra alierii oțelului moale în arcul cu elemente care să confere metalului depus rezistența la cavitație, Teza de doctorat, Timisoara, 1967.
8. **Kuzman A. F., -** Influența unor proprietăți fizice ale lichidului asupra incipienței şi eroziunii cavitaționale, Teza de doctorat, Timisoara, 1992.
9. **Scheffel M. s. a.,** - Dispozitive cu ultrasunete, Partea a II a, Editura Tehnica, Bucuresti, 1989.
10. *** Standard method of vibratory cavitation erosion test ASTM , Standard G 32 - 2010.

**ISSN 1454 - 8003**
**Proceedings of 2011 International Salon of Hydraulics and Pneumatics - HERVEX**
*9 – 11 November, Calimanesti-Caciulata, Romania*

# CONSIDERATII PRIVIND AVARIILE PRODUSE LA ARBORII TURBINELOR BULB DE LA PORȚILE DE FIER II

**Ilare BORDEAŞU, Mircea Octavian POPOVICIU**

**Rezumat:** In lucrare se prezintă şi analizează fisurile constatate la arborele turbinei de la Porțile de Fie II, după circa 130000-140000 ore de funcționare. Din cercetarea acestora rezultă ca principală cauză natura solicitării de oboseală şi mediul umed, coroziv, în care arbpore este obligat să funcționeze.

**Cuvinte cheie**: solicitare de oboseală, tubine hidraulice bulb, fisuri, coroziune,

## 1.Introducere

În timpul exploatării, arborele turbinei bulb este supus la solicitări specifice statice (întindere, compresiune, torsiune) şi dinamice (oboseală, vibrații aleatorii). Aceste solicitări sunt efectul forțelor şi momentelor hidraulice dezvoltate pe paletele rotorice, greutății rotorului (cu sau fără ulei), aflat în consolă, fig.1, şi vibrațiilor, inevitabile, create de masele aflate în mişcare de rotație şi distribuite inegal față de axa de simetrie a turbinei.

Observațiile realizate pe arborii turbinelor bulb de la CHE Porțile de Fier II au scos în evidență fisuri în zona de racord a flanşei arborelui ce-l cuplează cu rotorul turbinei. Examinarea acestor fisuri a condus la concluzia că acestea sunt specifice solicitărilor de oboseală inevitabile în exploatarea arborelui. Cum partea avariată este din zona fixată în consolă şi lucrează într-un mediu umed, care poate contribui la accelerarea procesului de fisurare, a impus analizarea comportării arborelui la solicitările specifice. Prin urmare, în cadrul lucrării, se face o prezentare a avariilor suferite de arborii turbinelor bulb de la CHE Porțile de Fier II, după un număr important de ore funcționare.

## 2. Parametrii de funcționare ai turbinei bulb. Date tehnice

În tabelul 1 sunt afişați parametrii de funcționare ai turbinei bulb şi datele tehnice culese din documentația aferentă.

**Tabel 1**. Parametrii de funcționare şi date tehnice necesare

| Parametrul | Simbol | Valoare |
|---|---|---|
| Căderea netă | H | 7,8 m |
| Debit | Q | 475 $m^3/s$ |
| Puterea utilă | P | 32,5 MW |
| Turația turbinei | $n_T$ | 62,5 rpm |
| Diametrul rotorului | $D_1$ | 7,5 m |
| Număr de palete | Z | 4 |
| Greutate paletă rotor | $G_{pal}$ | 7545 kg |
| Greutate subamsamblu rotor (fără ulei) | $G_{rotor}$ | 99,6 To |
| Volum ulei în butuc | $V_b$ | 4,5 $m^3$ |
| Densitate ulei | $\rho_u$ | 900 $kg/m^3$ |
| Poziția greutății rotorului față de flanşa arborelui | | 1650 mm |
| Lungime arbore | L | 7572 mm |
| Diametru arbore | d | 1200 mm |
| Diametru flanşe | D | 1700/2298 mm |

### 3. MATERIALULUI ARBORELUI TURBINEI

Arborele turbinei bulb este realizat din două componente, fig. 1: una turnată (formată din flanşa de cuplare cu rotorul turbinei şi o porțiune cilindrică) şi una forjată (formată din flanşa de cuplare cu arborele generatorului electric şi cea mai mare parte cilindrică, cu care se fixează şi în lagărul radial axial). Caracteristicile mecanice şi compoziția chimică ale oțelului arborelui 20 C sunt: rezistența mecanică la rupere $R_m$ = 470,88 N/mm$^2$, limtia de curgere $R_{p0,2}$ = 255.05 N/mm$^2$; C = 0,16…0,22%, Mn **=** 1…1,3 %, Si **=** 0,60…0.80%, Cr, Ni, Cu **<** 0,3%**,** S, P **<**0.03%.

Din analiza constituției chimice rezultă că materialul utilizat este un oțel slab aliat cu mangan. Proporția de crom şi nichel, (în special crom), este insuficientă pentru a conferi rezistență sporită la coroziune, inclusiv coroziune intercristalină. Având în vedere influența manganului asupra grăunților cristalini apreciem că elementul principal de aliere determină o structură grosolană a semifabricatului flanşei. În cazul semifabricatelor turnate această structură determină atât grăunți cristalini mari cât şi o oarecare neuniformitate a dimensiunilor acestora.

Considerăm că arborele retehnologizat, care este integral forjat, va prezenta față de arborele inițial (cu flanşă turnată), o rezistență mai mare la solicitările specifice, în special în zona de racordare a flanşei cu partea cilindrică.

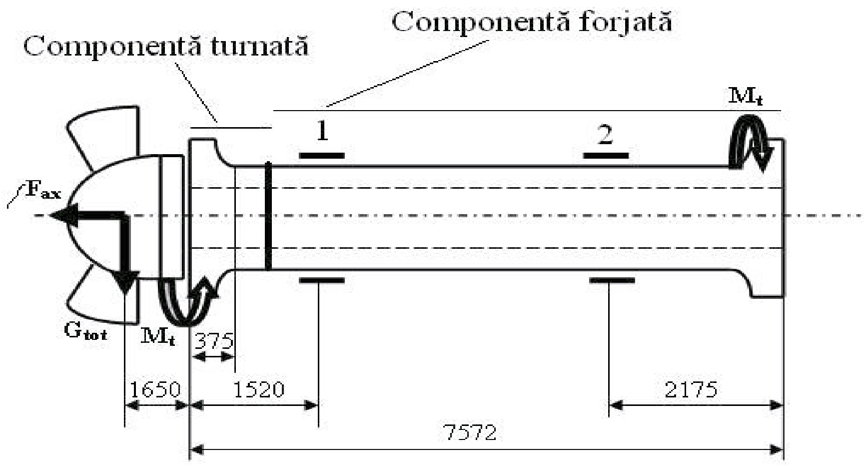


Fig. 1 Schița de principiu a arborelui turbinei

Păstrarea compoziției inițiale, cu procentaje mici de crom şi nichel, face ca rezistența la coroziune să rămână relativ redusă, ceea ce nu ameliorează propagarea fisurilor inițiate.

Din figura 2 se observă coroziunea, la suprafață, a arborelui inițial, determinată de slaba aliere, cu elemente chimice, ce pot spori rezistența la coroziune a materialului utilizat.

Fig.3 Coroziunea de suprafață şi punctele de coroziune dispuse preferențial după circumferință

În condițiile de solicitare la oboseală, specifice arborilor turbinelor bulb, coroziunile evidențiate în figura 2 constituie amorse de fisuri. De aemnea, se observă aşezarea punctelor corodate, preferențial, după linii circumferențiale. Această situație este deosebit de gravă, deoarece predetermină traseul de fisurare.

Având în vedere faptul că fisurile constatate au fost generate prin solicitări la oboseală se impun câteva considerații privind importanța finisării suprafețelor de racordare. Cu cât dimensiunile unei piese sunt mai mari cu atât costul operațiilor de finisare este mai ridicat. Rugozitățile mari ale pieselor solicitate la oboseală se comportă ca amorse de fisurare, motiv care impune o netezime sporită a zonelor supuse la asemenea solicitări. Din acest punct de vedere rugozitățile observate în figura 2 le apreciem ca fiind prea mari, ceea ce dezavantajează comportarea racordării flanşei la solicitări de oboseală. Din acest motiv se recomandă netezirea suprafeței folosind metode convenabile (de pildă finisare cu un polizor cu disc de pâslă, utilizând simultan şi pastă abrazivă); protejarea anticorozivă a suprafaței de racord şi cu expunere sa în aer.

## 4. ASPECTE ALE FISURĂRII ARBORILOR

### 4.1 Aspectul suprafețelor de rupere prin oboseală

Sintagma „oboseala materialelor” reprezintă descrierea procesului de inițiere şi propagare a uneia sau mai multor fisuri ca rezultat al aplicării repetate a unei solicitări, fiecare aplicare având valori insuficiente pentru a determina ruperea. Aspectul pieselor **rupte** prin oboseală prezintă următoarele trăsături caracteristice [Fractography and Atlas of Fractogaphs, Metals Handbook, vol 9, Metals Park Ohio, ATME 1986]:

- lipsa deformațiilor plastice macroscopice sau a modificărilor dimensionale (gâtuiri etc.);
- macroscopic, suprafața de rupere a piesei prezintă două zone: una cu aspect relativ neted (chiar lustruit) propriu propagării lente a fisurii iar cea de a doua are aspectul caracteristic ruperilor fragile (suprafață grunjoasă);
- zona netedă prezintă unele denivelări ce cresc progresiv cu îndepărtarea de la locul de inițiere al fisurii (zona cea mai bine lustruită se află în imediata vecinătate a punctului de inițiere);
- denivelările din zona propagării lente a fisurii prezintă o dispunere în arcuri concentrice, asemănătoare celor de pe suprafața unei valvule de scoică, denumite „linii de oprire”.

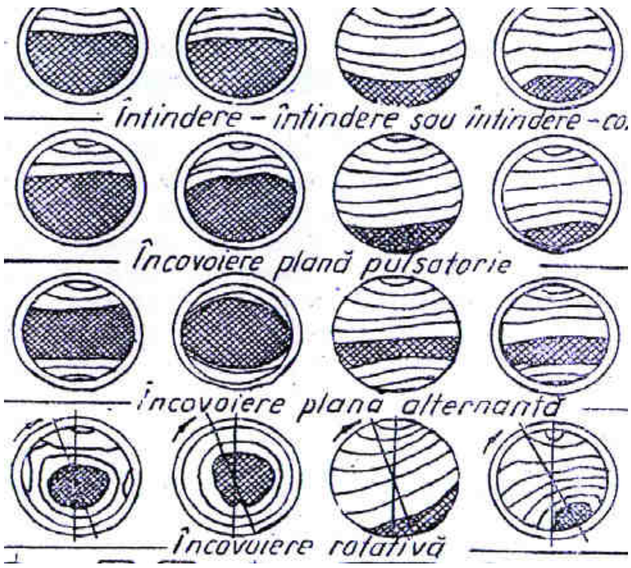

**Fig. 3 Aspectul suprafețelor rupte prin solicitări de oboseală [Fractography and Atlas of Fractogaphs, Metals Handbook, vol 9, Metals Park Ohio, ATMe 1986]**

În cazul oțelului, procesul de fisurare prin oboseală este transgranular. Fisurarea intergranulară se întâlneşte numai în acele cazuri în care oboseala este însoțită de fluaj sau coroziune fisurantă sub tensiune.

La secțiunile integral rupte prin oboseală se pot face aprecieri privind tipul şi nivelul solicitărilor care au determinat ruperea. În volumul „Fractography and Atlas of Fractogaphs, Metals Handbook, vol 9, Metals Park Ohio, ATMe 1986" sunt date aspecte tipice ale ruperilor prin oboseală. In figura 4 se prezintă cazul arborilor circulari solicitați la încovoiere rotativă.

De regulă, locul de inițiere al ruperii se află în apropierea unei suprafețe libere a piesei, acolo unde tensiunile rezultate din încovoiere sau torsiune ating valori maxime. Totodată, la suprafața piesei se exercită cel mai puternic acțiunea concentratorilor de tensiune rezultați din geometria piesei, din gradul de finisare a suprafeței acesteia sau ca urmare a unor eventuale deteriorări produse prin lovire, zgâriere, coroziune etc.

Atunci când tensiunea variabilă are valori mari există tendința apariției mai multor locuri de inițiere. Fronturile de fisurare pot să se unească sau nu într-un front unic. În cazul turbinei bulb din CHE Porțile de Fier II, într-o zonă critică sunt amorsate extrem de multe fisuri, în planuri paralele, care au lungimea de aproximativ 10...15 mm şi adâncimea de unu doi milimetrii. După opinia noastră această situație este generată de patru cauze principale:

- valoarea ridicată a tensiunilor variabile, în raport cu tensiunea medie;
- existența a numeroase amorse de fisură pe suprafața arborelui (rugozități din prelucrare şi puncte corodate), fig.2;
- insuficienta rezistență la coroziune a arborelui, fig.2;
- neuniformități ale structurii materialului.

### 4.2 Considerații privind condițiile de funcționare/exploatare a arborelui

Din cercetările efectuate a rezultat că fisurile au apărut după o perioadă de funcționare continuă a agregatelor, diferită de la un agregat la altul. De asemenea, exploatarea turbinelor a fost conformă regimurilor specifice, continuu supravegheată şi controlată. Ca urmare, zonele incriminate au fost verificate prin metode specifice nedistructive, la fiecare oprire a agregatelor româneşti. După controlul realizat la circa 130.000-140.000 de ore funcționare, în zona de racord a flanşei de cuplare a arborelui cu rotorul turbinei, au fost observate o rețea de fisuri circumferențiale. Acest aspect ne-a determinat face să apreciem că inițierea fisurilor a fost cauzată de solicitările specifice, constituția materialului, tehnologia de prelucrare şi condițiile de lucru (umiditate) şi a impus calculul şi modelarea, zonei respective, la solicitarea de oboseală.

### 4.3 Examinarea elementelor fisurate

Examinarea fisurilor este realizată pe baza fotografiilor efectuate pe arborii agregatelor bulb. Fotografiile realizate pe arborele de la hidroagregatul nr.6 (HA6), sunt folosite pentru fundamentarea cauzelor ce au dus la fisuri de o asemenea anvergură. În continuare se fac discuții şi observații pe baza imginilor de mai jos.

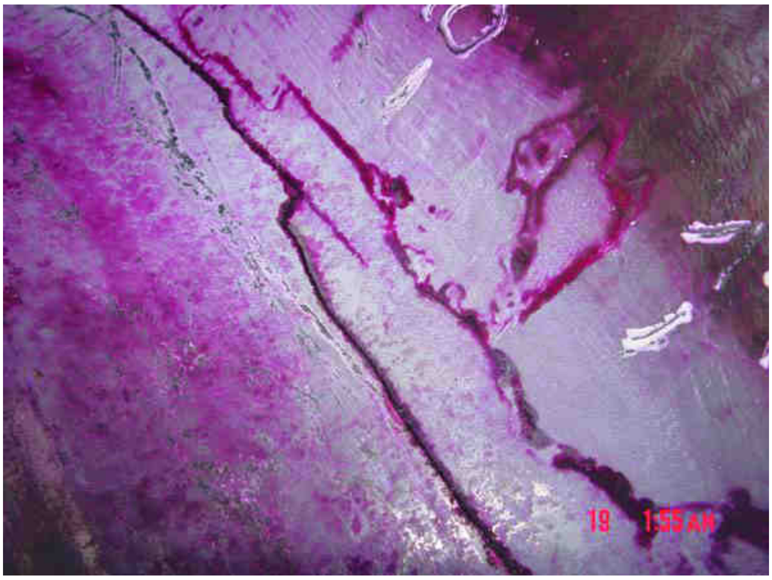


Fig. 4

Analizând imaginea din figura 4 se constată:
- forma zimțată a fisurii circumferențiale este mult mai evidentă, ceea ce reflectă existența unor microzone cu rezistență sporită care au necesitat ocolirea;
- coroziunea chimică a avut loc chiar şi sub stratul de vopsea protectoare;
- există fisuri şi în zone apropiate de cea de a doua rază de racordare (în dreptul săgeții). cest aspect arată gradul puternic de solicitare, generat de tensiunile ridicate induse prin solicitările mari la care este supusă partea arborelui, aflată în consolă;
- Fisurile s-au generat şi dezvoltat în planuri diferite; traseul de propagare a avut loc diferit probabil datorită, întâlnirii unor grăunți duri/legături intergranulare dure (impuse de prezență manganului ca principal element chimic de aliere) şi care au determinat schimbarea acestuia.
- Forma fisurilor este clar una specifică solicitării de oboseală; culoarea mai închisă a soluției folosite, pentru identificarea şi aprecierea gradului de avariere, arată că adâncimea fisurii este însemnată, care practic impune scoaterea arborelui din funcțiune şi remedierea defectului;
- inițial fisurile circumferențiare au început şi s-au dezvoltat în mai multe planuri; acest mod de formare şi dezvoltare este specific pieselor confecționate din semifabricate cu defecte structurale şi tehnologice de prelucrare (carburi de crom, grăunți cristalini mari şi neomogeni, prelucrare mecanică necorespunzătoare etc.) şi supuse la solicitări ciclice nesimetrice (cauzate de condițiile de montaj şi de distribuția maselor aflate în mişcarea compusă de rotație - încovoiere-compresiune +împingere axială);
- există zone în care fisurile au avut tendință să se dezvolte şi după generatoare conului, din zona de racordare; explicația este legată mai mult de calitatea semifabricatului flanşei; apreciem că acest arbore a fost cu deficiențe încă din faza de semifabricat;
- adâncimea fisurilor este mare în ambele planuri. Este evident că aici avem de-a face cu un material cu multiple defecte;

## 5. CONCLUZII FINALE

1. Apreciem că fisurarea produsă în zona de racord flanşă arbore - corp cilindric arbore este cauzată de solicitările specifice, constituția chimică şi structurală ale materialului, tehnologia de prelucrare şi condițiile de lucru (umiditate). Zona de racordare a flanşei în care apar fisurile lucrează în mediu umed, ceea ce implică şi o activitate corozivă, care contribuie la accentuare fisurării în timpul funcționării agregatului.

**2.** Dacă nu se fac operații de eliminare a fisurilor mici, acestea se pot dezvolta pe un arc de cerc din circumferința arborelui luând o formă neregulată, determinată de propagarea prin zone cu rezisență mai mică sau mai mare şi duc în final la ruperea arborelui.

**3** Inițierea şi dezvoltarea fisurilor circumferențiale se poate realiza în unul sau mai multe planuri. Acest mod de formare şi dezvoltare este specific pieselor confecționate din semifabricate cu defecte structurale şi tehnologice de prelucrare (carburi de crom, grăunți cristalini mari şi neomogeni, prelucrare mecanică necorespunzătoare, etc.) şi supuse la solicitări ciclice nesimetrice, cauzate de condițiile de montaj şi de distribuția maselor aflate în mişcarea compusă de rotație - încovoiere-întindere (împingere axială).

**4** Multitudinea fisurilor este determinată de amorsele inițiale, create, în primul rând, de tehnologia de prelucrare mecanică (nivelul rugozităților), dar şi de tenacitatea materialului.

## 6. RECOMANDĂRI

1. Arborele de la HA7 este, în prezent, retehnologizat, iar arborele de la HA8 este în program de retehnologizare, începând cu luna februarie 2009.
2. Pentru arborii cu fisuri se recomandă remedierea acestora prin strunjire şi finisare la o rugozitate de minim Ra=6,3 μm.
3. Pentru arborii cu durată de funcționare până la retehnologizare, se impune implementarea de noi soluții pentru etanşarea arborelui, care să scoată zona de racord din mediul coroziv, din prezent.
4. Se impune aplicarea unui sistem nou de etanşare, la coroziune, a zonei de racord, care sa conducă la creşterea fiabilității

## BIBLIOGRAFIE

[1]. Barsom J.M., Rolfe S. T., *Fracture and Fatigue Control*, Edition: 2, Prentice-Hall, 1987.

[2]. Bathias C., Paris P.C., *Gigacyclic Fatigue in Mechanical Practice*, Marcel Decker, New York, 2005.

[3] Rusu O. Teodorescu M., Laşcu-Simion N., *Oboseala metalelor*, vol.1, Editura Tehnică, Bucureşti, 1992.

[4] Mitelea I., Budau V., - *Studiul metalelor, Îndreptar tehnic*, Editura Facla, Timisoara, 1987.

[5] ***, *Fatigue Design Handbook*, Second Edition, SAE, Warrendale, 1988.

**ISSN 1454 - 8003**
**Proceedings of 2011 International Salon of Hydraulics and Pneumatics - HERVEX**
*9 – 11 November, Calimanesti-Caciulata, Romania*

# DYNAMIC PROCESSES MODELLING IN CLOSED LOOP ELECTROPNEUMATIC TRANSMISSION SYSTEM

**Hristo HRISTOV, Borislav GEORGIEV, Georgi ILIEV**

[1], Technical University of Gabrovo, Dep. Power Energy christo@tugab.bg

***Abstract:*** *In this paper is shown a mathematical model of dynamic processes in closed loop electro pneumatic transmission system. The model is based on nonlinear differential equations. The model was simulated on PC and results are shown in few graphics. Experimental test stand for dynamic process investigation is developed. Experimental step responses are shown.*

***Keywords:*** *electropneumatic system; dynamic processes; automatic controller*

## 1. Introduction

Electropneumatic transmission systems are widespread in many areas of industry. They are preferred for use in aggressive environments and fire. They have relatively high efficiency, less sensitive to external vibrations and have lower costs of operation. Compared with electrohydraulic, electropneumatic systems have significantly less output power and high speed inequality of the actuator. This disadvantage can be removed using additional speed hydraulic stabilizers [2].

Now, in many pneumatic systems are used rodless pneumatic cylinders. It offers flexible linear drives which can be simply and neatly integrated into any machine layout. Rodless pneumatic actuators are compact, high speed, no-lubrication cylinders to the complete linear system combining pneumatic or electric actuation with guidance and control modules.

Currently used mathematical models of such systems are mostly linear [1, 6], which prevents the production of results adequately reflect the processes in real electropneumatic driving systems. In work [2, 3, 7] a nonlinear mathematical model is developed and tested in the ongoing processes in electropneumatic drive system. Recently, in connection with the widespread introduction of the automated devices and machines, robots expand the scope of joint work of pneumatic systems and their control electronic devices. This causes an increase in research and theoretical developments and experimental applications of electropneumatic systems, becouse they have many positive qualities. Flexible control and the ability to easily form the necessary laws to regulate electronic devices achieved by combining best dynamic characteristics of pneumatic actuators.

Mostly used today pneumatic valves are with discreet action. This limits the field of their application for a special implementation of automated systems with open or closed circuit operation. In discrete control of flow is necessary to include various energetic point of wasteful elements, which reduces the overall efficiency of the system. In addition it can not provide the necessary fluency and precision of variation of pneumatic units. This requires a gradual transition to new constructive solution to the electropneumatic elements with an analog connection between the input and output signals. Many leading producers of pneumatic components such as Festo, Rexroth, Norgren, Schnaeider Kreuznach produce proportional and servo pneumatic valves. In the design of closed electropneumatic drive systems are widely used methods of computer modeling and simulation of processes occurring in different operating modes. In many cases it’s not possible to theoretically determine some important parameters and coefficients entering the equations of the mathematical model [4, 5].

## 2. Mathematical models

Fig. 1 shows a diagram of drive system with electro-pneumatic rodless cylinder. When input voltage $U_{IN}$ is supplied, electropneumatic servo valve spool start moove. As a result, compressed air passes through the valve and enters in the piston chamber of the cylinder 3 with load 7. The movement of the load registered with potentiometric sensor /feedback device/ 8, which output signal is voltage $U_{FB}$. Movement stops when equalizing voltages looming input device and feedback - $U_{IN}$ and $U_{FB}$.

The dynamics processes in electropneumatic closed system (Fig. 1) is described by the following equations:

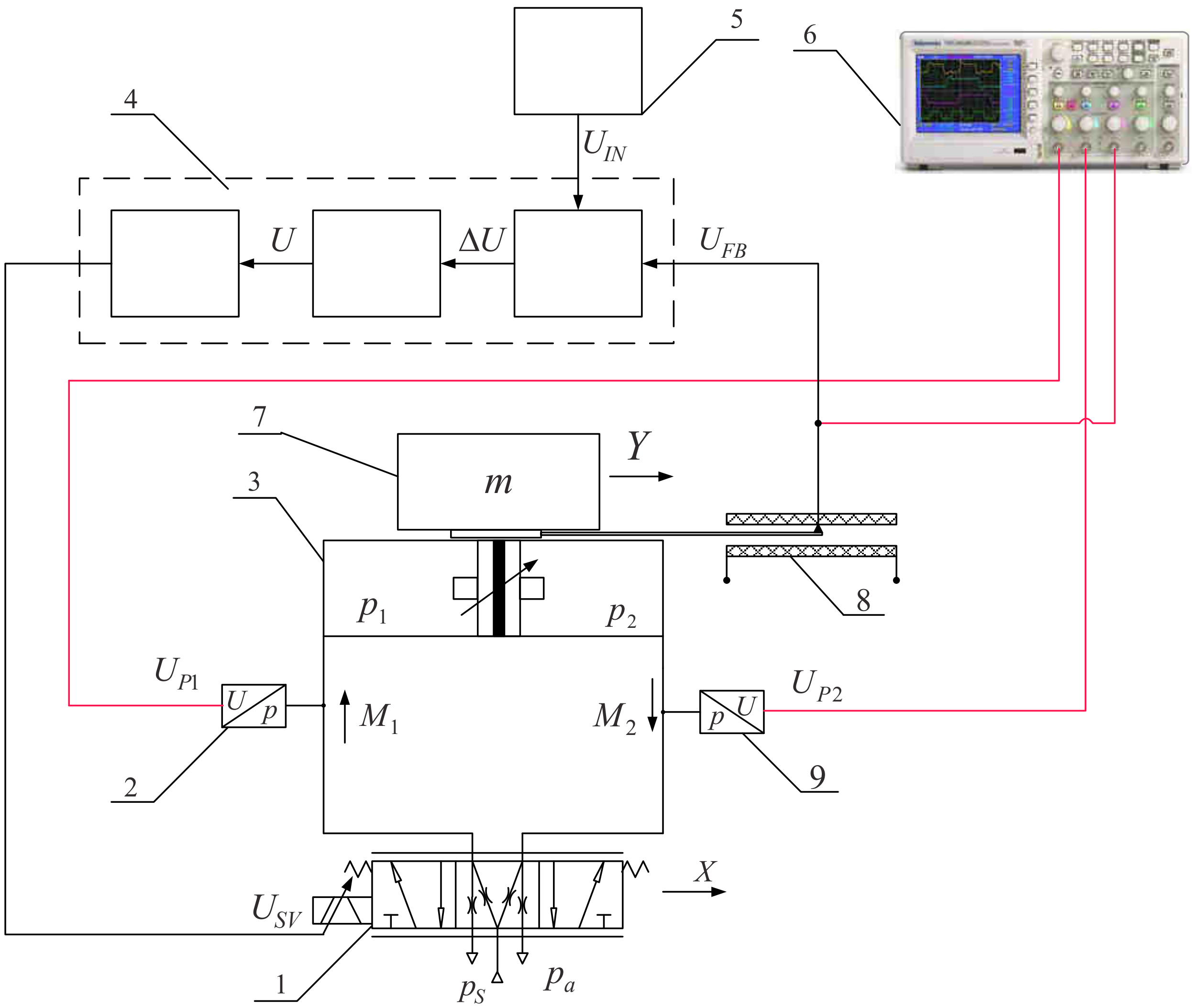


*Fig. 1. Schematic of electro-pneumatic system.*
*1 – pneumatic servo valves; 2 and 9 pressure sensors, 3 – pneumatic cylinder; 4 – electronic control unit servo valve 1; 5 – looming input device; 6 – oscilloscope, 7 – driven mass; 8 – potentiometric sensor for linear displacements; EP – electronic amplifier; EC – electronic controller; Σ – summing device.*

1. Equation of motion of the piston of the pneumatic cylinder:

$$m\frac{d^2Y}{dt^2} + k_T\frac{dY}{dt} + F_{Tc} = A(p_1 - p_2) \tag{1}$$

where:

$A$ – effective area of the piston of the pneumatic cylinder

$p_1$, $p_2$, – absolute pressure; operating in the chambers of the cylinder;

Y – moving the piston rod;

$m$, $k_T$ – mass of load and viscous friction coefficient;

$F_{Tc}$ – power of dry friction (Fig. 2);

The dependence of the force of dry friction is shown in Fig. 2.

Mathematical description of the force of dry friction $F_{Tc}$ is:

$$F_{Tc} = \begin{cases} \left(F_{T0} - k_{Tc}\frac{dY}{dt}\right) sign\left(\frac{dY}{dt}\right), & 0 < \left|\frac{dY}{dt}\right| \le v_0 \\ F_0\ sign\left(\frac{dY}{dt}\right), & v_0 < \left|\frac{dY}{dt}\right| \\ F_{T0}\ sign\left(\frac{d^2Y}{dt^2}\right), & \frac{dY}{dt} = 0 \end{cases} \tag{2}$$

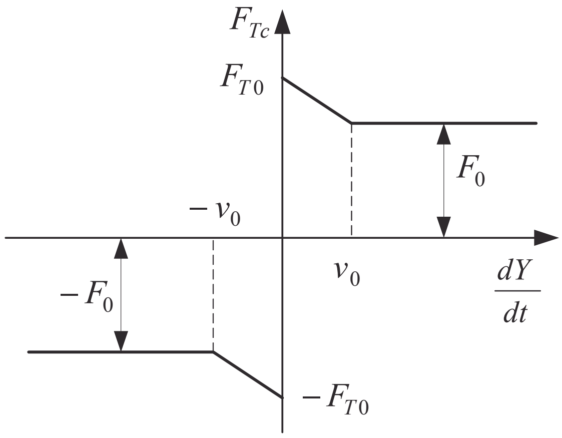


*Fig. 2 Characteristic of the power of dry friction*

2. Equations for incoming and outgoing mass flow in the cylinder

$$M_1 = \frac{1}{RT_1}\left[p_1A_1\frac{dY}{dt} + (V_{10} + A_1Y)\frac{dp_1}{dt}\right] \tag{3}$$

$$M_2 = \frac{1}{RT_2}\left[p_2A_2\frac{dY}{dt} - (V_{20} - A_2Y)\frac{dp_2}{dt}\right] \tag{4}$$

where:

$M_1$, $M_2$,– mass flow;

$R$ – gas constant;

$T_1$, $T_2$, $V_{10}$, $V_{20}$, – absolute temperatures and primary volumes of the spaces of left and right sides of the pneumatic cylinders;

3. Equations for mass flow passing through the valve:

for $X \ge 0$

$$M_1 = \mu_1 \pi \, dX \; p_S \sqrt{\frac{2k}{RT_1(k-1)}\left[\left(\frac{p_1}{p_S}\right)^{\frac{2}{k}} - \left(\frac{p_1}{p_S}\right)^{\frac{k+1}{k}}\right]} \tag{5}$$

$$M_2 = \mu_2 \pi \, dX \; p_2 \sqrt{\frac{2k}{RT_2(k-1)}\left[\left(\frac{p_a}{p_2}\right)^{\frac{2}{k}} - \left(\frac{p_a}{p_2}\right)^{\frac{k+1}{k}}\right]} \tag{6}$$

for $X < 0$

$$M_1 = \mu_1 \pi \, dX \; p_1 \sqrt{\frac{2k}{RT_1(k-1)}\left[\left(\frac{p_a}{p_1}\right)^{\frac{2}{k}} - \left(\frac{p_a}{p_1}\right)^{\frac{k+1}{k}}\right]} \tag{7}$$

$$M_2 = \mu_2 \pi \, dX \; p_S \sqrt{\frac{2k}{RT_2(k-1)}\left[\left(\frac{p_2}{p_S}\right)^{\frac{2}{k}} - \left(\frac{p_2}{p_S}\right)^{\frac{k+1}{k}}\right]} \tag{8}$$

where:

$\mu_1$, $\mu_2$ – flow rates coeficient;
$d$ – diameter of the of servo valve spool;
$X$ – servo valves spool displacement;
$k$ – adiabatic index ($k$ =1.4);
$p_S$ – supply pressure;

4. Equation of electronic PID controller:

$$U = k\left(\Delta U + \frac{1}{T_I}\int_0^t \Delta U dt + T_D \frac{d\Delta U}{dt}\right) \tag{9}$$

where:

$U$ – output voltage of the controller;
$\Delta U$ – voltage coming from the summing device;
$k$ – gain of the controller;
$T_I$, $T_D$ – time constant of integration and differentiation of the regulator;

5. Equation of electromechanical transducer:

$$T_{EC}\frac{dI_{SV}}{dt} + I_{SV} = k_u^{'} U \tag{10}$$

where:

$T_{EC}$, $k_u^{'}$ – time constant and gain of electromechanical transducer; $I_{SV}$ – output current of the electromechanical transducer.

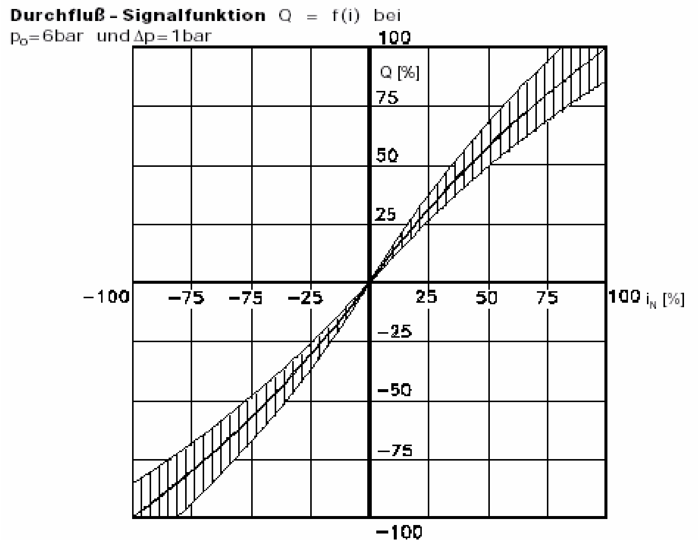


*Fig.3 Experimental static characteristics of the servo valves*

5. Equation for servo valves spool displacement:

The dynamics of the servo valves is described by a system of differential equations of relatively high order. Due to small amounts of some of the time constants of the equations, the order of the system can be reduced significantly. In Fig. 3 and Fig. 4 are show the experimentally obtained static and logarithmic frequency characteristics of the servo valves PVM 065. From these characteristics we can obtain approximations to second order differential equation:

$$T_{SV}^2 \frac{d^2X}{dt^2} + 2\xi_{SV} T_{SV} \frac{dX}{dt} + X = k_I I_{SV} \qquad (11)$$

where:

$T_{SV}$ , $\xi_{SV}$ , $k_I$ time constant, damping coefficient and the gain of the servo valves.

Values of the parameters of the servo valves - $T_{SV}$ , $\xi_{SV}$ , $k_I$ , can be determined by identifying the characteristics of Fig. 4.

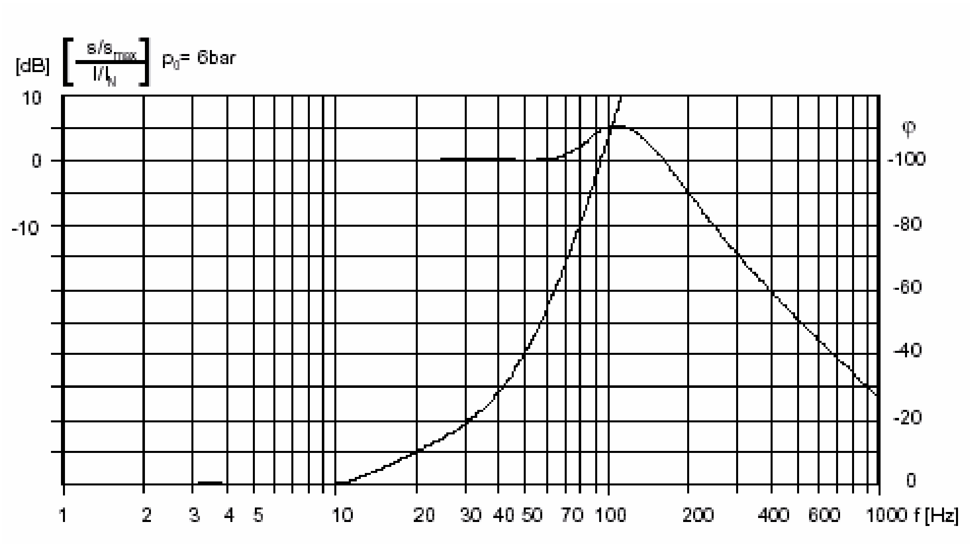

*Fig.4 Experimental frequency characteristics of the servo valves*

6. Equation of summing device:

$$\Delta U = U_3 - U_{FB} \tag{12}$$

where:

$U_3$ – input voltage;

$\Delta U = U_3 - U_{FB}$ – voltage difference.

7. Equation of feedback:

$$U_{FB} = k_{FB}^{'} Y \tag{13}$$

where: $k_{FB}^{'}$ – coefficient of feedback.

### 3. Modelling and simulation of the system

Based on the mathematical model of electropneumatic system was developed corresponding analog model. To simulate the processes in the system is used Matlab Simulink.

In Fig. 5 is shown developed analog model of the system in dimensionless type, and Fig. 6 presents the step responses of the input signal $U_{IN}$ .

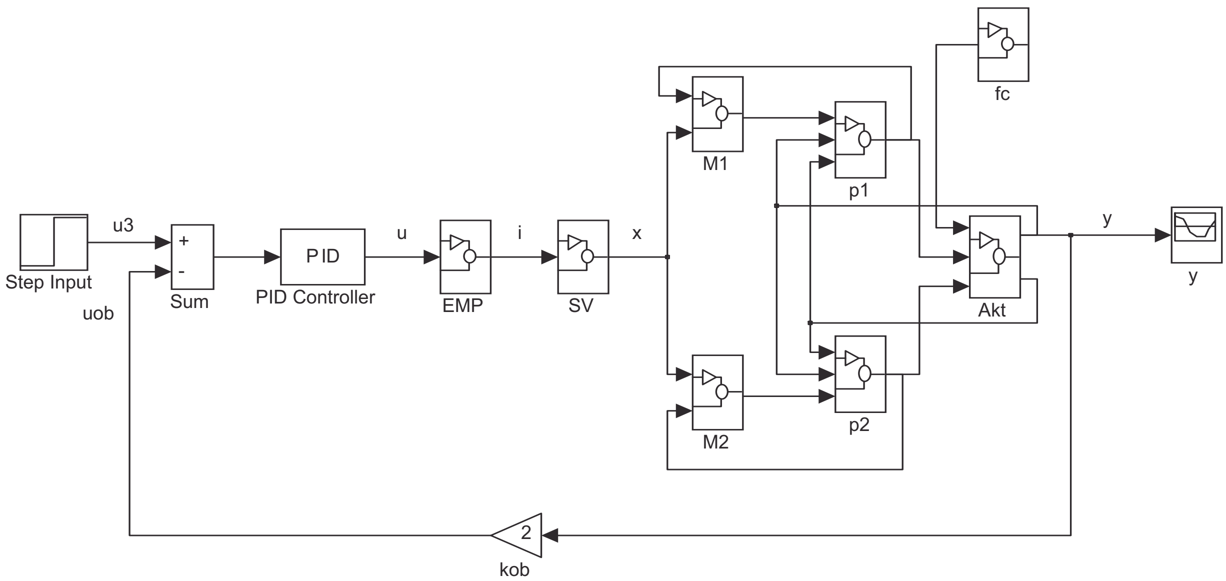


*Fig.5 Analog model of the system*

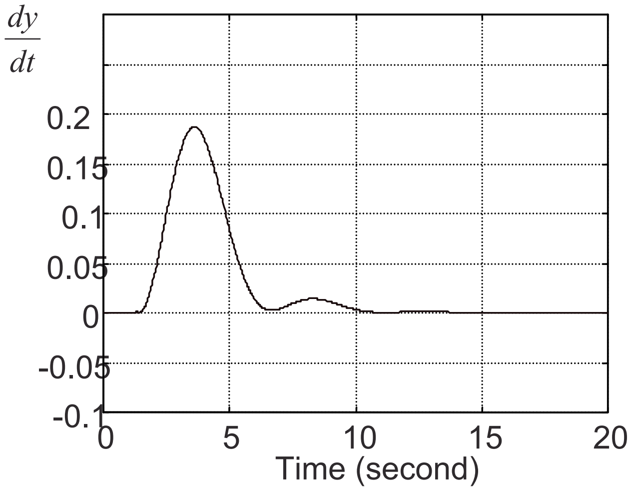
dy/dt
0.2
0.15
0.1
0.05
0
-0.05
-0.1
0
5
10
15
20
Time (second)

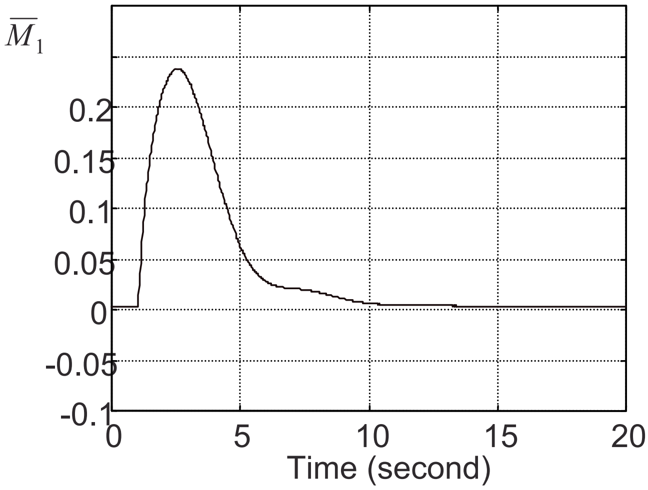
$\overline{M}_1$
0.2
0.15
0.1
0.05
0
-0.05
-0.1
0
5
10
15
20
Time (second)

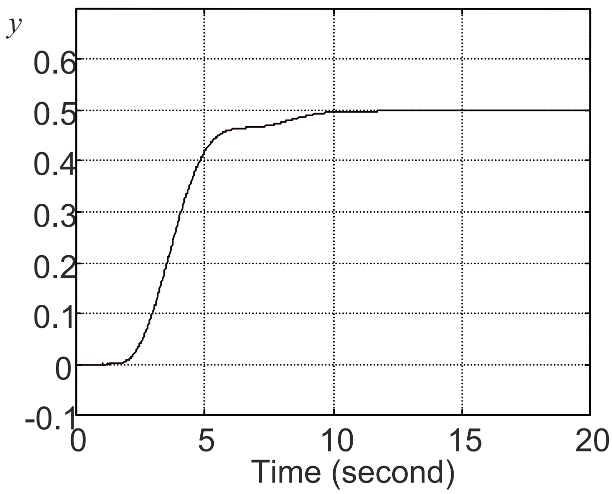
y
0.6
0.5
0.4
0.3
0.2
0.1
0
-0.1
0
5
10
15
20
Time (second)

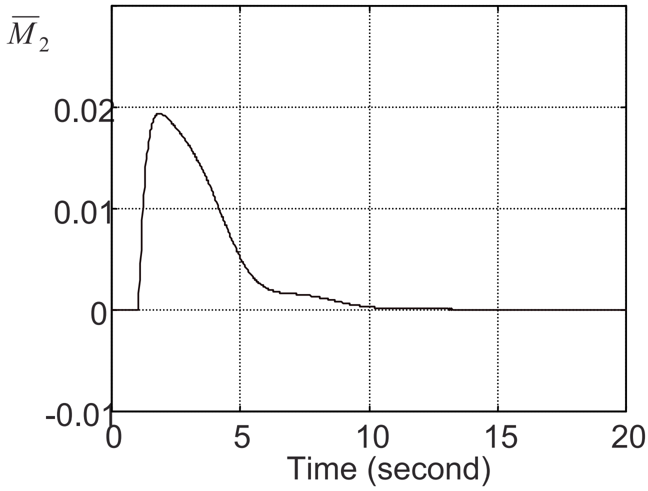
$\overline{M}_2$
0.02
0.01
0
-0.01
0
5
10
15
20
Time (second)

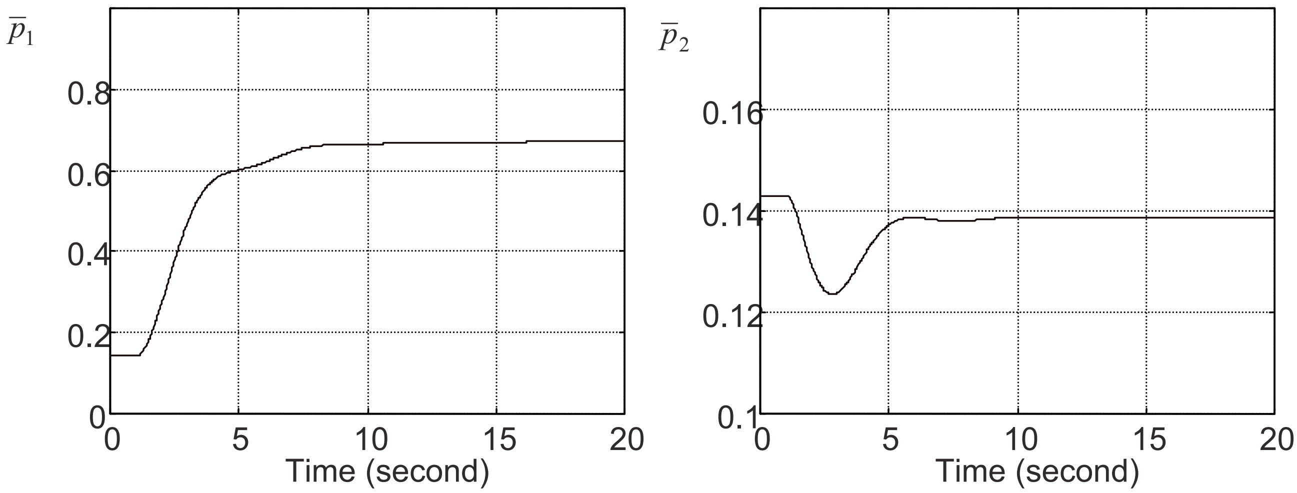


*Fig.6 Step responses in electro pneumatic closed system when changing the input signal u3***.**

**Experimantal results**

The developed mathematical model of electro pneumatic transmission system of Fig. 5 allows investigating the dynamic processes at different loads and initial conditions. The model include some important nonlinearities in the system: dependence of the force of dry friction in the actuator; dependencies on the mass flow passing through the throttling devices and forming the variables cameras of the operational cylinder; boundary conditions at the end of the stroke of the cylinder etc. As a result, obtained by simulations dynamic processes will correspond better to the processes in the real system. After recording a real dynamic responses it is possible to perform a verification of the model. Therefore is necessary to build an experimental stand, corresponding to the system of Fig.1, and need to be integrated measurement and control equipment, allowing to obtain experimental data in real time.

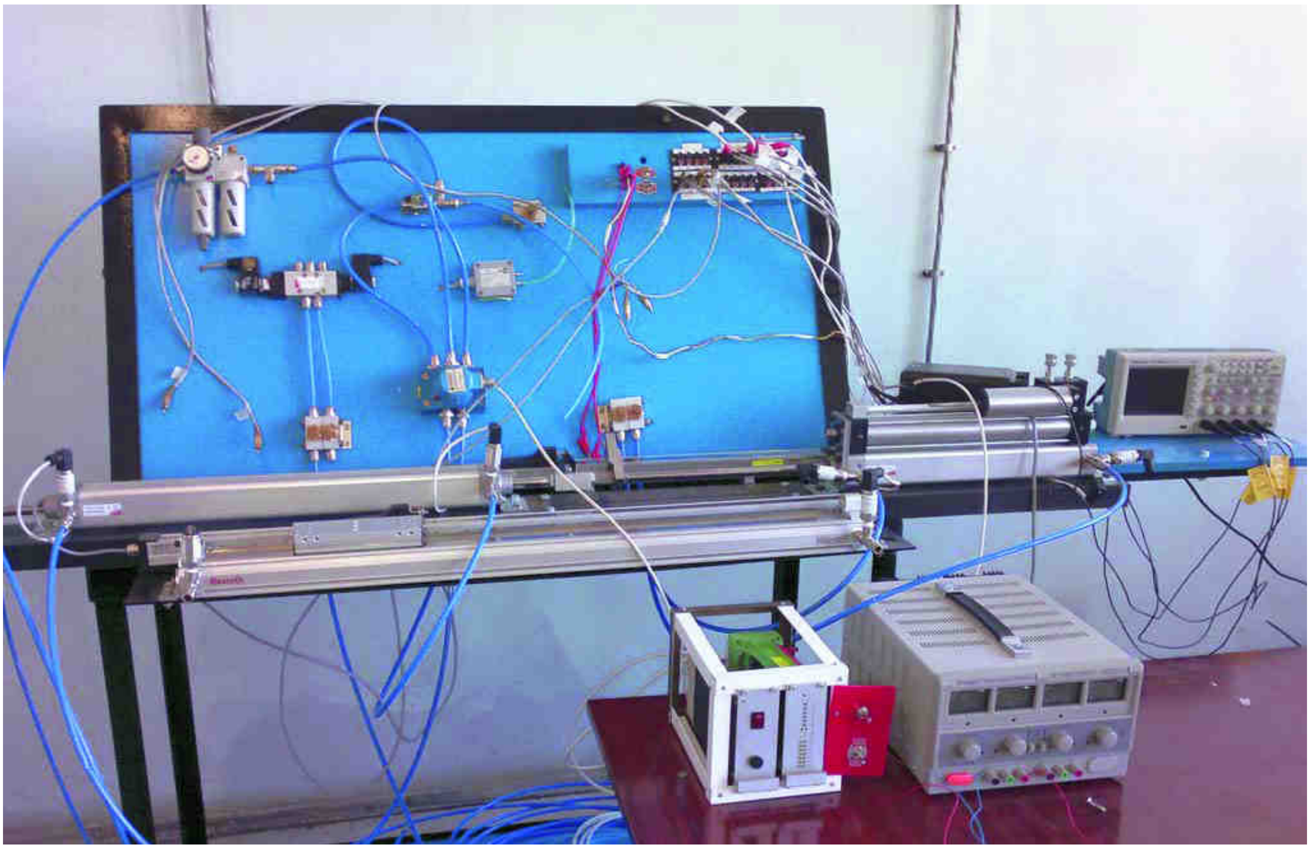

*Fig.7 Photo of experimental stand*

To specify the mathematical model and to obtain some unknown parameters, it s necessary to compare the results of computer simulation to those of real experiment For this purpose in Technical University of Gabrovo - department of “ Power Energy” was realized experimental test stand for investigating closed loop electro pneumatic system – Fig. 7. The main elements are pneumatic PVM 65 servo valve produced by Schnaeider Kreuznach, with electronic analogue PID controller, rodless cylinder Bosch Rexroth and, potentiometric sensor. The proportional, integral and differential form / P, I and D / can be changed and adjusted independently. Measuring electrical signals from sensors are recorded and displayed using a digital oscilloscope. The results of measurement using the oscilloscope except graphics is recorded as a file with the numerical values and displayed graphically.

The methodology for implementation of experimental studies is presented in [6].

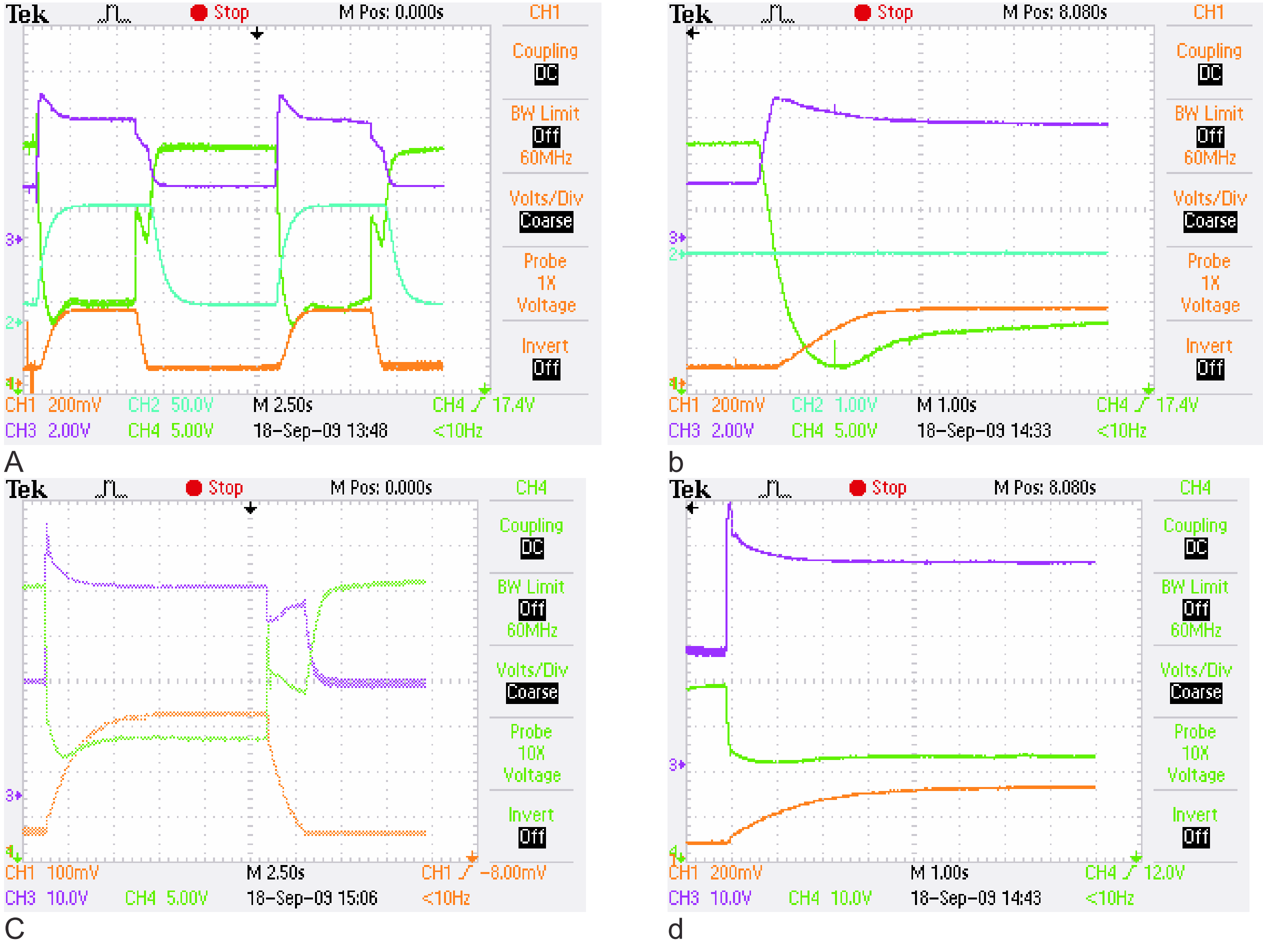


*Fig. 8 Experimental transitional processes with P controller /a, b/ and with PD controller /c, d/.*

## 5. Experimental results.

Some of the experimental results are presented in Fig. 8. The corresponding signals are as follows:

- channel CH1 – moving the rod of driving cylinder 3- $y$ .
- channel CH3 pressure in the piston chamber of the driving cylinder 3 - $p_1$;
- channel CH4 pressure in the rod chamber of the driving cylinder 3- $p_2$;

In Fig. 8 and shows the experimental transitional processes using the P and PD -controller in two-way movement of the pneumatic drive cylinder 3.

## 6. Conclusions

The obtained experimental results will be used to verify the mathematical model of the dynamics of closed loop electro pneumatic system. The experimental transient responses will be compared with those obtained from the simulation of mathematical model. By changing the parameters and structure of the model will be possible to achieve identity of experimental responses and responses obtained from simulation.

## REFERENCES

[1] Ivanov, P., Hr. Hristov, K. Ormandziev, Dynamic of automated hydro and pneumatic systems, Gabrovo, 2005.
[2] Hristov, Hr., Ivanov, P., K. Ormandziev, Step responses investigation in electropneumatic transmission system with hydraulic velocity actuator, „Machine №62, Series FH, Year XIV, Volume 1, TU- Varna, 2006, стр. 113 – 11.
[3] Ormandziev K., Hr. Hristov P. Ivanov, Computerized Modeling of nonlinear electropneumatic system, International Scientific Conference Unitex'08, 21-22 November 2008, Proceedings v. II, pp. II-437-442.
[4] Hristov, Hr., Ivanov, P., K. Ormandziev, Experimental Investigation of Dynamic processes in electropneumatic system, International Scientific Conference Unitex'08, 21-22 November 2008, Proceedings v. II, pp. II-443-448.
[5] Rusterholtz R., U. Widmer, Gundlagen-betrachtungen zur Auslegung pneumatischer Servoantriebe, O+P "Olhydraulik und pneumatik", 10/1985, Vol. 29, pp. 757 – 762.
[6] Hristov, Hr., Ivanov, P., K. Ormandziev, EXPERIMENTAL Investigation dynamic PROCESSES In closed loop electropneumatic transmission system, International Scientific Conference Unitex'09, 20-21 November 2009, Proceedings v. II, pp. II-443-448.
[7] Ormandziev K., Hr. Hristov P. Ivanov, Dynamic PROCESSES MODELLING In closed loop electropneumatic transmission system. Unitex'09, 20-21 November 2009, Proceedings v. II, pp. II-437-442.

**ISSN 1454 - 8003**
**Proceedings of 2011 International Salon of Hydraulics and Pneumatics - HERVEX**
*9 – 11 November, Calimanesti-Caciulata, Romania*

# MULTI-TIER APPLICATIONS FOR MONITORING AND CONTROLLING OF HYDRAULIC AXES

Marian BLEJAN, Petrin DRUMEA, Mircea COMES
Affiliation: Hydraulics and Pneumatics Research Institute, INOE 2000 – IHP,
No 14, Cutitul de Argint St., Bucharest, ROMANIA,
e-mail: blejan.ihp@fluidas.ro

**Abstract**

Hydraulic drives offer advantages in terms of precise control of forces and couples shareholders involving large values and aggressive working environments. Another advantage of hydraulic power drive is getting some great value in a very small geometric volume. Using principles of mechatronics development enables the obtaining of hydraulic drives consisting of mechanical components, hydraulics, electronics, sensors, software that can be naturally integrated into computerized testing stands.

The material presented refers at experimental research conducted by authors focused on integration of linear hydraulic axes into a computerized system. The original contribution regards the development of a digital servocontroler for monitoring and control of the position and force of a hydraulic axis and introduces the concept of "mechatronic tier" for an easy connection of a mechatronic device, hydraulic drive, with a computer system.

**Keywords**

hydraulic drive, robotics, mechatronics, position control, servocontroler

## Introduction

Hydraulic systems uses as work environment a liquid under pressure. They have appeared and developed rapidly, mainly due to the need to control and regulate the forces and moments large and very large with high precision, while they allow control of load position and velocity involved. Need to integrate the hydraulic systems is justified by the increasing complexity of automated technological facilities, increasing efficiency and productivity requirements ever higher rates as well as computerization of the manufacturing process. Widespread use of hydraulic machinery in manufacturing combined with production tracking systems requires complex measurements of parameters to be sent computerized systems. Integration of mechatronic assemblies in the hydraulic equipment allowing to measure and transmit the measurements to computer systems facilitates the manufacturing process. The evolution in "embedded systems" linked to the emergence of new types of sensors and methods of measurement of physical quantities specific hydraulic machinery allow these assemblies mechatronic approach in cooperation with European research units that have interests in these areas. Were developed technologies to build a computerized system that includes a layer of hydraulic equipment interface and a electronics "digital servocontroler" that monitors and controls the hydraulics. Based on original technology was implemented a multitier IT application layer containing a "mechatronic tier" that integrates hydraulic linear axis, the hydraulic axis is controlled and monitored by a digital servocontroler. The experimental results confirmed the achievement of outstanding performance in terms of static positioning accuracy.

Figure 1 shows the functional block diagram of the hydraulic stand used for experimental research to demonstrate the functionality and usefulness of the proposed solution. The hydraulic stand shown in figure 2 was purposefully created for testing dampers in order to determine the characteristics force speed, force stroke. The stand comprises a linear hydraulic axis controlled in position by means of a flow servo valve on the base of the data supplied by the position and force transducers. The stand electronics is realized as a standard electronic module with assemblying on DIN track, providing all the required operations for the control and monitoring of the hydraulic axis and the interface with the computer system.

**ISSN 1454 - 8003**
**Proceedings of 2011 International Salon of Hydraulics and Pneumatics - HERVEX**
*9 – 11 November, Calimanesti-Caciulata, Romania*

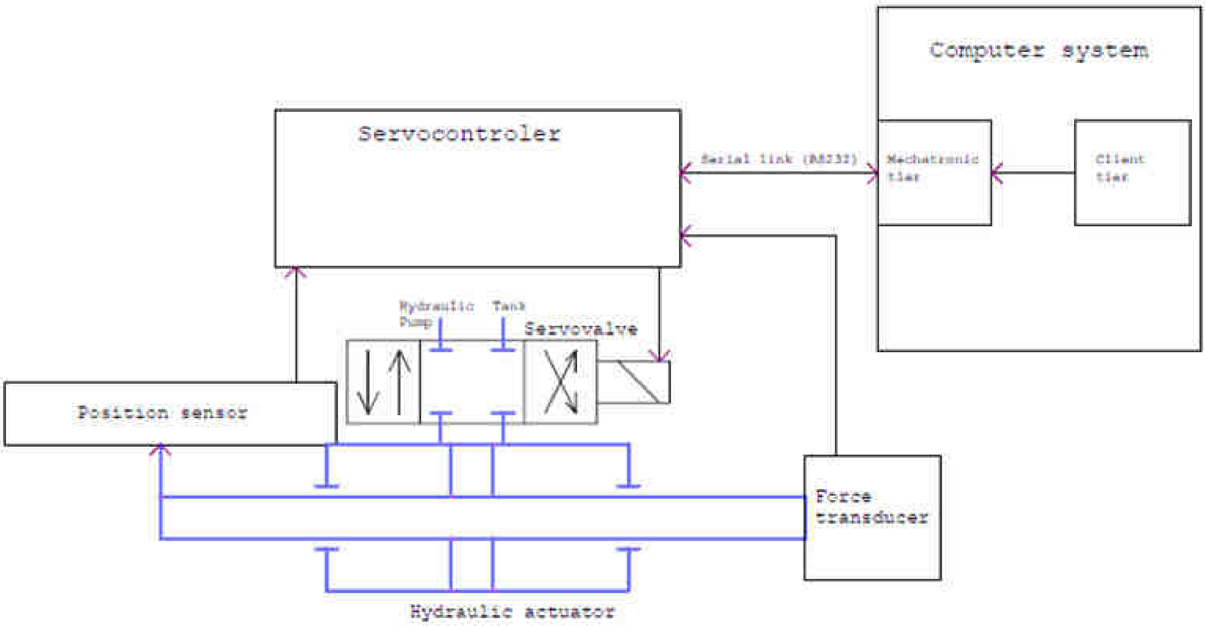


Figure 1: Functional block diagram

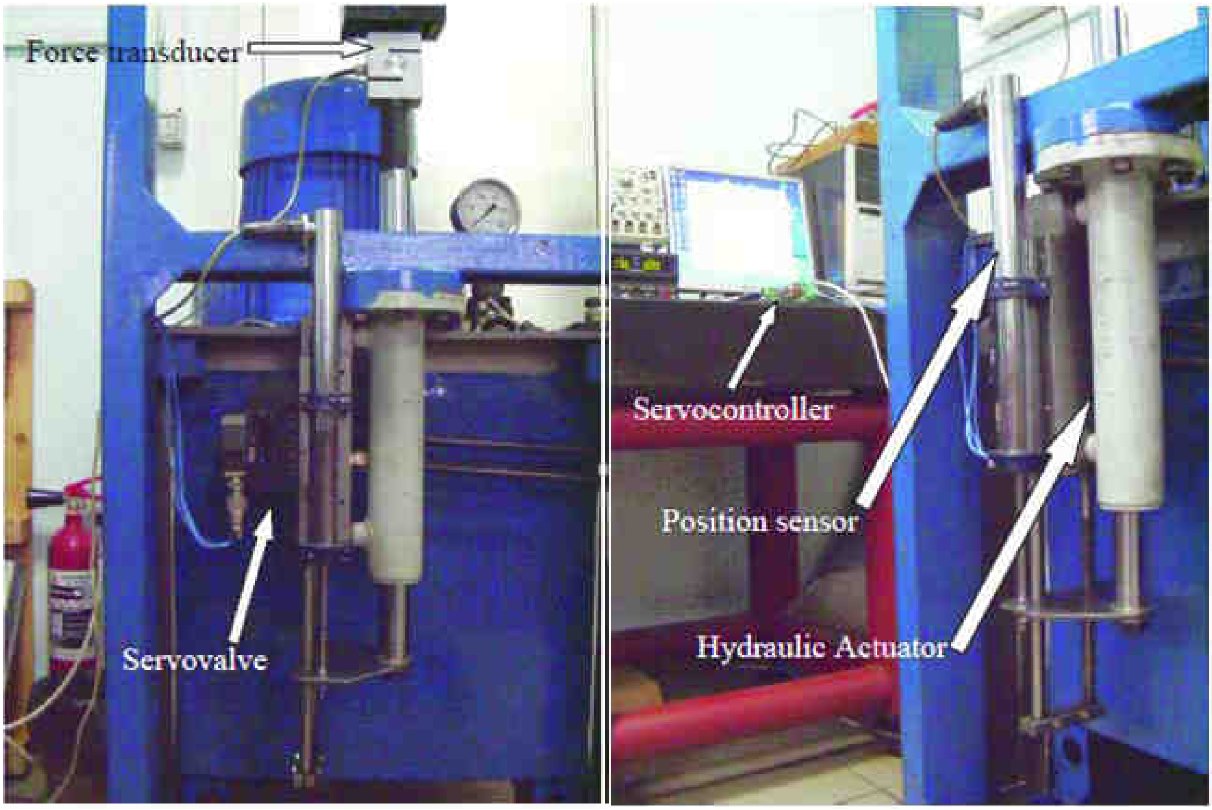


Figure 2: Experimental stand

**The hydraulics**

The driving ensemble, fig. 2, consists of a hydraulic cylinder with double rod. The cylinder is driven by a flow servo valve. Parameters of driving in the hydraulic cylinder rods are 200mm stroke, speed 0.66m/s, force 1100daN. Hydraulic power has the following parameters pressure 150bar and flow 90dm$^3$/min.

**The sensors**

On the rod of the hydraulic cylinder are mounted two sensors, fig. 3, one for measuring the rod position and another one for measuring the driving force. Position sensor is the LVDT (Linear Variable Differential Transformer) type having a fixed body and a sliding rod. The sensor body has two magnetically coupled coils by the rod. Coupling factor is altered by rod movement. The measuring range for the LVDT sensor is 0...200mm. The force transducer is a strain gauge load cells type with built-in electronics in the -5000daN...5000daN range.

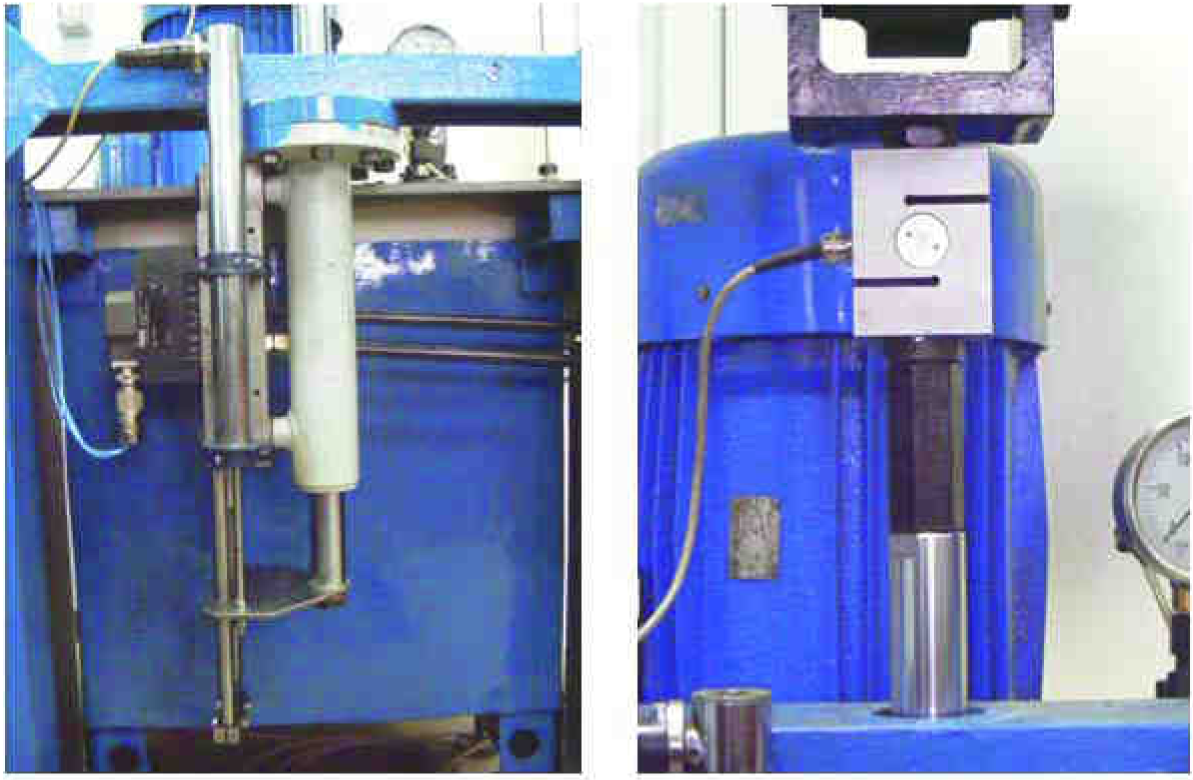

LVDT sensor    Force transducer

Figure 3: Sensors

**The electronics**

The electronic module, the digital servocontroller fig. 4 and 5, is based on an 8 bit microcontroller.

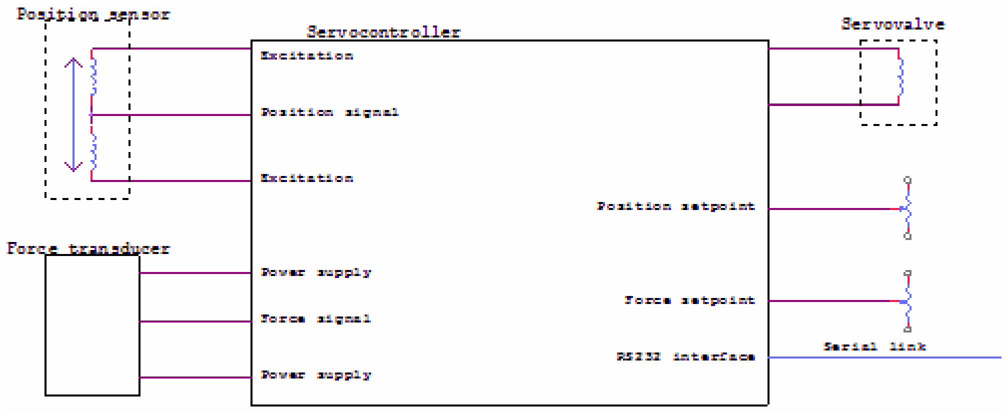


Figure 4: The electronics - functional block diagram

Figure 5: Electronics

The main functionality of the servocontroller is to provide the driving signal for servovalve to minimize the error between setpoint value and the measured value for the position (or force) of the cylinder rod. Another function is to interfacing the servocontroller with the position sensor and the force transducer and to converting the values of position and force in a numerical form. Force setpoint and position setpoint signals, is also converted into numerical values. Finally the servocontroller assure the physical link with informatics system.

**The software**

Multitier applications are used in implementing information systems that allow multiple users simultaneous access to the system and the data and the processing programs are separate, are a typical example web application. Multitier system architecture refers to a physical structuring mechanism for software modules (where the program runs).

The servocontroller runs a software that I ensure functionality. The software is build using event-driven technique in C programming language. At servocontroller level is assured a PID regulator for position and force. Also software calculates the speed value for cylinder rod.

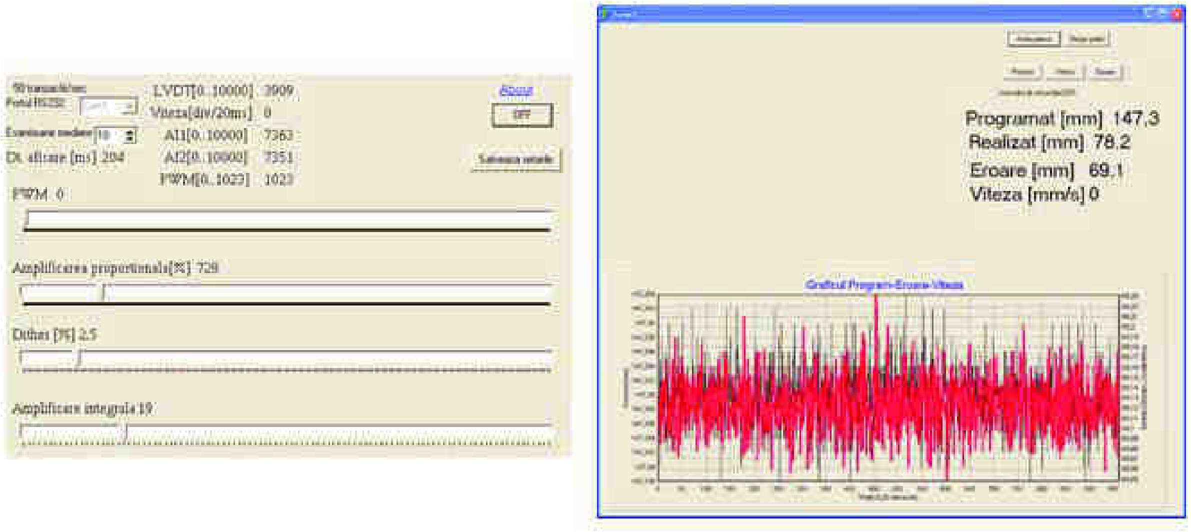


Mechatronic tier Client tier

Figure 6: Software

The PC software is designed as a multitier application, fig. 6. The top tier is “client tier” - the operator panel. The bottom tier is “mechatronic tier” which is a server application for the client tier. The mechatronic tier is developed using DCOM (Distributed Component Object Model) technology from Microsoft as an ActiveX component. The mechatronic tier assures the interface with the servocontroller.

The development of the applications operation client and parameterization of the hydraulic stand is substantially simplified through the incorporation of the implementation details of the physical and logic interface in the software components of the mechatronic tier

Multitier applications are used in implementing computer systems that allow multiple users simultaneous access to the system the data and the processing programs are separate, are a typical example web application. Multitier system architecture refers at a physical structuring mechanism for software modules (where the program runs).

## Experiments

Figure 7 and 8 shows the experimental characteristics of the rod position - positioning error at 1mms/s rod speed value.

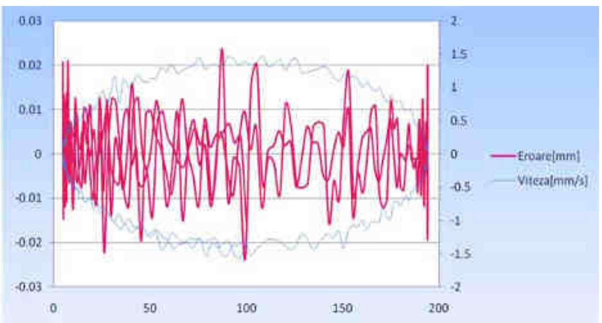


Figure 7: Sinusoidal excitation with a frequency of 2.5mHz value. On X axis is the rod position in mm

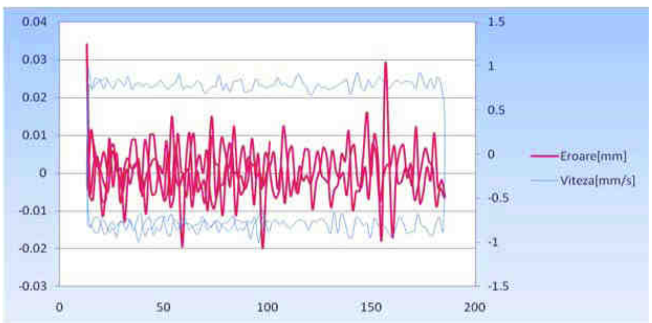


Figure 8. Triangle excitation with a frequency of 2.5mHz value. On X axis is the rod position in mm

## Conclusion

The experimental results confirmed a positioning accuracy of 0.1mm (0.05% of the actuator race), field monitoring of velocity of 1mm/s ... 1000mm/s and a link speed between computer and servocontroller of 50transactions/s. Experimental research conducted by the authors confirmed that the hydraulic axis performance allowing its use in robotics and informatics systems for manufacturing.

## Bibliography

[1] Test Point for Windows, Users Guide, Capital Equipment Corporation, Burlington, MA, 1994

[2] Mannesmann Rexroth, Hydraulic Trainer, vol 2, 1986

[3] MOOG (S.U.A. şi Germania), DOWTY (Anglia), BOSCH- REXROTH (Germania), PARKER (S.U.A.), VICKERS

[4] Carlo Ghezzi, “Fundamentals of Software Enginering”, 2003

[5] Joel de Vah, RUT - development manual 7.22 Design of Multi Tier Applications v1.5

[6] Marco Cantu, Mastering Delphi 7, Sybex © 2003

[7] http://java.sun.com/

[8] http://www.microchip.com/

[9] http://www.modbus.org/

ISSN 1454 - 8003
Proceedings of 2011 International Salon of Hydraulics and Pneumatics - HERVEX
*9 – 11 November, Calimanesti-Caciulata, Romania*

# EXPERIMENTAL STUDY CONCERNING THE FLOW OF BIOLOGICAL LIQUIDS IN ELECTRIC FIELDS

**Dan C. Badea[1], Alexandru Marin[2]**

[1] University POLITEHNICA of Bucharest – Material Strengths Dept., dancbadea@yahoo.com
[2] University POLITEHNICA of Bucharest – Hydraulics Dept., alexandru.marin@upb.ro

***Abstract:*** Paper is devoted to the experimental study of the biological liquids flow inside electric fields, respectively the influence of electrostatic field on the flow regime and designing a procedure for destroying microorganisms contained in the studied liquids

***Keywords***: *Biological liquids flow, Electrostatic field, Microorganisms*

## 1. Introduction

Liquid flow in electrostatic fields and their influence on different physical-chemical and biological were widely studied, but still some practical considerations should be clarified, in order to become useful in developing in-vivo applications.

## 2. Liquid flow in electrical field

If applying an electric field, a charged particle contained in a liquid is moving, as presented in Figure 1. This phenomenon is called “electrophoresis”.

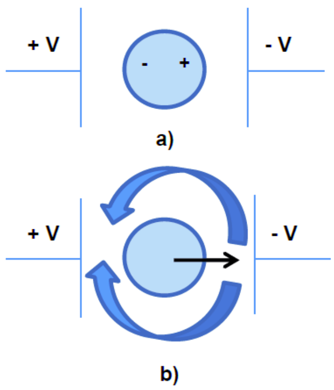


**Fig.1. Particle movement under electric field - electrophoresis**

Forces acting on the charged particle contained in a liquid, in an electric field, according to [7], are:

- Electrical force, $F_e = QE$ (1)
- “Friction” force in electrical field $F_{fe} = (Q-\varepsilon\xi d/2)E$ (2)
- Viscous friction force: $F = (\pi/8)C_R\rho_f d^2 w^2$ (3)

where: $Q$ = electrical charge of the particle, C
$\xi$ = electrical potential, V
$\varepsilon$ = liquid electric permittivity, F/m
$E$ = intensity of electric field, V/m (N/C)
$C_R$ = trail index
$d$ = diameter of the particle, m
$\rho_f$ = density of the liquid, kg/m$^3$

w = particle speed, m/s

The equilibrium forces equation, written for the particle is:

$$\vec{F}_e + \vec{F} + \vec{F}_{fe} = 0 \tag{4}$$

$$QE - \frac{\pi}{8} C_R \rho_f d^2 w^2 - \left( Q - \varepsilon\xi \frac{d}{2} \right) E = 0 \tag{5}$$

$$\frac{\pi}{8} C_R \rho_f d^2 w^2 = \varepsilon\xi \frac{d}{2} E \tag{6}$$

Depending on the Reynolds number, we have:

a) For Re < 1,

$$C_R = \frac{24}{\mathrm{Re}} = 24 \frac{\eta}{w d \rho_f} \tag{7}$$

where: η = liquid viscosity, Ns/m$^2$

and (6) becomes:

$$w = \frac{\varepsilon\xi E}{6\pi\eta} \quad \text{(m/s)} \tag{8}$$

known as *Huckel equation* [9].

b) For 1 < $R_e$ < $10^3$, according to [9]:

$$C_R = \frac{18{,}5}{(R_e)^{0{,}6}} = 18{,}5 (\eta / w d \rho_f)^{0{,}6} \tag{9}$$

and (6) becomes:

$$w = \left( \varepsilon\xi E / 4{,}62 \pi \eta^{0{,}6} \cdot \rho_f^{\ 0{,}4} \cdot d^{0{,}4} \right)^{0{,}71} \tag{10}$$

c) For $10^3$ < $R_e$ < $10^5$:

$$C_R = 0{,}44 \tag{11}$$

equation (6) becomes:

$$w = \left( \varepsilon\xi E / 0{,}11 \pi \rho_f d \right)^{0{,}5} \tag{12}$$

and is interesting to mention that the particle speed doesn't depend anymore on the viscosity of the liquid.

Concluding this paragraph, the particle speed inside the liquid, under electric field, is determined by: intensity of the electric field, viscosity and the size of the particle.

## 3. Considerations on electric permittivity of the liquids

For studying the optimal conditions of influencing the electric field on microorganisms, contained in biological liquids, we analyze the relation between electric permittivity of water and the associated electric energy stored in a certain liquid volume, V, done below:

$$W_T = \frac{1}{2} \varepsilon V E^2 \quad ,\mathrm{J} \tag{13}$$

So, if the volume V is small, than the energy $W_T$ and the influence on microorganisms is maximal, as desired in practical applications.

One of the procedures, destined to maximize the previous mentioned effect, is spraying the flowing water inside the electric field, the particles dimension being desired to be as close as possible to the dimensions of the microorganisms.

### 4. Biological stability of the liquids flowing inside electric fields

In order to make more efficient the microbiological influence on flowing electrolytic liquids, with $10^3 < Re$, we've done experiments with sprayed liquid in a high voltage electric field, respectively using the microorganism Escherichia Coli nr.11661 I.C.

The microbiologic characterization of the experimental probes was done by means of standard procedures and we determined the ratio corresponding to the efficiency of the process of destroying the microorganisms, done below:

$$\phi = \frac{N_i - N_f}{N_i} x100 \qquad ,\%$$

where: $N_f$ = final number of microorganisms, u/ml

$N_i$ = initial number of microorganisms, u/ml.

The process was studied on the equipment presented in Figure 4. The variable process parameter was the high voltage (0,5 – 25 kV). Actually, we used treatments at relative low levels (0,5 – 2 kV) and at high levels (5 – 25 kV), separately.

Table 1

| Voltage kV | Temperature $^0$C | $N_i$ u/ml | $N_f$ u/ml | $\phi$ % |
|---|---|---|---|---|
| 0,5 | 18 | 240 | 60 | 75 |
| 1,0 | 18 | 240 | 45 | 81 |
| 2,0 | 18 | 240 | 23 | 90 |
| 5,0 | 18 | 11000 | 5300 | 52 |
| 10,0 | 18 | 11000 | 3100 | 72 |
| 15,0 | 18 | 11000 | 2000 | 82 |
| 20,0 | 18 | 11000 | 1500 | 86 |
| 25,0 | 18 | 11000 | 1200 | 89 |

In Table 1, we presented the experimental results (average values). These show the "lethal" effect of the electrostatic field on the studied microorganisms.

At low voltage levels, is possible to destroy low concentration microorganisms, in the specific conditions of tissue culture medium.

In Figure 2 we present the variation of the destructive effect, depending on the high voltage values. The relationships are direct proportional.

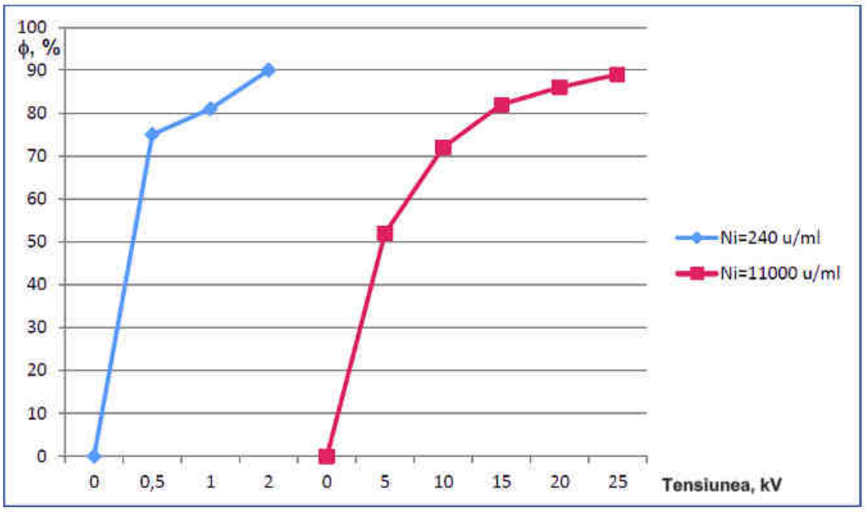


**Fig. 2. Electrostatic destroying for microorganism E. Coli**

For higher concentrations of microorganisms, it is necessary to use higher voltage levels – till 25 kV, in order to maintain the destructive efficiency.

In Figure 3, it is presented o photo image of the electrostatic destruction. The experiments were done at normal environment temperature, thus considering this procedure as "non thermal". Consequently, we preserve the vitamins and other useful substances from food products, and we reduce strongly energy consumption in such processes.

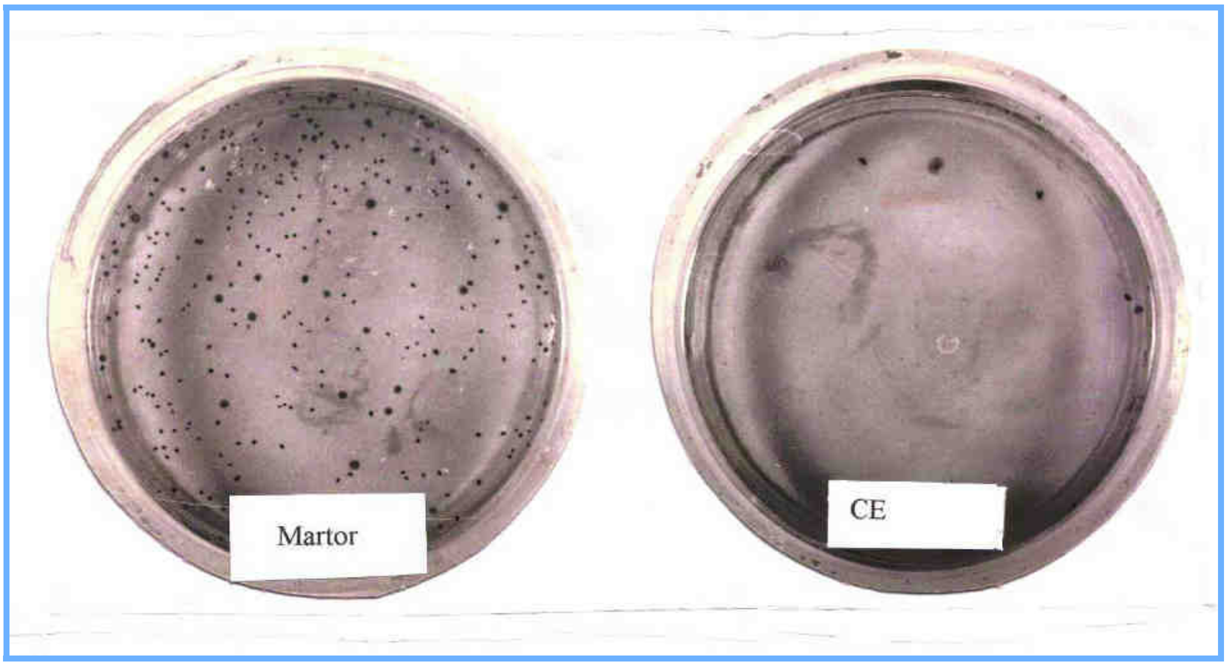


a) "Martor" – witness probe, with microorganisms    b) Treated probe

**Fig. 3. Photo image of the electrostatic destruction**

### 5. Experiments done with non – thermal treatment of beer

The procedure of electrostatic sprayed flow was applied to the non-thermal treatment of beer, by using a patented equipment, presented in Figure 4. The results proved fully the physical processes presented above, the application being very innovative.

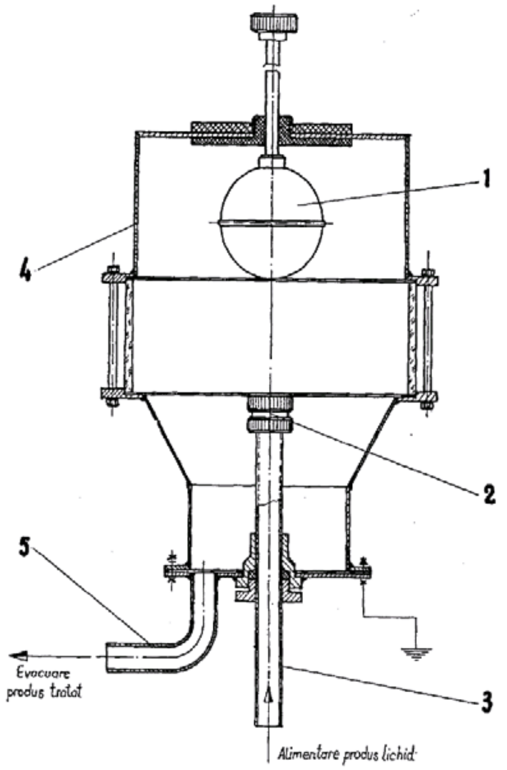


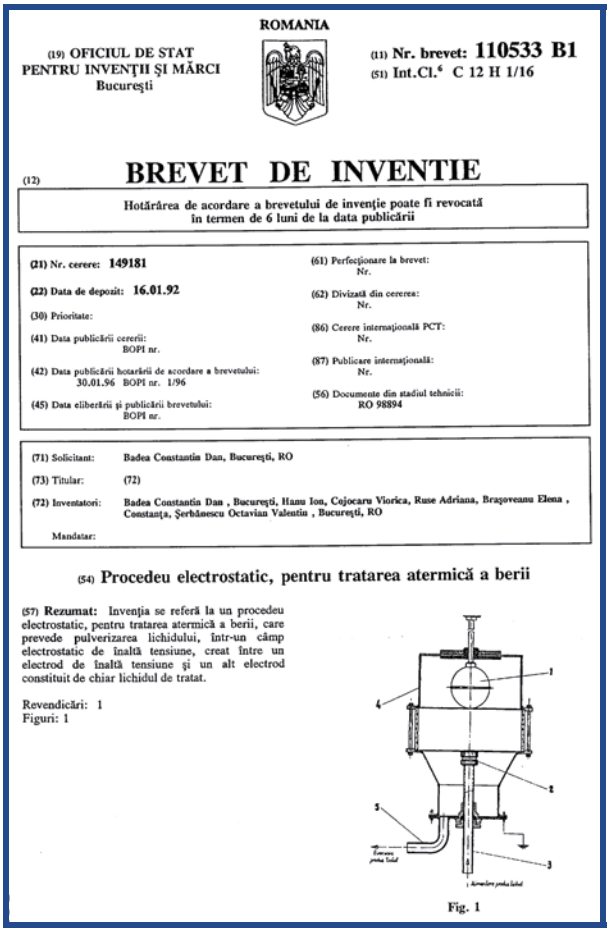

ROMANIA

(19) OFICIUL DE STAT PENTRU INVENŢII ŞI MĂRCI București

(11) Nr. brevet: 110533 B1
(51) Int.Cl.6 C 12 H 1/16

(12) BREVET DE INVENTIE

Hotărârea de acordare a brevetului de invenţie poate fi revocată în termen de 6 luni de la data publicării

(21) Nr. cerere: 149181
(22) Data de depozit: 16.01.92
(30) Prioritate:
(41) Data publicării cererii: BOPI nr.
(42) Data publicării hotarârii de acordare a brevetului: 30.01.96 BOPI nr. 1/96
(45) Data eliberării şi publicării brevetului: BOPI nr.

(61) Perfecţionare la brevet: Nr.
(62) Divizată din cererea: Nr.
(86) Cerere internaţională PCT: Nr.
(87) Publicare internaţională: Nr.
(56) Documente din stadiul tehnicii: RO 98894

(71) Solicitant: Badea Constantin Dan, București, RO
(73) Titular: (72)
(72) Inventatori: Badea Constantin Dan , București, Hanu Ion, Cojocaru Viorica, Ruse Adriana, Brașoveanu Elena , Constanţa, Şerbănescu Octavian Valentin , București, RO
Mandatar:

(54) Procedeu electrostatic, pentru tratarea atermică a berii

(57) **Rezumat:** Invenţia se referă la un procedeu electrostatic, pentru tratarea atermică a berii, care prevede pulverizarea lichidului, într-un câmp electrostatic de înaltă tensiune, creat între un electrod de înaltă tensiune şi un alt electrod constituit de chiar lichidul de tratat.

Revendicări: 1
Figuri: 1

Fig. 1

**Fig. 4. Patented equipment**

After 30 days, all witness probes were deteriorated – the beer was spoiled, while the treated ones were clear, tasty and a bit more foamy than the fresh product. All microorganisms were destroyed and the product was safe and healthy.

### Conclusions

The experimental research presented in this paper revealed clearly the existence of quantitative and qualitative correlations between the sprayed flow regimes, inside electric fields, and the destruction process of microorganisms, contained in biological liquids.

### Acknowledgments

This research was financed by means of a contract, signed with S. C. MALBERA S.A. from Constan  a - Romania.

**REFERENCES**

*[1] Badea C. Dan ş.a. - Procedeu pentru amestecarea electrostatică a lichidelor, Brevet România nr. 91707, 1987.*
*[2] Badea C. Dan ş.a. - Distrugerea electrostatică a microorganismelor patogene din alimente, Institutul de Chimie alimentară, ctr. 60, 1990-1992.*
*[3] Badea C. Dan ş.a. - Procedeu electrostatic pentru tratarea atermică a berii, Brevet RO nr. 110.533, 1996.*
*[4] Badea C. Dan ş.a. - Elaborarea unui procedeu electric de tratare a berii, Institutul de Chimie Alimentară, ctr. 81, 1991-1992.*
*[5] Firoiu C. - Tehnologia proceselor electrochimice, EDP, Bucureşti, 1983.*
*[6] Jitariu P. - Acțiunea câmpului magnetic şi electromagnetic asupra organismelor animale, Editura Academiei Române, Bucureşti, 1987.*
*[7] Moore A.D. - Electrostatics and its Applications, John Wiley & Sons, New York, 1973.*
*[8] Purcell E.M. - Cursul de fizică Berkeley, vol. II, Electricitate şi magnetism, EDP, Bucureşti, 1982.*
*[9] Schoen H.M. - New chemical engineering separation techniques, Interscience Publishers, New York, 1982.*
*[10] Tănăsescu F.T., Cramariuc R. - Electrostatica în tehnică, Editura tehnică, Bucureşti, 1977.*
*[11] Tănăsescu F.T., Antohi C. -Electrostatica în agricultură,Editura CERES, Bucureşti, 1988.*
*[12] Youjun Wu, Wei Yu, Chixing Zhou - The influence of electric field-induced orientation on the retraction of a liquid crystal droplet immersed in a flexible polymer matrix, Journal of Colloid and Interface Science 303 (2006) 546–551*
*[13] Dazhi Wang, Marin Sigurdson, Carl D. Meinhart - Experimental analysis of particle and fluid motion in ac electrokinetics, Experiments in Fluids 38 (2005) 1–10, DOI 10.1007/s00348-004-0864-5*

**ISSN 1454 - 8003**
**Proceedings of 2011 International Salon of Hydraulics and Pneumatics - HERVEX**
*9 – 11 November, Calimanesti-Caciulata, Romania*

# NEW APPROACHES REGARDING THE CREATION OF VIRTUAL ENTERPRISES IN THE NATIONAL NETWORK

**MARIAN TOPOLOGEANU[1], STEFAN VELICU[2],**

[1]**SC ICTCM SA Bucuresti;** [2]**POLITEHNICAL UNIVERSITY of Bucharest;** [1]mtopologeanu@ictcm.ro

**ABSTRACT**

*The paper presents a new concept of Virtual Enterprises (V.E.) in a complex approach as a regional network of economic entities as potential constitutes of a V.E. That make possible creation of a data base of technological, collaborative and behaviorist attributes allowing a selection process by clustering in the attribute space potential selections of V.E. groups able to produce the goal product.*

*The attributes classification is a good support to reengineering works, inside the network entities, to achieve organizational need imposed by the V.E. participation.*

**KEYWORDS:** virtual enterprise, entity, network.

## 1. INTRODUCTION

The Virtual Enterprise is an advanced form of associative and collaborative economic activity and the start is contemporaneous with first manufacturing production. One of actual definition of V.E. describes this concept like “a temporary network of independent companies, in relation any with other through informatics technology by which divided the competences, the infrastructure and the business process in the purpose to satisfy the requests of the market”. The definition of the network can be the “cooperation unofficial form which develop by change methods of informations, people and social norms”.

## 2. THE MODEL OF V. E.

The creation of V.E. is a initiative at competition of two primary requests:

- investors request to start the product in manufacturing and on market, with short production cycle and minimum costs;
- manufacturing economic entities request, the potential participants in the structure of V.E. is to fructify the production capacities on maximum.

The V.E has the life cycle divided on six stages:

- the conception – establish the relation and the strategy of V.E.;
- the competition – the primary test of the product on the market;
- the configuration –development and adaptation of the infrastructure and production capacities;
- the operative management – V.E manage the production, delivery and support product in profit conditions
- the final – the end of agreements and the results

## 3. CONCEPT OF NATIONAL NETWORK FOR V.E. – RENIV - PREMISES

The common development of V.E. pass following stages:creation

a) – seting the request of investitors and the definition of the object (product, service;

b) – extractions of technological and constructive dates of product ;

c) – appeal to potential participants, possessor of technologies, from lisr or by Internet on base of specialized portal, specify the technological requests;

d) – partners selection.

In these stages the approach by informatical product must make in c) stage.

The approach by national network concept of potential participants/partners in evolution of differents V.E. offers many advantages:

- creation of a data base of technological, collaborative and behaviorist attributes allowing a selection process
- are using only representations for technological attributes describe by „processes” (fractal approach) allowing a optimal selection by attributes clusters of potential partners;
- potential partners included in data base can to organize the technological processes in according with the requests by definition of attributes in network by reenginering works and virtual simulation;
- complex informaticl approach of registration process and selection of partners in network.

## 4. ASPECTS REGARDING THE SELECTION OF PARAMETERS FOR CREATION OF V.E. IN THE NETWORK

The success of V.E. like efficiency and finality depends by the partners quality and adequate of this for objective/object.The existence of data base of registration entities in network is a favored premise. The selection criterions must to vise the technological requests and behavioural/collaborative.

In esence the partners selection for V.E. with defined objective, attended by adequate informatic system crossing stages following:

- the representace of the object (product/service) of V.E. by technological attribute which defined him
- the entities selection from data base of network must make in two stages:

❖ Stage 1 – selecting in the technological attributes space, the attributes of object and to ensure that these find in attributes set declarate by the partners from network.

❖ Stage 2 – selections refining of stage 1 must make in the behavioural and collaborative attributes space.

## 5. INFORMATIC MECHANISM OF V.E. NETWORK

The informatics system V.E. will be a complex product which contains modulus:

- logging modulus in network;
- requirement modulus;
- communication modulus in network;
- operative modulus; selection tools of clusters;
- optimizing and modeling tools.

The public information, dissemination and access in system will be making by specialized site.

The realization of the product is the development result of parallel/sequential technological processes row, the architecture production system can be compound by working technological nucleus, with conceptual equivalent type holistic and fractorial.

**The working technological nucleus can be:**

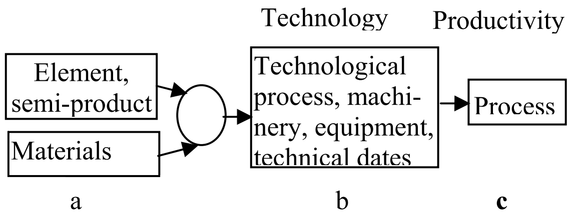


The feature **„ working technological nucleus”** is defined by 3 zones:

a) – **input** with defining of material type which enter in process or the product compounds of the product, semi-products or assembly entered in process;

b) – **technological zone** in which the technological concept reunites the technological process with specified operations, machineries and necessary equipments and the process features which is refer at processing requests, necessary qualities, production type;

c) – **output** from nucleus defined by processing compound, compound, manufacturing material, assembly, product.

Was defined in project 6 classes (A-F) with 14 parameters categories which will define the technological attributes frame like clustering space and a associated technological class (S).

The classes define: a) the technologies, b) operations and techniques, c) Compounds type, d) technological machineries, e) semi-product materials, f) technological dates, s) fabrication preparation
Example with development stages of a registration:

**6 TECHNOLOGICAL CLASSES AND SPECIFIED ATTRIBUTES**

| No. | Registration stage | CUMULATIVE TEXT | CUMULATIVE CODE | | | | | | | | | | | | | |
|---|---|---|---|---|---|---|---|---|---|---|---|---|---|---|---|---|
| | | | CT | $A_1$ | $A_2$ | $B_1$ | $B_2$ | C | $D_1$ | $D_2$ | $E_1$ | $E_2$ | $E_3$ | $F_1$ | $F_2$ | $F_3$ |
| *0* | *1* | *2* | *3* | *4* | *5* | *6* | *7* | *8* | *9* | *10* | *11* | *12* | *13* | *14* | *15* | *16* |
| 1 | 1 | Metal | 01 | | | | | | | | | | | | | |
| | 2 | Metal cutting | 01 | 08 | | | | | | | | | | | | |
| | 3 | Metal, cutting, turning | 01 | 08 | 01 | | | | | | | | | | | |
| | 4 | Metal, cutting, turning, horizontal spindle | 01 | 08 | 01 | 01 | | | | | | | | | | |
| | 5 | Metal, cutting, turning, automatic | 01 | 08 | 01 | 01 | 03 | | | | | | | | | |
| | 1 | 2 | 3 | 4 | 5 | 6 | 7 | 8 | 9 | 10 | 11 | 12 | 13 | 14 | 15 | 16 |
| | 6 | Metal, cutting, turning, automatic, spindle | 01 | 08 | 01 | 01 | 03 | 04 | | | | | | | | |
| | 7 | Metal, cutting, turning, automatic, CNC with automatic control automatic contr<br><br>automatic control | 01 | 08 | 01 | 01 | 03 | 04 | 05 | | | | | | | |

**ISSN 1454 - 8003**
**Proceedings of 2011 International Salon of Hydraulics and Pneumatics - HERVEX**
*9 – 11 November, Calimanesti-Caciulata, Romania*

| | | | | | | | | | | | | | | | | |
|---|---|---|---|---|---|---|---|---|---|---|---|---|---|---|---|---|
| | 8 | Metal, cutting, turning, automatic, CNC with automatic control | 01 | 08 | 01 | 01 | 03 | 04 | 05 | 02 | | | | | | |
| | 9 | Metal, cutting, turning, automatic, from carbon steel | 01 | 08 | 01 | 01 | 03 | 04 | 05 | 02 | 02 | | | | | |
| | 10 | Metal, cutting, turning, automatic, from carbon steel, usual | 01 | 08 | 01 | 01 | 03 | 04 | 05 | 02 | 02 | 01 | | | | |
| | 11 | Metal, cutting, turning, automatic, laminate bar | 01 | 08 | 01 | 01 | 03 | 04 | 05 | 02 | 02 | 01 | 02 | | | |
| | 12 | Metal, cutting, turning, automatic, diameter <10mm | 01 | 08 | 01 | 01 | 03 | 04 | 05 | 02 | 02 | 01 | 02 | 03 | X | |
| | 12 | Metal, cutting, turning, automatic and diameter 10–100 mm | 01 | 08 | 01 | 01 | 03 | 04 | 05 | 02 | 02 | 01 | 02 | 04 | X | |
| | 13 | Metal, cutting, turning, automatic, manufacturing precision IT 07 | 01 | 08 | 01 | 01 | 03 | 04 | 05 | 02 | 02 | 01 | 02 | 04 | X | 04 |

Example with two registrations:

| No. | CUMULATIVE TEXT | CUMULATIVE CODE | | | | | | | | | | | | | |
|---|---|---|---|---|---|---|---|---|---|---|---|---|---|---|---|
| | | CT | $A_1$ | $A_2$ | $B_1$ | $B_2$ | C | $D_1$ | $D_2$ | $E_1$ | $E_2$ | $E_3$ | $F_1$ | $F_2$ | $F_3$ |
| 1 | Metal, cutting, turning, horizontal spindle, automatic, spindles, machinery with high productivity, CNC with automatic control, carbon steel material, usual, from laminate bar, diameter Ø10mm, manufacturing precision IT 07 | 01 | 08 | 01 | 01 | 03 | 04 | 05 | 02 | 02 | 01 | 02 | 03 | X | 0 |
| 2 | Metal, cutting, turning, horizontal spindle, automatic, spindles, machinery with high productivity, CNC with automatic control, carbon steel material, usual, from laminate bar, diameter Ø10-100 mm, manufacturing precision IT 07 | 01 | 08 | 01 | 01 | 03 | 04 | 05 | 02 | 02 | 01 | 02 | 03 | X | 0 |

## 7.ECONOMIC, LOGISTIC AND BEHAVIORAL ATTRIBUTES

These sub serve at selections refining on technological attributes

| Parameter | expression |
|---|---|
| Dynamic of turnover | Percentage increase or decrease on 3 years on percentage scale |
| Dynamic of human resources | Percentage increase or decrease of human resources reported of dynamic turnover |
| Company near money | Percentage increase or decrease of near money in last years |
| Duty degree of company | Fluctuation in last 3 years. |

The weights are in unitary scales (1-4 or 1-5) with optimal value “1”

***Behavioral Parameters***

The administrator must check the declarations.

| Parameters | Scalar expression |
|---|---|
| The degree of completion of contractual business | Evaluation in 4 percentage scales according by economic entity |
| Contracts/orders weight/ with delay on delivery | Evaluation in 4 percentage scales |
| Weight of cancellation Contracts or cancellation orders from the contacts total | Evaluation in 4 percentage scales |

**Logistic parameters**

These parameters look at acquisition evaluation and delivery of partners in network.

**Acqusition Degree**

| | |
|---|---|
| Acquisition must be sure and qualitative with suppliers list | Evaluation YES/NO |
| Scheduled acquisition from market without suppliers list | YES/NO |
| Uncertain acquisition | YES/NO |

These registrations can be controlled by “network Administrator”.

**Delivery of the product**

| | |
|---|---|
| With respect of delivery diagram | Evaluation YES/NO |
| With delivery delays | Evaluation in 3 percentage scales |

**Management Parameters**

These parameters reflect the technical level of manager act.

| | |
|---|---|
| Informatics of all departments | Percentage evaluation of activities number, functional departments |
| Technological informatics | În 3 stages, one point for:<br>- designing informatics;<br>- production norm informatics;<br>- informatics of technical control and production automation |
| Commercial and marketing informatics | Evaluation: YES / PARTIAL (over 50%) /NO Declaration |

## 8.TECHNOLOGICAL CHARACTERIZATION

**The defining of functional dates** put the product in users zone who define not the technological parameters, first informations regarding requests like: human security, environment protection, the form, size, mass, medium (industrial processes, infrastructure, transport, personal use).

The importance of constructive date which determine technologic the products class present that the assembly operations, control, final testing are technological operations which must be in a specialized enterprise.

**The constructive levels of product**

The product is represent in this schedule:

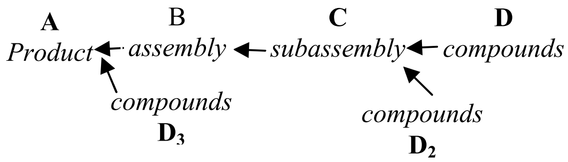


The diagram lattice points represent assembly operations specifically in AB lattice points and not in lattice points **BCD** and **CD**.

Regarding the production/realization of V.E. objective is important to tell the security source for production of assembly, subassembly, compounds.

For assembly, subassembly, compounds the source can be:

- acquisition from free market;
- partial realization in V.E.
- total realization in V.E.

The compounds can be:

- commune; usual assembly compounds from the market;
- specific – realize in product manufacturing

***Example of operation sheet for a compound***

For example we choose one type piece - connecting rod

**Date for Operation Sheet**
**Assembly**: heat engine
**Unit**: connecting road - link
**Compound:** connecting rod
**Compound weight:** 960 gr. (Fz: 03)
**Technological principal dimension**: Ø60 (F01: 04)[1] **Pieces/product Number** : 4
**Piece Material** : (example: OLC 45)
**Heat Treatment**: (example nitridation)

For execution of the piece is necessary the **TECHNOLOGICAL FLOW:**

1. Drop Forging;
2. Cutting (turning) of surface A;
3. Cutting (milling) of plane surface C;
4. Cutting (milling) of plane surface D;
5. Cutting (turning) of surface B;
6. Cutting (milling) of plane surface E;
7. Cutting(milling) of plane surface F;

8. Cutting (milling) of plane surface G;
9. Cutting (milling) of plane surface H;
10. Cutting (boring) of surface A;
11. Cutting (boring) of surface B;
12. Cutting(drilling) Ø5;
13. Heat Treatment (nitridation);
14. Cutting(grinding) of plane surface C;
15. Cutting(grinding) of plane surface E;
16. Cutting (grinding) of plane surface D;
17. Cutting(grinding) of plane surface F;
18. Cutting (grinding) of surface C;
19. Cutting(grinding) of surface B;
20. Cutting(grinding) for surface G balancing
21. Cutting (grinding) for surface H balancing;
22. Control.

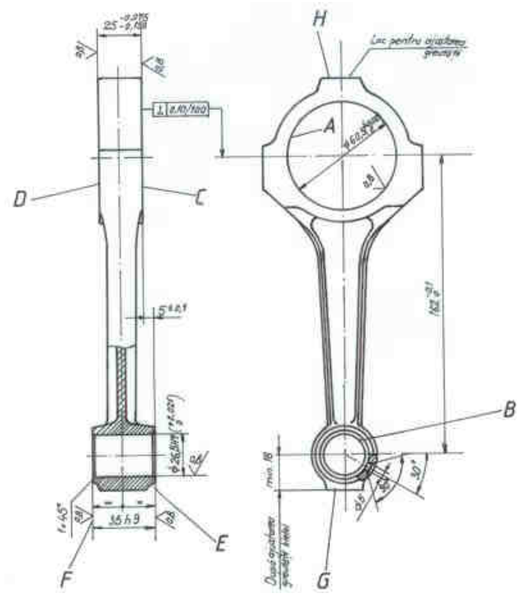

Connecting rod

***CUMULATIVE TECHNOLOGICAL OPERATIONS***

- Forging – operation: 1;
- Cutting – operations: 1, 5;
- Milling – operations: 3,4,6,7,8,9;
- Boring – operations: 10, 11;
- Drilling – operations: 12;
- Heat Treatment (nitridation) – operation: 13;
- Grinding – operations: 14, 15, 16,17,18,19,20,21;
- Control – operation: 22.

**Technological operations**: the 21 technological operations presented in technological sheet
**Cumulative technologies** : technological operations [2];
A … presented in technological sheet
**Special requests** : lot and quality mark [3];
**The definition of technological chain:**
Cumulative operations Chain: B… H
Free operation / independent: A. [4]

Operation Sheet of the compounds / section operation in cumulative code

| | | TECHNOLOGICAL OPERATIONS CODE | | | | | | | | | | | EXPERT NOTES | | | | | | | | | | |
|---|---|---|---|---|---|---|---|---|---|---|---|---|---|---|---|---|---|---|---|---|---|---|---|
| | | | | | | | | | | | | | EXPERT RECOMMANDATIONS | | | TYPE TOOLS | | COMPLEX TOOLS | | | | | |
| Compound: Connecting Rod / Cumulative code | | CT | $A_1$ | $A_2$ | $B_1$ | C | $E_1$ | $E_2$ | $E_3$ | $F_1$ | $F_2$ | $F_3$ | $C_2$ | $D_1$ | $D_2$ | $S_1$ | $S_2$ | 1 | 2 | 3 | 4 | 5 | |
| A | Forging | 01 | 04 | 03 | X | 07 | 02 | 02 | 02 | 09 | 03 | 10 | | | | 01 | 02 | | X | | | | |
| B | Cutting | 01 | 08 | 01 | X | 07 | 02 | 02 | 02 | 04 | 03 | 07 | 02 | 03 | 02 03 | | | | | | | | 1) |

| | | | | | | | | | | | | | | | | | | | | | | | |
|---|---|---|---|---|---|---|---|---|---|---|---|---|---|---|---|---|---|---|---|---|---|---|---|
| C | Milling | 01 | 08 | 02 | 01 | 07 | 02 | 02 | 02 | 08 | 03 | 08 | 02 | 03 | 02 03 | | | | | | | | 2) |
| D | Boring | 01 | 08 | 09 | X | 07 | 02 | 02 | 02 | 04 | 03 | 04 | 02 | 03 | 02 03 | | | | | | | | 3) |
| E | Drilling | 01 | 08 | 03 | X | 07 | 02 | 02 | 02 | 03 | 03 | 06 | 02 | 03 | | 03 | 01 | X | | | | | 4) |
| F | Heat treatment nitridation | 01 | 16 | 03 | X | 07 | 02 | 02 | 02 | 13 | 03 | X | | | | | | | | | | | 5) |
| G | Grinding | 01 | 08 | 06 | X | 07 | 02 | 02 | 02 | 04 | 03 | 04 | 02 | 03 | 02 03 | | | | | | | | 6) |
| H | Control | | | | | | | | | | | | | | | | | | | | | | 7) |

## 9 CONCLUSIONS

The regional approach makes possible creation of a data base of technological and behavioral attributes.

That makes possible selection by clustering of partners of V.E. on ask objectif.

The attributes classification is a good support to reengineering works, inside the network entities, to achieve organizational need imposed by the V.E. participation.

One informatics mechanism will assist the national network of V.E. in selection stage and in life cycle of creation entity.

## REFERENCE

**1 Adrian CURAJ**. The management of integrated manufacturing systems in virtual enterprise Ed. Didactica si Pedagogica. 2000 Bucharest;

**2. CEEX** Contract 13 I/07.10.2005. Development of an open wide of economic manufacturing entities, as a clustering dynamic space, to build up virtual enterprises defined by set of attributes–REINVIR. Project Manager -SC ICTCM SA ;

**3.** Virtual Enterprise in the concept of national network. *Constructia de Masini Revue*.Year No.1/2006.

**4** www.ictcm.ro/ceex2005/infosoc13-2005/;

5. www.ictcm.ro/projects in working

**ISSN 1454 - 8003**
**Proceedings of 2011 International Salon of Hydraulics and Pneumatics - HERVEX**
*9 – 11 November, Calimanesti-Caciulata, Romania*

# INTEGRATED CONCEPT AND DESIGN OF A COMPLEX TEST EQUIPMENT TECHNOLOGY OILFIELD TUBULAR MATERIAL

**Constantin CHIRITA [1], Andrei GRAMA [1], Adrian Constantin HANGANU [1]**

[1] "Gheorghe Asachi" Technical University of Iaşi, Faculty of Machine Manufacturing and Industrial Management, Department of Machine Tools, Hydraulic and Pneumatic Systems Engineering Department

***Abstract:*** This paper establishes from standards minimum design verification testing procedures and test acceptance criteria for casing and tubing connections for the oil and natural gas industries. These physical tests are part of a design verification process and provide objective evidence that the connection conforms to the manufacturer's claimed test load envelope and limit loads.
***Keywords****: tubular material, tubing conection, machine screwed - unscrewed*

## 1. Introduction (Arial, 11pt, Bold)

Prior to beginning a test, the manufacturer shall provide a connection data sheet for the product stating its intended connection assessment level, its geometry, and claimed performance properties in terms of tension, compression, internal pressure, external pressure, bending, and torque. The manufacturer shall provide a drawing, which is representative of the cross–sectional area of the connection. The manufacturer shall also provide the following in graphical form: 100 % Pipe Body Load Envelope, 95 % Pipe Body Load Envelope (or as otherwise agreed to between user and manufacturer), and claimed Test Load Envelope and should quantify limit loads. The manufacturer's own method of calculation should be used to derive the claimed test load envelope and to calculate the test loads. Performance data or the method described by which a manufacturer or user may estimate the test load envelope using a connection performance model based on capacities of specific critical cross–sections in the connection.

The manufacturer should define as completely as possible the limit loads for each connection. A user may also make an independent estimate of the limit loads. Limit loads shall be greater than the test load envelope.

It is critical that the combined load capacity described by the test load envelope be defined near and throughout the conditions where the dominant load sensitivity of the connection may change from pressure to axial force and/or bending or vice versa

Since casing and tubing connection designs and the resultant performance can vary widely, no overall requirement for the minimum number of values in a tabular data format can be mandated. However, it is expected that approximately 10 combined load values of pressure and axial force per quadrant should be sufficient to define the test and limit loads. If a connection design exhibits changes in load sensitivities, the loads at which the changes in load sensitivity occur shall be provided.

In the calculation of both pipe body and connection load capacities, it is the intent of this International Standard to test the specimens to as high a load or combination of loads as safely practical.

In the event that unanticipated events result in deviations to the detailed requirements and or procedures, such deviations shall be clearly identified in the documentation and test report.

ISSN 1454 - 8003
**Proceedings of 2011 International Salon of Hydraulics and Pneumatics - HERVEX**
*9 – 11 November, Calimanesti-Caciulata, Romania*

## 2. Connection Application Level (CAL) and qualification test procedures

Casing and tubing connections can be considered as concentrically layered mechanisms used to join lengths of pipe to form a casing or tubing string. Connections consist of threads, seals and/or shoulders on a body member. Connections can vary widely in design and function.

Casing and tubing strings are usually suspended and/or cemented in the well bore and are subject to five distinct types of primary loads:

a) fluid pressure — internal and/or external;
b) axial force — tension or compression;
c) bending — buckling and/or well–bore deviation;
d) torsion — make–up and rotation;
e) non–axisymmetric — area, line or point contact.

This International Standard only addresses the first three loading modes, which are primary in essentially all wells. The pipe body, as well as the casing or tubing connection, has to successfully withstand (contain and/or transmit) these loads in service.

The test load envelope of a pipe body can be mathematically defined as the various combinations of loads that produce a von Mises equivalent (VME) stress intensity in the pipe body equivalent to the tensile axial yield strength of the material. Similarly, the test load envelope of a connection can be defined as the various combinations of loads that define the sealing (pressure) integrity and structural capacity limits, in which the connection can cyclically operate.

A test load envelope consists of four quadrants:

— Quadrant I: axial tension plus internal pressure with possible bending;
— Quadrant II: axial compression plus internal pressure with possible bending;
— Quadrant III: axial compression plus external pressure with possible bending;
— Quadrant IV: axial tension plus external pressure with possible bending.

An example of the test load envelope of the pipe body and a connection is provided in Figure B.1.

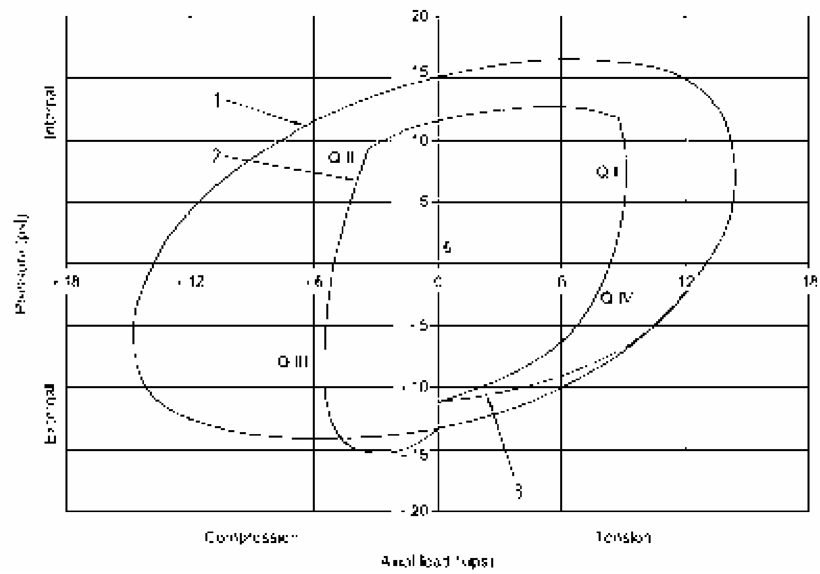


Key
1 100 % VME pipe body yield envelope
2 100 % test load envelope
3 100 % API collapse
Efficiency: 0,64 tension; 0,38 compression

Figure 1 — Pipe body and test load envelope at specified dimensions

ISSN 1454 - 8003
**Proceedings of 2011 International Salon of Hydraulics and Pneumatics - HERVEX**
*9 – 11 November, Calimanesti-Caciulata, Romania*

### 3. Procedures for testing casing and tubing connections

**Table 1 — Test matrix — Test series and specimen identification numbers**

<table>
<tr><th>Connection application level</th><th>Series A<br><br>4 quadrants with mechanical cycles</th><th>Series B<br><br>2 quadrants with mechanical cycles</th><th>Series C<br>Thermal cycling<br>Thermal/pressure and tension cycling</th><th>Bake and thermal cycle temperatur e</th><th>Internal test pressure medium (external is liquid)</th></tr>
<tr><td rowspan="2">IV<br><br>Total number of specimens= 8</td><td>At ambient temperature</td><td>Bending required at ambient temperature</td><td>5 mechanical at ambient temperature<br>50 thermal with pressure/tension*<br>5 mechanical at elevated temperature<br>50 thermal with pressure/tension*<br>5 mechanical at ambient temperature</td><td rowspan="2">180 C<br>(356°F)</td><td rowspan="2">Gas</td></tr>
<tr><td>Specimens<br>2,4,5,7</td><td>Specimens<br>1,3,6,8</td><td>Specimens<br>1,2,3,4</td></tr>
<tr><td rowspan="2">III<br><br>Total number of specimens= 6</td><td>At ambient temperature</td><td>Bending optional at ambient temperature</td><td>5 mechanical at ambient temperature<br>5 thermal with pressure/tension<br>5 mechanical at elevated temperature<br>5 thermal with pressure/tension<br>5 mechanical at ambient temperature</td><td rowspan="2">135 C<br>(275°F)</td><td rowspan="2">Gas</td></tr>
<tr><td>Specimens<br>2,4,5</td><td>Specimens<br>1,3,6,</td><td>Specimens<br>1,2,3,4</td></tr>
<tr><td rowspan="2">II<br><br>Total number of specimens=4</td><td rowspan="2">CAL II does not require external pressure test</td><td>Bending optional at ambient temperature</td><td>5 mechanical at ambient temperature<br>5 thermal with pressure/tension<br>5 mechanical at elevated temperature<br>5 thermal with pressure/tension<br>5 mechanical at ambient temperature</td><td rowspan="2">135 C<br>(275 F)</td><td rowspan="2">Gas</td></tr>
<tr><td>Specimens<br>1,2,3,4</td><td>Specimens<br>1,2,3,4</td></tr>
<tr><td rowspan="2">I<br><br>Total number of specimens=3</td><td rowspan="2">CAL I does not require external pressure test</td><td>Bending optional at ambient temperature</td><td rowspan="2">CAL I does not require thermal cycling test</td><td rowspan="2">CAL I does not require bake</td><td rowspan="2">Liquid</td></tr>
<tr><td>Specimens<br>1,2,3</td></tr>
</table>

| **Connection assessment level** | **Series A 4 quadrants with mechanical cycles** | **Series B 2 quadrants with mechanical cycles** | **Series C Thermal cycling<br><br>Thermal/pressure and tension cycling** | **Bake and elevated temperature tests** | **Internal test pressure medium<br><br>(external is liquid)** |
|---|---|---|---|---|---|
| IV | At ambient and elevated | Bending required at ambient and elevated temperatures | 10 thermal with pressure/tension<br>5 mechanical cycles at ≤ 35 °C (95 °F) | 180 °C (356 °F) | Gas |
| Total number of specimens 5 | Specimens 1, 2, 3, 4 | Specimens 1, 2, 3, 4 | Specimens 1,2,3,4 | | |
| III | At ambient and elevated | Bending required at ambient and elevated temperatures | 10 thermal with pressure/tension<br>5 mechanical cycles at ≤ 35 °C (95 °F) | 180 °C (356 °F) | Gas |
| Total number of specimens 5 | Specimen 1 | Specimens 1,2,3,4 | Specimens 1, 2 | | |
| III-Ambient A | At ambient | Bending required at ambient and elevated temperatures | 10 thermal with pressure/tension<br>5 mechanical cycles at ≤ 35 °C (95 °F) | 180 °C (356 °F) | Gas |
| Total number of specimens 5 | Specimen 1 | Specimens 1,2,3,4 | Specimens 1, 2 | | |
| II | At ambient (reduced cycles) | Bending required at elevated temperature | Not Applicable | 135 °C (275 °F) | Gas |
| Total number of specimens 3 | Specimen 1 | Specimens 1, 4 | | | |
| I-E | At ambient (reduced cycles) | At ambient with bending | Not applicable | Bake out not required ambient | Gas or liquid |

| | | | | | |
|---|---|---|---|---|---|
| Total number of specimens 2 | Specimen 1 | Specimen 1 | | | |
| I<br><br>Total number of specimens 2 | Not applicable | At ambient; no bending<br><br>Specimens 1 | Not applicable | Bake-out not required; ambient | Liquid |

**4. Main items for test equipment**

- Torque tool with monitoring/recording equipment
- Tension/compression test frame
- Hydraulic cylinders for tension/compression and bending
- Loadcells, straingauge equipment, displacement monitoring, plus control equipment
- Nitrogen pressure equipment, compressors, boosters plus control/recording equipment
- heating equipment (up to 180 degr C minimum) plus thermocouplers and controls/recording
- Water/Hydraulic oil pressure equipment, compressors, boosters, plus control/recording equipment
- leak monitoring system(s)
- external pressure autoclaves (design and seals)
- tensile test equipment at ambient and elevated temperatures
- Torque tool with hydraulics, control and monitoring/recording equipment
  • horizontal or vertical
  • own or rental
  • maximum torque capacity
- Tension/compression test frame
  • horizontal or vertical
  • dimensions (i.e capable of one sample or two sample testing)
  • load capacity (a direct function of casing size)
  • sample installation method
- Hydraulic cylinders
  • capacity tension/compression (double acting, capacity is a immediate function of maximum casing-size)
  • stroke
  • quality (small and large loads have to be precisely controlled, very slow moving so danger of slip-stick phenomena)
- Loadcells, straingauge equipment, displacement monitoring, plus control equipment
  • accuracy at small loads and high loads
  • personnel for straingauge application
- Nitrogen pressure equipment, compressors, boosters plus control/recording equipment
  • elaborate system requirements
  • accurate control and monitoring

- heating equipment (up to 180 degr C minimum) plus thermo couplers and controls/recording
  • equipment for baking
  • equipment for heating sample during tests
  • cooling system for sample
- Water/Hydraulic oil pressure equipment, compressors, boosters, plus control/recording equipment
  • Hydraulic oil for high temperature external pressure testing
  • very accurate pressure monitoring device required
  • Water can be used for CAL I tests only (all other CAL require > 100 degr; 135 degr CAL II or 180 degr CAL III/IV)
- leak monitoring system(s)
  • Conventional bubble method becomes difficult and can only be used for ambient temperature tests (i.e. CAL I only)
  • Pressure differential (drop or increase) monitoring in external (oil filled) chamber will be required for most applications, consequently the pressure monitoring on external chamber becomes critical
  • Alternative leak monitoring systems are under investigation.
  • external pressure autoclaves (design and seals)
  • The most difficult design will be the external autoclave design that will have to be able to:
  • Apply external pressure at temperatures up to 180 degr C
  • Maintain this pressure throughout the testing including bending
  • provide accurate monitoring of pressure changes indicating leakage.
  • Crucial design will be the seal.

## 4. Conclusions

In the integrated design and system design of a complex test equipment technology oilfield tubular material, SC HYDRAMOLD SRL Iasi has developed two devices, respectively: 68 000 Nm unscrewed screwed machine shown in Figure 2 and installation of tensile 400 tf shown in Figure 3.

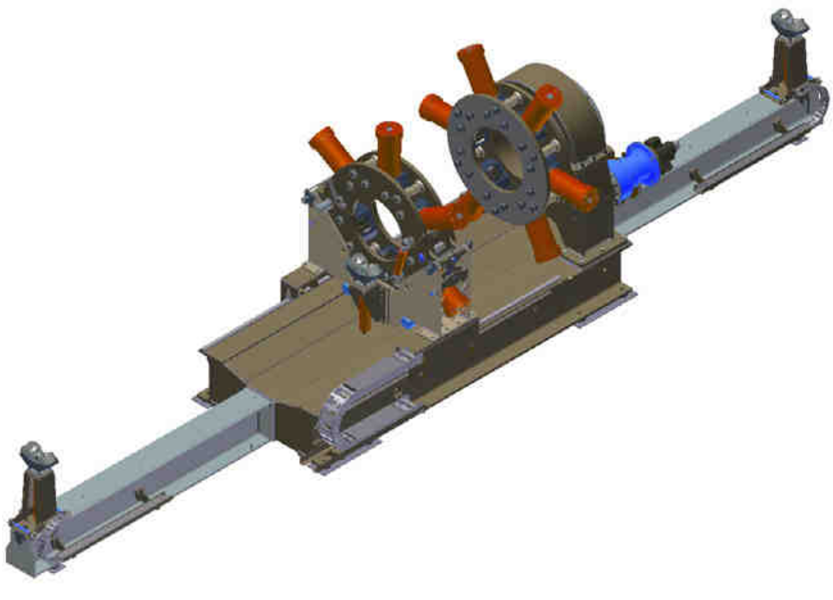

Figure 2 Unscrewed screwed machine 68 000 Nm

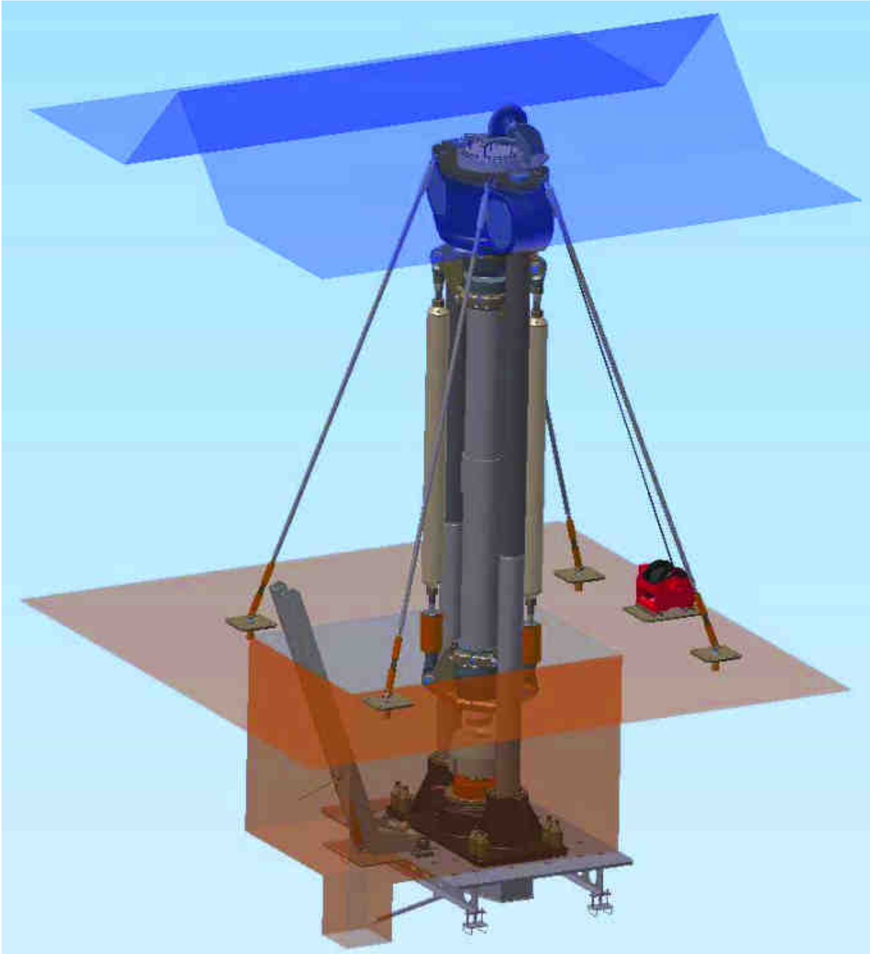

Figure 3. Installation of tensile 400 tf

## REFERENCES

[1] ISO 13679; 2002 Procedures for testing casing and tubing connections
[2] ISO FDIS 13679; 2011 Procedures for testing casing and tubing connections

**ISSN 1454 - 8003**
**Proceedings of 2011 International Salon of Hydraulics and Pneumatics - HERVEX**
*9 – 11 November, Calimanesti-Caciulata, Romania*

# STUDY ON DEFORMATION OCCURRING IN THE PROCESS OF HYDROFORMING

**Constantin CHIRIȚĂ [1], Bogdan VĂCEANU[1], Gheorghe NAGÂȚ [1], Andrei GRAMA [1]**

[1] "Gheorghe Asachi" Technical University of Iaşi, Faculty of Machine Manufacturing and Industrial Management, Department of Machine Tools, Hydraulic and Pneumatic Systems Engineering Department

***Abstract:*** *Need for the study of deformation of metallic materials in the process of hydroforming is necessary to know and to optimize constructive and functional elements that are made hydroforming system. In this paper we present the effects of plastic deformation occurring in the process of hydroforming type of metallic materials copper, aluminum, steel – for process wrinkle. Tests were performed on the integrated system developed by SC HYDRAMOLD SRL.*
***Keywords****: hydroforming, plastic deformation, wrinkled.*

## 1. Introduction

Hydroforming covers the process of forming defined as deep drawing and hydrostatic deformation of free-volume parts such as inner tubes. As a result, the process can be printed semi hydroforming plate type complex shapes that cannot be made generally by mechanical drawing or, if this is possible, the costs are unusually high.

Hydroforming is an unconventional method of obtaining parts formed by the direct or indirect (through a membrane) of a semi-fluid type on the board or pipe.

Machinery, equipment and technologies by forming an alternative hydroforming a growing interest in modern industry, the rapid changes in product conditions of construction vehicles, aircraft, consumer goods, but also in making parts that execution by other technologies would be difficult.

## 2. Tube Hydroforming Process

In FE modeling of any metal forming processes, a good understanding of the FEA code is as important as an understanding of the process itself. Typically, A THF process requires two motivational forces, i.e. axial force exerting on the tube ends and internal pressure acting normally to the tube inner surface. These two forces should be applied appropriately on the tube if a sound part is to be produced. In terms of process design, FEA is used to verify and refine loading paths. This section first gives an overview of the Y-shape hydroforming process. Then, FE modeling of the Y-shape hydroforming is discussed. PAM-STAMP is used throughout this work. There are some considerations in using any dynamic codes to simulate THF processes. These considerations are also discussed at the end of this section.

Y-shapes are (see Figure 1) commonly used as fitting parts in automotive exhaust manifolds. The parts are usually made of stainless steels A 304, which is rust resistant. Typically, in hydroforming of these Y-shapes, a counter punch is usually used to support the protrusion tip while it is growing. By this way, premature protrusion bursting is delayed and thus increasing the useful height of the protrusion. However, the use of a counter punch adds one more process parameter to be controlled properly with the axial feeds and internal pressure. The Y-shape studied in this work has a protrusion that is angled to the tube axis by 60 degrees. The detailed dimensions of the part are given in Figure 1. The load paths and tube material properties of this part will be discussed shortly in the next section.

In figure 2 shows pictures of Y-shape hydroforming procedure. These pictures are taken from Y-shape hydroforming experiments that are to be discussed later in this chapter. General specifications of the SPS hydroforming press used. Please note that in these forming

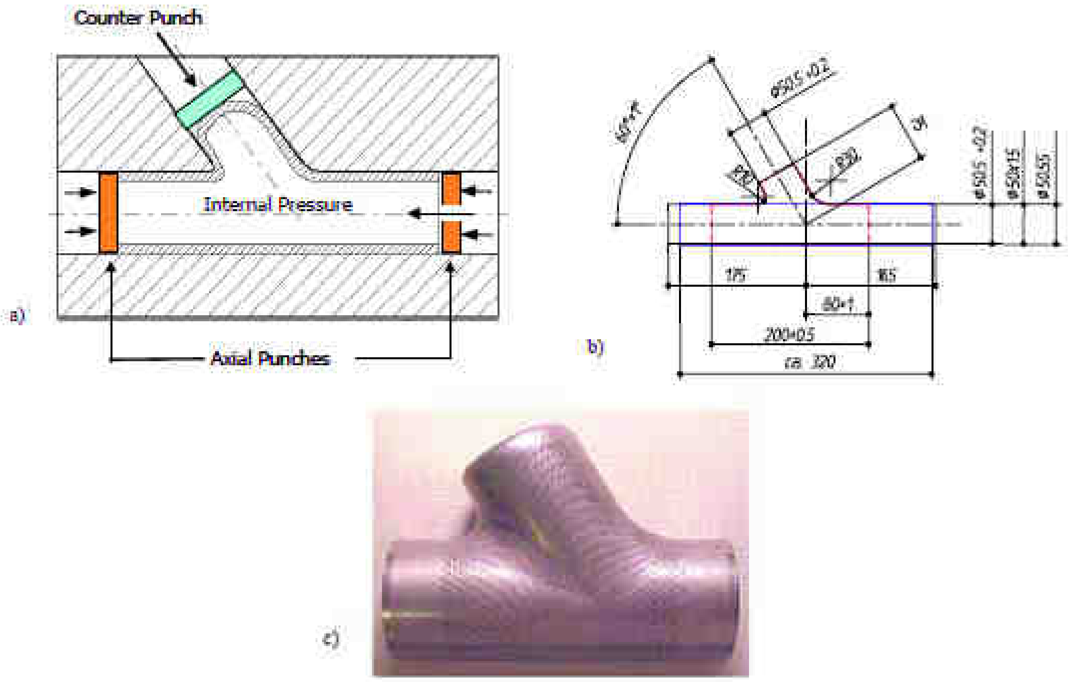


Figure 1: a) Schematic of hydroforming tooling of a Y-shape, b) dimensions of the Y-shape and c) a stainless steel (OL52) Y-shape hydroformed at SPS (Siempelkamp Pressen Systeme)

experiments, from which the photos are taken, the counter punch was not used. The process descriptions are given below.

1. Upper and lower die inserts were installed onto the press. The axial punches were connected to the pressure intensifiers with high-pressure hoses. Figure 2.a shows the lower die insert.
2. A rough drawing of the axial punch is shown in Figure 2.b. The punch has a conical shape at the tube-punch contact area. In this case, the tube blank has OD =50 mm, and to = 1.5 mm. For good sealing performance, the punches were designed to have 5 mm of sealing distance.
3. The tubes were spray-lubed with a solid film lubricant. The tubes were allowed to air-dry for about 2-3 hours.
4. Figure 2.b shows how a tube blank was placed and positioned in the lower die cavity. The axial punches were fully retracted to their home positions, while the counter punch axis was not in operation and rested at its home position.
5. Figure 2.c shows a completely formed Y-shape. It is shown that the length of the final part has been shortened due to the axial feeds. Axial feed was 40 mm and 80 mm on the left and right side, respectively. The maximum internal pressure was 600 bars. The protrusion height, Hp, was measured and considered as .formability index. in this study.

## 1. Process Parameter Adjustment Algorithms

This section mainly focuses on how the adaptive simulation program adjusts the pressure curve and axial feed curve using the wrinkle and fracture indicators developed in the previous section. The example application of the simple bulging continues here from the last section. A few important process parameter adjustment schemes are discussed. The details of each process adjustment schemes are given in the Appendix E to keep the chapter concise.

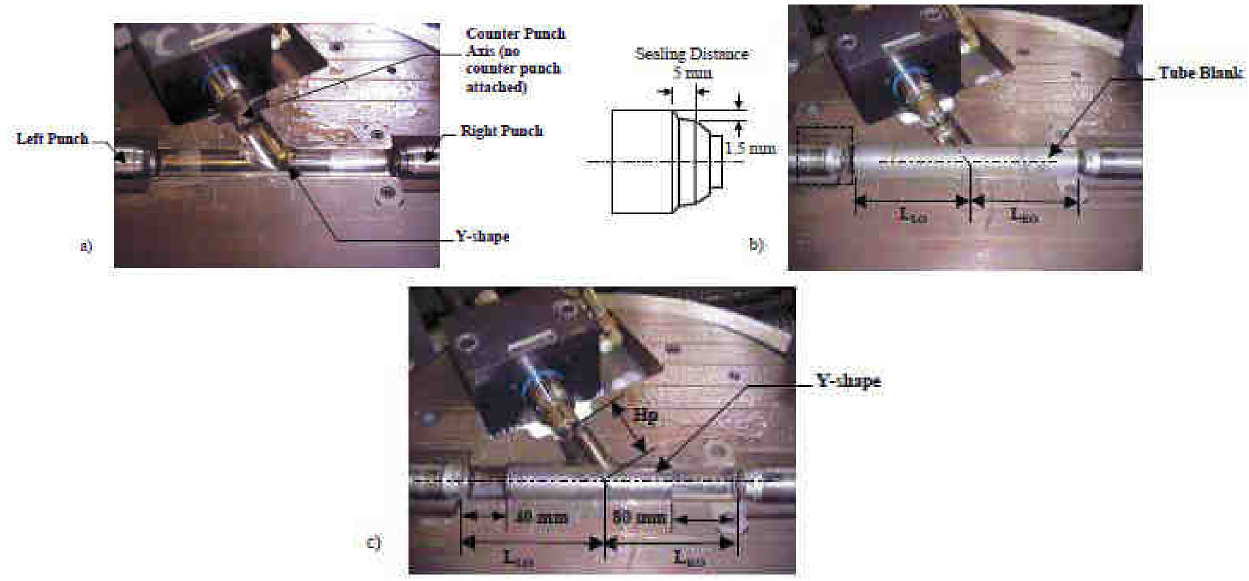


Figure 2: Y-shape hydroforming process procedure

The adaptive simulation program adjusts the pressure and axial feed curves at every control time steps (Tj) based on the part formability known at current simulation time step (ti). Figure 3 and Figure 4 show the part qualities and the adjusted process parameters, respectively, from an adaptive simulation run of the simple bulging. These curves will now be referred to repeatedly to explain how process adjustments are carried out in the AS program.

The part qualities considered in the current program are part wrinkles, part thinning, and part volume. Figure 3.a and Figure 3.b show the progress curves of the first two part qualities starting from the beginning to the end of the forming process. These curves are plotted against the normalized part volume, as it is a convenient way to indicate progress of the hydroforming process (V = 1 implies that the part is completely formed). However, the pressure and axial feed curves must still be applied into FE simulation in the time domain, see Figure 4. In this specific example of a simple bulge, the part volume progresses through the simulation time as shown in Figure 3.c.

## 2. Calibration Stage

In order to properly adjust the process parameters in any THF processes, it is important to first identify the two main forming stages: a) hydroforming and b) calibration. This can be done by using the normalized part volume versus time curve, Figure 3.c, to determine an appropriate time the start the calibration stage. Typically, the calibration stage should begin when the part is almost fully formed against the die cavity surfaces. This is to ensure that there is no large surface expansions of the part during the calibration, which will result in excessive part thinning or fracture.

In this example, the part volume of 90 % is chosen to be the calibration part volume cut-off, see Figure 3.c. From Figure 4, it can be seen that starting from the time when V = 0.9 the pressure is ramped up while the axial feed is stopped (axial feed velocity is zero) until the process ends where the part is completely formed, V = 1.

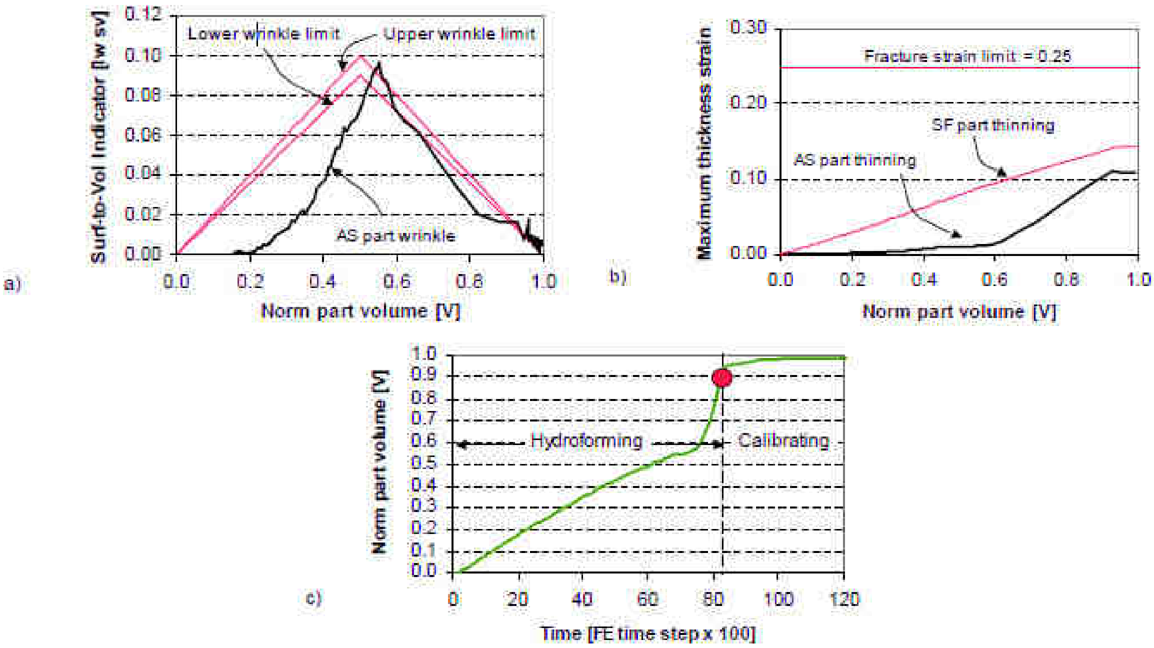


Figure 3: Part quality plots: a) surface area-to-volume wrinkle indicator versus normalized volume curves, b) fracture indicator versus normalized volume curves, and c) normalized volume versus simulation time step curve

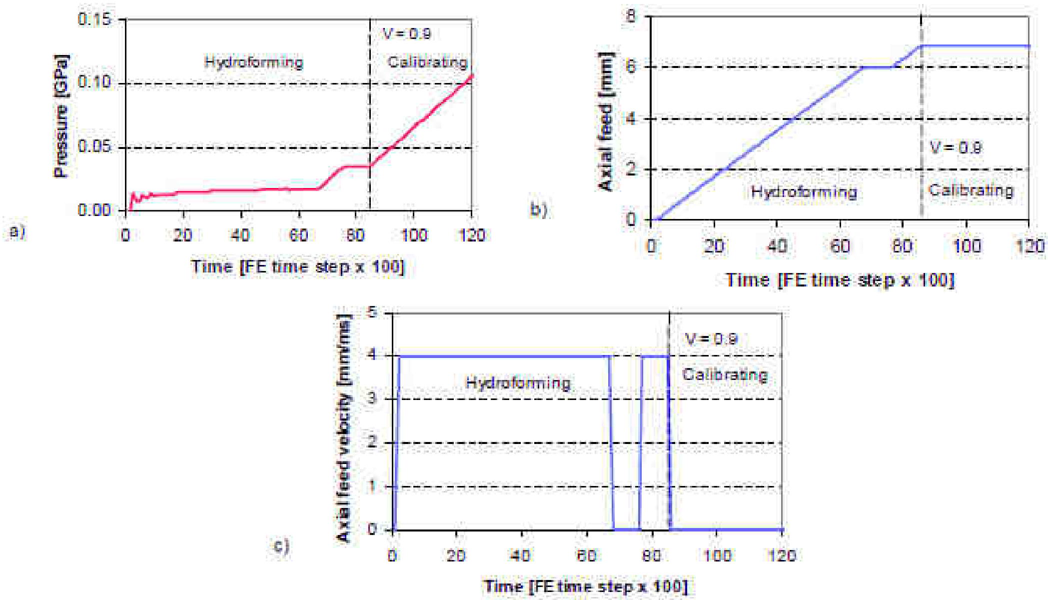


Figure 4: Adjustments of process parameters: a) internal pressure, b) axial feed displacement, and c) axial feed punch velocity versus time curves

## 3. Hydroforming Stage

During the period where the part forms with $0 < V < 0.9$, the process parameters should be applied such that the tube material be fed in as much as possible to prevent fracture without causing any part wrinkles. This has been the main concept in implementation of this adaptive simulation approach, as discussed earlier. From the general flow chart of AS procedure. Fortunately, applying maximized axial feed following the concept, stated above, should also result in minimized part thinning. Therefore, the part wrinkle is used as the main control state variable in this work.

Figure 3.a shows the winkle control trajectories (upper and lower limits) and an example of a wrinkle state plot of the simple bulging. These wrinkle control trajectories are derived from the optimum forming of the same part. The main goal here is to develop process control strategies that would form the part with the wrinkle state tracking closely along these wrinkle control limit trajectories. The physical meaning of tracking this triangle wrinkle trajectory is to adjust both pressure and axial feed at the control time step such that the part has some beneficial alive wrinkle during the forming and has none at the end of the process. On the other hand, if the wrinkle trajectory is flat, the tracking of this trajectory will result in a part that has no wrinkles at all time during the forming, i.e. part formed by pure expansion or self-feeding part of course, in practice these wrinkle control trajectories are not known a priory.

Experience gained from using this adaptive simulation on several different parts may be useful to approximate proper trajectories for resembling part geometries. Nevertheless, the shape of the trajectories should such that it allows some wrinkles during the forming process and allows no wrinkles at the process end, e.g. the triangle shape. The amount of the alive winkles allowed depends on the part formability. Some level of trial-and-error is, unfortunately, necessary here.

## 4. Wrinkle Control Strategy

The first process parameter adjustment scheme was first based only on the wrinkle control strategy, where the pressure is increased while the axial feed is stopped when the part wrinkle state exceeds the upper limit trajectory and the pressure is kept constant while the axial feed is increased when the part wrinkle state goes below the lower limit trajectory. This strategy results in the loading paths that are of a step-liked shape, see Figure 5.

It was found that this strategy could not handle the tracking of part winkle state during the first half of the process ($0 < V < 0.5$), where the trajectory demands the part to have increasing (or more severe) amount of wrinkles. The part always fractured due to the increased pressure during this period. This does not necessarily mean that the tracking of wrinkle state in the first half of the process is impossible. A better and more sophisticated control strategy is needed to achieve this task. As an alternative solution, the pure shear control strategy, discussed next, was developed to handle the process adjustment during the early forming stage, see Figure 5. The wrinkle control strategy was found to work better in the later forming stage, especially ($0.5 < V < 1$), when the wrinkle limit trajectory tapers down to zero, see Figure 3.a.

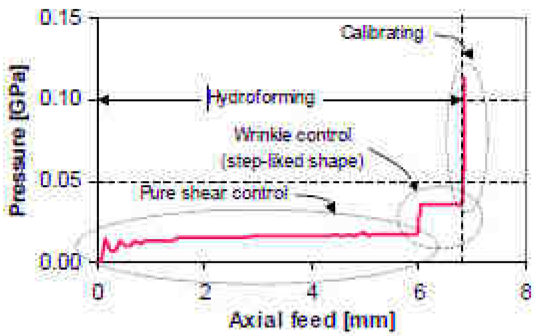


Figure 5: Loading path predicted by AS showing different stages of simple bulge hydroforming process and control strategies (from Figure 3 a and b)

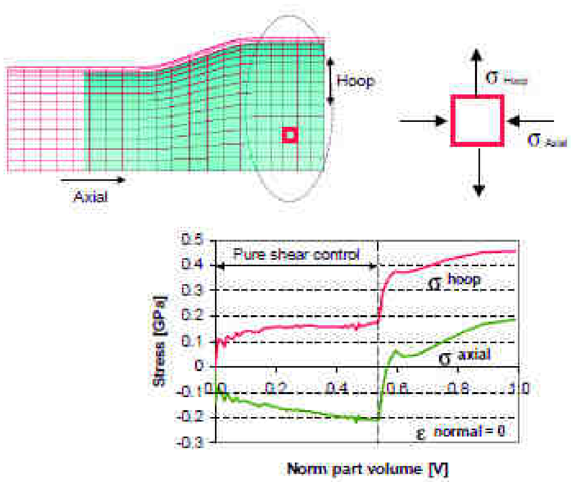


Figure 6: Plot of hoop and axial stresses showing pure shear control strategy

## 5. Pure Shear Control Strategy

It is well known, based on mechanics of sheet metal forming, that the pure shear state of stress will deform the sheet metal without changing the sheet thickness. This strategy attempts to regulate the pressure and axial feed such that the critical part area, see Figure 6, deforms with an in-plane pure shear state of stress at all time.

Theoretically, when applying this pure shear control strategy, the tubular part should form with that critical part area having the same thickness throughout the forming process. However, due to intrinsic sphere-liked shape of most THF parts while being expanded, the tensile biaxial state of stress tends to eventually dominate the critical area of the part. The pure shear state of stress will simply break down and be no longer possible to enforce it later in the process, when the tube has become sphere-liked. Therefore, this pure shear control strategy is only applied in the beginning of the process.

In this example, the pure shear control is active till the part wrinkle state exceeds the upper wrinkle limit, after which the wrinkle control strategy becomes active instead; see Figure 3.a and Figure 5. It should be pointed out, from Figure 3. a and b, that during period where the part volume is $0 < V < 0.6$, where the pure shear control is active, the part maximum thinning is kept quite small. This is the direct result of the pure shear control that tries to keep σ hoop = -σ axial, see Figure 5.

## 6. Modified Wrinkle Control Strategy

The wrinkle control strategy that gives a step-liked loading path, previously discussed, actually does not track the wrinkle control trajectory so well, see Figure 3.a. The part wrinkle state actually goes under the lower wrinkle limit trajectory (starting around V =0.7) until almost at the end of the process. This is because of the use of constant pressure while increasing axial scheme in and attempt to maximize the axial feed. This constant pressure level induces increased tensile hoop stresses the instance when the part grows larger in diameter that is caused by the pushing of the axial feed. This hidden shortcoming of the step-liked process adjustment strategy actually thins out the part unnecessarily.

The modified wrinkle control strategy, so called increased-decreased pressure process adjustment strategy, is developed to better track the wrinkle control limit trajectories. Figure 7 shows the part wrinkle state plot and the loading path of the same simple bulging process predicted by the same pure shear control strategy and the modified wrinkle control strategy. The comparison of maximum thinning curves of the parts, Figure 8, clearly shows that the modified control strategy reduces the maximum thinning consistently during 0.7 < V < 1.0. The only difference of the increased-decreased pressure control strategy from the step-liked control strategy is that the pressure is decreased while the axial feed is increased when the part wrinkle state goes below the lower wrinkle limit trajectory.

One may question the practicality of the rather zigzag loading path predicted. Figure 9 shows the smoothened loading path, which closely approximates the predicted one. From FE simulation results, this smoothened loading path forms this simple bulge successfully with the part maximum thinning of 8%.

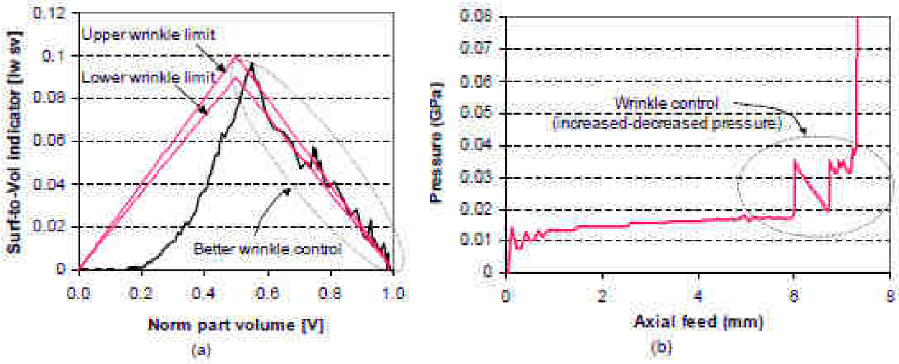


Figure 7: Adaptive simulation results using modified wrinkle control strategy: a) plot of part wrinkle state, and b) predicted loading path for the simple bulge

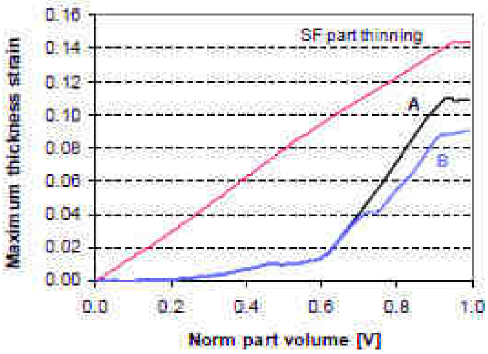


Figure 8: Comparison of maximum thinning evolutions of parts from all the adaptive simulation cases including the initial SF simulation: A – wrinkle control strategy and B - modified wrinkle control strategy

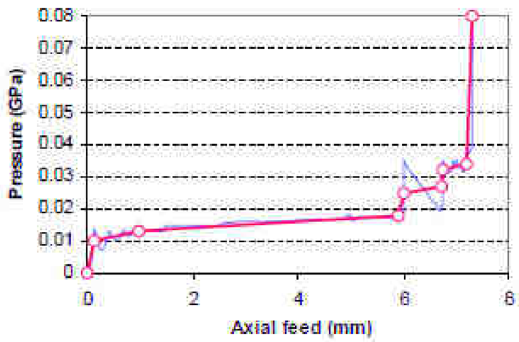


Figure 9: Smoothened loading path approximating the loading path predicted using the modified wrinkle control strategy for the simple bulging

## 7. Conclusions

This research work was intended to develop methodologies for design of part geometries and process parameters in tube hydroforming processes. The specific goals of this study were to develop a) part design guidelines for THF processes that facilitate engineers to bring conceptual THF part designs to production more efficiently and b) methodologies for design and optimize loading paths in THF using process FE simulation.

It was realized during this study that THF part geometries could vary so much from very simple to very complex. Thus, generating new THF part design guidelines (besides the guidelines already available in literature) seemed to be a very backbreaking task and may not be as useful. It was then realized that part geometry and process parameters were very much interrelated (i.e. design for manufacturing). Thus, the main goal was to focus only on developing systematic and time-efficient FE approaches to determine proper process parameters (i.e. loading paths). This could be used to evaluate THF part design for manufacturability, thus, in turn, fulfilling the part design guideline objective as well.

Through extensive applications of process FE simulation and some experimental work necessary, several design guidelines and advanced FE approaches for THF process designs have been developed. In this work, the main process FE simulation package used was PAM-STAMP. Simple bulge part geometry was used throughout this work in developing all the guidelines and methodologies. Also, many real THF parts (e.g. Tshape, Y-shape, Cross member, and sizable structural parts) taken from the automotive industry were used in the study.

## REFERENCES

[1] Rosa Di Lorenzo, Giuseppe Ingarao, Francisco Chinesta, Integration of gradient based and response surface methods to develop a cascade optimisation strategy for Y-shaped tube hydroforming process design, *Advances in Engineering Software*, *Volume 41, Issue 2*, *February 2010*, *336-348*

[2] Giuseppe Ingarao, Rosa Di Lorenzo, Fabrizio Micari, Internal pressure and counterpunch action design in Y-shaped tube hydroforming processes: A multi-objective optimisation approach, *Computers & Structures*, *Volume 87, Issues 9-10*, *May 2009*, *591-602*

[3] K. Saanouni , N.Belamri , P.Autesserre , Finite element simulation of 3D sheet metal guillotining using advanced fully coupled elastoplastic-damage constitutive equations, *Finite Elements in Analysis and Design*, *Volume 46, Issue 7*, *July 2010*, *535-550*

[4] M. Kadkhodayan∗, F. Moayyedian, Analytical elastic–plastic study on flange wrinkling in deep drawing process, *Scientia Iranica*, *Volume 18, Issue 2*, *April 2011*, *250-260*

**ISSN 1454 - 8003**
**Proceedings of 2011 International Salon of Hydraulics and Pneumatics - HERVEX**
*9 – 11 November, Calimanesti-Caciulata, Romania*

# MULTIPLICATOR HIDRAULIC DE PRESIUNE CU DUBLĂ ACTIUNE

**ZORIN BERCEA[1] si LIVIU VAIDA[2]**

[1,2] *Universitatea Tehnică din Cluj Napoca, Facultatea de Mecanică, Departamentul de Inginerie Mecanică, Cluj-Napoca, România*
[1] *e-mail*: Vasile.Bercea@termo.utcluj.ro;
[2] *e-mail*: Liviu.Vaida@termo.utcluj.ro

***Rezumat.*** *Autorii propun un nou model de multiplicator hidraulic de presiune cu dublă actiune (duplex), care permite alimentarea continuuă cu ulei hidraulic a unor receptoare hidraulice cu presiuni de functionare diferite de presiunea la care este livrat uleiul hidraulic de către pompa de ulei existentă, în conditii normale de functionare. Multiplicatorul este proiectat ca o constructie compactă si este alcătuit dintr-un motor hidraulic linear în interiorul căruia se prevede o pompă hidraulică cu piston, ambele functionând în sistem cu dublă actiune (duplex).*

*Avantajele prin care se evidentiază multiplicatorul propus, sunt:*

- *Proiectare novativă extrem de compact; pompa cu piston de ulei de înaltă presiune este înglobată în motorul hidraulic linear, cu o functionare cu dublă actiune (duplex, cu un transfer de putere hidraulică mare);*
- *Functionare automată, continuă, sigură, fără suprapresiuni sau socuri hidraulice, numai în conditiile existentei sarcinii hiraulice corespunzătoare pe circuitul de înaltă presiune. În lipsa acestei sarcini hidraulice, uleiul trece prin pompa de înaltă presiune ca printr-o rezisten ă hidraulică oarecare, fără ca motorul hidraulic să înceapă să functioneze. Presiunea minimă de livrare a uleiului hidraulic de către pompa de inaltă presiune este chiar presiunea de intrare a uleiului în agregat, iar cea maximă teoretică este presiunea de intrare a uleiului în agregat, înmul ită cu factorul de multiplicare a multiplicatorului;*
- *Alimentarea cu ulei a pompei de inaltă presiune se realizează automat din motorul hidraulic;*
- *Schimbarea sensului de functionare a motorului se realizează automat, de către un distribuitor, actionat de către un motor hidraulic liniar auxiliar, comandat de un sensor de diferentă de presiune prevăzut în corpul distribuitorului, pe baza diferentei presiunilor uleiului în diferitele incinte ale motorului si camera principală din distribuitor;*

***Cuvinte cheie:*** *Multiplicator hidraulic de presiune, motor hidraulic liniar, pompă hidraulică cu piston, distribuitor hidraulic de ulei cu actionare hidraulică.*

## 1. Introducere

Multiplicatorul de presiune cu dublă actiune (duplex) propus este alcătuit dintr-un motor hidraulic liniar în interiorul căruia este prevăzută o pompă hidraulică cu piston. Atât motorul hidraulic cât si pompa de înaltă presiune functionează cu acelasi tip de ulei hidraulic, iar prin proiectare, alimentarea cu ulei hidraulic a circuitului de înaltă presiune se realizează direct din camerele de lucru ale motorului hidraulic, iar acesta nu poate functiona fără existenta sarcinii hidraulice necesare pe circuitul de înaltă presiune, ceea ce permite presurizarea treptată, fără socuri hidraulice a acestuia. În caz de depresurizare bruscă a acestui circuit prin avarierea unor conducte sau elemente din circuit, motorul hidraulic nu mai poate functiona, iar uleiul hidraulic trece prin multiplicator ca prin orice rezistentă hidraulică.

## 2. Alcătuirea multiplicatorului hidraulic cu dublă actiune

În Figura 1 este prezentată o sectiune longitudinal prin multiplicatorul de presiune propus de autoris se prezintă cele mai importante subansamburi si repere din care este alcătuit:

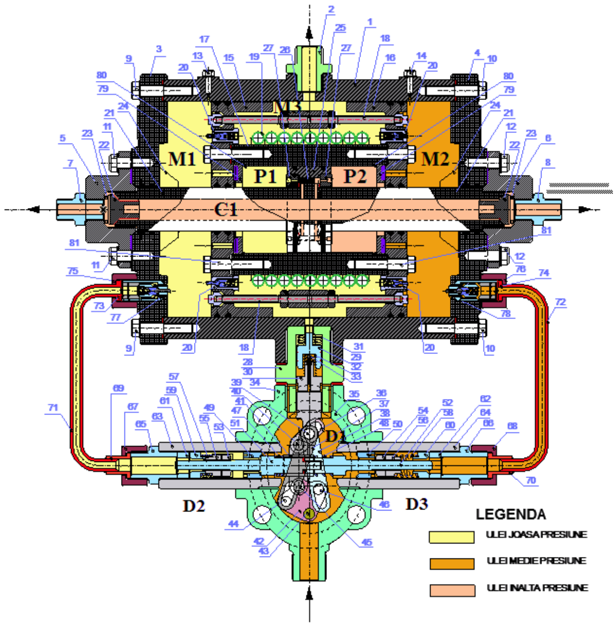


**Figura 1. Sectiune prin multiplicatorul de presiune cu dublă actiune propus.**

**Legenda:**
01 : Cilindrul motorului hidraulic; are diam.int.D1 [mm];
02 : Niplul racord de evacuare a uleiului hidraulic;
03 : Piesă de capăt 1 a motorului hidraulic;
04 : Piesă de capăt 2 a motorului hidraulic;
05, 06 : Capacele supapelor de sens ale pompei de înaltă presiune;
07, 08 : Nipluri racord de refulare a uleiului hidraulic la înaltă presiune;
09, 10, 11, 12, 81 : suruburi de îmbinare (tip pentru etan  are);
13, 14 : suruburi de dezaerare a incintelor 1 si 2 ale motorului hidraulic;
15,16 : Pistoanele 1 si 2 ale motorului hidraulic (sunt  i capace ale pompei de înaltă presiune);
17 : Cilindrul pompei hidraulice de înaltă presiune, are diametrul interior D2 [mm];
18 : Supape duble pentru motorul hidraulic; permite trecerea uleiului alternativ din incintele 1 sau 2 în incinta 3 de evacuare;
19 : Camere de comprimare din cauciuc, presurizate ini  ial cu azot;
20 : Ventile de descărcare a presiunii si de blocare;
21 : Coloana principală suport a pistonului pompei de înaltă presiune, care este fixă;
22 : Supape de sens de înaltă presiune;
23 : Arcurile disc ale supapelor de sens 22;
24 : Arcuri disc de fortă;
25 : Pistonul pompei cu dublă ac  iune de înaltă presiune;
26 : Supapă principală de comutare pentru cele două incinte ale pompei de înaltă presiune;
27 : Piuli  e care fixează pistonul pompei duplex de inaltă presiune, 25;
28 : Corpul pistonasului si a senzorului de diferen  ă de presiune dintre M3 si D1;
29 : Senzor de diferentă de presiune dintre D1  i M3;
30 : Pistonul motorului hidraulic liniar auxiliar, ac  ionează prin ambielaj supapele de alimentare cu ulei a motorului hidraulic principal si permite schimbarea sensului de deplasare a motorului hidraulic;

31 : Arcul dublu spiral al senzorului de presiune 29;
32 : Arcul spiral al pistonului 30;
33 : Supapa de descărcare pentru pistonaul 30 (permite coborârea acestuia imediat si bascularea supapelor, dupa ce este actionat de presiunea uleiului din corpul 35);
34 : Corpul principal al distribuitorului (camera mecanismelor de actionare si de comutare a distribuitorului);
35 : Capacele corpului principal al distribuitorului;
36 : Biela de împingere si de blocare a man  onului alunecător 41, de către pistonaul 30;
37,38 : Biele de tragere a platourilor de basculare 42 de catre pistonul 30;
39, 40, 44, 45, 46 : Bolturi mobile de legătura ambielaj;
41 : Manson alunecător; permite actionarea si blocarea supapelor duplex;
42 : Platouri de basculare a mansonului alunecător 41 si a supapelor 51 si 52;
43 : Bolt fix pentru realizarea basculării platourilor 42;
47, 48 : Arcuri pentru pozitia de echilibru a man  onului alunecător 41;
49, 50 : Scaunele supapelor principale 51 si 52 ale distribuitorului;
51, 52 : Supapele principale care prin construc  ie func  ionează interconectate, în sistem duplex;
53, 54, 61, 62 : Ghidaje ale supapelor principale 51 si 52;
55, 56, 59, 60 : Suporturile arcurilor de echilibru ale supapelor 51 si 52; permite reglarea tensiunilor în arcuri;
57, 58 : Arcurile supapelor principale 51 si 52;
63, 64 : Camerele supapelor principale 51 si 52;
65, 66 : Nipluri de legatură dintre camerele supapelor 63 si 64 si conductele de alimentare cu ulei ale motorului hidraulic;
67, 68, 69, 70, 71, 72, 73, 74, 75, 76 : Elemente de legătură si conducte de alimentare cu ulei ale motorului hidraulic;
77, 78 : Ventile de sens cu descărcare prin ac  ionare directă pentru alimentarea cu ulei a motorului hidraulic principal;
79 : Supape pentru alimentarea cu ulei din incintele 1 si 2 ale motorului hidraulic, ale incintelor 1 si 2 ale pompei de înaltă presiune;
80 : Arcurile disc ale supapelor 79;

Multiplicatorul prezentat în Figura1, este alcătuit din următoarele blocuri functionale:

- motorul hidraulic liniar, cu dublă actiune (duplex) cu două incinte active, M1 sI M2 si o cameră de colectare a uleiului utilizat si acumulator hidraulic , M3 este alcătuit din următoarele repere:
  - corpul motorului si cilindrul cu dublă ac  iune: reperele 1, 3, 4, îmbinate cu suruburile 9, 10;
  - grupul de pistoane 15, 16, fixate de cilindrul 17, cu  uruburile 81;

  Din figura 1, se observă că reperele 1, 3, 15 si 21, mărginesc incinta M1, iar reperele 1, 4, 16 si 21, mărginesc incinta M2. Parametri principali ai incintelor M1 si M2 de formă toroidală, sunt:
    - diametrul exterior al incintelor  M1 si M2, este $d_1$;
    - diametrul interior al incintelor , este $d_3$;
    - înăltimea cilindrilor (generatoarea cilindrilor determinati de deplasarea pistoanelor) este distanta fizică între pozitiile aceluiasi punct de pe fata unui piston, la cele două capete de cursă, $h_{m1}$. De precizat că nu toată această distantă parcursă este activă, la presiune nominală de functionare, pe o portiune producându-se frânarea si oprirea grupului de pistoane si inversarea sensului de deplasare a acestora; denumim deplasarea activă cu $h_{ma}$;
  - camera de colectare a uleiului utilizat M3 este mărginită de reperele 1, 15,16  i 17. De observat că această cameră este si cameră de frânare si acumulator hidraulic, în ea fiind prevăzute camerele de comprimare 19, din cauciuc, presurizate ini  ial cu azot;

  Alimentarea cu ulei hidraulic se realizează din distribuitorul hidraulic automat, prin supapele de sens cu descărcare 77  i 78, iar evacuarea uleiului se realizează prin orificiul de evacuare  i racordul 2, care sunt obturate la capăt de cursă de către pistoanele 15 sau 16, permi  ând echilibrarea presiunilor în camerele motorului si o mai u oară comutare a supapelor distribuitorului de ulei ( ca să nu lucreze sub sarcină).

- pompă hidraulică cu piston de înaltă presiune, cu dublă actiune, înglobată în motorul hiraulic mai sus descris, are în compunere două incinte active P1 si P2, colectorul central C1 i este alcătuită din:
  - corpul si cilindrul pompei: reperele 17, 15, 16, îmbinate cu suruburile 81;
  - pistonul pompei: reperele 21, 25, îmbinate cu reperele 27.

  La acest model de multiplicator, corpul si cilindrul pompei este mobil, iar pistonul pompei, este fix.

  Din Figura 1, se observă că reperele 17, 15, 21, 25 si 27, mărginesc incinta P1, iar reperele 17, 16, 21, 25 si 27 mărginesc incinta P2. Parametri relevanti ai incintelor P1 si P2, de formă toroidală, sunt:
    - diametrul exterior al incintelor P1 si P2, este $d_2$;
    - diametrul interior al incintelor , este $d_3$;
    - inăl imea cilindrilor (generatoarea cilindrilor determina i de deplasarea pistoanelor) este distan a fizică între pozitiile aceluiasi punct de pe fa a unui piston, la capete de cursă, $h_{p1}$. De precizat că nu toată această distan ă parcursă este activă, la presiune nominală de functionare, pe o por iune producându-se frânarea si oprirea grupului de pistoane si inversarea sensului de deplasare a acestora; denumim deplasarea activă cu $h_{pa}$. Trebuie să observăm că grupul pistoanelor motorului înglobează corpului pompei, prin urmare evident, se deplasează împreună, deci $h_{m1} = h_{p1}$. Este interesant de comparat $h_{ma}$ si $h_{pa}$, ambele fiind deplasari active. Eventualele diferen e exprimă diferen ele temporale dintre intervalele de timp în care motorul hidraulic produce energie mecanică i cel în care aceasta se consumă de către pompă, ceea ce presupune înmagazinarea energiei sub formă de energie poten ială, respectiv cedarea acestei energii poten iale de către acumulatorul hidraulic prevăzut.

  Alimentarea cu ulei a pompei de înaltă presiune se realizează din incintele M1 sau M2 ale motorului, care nu sunt în acea secven ă sub presiunea normală de lucru, prin supapele 79, ac ionate de arcurile disc 80. Evacuarea uleiului se realizează prin supapa alcătuită din reperele 26 si 27, pistonul 25, în colectorul central C1 – reperul 21, din care uleiul este refulat în circuitul de înaltă presiune prin supapele 22, actionate de arcurile disc 23 si racordurile 7 i 8.
- distribuitorul de ulei pentru motorul hidraulic, care permite i schimbarea sensului de deplasare a grupului de pistoane, are în compunere următoarele subansamble:
  - un motor hidrulic auxiliar cu simplă ac iune (reperele 28, 30), comandat de senzorul de presiune 29 si reperele 31, 32, 33. Sub actiunea diferen elor de presiune a uleiului dintre camera centrală a distribuitorului D1 si incinta de evacuare a uleiului din motorul hidraulic M3, motorul hidraulic auxiliar, comandat de senzorul de presiune 29, actionează supapele de alimentare ale motorului prin ambielajul din camera mecanismelor D1;
  - camera centrală de distribu ie, care este si camera mecanismelor D1, alcătuite din reperele: 34,35, 36, 37, 38, 39, 40, 41, 42, 43, 44, 45, 46, 47 si 48.
  - camerele supapelor D2 si D3 sunt reperele 63 si 64 si contin reperele: 51, 52, 49, 50, 53, 54, 55, 56, 57, 58, 59, 60, 61, 62. Supapele 51+52 ac ionează simultan si comandă deplasarea grupului piston al motorului într-un sens sau în sens opus;
- conducte i elemente de legătură între blocul distribuitorului (camerele supapelor D2 si D3) si supapele de sens si descărcare (pentru alimentarea cu ulei a motorului) 77 si 78 sunt alcătuite din reperele: 65, 66, 67, 68, 69, 70, 71, 72, 73, 74, 75, 76.

## 3. Func ionarea multiplicatorului hidraulic cu dublă ac iune

ISSN 1454 - 8003
Proceedings of 2011 International Salon of Hydraulics and Pneumatics - HERVEX
9 – 11 November, Calimanesti-Caciulata, Romania

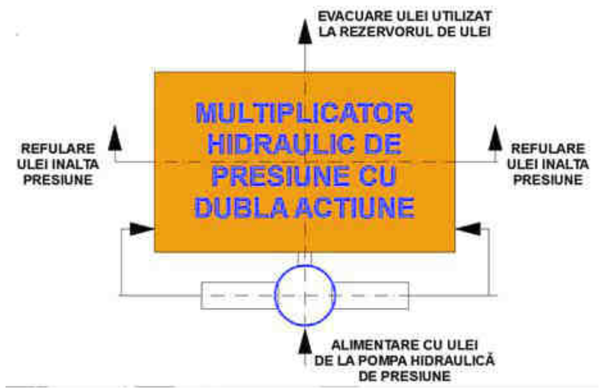


**Figura 2. Schema bloc a multiplicatorului hidraulic de presiune cu dublă actiune**

Punerea în func iune a multiplicatorul hidraulic propus, se realizează în două etapei:

- umplerea cu ulei a instalatiei, la o presiune inferioară celei de func ionare normală. De subliniat că umplerea cu ulei a circuitului de înaltă presiune se realizează direct din multiplicator;
- func ionarea normală a multiplicatorului de presiune, cu alimentarea cu ulei de la o pompă de ulei de medie presiune si livrarea uleiului de inaltă presiune pe o sarcină hidraulică corespunzătoare. În situatia în care rezisten a hidraulică de pe circuitul de înaltă presiune este prea mică si nu permite cre terea presiunii, functionarea este defectuoasă sau imposibilă. Până la presurizarea circuitului la o presiune apropiată de presiunea de alimentare cu ulei a multiplicatorului, multiplicatorul functionează ca o rezisten ă hidraulică, uleiul trecând pur si simplu prin el; după egalarea presiunilor de pe circuitul de înaltă presiune cu cea de alimentare, livrează ulei la o presiune cu o valoare depinzând de rezistenta hidraulică de sarcină a receptorului de înaltă presiune, până la presiunea maximă posibil de livrat, care este presiunea de alimentare cu ulei a utilajului, înmultită cu factorul de multiplicare, care pentru acest model este 8.

3.1. Umplerea cu ulei a instalatiei

A a cum s-a arătat mai sus, procesul are loc la o presiune redusă, pentru a permite aerului să iasă i a realiza o umplerea cât mai completă a instalatiei. Evacuarea aerului (dezaerarea) se realizează prin racordurile de evacuare a uleiului si cele două suruburi de dezaerare prevăzute la partea superioară a corpului motorului hidraulic, cîte unul pentru fiecare incintă. Aerul nu poate fi evacuat complet imediat, asa că e bine ca procesul să se repete după câteva curse efectuate de grupul de pistoane al motorului (care este si cilindrul pompei de inaltă presiune).

Este indicat ca umplerea circuitului exterior de înaltă presiune să se realizeze odată cu procesul de umplere a multiplicatorului, aerul continut de conductele si armăturile, dar si de receptorul hidraulic de înaltă presiune, fiind evacut prin sistemele de dezaerare prevăzute în puncte cu o cotă geodezică superioară zonei învecinate prevăzute în acest scop. Se va avea grijă ca si pompa de ulei si conductele care alimentează cu ulei multiplicatorul să fie umplute cu ulei fără incluziuni de aer.

3.2. Functionarea multiplicatorului de presiune

Rolul multiplicatorului de presiune este acela de a livra ulei hidraulic la o presiune superioară aceleia livrate de pompa de ulei hidraulic care alimentează sistemul i limitată superior ca valoare la presiunea de alimentare a multiplicatorului înmul ită cu factorul de multiplicare ( care pentru modelul prezentat în Figura 1 este 8), valoarea sa depinzând de sarcina din acest circuit.

După umplerea multiplicatorului cu ulei hidraulic, conectarea sarcinii hidraulice de pe racordul de înaltă presiune i a racordului de refulare la tancul de colectare, verificarea armăturilor i a aparatelor de măsură  i control, se trece la punerea în func iune a multiplicatorului de presiune. Pozi ia supapelor principale din distribuitorul D este aleatoare, cea rezultată după umplerea sistemului cu ulei, iar a pistonului dublu a motorului principal (15+16+17) este undeva între arcurile disc 24 (de subliniat că această pozi ie nu poate fi la capete de cursă unde actionează unul din arcurile disc de fortă 24, pentru că acesta ar impinge pistonul pînă la completa detensionare a arcului). În cele ce urmează vom considera ca moment initial pozitia pistonului si a supapelor principale din distribuitorul dublu D, din Figura 3.

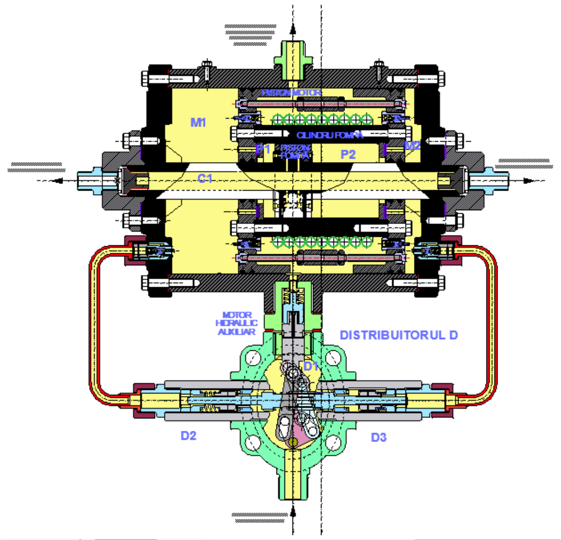


**Figura 3. Pozitia elementelor multiplicatorului înainte de punerea în functiune.**

**Functionarea motorului.** Prin racordul de alimentare a utilajului se alimentează utilajul cu ulei la presiunea nominală de func ionare si motorul auxiliar 29 si piesa 30 intră în functiune si se deplasează spre incinta M3, pozitie în care rămâne piesa 30. Presiunile de pe cele două fete ale pistonului 29 se egalează prin canalele prevăzute în 28 si prin supapa 33, si 29 este împins spre D1 de către arcul 31, producînd bascularea supapelor principale din distribuitorul dublu D prin ambielajul din camera D1, ceea ce face ca distribuitorul D3 să permit accesul uleiului spre M2, iar D2 închide accesul uleiului spre M1. Începe alimentarea cu ulei a motorului principal si multiplicatorul intră în functiune normal. Pistonul dublu al motorului (15+16+17) se deplasează spre stânga, incinta M1 se micsorează ca volum, iar uleiul din această incintă intră în P1 respectiv M3. Apropierea pistonului dublu al motorului de capătul cursei obturează evacuarea incintei M3 spre tanc, ceea ce face să crescă presiunea în M3. Această cre tere de presiune se transmite si în M1, ceea ce încetine te mi carea pistonului dublu, mi care amortizată si de arcul disc 24. Egalizarea presiunilor din motorul hidraulic cu presiunea din distribuitorul D determină coborârea piesei 29 si pregătind motorul auxiliar pentru ac iune. Arcul disc 24, comprimat de pistonul dublu sub ac iunea presiunii din motor, începe să se destindă si să împingă spre dreapta pistonul dublu, ac iune care deblochează evacuarea incintei M3 spre tanc si scăderea bruscă a presiunii. Diferenta de presiune dintre distribuitorul D si incinta M3, determină intrarea în functiune a motorului auxiliar si pistonul 30 împinge supapa 29 spre M3, pozitie în care si rămâne. Presiunile de pe cele două fete ale pistonului 29 se egalează prin canalele prevăzute în 28 si prin supapa 33, si 29 este împins spre D1 de către arcul 31, producînd bascularea supapelor principale din distribuitorul dublu D prin ambielajul din camera D1, ceea ce face ca distribuitorul D2 să permit accesul uleiului spre M1, iar D3 închide accesul uleiului spre M2. Se schimbă sensul de deplasare a pistonului motorului si începe deplasarea acestuia spre dreapta si evenimentele se desfă oara ca mai sus, dar în sens invers. La capetele de cursă ale motorului si a pompei, se realizează schimbarea automată a sensului de deplasare a pistonului dublu (principal) al motorului (grupul 15+16+17).

**Funcţionarea pompei.** După începerea funcţionării motorului hidraulic, incinta M2 se măreşte ca volum, supapa 79” se închide, iar incinta P2 a pompei se micşorează ca volum, uleiul comprimându-se. Incinta M1 se micşorează ca volum, iar volumul incintei P1 crette, presiunea uleiului din P1 scade şi supapa 79’ se deschide permiţând alimentarea cu ulei a incintei P1 . Diferenţa de presiune dintre P2 şi P1 determină bascularea supapei 26, permitând uleiului presurizat din P2 să pătrundă în colectorul C1, pe care îl pune sub presiune. Supapele 22 se deschid şi începe livrarea uleiului la înalta presiune pe circuitul exterior. Apropierea pistonului dublu al motorului de capătul cursei şi apoi oprirea acestuia la capăt, determină oprirea funcţionării pompei, supapele 22 acţionate de arcurile 23 se închid şi colectorul C1 este izolat de circuitul exterior.

Schimbarea sensului de deplasare a pistonului dublu al motorului, determină reluarea secvenţei de mai sus, în sens opus. Adică incinta M1 se măreşte ca volum, supapa 79’ se închide, iar incinta P1 a pompei se micşorează ca volum, uleiul comprimându-se. Incinta M2 se micşorează ca volum, iar volumul incintei P2 creşte, presiunea uleiului din P2 scade şi supapa 79” se deschide, permiţând alimentarea cu ulei a incintei P2 . Diferenţa de presiune dintre P1 şi P2 determină bascularea supapei 26, permitând uleiului presurizat din P1 să pătrundă în colectorul C1, pe care îl pune sub presiune. Supapele 22 se deschid si începe livrarea uleiului la înalta presiune pe circuitul exterior. Apropierea pistonului dublu al motorului de capătul cursei şi apoi oprirea acestuia la capăt, determină oprirea funcţionării pompei, supapele 22 actionate de arcurile 23 se închid si colectorul C1 este izolat de circuitul exterior.

## 4. Parametri constructivi ai multiplicatorului de presiune prezentat

Elementele dimensionale ale modelului prezentat în Figura 1, sunt:

$d_1$ = 200 mm; $d_2$ = 80 mm; $d_3$ = 40 mm; $h_{m1} = h_{p1}$ = 82 mm; $h_{ma} = h_{pa}$ = 76 mm; $p_n$ = 30÷50 daN/cmp.

Din analiza modului în care este proiectat multiplicatorul, constatăm că pistonul motorului înglobează cilindrul pompei ( care este aici mobil). Prin urmare forţa de împingere a pistonului motorului este transmisă direct pompei, cu pierderi prin frecare neglijabile.

Determinăm forţa de împingere produsă de pistonul motorului:

$$F_m = p_n * A_{\text{pistonului motorului}} \quad [N] \tag{1}$$

unde: $p_n$ este presiunea nominală de alimentare a multiplicatorului.

$$A_{\text{pistonului motorului}} = (\pi\, d_1^2/4 - \pi\, d_3^2/4) = \pi/4\,(d_1^2 - d_3^2) \tag{2}$$

$$F_m = \pi/4 * p_n\,(d_1^2 - d_3^2) \tag{3}$$

Aceasta este egală cu forţa transmisă pompei cilindrului pompei:

$$F_m = F_p \tag{4}$$

$$F_p = p_p * A_{\text{pistonului pompei}} \quad [N] \tag{5},$$

Unde $A_{\text{pistonului pompei}} = (\pi\, d_2^2/4 - \pi\, d_3^2/4) = \pi/4\,(d_2^2 - d_3^2)$ (6)

Din (1,4,5), rezultă:

$$p_n * A_{\text{pistonului motorului}} = p_p * A_{\text{pistonului pompei}} \tag{7}$$

Denumim $p_p/p_n$ coeficientul de multiplicare a presiunii $c_{mp.}$ Acesta reprezintă deci raportul dintre presiunea maximă refulată de pompă şi presiunea de alimentare a motorului hidraulic ( pentru modelul prezentat, se poate spune, a multiplicatorului de presiune).

Rezultă $c_{mp} = p_p/p_n$ (8)

Din (7 şi 8) rezultă: $c_{mp} = p_p/p_n = A_{\text{pistonului motorului}} / A_{\text{pistonului pompei}}$ (9)

Din (2, 6 şi 9) rezultă:

$$c_{mp} = [\pi/4\,(d_1^2 - d_3^2)]/[\pi/4\,(d_2^2 - d_3^2)] = (d_1^2 - d_3^2)/(d_2^2 - d_3^2) \tag{10}$$

Înlocuind în (10) cu valorile reale ale dimensiunilor elementelor multiplicatorului, se obţine:

$$c_{mp} = (200^2 - 40^2)/(80^2 - 40^2) = 8 \tag{11}$$

Se calculează debitul de ulei utilizat de motorul hidraulic (pentru presiunea la care lucrează motorul, se neglijează compresibilitatea uleiului):

$V_{\text{total ciclu motor}} = 2 * A_{\text{pistonului motorului}} * h_{m1} = 2* \pi/4\ (d_1^2 - d_3^2) * h_{m1} = 0{,}004946\ mc = 5\ dmc$ (12)

$V_{\text{util ciclu motor}} = 2 * A_{\text{pistonului motorului}} * h_{ma} = 2* \pi/4\ (d_1^2 - d_3^2) * h_{ma} = 0{,}004584\ mc = 4{,}56\ dmc$ (13)

$_{\text{volumic motor}} = V_{\text{util ciclu}} / V_{\text{total ciclu}} = 0{,}004584/0{,}004946 = 0{,}9268$ (14)

Pentru func ionarea la o frecven ă de cca. 2 cicluri/s, debitul de ulei hidraulic utilizat este:

$Q_{\text{ulei utilizat}} = V_{\text{consumat}} /t = n_{\text{cicli/s}} * V_{\text{total ciclu motor}} /1 = 2 * 0{,}005 = 0{,}01\ mc/s = 10\ dmc/s$ (15)

Se calculează debitul ulei livrat de pompa de înaltă presiune. Se neglijează compresibilitatea uleiului.

$V_{\text{total ciclu pompă}} = 2 * A_{\text{pistonului pompă}} * h_{m1} = 2* \pi/4\ (d_2^2 - d_3^2) * h_{p1} = 0{,}00064\ mc = 0{,}64\ dmc$ (16)

$V_{\text{util ciclu pompă}} = 2 * A_{\text{pistonului pompă}} * h_{ma} = 2* \pi/4\ (d_2^2 - d_3^2) * h_{pa} = 0{,}00057\ mc = 0{,}57\ dmc$ (17)

$_{\text{volumic pompă}} = V_{\text{util ciclu}} / V_{\text{total ciclu}} = 0{,}00057/0{,}00064 = 0{,}89$ (18)

Pentru func ionarea la o frecven ă de cca. 2 cicluri/s, debitul de ulei hidraulic livrat este:

$Q_{\text{ulei livrat}} = V_{\text{livrat}} /t = n_{\text{cicli/s}} * V_{\text{util ciclu pompă motor}} /1 = 2 * 0{,}00057 = 0{,}00114\ mc/s = 1{,}14\ dmc/s$ (19)

Presiunea uleiului cu care se alimentează multiplicatorul hidraulic este:

$p_n = 30\ daN/cmp = 3000000\ N/mp$ (20)

Se calculează puterea hidraulică consummate pentru func ionarea multiplicatorului de presiune la parametri indica i mai sus:

$P_{\text{consumat}} = Q_{\text{ulei utilizat}} * p_n$ [W] (21)

$P_{\text{consumat}} = 0{,}01 * 3000000 = 30000\ W = 30\ KW$ (22)

Se calculează puterea hidraulică livrată de pompa de înaltă presiune din multiplicatorului de presiune, la parametri indicati mai sus (se neglijează în acest exemplu pierderile de presiune interioare ale pompei de ulei si compresibilitatea acestuia ):

$P_{\text{util}} = Q_{\text{ulei util}} * p_n {}^* c_{mp}$ [W] (23)

$P_{\text{util}} = 0{,}00114 * 3000000 * 8 = 27360\ W = 27{,}36\ KW$ (24)

Se calculează randamentul hidraulic al multiplicatorului, care nu ine seama de scăderea presiunii pompei în func ionare, de compresibilitatea i elasticitatea uleiului, de eventuale incluziuni de aer, de elasticitatea elementelor mecanice de construc ie a pompei hidraulice. Se poate afirma că este randamentul maxim al multiplicatorului:

$_{\text{hidraulic multiplicator}} = P_{\text{util}} / P_{\text{consumat}} = 27{,}36/30 = 0{,}912$ [ - ] (25)

## 5. Reglarea parametrilor de functionare a multiplicatorul hidraulic

Reglarea parametrilor de alimentare cu ulei la înaltă presiune pe sarcina hidraulică din acest circuit se poate realiza în mai multe moduri:

- reglarea directă a căderii de presiune a uleiului pe sarcina hidraulică în circuitul de înaltă presiune se poate realiza prin intercalarea unui ventil de reduc ie a presiunii;
- reglarea presiunii de alimentare a multiplicatorului (deci i a motorului hidraulic integrat):
  - alimentarea multiplicatorului cu diferite trepte de presiune;
  - intercalarea pe circuitul de alimentare cu ulei a unui ventil de reductie a presiunii ;
  - alimentarea discontinuă a multiplicatorului cu ajutorul unui distribuitor si intercalarea pe circuitul de alimentare a unui accumulator de presiune pentru atenuarea oscila iilor de presiune si mentinerea constantă a presiunii. Metoda permite acoperirea unei necesită i de volum mare de ulei în timp scurt si în anumite situatii ( de consum fluctuant de ulei la înaltă presiune) a utilizării unei surse de alimentare cu o putere hidraulică mai redusă decât puterea nominală a multiplicatorului;
- reglarea presiunii de evacuare a uleiului din multiplicatorul de presiune, este o solu ie acceptabilă pentru a asigura presiunea maximă în circuitul de înaltă presiune, la un debit mai redus. Poate fi utilizată pînă la presiuni în incinta M3 care să permit bascularea distribuitorului

D ( diferenta de presiune între D1 si M3 să fie suficientă ca să permită functionarea motorului hidraulic auxiliar).

## 6. Concluzii

1. Multiplicatorul de presiune prezentat de autori este o construc ie compactă, având *pompa cu piston de ulei de inaltă presiune înglobată în motorul hidraulic linear si o functionare cu dublă actiune (duplex, cu un transfer de putere hidraulică mare);*
2. *Functionarea automată, continuă, sigură, fără suprapresiuni sau socuri hidraulice, se produce numai în conditiile existentei sarcinii pe circuitul de înaltă presiune, în caz contrar uleiul trece prin pompa de înaltă presiune ca printr-o rezisten ă hidraulică oarecare, fără ca motorul hidraulic să înceapă să func ioneze.*
3. *Presiunea minimă de livrare a uleiului hidraulic de către pompa de inaltă presiune este chiar presiunea de intrare a uleiului în agregat, iar cea maximă teoretică este presiunea de intrare a uleiului în agregat, înmultită cu factorul de multiplicare a multiplicatorului;*
4. *Schimbarea sensului de functionare a motorului se realizează automat, de către un distribuitor, actionat de către un motor hidraulic linear auxiliar, comandat de un sensor de diferentă de presiune prevăzut în corpul distribuitorului, pe baza diferentei presiunilor uleiului în diferitele incinte ale motorului si camera principală din distribuitor;*

***Mulțumiri.*** Această lucrare a fost sustinută de proiectul "Îmbunătățirea calității studiilor de doctorat în studii de inginerie pentru dezvoltarea societății bazate pe cunoaştere - QDOC" Contract nr. POSDRU/107/1.5/S/78534, proiect cofinanțat de Fondul Social European prin programul Operațional Sectorial al Resurselor Umane 2007-2013.

### B I B L I O G R A F I E

[1]. C ă l i n o i u, C., *Senzori si traductoare*, volume I, Editura Tehnica, Bucure ti, 2009.
[2] C h e r v a s e, M., V a i d a, L., O p r u t a, D., *Mecanica Fluidelor- elemente tehnice*, Ed. SITECH, Craiova, 2006.
[3] D e a c u, L., P o p, I., *Hidraulica masinilor-unelte*, Lito.IPCN, Cluj-Napoca, 1983.
[4] M a r i n, V., M a r i n, A., *Sisteme hidraulice automate–constructive, reglare, exploatare*, Editura Tehnica, Bucuresti, 1987.
[5] O p r e a n, A., s.a., *Acționări şi automatizări hidraulice, modelare, simulare, încercare*, Editura Tehnica, Bucuresti, 1989.
[6] O p r u t a, D., V a i d a, L., *Dinamica fluidelor*, Editura Mediamira, Cluj Napoca, 2004.
[7] O p r u t a, D., V a i d a, L., G i u r g e a, C o r i n a , N ă s c u t i u, L u c i a n, *Mecanica fluidelor*, Lucrări practice, Editura Todesco, Cluj Napoca, 2004.
[8] Prodan, D., s.a., *Masini-unelte şi prese. Elemente hidrostatice*. Editura Tehnica, Bucuresti, 2001.
[9] V a i d a, L., O p r u t a, D., C h e r v a s e, M., G i u r g e a, C o r i n a, Mecanica fluidelor - Elemente teoretice, Editura Universită ii din Oradea, 2000.
[10] V a i d a, L., D e a c u, L., O p r u ț a, D., *Asupra pierderilor de putere în acționările hidraulice*, în Revista „Hervex 2002”, Noiembrie 2002, Râmnicu-Vâlcea, pag. 275 -280.
[11] Velescu, C., Aparate si echipamente hidrostatice proportionale, Editura MIRTON, Timisoara, 2003.

**ISSN 1454 - 8003**
**Proceedings of 2011 International Salon of Hydraulics and Pneumatics - HERVEX**
*9 – 11 November, Călimăneşti-Căciulata, Romania*

# ANALIZA CFD A CURGERII UNUI FLUID PRINTR-O REZISTENȚĂ HIDRAULICĂ CU SERTAR CILINDRIC ŞI BUCŞĂ

**Drd. Ing. Ioana Sfârlea[1], Dr. Ing. Florin Bode[2] , Prof. Dr. Ing. Dan Opruța**
[1]Universitatea Tehnică Cluj-Napoca, Departamentul Inginerie Mecanică, Ioana.Sfârlea@termo.utcluj.ro
[2]Universitatea Tehnică Cluj-Napoca, Departamentul Inginerie Mecanică, Florin.Bode@termo.utcluj.ro
[3]Universitatea Tehnică Cluj-Napoca, Departamentul Inginerie Mecanică, Dan.Opruța@termo.utcluj.ro

***Rezumat:*** *Lucrarea prezintă un studiu de tip Computational Fluid Dynamics (CFD) a simulării curgerii unui fluid printr-o rezistență hidraulică cu sertar cilindric şi bucşă. Rezultale obținute vor fi de folos in optimizarea constucției geometrice a sertarului şi a orificiilor bucşei astfel încât toate aspectele ce se cer studiate în cazul acestui tip de rezistență hidraulică să fie soluționate.*

***Cuvinte cheie****: rezistență hidraulică, cavitație, simulare, CFD*

## 1. Introducere

În acest articol se prezintă un studiu de tip Computational Fluid Dynamics (CFD) a curgerii unui fluid printr-o rezistență hidraulică cu sertar cilindric şi bucşă.
Literatura de specialitate [1][2][3][4] prezintă mai multe cercetări asupra rezistențele hidrulice cu piston fără bucşă decât asupra celor cu bucşă. Aspectele ce trebuie studiate sunt aceleaşi la ambele tipuri de rezistențe. Diferența dintre acestea este că pentru deschideri mari de comandă ale sertarului la rezistențele cu bucşă aria de curgere este aceeaşi ca la deschideri mici ale pistonului la rezistențele fără bucşă. Acest lucru dă posibilitatea unui mai bun control asupra debitului, aşa cum reiese şi din ecuația debitului a curgerii printr-o rezistență diafragmatică:

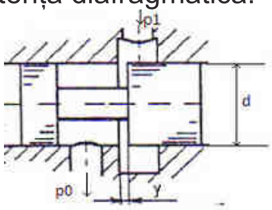


$$Q = \alpha A \sqrt{\frac{2\Delta p}{\rho}} \qquad (1)$$

unde: Q-debit, $\Delta p = p_1 - p_0$, α-coeficient de debit, ρ- densitatea fluidului, A-aria secțiunii de curgere

Cerințele ce trebuie îndeplinite pentru un comportament static şi dinamic mai bun al rezistențelor sunt:

- coeficient de debit α, ca măsură a pierderilor hidraulice, cât mai apropiat de valoarea 1
- număr Reynolds critic cât mai mic, ceea ce conduce la obținerea unui coeficient α constant pentru debite mici
- reducerea forțelor hidrodinamice, ale căror tendință este de a „închide" rezistența, fiind cu atât mai mari cu cât debitul este mai mare. Acestea au o influență majoră asupra performanțelor aparatelor, dar şi asupra posibilității de comandă a debitului
- reducerea fenomenului cavitațional care apare din cauza scăderii presiunii sub presiunea de vaporizare. Din ecuația lui Bernoulli reiese că la debit constant, dacă secțiunea de curgere se micşorează viteza de curgere creşte, iar presiunea scade (diferența de presiune este mare).Acest lucru indică posibilitatea apariției cavitației. Din investigațiile de pănă acum se constată că modificarea configurației geometrice a rezistențelor conduce la o reducere a fenomenului cavitațional.

Rezistențele hidraulice cu sertar cilindric şi bucşă au mai multe forme constructive (figura 1). Prezenta analiză se axează pe rezistențe cu bucşă cu orificii circulare (figura 1c), dar acestea pot fi de diferite forme.

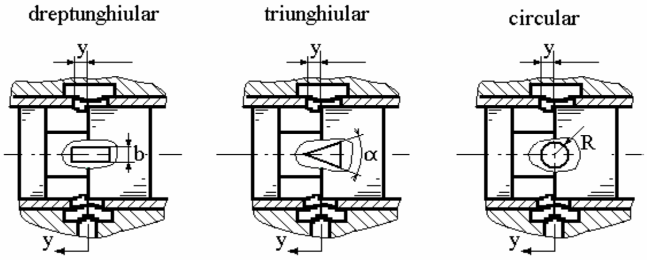


Figura 1. Rezistențe hidraulice cu sertar cilindric şi bucşă

Lucrarea [2] prezintă un amplu studiu asupra rezistențelor hidraulice cu sertar cilindric. S-a urmărit scăderea cifrei Reynolds, de la care, în sus, coeficientul de debit să fie constant, s-au determinat valori ale coeficientului de debit pentru diferite forme de rezistențe, s-a încercat micşorarea forțelor hidrodinamice şi s-a studiat fenomenul cavitațional.
Analizele de tip CFD au fost dezvoltate, în principal, pentru vizualizarea proceselor complexe sau a curgerilor prin geometrii complicate. Ajută foarte mult în procesul de producție, prin reducerea costurilor de realizare fizică a modelelor studiate. Un astfel de exemplu este studiat de An, Kim şi Shin [5] care au realizat o simulare numerică pe mai multe tipuri de supape de control având geometrii diferite. S-au investigat şi analizat căderile de presiune, efectul cavitațional precum şi variația coeficientului de debit. Comparând o supapă convențională cu una nou proiectată, utilizând metoda CFD, se observă o îmbunătățire a câmpului de curgere, cu cavitație redusă şi creşterea performanțelor la aceasta din urmă.
Studiul realizat în cadrul prezentei lucrări reprezintă primul pas dintr-o serie de simulări ce au ca scop optimizarea configurației geometrice a rezistențelor hidraulice cu sertar cilindric şi bucşă. Vor fi analizate căderile de presiune, câmpul vitezelor şi fenomenul cavitațional pentru mai multe deschideri de comandă ale rezistenței.

## 2. Modelarea geometrică

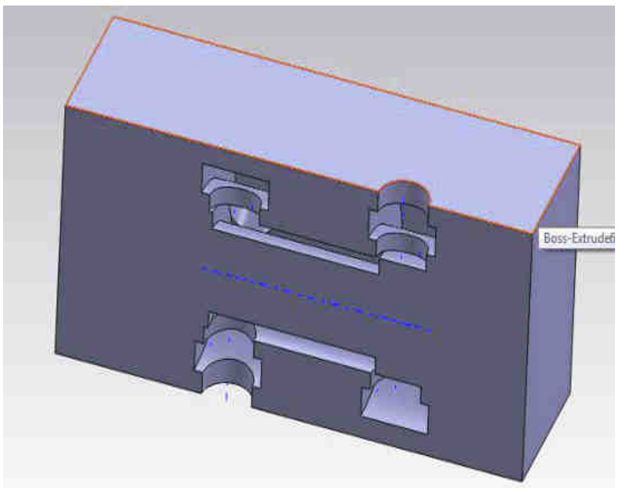


Figura 2. Modelul geometric

Modelul geometric al rezistenței hidraulice studiate a fost realizat cu ajutorul softului Solid Works 2011. S-a construit un bloc cu dimensiunile de 30x50x30 (l x L x h) în care s-a realizat sertarul cilindric, bucşa cu 6 orificii a 6 mm diametru şi canalele din corpul distribuitorului, cu o lătime de 8 mm. Orificiile de intrare şi ieşire au tot 6 mm diametru, iar deschiderea de comandă pentru care s-a făcut simularea este de 0,45 mm. S-au ales deschideri mici deoarece se doresc studiate atât apariția forțelor hidrodinamice, care perturbă comportarea dinamică a rezistenței, cât şi apariția fenomenului de cavitație, ce rezultă din scăderea presiunii sub presiunea de vaporizare. Acest lucru se intâmplă din cauza îngustării bruşte a secțiunii de curgere.

**ISSN 1454 - 8003**
**Proceedings of 2011 International Salon of Hydraulics and Pneumatics - HERVEX**
*9 – 11 November, Călimăneşti-Căciulata, Romania*

Geometria astfel proiectată, a fost importată in Ansys 12.1. Aici s-a creat stratul de fluid care mai apoi a fost discretizat. În zona de interes s-a realizat o discretizare mai fină, aceasta rărindu-se pe măsură ce se apropie de pereți. Discretizarea se poate observa în figura 3.

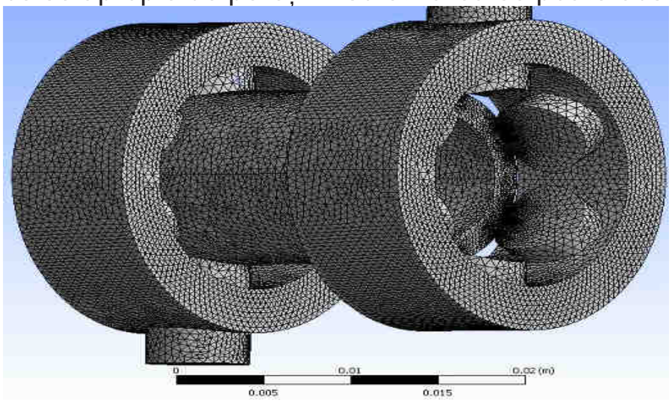


Figura 3. Discretizarea stratului de fluid

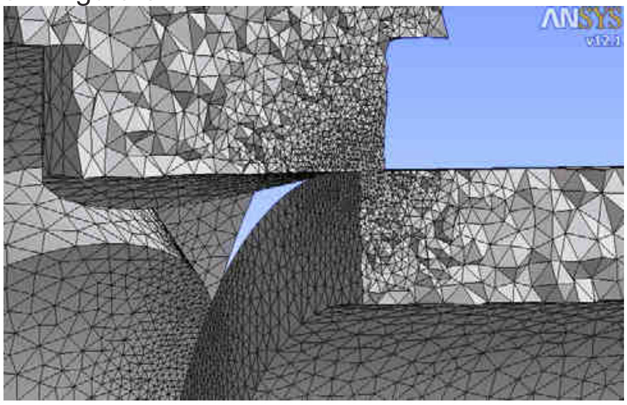


Figura 4. Detaliu mesh 3-D

În zona deschiderii de comandă a rezistenței s-a realizat o discretizare mai fină (partea mai întunecată).
Pentru o mai bună vizualizare a curgerii, s-a creat un plan median prin rezistență şi s-a creat un detaliu al discretizării, tocmai pentru a se observa mai bine dimensiunea celulelor folosite (Figura 4).
Pentru discretizarea întregului strat de fluid au fost nevoie de 1.7 milioane celule.
Din punct de vedere al condițiilor la limită, s-a impus fluidul care curge prin rezistență,un ulei hidraulic HPE 46 (cu o densitate de 850 km/m$^3$ şi o vâscozitate cinematică la 40º C de 46 cSt). S-a mai impus căderea de presiune pe rezistență de 20 bar.

### 3. Modelarea numerică

Pentru investigarea curgerii există mai multe modele de turbulență. De exemplu, dacă în timpul curgerii densitatea fluidului rămâne constantă se recomandă cu succes metoda Reynolds (1895). În schimb, dacă densitatea fluidului variază, metoda de utilizat este cea propusă de Favre. [6]
Modelul de turbulență ales pentru această simulare este RNG k-ε. Modelul de turbulență k-ε se încadrează în clasa modelelor de turbulență des folosite pentru rezolvarea calculelor hidraulice. Este un model robust, economic si cu precizie mare pentru o gama largă de curgeri turbulente. Modelul standard k-ε este un model semi-empiric bazate pe ecuațiile de transport ale energiei cinetice k şi rata de disipație turbulentă a acesteia.
Modelul RNG k-ε, derivă din modelul standard k-ε folosind o riguroasă tehnică statistică numită „renormalization group theory”. Acesta implică includerea unui termen în plus la ecuația ratei de disipație turbulentă, fapt care îmbunătățeşte simțitor calculul curgerii prin secțiuni mici. De asemenea creşte performanțele în cazul curgerilor turbionare şi este folosit cu succes în curgerile turbulente la numere Reynolds mici.
Simularea a fost făcută pe presupunerea că fluidul de lucru este incompresibil şi s-au ignorat influențele gravitațională şi cea de plutire. Notând cu u viteza de curgere, modelarea numerică are la bază ecuațiile ce guvernează curgerea. De regulă, acestea constau în ecuația de continuitate (relația 2 ), ecuația de conservare a impulsului sau ecuația de mişcare pe o direcție i ( relația 3)

$$\frac{\partial u_x}{\partial x} + \frac{\partial u_y}{\partial y} + \frac{\partial u_z}{\partial z} = 0 \qquad (2)$$

ISSN 1454 - 8003
Proceedings of 2011 International Salon of Hydraulics and Pneumatics - HERVEX
9 – 11 November, Călimăneşti-Căciulata, Romania

$$u_x \frac{\partial u_i}{\partial x} + u_y \frac{\partial u_i}{\partial y} + u_z \frac{\partial u_i}{\partial z} = -\frac{1}{\rho}\left(\frac{\partial p}{\partial x_i} + \frac{\partial p}{\partial y_i} + \frac{\partial p}{\partial z_i}\right) + \nu\left(\frac{\partial^2 u_i}{\partial x^2} + \frac{\partial^2 u_i}{\partial y^2} + \frac{\partial^2 u_i}{\partial z^2}\right), \qquad (3)$$

unde ρ reprezintă densitatea fluidului,
p – presiunea fluidului
ν – vâscozitatea cinematică
şi ecuația de transport (relația 4):

$$u_x \frac{\partial t}{\partial x} + u_y \frac{\partial t}{\partial y} + u_z \frac{\partial t}{\partial z} = a\left(\frac{\partial^2 t}{\partial x^2} + \frac{\partial^2 t}{\partial y^2} + \frac{\partial^2 t}{\partial z^2}\right) \qquad (4)$$

Pentru rezolvarea modelului de curgere turbulentă k-ε, mai avem nevoie de două ecuații. Dar pentru această simulare s-a ales modelul de turbulență RNG k-ε, care spre deosebire de modelul convențional k-ε, s-a dovedit a fi mai precis în calculul turbulențelor. Relațiile care se adaugă sistemului de ecuații ce definesc complet curgerea în modelul de turbulență ales (RNG k-ε) sunt:

$$\frac{\partial}{\partial \tau}(\rho k) + \frac{\partial}{\partial \chi_i}(\rho k u_i) = \frac{\partial}{\partial \chi_j}\left(a_k \mu_{eff} \frac{\partial k}{\partial \chi_j}\right) + G_k - \rho\varepsilon + S_k \qquad (5)$$

$$\frac{\partial}{\partial \tau}(\rho \varepsilon) + \frac{\partial}{\partial \chi_i}(\rho \varepsilon u_i) = \frac{\partial}{\partial \chi_j}\left(a_\varepsilon \mu_{eff} \frac{\partial \varepsilon}{\partial \chi_j}\right) + C_{1\varepsilon} G_k \frac{\varepsilon}{k} - C_{2\varepsilon}\rho \frac{\varepsilon^2}{k} - R_\varepsilon + S_\varepsilon \qquad (6)$$

$G_k$ – coeficient de generare a energiei cinetice turbulente
$S_k$, $S_\varepsilon$ – termeni definiți de utilizator
$C_{1\varepsilon}$=1,42, $C_{2\varepsilon}$ =1,68 – constante specifice modelului de turbulență [8]
$R_\varepsilon$ – din ecuația ε este exact termenul care face diferența între modelul standard k-ε şi modelul ales RNG k-ε şi este de forma:

$$R_\varepsilon = \frac{C_\mu \rho \eta^3 \left(1 - \frac{\eta}{\eta_0}\right)}{1 + \beta\eta^3} \frac{\varepsilon^2}{k} \qquad (7)$$

unde $\eta \equiv S_k/\varepsilon$; $\eta_0$= 4,38; β=0,012

**4. Rezultatele simulării**

Având în vedere faptul că domeniul deschiderilor mici ale rezistențelor hidraulice pune cele mai multe probleme din punct de vedere a comportării dinamice a sistemelor hidraulice, prezenta simulare ne oferă o imagine de ansamblu a fenomenelor care apar în interiorul rezistenței. Investigațiile s-au concentrat doar pe distribuția câmpurilor de presiuni şi viteze.
Astfel, în figura 5 este prezentat conturul presiunilor pe rezistență; în ambele figuri (5a şi 5b) se observă diferența de presiune care apare la îngustarea secțiunii de curgere. Conform ecuației lui Bernoulli, o dată cu micşorarea ariei de curgere, la debit constant, viteza de curgere creşte, iar presiunea scade. În figura 5a se observă că scara de valori a presiunii atinge şi valori negative. Acest lucru este practic imposibil, dar el se traduce prin apariția unei puternice scăderi de presiune, posibil cavitațională în apropierea pereților. Figura 5b are scara de valori a presiunii exprimată în atmosfere. Ținând cont de condițiile la limită impuse, se observă că circuitul fluidului este unul de la pompă spre rezervor, fără recircularea acestuia.

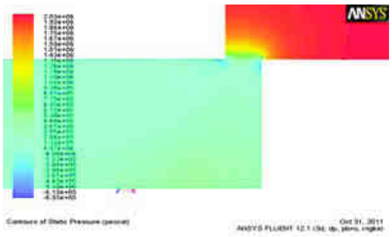

a. Detaliu in plan longitudinal a conturului de presiuni

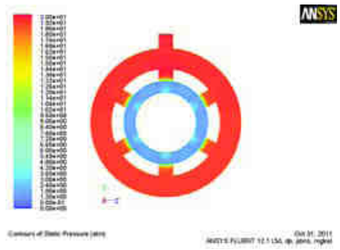

b. Secțiune transversală prin mijlocul jetului

Figura 5. Conturul de presiuni

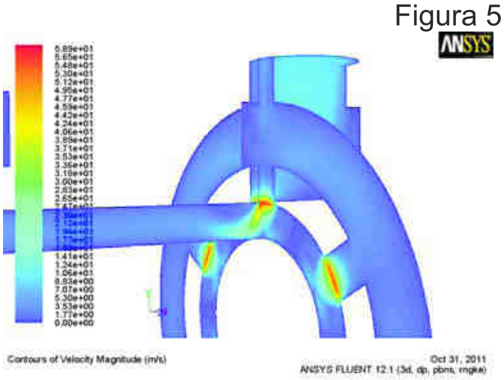


a. Distribuția 3-D a câmpului de viteze

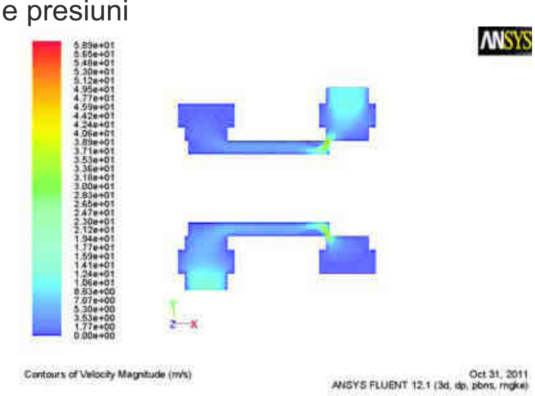


b. Secțiune longitudinală a câmpului de viteze

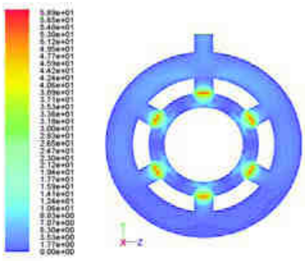

c. Secțiune transversală prin mijlocul jetului de fluid

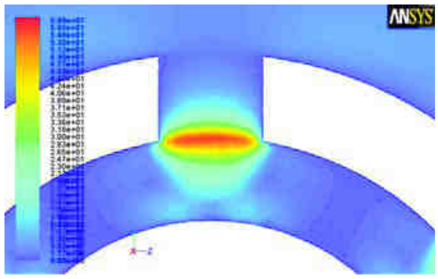

d. Detaliu secțiune transversală

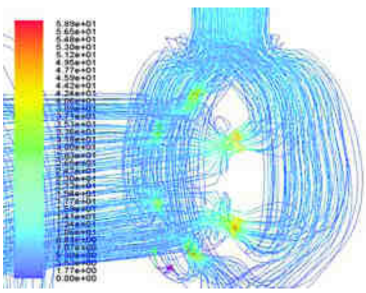

e. Distribuția vitezelor (linii de curent)

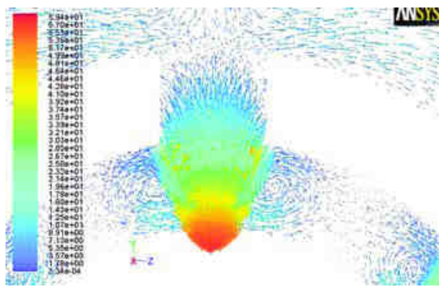

f. Vectori de viteză (detaliu deschidere de comandă)

Figura 6. Distribuția câmpului de viteze

Ţinând cont de aceeaşi ecuaţie a lui Bernoulli, figura 6 prezintă creşterea vitezei de curgere în zona de deschidere a rezistenţei. S-au prezentat mai multe imagini din care rezultă o valoare de până la aproape 60 m/s a vitezei în mijlocul jetului de fluid. În figura 6a este redată o imagine 3D a câmpului de viteze, care confirmă, intr-o oarecare măsură, rezultatul obţinut în lucrarea [2]. Concluzia [2] a fost ca la un unghi de intrare al jetului de fluid de aproximativ 69º configuraţia geometrică este optimă. În urma măsurării unghiului jetului a reieşit o valoare de ≈60º. Figurile 6b, 6c şi 6d redau secţiuni prin jetul de fluid astfel: 6b – secţiune longitudinală mediană prin corpul rezistenţei; 6c şi 6d – secţiune transversală prin mijolcul jetului de fluid, vedere de ansamblu, respectiv detaliu pe un orificiu al bucşei. Figurile 6e şi 6f prezintă o imagine 3D a liniilor de curent urmate de jetul de fluid, observându-se fenomenul de creştere a vitezei in secţiunea de îngustare, respectiv o imagine detaliată a vectorilor câmpului de viteze pe un singur orificiu al bucşei.

## 5. Concluzii

În urma analizei CFD a curgerii printr-o rezistenţă hidraulică cu sertar cilindric şi bucşă, s-a observat că la îngustarea bruscă a secţiunii de curgere, datorită creşterii vitezei jetului, presiunea scade brusc, iar în zonă poate apărea cavitaţia. Acest lucru este confirmat de rezultatele experimentale din literatura de specialitate. Pornind de la această simulare se vor face studii şi analize mai amănunţite pentru a determina o formă geometrică a orificiului bucşei sau a sertarului care sa îmbunătăţească performanţele dinamice ale aparatelor de comandă a energiei hidraulice.

**MULŢUMIRI:** Această lucrare a fost realizată cu sprijinul acordat prin proiectul " QDOC - Cre  terea calită  ii studiilor doctorale în   tiin  e inginere  ti pentru sprijinirea dezvoltării societă  ii bazate pe cunoa  tere” contract nr. POSDRU/107/1.5/S/78534, proiect cofinan  at din Fondul Social European prin Programul Opera   ional Sectorial pentru Dezvoltarea Resurselor Umane 2007-2013.

## BIBLIOGRAFIE

[1] T. Canta, „Acţionări hidrulice şi pneumatice”, IPCN, 1982
[2] D. Opruţa, „Optimizarea constructivă a comportării statice şi dinamice a aparatelor de comandă a energiei hidraulice”, Cluj-Napoca, Teză doctorat, 1998
[3] W. Backe, „Servohydraulik”, RWTH, Aachen, 1984
[4] I. Deacu, D. Banabic ş.a. – Tehnica Hidraulicii Proporţionale, Editura Dacia, Cluj-Napoca, 1989
[5] Y. J. An, B. J. Kim, B. R. Shin, „Numerical analysis of 3-D flow through LNG marine control valves for their advanced design”, Journal of Mechanical Science and Tehnology 22, 2008; p. 1998-2005
[6] R. Farmer, R. Pike, G. Cheng, „CFD analysis of complex flow”, Computers and Chemical Engineering 29, 2005; p. 2386-2403
[7] G. Zhang, M. Tian, S. Zhou, „Simulation and analysis of flow pattern cross-corrugated plate heat exchangers”, Journal of Hydrodynamics, Ser.B, 2006, 18(5); p. 547-551
[8] W. Rodi, „Turbulence models and their application in hydraulics” IAHR, Olanda, 1984; p. 9-46
[9] Ansys 12.0 Theory Guide

**ISSN 1454 - 8003**
**Proceedings of 2011 International Salon of Hydraulics and Pneumatics - HERVEX**
*9 – 11 November, Calimanesti-Caciulata, Romania*

# SIMULARE CFD A CURGERII PE O PLACĂ ONDULATĂ

**Oana Giurgiu Irimieş[1], Florin Bode[2], Dan Opruța[3]**

[1] Universitatea Tehnica Cluj-Napoca, Departamentul de Inginerie Mecanica, e-mail: Oana.Giurgiu@termo.utcluj.ro

[2] Universitatea Tehnica Cluj-Napoca, Departamentul de Inginerie Mecanica, e-mail: Florin.Bode@termo.utcluj.ro

[3] Universitatea Tehnica Cluj-Napoca, Departamentul de Inginerie Mecanica, e-mail: Dan.Opruța@termo.utcluj.ro

***Rezumat:*** *Lucrarea prezintă un studiu numeric de tip Computational Fluid Dynamics (CFD) asupra plăcilor schimbătoarelor de căldură. Studiul a fost realizat pe o placă ondulată, având unghiul de înclinare $\beta = 60^o$. Modelul analizat a fost creat în programul Solid Works, importat în Ansys – Design Modeller, unde s-au creat straturile de lichid (apa caldă și apa rece, de o parte și de alta a plăcii studiate numeric) și s-a făcut discretizarea geometrică după care s-au introdus condițiile la limită în vederea realizării simulării numerice. Pentru simularea numerică s-a utilizat softul Fluent 6.2.*

***Cuvinte cheie***: *simulare numerică de tip CFD, schimbătoare căldură, placă ondulata, Fluent.*

## 1. Introducere

Schimbătoarele de căldură reprezintă aparate care au drept scop transferul de căldură de la un fluid la altul, în procese de încălzire, răcire, recuperare de căldură, condensare, evaporare sau alte procese termice în care sunt prezente două sau mai multe fluide cu temperaturi diferite.
Pe plan mondial schimbătoarele de căldură cu plăci au început să fie introduse în fabricație încă din anul 1948, când a fost finalizat primul proiect al noii generații de schimbătoare cu plăci, având performanțe mult înbunătățite. Pe plan național, schimbătoarele de căldura cu plăci au fost introduse în fabricație după anul 1990. [1]
Cel mai comun tip de schimbător cu suprafață primară este **schimbătorul cu plăci şi garnituri** (SCP-G). Aplicațiile acestor schimbătoare sunt limitate de către presiunea maximă de funcționare, precum şi de către diferența de presiune dintre cele două fluide. Sunt concepute şi realizate SCP-G capabile să reziste unei presiuni de 25 bar şi unei diferențe de presiuni de 25 bar. Se admit astăzi, în mod frecvent, presiuni de funcționare cuprinse între 16–20 bar. Temperatura maximă de funcționare limitează domeniul de utilizare al SCP-G, în funcție de natura garniturilor, admițându-se ca limită superioară de utilizare la garniturile standard, o temperatură de 150°C.
**Schimbătoarele cu plăci sudate** permit utilizarea suprafețelor primare de schimb de căldură, cu nivele de presiuni şi temperaturi mai ridicate decât la SCP-G. Unele variante pot funcționa între $-80^0$C şi $+450^0$C, respectiv 100 bar.
**Schimbătoarele cu plăci semisudate** sunt aparate utilizate în aplicații speciale în care unul dintre agenții termici de lucru necesită un circuit ermetic, iar celălalt circuit trebuie să permită curățarea manuală.
**Schimbătoarele cu plăci brazate** sunt utilizate în cazul agenților frigorifici care lucrează la temperaturi pozitive şi negative, cu schimbare de fază. În ultima perioadă, având în vedere prețurile lor de achiziție relativ scăzute, aceste utilaje sunt folosite pe scară largă la încălzire şi preparare de apă caldă menajeră, dacă agenții de lucru sunt curați.
Cercetările actuale se concentrează pe creșterea performanțelor schimbătoarelor de căldură, o direcție în acest sens o reprezintă optimizarea geometriei plăcilor știind că regimul de curgere și unghiul de înclinare al canalului de curgere pentru o placă ondulată au o importantă influență asupra coeficientului global de transfer de căldură. [2]

Plăcile ondulate ale schimbătoarelor de căldură au fost studiate și analizate experimental. In această lucrare se prezintă o abordare a curgerii peste o placă ondulată a unui schimbator de căldură din punct de vedere CFD, mai puțin tratată în literatura de specialitate.
In acest scop s-a creat un model de placă cu un unghi de înclinare $\beta = 60°$, utilizând o combinație de trei softuri comerciale disponibile: Solid Work pentru modelare, Ansys – Design Modeller pentru generarea mesh-ului și Fluent pentru simularea CFD.
Studiile efectuate [3], utilizând software - ul CFD au arătat că înclinația ondulării are un efect asupra schimbărilor regimului de curgere și s-a demonstrat că regimul de turbulență apare la creșterea unghiului de înclinare $\beta$. Efectele ondulării asupra coeficientului global de transfer de căldură cât și asupra pierderilor de presiune, au fost studiate cu ajutorul simulării numerice de tip CFD, utilizandu-se modele geometrice simplificate. [5, 7,8] Pentru simulare s-a utilizat modelul de turbulență $k=\omega$ SST. Acest model este cel mai potrivit pentru simularea curgerii pentru aceste tipuri de geometrii. [9.]
Cele mai recente cercetări cu privire la schimbătoarele de căldură cu plăci s-au axat pe corelații între numărul Nusselt şi coeficientul de frecare, datorită faptului că pot fi determinați experimental pentru toate modelele de schimătoare de căldură. [4]. Pierderile de presiune şi coeficientul de transfer de căldură depind de modul de distribuire a curgerii fluidului prin canalele schimbătorului de căldură. [6].
Scopul prezentei lucrări este de a face o simulare numerică de tip CFD în vederea analizei distribuției curgerii fluidelor în lungul plăcii și a modului în care se realizează transferul de căldură pentru modelul de placă propus.

## 2. Modelul geometric.

Modelul geometric (figura 1) constă într-o placa ondulată, având unghiul de înclinare $\beta = 60^0$, lungimea activă a plăcii L=50 mm, lățimea activă a plăcii l = 100 mm, pasul de ondulare p = 3 mm, înălțimea ondulării e = 0.5 mm, înălțimea canalului sau înăltimea de ondulare $H_0$ =2.5 mm. Modelul a fost realizat în programul Solid Works 2011 și a fost importat în Ansys, unde s-au creat straturile de lichid (figura 2) și zonele de lucru: z1 – intrare apă rece; $z_2$ – ieșire apă rece; $z_3$ – intrare apă caldă; z4 – ieșire apă caldă; z5 – interfață placă, după care s-a discretizat modelul. Discretizarea geometrica - mesh (figura 3) a fost realizată în programul Ansys – Design Modeller, utilizându-se în jur de 450000 elemente tetraedrale.

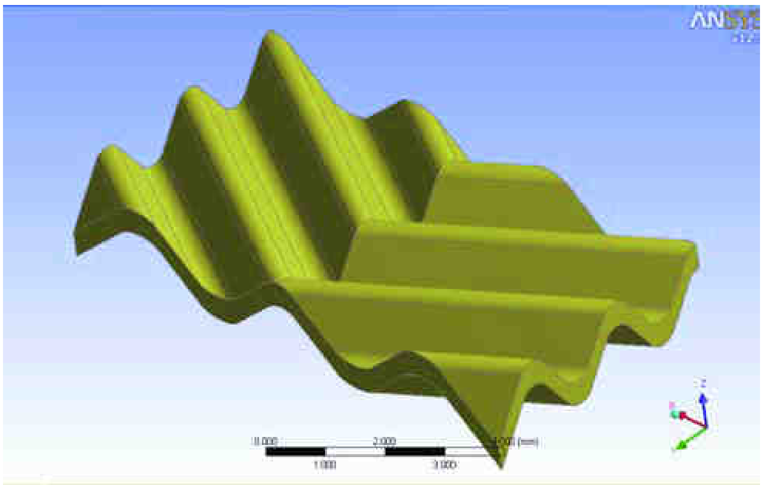

**Fig. 1** Modelul geometric

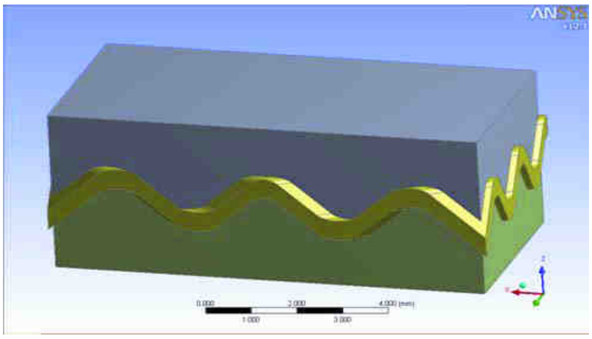

**Fig. 2** Crearea stratului de lichid

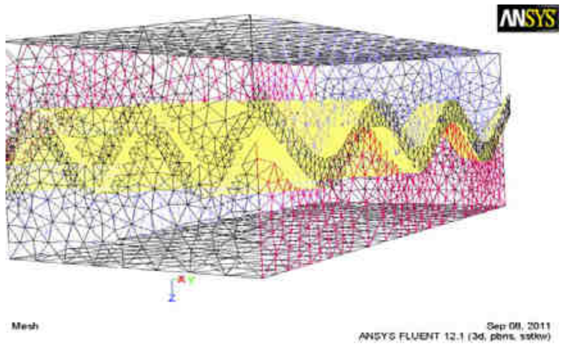


**Fig. 3** Discretizarea geometrică

## 3. Modelul matematic

Literatura de specialitate [9, 10] recomandă pentru simularea numerică a curgerii peste plăcile schimbătoarelor de căldură utilizarea modelului de turbulență k-ω SST (**S**hear **S**tress **T**ransport). Model se folosește la simulări în care atât zonele de centru cât și cele de la perete trebuiesc modelate în detaliu, la fel ca și în cazul plăcilor ondulate, pentru a obține rezultate cât mai reale.
Acest model este un amestec între modelul standard k- ε şi modelul k-ω. Modelul foloseşte o formulare k - ε pentru zona curgerii libere, evitând astfel dezavantajele majore ale lui k-ω privind condițiile inițiale şi un model k- ω pentru stratul limită. Acest lucru este realizat prin formularea modelului k - ε în manieră k - ω. Trecerea graduală între cele două zone este asigurată prin definirea unor funcții de „amestec” care activează formularea k - ω sau k - ε în funcție de zonă şi prin introducerea unui termen difuziv în ecuația de transport a lui ω.
Modelul k - ε şi-a demonstrat eficiența, fiind cel mai popular model testat pe o clasă largă de aplicații. Unul dintre cele mai importante avantaje ale modelului este reprezentat de necesarul redus de resurse de timp şi de putere de calcul. O simulare numerică ce utilizează acest model este o simulare simplă fără clauze adiționale ca în cazul altor modele numerice. Acesta este principalul motiv pentru care modelul k - ε a fost adoptat pe scară largă şi folosit în numeroase aplicații industriale.
Modelul k – ω standard este un model empiric bazat pe modelarea ecuațiilor de transport pentru energia cinetică (k) și rata de disipație turbulentă (ω).
Ecuațiile care stau la baza modelului de turbulență k-ω SST [10] sunt:

- Ecuațiile Navier – Stokes

$$u_x \frac{\partial u_i}{\partial x} + u_y \frac{\partial u_i}{\partial y} + u_z \frac{\partial u_i}{\partial z} = -\frac{1}{\rho}\left(\frac{\partial p}{\partial x_i} + \frac{\partial p}{\partial y_i} + \frac{\partial p}{\partial z_i}\right) + \nu\left(\frac{\partial^2 u_i}{\partial x^2} + \frac{\partial^2 u_i}{\partial y^2} + \frac{\partial^2 u_i}{\partial z^2}\right) \quad (1)$$

Unde: ρ reprezintă densitatea fluidului, p – presiunea fluidului, v – vâscozitatea cinematică

- Ecuațiile de transport

$$u_x \frac{\partial t}{\partial x} + u_y \frac{\partial t}{\partial y} + u_z \frac{\partial t}{\partial z} = a\left(\frac{\partial^2 t}{\partial x^2} + \frac{\partial^2 t}{\partial y^2} + \frac{\partial^2 t}{\partial z^2}\right) \quad (2)$$

- Ecuațiile de continuitate

$$\frac{\partial u_x}{\partial x} + \frac{\partial u_y}{\partial y} + \frac{\partial u_z}{\partial z} = 0 \quad (3)$$

- Ecuațiile de transport pentru energia cinetică

$$\frac{\partial(\rho k)}{\partial t}+\frac{\partial(\rho k u_i)}{\partial x_i}=\frac{\partial}{\partial x_j}\left(\Gamma_k\frac{\partial k}{\partial x_j}\right)+G_k-Y_k \tag{4}$$

- Ecuațiile de transport pentru rata de disipație turbulentă

$$\frac{\partial(\rho\omega)}{\partial t}+\frac{\partial(\rho\omega u_i)}{\partial x_i}=\frac{\partial}{\partial x_j}\left(\Gamma_\omega\frac{\partial\omega}{\partial x_j}\right)+G_\omega-Y_\omega+D_\omega \tag{5}$$

Unde: $G_k$ este coeficientul de generare a energiei cinetice turbulente, datorită gradienților vitezei mediei, $G_\omega$ reprezintă rata specifică de disipare a energiei cinetice turbulente. $\Gamma_k$ şi $\Gamma_\omega$ reprezintă difuzia efectiva a lui k, respectiv ω. $Y_K$ şi $Y_\omega$ reprezintă difuzivitățile efective ale lui k şi respectiv reprezintă ω. $D_\omega$ este un coeficient de difuzie.

## 4. Simularea numerică.

Pentru a ajunge la o varianta optimă de placă trebuie efectuate teste pe diferite modele de plăci, având unghiuri de înclinare diferite. Datorită costurilor ridicate de producție pentru fiecare model de placă ce ar trebui studiat experimental, se va utiliza simularea numerică, ce permite studiul diverselor geometrii fără ca acestea sa fie realizate fizic. In urma rezultatelor simulării se va alege varianta optimă de placă – cea pentru care transferul global de căldură este mare și pierderile de presiune sunt mici.
Această simulare reprezintă un prim pas în vederea optimizării parametrilor geometrici necesari la construcția plăcilor schimbătoarelor de căldură. Studiul s-a axat pe determinarea transferului de căldură peste o placă ondulată (figura 1) între cele două zone de lichid ce străbat placa reprezentate de apa rece și apa caldă.
Conform celor amintite in capitolului 2, simularea se va face utilizand softul FLUENT – modelul de turbulență k-ω SST. Literatura de specialitate recomandă utilizarea modelului de turbulență amintit pentru acest tip de geometrie. [9, 10]
Pentru simulare s-au impus urmatoarele condiții la limită:

- Temperatura de intrare apă rece $t_{iar}$ = 293 K;
- Temperatura de intrare apă caldă $t_{iac}$ = 353 K;
- Viteza de intrare a apei în domeniul de interes, atât pentru apa caldă cât și pentru apa rece a fost $v_{ar} = v_{ac}$ = 0.2 m/s;
- S-a considerat că pereții exteriori sunt adiabați;
- Tipul de curgere ales este în contracurent.

S-a urmărit distribuția temperaturilor pe placă în 4 plane: primul plan a fost situat pe placă, al doilea într-un plan situat la 1 mm față de placă în zona rece, al treilea plan la 1 mm față de placă în zona caldă și al patrulea plan a fost unul longitudinal. Rezultatele simulării sunt redate în continuare.

- Distribuția temperaturii pe placă – din simularea numerică se observă importanța canalelor ondulate care ajută la creștere zonelor turbulența. Acest lucru se reflectă în creșterea coeficientului de transfer de căldură.

**ISSN 1454 - 8003**
**Proceedings of 2011 International Salon of Hydraulics and Pneumatics - HERVEX**
*9 – 11 November, Calimanesti-Caciulata, Romania*

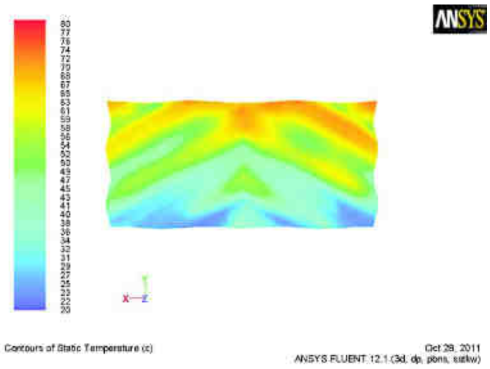


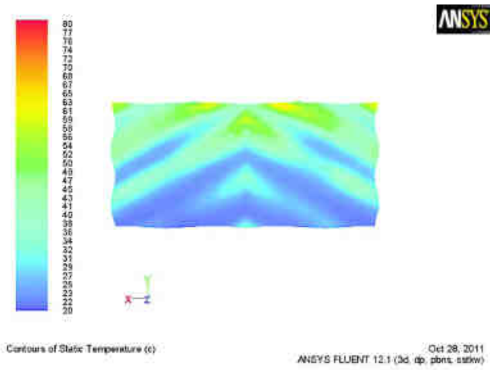


Fig. 4 Distribuția temperaturilor

a. apa caldă b. apa rece

In figura 4 este prezentată distribuția de temperatură pe zona de curgere a fluidului 4.a – cald, respectiv 4.b – rece. Se observă modul de transfer de căldură de la fluidul cald la cel rece (apa caldă pe parcursul trecerii peste placă se răcește, iar apa rece se încălzește).

- Distribuția temperaturilor într-un plan situat la 1 mm fața de placă în zona caldă respectiv zona rece

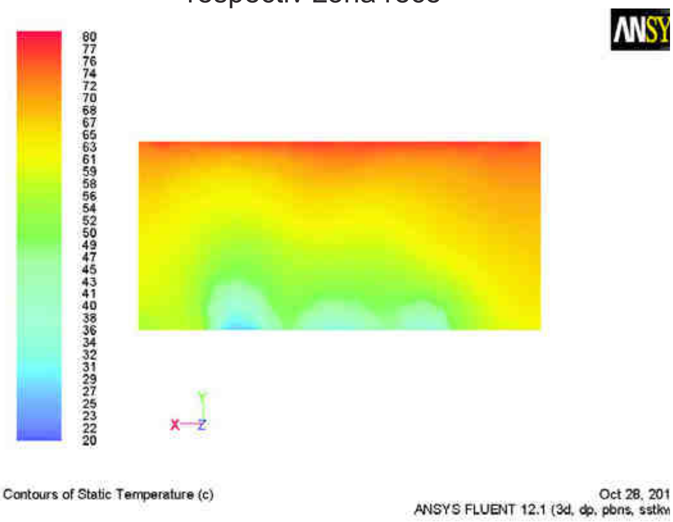


Fig. 5 Distribuția temperaturilor într-un plan situat la 1 mm față de placă în zona caldă

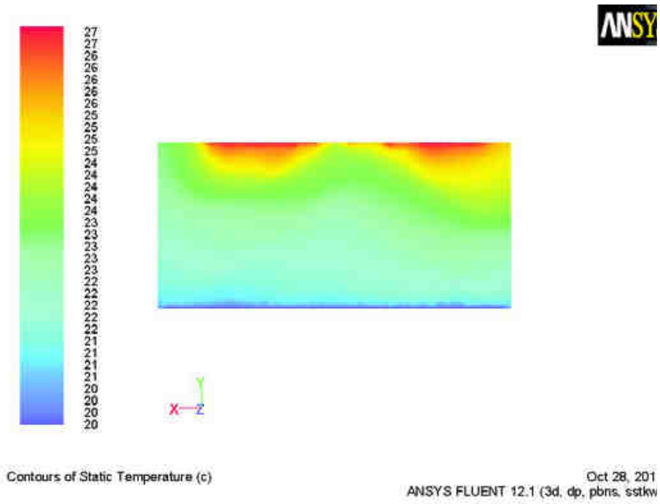


Fig. 6 Distribuția temperaturilor într-un plan situat la 1 mm față de placă în zona rece

Din câmpul de temperatură figura 5 se poate observa că în zona de intrare (cea de sus), gradientul de temperatură este maxim datorită regimului de curgere turbulent și începe să scadă până la ieșirea din domeniul studiat. In figura 6, gradientul de temperatură are valoarea cea mai mică în zona de intrare a fluidului rece și incepe să crească, în timp ce se realizează transferul de căldură de la apa caldă la cea rece.Valoarea maximă a temperaturii apare în zona de intrare a lichidului cald (figura 5), în timp ce cea mai scăzută temperatură apare în zona de intrare a fluidului rece (figura 6).

- Distribuția temperaturilor în plan longitudinal evidențiază cele doua zone de curgere a fluidelor separate de placă

**ISSN 1454 - 8003**
**Proceedings of 2011 International Salon of Hydraulics and Pneumatics - HERVEX**
*9 – 11 November, Calimanesti-Caciulata, Romania*

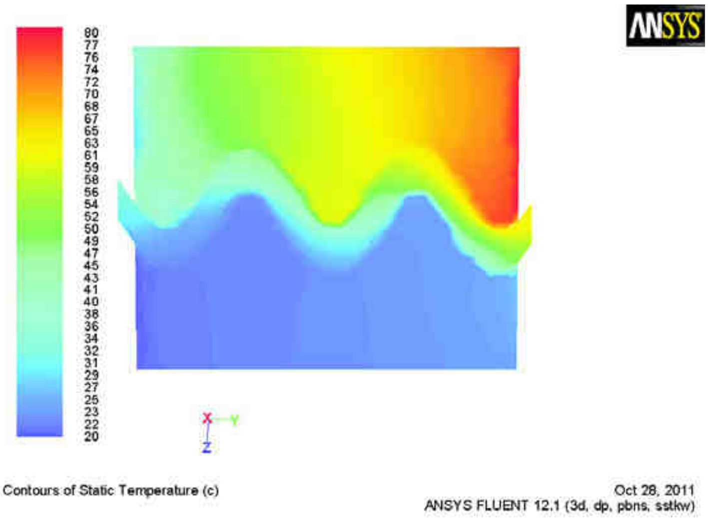


Fig. 7 Distribuția temperaturilor în plan plan longitudinal

## 4. Concluzii

Simularea numerică de tip CFD ofera soluții optime în studiul curgerii fluidelor pe o placă, în vederea găsirii geometriei pentu care raportul dintre coeficientul global de transfer de căldură și pierderile de presiune să fie optim. Această analiză constituie un prin demers pentru simularea curgerii prin schimbătoarele de căldură. Modelul geometric s-a realizat la scara 1:1 respectând dimensiunile unui model de placă existent. Datorită faptului că la discretizarea modelului geometric s-au utilizat un numar mic de elemente, rezultatele obținute în urma simulării nu au fost satisfăcătoare în zona de fluid rece. Acest fapt s-a datorat apariției unor zone de turbulență care au făcut ca lichidul rece să fie direcționat spre zona de intrare. In schimb, în zona caldă transferul de căldură s-a realizat, iar rezultatele au fost asemănătoare cu cele precizate în literatura de specialitate. Viitoarele simulări vor avea ca bază de pornire prezentul studiu, cu specificația că geometriei existente i se vor adăuga două zone netede, una de intrare și una de ieșire, necesare distribuției uniforme a fluidului în canalele de curgere ale plăcii schimbătorului de căldură. In acest mod se vor evita zonele turbionare ce fac ca fluidul să fie impins spre zona de intrare.

**MULȚUMIRI:** Această lucrare a fost realizată cu sprijinul acordat prin proiectul " QDOC - Creșterea calității studiilor doctorale în științe inginerești pentru sprijinirea dezvoltării societății bazate pe cunoaștere" contract nr. POSDRU/107/1.5/S/78534, proiect cofinanțat din Fondul Social European prin Programul Operațional Sectorial pentru Dezvoltarea Resurselor Umane 2007-2013.

## BIBLIOGRAFIE

[1] Plesa A., Metodologia cerectarilor teoretice privind utilizarea schimbatoarelor de caldura cu placi in instalatiile frigorifice, UTC-N 2003
[2] Z.N. Zhao, "Effects of the corrugated inclination angle on heat transfer and resistance performances of plate heat exchangers", vol. 5, pg. 2–3, 2001 [Petro-Chemical Equipment]
[3] G.M. Zhang, M.C. Tian, "Simulation and analysis of flow pattern in cross-corrugated plate heat exchangers", vol. 18(5), pg. 547–551, 2006 [Journal of Hydrodynamics]
[4] A.W.G. Jorge, J.M. Pinto, Modeling of plate heat exchangers with generalized configurations, Internatonal Journal of Heat and Mass Transfer 46 (2003) 2571–2585.
[5] Y.C. Tsai, F.B. Liu, P.T. Shen, Investigations of the pressure drop and flow distribution in a chevron-type plate heat exchanger, vol. 36, pg. 574–578, 2009 [International Communications in Heat and Mass Transfer]

[6] Y.M. Raquel, C.C.G. Flavio, C.T. Carmen, A.W.G. Jorge, “The effect of flow arrangement on the pressure drop of plate heat exchangers”, vol. 63, pg. 5386–5393, 2008 [Chemical Engineering Science]
[7] Xiao-Hong Han, Li-Qi Cui, Shao-Jie Chen, Guang-Ming Chen, Qin Wang, “A numerical and experimental study of chevron, corrugated-plate heat exchangers”, vol. 37 ,pg. 1008-1014, 2010, [International Communications in Heat and Mass Transfer]
[8] Pelletier, O., Strömer, F., Carlson, A., “CFD simulation of heat transfer in compact brazed plate heat exchangers”, vol. 111(1) pg.846-854, 2005. [ASHRAE Transactions]
[9] Kanaris, A.G., Mouza, A.A., and Paras, S.V., 2005, Flow and heat transfer in narrow channels with corrugated walls CFD code application, Chemical Engineering Research and Design, 83 (5 A):460-468.
[10] www.fluent.com – Fluent Users Guide

**ISSN 1454 - 8003**
**Proceedings of 2011 International Salon of Hydraulics and Pneumatics - HERVEX**
*9 – 11 November, Calimanesti-Caciulata, Romania*

# EXPERIMENTAL RESEARCH A CONTROL SYSTEM OF CAPACITY RADIAL PISTONS PUMPS

PhD.Eng.Ioan LEPĂDATU[1], Dipl.Eng. Liliana DUMITRESCU[1], PhD.Eng.Cătălin DUMITRESCU[1]

[1]Hydraulics and Pneumatics Research Institute in Bucharest

**Abstract**
The rotary volumetric pumps with radial pistons used in hydraulics have been very little studied in Romania and when the issue was approached it was only theoretically.
The paper presents the results of the experimental studies performed by the author on a positioning servo mechanism used for regulating the geometrical volume of the pumps with radial pistons.
For developing the research, the author has projected and realized the experimental model of the mechatronic positioning system and the test stand.
In this first paper presents experimental measurements carried out on servo static.

**Key words**: mechatronic system, positioning servo mechanism, volumetric pump, flow regulation

## 1. Introduction

The hydraulic power systems use as a working medium a fluid under pressure. The generators of hydrostatic energy, named currently volumetric pumps have the role of supplying the pressure power for the operational fluid. This is then used by the hydraulic motors for producing mechanical work for power mechanisms. A volumetric pump is energetically efficient if it supplies only the flow required by the system [1], which means that it must be capable to change continously its geometric volume.

At modern pumps the regulation of the geometric volume is achieved by means of mechatronic positioning systems.

In fig. 1 is shown a functional scheme of such a mechatronic system which operates with hydraulic power [2].

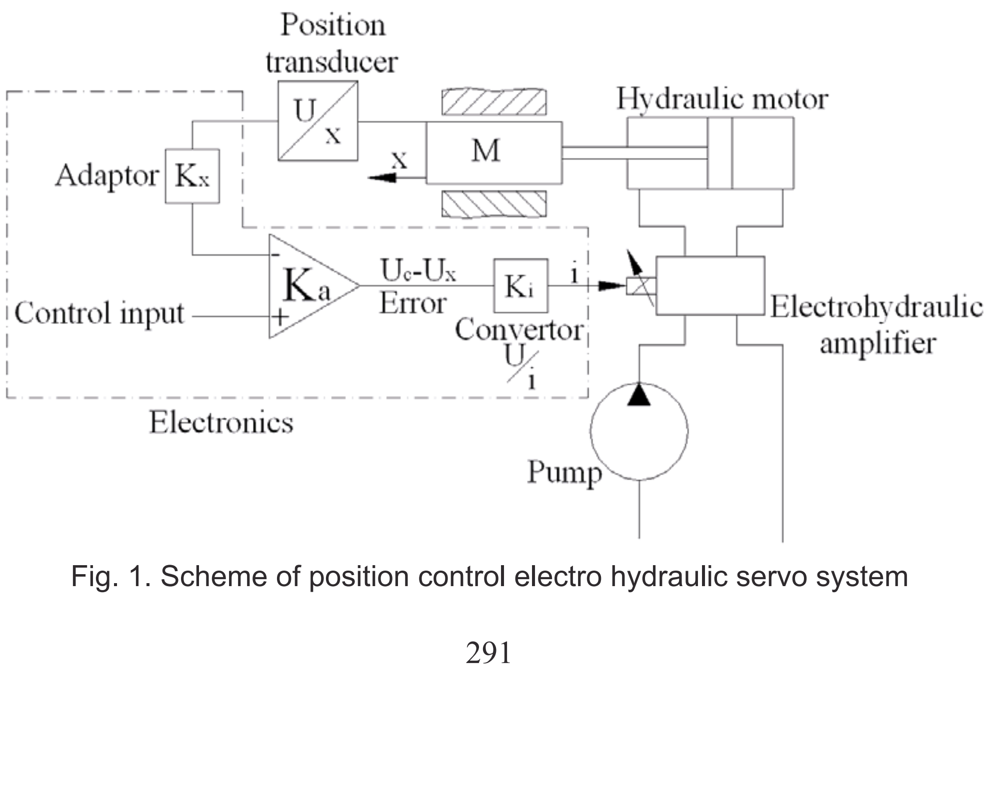


Fig. 1. Scheme of position control electro hydraulic servo system

M – load mass, x – piston displacement, $k_x$ – calibration coefficient position information, $k_i$ – conversion coefficient voltage / current, $k_a$ - error amplification factor

The system includes the following components:
- linear hydraulic motor which may be a double or single-acting hydraulic cylinder;
- electrohydraulic amplifier which may be servo valve or proportional distributor;
- displacement or position transducer;
- electronics.

## 2. The experimental model of the servo mechanism

In fig. 2 is presented the scheme of the functional model tested experimentally and in fig. 3 is given a photo of the realized physical model.

The structure of the servo mechanism is the classic one used by all the manufacturers of pumps with blades or radial pistons. The experimental model was realized using the electrohydraulic amplifier D 930 MOOG with integrated electronics [3]. The mechanical components of the positioning system and the linear hydraulic motor were designed and realized by the author at the institute (INOE 2000 IHP).

The influence of the various parameters (the diameters of the pistons, clearances of the hydraulic motor, the constant of springs, the supply pressure etc.) on the dynamics of the system was determined by numerical simulation. It was used the software package AMESim of the French company „Imagine" [4].

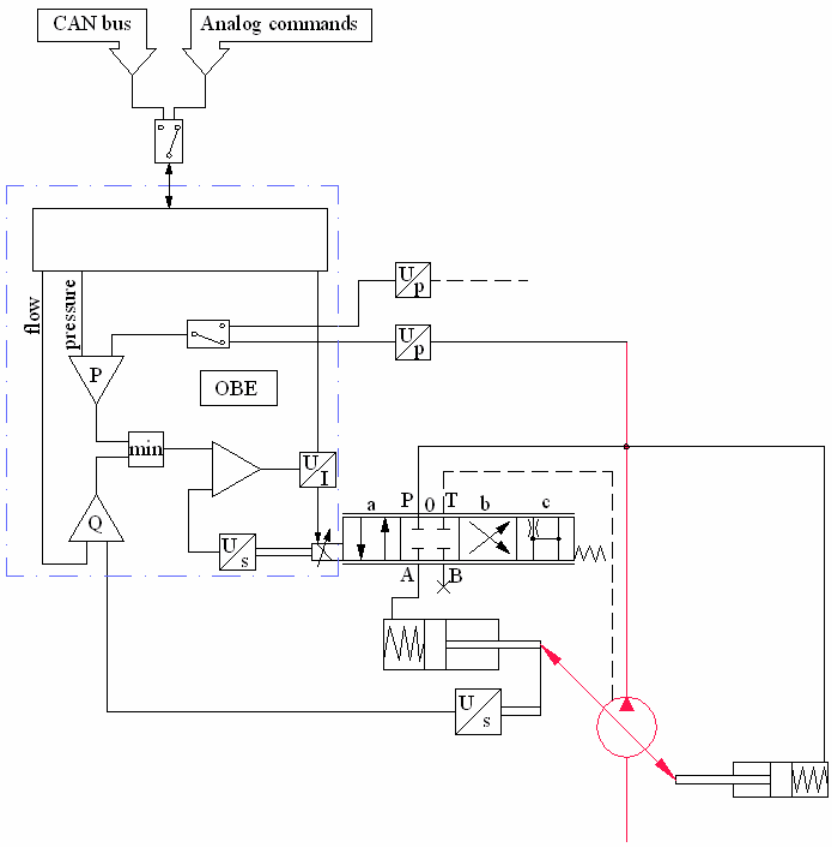


Fig. 2. Diagram of functional model of positioning servomechanism
CAN (Controller Area Network), OBE (Integrated (On Board) Control Electronics)

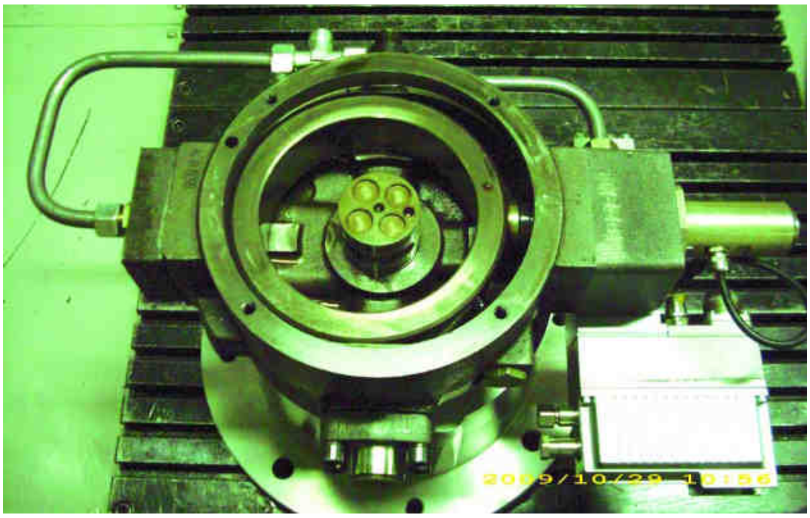


Fig. 3. Functional model of positioning servomechanism

## 3. Test stand

The scheme of the stand used for experimental research is shown in fig. 4 The source of hydraulic energy consists of: a pump (P) powered by an electric motor, a safety valve used for regulating pressure (SS) and a high fineness filter (F).

The integrated control electronics compares and processes signals received from the stroke transducer and the generator of functions (GFA) by means of which the positioning tracks are programmed based on the electric power which supplies the proportional distributor. All the measured electric signals, processed in the system are gathered by a data acquisition system (SAD) and send to a computer where are memorized in a standard format system, as database.

The voltage source (STT) sends signals to the electronic amplifier to simulate the set pressure reaching by the pump on which is mounted the positioning device already tested.

Technical parameters:

a) The positioning mechanism:

| | | |
|---|---|---|
| - positioned mass | M = 3,05 kg | |
| - large area piston | D = 32 mm | A = 804,25 mm$^2$ |
| - small area piston | d = 22 mm | a = 380,13 mm$^2$ |
| - eccentricity range | e = -5…+5 mm | |

b) Control circuit:

| | |
|---|---|
| - flow | 6 l/min |
| - pressure | 20 bar |

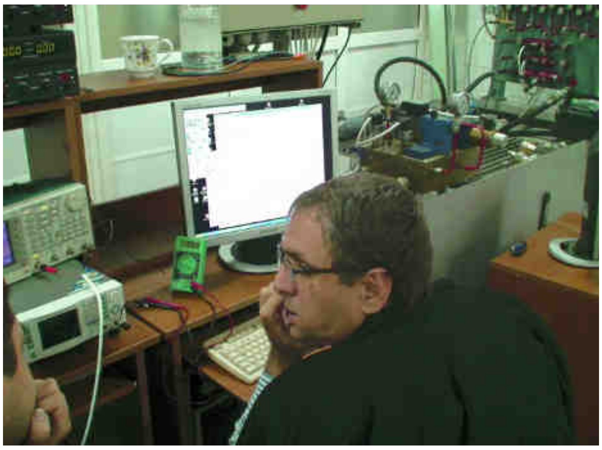

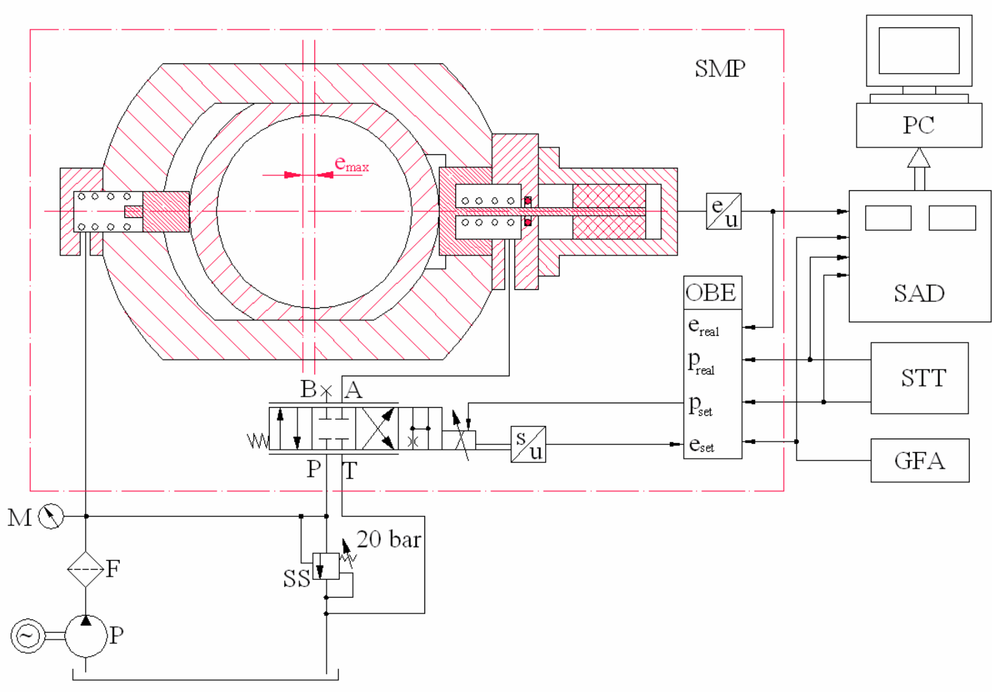


Fig. 4. Diagram of the experimental research stand

SMP-mechatronic positioning system
SAD-data acquisition system
STT-stabilized voltage source
GFA-generator of aleatory functions
SS-safety valve
OBE-on board electronics

F-filter
M-manometer
P-pump
$e_{set}$-set eccentricity
$e_{real}$-reached eccentricity
$p_{set}$-set pressure
$P_{real}$-reached pressure

## 4. Quasi – static experimental tests

For finding the behavior in static operational state of the positioning system were applied control signals $U_c$ in the range between 0...10 V increasing and decreasing, of various shape and a range of frequencies of 1; 0,7; 0,35 and 0,1 Hz.

### *4.1. The response to the signal in the increase/decrease range*

The tests were performed for control signals with max. amplitude and frequencies of 1; 0,7; 0,35 and 0,1 Hz .The results for the values of 1 Hz and 0,1 Hz are shown in the diagrams from the fig. 5. In the table is shown the delay between specified and reached for ups and downs at a certain moment chosen at random T.

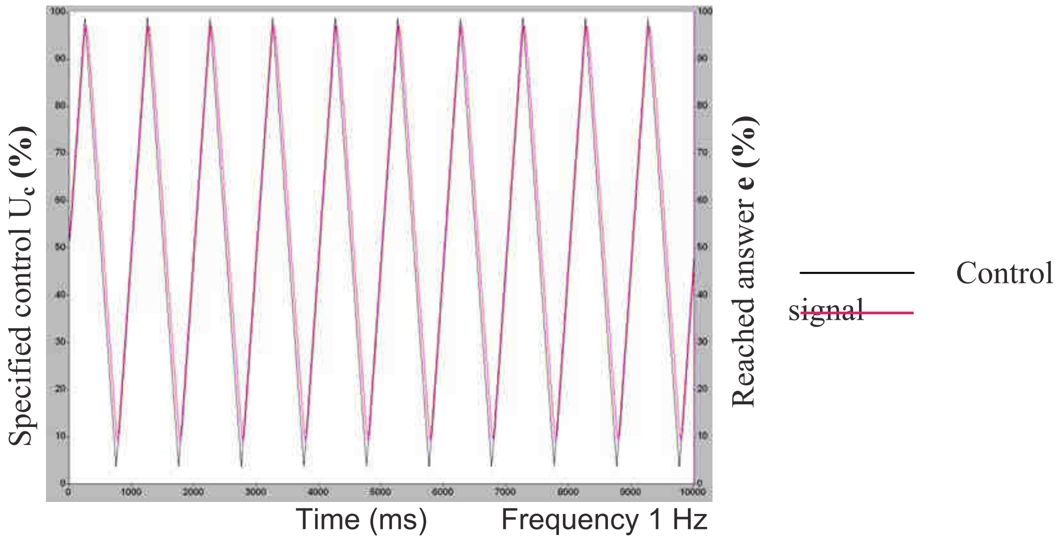


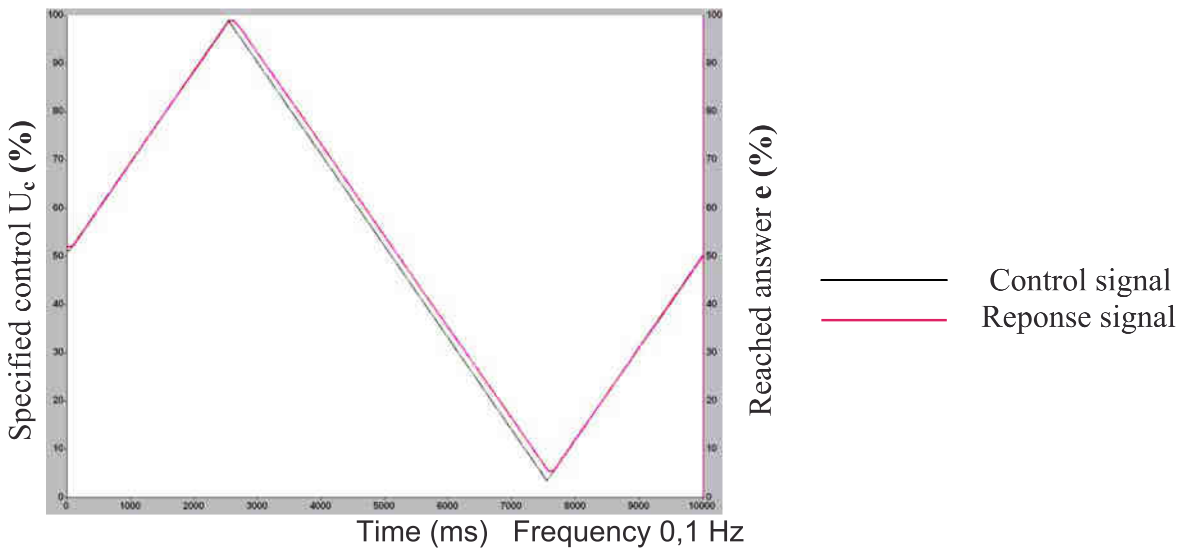


Fig. 5. Response of the positioning system to increasing/decreasing ramp-type signal

*Table 1*

**Lag between preset and obtained value in case of an increasing /decreasing ramp-type signal**

| **Time (ms)** | **Sense** | **Specified (%)** | **Reached (%)** | **Difference (%)** |
|---|---|---|---|---|
| 1000 | upward | 49.7370986415577 | 46.9134193908708 | 2.82% |
| 1500 | downward | 52.7455696644891 | 59.8680415163945 | 7.12% |

Frecvența 1 Hz

| **Time (ms)** | **Sense** | **Specified (%)** | **Reached (%)** | **Difference (%)** |
|---|---|---|---|---|
| 2000 | upward | 88.5573180303273 | 88.6701482377609 | 0.11% |
| 4000 | downward | 71.1325538819081 | 73.2525682022705 | 2.12% |

Frecvența 0,1 Hz

It is found that the delay between specified and reached increases in the same time with the frequency and is higher donwards than upwards.

**ISSN 1454 - 8003**
**Proceedings of 2011 International Salon of Hydraulics and Pneumatics - HERVEX**
*9 – 11 November, Calimanesti-Caciulata, Romania*

### *4.2. The response to the low frequency sinusoidal signal*

The tests were made for prompts with max amplitude and frequencies of 1; 0,7; 0,35 and 0,1 Hz.

The results obtained for the values of 1 Hz and 0,1 Hz are shown in the diagrams from 6. In the table 2 is presented the delay between specified and reached for ups and downs at a certain moment chosen at random T.

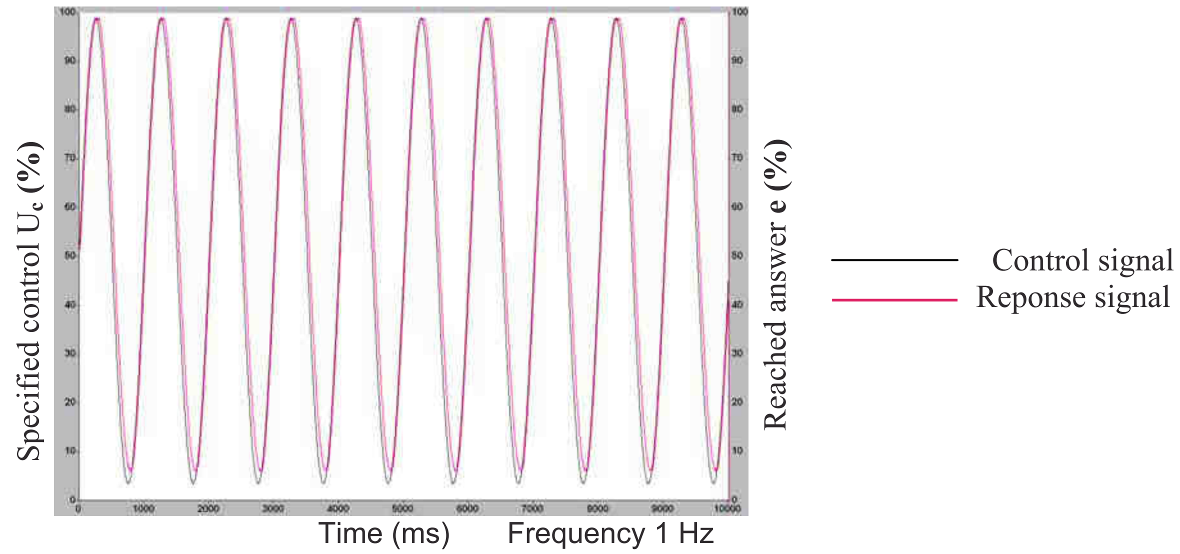


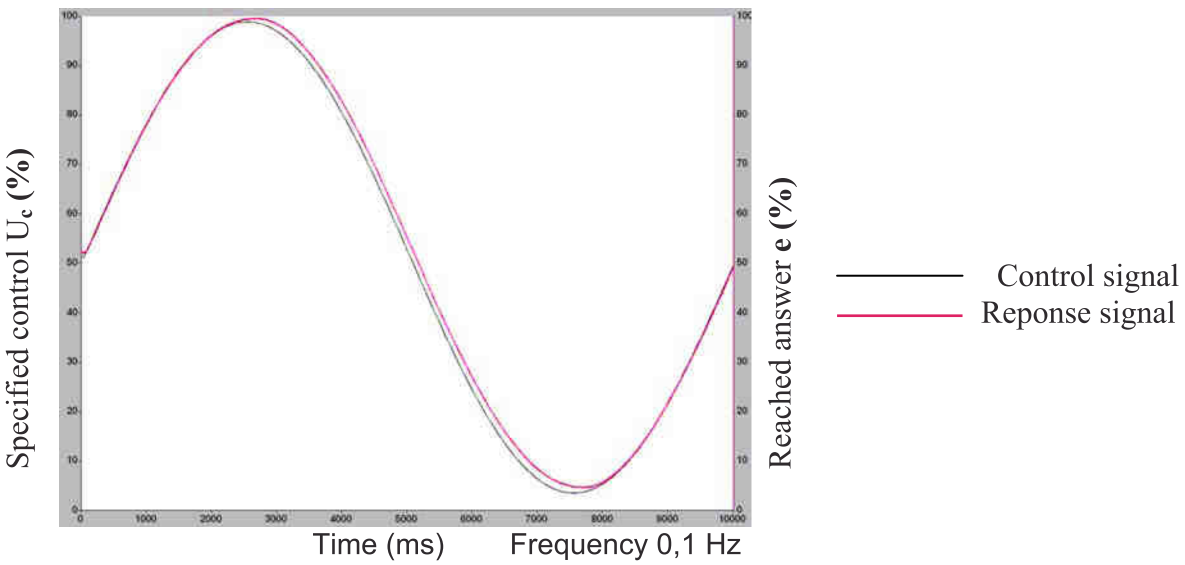


Fig. 6. Reponse of the positioning system to low frequency sinusoidal signal

*Table 2*

**Lag between preset and obtained value in case of a low-frequency sinusoidal signal**

| Time (ms) | Sense | Specified (%) | Reached (%) | Difference (%) |
|---|---|---|---|---|
| 1000 | upward | 48.3726078410567 | 44.0732337721616 | 4.3% |
| 1500 | downward | 54.1412259937081 | 64.1677742408697 | 10.03% |

Frequency 1 Hz

| Time (ms) | Sense | Specified (%) | Reached(%) | Difference (%) |
|---|---|---|---|---|

| | | | | |
|---|---|---|---|---|
| 2000 | upward | 96.0911535185473 | 96.2432511385023 | 0.15% |
| 4000 | downward | 80.428514170209 | 82.5280050154415 | 2.1% |

Frequency 0,1 Hz

It is found that the delay between specified and reached increases in the same time with the frequency and it is higher downwards than upwards.

### *4.3. The static characteristic of the system*

The relation between the specified prompt and the response of the system was determined for a control signal of an increasing decreasing range of frequencies between 0,1 and 0,0005 Hz (fig. 9).
It is found that the hysteresis decreases with the frequency.

Reached response **e (%)**

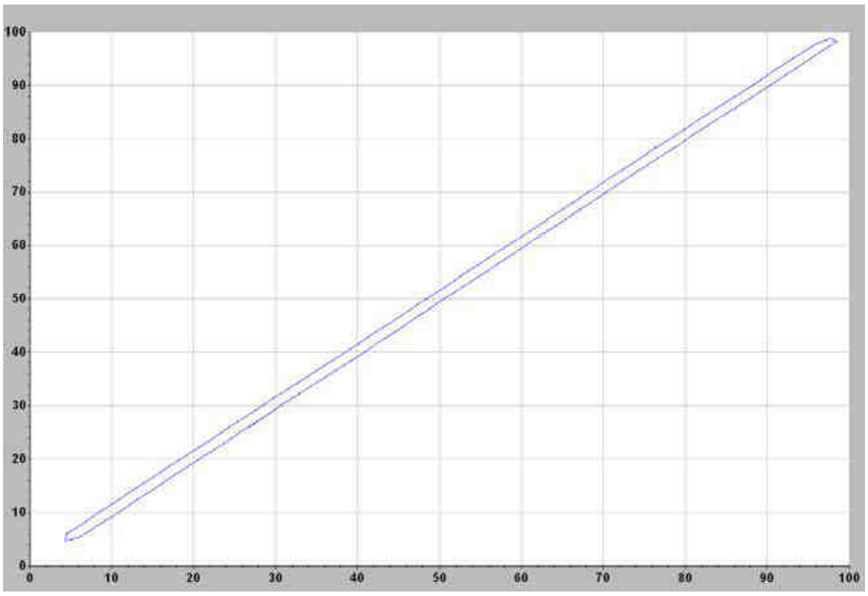


Frequency 0,1 Hz

Specified control $U_c$ **(%)**

Reached response **e (%)**

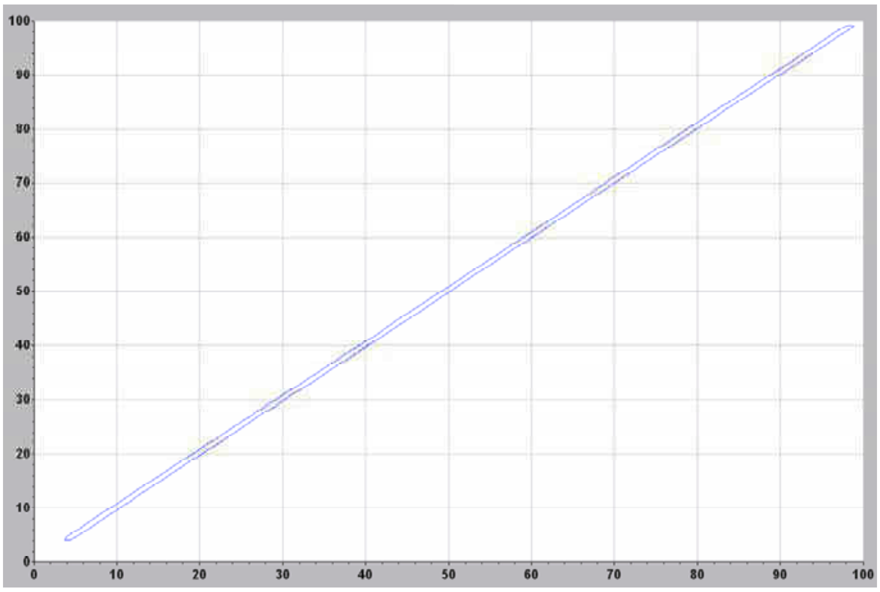


Frequency 0,03 Hz

Specified control $U_c$ **(%)**

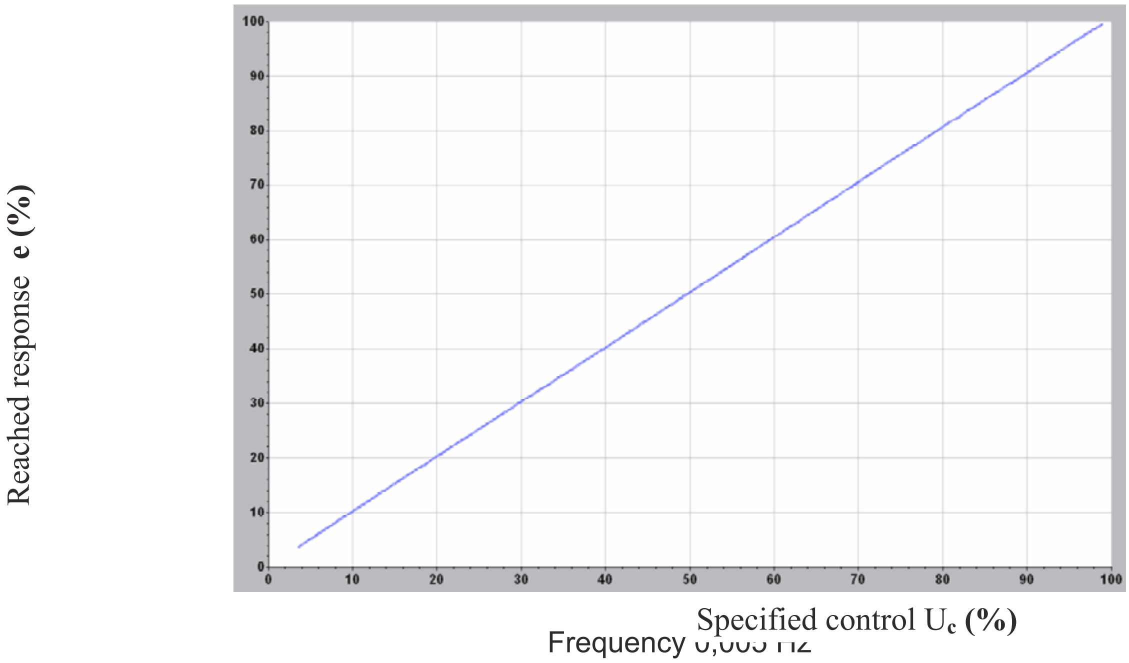


Fig. 7. Static characteristic of positioning system

## 5. Conclusions

The experimental model projected and realized by the author at the institute INOE 2000 IHP (The R & D Institute of Hydraulics and Pneumatics) was in accordance with the functional requirements of a positioning mechanism used for regulating the geometrical volume of the pumps with radial pistons.
The test stand designed and realized by the authors was used for performing on it the experimental studies in static and dynamic conditions of the system.
Under dynamic experimental research conducted by the authors will be presented in the future paper.

## B I B L I O G R A P H Y

[1]. *Alexandrescu, N.* – Mechatronic Positioning System with Hydraulic Actuation - Proc International Conference on Multidisciplinary Desing in Engineering, Montreal, Canada, 2001
[2]. Mannesmann Rexroth – Hydraulik Trainer Vol 2, Schleunung Druk SD GmbHCo, 1986
[3]. *** - MOOG Cataloague – Hydraulics Components, 2008/09
[4]. *** - AMESIM Catalogue – www.amesim.com/

**ISSN 1454 - 8003**
**Proceedings of 2011 International Salon of Hydraulics and Pneumatics - HERVEX**
*9 – 11 November, Calimanesti-Caciulata, Romania*

# MATHEMATICAL MODELING AND NUMERICAL SIMULATION APPLIED OF HYDRAULIC SYSTEMS IN ORDER TO IMPROVE EFFICIENCY THROUGH CONVERSION AND ENERGY RECOVERY

Adrian Georgian PANTIRU[1], Bogdan MIHALESCU[2], Petrică KREVEY[3], Constantin CĂLINOIU[4]

[1]. Hydraulics & Pneumatics Research Institute of Bucharest, Romania
[2]. University POLITEHNICA of Bucharest, Romania
[3]. Hydraulics & Pneumatics Research Institute of Bucharest, Romania
[4]. University POLITEHNICA of Bucharest, Romania

**Key words:** conversion, hydraulic drives, simulation, AMESim

**Abstract:** The paper approaches the study of a hydraulic device with mixt adjustment which is present in the equipping of the INOE 2000-IHP Bucuresti laboratory, comprising primarly a MOOG servopump and secondarly a BOSCH servomotor. The main original aspect of the paper consist in the realization of some simulation models in AMESim, specific for the servopump and transmission.

The objectives of the paper:
- study the behavior of a volumetric hydraulic pump with adjustable volume equipped with a numerical electronic module which may be giben configuration for various types of compensators (for flow,pressure,power and minimal compensator)
- study the behavior of the stand used for recoverying the hydrostatic energy realized with equipment for primary and secondary adjustments

Simulations were performed by means of the package of AMESim simulation programs. By the numerical simulation of the running of the volumetric pumps equipped with numerical electronic control block, pressure and displacement transducers for the indirect measurement of the pump capacity were put into evidence the possibilities of configuration of the electronic block for obtaining various types of compensators, without being necessary to modify the pump structure. Simulations were performed for pumps equipped with numerical flow, pressure, power and minimal compensators.

The results are presented in graphical form. Simulations regarding the work of the volumetric pump equipped with the minimal compensator put into evidence the fact that this compensator valuates efficiently the Load sensing mechano hydraulic device. This type of compensator has the advantage that eliminates hydraulic throttle from the discharge pipe of the pump required for measuring flow and in this way are eliminated load and energy losses from the system. The results obtained during simulation of the work of the experimental model of the stand performed in the lab allow us to assume that the fluid power installations offer the possibility of performing some complex experiments for studying various phenomena which may appear in the hydraulic drive system with secondary adjustment and recovery of energy.

## 1. Introduction

Mechatronics is a combination of multiple well known engineering domains: mechanics electronics computer science, therefore it does not represent a new engineering domain but a concept which is based on the integration and interaction of the specific engineering domains mentioned above.

The integration on wide scale micronisation the technology of the components mounted on the surface SMT made possible the integration of the electronic modules specific for sensors into their structure. The use of new materials and technologies at making actuators allow reaching high performance at minimal volume. The operational mechanism comprises both afferent sensors and the adaptation electronics and also the actuators and electromechanical convertors and their drivers.

It should be mentioned that the electronics of the sensor and of the actuator may be equipped with microcontrollers having implemented a purposefully created software so that the entire system becomes smart. In this case it may communicate directly with the process manager or other smart subszstems. This kind of smart mechatronic systems become increasingly used on large scale.

The hydraulic regulation apparata are elements which allow the regulation of certain specific parameters in the installations with hydraulic drive from the industrial field. Initially the command of these apparata was performed manually by means of mechanical elements. Then this was replaced by electric devices(electromechanic convertors) These devices required electronic blocks which provided electric supply at desired parameters (voltage current etc.) and were attached to the control panels of the installation.

The advantage of these systems was the transmission of the prompt of the hydraulic drive element through electric cable allowing remote control.

The volume of a volumetric pump is defined as theoretical volume which is aspired and discharged from it at a complete revolution.

At first generation of volumetric pumps the volume or the geometrical volume could not be adjusted which meant that at a constant drive revolution the flow of the pump is approximately constant. These type of pumps is efficient in those applications at which the speed of the hydraulic motor supplied by the pump with constant volume has a very slight variation. If the distance between the max and the min speed of the motor is big then these pumps are no more efficiently working energetically cause the difference betweeen the flow discharged by the pump and that accepted by the motor turns back in the reservoir of the installation at the operational pressure.

That part of the hydraulic power (flow x pressure) supplied by the pump and not consumed by the hydraulic motor is lost in the form of heat stored in the fluid operational field and then is dissipated in the environment. The need for reaching an increased energetic efficiency of the high power pumps led to the development of a second generation of generators of hydrostatic energy that of the pumps with adjsutable cylinder volume. For the adjustment of the volume of this type of pumps was conceived a wide variety of devices which may be classified into two groups:
● control and servo control devices; manual, mechanical, hydraulic, etc.;
● regulation devices for pressure flow power, load-sensing etc.

## 2. Mathematical modelling

It was made for a hydraulic drive installation with secondary adjustment comprising in its structure the following main subassemblies
- pressure source (volumetric pump with fix volume driven at constant speed;
-hydraulic motor with adjustable capacity;
-module for simulating the load (volumetric pump with fix volume and proportional valve for adjusting pressure).
- safety regulation and control element

For performing the mathematical modelling were written the characteristic equations for each equipment and the relationships between the different equipment. This apparata was realized in the Laboratory for Hydraulic Drives of INOE 2000-IHP. The Operational diagram of the apparata is shown in fig.1.

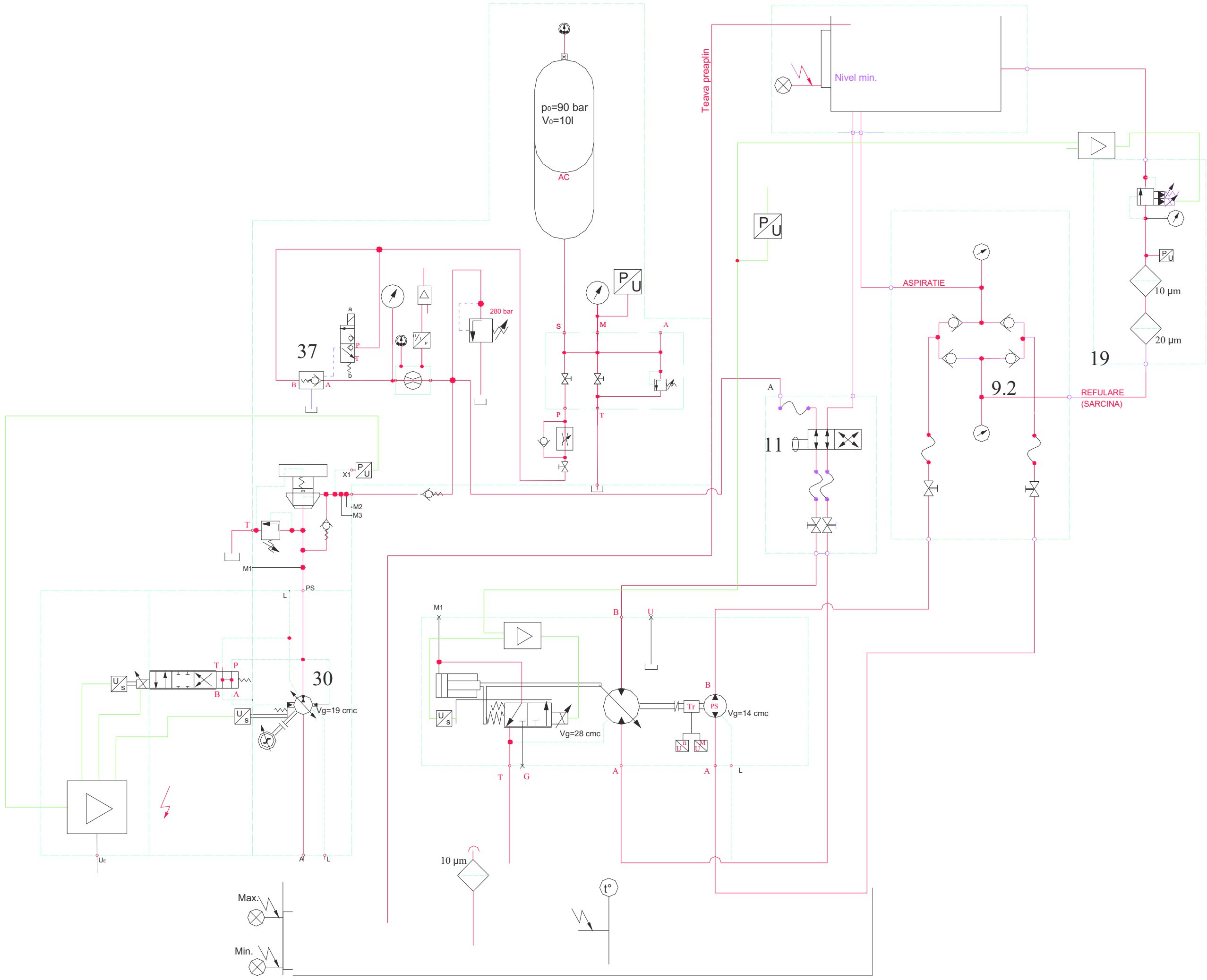


Fig.1 operational diagram of the hydraulic drive installation with secondary adjustment

The mathematical model comprises the following equations:

– The theoretical flow discharged by the pump: $Q_{tp} = V_p \cdot N_p$;

– Leak flow of the pump : $Q_{sp} = K_{sp} \cdot P$;

– Real flow discharged by the pump $Q_p = Q_{tp} - Q_{sp}$;

_ Theoretical flow of the hydraulic motor: $Q_{tm} = V_m \cdot N_m \cdot X$;

_ Leak flow of the motor: $Q_{sm} = K_{sm} \cdot P$;

– Flow consumed by the hydraulic motor: $Q_m = Q_{tm} + Q_{sm}$;

– Equation of continuity: $Q_p - Q_m = \frac{V_0}{E_e} \cdot \frac{dP}{dt}$;

– Torque developed by the hydraulic motor: $M_m = \frac{V_m \cdot P}{2 \cdot \pi}$;

- Equation of the moments balance: $\frac{V_m \cdot P(s)}{2 \cdot \pi} = J \cdot \frac{d^2\theta}{dt^2} + K_f \cdot \frac{d\theta}{dt} + M_r$;
- The characteristic of the valve for limiting pressure: $p = k_s U$ ;
- The characteristic of the speed transducer: $U = k_t N$ ;
- Characteristic of the moment transducer: $U = k_m M$;
- Characteristic of the hydro accumulator: $pV^k = ct.$

**3. Numerical simulation**

The numerical values

The numerical values of the parameters of the equipment composing the installation structure are shown in table 1. Simulations were performed on the base of the assumption that the main pump has a fix capacity for putting into evidence the variation of the hydraulic motor capacity.

Table 1

| Nr. crt | The name of the parameter | Value | Remarks |
|---|---|---|---|
| 1 | Max capacity of the main pump Vp [cm$^3$/rot] | 19 | |
| 2 | Pump revolution $N_p$*[rot/min]* | 1450 | |
| 3 | Nominal discharge pressure of the pump $P_{pnom}$ *[bar]* | 315 | |
| 4 | pump leek flow at nominal pressure $Q_{scp}$*[l/min]* | 0,5 | |
| 5 | Motor capacity $V_m$ *[cm$^3$/rot]* | 28 | variable |
| 6 | Motor revolution $N_m$*[rot/min]* | - | variable |
| 7 | Nominal supply pressure of the motor $P_{mnom}$*[bar]* | 315 | variable |
| 8 | Motor leek flow at nominal pressure $Q_{scm}$*[l/min]* | *1* | |
| 9 | Inertial moment of the parts driven by the motor *J[Kg.m$^2$]* | 0,05 | |
| 10 | Under pressure oil volume $V_0$ *[l]* | 5 | |
| 11 | The equivalent compresibility module $E_e$*[bar]* | 14.000 | |
| 12 | The volume of the hydro accumulator $V_h$ *[l]* | 2,5 | |
| 13 | Nominal tension of control of the valve *U [V]* | 10 | variable |
| 14 | The capacity of the pump load $V_p$ *[cm$^3$/rot]* | 14 | |

For validating the results of the theoretical research regarding the conversion, recovery, storage and reuse of the hydrostatic energy in the hydraulic drives was realized a mechatronic device for converting mechanical energy into hydrostatic and of the hydrostatic energy into mechanical, this device comprising the following main components>

- Main volumetric pump with adjsutable volume and electronic compensator block
- Volumetric hydraulic motor with adjustable capacity
- Volumetric pump with fix capacity
- Oil reservoir
- Hydraulic bridge with directional valves
- Hydro accumulator for storing hydraulic energy
- Sensors and transducers
- Data acquisition system
- Control system

For performing simulations was realized the simulation network shown in fig.2 The main objective of the activity of numerical simulation was to find the device regulation parameters for keeping constant the speed of the hydraulic motor when the moment from its arbor is variable in time.

- The simulation network comprises the following main hydraulic blocks:

- Volumetric hydraulic pump with adjustable capacity equipped with pressure compensator
- Volumetric hydraulic motor with adjustable capacity
- Secondary volumetric pump for the simulation of the hydraulic motor load
- Hydraulic bridge with directional valves
- Hydro accumulator
- Pressure transducer
- Revolution transducer
- Valve for limiting pressure in the hydraulic circuit of the main pump

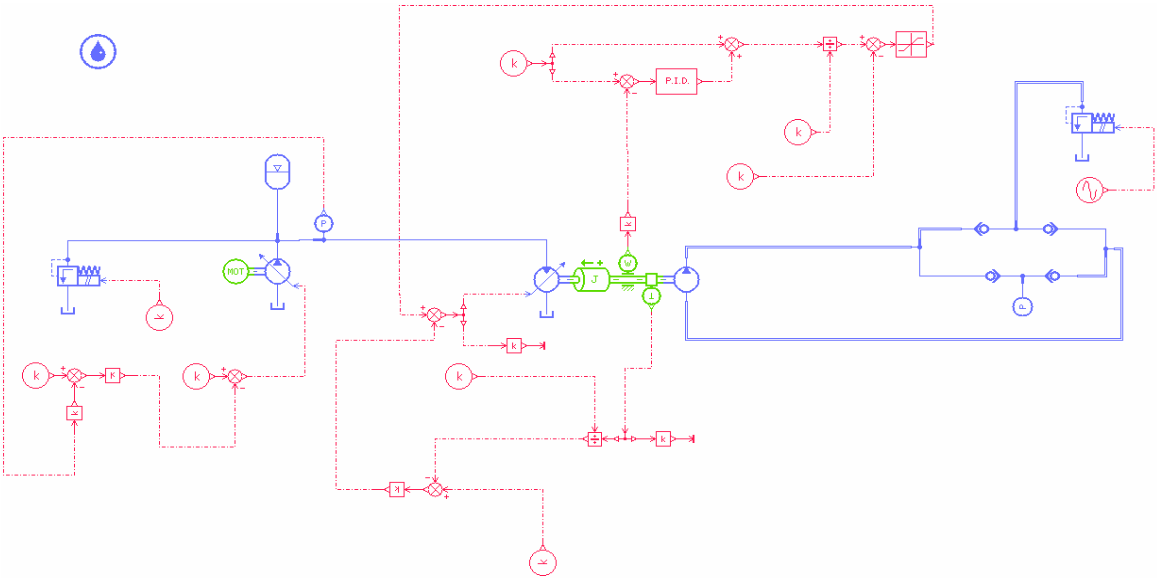

Fig. 2. Scheme of the simulation network

The oil flow discharged by the main pump is used for supplying a hydraulic motor which has coupled at its arbor a volumetric pump with fix capacity. The main pump which has an adjustable capacity is driven by an electric motor with fix revolution. The modification of the resistant moment from the arbor of the hydraulic motor is made by the modification of the discharge pressure of the secondary volumetric pump with fix capacity.

The active moment developed by the hydraulic moment is proportional with the result between the value of its capacity and the value of the pressure drop between its energetic hydraulic couplings. Therefore the attainment of an active moment at the arbor of the motor which to defeat the resistant moment variable in time is realized by modifying the pressure of the supply oil of the motor and by modifying the capacity of the hydraulic motor. In the same time it must be maintained constant the revolution at the arbor of the hydraulic motor and must be modified the value of the oil flow which supplies the hydraulic motor.

All these adjustments must be done in the conditions in which the valve that limits pressure in the main hydraulic circuit it remains shut, there is no oil discharge from the reservoir and no dissipate energy losses.

In figures 3...9 are shown synthetically the results of the simulations performed for maintaining constant the revolution speed of the hydraulic motor when the resistant moment from its shaft is variable in time.

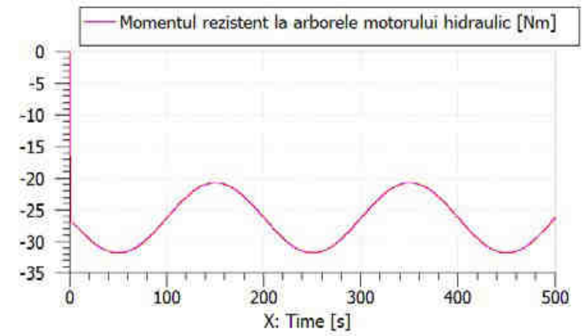


Fig. 3. Variation in time of the resistant moment at the shaft of the hydraulic motor

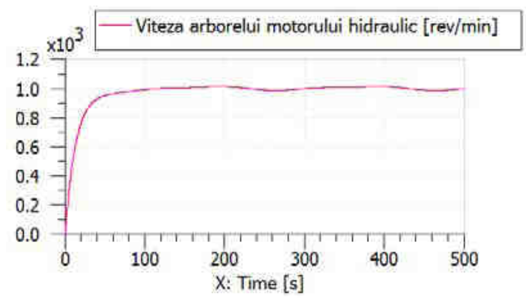


Fig. 4. Variation in time of the speed of the hydraulic motor shaft

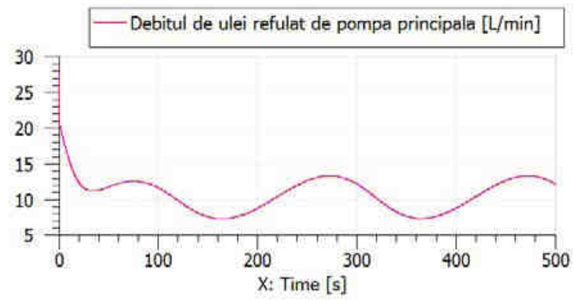


Fig. 5. Variation in time of the oil flow discharged by the main pump

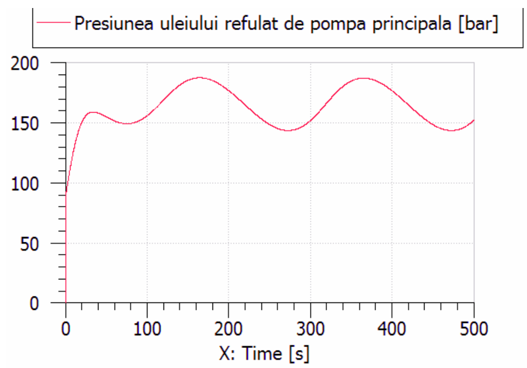


Fig. 6. Variation in time of the pressure of the oil discharged by the main pump

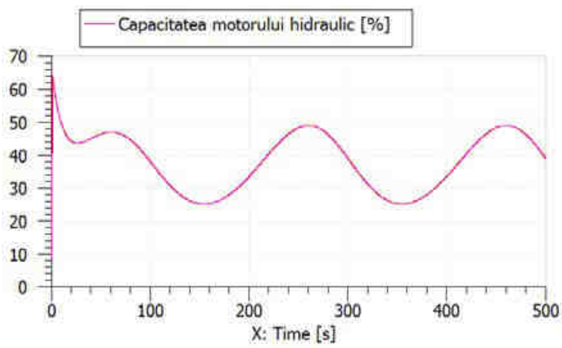


Fig. 7. Variation in time of the hydraulic motor capacity

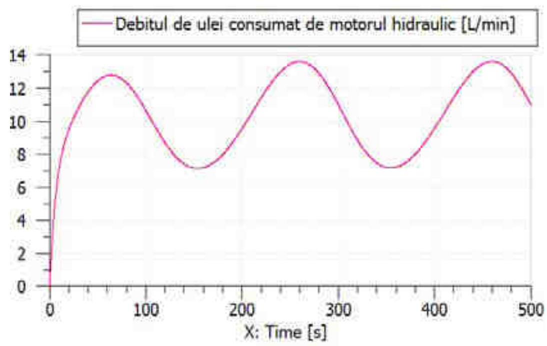


Fig. 8. Variation in time of the oil flow consumed by the hydraulic motor

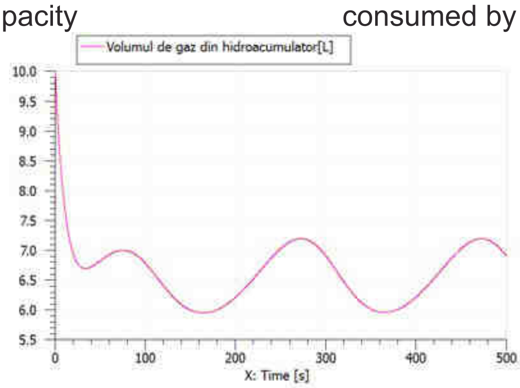


Fig. 9. Variation in time of the gas volume stored in the accumulator

ISSN 1454 - 8003
Proceedings of 2011 International Salon of Hydraulics and Pneumatics - HERVEX
*9 – 11 November, Calimanesti-Caciulata, Romania*

**4. Calculation of the energetic efficiency improvement due to the use of mehatronic components in hydraulic drives**

The improvement of the energetic efficiency in the process of conversion of the mechanical energy into hydrostatic and of the hydrostatic energy into mechanical, its accumulation, storage and reuse, represent the main concerns in the field of hydraulic drives which equip various fix and mobile installations.

Using the formula : $\Delta T = 0{,}055\,\frac{\Delta p}{\eta}$ in which,

ΔT - the increase of the fluid temperature in [ºC];
Δp - operational pressure in [bar];
η - total output of the hydraulic machine.
The amount of heat dissipated by a unit with radial pistons will be:
Q = mcΔT = ρDcΔT in which,
P - density of the hydraulic oil [kg/dm³];
D - flow of the hydraulic machine [l/min];
c - hydraulic oil specific heat [kcal/kg ºC]
For exemplification will take into accountthe following data:
Δp = 300bar; η = 85%;
it results: $\Delta T = 0{,}055\,\frac{300}{0{,}85}$ = 19,4°C, and for
ρ = 0,86 kg/dm³;
D = 26l/min;
c = 0,5 kcal/kg°C;
Q = 0,86*26*0,5*19,5 = 13080,6 kcal/h, in the case in which the flow of the pump is not reduced at minimum by means of the electrohydraulic devices in the inactive work stages of the process.

Taking into account that the caloric power of a kg of conventional fuel is of 7000 kcal/h, it results a saving of 1,86 kg c.c during the inactive work phases of the process.

For the accumulation, storage and reuse of the hydrostatic energy it is presented the calculation methodology for a battery of hydro pneumatic accumulators of V = 25 l each considered as the most recommended for solving the matter. For the exemplification of the calculation it was chosen the situation in which the parameters are those from the experimental stage, the vehicle wheeling with optimum speed, brakes and stops after it covered a certain distance. The set of equations which define the studied process are:

$$\frac{m\,V^2 opt}{2} = L_{12} + Q_{12} \tag{4.1}$$

$$L_{12} = \frac{p_1 v_1 - p_2 v_2}{n-1} \tag{4.2}$$

$$Q_{12} = \frac{\chi - n}{\chi - 1} x L_{12} \tag{4.3}$$

$$\frac{m\,V^2 opt}{2} = \frac{p_1 v_1 - p_2 v_2}{n-1} + \frac{\chi - n}{\chi - 1} x \frac{p_1 v_1 - p_2 v_2}{n-1} \tag{4.4}$$

$$v_2 = \frac{p_1}{p_2} x v_1 - \frac{m}{2} \cdot \frac{n-1}{p_2} \cdot \frac{1}{1 - \frac{1-n}{\chi - 1}} V_{opt}^2 \tag{4.5}$$

Below is presented a method of use of the calculation formula for a real application the jeep ARO 243. The initial data of the problem are :

a) the weight of the car 1800 (kg)
b) the wheeling mode $V_{opt}$ = 60 km/h = 16,6 m/s
c) $p_0$ – the load pressure of the accumulator
$p_0$ = 70 bar
$p_1$ – min operational pressure of the accumulator
$p_1$ = 100 bar
$p_2$ – max operational pressure of the accumulators
$p_2$ = 200 bar
$v_1$ – the summed initial volume of the accumulators
$v_1$ = 50 l

$\frac{m \quad V^2}{2} = \frac{p_2 v_2 - p_1 v_1}{1-K}$ where K = 1,4 for the adiabatic

$v_2 = \frac{mV^2}{2} \cdot \frac{(1-K)}{p_2} + \frac{p_1}{p_2} v_1$ in which replacing the values from above it results :

$v_2$ = 521 l

The energy stored in the accumulators is of 248000 J = 892800 kWh and considering a coefficient of service/year $k_s$ = 1/30, it results an amount of recoverable energy equal with 29760 kwh/year. Making a calculation for a year and energy costs, taking into account the price of a Kwh of 0,48 lei, it results a saving of 14284 lei/year, which is significant. It is aimed to use this saved energy for driving the car in the reverse sense to that in which it was made the recovery.

## 5. Conclusions

By numerical simulation of the operation of the voumetric pumps equipped with numerical electronic control block, pressure and displacement transducers for measuring indirectly the capacity of the pump, were spotlighted the possibilities of configuration of the electronic block for obtaining various types of compensators, without being needed the modification of the pump strucre. Simulations were performed for pumps equipped with numerical compensators of flow, pressure, power and minimal compensators.

Simulations regarding the work of the volumetric pump equipped with the minimal compensator put into evidence the fact that this type of compensator valuates very well the Load sensing mechano hydraulic device. This type of compensator has the advantage that it eliminates the hydraulic throttle from the discharge pipe of the pump required for measuring the flow and are eliminated the load and energy losses from the system.

The results obtained after the numerical simulation of the work of the experimental model allow us to estimate that the hydraulic drive installations offers the possibility of performing some complex experiments for studying various phenomena which may occur in the systems with secondary regulation and energy recovery.

The saving of energy obtained as a result of using the volumetric hydraulic pumps equipped with numerical block of regulation and control is put into evidence by the value of the flow transited through the valve for adjusting the pressure from the main circuit. For maintaining relatively constant the revolution speed of the hydraulic motor independently of the load variation at exit, is realized by modifying the capacity of the hydraulic motor correlated with the value of the supply pressure and the oil flow discharged by the main pump. This thing allows the the maintaining of the supply pressure at a minimum value so that the energy saving to be maximum.

The use of the multiple regulation loops and of a PID electric compensator in the loop for regulating the speed reduces significantly the speed variation range value without affecting the dynamic performances regarding the developed torque shaft.

ISSN 1454 - 8003
Proceedings of 2011 International Salon of Hydraulics and Pneumatics - HERVEX
*9 – 11 November, Calimanesti-Caciulata, Romania*

# EXPERIMENTAL RESEARCH ON POSITIONING LINEAR ELECTROHYDRAULIC SERVO SYSTEMS

**Corneliu CRISTESCU, Petrin DRUMEA, Catalin DUMITRESCU, Ioana ILIE and Iulian DUTU**
institution of the author, e-mail address (Arial, 10pt, Regular)

Hydraulics and Pneumatics Research Institute, INOE 2000-IHP, Bucharest, Romania

***Abstract:*** *The paper presents the results of conducting experimental research on factors influencing the positioning precision/error of linear electrohydraulic servomechanisms. Based on the mathematical model and preliminary experimental research conducted there have been identified factors that influence the positioning accuracy, and have been proposed some measures to control it in normal limits. The experimental results obtained highlight interesting aspects from the scientific point of view; they can be used to optimize the positioning precision of linear electro hydraulic servomechanismsre*

***Keywords****: experimental research, dynamic behaviour, electro hydraulic servomechanisms, positioning servo system, positioning precision, positioning error.*

## 1. Introduction

Systems for automatic control of physical parameters and for automatically maintaining the parameters adjusted to the a priori programmed limits represent one of the newest and most dynamic components of industrial automation in various fields: automotive industry, aviation, industrial robots, manipulators etc. Automatic hydraulic systems are the class of automated systems performing amplification, by hydraulic means, of the control quantity to the level required for the operation quantity. Automatic adjustment hydraulic systems are designed in particular to control the modification of an output quantity of a certain physical system, under the influence of programming and disturbing input quantities of a system, and to precisely adjust the amount of an output quantity, depending on the value of the input quantities [1], this functional role being performed by reaction hydraulic automatic systems containing servo parts hydraulic equipment. Proportional hydraulics technique allows obtaining important benefits, covering the possibility for increasing speed of operative elements, increased *precision of operation* of operative elements, including the absence of shocks to the reversal of direction of movement of the engines.

Servo hydraulics is a complex, interdisciplinary science and it is a system technique itself.

Linear positioning electrohydraulic servomechanisms represent just one special class of these automatic hydraulic systems, and they consists in principle of an *adjustment device*, which consists of the regulator that contains a comparator and an amplifier, as well as a *hydraulic servo cylinder*, consisting of a hydraulic cylinder, an electrohydraulic servo valve and, also, a position measuring system [2]. Hydraulic and electrohydraulic servo valves are used, preferentially and rationally, for *positioning in variable place* a hydraulically driven mechanism, by command, in closed circuit, in closed loop or feedback loop, from a displacement transducer of a servo valve or hydraulic cylinder, in particular, when the positioning precision required is high.

Therefore, research on static and dynamic behavior and, above all, testing of the stability and positioning accuracy of these electrohydraulic servo systems should be made in accordance with specific procedures, they having a decisive influence on the functioning of equipment to which they belong [3].

## 2. Structure of an Electrohydraulic Positioning Servomechanism

Automatic electrohydraulic systems or electrohydraulic servo systems are automatic adjustment systems that are composed of an operative element of hydraulic origin, performing amplification of the control parameter to the size required by the operative part of the physical system it controls/adjusts. Electrohydraulic positioning systems, or systems for automatic control of displacement, are designed to achieve and monitor continuously the position in space of mechanisms controlled (output parameter), based on a signal generated by specialized programming component (signal/ input programming parameter). For the positioning error to be as small as possible, positioning systems operate in closed circuit or in closed loop [4].

The basic structure of an electrohydraulic positioning servo system is shown in Figure 1, which shows that the input parameter $X_i$, which may be a voltage $U_i$, is compared by the electronic comparator EC to the output parameter $U_e$, resulted from the action of the converter CS on the signal CS, then amplified by the signal amplifier AS, derived from the displacement sensor SD, which measures the output parameter $X_e$, which is a displacement/stroke at the linear hydraulic motor LHM shaft, as the operative element on the driven load within the adjusted process PR. The difference between the preset parameter and the size of the output parameter measured by the displacement sensor SD, $DU=U_i-U_e$, is amplified by an electronic amplifier EA, which controls through a corresponding control current IC, with a positive or negative value, the hydraulic proportional distribution element PHE, which usually is a servo valve SV, and produces a flow Q, which is the parameter to be adjusted within the system, and which generates at the linear hydraulic motor LHM a displacement of its shaft, which is the output parameter of the control system $X_e$, with a value fully consistent with the input parameter $X_i$, respectively DU, which produces, ultimately, a corresponding displacement of the load AT, making thus the adjustment by positioning to the desired point, even if random disturbing forces interfere with the operative element (Z), [5].

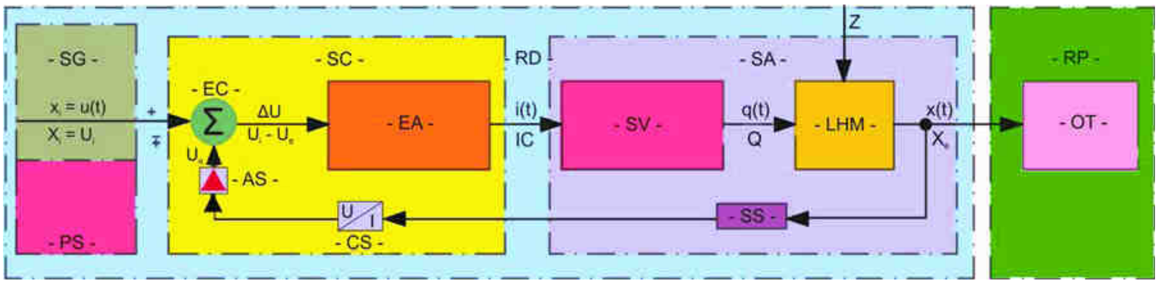


Fig. 1: Basic structure of electro hydraulic positioning servo systems.

Electrohydraulic adjustment servo systems must meet high stability, speed, precision and efficiency requirements. With a start signal there is initiated, on the function generator, a ramp function corresponding to the rated value of the desired position in space. The output signal of the ramp function generator increases over a time set for ramp creation, from 0 V up to the voltage set by a potentiometer for ratings. Ramp time set here corresponds to speed of displacement, through which the process is adjusted. Physical development of a servo-actuator is shown in Figure 2.

Fig. 2: Servo-actuator with MOOG electrohydraulic servo valve.

## 3. Positioning Precision of a Linear Electrohydraulic Servomechanism

Displacement sensors, existing in the structure of linear hydraulic positioning servo systems, have a critical role in performing the automatic adjustment of the desired and programmed position. The precision that positioning servo system ensures can not be greater than the precision of the position measuring system. Their accuracy is related to the maximum size of measured parameter and, consequently, the relative precision of the sensor decreases with increasing length of displacement of linear hydraulic motor shaft [6]. In operation of an electrohydraulic positioning servo system there is possible that between theoretical output parameter ($e_t$) and the actual one $(e_r)$ for some deviations to occur in stationary state $(\Delta e)$.

In this situation it can be considered that the positioning accuracy is given by the difference between the two output parameters, the theoretical one and the actual measured one [1].
In systemic approach, inaccuracy of a system is not due to construction flaws, but it is related to the structure of the system, and it is considered dependent on the value in stationary state (at $t \to \infty$) of the drive parameter $a_\infty$ (also called stationary error).

As it is known, the error $a_\infty$ depends on the order $\alpha$ of astatism of the system and on the control mode (input type step, or ramp, or parabola). Calculation procedure is relatively simple: to identify – for the investigated system - *fdt* in open circuit $T_d(s) = R(s)/A(s)$; extract in common factor the terms *s* at the maximum power possible, for both *R(s)* and $A(s)$, and thus could be made transcription of $T_d(s)$ in the form of relation:

$$T_d(s) = \frac{K}{s^\alpha}\frac{R_p(s)}{A_q(s)} = \frac{K}{s^\alpha}T_{d_\alpha}(s) \text{ (Where: lim } T_{d_\alpha}(s) = 1\text{);} \tag{1}$$

There is identified the control mode $i(t)$, respectively $I(s)$; it is calculated:

$$a_\infty = \lim_{s\to 0}\frac{sI(s)}{1+\frac{K}{s^\alpha}} = \lim_{s\to 0}\frac{s^{\alpha+1}}{s^\alpha + K}\cdot I(s) \tag{2}$$

As for the means of correcting precision, there are essentially two ways to increase the precision of a system, so the decrease the value of $a_\infty$, namely:

- *increasing the amplification factor* K, which has to be made only to the extent where the system begins to lose its reserve of stability, or even becomes unstable, or:
- *increasing the astatism order* $\alpha$ *of the system* by introducing *in direct loop* an integrator-type regulator. In practice there are not used corrections of type ***I***, that is regulators with *fdt: K/S*, but of type *PI*, regulators with *fdt*: $K_1 + \frac{K_2}{s}$, to avoid reducing the degree of stability.

Experimental research, presented below, was conducted in this way.

## 4. Presentation of the Investigated Electrohydraulic Positioning Servo System

To analyze the static and dynamic behavior of the electrohydraulic positioning servo system for detecting the *factors* leading to *increased accuracy of positioning* was necessary to create/invent an *experimental electrohydraulic positioning servo system*, which, by mounting on a suitable stand in Laboratory of servo-systems of INOE 2000-IHP, to enable development, in good conditions, of the experimental research. The electrohydraulic experimental positioning servo system is shown in Figure 3 and Figure 4 and consists, in turn, of two main parts, namely:

- the *hydraulic part of servo system* or servo cylinder, consisting of a hydraulic cylinder with a bilateral rod and an *electrohydraulic servo valve* for control of servo system, represented by places 10, 11, 12,
- the *mechanical part of servo system*, composed of mechanical parts attached to the hydraulic cylinder rod, the *spring* or *set of springs* with its connecting parts to the rod of cylinder, respectively, the *force transducer*, represented by places 1, 2, 3, 4, 5, 6, 7, 8 and 9.

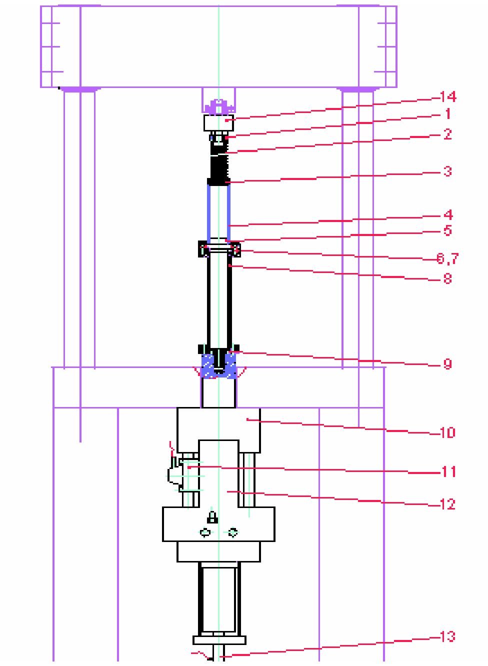


Fig. 3 Diagram of the experimental servo system.

Fig. 4 Mounting of the servo system on existing frame

In addition to hydraulic and mechanical components of the device, it also contains three transducers, which interface the mechanical-hydraulic part to the electronic part of the measurement system of experimental stand used, namely: *Stroke transducer*, place 13, which is integrated in the structure of servo cylinder; *Force transducer*, place 14, which is mounted between the fixed part of the stand (upper crossbar) and extension of cylinder rod and *Pressure transducer*, which shows the pressure at the input of servo valve.

*Hydraulic cylinder*, which is controlled by an electrohydraulic flow *servo valve*, was supplied from a hydraulic station capable of delivering a maximum *admitted* pressure, at a maximum proper flow, which allowed obtaining a convenient maximum speed and strength permitted, controlled at the hydraulic cylinder rod. Cylinder rod position is monitored by a *stroke transducer* TC, with measuring range compatible with that of the hydraulic cylinder. The value of force at the cylinder rod is monitored through the *stroke transducer* TC, with a convenient range of measurement, in extension and compression [5].

## 1. Presentation of Experimental Assembly for Research on the Servo System

Conducting experimental research on the factors leading to increased positioning precision imposed design and development of an *experimental assembly*, where *the experimental electrohydraulic positioning* servosystem be mounted in, which is a functional group of components, equipment, devices and proper instrumentation, including stands or parts of existing stands, aimed at allowing development of the necessary experimental research in which to highlight the main factors leading to increased positioning accuracy.

The hidro-mechanic schema of an *experimental assembly* is presented in Figure 5,

An overview of the experimental assembly is shown in Figure 6, where it can be seen that, in addition to the experimental electrohydraulic servo system presented, this assembly also includes a hydraulic power station to supply the positioning servo system, as well as a computer and a data acquisition board, which form the data acquisition and processing system **SAD**, which also provides the output, in graphic or tabular form, for the parameters of interest: stroke, load/force, pressures and positioning error of the tested servo system for various levels of pressure and flow. Specialized software was installed on computer, that allowed acquisition, storage and processing of data acquired by the acquisition board, taken from the stroke, force and pressure transducers specified above. Some of the experimental results are shown below in graphic form.

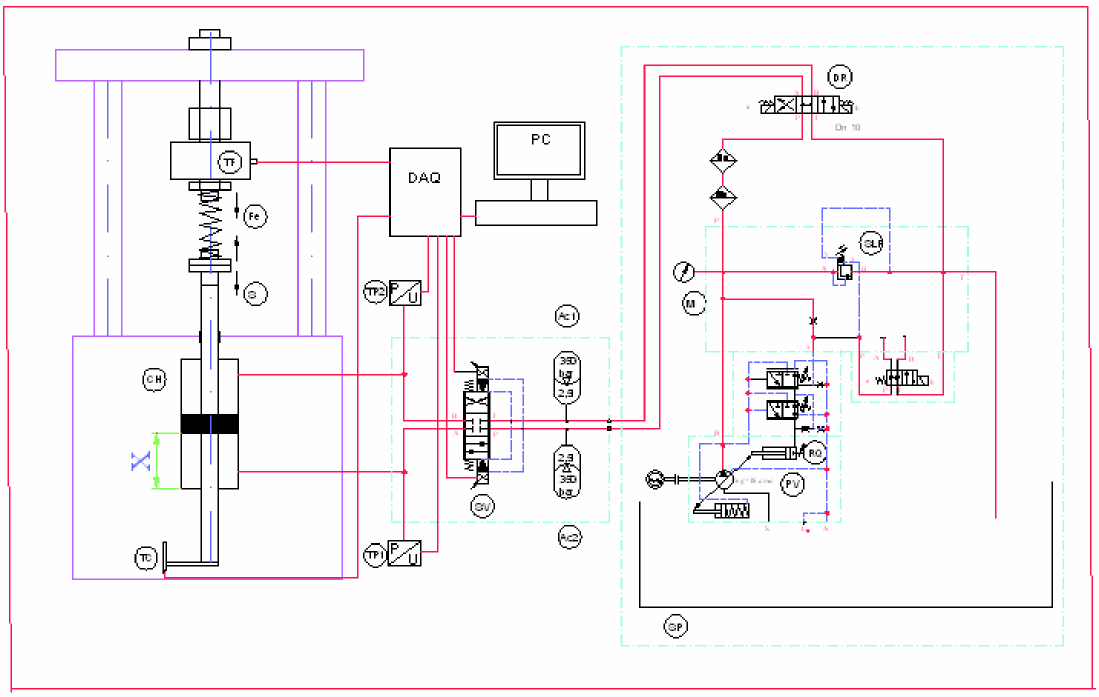


Fig. 5 The hidro-mechanic schema of an *experimental assembly*

**ISSN 1454 - 8003**
**Proceedings of 2011 International Salon of Hydraulics and Pneumatics - HERVEX**
*9 – 11 November, Calimanesti-Caciulata, Romania*

Thus, Figure 7 presents the panel for display on PC monitor screen, where can be seen graphs of the parameters of interest, mentioned above. Stroke programmed by stage-type signals, and system response, which looks like a delay system of-order 1, can be seen in Figure 8, where there are presented both the upward and the downward stroke. Figure 9 shows the variation of positioning error during a complete cycle, where it can be noted that for about 90% of the stroke, positioning error approaches the one which can be ensured by the stroke transducer. Figure 10 presents, for a total of 24 points, the curves of variation of the positioning error to both descending (top curve, in black) and ascending stroke (bottom curve, in red). It is noted that for the investigated servo system the average positioning error, at downward stroke, is 0.25 mm, similar to the error of stroke transducer, and at upward stroke it is 1.2 mm. If there is represented an average cumulative positioning error for both strokes, so for a double total of points (48 points), the average cumulative error is about 0.7 mm, which was expected, as shown in Figure 11 .

Fig. 6 Experimental assembly of servo system.

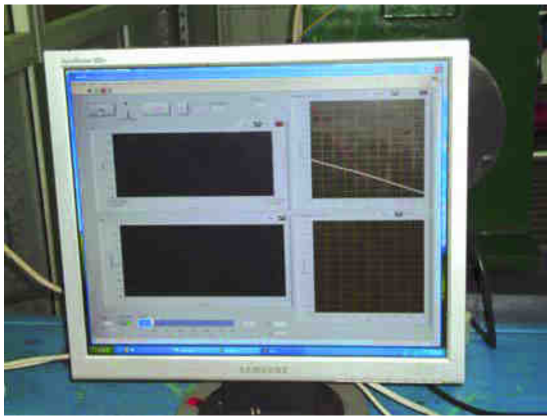

Fig. 7 Display panel on PC.

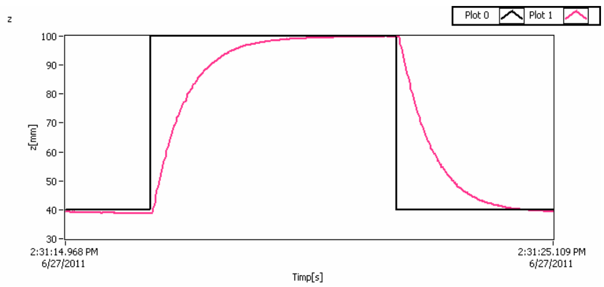


Fig. 8 Controlled stroke and response stroke.

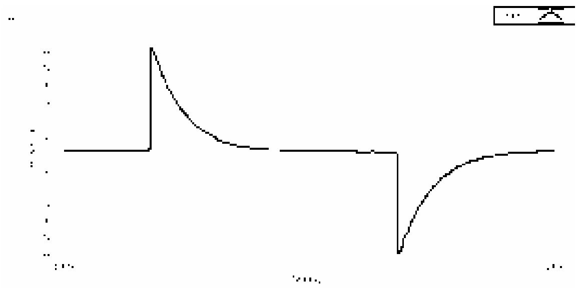

Fig. 9 Variation of positioning error.

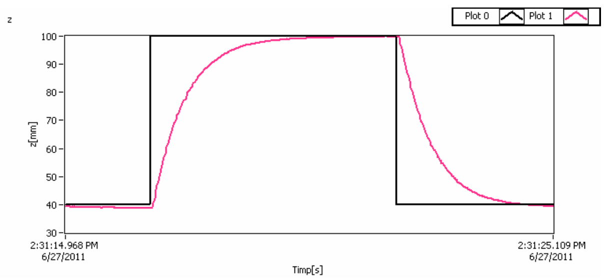


Fig. 10 Variation of positioning error

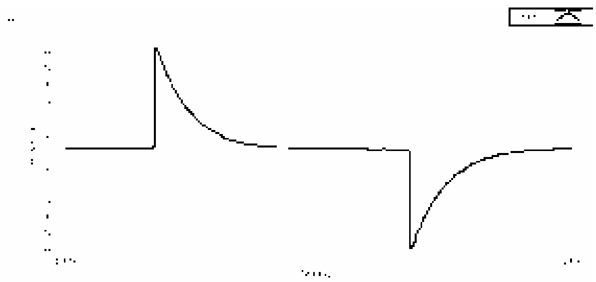

Fig. 11 Variation of cumulative positioning error.

## 6. Conclusions

Linear electrohydraulic positioning sservo systems are typical systems for automatic adjustment of current position in a particular straight course of work. The dynamic response of servo system is a typical response of a delay adjustment system of order 1, and after 90% of the set stroke is covered, the positioning error of the servo system gets close to the acceptable one, given by the stroke transducer installed. Variation of positioning error, which is great at first, decreases as the closed-loop control system is approaching the final stroke and the error at upward stroke is greater than the one at the downward stroke.

Increasing the positioning precision of electro hydraulic servo systems can be done by *increasing the amplification factor* $K_p$, but only to the extent where the servo system loses its stability reserve.
Also, increasing positioning accuracy and improving servo system stability can be achieved by *increasing the astatism order of the system*, by introducing *in direct loop* a *proportional-integrator* regulator.

## 2. REFERENCES

[1] Marin V., Marin Alex. *Sisteme hidraulice automate–constructie reglare exploatare* (Automatic hydraulic systems-building control operation)–, Technical Printing House, Bucharest, 1987

[2] Mannesman Rexroth, Hydraulic Trainer, Vol. 2, RRUU 00303/10.86, Printed by SchleunungDruckSD, 1986.

[3] Al. Dorin, Tb. Dobrescu, A. Bucuresteanu. *Hydraulic driving of the industrial robots.* House Publisher Bren, Bucharest, 2008.

[4] Corneliu Cristescu, Petrin Drumea, Catalin Dumitrescu, Ioana Ilie and Iulian Dutu. *Experimental Research on Factors Influencing Positioning Precision of Linear Electrohydraulic Servo Systems*. In: Proceedings of The 2nd IACSIT International Conference on Mechanical Engıneerıng, Robotics and Aerospace-ICMERA 2011, October 20 - 22, 2011, Bucharest, Romania, **pp. 205 - 210**, ISBN 978-981-07-0420-9, Edited by Jiang Xiaolan, IACSIT PRESS, Singapore, ISSN 2010-460X, Full text availabile at: http://www.ipcsit.com.

[5] C. Velescu. Aparate si echipamente hidraulice proportionale (Aparatus and Hydraulic proportional equipments), House Publisher Mirton, Timisoara, 2003.

[6] *C. Calinoiu, Senzori si traductoare (*Sensors and transducers), vol. I, Technical Printing House, Bucharest, 2009.

ISSN 1454 - 8003
Proceedings of 2011 International Salon of Hydraulics and Pneumatics - HERVEX
*9 – 11 November, Calimanesti-Caciulata, Romania*

# The geometry of unconventional power transmission

**Drd. Liviu BĂRNUȚIU, Prof. Univ. Em. Dr. Ing. Ioan I. POP**

*Takata-Petri RO, Zona Industriala Vest Arad, Str. III, Nr. 9, 310375 Arad, e-mail: Liviu:Barnutiu@eu.takata.com
**Catedra de Maşini unelte şi Roboți Industriali, Universitatea Tehnică Cluj, B-dul Muncii nr. 103-105, Cluj-Napoca, e-mail: ioanpop@yahoo.com

***Abstract:.***
*Transmission problem defined broadly as shown in the figure above is, as a primary shaft which rotates continuously driven by a prime mover, to transmit power to another shaft called the secondary, so that regardless fluctuations in torque and speed of the spindle secondary mover power to develop naturally with maximum efficiency*

***Keywords***: *Mobile mechanical sistem, quadrilateral pendulum, transmitting report*

## 1. Introduction:

Mechanisms (Mobile Mechanical Systems - EMS) used in construction machinery and equipment classes are mostly, desmodromic present case I, with the degree of mobility M = 1 and with one engine coupling. Complex structures are obtained by composing the basic EMS series connection (for example in building robots) or parallel (eg CNC machine work, parallel robots, etc.).These processes are obtained mechanical structures "with several axes", a term which defines the number of independent movements characteristic of EMS point to the reference system. EMS command and control is done by imposing these laws of motion (space, linear or angular velocity and acceleration versus time) the coupling / motor couplings

## 2. Problem description:

This version of EMS undesmodrom proposed to build an automatic gearbox which dynamically adjusts the transmission ratio depending on the time led resistant element (Fig. 2.1), consists of two articulated quadrilateral mechanisms - ABCD and DFGH - a common element, DF lever (4), which acts as articulated quadrilateral ABCD and rocking to the crank for DFGH. (Space, linear or angular velocity and acceleration versus time) the coupling / motor couplings.

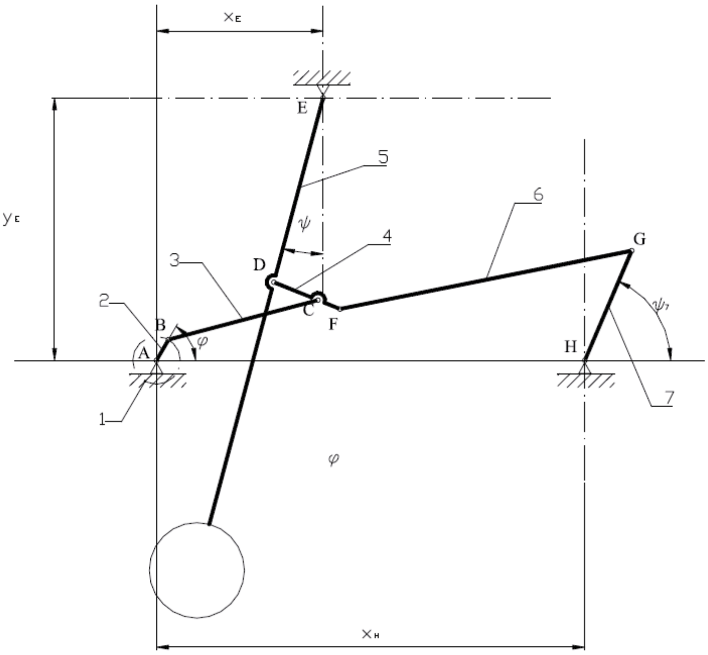


***Fig. 2.1 - Unconventional system of power transmission***

DF is the pendulum articulated lever 5. If it is blocked, EMS operates as a dual mechanism articulated quadrilateral numbered and transforms the rotation around the coupling element a motor engines alternative rotating element driving tee 7, around the coupling H.

$$i(\varphi_1) = \frac{\omega_1}{\omega_7(\varphi_1, M_r)} \tag{2.1}$$

$$i_{1,7} = \frac{2\pi}{\Delta\psi_7(M_r)} \tag{2.2}$$

.

Where:

$\Delta\psi_7$ is the angle of oscillation of the beam 7, variable resistance depending on when $M_r$.

Continuity of movement is obtained by fitting the input shaft parallel on the same two mechanisms are identical, but out of phase by 180 °. Led elements of the two mechanisms are mounted on the same shaft output, and submit its successive movements through valve couplings.

The degree of mobility of the mechanism is determined by the relationship:

$$M = 3 \cdot (n-1) - 2 \cdot C_5 = 3 \cdot (7-1) - 2 \cdot 8 = 2$$

which means that the mechanism will move according to two independent parameters, engine crank rotation and resistant when driven shaft. EMS is not static but determines its equilibrium position and a dynamic condition.

Input data's:

Geometry modeling CAD program SolidEdge mechanism was used, and for mathematical modeling, Mathcad.

For geometric and kinematic study the following parameters were used:

Rated speed input $n_{i\,nom} = 3000 \dfrac{rot}{\min}$

Resistant when output (for a system operating) $M_{re} = 50 N \cdot m$

Mass of the counterweight $m_5 = 100\,kg$

Baseline dimensions chosen mechanism (to be final by optimization)

| | |
|---|---|
| Crank length 2 | $l_{AB} = 10\,mm$ |
| Rod length 3 | $l_{BC} = 70\,mm$ |
| The length of the lever 4 | $l_{DF} = 30\,mm$ |
| Joint position C on lever 4 | $l_{CD} = 20\,mm$ |
| Length of balance 5 | $l_5 = 500\,mm$ |
| Length of balance 7 | $l_{GH} = 50\,mm$ |
| Rod lenght 6 | $l_{FG} = 125\,mm$ |
| Joint position Don on balance 5 | $l_{DE} = 80\,mm$ |

Coordinates joint mechanism

Fixed joints:

**A** (head shaft axis) $x_A = 0\,mm; \quad y_A = 0\,mm$

**H** (driving shaft axis) $x_H = 200\,mm; \quad y_H = 0\,mm$

**E** (Universal joint of balance rod counterweight) $x_E = 75\,mm; \quad y_E = 110\,mm$

Mobile joints parameters

- $\varphi_2$ crank angle of rotation of the motor shaft 2
- $\psi_5$ oscillation of the rocking angle 5

**B** (coupling adapter) $x_B(\varphi) = l_{AB} \cdot \cos(\varphi); \quad y_B = l_{AB} \cdot \sin(\varphi)$

**D** (coupling of the rocking lever 4 and 5) $x_D(\psi) = x_E - l_{DE} \cdot \sin(\psi); \quad y_D = y_E - l_{DE} \cdot \cos(\psi)$

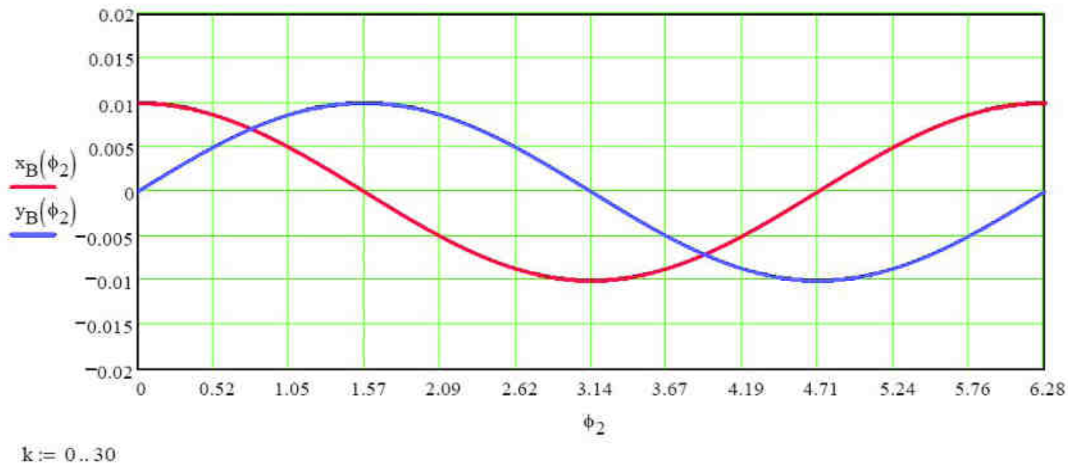


***Fig. 2. 2 Coupling coordinates B***

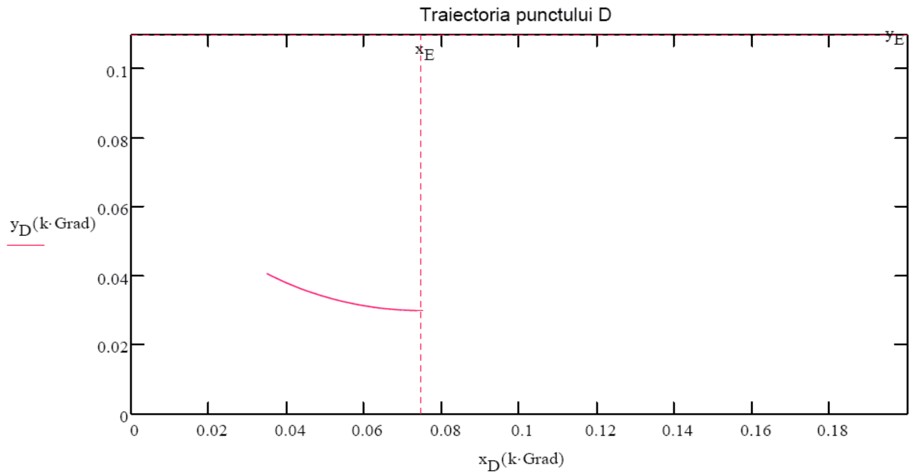


*Fig. 2.3. - Coupling path D*

C (coupling of the rod 3 and lever 4) on the positions of joints B and D snapshots are at the intersection of circles with centers in B and D and radius, respectively.

The coordinates of point C are solution abscissa and ordinate major minor system of equations of the two circles.

$$A_C(\varphi,\psi) = (x_D(\psi) - x_B(\varphi))^2 - (y_D(\psi) - y_B(\varphi))^2 \qquad (2.4)$$

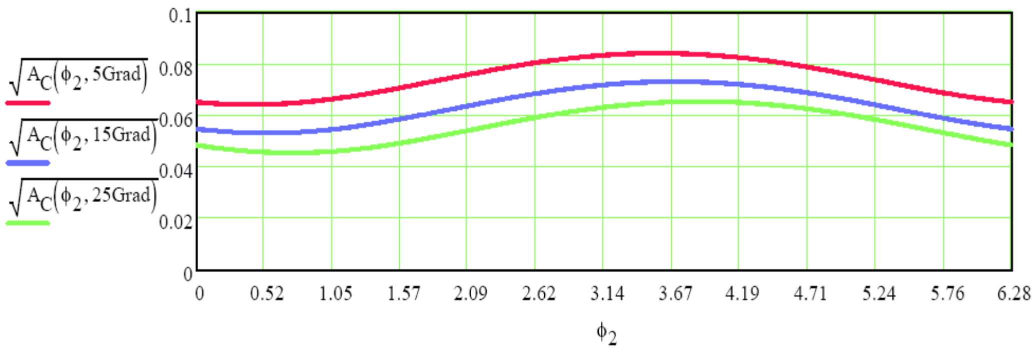


***Fig. 2. 4 - Change of distance between points B and D to a rotation of the crank***

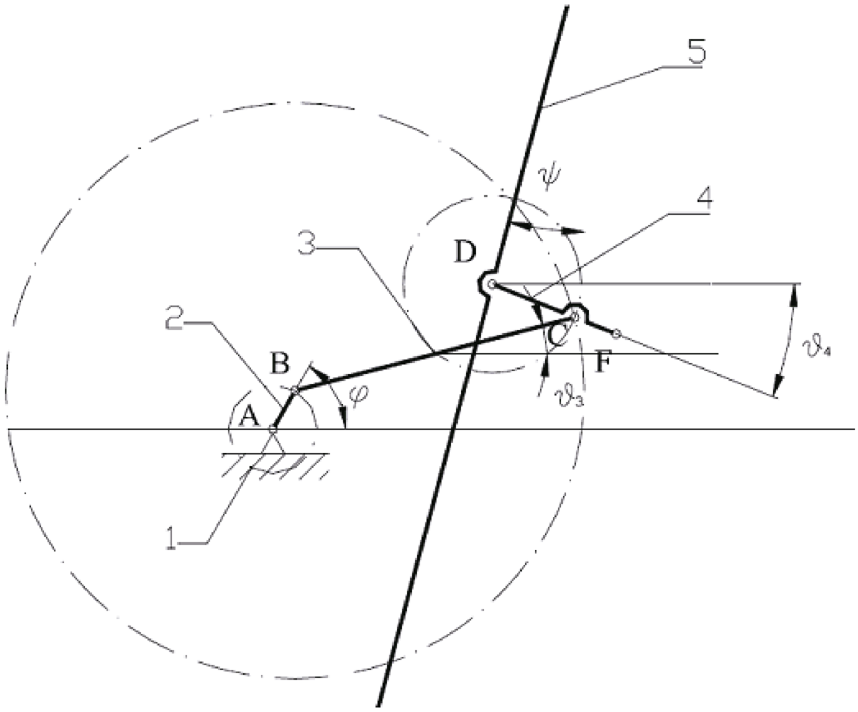


***Fig. 2.5 - Diagram for determining coordinates p. D***

Degree 2 equation parameters that determine the coordinates of the point D:

$$\lambda_C(\psi) = l_{BC}^2 - l_{CD}^2 - l_{AB}^2 + x_D^2(\psi) + y_D^2(\psi) \tag{2.5}$$

$$B_C = -\{2 \cdot [(y_D(\psi) - y_B(\varphi)) \cdot (x_B(\varphi) \cdot y_D(\psi) - x_D(\psi) \cdot y_B(\varphi))] + (x_D(\psi) - x_B(\varphi)) \cdot \lambda_C(\psi)\} \tag{2.6}$$

$$C_C(\varphi,\psi) = \frac{1}{4} \cdot \lambda_C^2(\psi) + (l_{AB}^2 - l_{BC}^2) \cdot (y_D(\psi) - y_B(\varphi))^2 - \lambda_C(\psi) \cdot (y_D(\psi) - y_B(\varphi)) \tag{2.7}$$

$$\Delta_C(\varphi,\psi) = B_C^2(\varphi,\psi) - 4 \cdot A_C(\varphi,\psi) \cdot C_C(\varphi,\psi) \tag{2.8}$$

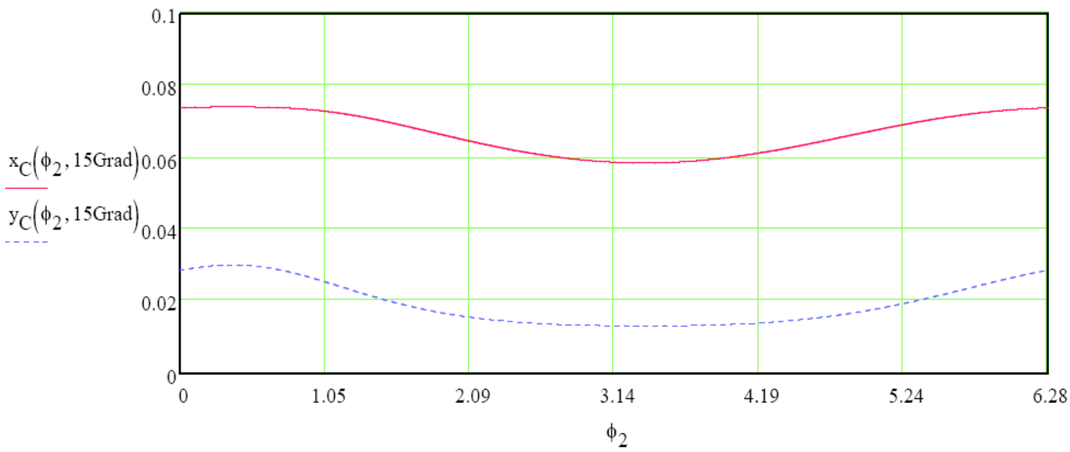


***Fig. 2.6 - The coordinates of the point C for the pendulum angle of 15 °***

The coordinates of the point C

$$x_C(\varphi,\psi)=\frac{-B_C(\varphi,\psi)+\sqrt{\Delta_C(\varphi,\psi)}}{2\cdot A_C(\varphi,\psi)} \tag{2.9}$$

$$y_C=\frac{\lambda_C(\psi)}{2\cdot(y_D(\psi)-y_B(\varphi))}-\frac{x_D(\psi)-y_B(\varphi)}{y_D(\psi)-y_B(\varphi)}\cdot x_C(\varphi,\psi) \tag{2.10}$$

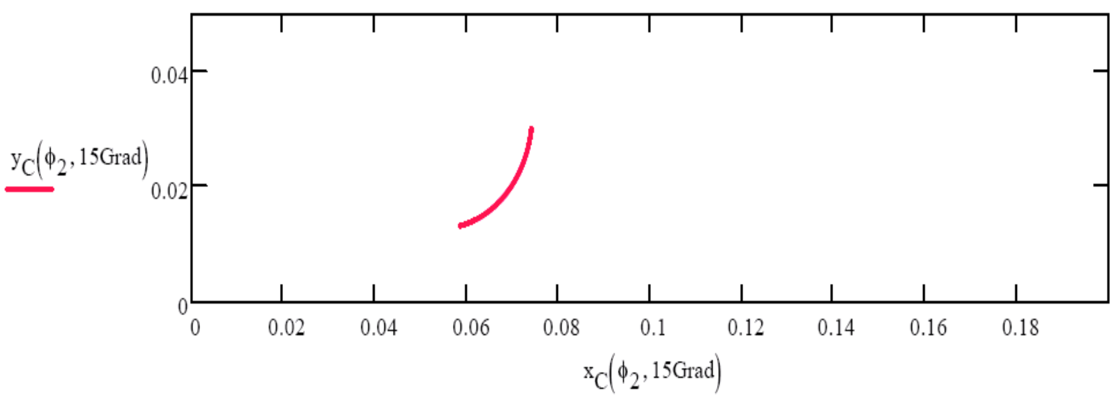


***Fig. 2.7 -. The trajectory of the point C with ballast hung at 15 °***

The coordinates of point F :

$$x_F(\varphi,\psi)=x_D(\psi)-\frac{l_{DF}}{l_{CD}}\cdot(x_D(\psi)-x_C(\varphi,\psi))$$
$$y_F(\varphi,\psi)=y_D(\psi)-\frac{l_{DF}}{l_{CD}}\cdot(y_D(\psi)-x_C(\varphi,\psi)) \tag{2.11}$$

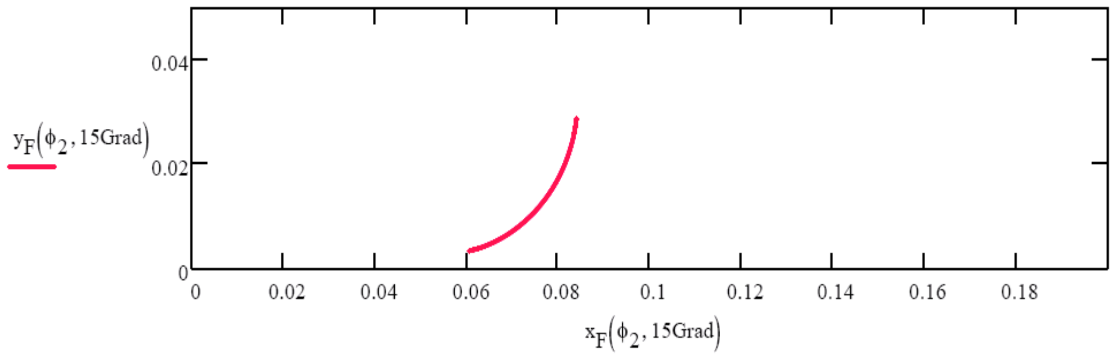


***Fig. 2.8 - Trajectory point F with ballast hung at 15 °***

The coordinates of the point G major are the solution of the abscissa and ordinate major equations of the two circles.

ISSN 1454 - 8003
Proceedings of 2011 International Salon of Hydraulics and Pneumatics - HERVEX
*9 – 11 November, Calimanesti-Caciulata, Romania*

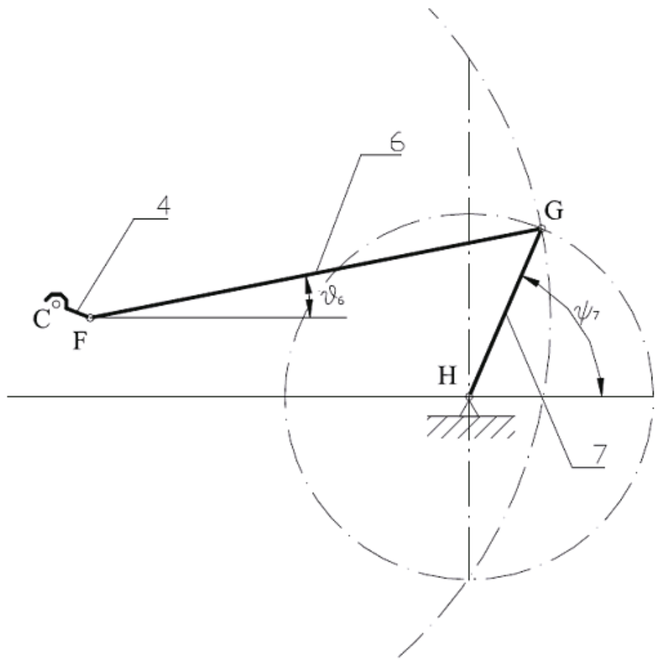


***Fig. 2.9 - Diagram for determining the coordinates of point G***

$$A_G(\varphi,\psi)=\left(x_H-x_F(\varphi,\psi)\right)^2+\left(y_H-y_F(\varphi,\psi)\right)^2 \tag{2.12}$$

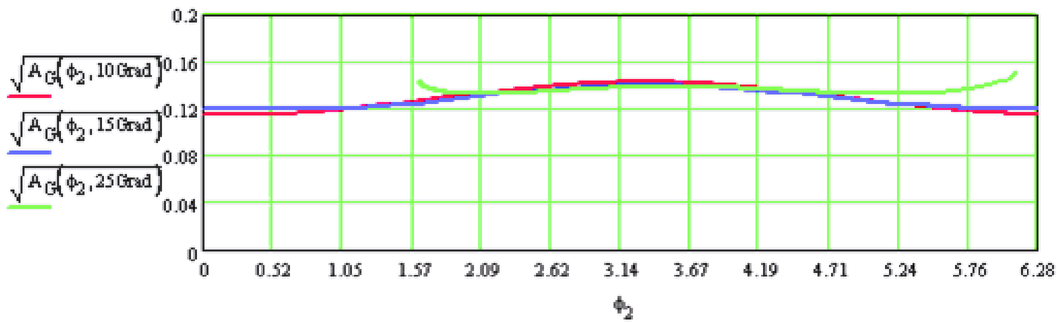


***Fig. 2.10 - The variation in distance between F and H a rotation of crank***

Second Degree equation parameters that determine the coordinates of the point G:

$$\lambda_G(\varphi,\psi)=l_{FG}^2-l_{GH}^2-x_F^2(\varphi,\psi)-y_F^2(\varphi,\psi)+x_H^2+y_H^2 \tag{2.13}$$

$$B_G(\varphi,\psi)=-\left\{\begin{array}{l}2\cdot\left[\left(y_H-y_F(\varphi,\psi)\right)\cdot\left(x_F(\varphi,\psi)\cdot y_H-x_H\cdot y_F(\varphi,\psi)\right)\right]\\+\left(x_H-x_F(\varphi,\psi)\right)\cdot\lambda_G(\varphi,\psi)\end{array}\right\} \tag{2.14}$$

$$\begin{gathered}C_G(\varphi,\psi)=\frac{1}{4}\cdot\lambda_G^2(\varphi,\psi)+\left(x_F^2(\varphi,\psi)+y_F^2(\varphi,\psi)-l_{FG}^2\right)\cdot\left(y_H-y_F^2(\varphi,\psi)\right)^2\\-\lambda_G(\varphi,\psi)\cdot\left(y_H-y_F(\varphi,\psi)\right)\cdot y_F(\varphi,\psi)\end{gathered} \tag{2.15}$$

$$\Delta_G(\varphi,\psi) = B_B^2(\varphi,\psi) - 4 \cdot A_G(\varphi,\psi) \cdot C_G(\varphi,\psi) \tag{2.16}$$

The coordinates of the point G

$$x_G(\varphi,\psi) = \frac{-B_G(\varphi,\psi) + \sqrt{\Delta_G(\varphi,\psi)}}{2 \cdot A_G(\varphi,\psi)} \tag{2.17}$$

$$y_G(\varphi,\psi) = \frac{\lambda_G(\varphi,\psi)}{2 \cdot (y_H - y_F(\varphi,\psi))} - \frac{x_H - x_F(\varphi,\psi)}{y_H - y_F(\varphi,\psi)} \cdot x_G(\varphi,\psi) \tag{2.18}$$

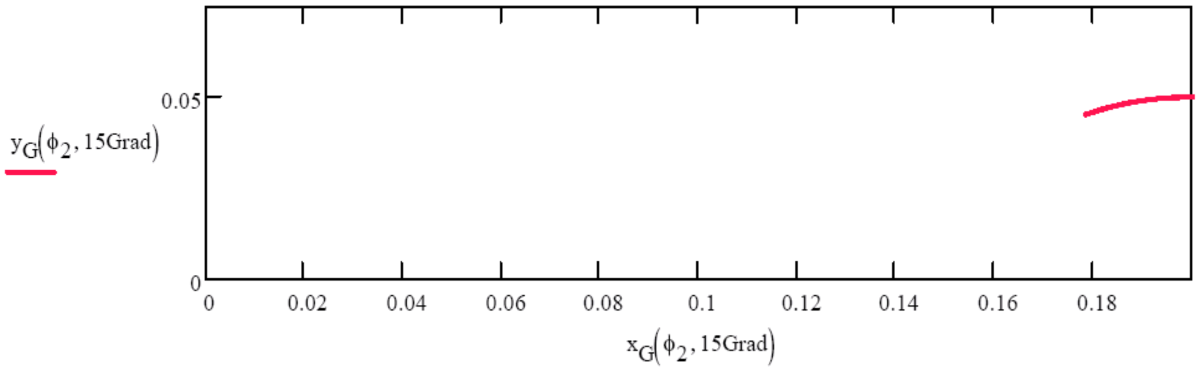


***Fig. 2. 11 - The trajectory of the point G with ballast hung at 15 °***

The angles made by connecting rod and balansiere with the axis x-x

$$\theta_3(\varphi,\psi) = a\tan\left(\frac{y_C(\varphi,\psi) - y_B(\varphi)}{x_C(\varphi,\psi) - x_B(\varphi)}\right)$$
$$\theta_4(\varphi,\psi) = a\sin\left(\frac{y_D(\psi) - y_C(\varphi,\psi)}{l_{CD}}\right) \tag{2.19}$$
$$\theta_6(\varphi,\psi) = a\tan\left(\frac{y_G(\varphi,\psi) - y_F(\varphi,\psi)}{x_G(\varphi,\psi) - x_F(\varphi,\psi)}\right)$$

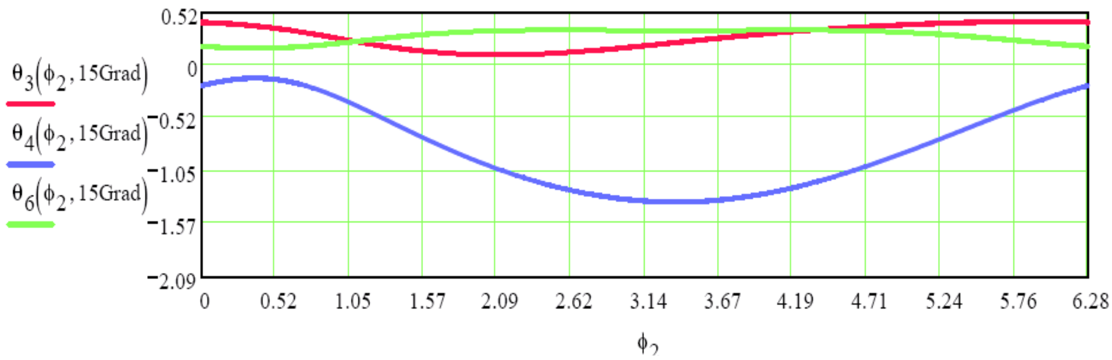


***Fig. 2.12 -The angles made by connecting rod and balansiere with the axis x-x***

Angle of rod 7: (oscillation)

$$\psi_7(\varphi,\psi) = a\cos\left(\frac{x_G(\varphi,\psi) - x_H}{l_{GH}}\right) \tag{2.20}$$

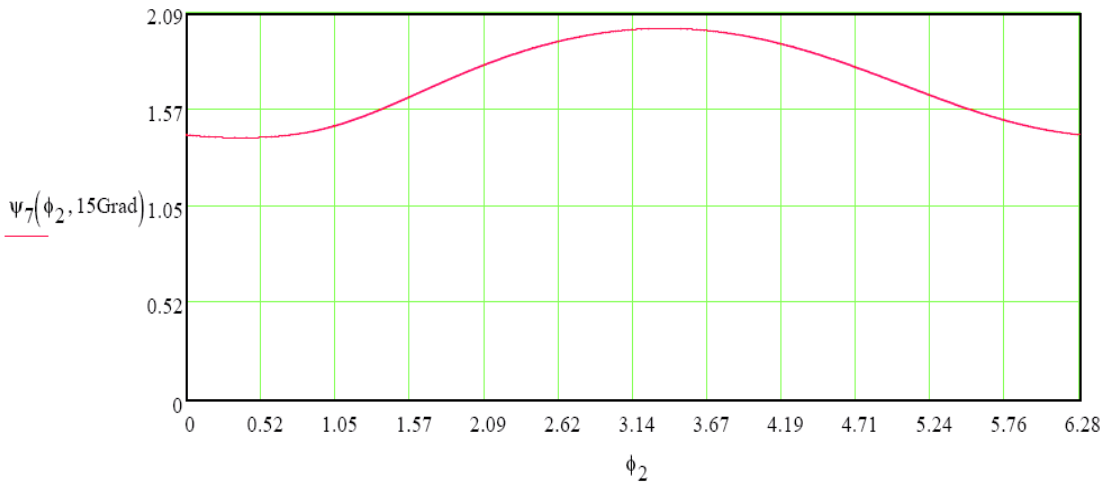


***Fig. 2.13 - Oscilatie angle of rod 7***

Rotation shaft driven by th rod 7 by coupling the effect is obtained by removing the rod interval rotates freely in the sense of the coupling, i.e., the speed of about is negative:

$$\psi_8 = \psi_7(\kappa,\psi)\cdot\left(\frac{d}{d\varphi}\psi_7(\varphi,\psi) > 0\right) \tag{2.21}$$

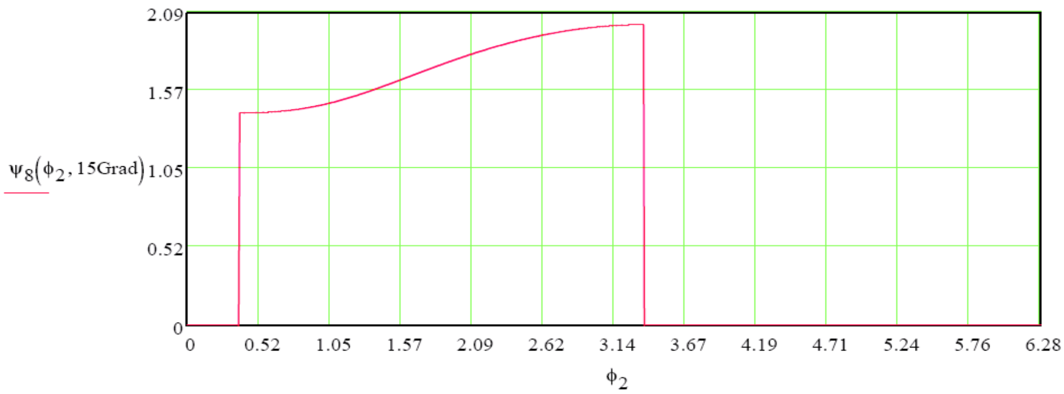


***Fig. 2.14 - Driven shaft rotation***

In this way is determined the dependence between the oscillation of the led-rod 7-shaft driven, respectively, and position angles of lever engines 2 and 5 of the pendulum. Dependence on the angle of the position of the pendulum of time resistant position and angle of the lever engines will be determined by analysis of kinetostatic and dynamic system.

**3. Conclusions:**

It is necessary to the design and realization of such automatic gearboxes, vast inertial, enabling the functionality of such innovative solutions as well as verifying the existence of correlations of data from the mathematical model with the data to be collected during the operation of the mechanism. From the analysis of geometric, kinematic and dynamic of this piece, it appears that the best solution both in terms of the possibilities of designing, implementing and integrating mechanism for power transmission on a vehicle. On this model will be tested for functionality this innovative solutions on a motor vehicle, the behaviour of the transfer of energy (work) from the engine to the led, the study of the reaction mechanism of energy, efficiency, noise and vibration that you produce, advantages, disadvantages, etc.

**REFERENCES**

[1] POP, I.I., Tratat de teoria sonicităţii, Editura Performantica, Iaşi, 2006

[2] POP, I.I., ş.a., Integrala invenţiilor, Vol. I, Editura Performantica, Iaşi, 2006

[3] POP, I.I., ş.a., Integrala invenţiilor, Vol. II, Editura Performantica, Iaşi, 2006

[4] POP, I.I., ş.a., Integrala invenţiilor, Vol. III, Editura Performantica, Iaşi, 2006

[5] POP, I.I., ş.a., Integrala invenţiilor, Vol. IV, Editura Performantica, Iaşi, 2006

**ISSN 1454 - 8003**
**Proceedings of 2011 International Salon of Hydraulics and Pneumatics - HERVEX**
*9 – 11 November, Calimanesti-Caciulata, Romania*

# Unconventional system of transmission and power conversion

**Drd. Liviu BĂRNUȚIU, Prof. Univ. Em. Dr. Ing. Ioan I. POP**

*Takata-Petri RO, Zona Industriala Vest Arad, Str. III, Nr. 9, 310375 Arad, e-mail: Liviu:Barnutiu@eu.takata.com
**Catedra de Maşini unelte şi Roboți Industriali, Universitatea Tehnică Cluj, B-dul Muncii nr. 103-105, Cluj-Napoca, e-mail: ioanpop@yahoo.com

***Abstract:***

*Transmission problem broadly defined, is, as a primary shaft which rotates continuously driven by a prime mover, to transmit power to another shaft called the secondary, so that regardless of fluctuations in torque and speed of the spindle secondary primary engine power to develop naturally with maximum efficiency.*

***Keywords****: Transmission damping cylinder, drosel*

## 1. Introduction:

Converter made of Gogu Constantinescu differs from the classic gearboxes that do not appear in the construction of the converter gears, power transmission from main engine driven shaft is accomplished by using inertia of oscillating masses arranged in such a way as to not obtain a decreasing rate with increasing torque-resistant.
The assembly is equipped with a transmission mechanism comprising a lever which oscillates and is linked to two different points (one point connects with the shaft to operate and liaise with other coupler valve). At the same time, this lever is under the direct influence of inertial mass, which can perform a reciprocating or oscillatory. Following the operation, oscillatory motion is converted with a valve coupling rotating, acted in every half rotation.
If resistance to rotation of the driven shaft is small, inertial mass will oscillate about the leverage position than the average and maximum stroke is unidirectional mechanisms as long as the resistance to rotation is 0.
Since the resistance to rotation of the shaft increases, the inertial mass start to grow .
One of the objectives of Gogu Constantinescu converter is transmitting power from the motor driven shaft so that an increase in resistive moment the shaft leading to lead to an increase in engine speed so that the engine output may not decrease when with increasing resistive moment is resolving the problem of converting a unidirectional rotary motion in a rotating flashing in one direction.
The principle of transmitting power from a main motor shaft to be rotated at a time against a variable resistance is achieved by dividing or alternating sinusoidal motion, uniform motion derived from a shaft, alternating movements of the same frequency components, one of the components alternating movement is responsible for movement of a mass and the other component is responsible for movement of a pair of devices alternating one-way working in opposite phase, turning the shaft.
The converter can be composed of an automatic mechanism, which transmits an output variable from a shaft that has a constant speed in a shaft is called a variable torque-resistant, the division between a ruling movement of cranks oscillating and oscillating mass elements moving mechanism leads to unidirectional, arranged so that each complete oscillation of the shaft head, to produce at least two engine impulses oscillating element.
It was found that the converter can achieve a combination of different links, tables and unidirectional mechanisms, provided essential that oscillatory motion derived from the uniform rotation of a main engine shaft is divided into two oscillatory movements of the same frequency, one acting on the mechanisms of weight and a unidirectional, acting at least two pulses on the secondary shaft at each

oscillation produced by the main motor shaft, so that when the mass movement amplitude increases, the rotor speed decreases and vice versa.
Fundamental frequency of all moving points should always be the same for each part of the mechanism. Another important condition is that such systems should not be prevented, so that movement of parts to determine the movement of all other parties should be free to position themselves in a state of stability around a mean position well defined and practically fixed, such a position is determined by internal forces developed in the mechanism.
To obtain all other forms of mechanism, is sufficient connection between the shaft trimming system which rotates uniformly oscillating masses and mechanisms operating unidirectional secondary shaft, so as to describe the oscillating masses over a period, an elliptical orbit, closed, wherein at least one of the main axis is maximum when the rotor is stationary and stationary masses, or to describe the closed orbits at least one of the main axes is zero or minimum when the rotor reaches full speed.

Unconventional system of power transmission and conversion studied, is part of the automatic transmission, as it provides a continuous change of speed and when transmitted to the wheels, while achieving optimum correlation between speed and time at a speed of input resistance which may change the low limit. Thus, by means of oscillating masses, when a driver shaft that rotates uniformly, is transmitted to a shaft drive, moving against a time variable angle, increasing the ratio of self-management and the shaft speed increases led , and also to decrease, the ratio is reduced.

## 2. Problem description:

This reduction is variable gear ratio based on the action and the inertia of bodies.

Gearbox subassembly consists mainly of input shaft and output shaft subassembly. Input shaft, 031 is provided with two eccentric offset in $180^0$ on which are mounted two leaflets, 022, by means of bearings. These leaflets are connected by rods rigid arm 018 located on the output shaft 017.
Between arm 017 and shaft 021 is a coupling valve that allows the transformation of the oscillation movement of the arm 017 rotating shaft 021 with the transmission ratio of 1:1. At a rotating input shaft flywheel running a complete oscillation, as well as arm 017, so half of his movement is moving engines. For this reason, to take out a permanent rotating the two eccentric is shifted to $180^0$, each contributing half of the leaflets of a rotating output shaft parts.

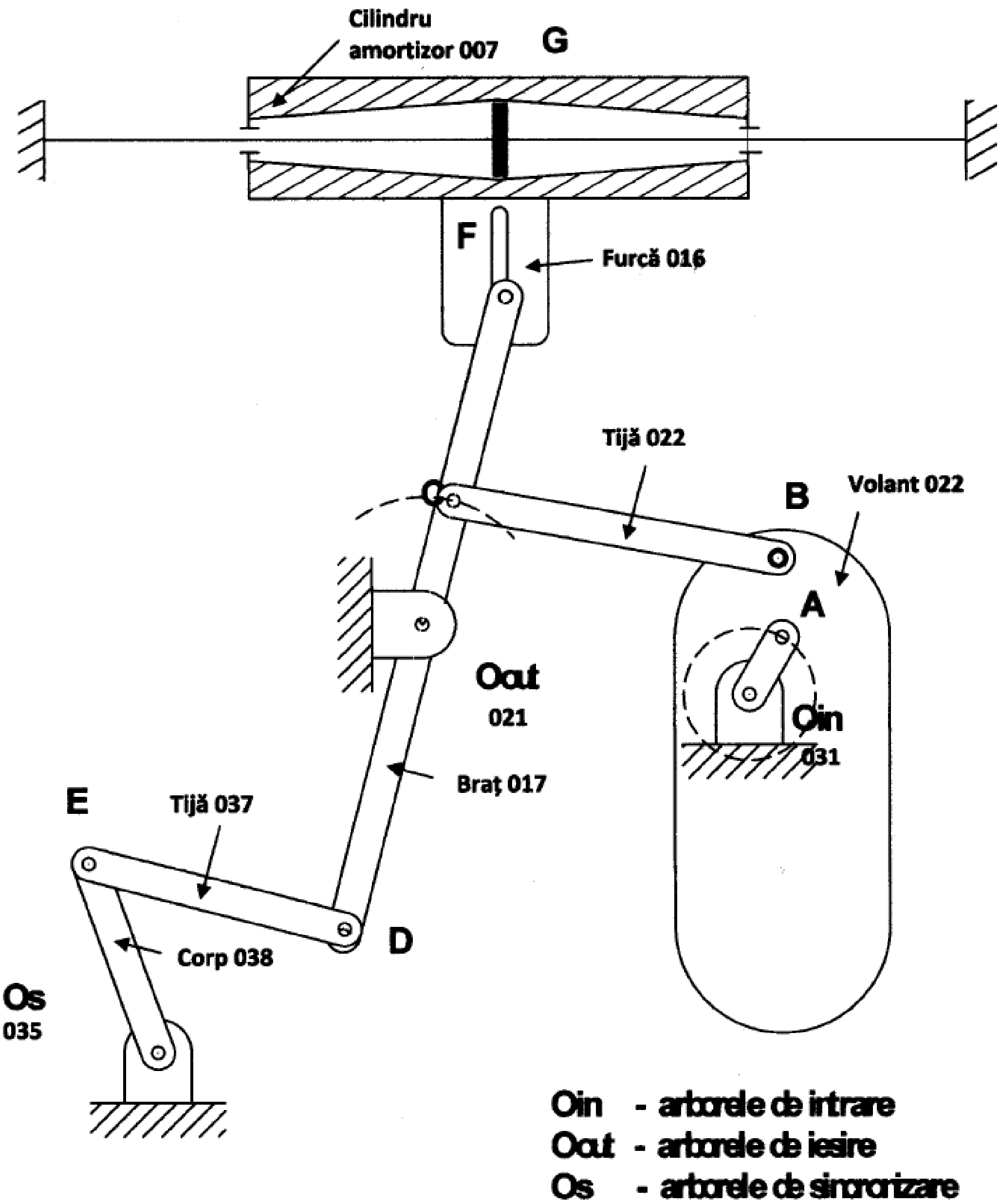


*Fig. 2.1 –Kinematic scheme*

To better understand how this reduction, suppose (purely theoretical) that the point of articulation of the rod 018 and flywheel 022 does not move either left or right, only up and down (+ /-10mm from the mean). In this case the flywheel 022 will perform an oscillation around the joints mentioned, the arm 017 with a barely perceptible oscillation. This oscillation of the flywheel 022 is produced by rotating the input shaft so on his work with a force dependent on its mass, eccentricity and frequency. This force is acting in joint reaction force, it is the maximum that may occur and therefore maximum driving forces. The amplitude of oscillation depends on the load arm 017 from the output shaft, how much load is greater his speed is lower.

To always be a mismatch between the movements of 1800 parts 017, has introduced a synchronization shaft, 035, 017 connected rigid parts.

When force is very low or high speed is compared to the required tasks, is the possibility of large swings, uncontrollable elements can hit each other. To avoid it, this movement is limited, that limitation has as effect and limit the maximum ratio between output and input speed.

To avoid shocks when the race limit has created a damper cylinder (Figure 2.2). With this cylinder is achieved when maximum braking speed oscillations of the last quarter of a moving swing. Thus all oscillations with amplitude greater than 0.75 of maximum amplitude, and they will have a brake on this portion.
Figure 2.2 is shown the link between components of the input shaft and output shaft damper cylinder.

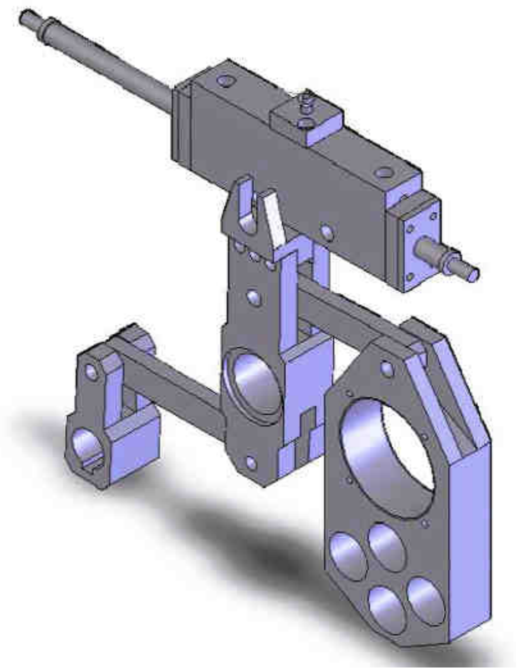

***Fig. 2.2 –Ddamper cylinder  assembly / components and output shaft intrares***

In figures 2.3 and 2.4 are presented in the body of the damper cylinder (007) and piston (010) used to avoid the occurrence of shocks when limiting race driving jib (017).

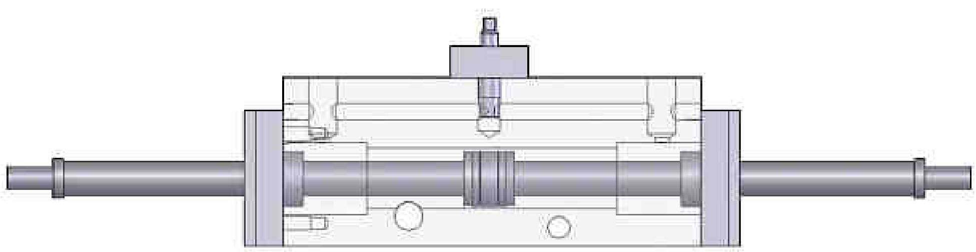

***Fig. 2.3 –Cylinder damper***

Braking is achieved by two fixed chokes, one result of the construction of the cylinder and one adjustable damper. To avoid that and when you start the movement in the opposite direction after having been reversed, the movement are still braked, was made into a valve, the detail of the X-X-D section D.

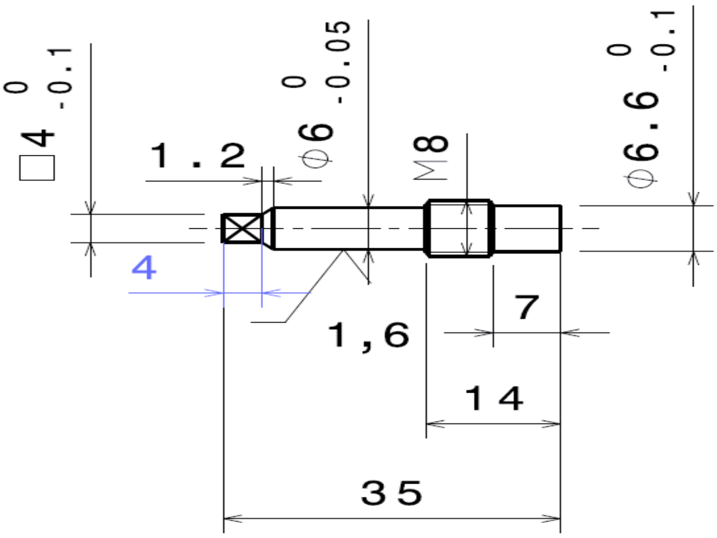


*Fig. 2.4 –__Drosel brake__*

## 3. Conclusions

As is apparent, S.N.T.P. requires a simple construction, different from the classical case, in that there are toothed, sincroane and no clutch. Also, starting from a basic principle in Physics (F = m ·a) we can say that when we have a small number of rotations to the input shaft, the vast inertial force of contragreutății F will be less, in consequence a greater amplitude. As the number of turns in the main tree grows, the vast inertial force of oscillating mass becomes increasingly more important, it may be in such notice a decrease of oscillation amplitudes of contragreutății. In this case, you may observe alternating component obtained from the Division of the movement from the input shaft, an increasing trend, thus yielding a number of rotations on increased output shaft.

## REFERENCES

[1] Transmission (mechanics) - http://en.wikipedia.org/wiki/Transmission_(mechanics)

[2] Torque converter - http://en.wikipedia.org/wiki/Torque_converter

[3] Gears - Gearboxes - http://www.roymech.co.uk/Useful_Tables/Drive/Gears_Gearboxes.html

[4] Gearboxes - http://www.gears-manufacturers.com/gearboxes.html

[5] POP, I.I., Tratat de teoria sonicității, Editura Performantica, Iaşi, 2006

[6] POP, I.I., VIDICAN M.P., "Sonicitate" mecanică , Editura Performantica, Iaşi, 2010

[7] POP, I.I., ş.a., Integrala invențiilor, Vol. I, Editura Performantica, Iaşi, 2006

[8] POP, I.I., ş.a., Integrala invențiilor, Vol. II, Editura Performantica, Iaşi, 2006

[9] POP, I.I., ş.a., Integrala invențiilor, Vol. III, Editura Performantica, Iaşi, 2006

[10] POP, I.I., ş.a., Integrala invențiilor, Vol. IV, Editura Performantica, Iaşi, 2006

**ISSN 1454 - 8003**
**Proceedings of 2011 International Salon of Hydraulics and Pneumatics - HERVEX**
*9 – 11 November, Calimanesti-Caciulata, Romania*

# INNOVATIVE ASPECTS REGARDING THE REALIZATION EQUIPMENT TO MAKE PRESTRESSED CONCRETE STRUCTURE

**Constantin CHIRIȚĂ[1], Andrei GRAMA[1], Adrian Constantin HANGANU,**

[1] "Gheorghe Asachi" Technical University of Iaşi, Faculty of Machine Manufacturing and Industrial Management, Department of Machine Tools, Hydraulic and Pneumatic Systems Engineering Department

***Abstract:*** *(The development of new products represents the main problem, with which problem an organization may remain on the market and may also win new market share. Thus, for structures of prestressed concrete it was concived a device for tensioning of armature and hydraulic source attached to this device both products were placed on a frame forming a mobile reinforcement tension device. The presented equipments have an innovative character on national level due to the fact that such elements never have been made in Romania till present and they represent proposals of inventions.*
***Keywords****: Device for tensioning, hydraulic sources, pretensioning*

## 1. Introduction

The realizing of new products represents the success and the increase of profit in a organization.

Developing a new product is necessary for maintaining an organization on the market. The basic theory of marketing settles that a product has a life cycle composed from the following phases: growing, maturity and decline. When the product reaches maturity and decline is imperative necessarily that the organization plays an active role at:

- the extent of the offered product line and of life cycle;
- redesigning of the product in order to obtain superiority on the market;
- the development of new products for obtaining profits.

Even though innovation is a great success, and its absence may represent a failure, the placing of new products on the market is risky.

Developing a new product is expensive. The investments in research development, engineering, marketing researches, marketing developments and testing should be done before placing the product.

The main factors of initiation of new products are represented by: financial purposes, the increase sales, the competitive position, the life cycle of the product, the technology, the globalization, material's costs, inventions, and clients' necessities.

For realizing a new product an organization has the option to choose from a series of alternative strategies. One of the strategic decisions is if the product should be either reactive or proactive.

On the reactive product the strategy is realized by focusing the ascertainments made on the realized product. In the case of the proactive product the strategy is based on resource allocation in order to prevent unpleasant event and to ensure the realization of purposes.

For a better comprehension of the two strategies above we offer the following examples: the reactive product is the mode of seeing the competitors followed by expectation till the competitors introduce a product and if the product is a successful one the next step is to copy the product. The proactive product bases on the forestall of competitors by being the first on the market to introduce a competitive product, thus the competitors will find it difficult to realize or to improve it.

Analyzing the two strategies we can conclude that the reactive product is easier to realize than the proactive one, but regarding the innovation the proactive product offers a larger source of ideas, fact that may lead to the innovative character of the product.

The sources of ideas are coming from the initial alternative forces which are generated by the initiation factors earlier presented. Thus, we can distinguish the following sources of ideas: the new requirements of the market, the changing of technology, new materials or new availabilities of the supplier, patented inventions and the actions of the competitors. These forces are sources of ideas but for to be efficient the organization needs to consider all sources of ideas, not only the initial, especially when referring to proactive products.

For the designing of the product a certain number of good and bad ideas is generated, their distribution being a normal one.

The first idea may not reflect a great innovation on the market, it is very important to pay a substantial creative attention to the development of products that may revolutionize the market. This product may realize the structure of the markets by adding new dimensions at the product's performances, by technology or by creating a new market share. In order to find these major innovations the market has to be stimulated with new major ideas of concepts or prototypes.

If the invention consists of creating new products or processes by the development of new knowledge or the combining of the existent knowledge, the innovation represents the initial commercialization of the invention by products and selling of new products or services or by using a new method of production. Once introduced the innovation realizes the scattering through initiation or absorption of the innovative product (fig. 1).

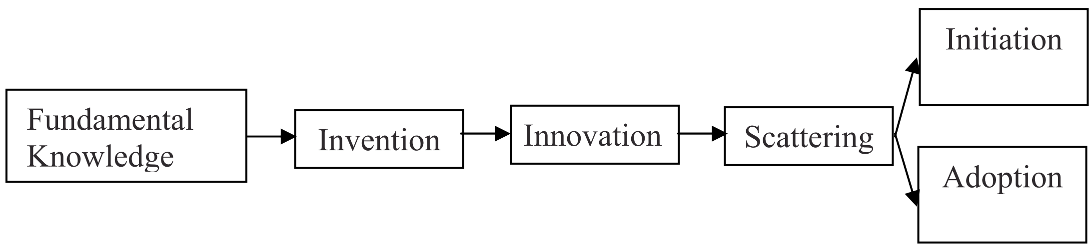


Fig. 1. The graphical representation of innovation

Given the innovation requirements in realizing the products, in DISAHP from Techical University "Gheorghe Asachi" Iassy was realized an innovative system for obtaining prestressed concrete by prestressing, system that includes invention proposals and satisfies the high level of performances requested by the market.

**The structure of hydraulic equipments in order to obtain prestressed concrete**

To highlight the components of the prestressed concrete production by stressing shown in Fig. 2 the general structure of production of the prestressed concrete tendon strain tendon with straight tendons, structure built by the firm Paul Machinenfabrik GmbH [7].

Equipment used for this purpose should be to make the operation of tensioning the reinforcement, to maintain this situation by pouring concrete and reinforcement, after allowing reinforcement slow releaseation, during which efforts to spread the concrete structure is transmitted by pin or by marginal anchoring systems, creating compression in this effort. At any point of the route prestressed reinforcement, which may be straight or curved, paralleled in Unladen concrete structure which balances the two efforts: the extent of compression reinforcement and concrete.

Reinforcement of the concrete structure can be achieved in a number of strands (strand ropes steel strand) with diameters ranging from 9 mm and 16 mm toroanele are placed at intervals, for prestressed concrete slab, or beam, for concrete beams. Normally, if the plates, pre is done individually, strand after strand and strands strands is pretensionează group, releaseation fittings are done but, always, for all toroanele the same time, thus avoiding production of undesirable deformation different tension concrete structure due to a strand or another.

The general pattern of stands of pretensioning / release / casting prestressed concrete structures is shown in Fig. 2. The first stage is placed toroanele 1 which are arranged in coils of image and guided by cutting and pointing device 8. Strands 1 are anchored at the left end of fixed collected at 2 and right free ends pass through abutment 7 is located on 5 stands using fixture and releaseation cylinders 6, and then crashes through bushes anchor.

In the next phase - bringing toroanelor - is done with a stressing jack (hydraulic jack) 9, powered by high-pressure hydraulic unit 11. Stressing can be accomplished in one working cycle of the device 9 (if race has its cylinder strand extent of the achievement of force necessary) or a sequence of working cycles (depending on the force required pretensioning and strand length).

After stressing and anchoring all strands the bushes blocking the abutment 7, pass the following stages pouring concrete and its reinforcement.

Concrete is poured into the desired shape and leave 3 to strengthen as necessary. After the time of hardening, is passed to the relief of the structure, namely the transfer voltage spread in mass concrete.

It is to operate the system to release with members hydraulic cylinders 6, place the brackets 5 and whose piston is initially positioned the rod tip back down to the furniture collected 7, leading thus its position during prestresing and anchoring strands tension, 6 hydraulic cylinders are powered by high-pressure hydraulic unit 10.

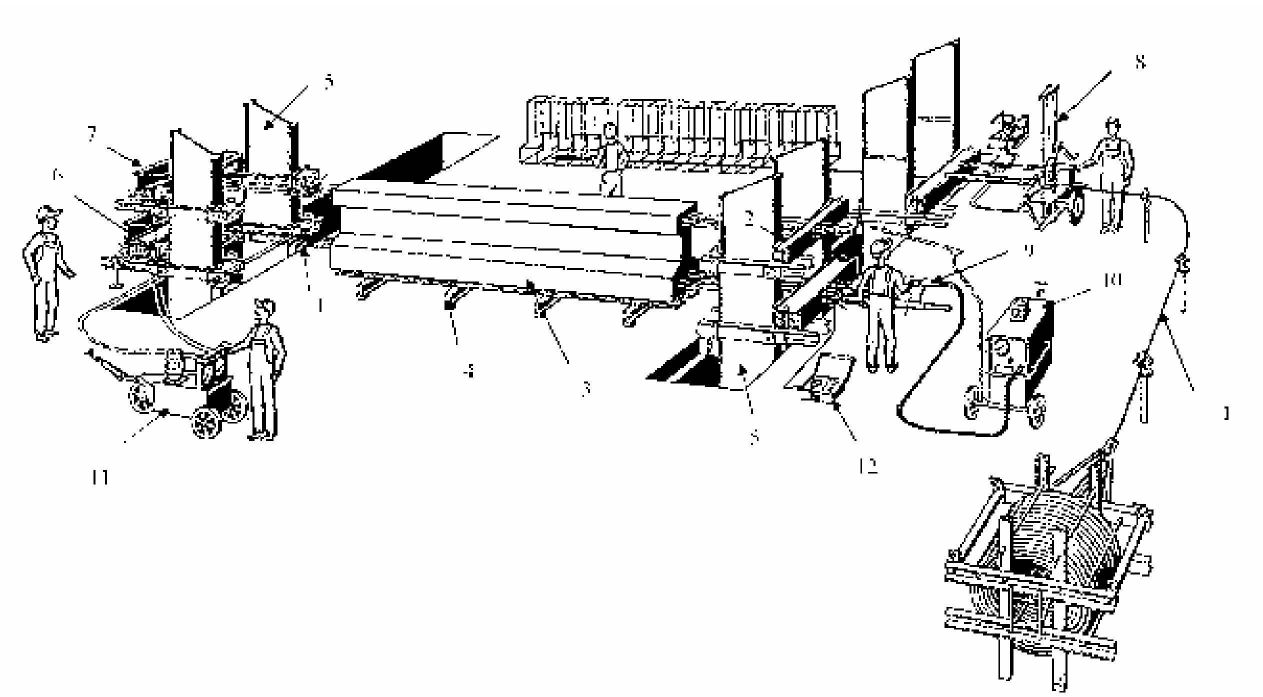


Fig. 2. - Overall structure of the stand of making prestressed concrete structures by stressing: 1 - strands, 2 - Fixed collected; 3 - plates, 4 - pedestal, 5 - Racks, 6 - hydraulic cylinders, 7 - abutment, 8 - device turned and charged; 9 - stressing jack; 10 - High pressure hydraulic unit, 11 - High pressure hydraulic unit, 12 - measuring and control system [7]

For releaseation toroanelor is unblocked while rods and hydraulic cylinders 6, the controlled discharge of fluid behind the piston, is to withdraw the rods to the left with speed and controlled, while moving to the left and abutment 7, the releaseation producându and induction of compression to tension concrete structure, speed of releaseation is determined by the speed of induction in mass concrete efforts compression without producing deformation or even destruction of its potential for high speed relief or relief of sudden.

The power of the strands is measured using measurement and control system 12 and the tension becomes zero, the strands heads cut off. Cutting strands usually run hydraulic cutting or flame cutting. After cutting heads, the concrete structure is handled by cranes in the reception and storage.

Remove the ends left over after cutting the lock collected and bushes, can proceed to repeat the cycle for developing a new beams.

These devices made in fittings tension structure prestressed concrete with forces ranging between 6.3 and 25 Tf on each fixture tense. Strain of concrete structures is achieved with minimum lengths of 6 meters to 25 meters. For very long beams are used for tensioning of high tension by 25 Tf requiring and achieving drawing from several races of dipozitivului tensioning. An important role is to release and stroke cylinders, which should increase the length and the structure and tasks to which it is subject.

Loss of pre-tensioning is defined as the difference between the tension applied wires and pretensioning of the element itself. This definition concerns the loss and the instant in time.

Most of these are in some way subject to "slip", under the action of a sustained standing tasks, tends to show a certain plasticity in the material so that material is not entirely in original form if it removes the burden. It is produced or retained as an irreversible deformation, known as "slip."

Contraction of concrete and "slip" of concrete and wires are potential sources of losses for pretensioners and the design and implementation of pre-tensioned concrete elements to take account of these contraction.

Contraction intensity may rise to 0.02% depending on environmental conditions and type of concrete. If pretensioned concrete, contractions begin immediately after casting concrete, while for post-tensioned concrete element they "consume" some of the contractions before the tendon tension, and thus power losses caused by contractions are lower.

Releasing pretensioning reinforcement compression (shortening) of concrete and the phenomenon of "release" of concrete. It should be added to the contraction of concrete.

The tension steel tendons, the effect of "releasing" is lengthening tendon, leading to a further loss of blood. Extent for all pre-tensioning system using wedge type attachments, expected some degree of stretching in one or both ends of a pre-bed. Under normal conditions, the most common devices, the spread is 3 - 13mm.

**The mobile equipment of prestressed reinforcement**

Mechanical or hydraulic pulling equipment mono or multi-wire wich anchor cabstan system that sequentially grip and pulling the wires in different variants have been used to pre-tension prestressed concrete elements. To be operated devices are used to carry hydraulic pressure required to achieve the tensioning force. At first these were mechanical equipment in time due to progress in hydraulic research and were replaced by electro-hydraulic sources of force ordered by remote control. The main disadvantage of these devices presents the weight to be handled in the correct tool to guide the tensioning of the abutment locking system where wires are located.

To facilitate the process of achieving pretensioning wires in order to obtain pre-stressed concrete structures, has developed a mobile tensioners equipment see Fig. 4. This equipment provides cross both the horizontal and acclive tensioning device. Mobile equipment, and prestressed reinforcement provided hydraulic power source associated single-wire pretensioning device.

Mobile equipment is made up of tension reinforcement a cariage **A**, made of a resistant metal construction, fitted with a lock on the position commonly known baking frame **B**. Cariage down a metal frame is equipped with rubber wheels to facilitate displacement where you want it to pre-tension wires. The carriage **A** is equipped with rubber wheels to facilitate it's dispascement to where you want to pretension wires. For handling the carriage equipment has a handle, which is coupled to the rear wheel without changes, in order to facilitate rotation of the mobile tensioners system. The vertical baking frame **B**, is provided with a camp at the top to allow rotation in a horizontal plane at $360^0$ beam **1**, beam **1** is handled by the system **2**. System **2** is designed to index a beam, the steps referred to throughout the circumference of the baking frame **B** at $30^0$, horizontally. On a beam, placed slide **3**, where a hoist hanging hook **4** at one pulley tracker **C**, which is attached to the tensioning device **D**. On the baking frame **B**, place a hydraulic power source of force **E**, which is located conveniently on the carriage has equipment to ensure stability. Hydraulic power source of force **E**, tensioning device **D** acts.

The main role of the hoist beam **1** and pulley tracker **C**, can easily manipulate single-tensioning device **D**, both horizontally and vertically to achieve a beam tensioning tendons. The role of the system **2**, is the mobile equipment can be used both for a stand that is made of prestressed concrete beams and other stands in the working area of mobile equipment.

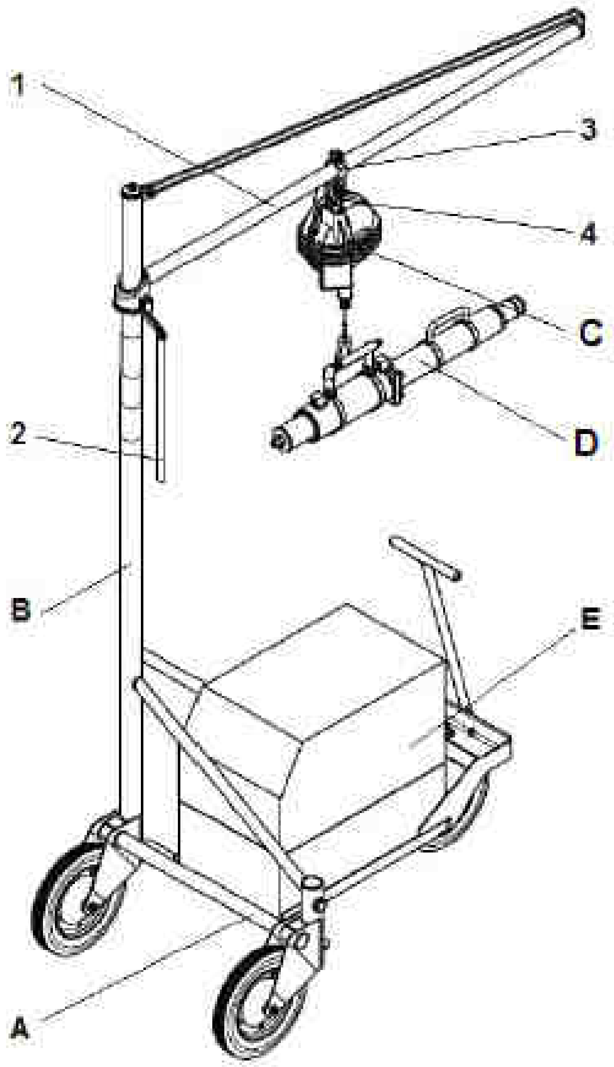


Fig.4. The mobile equipment of tension reinforcement
A – cariage, B - baking frame, C - pulley tracker, D - single-tensioning device, E - hydraulic power source of force
1 – beam, 2 – system of rotation, 3 – slide, 4- hanging hook.

The mobile equipment of tension reinforcement, is in turn composed of innovative products that will be presented below.

## Conclusion

After achieving and experimenting of the mobile equipment of tension reinforcement presented in the paper, the following conclusions can be drawn:

Mobile equipment of tension reinforcement can be used on level ground and injured both the level due to being equipage with rubber wheels.

Due to the large mass of tension devices, they can be used properly by using a hoist device tensiont mass.

Because the hydraulic power source is electrically operated, should consider using a power cable long enough to facilitate its binding to a power source.

Using an anchor carriage system in the composition of the mobile system pretensioners, can achieve a better balancing of the system and use several different weights tensioning devices.

He noted the flexibility to work on multiple staanduri tensioners, using the rotation system provided for the indexing lever $30^0$.

## REFERENCES (Arial, 11pt, Bold)

[1] D. Zetu, C. Chiriță, A. Grama, M. Afrăsinei, „Research Concerning the Technology and the Equipment to Make Prestressed Concrete Structure" Buletinul I.P. Iaşi, publicat de U.T. „Gheorghe Asachi", Iaşi, Tomul LV (LIX), Fasc. 1, **(2009)**, Secțiunea Construcții de maşini, pag. 71-76

[2] C. Chiriță, D. Zetu, A. Grama, M. Afrăsinei, „Device for Tensioning of Strands of Prestressed Reinforced Concrete Structures" Buletinul I.P. Iaşi, publicat de U.T. „Gheorghe Asachi", Iaşi, Tomul LV (LIX), Fasc. 1, **(2009)**, Secțiunea Construcții de maşini, pag 65-70

[3] C. Chiriță, A. Grama, D. Zetu, „High Pressure Hydraulic Unit Used in Making Presstresed Reiforced Concrete Structure" Buletinul I.P. Iaşi, publicat de U.T. „Gheorghe Asachi", Iaşi, Tomul LVI (LX), Fasc. 1, **(2010)**, Secțiunea Construcții de maşini, pag 213-222

[4] Glen L. Urban & John R. Hauser "Design and Marketing of New Products", Prentice Hall, Englewood Cliffs, New Jersey, 2002.

[5] C. Chiri ă, L. Damian, A. C. Hanganu, D. Calfa "Echipament mobil de pretensionat armaturi" A/00889/24.09.2010 HYDRAMOLD SRL, SC HYDRAMOLD SRL

[6] Paul Maschinenfabrik GmbH&Co. KG "Operating Manual – Pump Unit – Mach. No.:07196878/2", Max-Paul-Straße 1 88525 Dürmentingen/Germany

**ISSN 1454 - 8003**
**Proceedings of 2011 International Salon of Hydraulics and Pneumatics - HERVEX**
*9 – 11 November, Calimanesti-Caciulata, Romania*

# INNOVATIVE ASPECTS REALIZATION EQUIPMENT TO MAKE PRETENSIONING CONCRETE STRUCTURE

**Andrei GRAMA[1], Constantin CHIRIȚĂ[1] , Dumitru ZETU[1],**

[1] "Gheorghe Asachi" Technical University of Iaşi, Faculty of Machine Manufacturing and Industrial Management, Department of Machine Tools, Hydraulic and Pneumatic Systems Engineering Department

***Abstract:*** *The development of new products represents the main problem, with which problem an organization may remain on the market and may also win new market share. The rise of resistance at stretching of reinforced concrete is obtained by prestressing it. The presented equipments have an innovative character on national level due to the fact that such elements never have been made in Romania till present and they represent proposals of inventions.*
***Keywords****: Device for tensioning, hydraulic sources, pretensioning*

## 1. Introduction

Stuctural concrete or even reinforced concrete is characterised by reduced resistance at stretching in contrast with the resistance at compression. This means that these kinds of concrete should be used only for building foundations, foundations for heavy machine tools, foundations for heavy tanks etc. The concrete structures subjected to very powerful stretching loading need the stressing of the reinforcement, producing the prestressing of the concrete and finally the growth of resistance at streching. This solution is necessary for the execution of big roofs for large industrial assembly rooms, concrete bridges, platforms of multistoried parking lots, etc

The structure of uncompressed reinforced concrete subjected to strong stretching behaves as in Fig. 1a, where we can notice that under the action of the loading, cracks appear in the beams or the plates simply suported or in console, which can have an unfavourable evolution. In Fig. 1.b, the shape of the compressed structure is noticed, and in Fig. 1.c, the situation of beams or plates under the loading pressure is shown, a situation in which the lack of cracks is noticed even if the loading has much higher values.

An intermediate solution which bridges the gap between the reinforced concrete and the prestressed one, can be obtained through a partial prestressing of the concrete structure. If the reinforced concrete is expected to crack when the loading is applied and the prestressed concrete doesn't crack, the partially prestressed concrete can crack by the amplification of the loading at the value that surpasses "the decompression moment", moment when the tension in the extreme fibres of the concrete structure surpasses the resistance to stretching.

Prestressing can be achieved by using steel wires and products of steel wire: bars, strands and cables, which are greffered to in general steel „tendons". In most of the applications, these tendons aren't covered for the protection to corrosion, but there are also solutions of strands covered with epoxy resin. In other cases, other materials can be used, having in their composition non-metal fibres with high level of resistance at stretching and which are stable in alkaline environment.

The prestressing of reinforced concrete structure can be achieved in two ways:

- by pretensioning
- by posttensioning

In the case of prestressed structures, which normally are achieved in industrial rooms, reinforcement strands are subjected to stretching against a retention head before casting the concrete. After the concrete has been casted, it is left to strengthen and to reach the necessary resistance, then the release of strands from the wires is produced and their force is transferred to the concrete structure, compressing it.

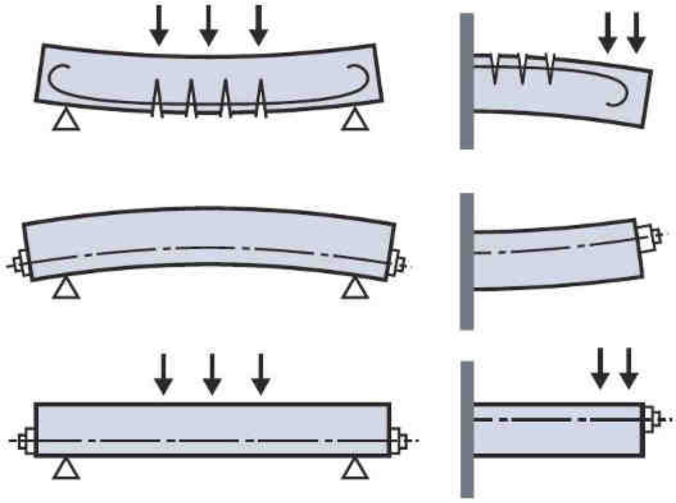


*Fig.1- Behaviour of beams/plates of reinforced concrete and prestressed under load a - reinforced concrete; b – prestressed reinforced concrete without load. c – prestressed reinforced concrete under load;*

The posttensioning is especially achieved, “in situ”, involving the installation and the tensioning of the wire strand or of some tendons under the shape of bars only after the concrete has been cast, has solidified and has reached a minimum resistance to compression.

The plates and beams precompressed through prestressing are used almost exclusively for building industrial assembly rooms or storied parking lots, while posttensioning is especially used for building „ in situ”, of concrete bridges and viaducts; the stressing of anchorage systems is exclusively achieved through posttensioning.

**2. The structure of hydraulic equipments in order to obtain prestressed concrete**

The prestressed of the reinforced concrete structure (plates, beams) through prestressing is achieved in proper industrial rooms, on complex casting bed installation which allow the execution of all technological operations necessary in this case. The equipments used for this purpose must achieve the stressing process of the reinforcement, in order to maintain this situation until the casting and solidification of the concrete is achieved, after which the release of the reinforcement is allowed, during which the stretching efforts are transferred to the concrete structure, through adherence or through marginal anchorage systems, creating in this compression efforts. At any point of the route of the prestressed reinforcement, route which can be straight or curved, there coexists two kinds of efforts in the uncharged concrete structure which balance themselves: the stretching in the reinforcement and the copression in the concrete.

The reinforcement in the concrete structure can be achieved in a number of strands (multicore cables from steel wire), of diameters from 9mm to16mm; the strands are placed at certain distances, in the case of prestressed concrete plates or in strands wire, in the case of concrete beams. Normally, in the case of plates, prestressing is achieved individually, strand by strand, and the cluster of strands are prestressed in groups; but the release of the reinforcement is always achieved for all the strands at the same time, avoiding thus the production of undesired deformations of the concrete structure due to different stressing of one strand or another.

The general structure of the prestressing /release/casting stand of the precompressed concrete structures is presented in Fig. 2. Strands 1 are anchored at the left end to the abutment anchor 2 and at the free ends in the right pass through the abutment 7 and the travers anchorage plate 8 for socket anchorages after prestressing. The prestressing is achieved with the help of a single-wire pretensioning devices 9, fed from a hydraulic unit of high pressure 11. The prestressing can be achieved only during one working cycle of the single-wire pretensioning devices 9 (if the stroke of its cylinder allows the achievement of the strand with the necessary strength) or in a sequence of strokes (depending on the strength demanded by prestressing and the length of the strand).

After the prestressing and achoring of all the strands in the socket anchorage in slab 8, the concrete is cast in the desired shape 3 and it is left to solidify as long as it is necessary. After the time is up the system of release is operated having hydraulic relaxation cylinders 6, placed on the bolsters 5 and whose pistons are initially placed with the end of the branch rods on the abutment 7, thus determining its position during prestressing and anchoring of the stressed strands; the hydraulic relaxation cylinders 6 are fed from the hydraulic unit of high pressure 10.

To release of the strands, the rods of the hydraulic relaxation cylinders 6 are instantaneously released and through the controlled evacuation of the fluid behind the pistons, it is allowed the withdrawal of the rods to the left with a controlled speed and at the same time it also moves to the left the abutment 7 and the slab 8, producing the release and the transfer of the compression tensions towards the structural concrete; the release speed is determined by the transfer speed in the concrete mass of the compression efforts without producing its deformation or even its destruction, which may happen in the case of a release at high speed or of a sudden release. As results from Fig. 2 in order to achieve structures from prestressed concrete, two hydraulic equipments of high pressure are necessary: the stressing equipment of the reinforcement and the release equipment. Normally, if it is necessary to achieve the stressing strength at high precision and the on-line monitoring of the working and technological parameters of the equipment, then there will also be necessary to introduce a monitoring and controlling equipment of the stressing strength.

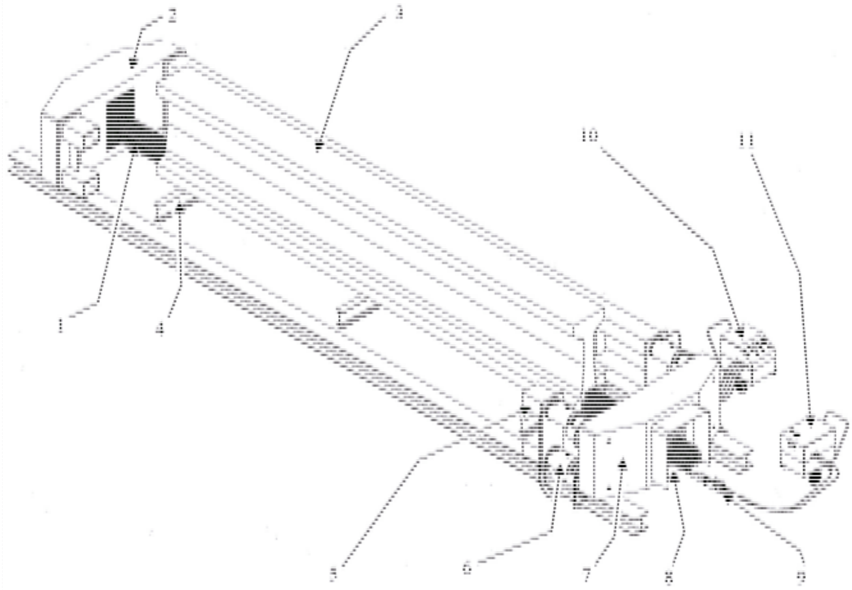

Fig. 2. – General structure of the stand to achieve prestressed concrete through prestressing
1 – strands; 2 - abutment anchor; 3 – mould; 4 – support; 5 – bolsters; 6– hydraulic relaxation cylinders; 7 – abutment; 8 – slab; 9 – single-wire pretensioning device; 10 – high pressure hydraulic unit for release; 11 - high pressure hydraulic unit for pre-tensioning;

In DISAHP from Techical University “Gheorghe Asachi” Iassy was realized an innovative system for obtaining prestressed concrete by prestressing, system that includes invention proposals and satisfies the high level of performances requested by the market.

### 3. The innovative structure of the tensioning device

The tensioning devices of reinforcements used to obtain prestressed concrete is achieved in different constructive ways, offering each time the creating of an innovative structure of the device. All these devices are portable; those having weights up to 20daN can be manually manipulated, while those with weights over 20daN (for example, the devices for the tesioning of strands placed in clusters) are placed on carriages and moved in the position in which the technological process is achieved.

The work phases of the tensioning device of a single strand are represented in Fig. 3 and defined as follows.

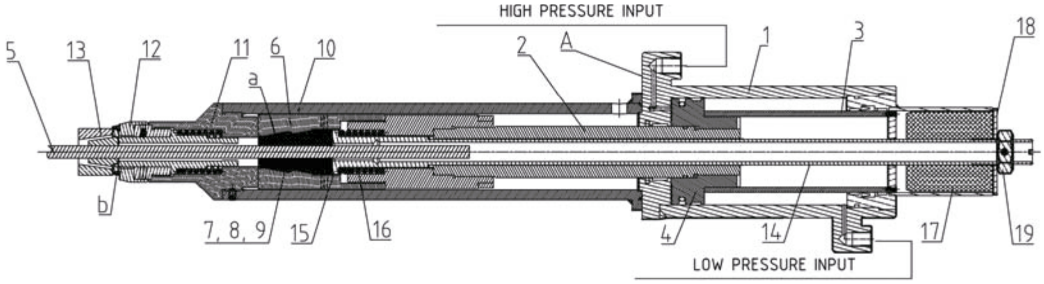


Fig. 3. Tensioning device with mechanically driven blockings
1. Cylindrical frame; 2. Left hollow rod; 3. Right hollow rod; 4. The cylinder piston; 5. Strand; 6. Bushing; 7, 8, 9 Wedge grips, strand blocking system; 10. Pipe frame; 11. Bushing; 12. Abutment cup; 13. Bushed bearing with mantle corbel; 14. Guiding strand pipe; 15. Flange; 16. Arc; 17. Protection bushing; 18. Shutter disk; 19. Nut with blocking spline to insure the set position.

The work phases of the tensioning device of a single strand are represented in Fig. 4 and defined as follows.

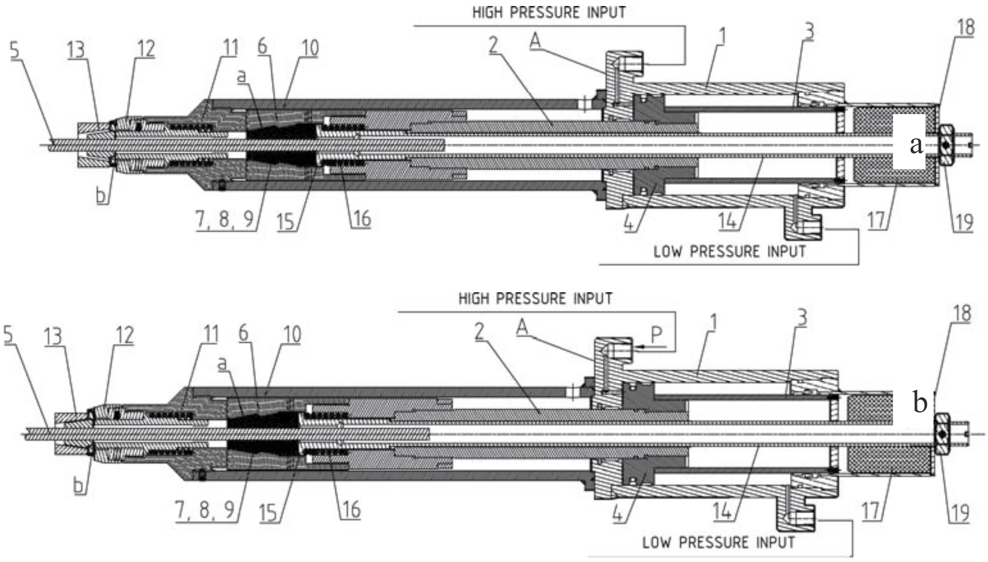

ISSN 1454 - 8003
**Proceedings of 2011 International Salon of Hydraulics and Pneumatics - HERVEX**
*9 – 11 November, Calimanesti-Caciulata, Romania*

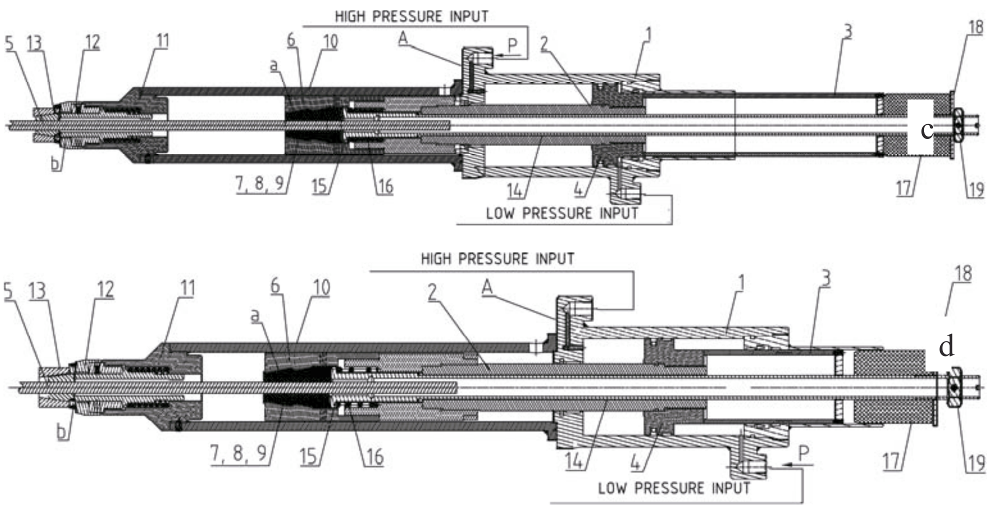


Fig. 4 Functioning phases of the tensioning device of a single strand with mechanically driven blockings

a - phase I, b – phase II, c – phase III, d – phase IV

Phase I: The introduction of the device on the free end strand 5 until the abutment cup 12, through the rams “b”, is supported on the block wedge grips 13; the inside arc of the bushing 11 will be in compressed state after achieving the contact between the alignment piston of the wedge grips and the blocking wedge grips. In this moment, the device with mechanically driven blockings will be concentrically positioned with the strand that must be tensioned;

Phase II: The coupling of the high pressure fluid entrance in the chamber on the left of the piston 4, producing, in the first phase, the pulling towards the right side of bushing 6 and the blocking of wedge grips 7, 8 and 9 on strand 5 due to the action of the dual cone-shaped surface on the mantle corbel; the permanent contact between the surface “a” of the wedge grips and bushing 6 is maintained because of the action of arc 16. To better control of the contact between the wedge grips surface and bushing 6, a gripping of nut 19 is performed until this is blocked by the shutter disk 18, whereupon the nut is secured with the help of a blocking spline;

Phase III: Pulling of the strand to the right until the achievement of necessary stretching force is performed. This is achieved until piston 4 reaches the right end of its stroke. If there are long strands, in order to straighten the strand and then to stretch it with the desirable stretching strength it is necessary to perform more strokes of the piston because the stroke of a tensioning device of strands can’t exceed the values 500 ÷ 600 mm.

To use cylinders with reasonable strokes (300-500 mm) even in the case of a longer strand, the pulling cycle is repeated until it reaches the necessary tensioning force.

Phase IV: The bring back of wedge grips for a new pulling is done by stopping the high pressure fluid entrance and strand 5 is blocked in the mantle corbel 13; then the low pressure entrance is coupled and piston 4 and bushing 6 are moved towards the left, releasing the wedge grips 7, 8 and 9. Now the system moves towards the left side until it reaches the position from phase II.

The back in the initial position the cycle is repeated according to the above-mentioned phases.

After repeating the cycle until it reaches the demanded value of the strand stretching force, the device is back in the initial position and it is removed from the strand, this remaining blocked in the mantle corbel 13 and goes then to the next strand in the same way.

The flexibility of these devices, demanded by various applications, is insured by the possible modification, mainly, of the two parametres but also of the different constructive parametres demanded by the application requirements, such as: the strand diameter (9, 12, 15, 18 mm), the minimum length of free end of strand etc. The pressure parameter of the high pressure unit is insured by the possibility of using some pressure pumps up to 700 bar, with different steps of necessary pressure useful in various phases of the tensioning cycle. With the hydraulic controlling panel of the device, we must insure not only the feeding at diffrent pressure in the various phases of the work cycle but also the necessary blockings in case of accidental disconnecting of the pressure in the feed circuit. Also, the logical structure of the controlling system must exclude the possibility to transmit a wrongly controlling signal for the normal sequence of the working phases.

As far as the tensioning strength of the reinforcement is concerned, this can be monitored on-line by supervising the value of the feed pressure of the pulling cylinder with the help of an air gauge in strength values standard and the display of these values. The command to stop feeding can be done manually, after observing on the air gauge of strength value, or automatically, by introducing in the feed circuit a pressure relay, programmed to trigger when reaching the suitable corresponding tensioning strength.

**4. The innovative structure of the hydraulic power source**

For realizing a prestressing operation of the prestressed concrete structures through pretensioning or post-tensioning it is necessary the development of a high strength and of a high work speeds, that in the present moment is realized with the help of the hydraulic actions of high pressure. The system embeds o series of independent components that have the role to produce, take, transform and transmit the energy to the execution element, see fig. 5

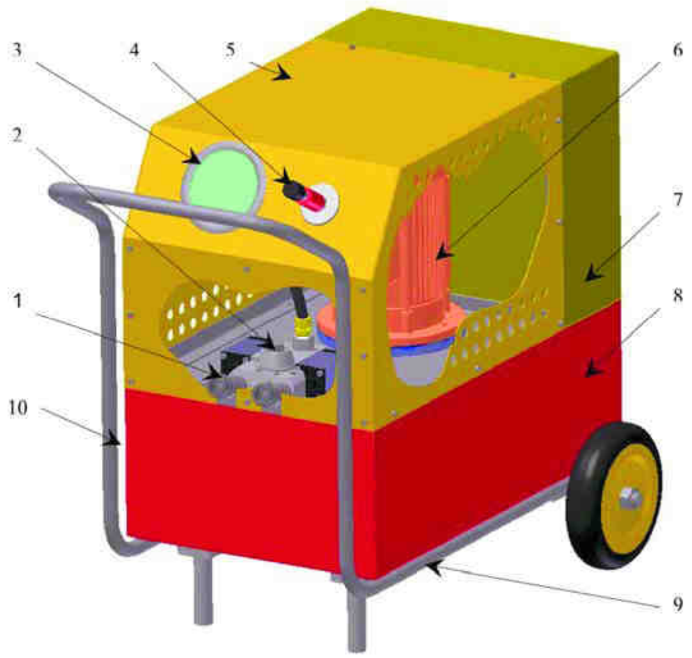


Fig 5. The structure of the high pressure hydraulic unit

1. The main semi thimble 2. Double action multiplier, 3. Manometer, 1000 bars 4. Regulation pressure valve 5. Pad 6. Electro pump( electric engine and PRD pump), 7. Electrical panel 8.Oil storage, 9. Support and operating gantry (with wheels), 10. Oil level indicator [3]

The electro pump Ep1 is formed of the pump with gears P which is powered with the electric engine ME. The bound between the pump and the engine is ensured by a gearing with elastic materials. The pump P has a suction filter F1. The electro pump is placed on the store, in a vertically position, with the pump and the suction filter dipped in oil.

The command, regulation and control panel is placed on the superior side of the hydraulic multiplier and on this are placed the following hydraulic device: D1 and D2 distributors, the fast connecting bins of the consumers and the movable direction valve SD.

The hydraulic multiplier is a compact construction that which contains the multiplying system (piston, bar, direction valve) and at the exit it has placed the direction valve S1, S2. It is placed on the store of the group and is partially dipped in oil. At the superior side we can see the command, regulation and control panel.The work principle of the electro-hydraulic high pressure group is presented in Fig 6.

For starting the electro-hydraulic group it is put under stress. In this phase, the hydraulic linkage is: The oil from the store is swept by the F filter, by the pump with gears with double section P and cranked back into the store. This operation takes about 10 minutes for stimulating the oil in electro pump oil and the homogenization of the hydraulic oil.

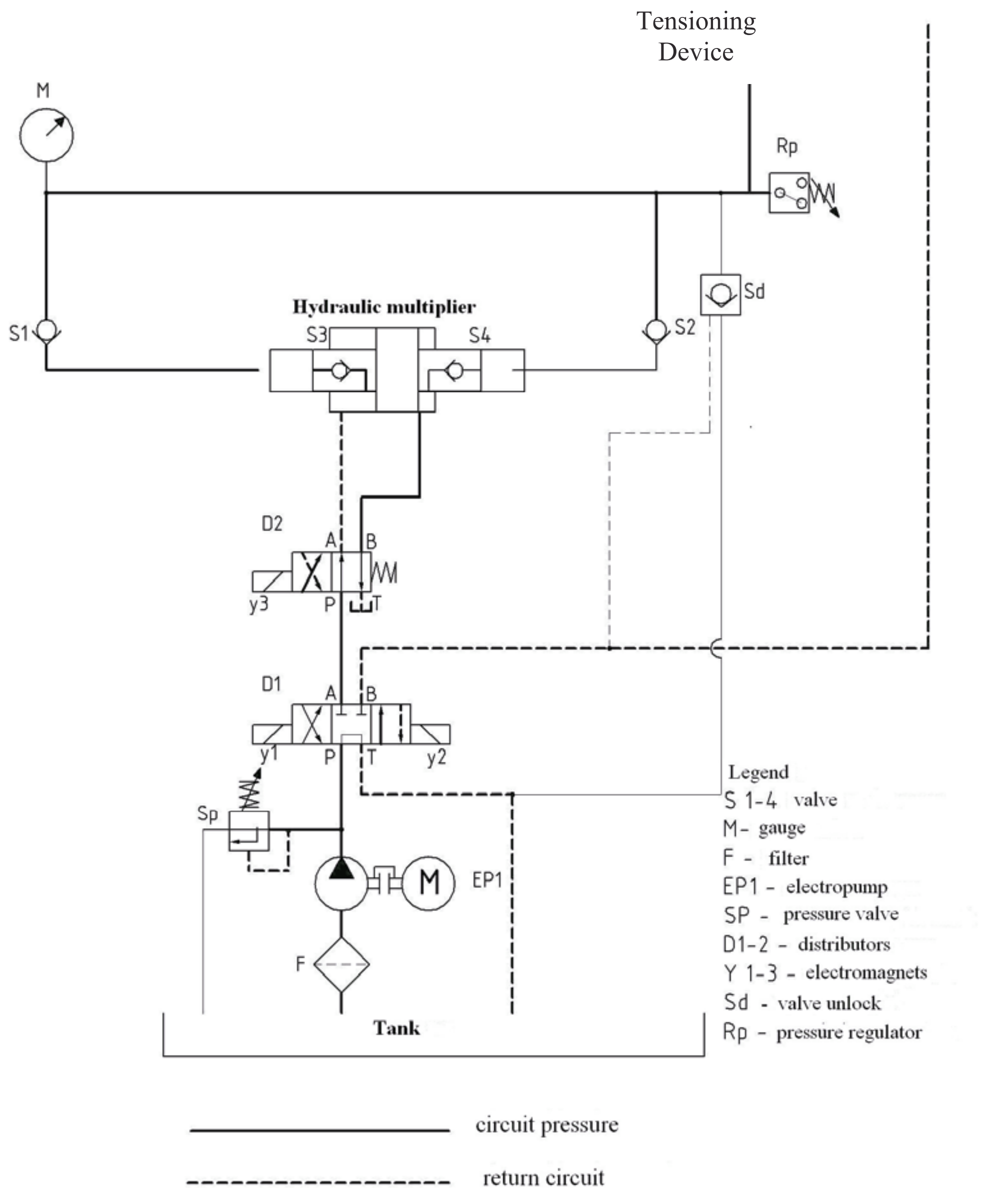


Fig. 6 Hydraulic scheme of high pressure hydraulic unit

In the next phase the linking of the tendon and the stroke of it by the tensioning device takes place. The direction of the hydraulic circuit is: the oil from the store is swept, through filter FA1, by the pump with gears with double section P and cranked back in the hydraulic installation through D1 distributer. (The electromagnet y2 is activated) and through the distributer D2 ( the electromagnet y3 in inactivated) at the hydraulic multiplier with double section. The oil transverse the hydraulic multiplier also through the direction valve S1 and it is transmitted to the fast thimble RP and the pressure hose reaches the consumer. The fast movement is realized till the pressure from the system reaches 100 bars, value at which the pressure valve SP was set, moment in which the multiplying process begins.

For bringing the hydraulic multiplier at the initial position after the piston inside realizes a stroke, has the following hydraulic path: the electromagnet y3 of the distributer D2 is activated, it realizes the changing of the pressure circuit from the tube A on tube B and the oil from the tube A and inside the hydraulic multiplier is transmitted to the oil storage.

The stroke of the cylinder inside the hydraulic multiplier is determined with the help of some electromagnets that are in contact with the bottom walls of the hydraulic multiplier. During the drawing, due to the low volume of oil that gets out from the multiplier leads to the realization of gradually movement of the piston inside the cylinder from the tensioning device.

Forward, after realizing the drawing of the tendon till the end of cylinder stroke of the drawing device, takes place the returning to the initial position, fact that allows the release of the tendon. From hydraulic point of view implies the activation of distributer D1 ( the electromagnet y1 is activated), fact that leads to the stop of using the hydraulic multiplier and the bringing of oil under pressure in the cylinder of the tensioning device, the oil gets in the storage through the movable valve Sd.

When getting back to the initial position the piston of the tensioning device has the same gradually move due to the action of the movable valve Sd on all the realized circuit. Stopping and activating the movable valve Sd is fast realized, the process can't be seen by the human eye.

## 5. Conclusion

After achieving and experimenting of the tensioning device presented in the paper, the following conclusions can be drawn:

The tensioning device in Fig. 1 having a load of about 20 daN, can be used both in applications of prestressing the concrete through pretensioning and through posttensioning, when the operation is done"in situ";

Fed from a high pressure hydarulic source (700 bar), the device can produce the tensioning strength of a single strand up to 25 tf;

The tensioning device shows special security during the work, security due both to the constructive execution and to the hydraulic controlling panel of the device which insures the necessary blocking in case of accidental disconnection of the pressure in the feeding cycle;

A special flexibility has been noticed in using the device as it can be used to tension some strands of various lengths, due to the possibility to work in repetitive cycles, but also of different diametres, due to the possibility to change the blocking and the pulling wedge grips;

Following a number of repetitive attempts, we reached the conclusion that both in the construction of the pulling and blocking wedge grips and their thermal treatment, must be achieved in such a way as to insure the frictional force between the wedge grips and the strand at values which should not allow the slipping between them during the work or during the blocking of the tensioned strand.

After achieving and experimenting of the high pressure hydraulic unit presented in the paper, the following conclusions can be drawn:

The unit can be used electro submitted applications both in specialized factories and "in situ" for both the prestressed concrete structures pretension and by postension.

Because of the way he has, the unit can carry high-pressure hydraulic tensioning devices on supports of their settlement on the mount.

Because the device pulling heavy loads, high pressure hydraulic unit can attach a system to maintain its working position for ease of handling and working with it.

To acquire data on achievements stages firing, high pressure hydraulic unit can be fitted with measuring and storage system working pressure hydraulic circuit.

Due to variations of pressure what extent they wish to wires, control panel buttons can be introduced to limit the pressure to the desired value, so that their drawings to achieve the best conditions.

High pressure hydraulic unit may be used drawing as a device that presented in the paper. You can also use two or three devices can work simultaneously or separately, the changes to the hydraulic circuit, electrical panel and the control.

## REFERENCES

[1] D. Zetu, C. Chiriță, A. Grama, M. Afrăsinei, „Research Concerning the Technology and the Equipment to Make Prestressed Concrete Structure” Buletinul I.P. Iaşi, publicat de U.T. „Gheorghe Asachi”, Iaşi, Tomul LV (LIX), Fasc. 1, **(2009)**, Secțiunea Construcții de maşini, pag. 71-76

[2] C. Chiriță, D. Zetu, A. Grama, M. Afrăsinei, „Device for Tensioning of Strands of Prestressed Reinforced Concrete Structures” Buletinul I.P. Iaşi, publicat de U.T. „Gheorghe Asachi”, Iaşi, Tomul LV (LIX), Fasc. 1, **(2009)**, Secțiunea Construcții de maşini, pag 65-70

[3] C. Chiriță, A. Grama, D. Zetu, „High Pressure Hydraulic Unit Used in Making Presstresed Reiforced Concrete Structure” Buletinul I.P. Iaşi, publicat de U.T. „Gheorghe Asachi”, Iaşi, Tomul LVI (LX), Fasc. 1, **(2010)**, Secțiunea Construcții de maşini, pag 213-222

[4] Glen L. Urban & John R. Hauser “Design and Marketing of New Products”, Prentice Hall, Englewood Cliffs, New Jersey, 2002.

[5] C. Chiri ă, L. Damian, A. C. Hanganu, D. Calfa, A. Grama “Cap tensionare armături” A/01016/04.12.2009 SC HYDRAMOLD SRL, SC HYDRAMOLD SRL

[6] Paul Maschinenfabrik GmbH&Co. KG “Operating Manual – Pump Unit – Mach. No.:07196878/2”, Max-Paul-Straße 1 88525 Dürmentingen/Germany

**ISSN 1454 - 8003**
**Proceedings of 2011 International Salon of Hydraulics and Pneumatics - HERVEX**
*9 – 11 November, Calimanesti-Caciulata, Romania*

# DEVICE TO FACILITATE START INTERNAL COMBUSTION ENGINES

**Andreea BRODEALA[1], Bogdan MIHAILESCU[1], Vasile ALEXANDRU[1], Paul SVASTA[1], Mihaela PANTAZICA**

1Center for Technological Electronics and Interconnection Techniques, University “Politehnica” of Bucharest, Romania

e-mail address: andreea.brodeala@cetti.ro

***Abstract***: *“Electrochemical Double Layer capacitors” – EDLC, supercapacitors or ultracapacitors are the terms currently used for the passive components where the accumulation of charge takes place in the double layer at the atomic level. EDLCs are different from lead batteries which have very high charging current. This current can reach values of 1000A. EDLC operation is similar, in a first analysis, to the conventional electrolytic capacitors. Another parameter is the leakage current, which defines the maximum energy stored and maintained as energy losses [1]. Modern technologies used to achieve low electrical resistance materials and processing their surfaces enabled the realization of the EDLC cells (based on an invention which took place 150 years ago). These are able to store more energy as electric charge. Supercapacitors are able to store a quantity of electricity compared with the accumulator. Batteries store electric charge a long time under constant voltage and relatively small current, but they require charging with very high currents.*

***Keywords***: *EDLC, start, internal, combustion, engine*

## 1. Introduction

Modern technologies used to achieve low electrical resistance materials and processing their surfaces enabled the realization of the EDLC cells (based on an invention which took place 150 years ago). These are able to store more energy as electric charge. Supercapacitors are able to store a quantity of electricity compared with the accumulator. Batteries store electric charge a long time under constant voltage and relatively small current, but they require charging with very high currents see fig. 1.

Vezi la review sau ceva similar pentru office 2003 unde scrie Accept all changes sau modifications.

## 2. Supercapacitors technologies and performances versus lead acid batteries

Lead-acid batteries are relics that haven’t changed much since their invention nearly 150 years ago. Heavy and unable to withstand rapid charge-discharge cycles, they are unsuitable for the automotive world’s killer app, hybrid-electric vehicles. Hybrids instead use expensive nickel-metal hydride (NiMH) batteries or, experimentally, lithium batteries. But a new, souped-up version of lead-acid batteries could change that, cutting the cost of hybrids and also improving the function of power grids and a range of other applications. The new design combines lead-acid chemistry with supercapacitors, energy-storage devices that can quickly absorb and release a lot of charge, which they store along the roughened surface of their electrodes. Unlike ordinary lead-acid batteries, which are slowed by the movement of chemicals within them, these could provide quick bursts of power for acceleration and then recharge during braking, a must for hybrid-electric and electric vehicles. A hybrid’s rapid recharging cycles and high currents would destroy the lead electrodes in standard batteries, because lead sulfate would build up on them. The new batteries can go through at least four times as many charging cycles as lead-acid batteries, and, crucially, would cost about a quarter of NiMH batteries [2].


EDLC cells with values of 1200F/2,5V and 600F/2,5V


Lead acid battery

Fig. 1.

The new batteries advantage over standard lead acid batteries comes from simple tweaks of the negative electrode. Instead of a lead plate, the electrode are made from activated carbon, the highly porous, spongelike material used in supercapacitors electrodes. When a regular battery discharges, the lead electrode reacts with sulfate ions, forming lead sulfate and creating protons and electrons. Supercapacitors activated carbon electrode directly releases and adsorbs protons from the sulfuric acid electrolyte during discharging and charging. The batteries recharge four times as fast as conventional ones [2].

Advantages of EDLC versus batteries could be enumerated:

a. loading and cutting discharging current that can reach values of 1000A
b. working regardless of position
c. 500.000 cycles of charge/discharge, compared to the accumulator, which guarantees only a few hundred charge/discharge cycles. However the lifetime is limited to 10 years.
d. report task/ low weight charge/low weight were reported
e. usage at temperature below -50$^{o}$C
f. reducing lead
g. environmentally friendly.

### 3. Operating principle

**ISSN 1454 - 8003**
**Proceedings of 2011 International Salon of Hydraulics and Pneumatics - HERVEX**
*9 – 11 November, Calimanesti-Caciulata, Romania*

Charge transport phenomena occurring in double-layer materials have led to the development of high capacity capacitors. EDLC store energy in the same way as aluminum electrolytic capacitors, that is charge is not only gained at the two plates but also at the interface between conductor surface and an electrolyte solution The charge accumulated thus, forms a double layer that is electrically charged, the separation between each layer being of a few Angstroms. EDLC cells are composed of two plates, forming two layers, one at each interface electrode/electrolyte, which leads to the formation of two "capacitors connected in series". A membrane separates the two layers and does not allow electric contact between them. The membrane allows ions to pass through, from one side to the other [3], see fig.2

Products are available on the market as EDLC cells with rated voltage of 2.5 V or as supercapacitors modules. Modules are obtained by connecting cells in series to obtain voltages up to 300V [4]. The maximum capacity of an existing commercial supercapacitor cell is currently 5000 F.

The EDLC cell from fig. 2 contains two thin film aluminium foils coated with a black carbon-based film and an electrolyte solution izobutironitril. Active treatments applied to the carbon influence the porous structure of the plate surface and the electrolyte adherence to these pores is very important.

Storing charge in double layer is a surface process, so it can be concluded that the characteristics of the plate surface bear a direct influence on the capacitance value of the supercapacitor. The material that is most widely used for the plates is carbon, but research in the field point to metallic oxides and conducting polymers as interesting alternatives.

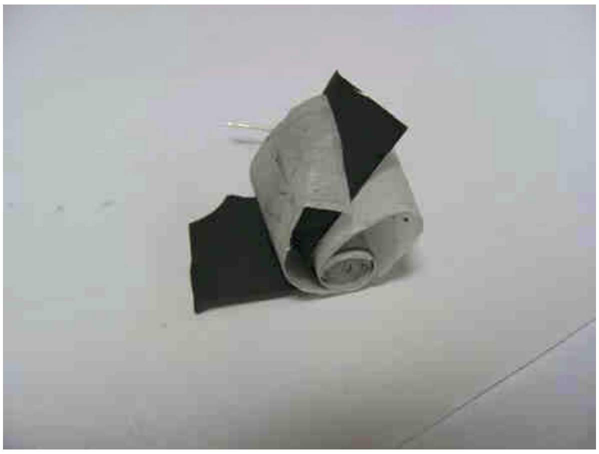

Fig. 2 opened supercapacitor cell

The plates are realized from materials with an effective surface processed to increase the surface of the double layer: porous carbon, carbon aerogels. High energy density's can be obtained due to the high specific capacitance. This capacitance values are obtained through:

- The existence of the plate/electrolyte interface on the plates;
- The existence of the thin layer (of atomic dimensions) that separates the charge.

In many cases a given type of carbon with a smaller useful area can have a higher specific capacitance than a carbon type with a higher useful area. This occurrence is due to the process of carbon processing and to the direct dependency of the double layer capacitance of these processes.

Active treatments applied to the carbon layer influence the porous structure of the plate surface and the electrolyte adherence to these pores is very important.

Metallic oxides represent an alternative, mainly due to their high specific capacitance and low electrical resistance, thus allowing the fabrication of EDLC's with high power and energy density [5].

The separator with its meshed configuration prevents the apparition of an electric contact between the two plates but allows the ionic load transfer. Paper and some polymers are used as separators in the case of organic electrolyte solutions. In the case of aqueous electrolyte solutions ceramic materials or glass fiber are used as separators. To obtain high performances the separator must be thin and must have high electrical resistance and high ionic conduction capacity [5].

## 4. Measurement and results obtained using EDLC battery

### 4.1. EDLC Battery

Since EDLC have very low nominal voltages (2,5-2,7V) in order to employ them at customary industrial applications and consumer voltages (5V, 12V, 24V etc.) it is necessary to connect them in series. Connecting capacitors in a series configurations has some disadvantages such as a reduction of the total capacitance (for example 6 capacitors, each with a capacitance value of 600F, connected in series will have the equivalent capacitance C/6=100F) [6].

An EDLC's battery shall not be able to store enough energy for working condition with average currents over a long period of time. Similarly a lead battery should be over-sized, so that it would be able to deliver the peak power needed for the high current regime. Over-sizing a lead battery would increase the system weight and overall cost. A hybrid source composed of a capacitor battery with load accumulators system reduces weight by nearly 60% and leads to a significant reduction in cost [6].

For this work we propose a battery that consists of six EDLC's cells of 600F each connected in series. In this case it is very important to maintain all capacitors within the limits imposed by the rated voltage. In order to maintain an even voltage at the capacitors terminals, resistors are used. These resistors are called equalization resistors and are connected in parallel with each series connected capacitor see fig. 3.

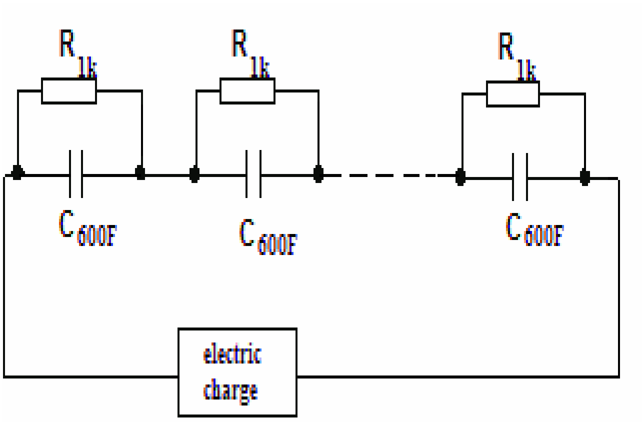


Fig. 3. Equalization voltage EDLC in series grouping – elect switching devices.

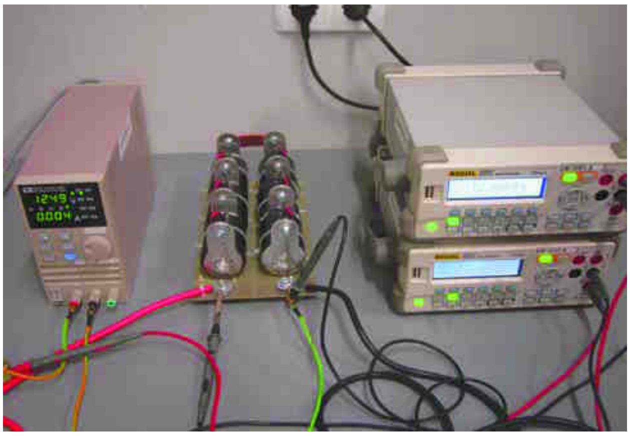

Fig. 4. Set-up measurement

When connected in series, care must be taken to ensure the capacitor voltages are balanced to prevent overloading either of them. Equalization resistors can be used in parallel on each capacitor, see fig.3 this solution has the disadvantage that it drains the capacitor when the charging circuit is disabled. Using an electronic circuit eliminates this disadvantage. Equalization resistors are used in order to maintain an even voltage at the EDLC terminals. When the voltage across an EDLC increases balancing due to current loss resistance decreases. This happens for every EDLC cell.

The advantage of using this tandem - car battery with EDLC - is to reduce weight/unit of energy. For example we can use in place of a 60A/h accumulator, with a circuit current of 500A, a system employing a 25Ah lead battery, with a short circuit current of 100A, and an EDLC with a maximum of 400A/h [6].

### 4.2. Measurements and results

Processing and results of measurements made with the platform from fig. 4. EDLC's battery was powered at 15V and 2A of the power supply. On the battery were measured output voltage and leakage current. Leakage current is that which exists in battery after it has stabilized at loading see fig.5. Note that EDLC's battery was charging in about 15min and the leakage current can be read after 12hours. The equalization resistors R are axial resistors 1K with metal oxide film. The equalization resistors are designed to stabilize voltage on each EDLC cell.

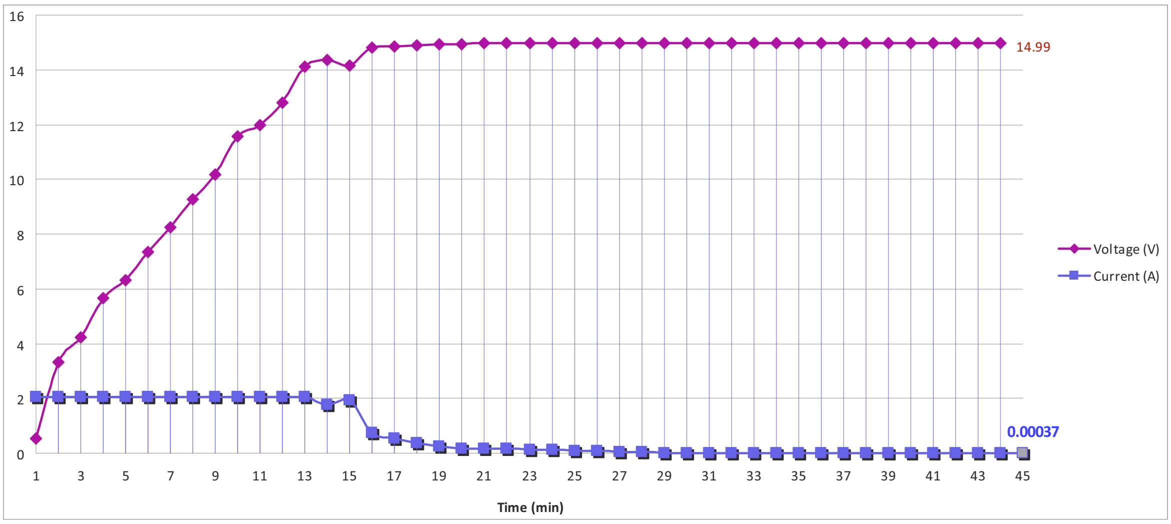


Fig. 5.a. Charging the EDLC batteries.

The charging voltage starts at 0.53mV and after 13min the voltage is 14.37V see fig.5.a. The current begins to drop from 2A to 1.76A. This decrease continues about 12hours, the last value 0.37mA is considered to be leakage current seefig.5.b.

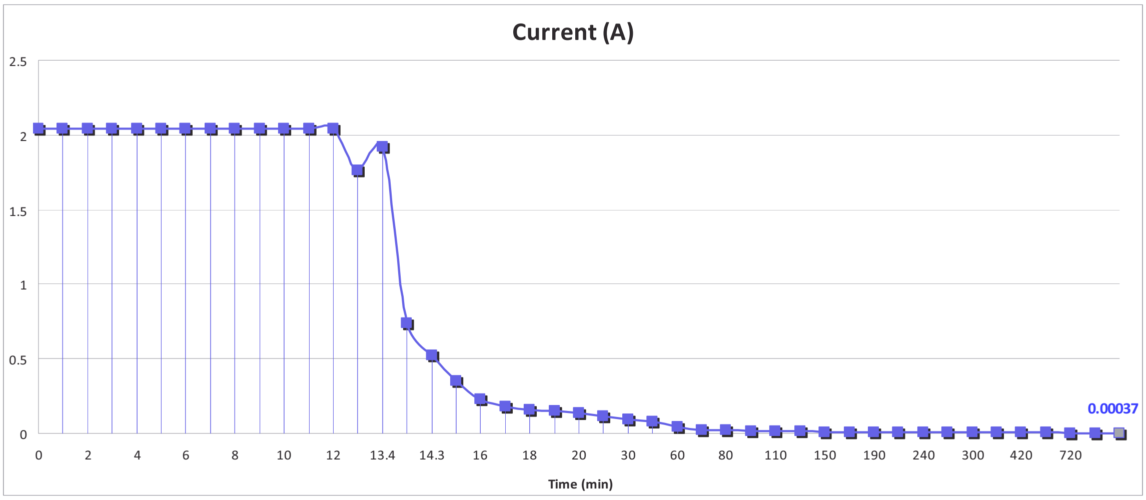


Fig. 5.b.Charging the EDLC batteries.

## 5. Conclusions:

- Constructive elements of EDLCs that have a direct impact on its performance are the electrolyte, separator and fixtures. Surface properties of a material used to manufacture have a significant impact on the specific capacity of the capacitor;
- The electrolyte and the separator influence directly the specific capacitance and have a direct impact on energy density.
- The advantage of using equalization resistors is to decrease current loses.
- The advantage of using this tandem - car battery with EDLC - is to reduce weight/unit of energy.

## Acknowledgment

The work has been funded by the Sectoral Operational Programme Human Resources Development 2007-2013 of the Romanian Ministry of Labour, Family and Social Protection through the Financial Agreement POSDRU/6/1.5/S/16 and through the Financial Agreement POSDRU/88/1.5/S/60203.

## References

[1] B.E. Conway, "Electrochemical Supercapacitors, Scientific Fundamentals and Technological Applications", Kluver Academic, 1999.
[2] http://spectrum.ieee.org/green-tech/advanced-cars/a-batterycapacitor-hybridfor-hybrids
[3] P. Svasta, A. Vasile, C. Ionescu, V. Golumbeanu, "Condensatoare", Cavallioti, Bucharest 2010.
[4] http://www.imt.ro/tehnanoconel/tehn.htm

[5] Andreea Brodeală, Alexandru Vasile, Emilian Ceuca, Paul Svasta, Cristina Marghescu Ciprian Ionescu - EDLC Characterization Platform SIITME 2010 Pitesti 2010.

[6] Alexandru Vasile, Andrei Drumea, Paul Svasta, Andreea Brodeala, Ciprian Ionescu, Cristina Marghescu – „Dispozitive moderne pentru acumularea de sarcină electrică şi aplicații specifice, Hervex 2010

ISSN 1454 - 8003
Proceedings of 2011 International Salon of Hydraulics and Pneumatics - HERVEX
*9 – 11 November, Calimanesti-Caciulata, Romania*

# ELECTRONIC SOFT STARTER FOR THE CONTROL OF ELECTRIC PUMPS UP TO 2.2 KW

**Bogdan MIHAILESCU[1], Andreea BRODEALA[1], Alexandru VASILE[1] si Paul SVASTA[1]**

[1] Centre for Technological Electronics and Interconnection Techniques, "Politehnica" University of Bucharest,

e-mail: bogdan.mihailescu@cetti.ro

***Abstract:*** *One of the main problems that occur frequently in a water distribution system involves the start-up, but especially the stopping of the electric pumps. The clash of water with the system pipes can cause premature wear of both the pump and the distribution network. This paper presents a proprietary solution of electronic controlling the single phase electric pumps with nominal power ratings up to 2.2 kW in order to eliminate the wear caused by the sudden start and stop of the system. The developed electronic module allows the control of energy transmitted to the pumping equipment and to program the parameters of the system depending on the application. It can also change that starting and the stopping ramp of the entire system. The method used has minimal electromagnetic disturbances due to switching of the power semiconductor device as it passes through zero voltage of the mains.*

***Keywords****: electric pump control, soft starter, electric motor control*

## 1. Introduction

In a water distribution system every pump must be properly controlled in order to avoid accidents. The paper presents an economical solution for electronic control of a single phase electric water pump in order to avoid the problems that most often appear when starting and stopping a water distribution system. When the system sudden stops the clash of water with the system pipes can cause premature wear of both the pump and the distribution network. In severe situation can even lead to physical damage of the valves and pipes that would require costly repairs. The proposed electronic module can be used to control single phase water pump with up to 2.2 kW nominal rated power. It was designed as an energy efficient electronic prototype which is based on a solid-state relay (SSR) as the switching element with the role to actively control the injection of power in a system, in this case the electric pump. The main feature of the module is the capability of switching between the on-phases and the off-phases during the zero-crossing of the AC mains, which offer the premises of very low electromagnetic emissions, which are necessary in order for the device to not interfere with other, more electromagnetically susceptible electronic devices also part of the controlling block of the system.

The paper describes the electronic module prototype operating principles, the experimental tests performed in order to validate and optimize the solution, laboratory tests for electromagnetical compatibility and determining the maximum radiated emissions in the frequency domain and validation of the results by experiments made in semi-anechoic chamber.

## 2. Electronic Control Module Operating Principles

The process control module block diagram is presented in figure 1. A PIC16F690 RISC micro-controller was used in order to minimize the costs, the dimensions and the power consumption. A solid-state relay SSR (S102S02-Sharp) was chosen as switching element (power switch block), offering an isolated interface between the high voltage AC input and the low voltage DC control

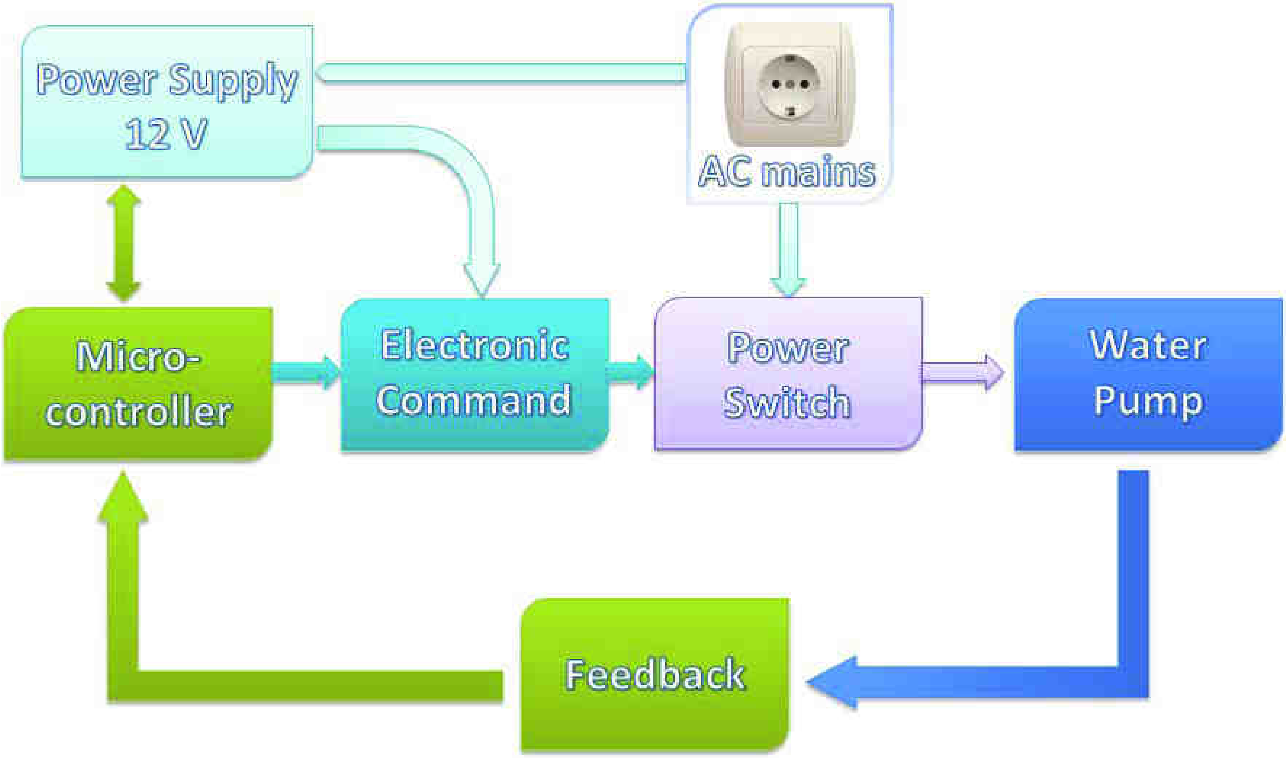


**Figure 1** Schematic block of the electronic control module

circuitry. The power supply delivers a continuous voltage of 12V to the micro-controller and the command block. The water pump block represents the load whose operating parameters values is returned to the micro-controller for analysis through the feedback loop for assessment in oreder to decide the next command to be given.

An important feature of the SSR named above is the zero cross detection [1]. There are two conditions necessary for a SSR to switch:

- a zero crossing of the voltage by its internal detector;
- an enable signal on its input circuit (an infrared, IR, LED and a photovoltaic detector).

Therefore, the first investigation was to emphasize the switching at the zero crossings of the mains voltage on different resistive loads (40W, 2.2kW). It was analysed the delay of the switching due to the SSR. As seen in figure 2, a 500μs delay exists between the zero crossing of the voltage sine wave and the switching of the SSR, regardless of the load.

The control block should be able to detect the zero crossings in order to assure the SSR enable command and to count the signal periods, at the same moment. This is obtained by connecting the AC mains through a 1 MΩ resistor directly to a microcontroller pin that can be programmed as an interrupt-on-change input (e.g. RA2). Using a 4 MHz clock oscillator, meaning 1 μs per instruction, the delay between the zero crossing and the command for the IR LED is much less than the hardware delay introduced by the SSR (500 μs as mentioned above), being directly proportional to the number of instructions from the interrupt subroutine treating that request (20-25 instructions).

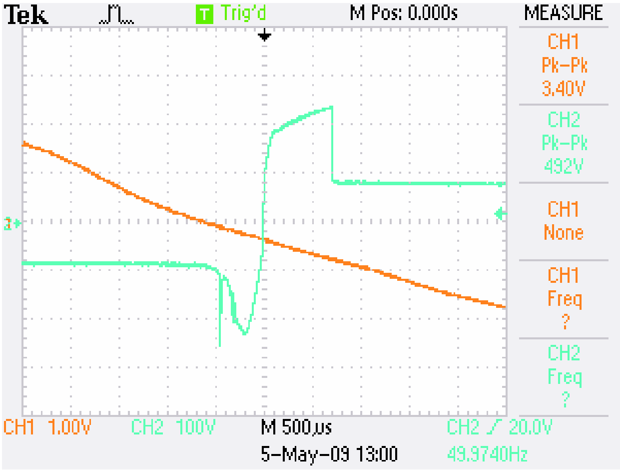


**Figure 2.** Zero cross detection of the SSR and switching delay

The microcontroller was instructed to run a test program which enabled the SSR to pass five times (m fom n) sines (or to stop passing n-m from n sines), where m is a string of numbers. In figure 3 it is presented the command signal on the IR LED on the SSR, as seen on an oscilloscope, when the n = 10, and m = 3, 3, 4, 4, 5, 6, 7, 8, 9, 9. It can be observed the pattern of five similar shapes which proves the accurate generation of the command signal. This is the principle on which is based the control of the energy transferred to the load.

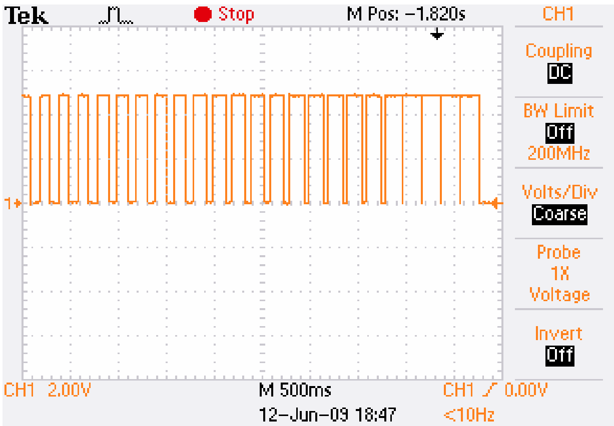


**Figure 3.** Example of the switching principle of the electronic module

In this stage, the communication between the electronic module and his operator was reduced to a data transfer between a PC and the module through RS232 serial port. This gives the possibility of programming the microcontroller to suit different parameters depending of the application. For example the maximum starting current necessary for the electric pump can be limited to any value between 1 Amper and 10 Ampers. Also the time in which the pump is stopped and is started can be programmed values between 1 second and 360 seconds. Specific programs can be created to accommodate a wide range of applications and many types of electric pumps

## 3. Electromagnetical Compatibility Tests

In order to test the principle that switching at the zero crossing of the mains voltage produces very low electromagnetical disturbances, upon the electronic module ware performed electromagnetic compatibility tests. The electronic module prototype was enlisted as class B equipment because it operates while being connected to a 230V power network and all tests were setup and performed according to CISPR 22 [5] for Information technology equipment using a 2.2 kW resistive load in order to reach nominal power output and 40W inductive load. For validation of the design and construction of the process control module the tests were initially done in a 3m semi-anechoic chamber using a Line Impedance Stabilization Network (LISN), an EMI Test Receiver, calibrated RF cables and antennas. For the mains terminal disturbance voltage tests the EUT was placed on a 0.8 meters height non-conductive table and was connected to the LISN. Table 1 shows the recorded maximum levels of conducted emissions. [3]

**Table 1. Quasi-peak levels of conducted emissions**

| PEAK | FREQ. *(MHz)* | LEVEL *[dB(µV)]* | LIMITS *(CISPR 22)* |
|---|---|---|---|
| PEAK 1 | 2.02 | 70.75 | 56 dB(µV) |
| PEAK 2 | 4.25 | 93.80 | 56 dB(µV) |
| PEAK 3 | 5.25 | 47.82 | 56 dB(µV) |
| PEAK 4 | 8.33 | 39.69 | 60 dB(µV) |

a. frequency band from 0.15 MHz to 30 MHz (load = 2.2kW)

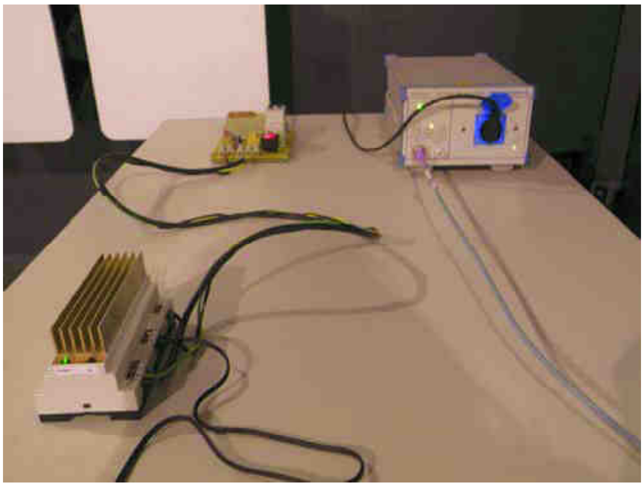

**Figure 4.** View of the electronic module being tested for conducted disturbances in a semi-anechoic chamber

For the electromagnetic radiation disturbance tests seen in figure 5, the EUT was placed on the non-conductive table in front of the log-periodic antenna (horizontal and then vertical polarized) which measured the emissions from 3m away. [4] The turn-table and the antenna mast were controlled in order to record the maximum radiated emissions levels for the operating mode of the device. Table 2 compares the noted emission levels with the limits from the standard.

**Figure 5.** View of the electronic module being tested for radiated disturbances in a semi-anechoic chamber

**Table 2.** Quasi-peak levels of radiated emissions

| PEAK | FREQ. *(MHz)* | LEVEL *[dB(µV)]* | LIMITS *(CISPR 22)* |
|---|---|---|---|
| PEAK 1 | 4.02 | 32.43 | 40 dB(µV)/m |
| PEAK 2 | 3.64 | 28.43 | 40 dB(µV)/m |
| PEAK 3 | 4.31 | 27.20 | 40 dB(µV)/m |

b. frequency band from 0.15 MHz to 10 MHz (load = 2.2kW)

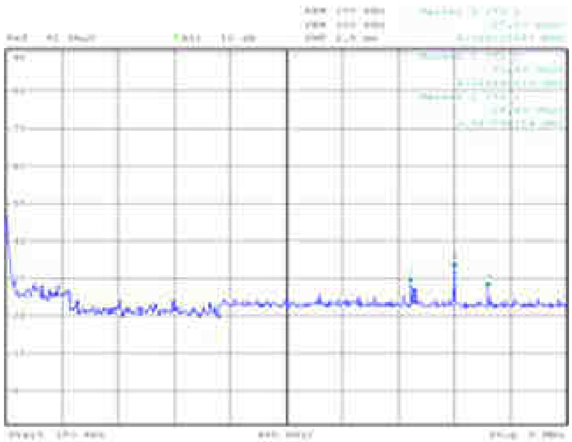

**Figure 6** Recorded radiated emissions of the electronic module

## 4. Results

The possibility of variation of the switched power was put in evidence by commanding the light intensity of an electric bulb; also, it was tested by commanding the soft start and stop of an AC motor. The results were encouraging, but proved the necessity to improve the pattern for the command signal, at least for motor control applications and for specific electric pump operation.

Electromagnetic compatibility tests in laboratory have shown that the emissions levels recorded for mains terminal disturbance voltage exceeds the CISPR 22 limits in the 0.15 MHz to 5 MHz range. Above 5 MHz conducted emissions fall below the specified limits. The recorded levels of radiated emissions are well below the specified limits for the entire 0.15 MHz to 30 MHz bandwidth.

The electronic module was manufactured in-house as a prototype (figure 7).

**Figure 7.** The prototype of the electronic module

## 5. Conclusions

The experiments made evident the switching and temperature characteristics of the choosed SSR in permanent and controlled switched working conditions. The SSR presents a very well behaviour in switched mode, residual voltage being around 1V. The switch delay is minor and does not affect the current transfer in the load. The power dissipation is low, even at 2.2kW, its maximum value is 12W (for a load current of 10A and a 12V power supply for logic circuits). However, by using a by-pass relay the power dissipation is drastically reduced. Measurements taken in the laboratory emphasized the importance of a below 5 MHz differential filter present in the supply block of the electronic module. Quasi-peak levels of radiated emissions recorded by the log-periodic antenna were below 33 dB(μV)/m emphasizing that the switching at the zero crossing of the mains does produce much less radiated disturbances than conventional switching methods.

The programmable nature of the electronic device recommends it for usage with different types of electric pumps and applications.

## ACKNOWLEDGMENT

The authors would like to thank EMCLab- Electromagnetic Compatibility Laboratory from “Stefan cel Mare” University of Suceava represented by professor Eugen Coca and Georgiana Buta, Ph. D. student, for the EMC tests performed.

The work has been funded by the Sectoral Operational Programme Human Resources Development 2007-2013 of the Romanian Ministry of Labour, Family and Social Protection through the Financial Agreement POSDRU/6/1.5/S/16 and through the Financial Agreement POSDRU/88/1.5/S/60203.

## REFERENCES

[1] I. Plotog, P.Svasta, B.Mihailescu, G.Varzaru and I. Busu., “Electronic module for controlling the energy in a vapour phase soldering machine”, Conference proceedings 15th International Symposium for Design and Technology of Electronic Packaging, pp. 383-386 , 1st edition 2009, ISBN 978-1-42445133-3, Gyula, Hungary, September 2009.

[2] B. Mihailescu, I. Plotog, P. Svasta and M. Vladescu, „The Modeling & EM Simulation Assessment as Part of DFX Methodology”, Conference proceedings 33rd International Spring Seminar on Electronics Technology, ISSE 2010, pp. 206-207, ISBN 978-83-7207-870-4, Var ovia, Polonia, Mai 2010. (ISI)

[3] G. Buta, B. Mihailescu, E. Coca, I. Plotog and P. Svasta, “EMC Assessment for VPS technology process control module”, Conference proceedings 6th International Workshop of Electromagnetic Compatibility, CEM 2009, Constanta, Romania, November 2009.

[4] B. Mihailescu, I. Plotog, P. Svasta and M. Vladescu, ”Electromagnetic Compatibility Evaluation and 3D EM Simulation of VPS process control module”, Conference proceedings 7th International Workshop of Electromagnetic Compatibility, Odoheiu Secuiesc, Romania, Septembrie 2010.

[5] EN 55022 - "Information Technology Equipment. Radio Disturbances Characteristics. Limits and methods of measurement", 2007;

**ISSN 1454 - 8003**
**Proceedings of 2011 International Salon of Hydraulics and Pneumatics - HERVEX**
*9 – 11 November, Calimanesti-Caciulata, Romania*

# EXPERIMENTAL STAND TO TEST ADJUSTABLE HYDRAULIC PUMPS

**Daniel BANYAI[1], Liviu VAIDA[2], Lucian MARCU[3], Ioan CRETA[4]**

[1] Technical University of Cluj-Napoca, Department of Mechanical Engineering, daniel.banyai@termo.utcluj.ro
[2] Technical University of Cluj-Napoca, Department of Mechanical Engineering, liviu.vaidai@termo.utcluj.ro
[3] Technical University of Cluj-Napoca, Department of Mechanical Engineering, lucian.marcu@termo.utcluj.ro
[4] Technical University of Cluj-Napoca, Department of Mechanical Engineering, cretaioan@yahoo.com

***Abstract:*** *Used in a large number of applications, hydraulic systems must be more efficient which leads to the need of designing a universal test stand for adjustable hydraulic machines to improve energy efficiency. The paper presents information needed to achieve such a test stand and the tests possibilities that it offers, namely drawing the characteristic curves, allows analysis of dynamic behavior in different operating regimes being able to choose for any control structure.*
***Keywords****: variable displacement pumps, dynamic behavior of adjustable pumps, hydraulic testing stand*

## 1. Stand presentation

High power, drives namely hydraulic systems, pursuing a high degree of automation, minimum power consumption, adaptability to a large range of industrial applications and perturbations becoming flexible systems.

The concept of flexible system requires the ability to adapt to changes in the working regime and adaptation in relation to any environmental disturbing factor, collected into a comprehensive system in which human operator intervention is minimized or not necessary.

Reduction of energy consumption for hydraulic systems, is obtained by using in the main circuits whenever it's possible adjustable hydraulic machines, based on volumetric dosing principle of energy, the resistive principle are only in control circuits of the variable displacement pump or motor. Thus the pump will ensure, ideally, the energy absorbed by the motor.

Variable displacement pumps allow easy control of system parameters (pressure, flow, power, or combinations between them). Their technical characteristics make them become the best option for most applications from machine tools to mobile devices.

Given these tendencies the purpose of the paper is the optimization of the adjustment structure of hydraulic parameters, their control in the system to which they belong assemblers and testing the assembly pump-adjustment system.

To achieve these objectives it was designed and created a stand capable to test the performances of adjustable pumps working under pressure control, flow, power or combination of them.

The overall picture and a schematic representation of the experimental plant is found in Fig. 1.

The main subassemblies of the plant are: 1. pump with electro-hydraulic adjustment system, 2. hydraulic energy source for control supply, 3. specific sensor 4. Electric supply and control system for: proportional distributor, sensors and the distributor to simulate the load, 5. acquisition and control hardware system, 6. command and control interface 7. load simulator.

The test pump is trained at constant speed of 1450 rev / min, with a three-phase asynchronous electric motor with 15 kW rated power.

To increase the universality of the stand it was provided with a hydraulic group with pump for control flow supply. Flow requirements (any sizes) is 2.5 - 3 l / min.

Hydraulic group for the command supply (Figure 2) contains the following: gear pump (PRD 1-217 - Plopeni UM), providing a flow of 3.75 l / min at a pressure set in the range 20-100 bar, filter; pressure limiting valve and pressure gauge. The supply of the control circuites in this way is advantageous in terms of energy balance, because the control circuites of the pump are working in resistive maner.

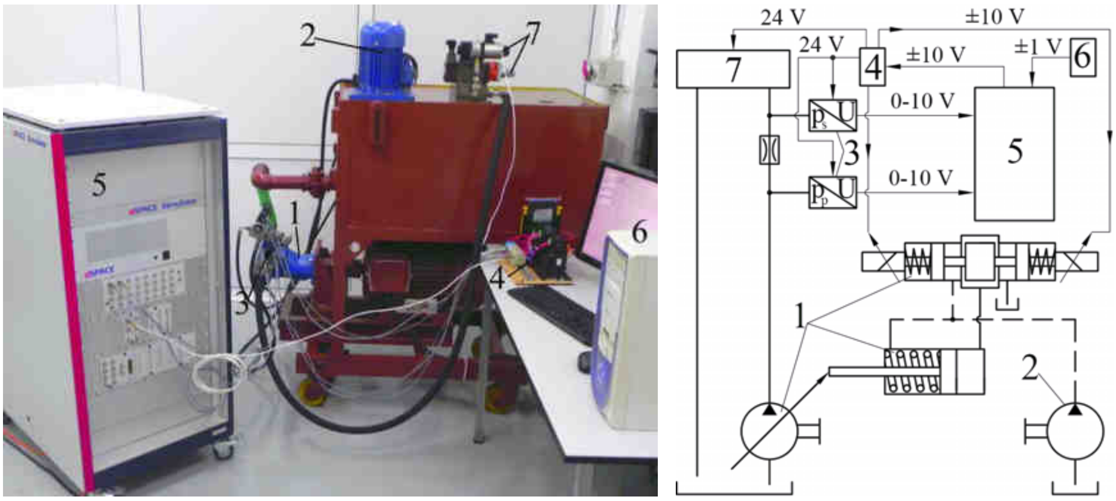

Figure 1. Stand overview


Figure 2 Hydraulic unit

To measure the load pressure was choose a transducer specific to fluid power systems, high working pressure (400 bar) and compatible with the working environment according to DIN 51524 ... 535. The transducer is witch deformable elastic membrane (Figure 3). Membrane strain measurement is made with strain gauges and with circuits dedicated to this type of measurement. The supplied signal is analog, voltage between 0-10 V.

Figure 3 Pressure transducer (Wika A10)

ISSN 1454 - 8003
**Proceedings of 2011 International Salon of Hydraulics and Pneumatics - HERVEX**
*9 – 11 November, Calimanesti-Caciulata, Romania*

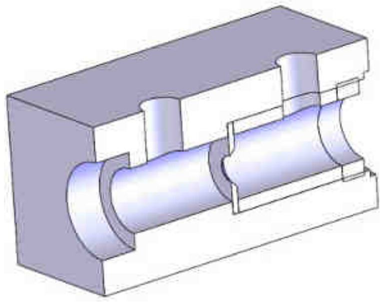

Figure 4 Diaphragm block

For flow measurement were used two identical pressure sensors, mounted in a block, one before and one after the diaphragm.

In order to have an apropiate value between the measured flow and the real value for the flow, was required an sensor calibration and filtering of signals with low-pass filter of second order. It was conditioned the signal given by the sensor located downstream of the diaphragm when between the sensors the diaphragm is missing so that the voltages generated be equal. The difference between the signals, the square root of the pressure variation on the diaphragm and the multipication with the diaphragm constant were made in the automation and control software developed in Matlab Simulink. The systems for processing and conditioning the signals from transducers were realized by software processing because the facilities and simplicity of implementation that DSpace system provides and not analog processing that requires a large number of electronic components and difficulties in achieving these circuits.

The signal that represents the power given by the pump was obtained by multiplying the signal from pressure sensor located downstream of the diaphragm and the signal representing the flow. The operation was performed also in the automation and control software.

To create a workload were used two adjustable throttle and a way valve mounted on a block (Figure 5), thus, if the distributor is unpowered, the flow passes through the first drosel, and when is powered flow passes through the resistance created by throttle 2, creating a disturbance.

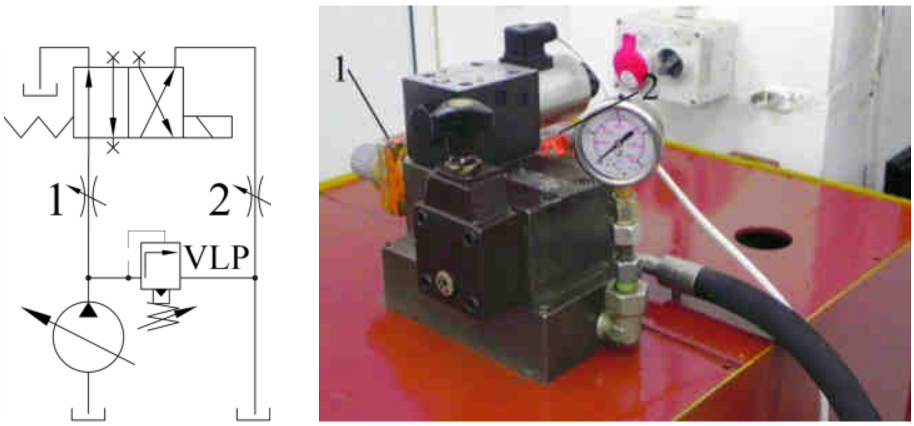


Figure 5. Load simulator

This simulating solution of the load is justified given that in an automatic adjustment circuit, the output size (adjusted) is influenced primarily by the size of the input (driving) and other disturbing sizes. The most common disturbance seen in hydraulic pumps and motors is caused by the pressure load.

## 2. The software application

The data acquisition and control system DSpace is modular and with Control Desk software and Matlab - Simulink form a complete equipment for control and monitoring machinery, installations and industrial robots. This equipment is the type of "stand alone" and was designed for research and development of applications in the laboratory.

The software package (associated to DSpace system) contain libraries that make possible to access the physical modules directly from the programming environment Matlab - Simulink. Applications for acquisition and signal generation, as well as monitoring and control, are done through the Simulink graphical programming. By compiling these files are generated applications for real-time processor, which are transferred to it by a optical fiber bus for high-speed. Real-time applications are running on CPU integrated in DSpace, while graphical, control and monitoring interfaces are running on the computer attached to Dspace system.

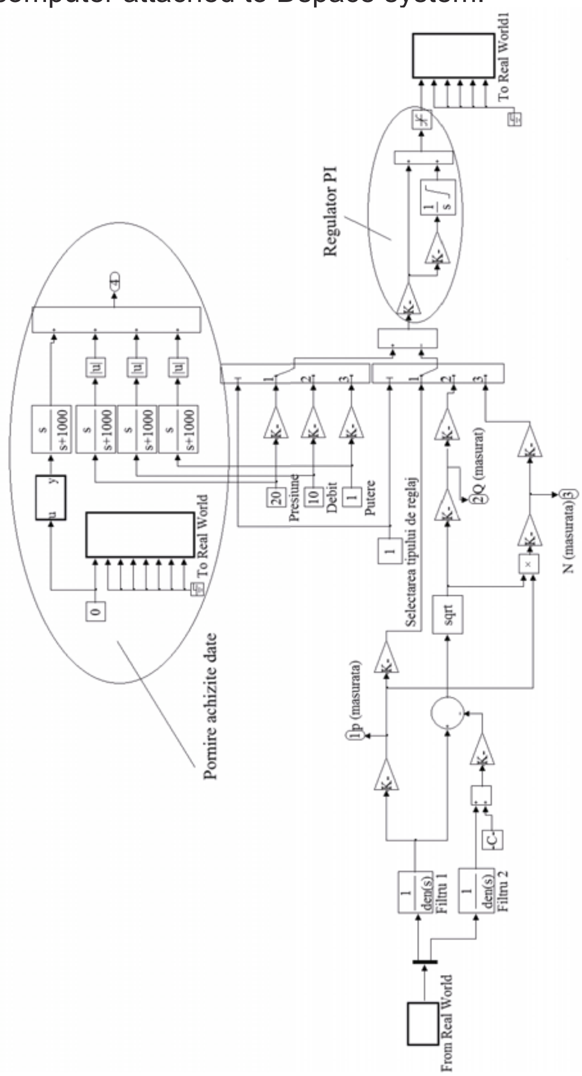

Figure 6 Software for command and control

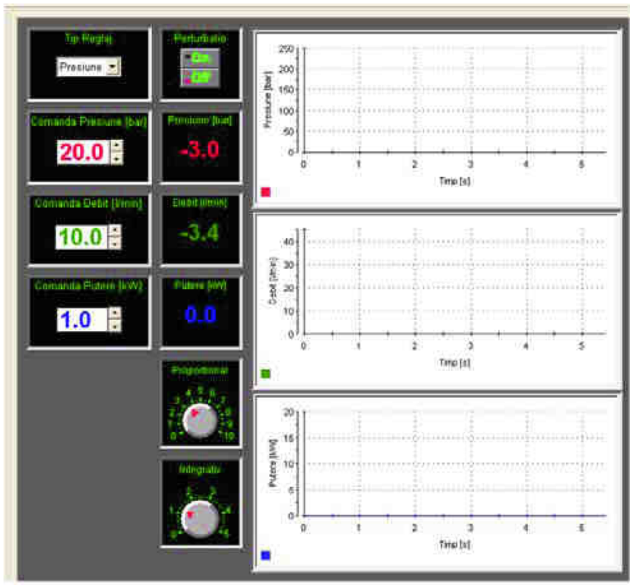

Figure 7. The command and control graphic interface

In figure 6 is presented the software for command and control adjustable pumps made in Simulink. The signals from the two pressure sensors are filtered (signal sensor 2 is corrected by sensor 1), then calculates the flow and the power. The value of the system pressure is measured by sensor 1 after filtration.. Signals corresponding to desired value for pressure, flow and power, are compared with the setpoint of these parameters in a differential block (constant blocks marked with: pressure, flow, power). The signal resulting from the operation of difference is inserted into a PID controller, the output signal is available at the analog exit port of DSpace system.

The selection of the adjustment type, the command value and the real value of the adjusted hydraulic parameter, are made using two programmable switches.

Data acquisition is started when is given an command for pressure, flow, or when the disturbance is on.

Using Control Desk software was made a GUI for command and viewing the adjusted parameters. Like Figure 7, the interface contains a selector for the desired setup type, a switch (On / Off) to enable or disable the disturbance, three buttons for insterting the desired value for pressure, flow and power, three oscilloscopes to view evolution parameters pump in real time, three alphanumeric display showing instantaneous value of the parameters and buttons for changing the regulator parameters, if is necessary.

## 3. Results

While maintaining pressure load at constant value, the flow changes proportional to the section of the diaphragmatic resistance that simulates load. As the load can vary within very large limits in a hydraulic system that serves a technological process, the purpose was to determine how the pumps with variable displacement respond to changes in load. After the analyze of the step response curves, it can be concluded that the damping increases with decreasing load resistance, respectively with increasing flow required by the system.

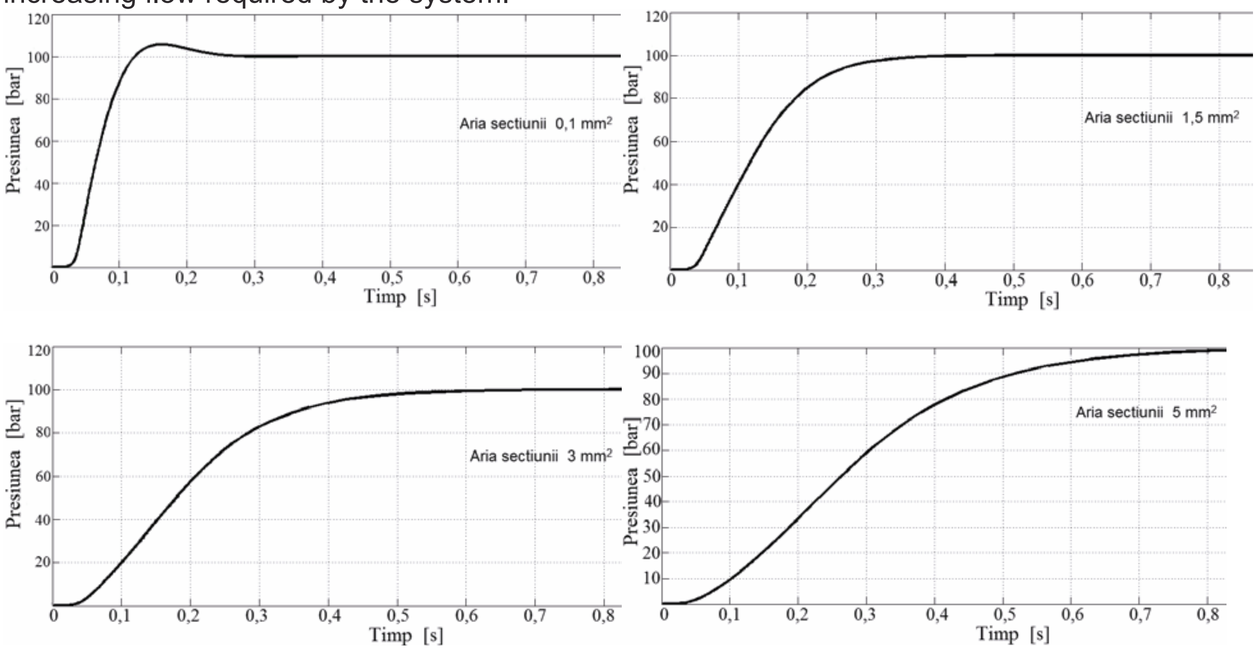


Figure 8 Step response of system to changes in load

Experimental investigations on the dynamic behavior of the pump with an control system existing on stand are shown in Figure 9, for all three types of possible adjustment structures. Result from the graphs that electro-hydraulic control system, measurement and control system of hydraulic parameters made for the presented stand, meets the required performance for testing the variable displacement pumps.

**ISSN 1454 - 8003**
**Proceedings of 2011 International Salon of Hydraulics and Pneumatics - HERVEX**
*9 – 11 November, Calimanesti-Caciulata, Romania*

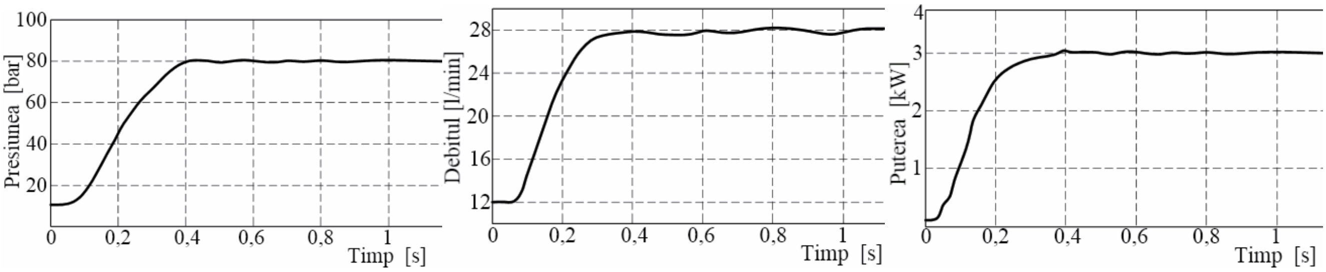


Figure 9 Step response of system for power flow and pressure control

## REFERENCES

[1] Banyai D., Vaida L., Electro-Hydraulic Control System for Variable Displacement Machines, 12th International Conference „Automation in Production Planning and Manufacturing“, p. 50-58, Zilina, Slovacia, 2011.
[2] Năşcuțiu L., Banyai D., Marcu I.L, Control system for hydraulic transmissions specific to wind machines, DTMM 2010, Buletinul Institutului Politehnic din Ia i, ISSN 1244–7863, Ia i, 2010.
[3] Năşcuțiu L., Banyai D., Opruța D., Measurement of hydraulic parameters, DTMM 2010, Buletinul Institutului Politehnic din Ia i, ISSN 1244–7863, Ia i, 2010.
[4] Opruța D., Optimizarea constructivă a comportării statice i dinamice a aparatelor de comandă a anergiei hidraulice, Teză de doctorat, Cluj-Napoca, 1998.
[5] Vaida L., Comanda proporțională a pompelor reglabile, Teză de doctorat, Universitatea Tehnică Cluj-Napoca, 1999.
[6] Vaida L., Năşcuțiu L., Deacu L., Stand experimental pentru determinarea caracteristicilor motoarelor hidraulice, Buletin informativ HIDRAULICA, Institutul de Cercetări pentru Hidraulică şi Pneumatică, ISSN 453-7303, Bucureşti, 1999.
[7] Opruța Dan, Vaida Liviu, Dinamica fluidelor, Ed. Mediamira, Cluj-Napoca, 2004, ISBN 973-713-044-8.
[8] www.dspace.de

**ISSN 1454 - 8003**
**Proceedings of 2011 International Salon of Hydraulics and Pneumatics - HERVEX**
*9 – 11 November, Calimanesti-Caciulata, Romania*

# STAND AND EQUIPMENTS FOR DETERMINING THE DYNAMIC PERFORMANCES OF ELECTROHYDRAULIC PROPORTIONAL DIRECTIONAL CONTROL VALVES

**Radu Iulian RADOI[1], Iulian DUTU[1], Marian BLEJAN[1]**

[1] Hydraulics and Pneumatics Research Institute INOE 2000 – IHP Bucharest

***Abstract:*** *The nonperforming poportional electro hydraulic equipment may affect the performance of an entire installation. Nowadays the technique of proportional electrohydraulic control requires thorough study, because there are still unsolved theoretical and practical problems. The article presents the structure of the stand and related equipment to carry out determinations on the dynamic performance of the proportional electrohydraulic devices. Among the related equipment can be found testing device made of hydraulic cylinder with high dynamic response, data acquisition system and software for data conditioning and storage and a SR-780 FFT Spectrum Analyzer produced by Stanford Research Systems. The tests that can be performed is to determine the frequency response and step response of the electrohydraulic proportional directional control valves with or without on board electronics (OBE).*

Key words: **proportional control, dynamics, electrohydraulic, data acquisition**

## 1. Introduction

Electrohydraulic control elements has appeared after growth of complex machinery which required new performances from hydraulic driving, related to reaching and mentaining of some pameters, independent of disturbing factors.

The basic role of control elements is to establish and maintain the output parameter value (flow rate, pressure), depending on input parameter value (voltage or electric current).
Applications with electrohydraulic proportional directional valves are found in the industrial field and that of mobile installations. These equipment satisfy the special requirements of the industrial and mobile installations. They have known an increasing development lately and the use of electronics and microprocessors contributed to the improvement of their dynamic performances. The progress registered in the domain of proportional electrohydraulic directional valves enhanced their performances which approached those of the servo valves. The performant proportional valves are used in application of control in close loop with a low price and low maintenance needs. In this paper are presented facilities for testing such devices in terms of dynamic performances.

## 2. Electrohydraulic proportional directional control valves

From point of view of needed facilities, in order to test them, electrohydraulic proportional directional control valves can be classified as follows:

- direct operated without on board electronics or position transducer for valve spool;
- direct operated with on board electronics and/or position transducer for valve spool;
- piloted without on board electronics or position transducer for valve spool;
- piloted with on board electronics and/or position transducer for valve spool.

### 2.1. Direct operated proportional directional valve

In this directional valve the proportional electromagnet acts directly on command spool.

The main components of directional valve are: case, one or two proportional electromagnets, position sensor for some models , command spool, and one or two springs for centering spool.
If electromagnets are not activated, the command spool is maintained through centering springs to middle position.
At command spool from fig. 1 the connection between P, A, B and T is closed. For example, if the left electromagnet (A) is activated, he move command spool to the right. Thus are created connections between P – B and A – T. As the signal comming from electronic controller is higher the more is pushed the command spool to the right. The stoke is so proportional with electric signal. As the spool stroke is higher the more is flow section and more is volumetric flow rate.
The left electromagnet from fig. 2 is equipped with inductive position senzor, this setting out real position of command spool and "announce" it as electric signal (volts), proportional with stroke, to the electronic amplifier.
Translation sensor is executed with double stroke and so are monitored both control directions.

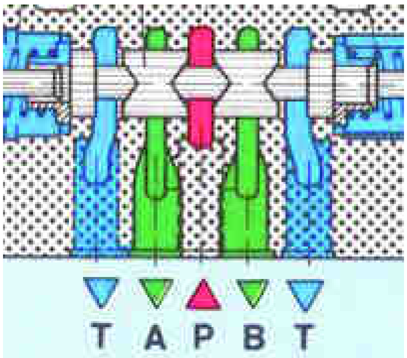


Fig. 1 Spool of proportional directional valve and connection

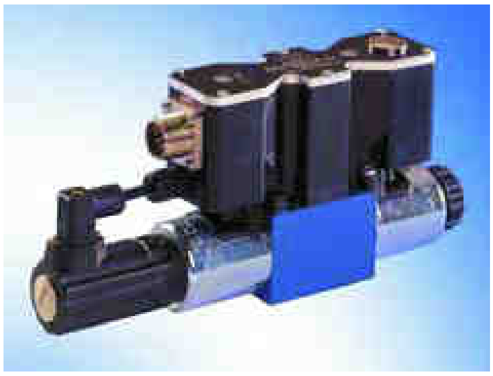

Fig. 2 Distribuitor proporțional direct comandat cu revenire electrică produs de Rexroth-Bosch

**2.2. Pilot operated proportional directional valve**

Proportional directional valves with greather nominal sizes are piloted. Reason is due to active forces necessary for main command spool displacement.
Usually the proportional directional valves with sizes up to 10 and icluding are direct operated and starting with size 10 they are pilot operated.
An pilot operated proportional directional valve (fig. 3), consist from a pilot valve with proportional electromagnets, main stage containing the main spool and its centering springs.
As proportional electromagnets are used those with current-force behavior.
To get an overview is described simplified operation.
Electrical control signal is transformed by the proportional electromagnet into a proportional force. Corresponding with force is obtained to the outlet of pilot valve a pressure. This pressure acts on the spool surface and move him to the opposite spring until the spring force and the pressure force are equal. Spool stroke and thus the flow section are dependent on the size of active pressure on the surface at the end of the distribution spool. To limit the piloting pressure can be used a pressure reducer.
The pressure control valve with 3 way used for piloting consist, essentially, from: body, two electromagnets and two spools for proportional pressure adjust.
Through the piloting valve is varied the pressure in A or B inlets proportionally with electrical signal from the input.

**ISSN 1454 - 8003**
**Proceedings of 2011 International Salon of Hydraulics and Pneumatics - HERVEX**
*9 – 11 November, Calimanesti-Caciulata, Romania*

If in the spaces from the ends of the main spool is no pressure, ie A and B inlets of the pilot valve, main spool is maintained by the centering springs in the middle position.

If is activated one of the electromagnets is forming a pressure proportionally with the input signal. The resulting pressure force move the main control spool against centering spring until the spring force and pressure force are equal. The size of command pressure determine the spool position and thus the flow rate.

Fig. 3 Distribuitor proportional pilotat produs de Parker

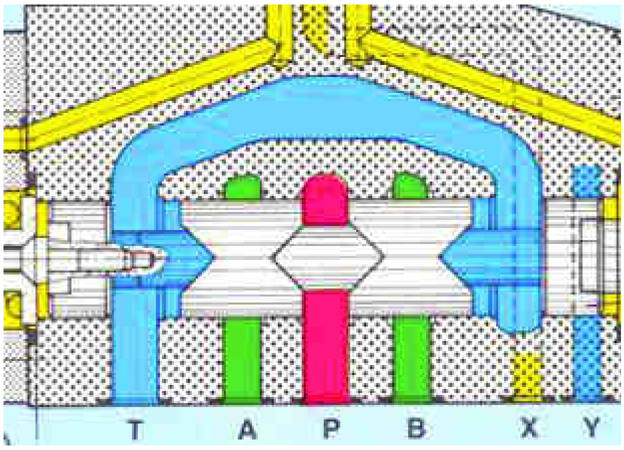


Fig. 4 Sertarul si camerele de comanda ale distribuitorului proportional pilotat

3**. Dynamic characteristics** of electrohydraulic proportional directional valves are the following:

- Step response, defined by the following parameters
  - delay time $t_d$ - the time when output value reaches 0.5 size of the stabilized output value;
  - stabilization time $t_s$ - the time in which the variations of output value are less than ± 5% of stabilized output size;
  - Override, or maximum deviation of the output value;
- response to sinusoidal signal defined by the characteristic of attenuation, according to frequency and phase shift according to frequency.

Besides the dynamic characteristics, for proportional directional valves can be determined and the following parameters:

- hysteresis, the difference between the command size, usually a current within 200 ... 800 mA, required to achieve a flow rate variation in upwards with the input level , from minimum to maximum, and the control level necessary to obtain same flow rate at a command size variation in downward from maximum to minimum;
- linearity, determined by the maximum value of difference between command level from real diagram and that obtained on theoretical diagram (drawn between extreme points from the hysteresis diagram)
- repetability, maximum difference between values obtained at the same level of command value;
- sensitivity, defined by the ratio between output amount variation and the corresponding variation of input amount, in case of lineary static characteristic
- the characteristic of flow rate – command level from input (usually a current within 200 ... 800 mA) at a constant pressure drop;
- the characteristic of pressure-flow rate at a constant command level at input;

- minimum working pressure, which represent the minimum value of pressure from sistem at that can be adjusted the flow rate on entire domain

## 4. Stand and equipments

**4.1 The testing stand** is configured so as to allow for experiments to obtain dynamic response characteristics of electrohydraulic proportional directional valve.
To achieve tests for proportional directional valves without position transducer for spool is used a testing device equipped with dynamic response cylinder with a piston with friction and weight reduced. In fig.5 it can be seen the scheme for data acquisition and hydraulic instalation, established to carry out experiments.

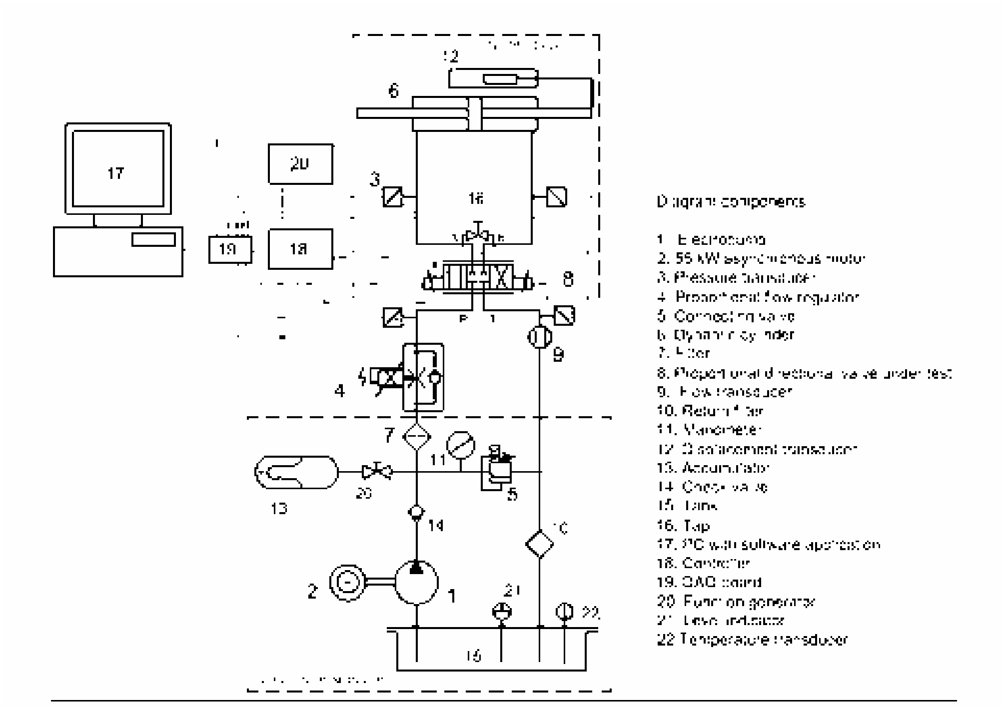


Fig. 5 Stand diagram

Stand characteristics:

- Maximum operating pressure = 300 bar
- Max. flow rate= 120 l/min
- Filtration 10 $\mu$m
- Pressure, flow, temperature and displacement transducers
- Controller
- Function generator
- Data aquizition board
- PC and software

### 4.2 Equipments

**Testing device**

The testing device (fig. 6) contains the fixation plate for proportional directional valve and the hydraulic cylinder with dynamic response equipped with displacement transducer. Thru fixation plate are realized connections between directional valve inlets and hydraulic stand inlets.

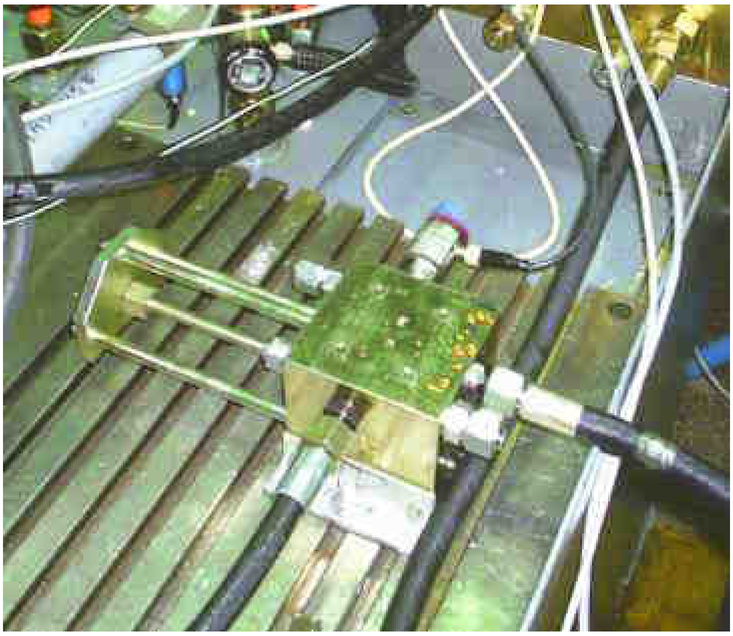

**Fig. 6 Testing device**

**Software application for data acquisition of experimental results**

The experiments are realized with help of an application made in TEST POINT software.
Panels of applications for determining frequency response and step response are presented in Fig. 7 and Fig. 8. To generate control signals corresponding to the tests is used a Tektronix AFG 3022B function generator which is set for each type of test as in figures 7a and 8a.
Pressing the start button from the software application panel, is sent trigger signal through an output channel of data acquisition card (fig. 9) to the trigger input from the functions generator. Following this command the function generator triggers the step signal or sweep frequency signal depending on the test carried out. Thru an analog input channel is acquired the signal from the function generator, and thru another the response signal from proportional directional valve. The frequency response test lasts 10 seconds, and step response test lasts 100 miliseconds, which time are aquired 25000 points for every channel. After tests are finished each application puts on a chart the values acquired.The recorded data can be saved, after tests, into a file which contains columns with values for time, command signal and response of proportional directional valve. This data can be imported in other programs for charts drawing or other numerical calculations.

ISSN 1454 - 8003
Proceedings of 2011 International Salon of Hydraulics and Pneumatics - HERVEX
*9 – 11 November, Calimanesti-Caciulata, Romania*

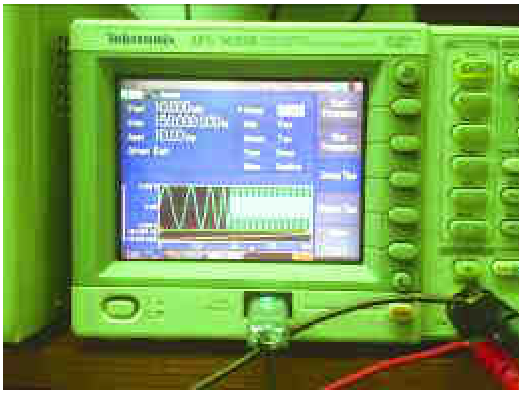

a

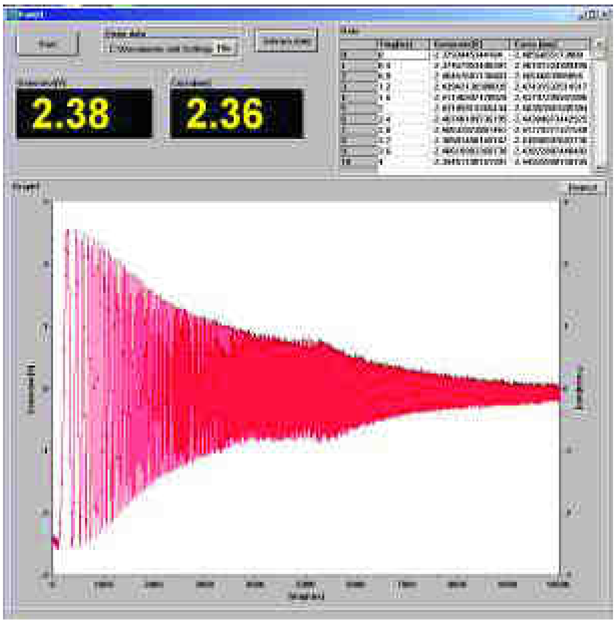


b

Fig. 7 Software application for frequency response testing

a

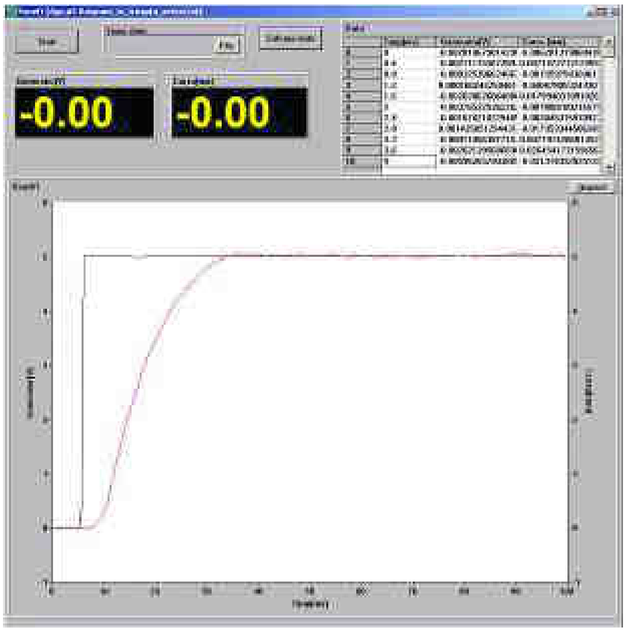


b

Fig. 8 Software application for step response testing

Fig. 9 National Instruments USB-6218 DAQ board

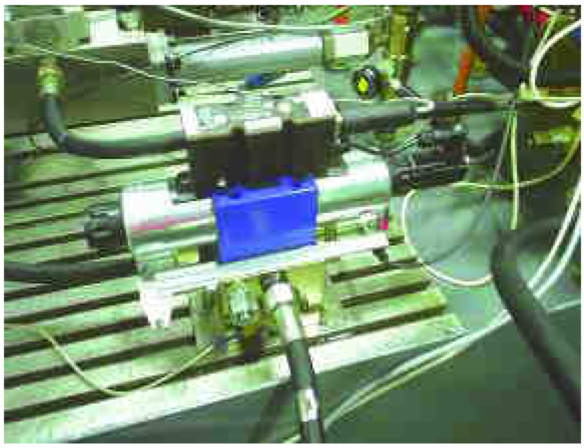

Fig.  10 Proportional directional valve during tests

In fig. 11 is presented the chart of step response, and in fig. 12 is presented the characteristic amplitude-phase-frequency for proportional directional valve tested.
Response attenuation of directional valve at a particular frequency is expressed in dB by this ratio:
A(dB)= 20 lg($U/U_o$) ,where:
U- amplitude of response signal;
$U_o$- amplitude of reference signal;

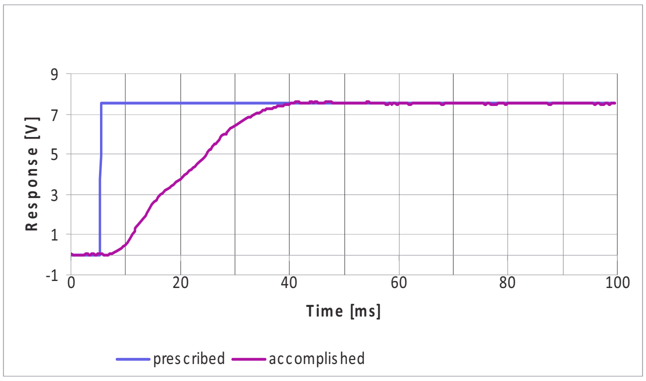


Fig. 11

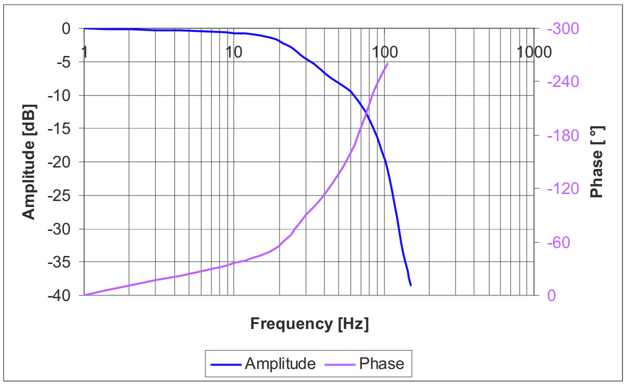


Fig. 12

For transfer function determination of proportional directional valve with on board electronics which provide the signal for position transducer of spool, can be used FFT analyzer type SR 780 made by the Stanford Research Systems (fig. 13).

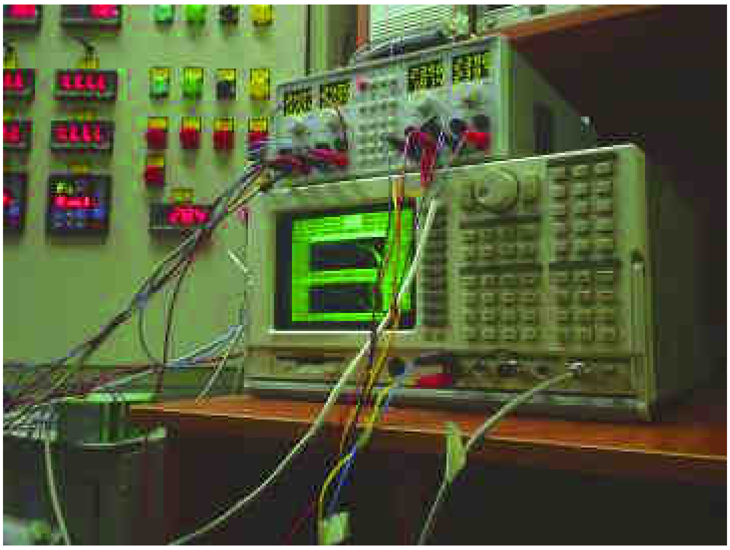

Fig. 13 Determining the transfer function using
a Network Signal Analyzer type SR780 produced by the
Stanford Research Systems

Signal generated by the signal source of the analyzer is applied to control input of proportional directional valve and in one of the inputs in the analyzer.

Response signal from spool position transducer of directional valve , signal which is in volts, is applied to the second input of the analyzer, resulting the diagrams from fig. 14.

With the help of cursors from the analyzer screen can be inspected and extracted values for the phase and attenuation depending on frequency. With these values cab be drawn the Bode diagrams.

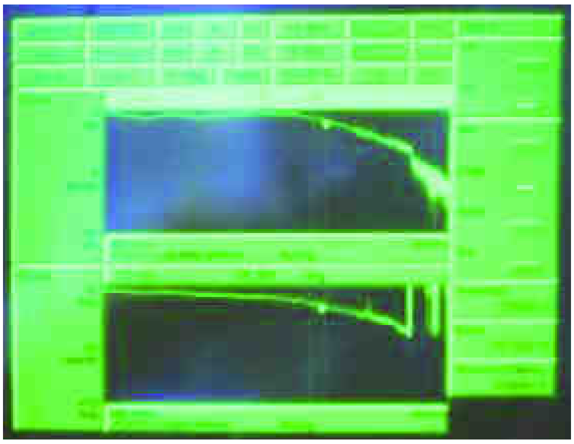
Input signal sinus with amplitude of 2,5 V

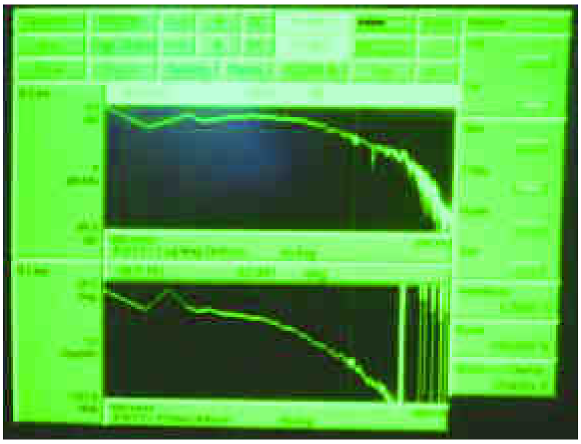
Input signal sinus with amplitude of 2,5 V

Fig. 14

## 5. Conclusions

Using the stand and related equipment can be determined both dynamic performance of proportional directional valves without transducer for spool position and on board electronics as well as for those with integrated electronics and electrical reaction.

Software applications allow recording and storing data in order of some numerical processing or drawing diagrams.

## REFERENCES

[1]. L. Deacu, D. Banabic, M.M. Rădulescu, C. Rațiu, Tehnica hidraulicii proporționale, Dacia publishing house, Cluj-Napoca, 1989
[2]. Merritt H., Hydraulic Control systems, John Wilez and Sons, 1967
[3]. Cornel Velescu, Aparate şi echipamente hidraulice proporționale, Mirton publishing house , Timişoara, 2003
[4]. V. Marin, R. Moscovici, D. Teneslav, Sisteme hidraulice de reglare automată – Probleme practice, Tehnica publishing house , Bucharest, 1981
[5]. Ion Mazilu, Virgil Marin, Sisteme hidraulice automate, Romanian academy publishing house , Bucharest, 1982
[6]. Backe W., Servohydraulik, RWTH, Aachen, 1984
[7]. Blackburn J.F., Fluid Power Control, MIT Press, Boston, 1969
[8]. Hydraulik trainer, Mannesmann Rexroth, vol. II, 1986
[9]. http://www.thinksrs.com/downloads/PDFs/Manuals/SR780m.pdf

ISSN 1454 - 8003
Proceedings of 2011 International Salon of Hydraulics and Pneumatics - HERVEX
*9 – 11 November, Calimanesti-Caciulata, Romania*

# EXPERIMENTAL INVESTIGATION OF ELASTOMERIC U ROD SEALS FRICTION DURING TRANSIENT CONDITIONS

**M. Crudu[1], C.Cristescu[2], S. Cananau[1], A. Pascu[1]**

[1]Machine Elements and Tribology, University "Politehnica" of Bucharest, Romania, crudumonica@yahoo.com, s_cananau@yahoo.com, apascu@omtr.pub.ro
[2]*INOE 2000 IHP, Bucharest, Romania, cristescu.ihp@fluidas.ro*

***Abstract:*** *This research is focused on reciprocating "U" seals, usually used in hydraulic actuators applications. In order to simulate reciprocating seals behavior in real conditions, an original experimental device was conceived. The experimental device provides friction force measurements for a couple of "U" seals reciprocated against a steel rod, during transient conditions. A stick slip phenomenon is observed at start-ups and when the direction of motion is changed. According to measurements this phenomenon is a function of standing time and reciprocating speed. The effects of these two parameters are discussed in order to find solutions to reduce this negative phenomenon affecting the service life of hydraulic systems. The stick slip phenomenon is accentuated with the standing time while reciprocating speed seems to have a diminishing effect.*

***Keywords***: *reciprocating seals, friction, stick slip phenomenon*

## 1. Introduction

The sealing may be fixed or mobile, and the mobile ones, from the point of view of the relative motion between the sealing surfaces, may be with rotation or translation motion, the last ones being the subject of the present article. The mobile translation sealings are specific to the hydraulic cylinders, Fig. 1, where realize the sealing on the rod with diameter *d*, being in reciprocating translation motion on the stroke, of the fluid with the constant viscosity $\eta$ and under pressure *p*. In the Fig. 1, *d* is the rod diameter, *S* is the rod stroke, *v* and $v_r$ are the velocities, in the both senses.

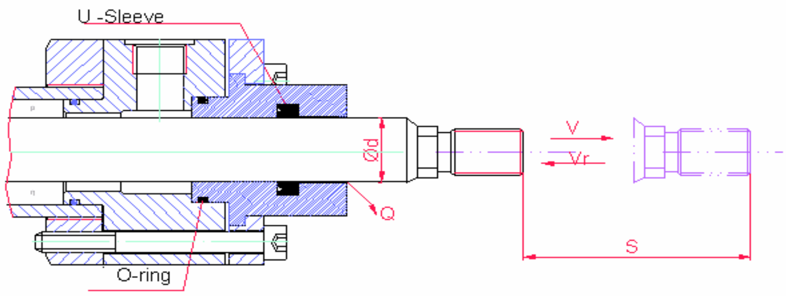


*Fig 1: The sealing of the hydraulic cylinders rod*

Performing optimum mobile sealings represent a key factor for providing the reliability of the drive systems to which they belong, inclusively for reducing hard wears, caused by the modification of the kind of lubrication used. At the mobile with contact sealings, with component parts in relative motion, matter much the modality of obtaining compression needed for sealing, usually due to external or internal forces. In the hydraulic power systems are used mainly sealings realized under the internal forces effect, more precisely of internal pressure which is sealed by different kinds of gasket
The sealing process is influenced, beside the phenomena, from the sealing interstice, by the gasket type, material and shape and the characteristics of the sealed medium.

## 2. Experimental device description

In order to evaluate the friction forces from the sealing of the hydraulic cylinders, was projected and realized an experimental device**.** This experimental device is conceived purposefully for working by mounting it on a stand which provides operational strokes. The adopted technical solution was the replacement of the rod cylinder head sealing, Fig. 2, with one double sealed guidance bushing, which to contain 2 U type sealings, fixed with the wings facing one another, see Fig. 3.The operational fluid is injected between these two sealing elements, identical with that of a hydraulic cylinder running and can be measured by means of one *pressure transducer*.

Fig. 2: The rod cylinder head sealing

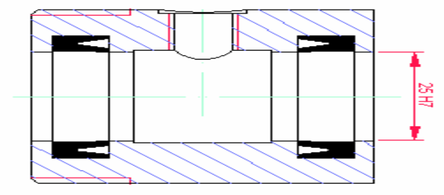

Fig. 3. The double sealed bush

The experimental device is presented in the Fig. 4. In the schematic representatio*n, it* can see that, the rod (1) being fixed and suspended on the upper bridge of the stand, by means of a threaded bush (2), by the force transducer (3), connected at the other side by the up catching stationary head (4) of the existing stand. Downside, the rod crosses the double sealed bush (5) assembled by means of a nut (6), from the used cylinder, by its liner (7). The cylinder liner is used just for supporting the double sealed bush and for making pace necessary for performing the operational strokes of the cylinder rod. Downside, the cylinder liner is connected to the mobile rod (8) of one the hydraulic cylinder, of the existing stand where is mounted, by means of a connection part (9) and a nut (10). The experimental device, Fig. 5, operates in vertical position and need the mounting the liner of the experimental device on the mobile rod of the hydraulic cylinder of existing stand, Fig. 6.

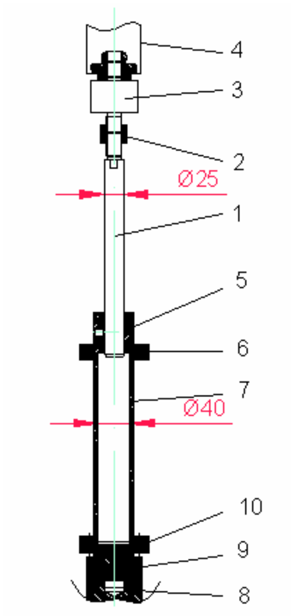


Fig. 4: Schematic representation

Fig. 5. The experimental device

Fig. 6: The existing bench test

This stand, by plant hydraulic own, provides the motion of the cylinder liner, together with the double sealed bush, up and down and, also, the measuring of the stroke with an stroke transducer. The rod of the cylinder, which passes through the double sealed bush, is immobile. In this manner, will be eliminate the risk of additional inertial force which can perturb the force transducer

## 3. Test procedure

The experimental device provides friction force variation in time, at constant speed, temperature and pressure, during transient conditions. The friction force recorded by the force transducer represents a sum of friction forces from seals tested, one experiencing instroke and the other outstroke. The friction force variation in time was measured during three consecutive cycles for various input pressures, between 0 and 20 MPa at two reciprocating speeds: 43 and 80 mm/s. The testing temperature was maintained constant at 15 º C. The tests were carried out during multiples days and for the same test conditions, tests were repeated three times. In Tab.1 are presented the test parameters utilized in the experiments.

Tab.1 Test parameters

| | |
|---|---|
| Type of seals tested | U type rod seals |
| Seals materiel | HNBR |
| Seals thickness | 7.5 mm |
| Rod materiel | Steel |
| Oil viscosity | 0.1455 Pa*s |
| Stoke length | 140 mm |

## 4. Results and discussions

In Fig. 7 is represented a typical example of friction force measurement recorded by the force transducer during tests. During instroke measurements, the friction force registered is much higher than the friction force registered during outstroke. The measurements considered correct are those registered during outstroke, because during outstroke the rod and the test cell, containing the elastomeric seals, are better aligned. The outstroke measurements are those represented in the positive region of the scatters. A stick slip phenomenon is observed at the beginning as well as at the changing of the stroke. Analyzing the measurements it was observed that this phenomenon is a function of standing time and speed. The effects of these two parameters will be further presented and discussed.

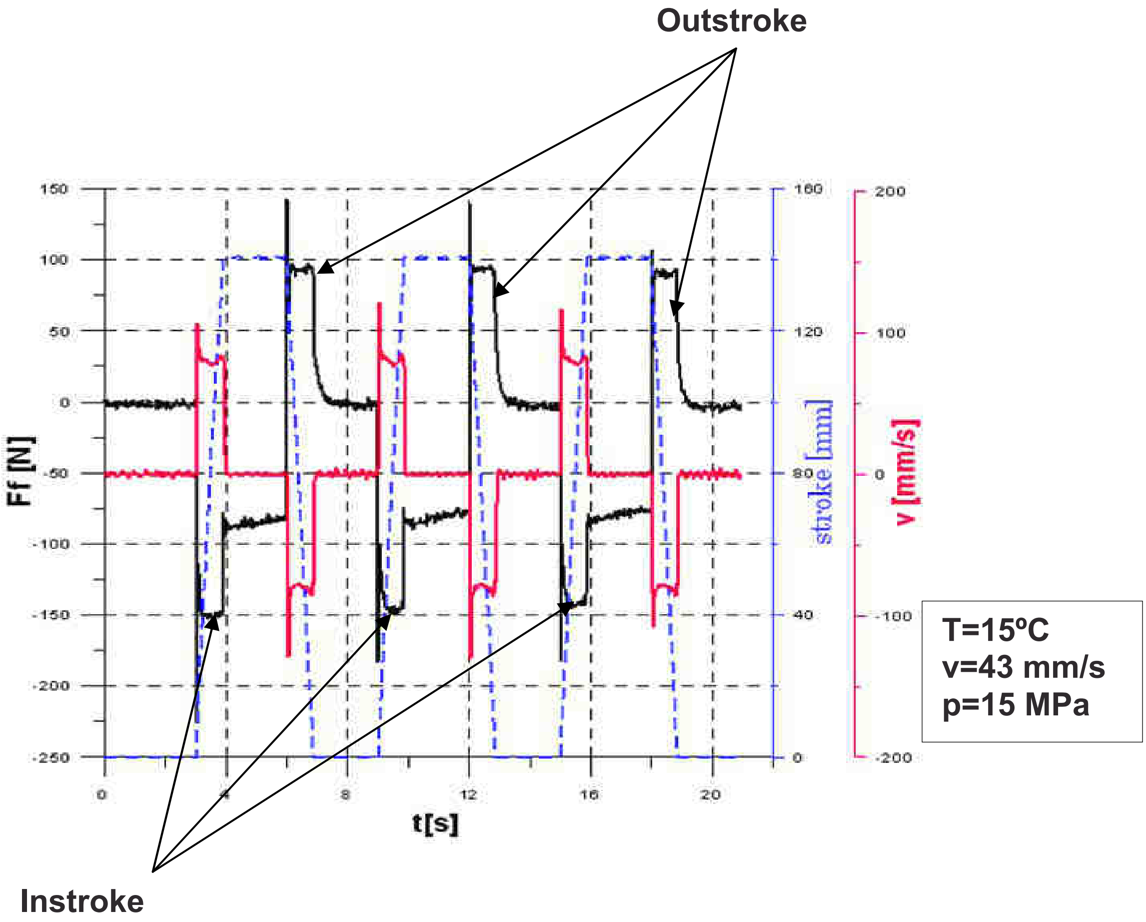


Fig.7 Typical experimental measurement

### 4.1 The effect of standing time

In order to highlight the effect of the standing time period before start-ups on the stick slip phenomenon, the first two measurements (Fig. 8,9) recorded in the same conditions, after a long period of standing time of the experimental device are presented. In Fig 8 a strong stick slip phenomenon is registered at start up. On the second friction variation measurement, although the conditions of measurements were conserved, the stick slip phenomenon recorded at start-up is almost three times smaller (Fig.9). The explanation for this phenomenon is the natural tendency of seals to squeeze lubricant out of the contact, during standing period. So when the device was start up after a long period of standing, the seals worked in almost dry conditions of lubrication, while during the second friction variation measurement, boundary lubrication is encountered. A first conclusion is that the stick slip phenomenon depends strongly on the system standing time.

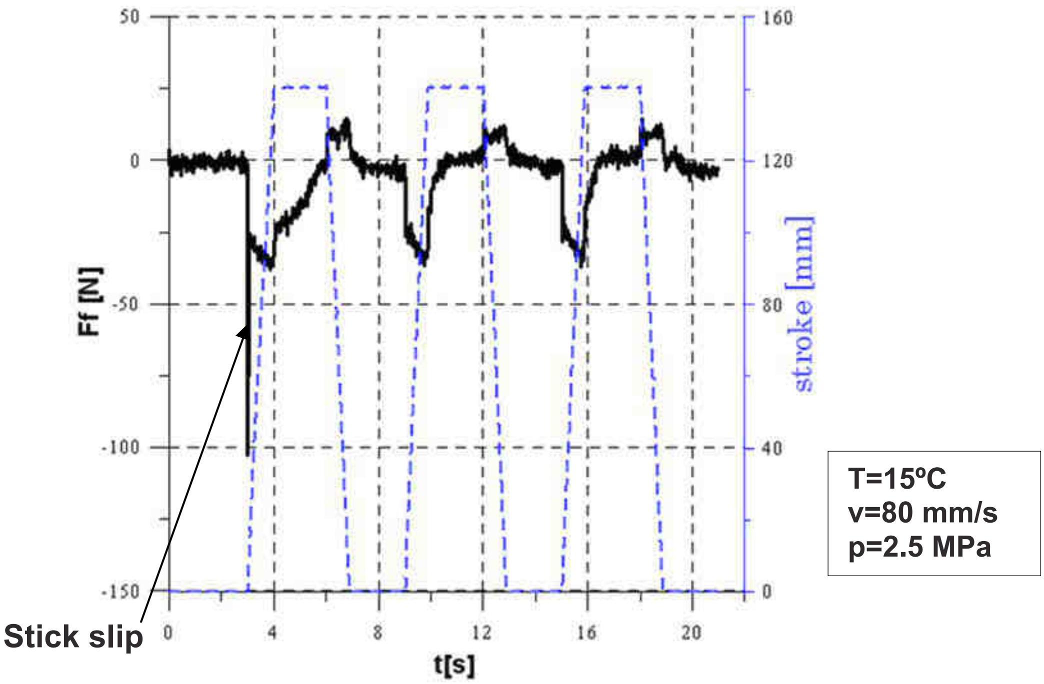


Fig.8 First friction force measurement recorded after a long period of standing time of the experimental device

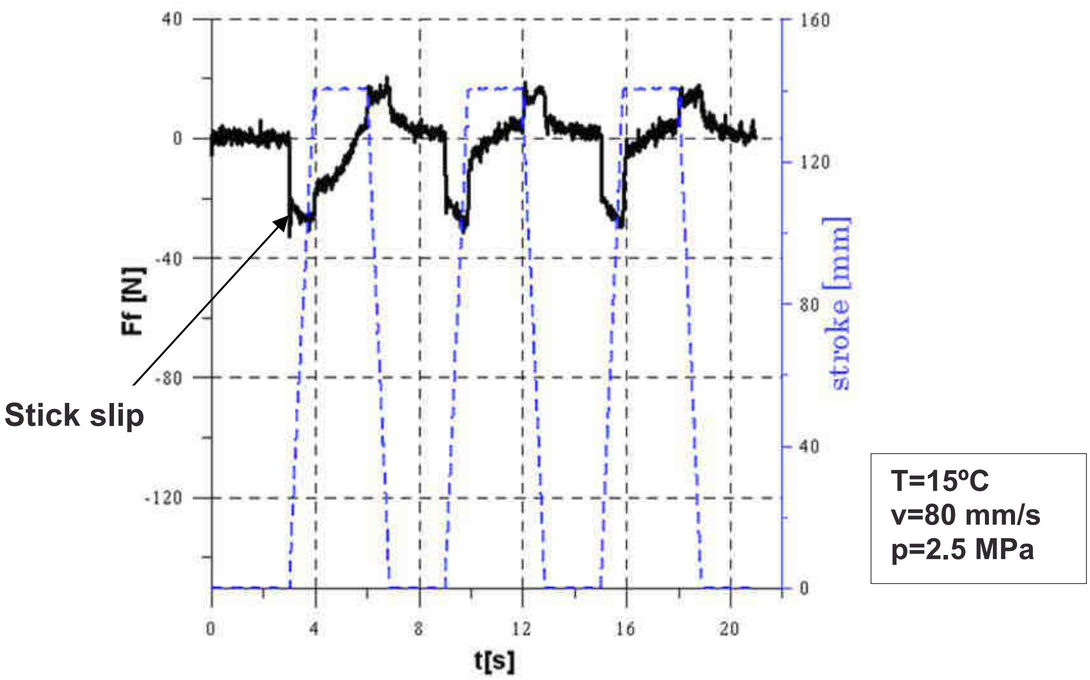


Fig.9 Second friction force measurement recorded after a long period of standing time of the experimental device

### 4.2 The effect of reciprocating speed

In hydraulic industry, when refer to seal friction, usually two types of friction are distinguished: breakout and running friction. Breakout friction is encountered at the beginning (ending) of an operational stroke, when the movement of the seals against the rod is initiated while running friction is encountered after the breakout period, when the seals are in motion. The significant drop in friction recorded within one stroke; signify the crossing from breakout to running stage of seals friction. The breakout friction is almost two times higher than the running friction. This is because a bigger force is required to overcome the adhesion forces acting between the seals and the rod in order to put the seals in motion. In the breakout stage, dry/ boundary lubrication regime is encountered and as the lubricant film forms in the contact, a drop in friction is recorded, meaning the seals are experiencing running friction. The formation of the fluid film depends strongly on the reciprocating speed so from this point of view, the breakout stage friction period is expected to be reduced as the reciprocating speed increases.

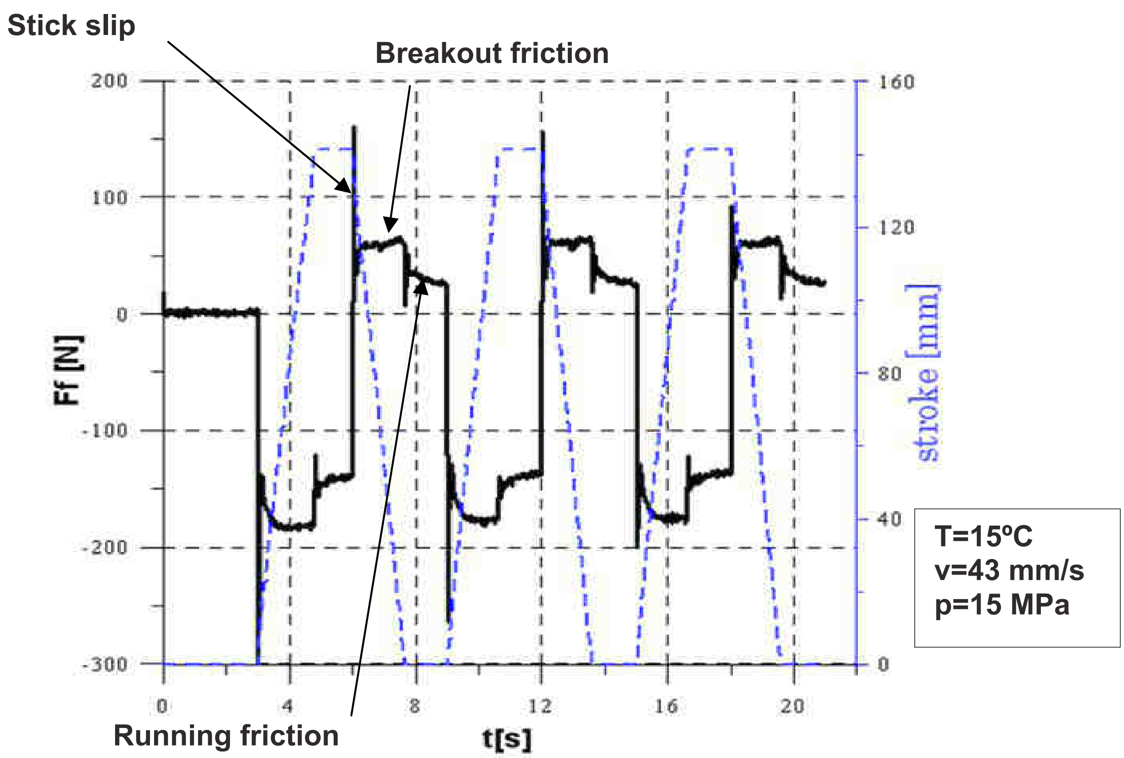


Fig. 10 Friction force variation at small reciprocating speed

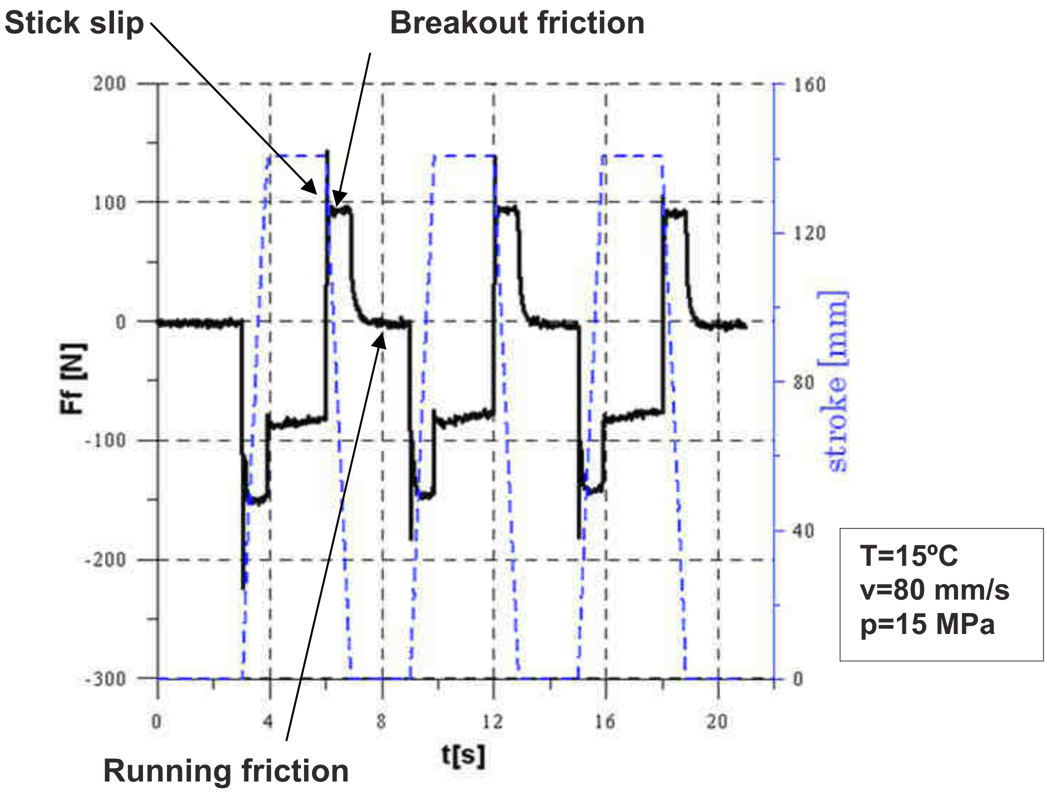


Fig. 11 Friction force variation at high reciprocating speed

Analyzing Fig. 10 and Fig. 11, it is clear that speed reduces almost twice the breakout stage friction period as well as the magnitude of friction recorded during both stages. Stick slip phenomenon is also reduced with increasing the reciprocating speed. It was observed that stick slip is attenuated during consecutive cycles. This behavior is a consequence of better lubrication and reduced standing time.

## 5. Conclusions

Friction force measurements during transient conditions were carried out using an original experimental device conceived by INOE 2000 IHP. A stick slip phenomenon was observed at starts-up and when the direction of motion is reversed. This phenomenon depends strongly on the standing time of the device. The explication is the natural tendency of seals to squeeze out of the contact the oil, during standing periods. So in order to reduce the stick slip phenomenon shorter standing time between consecutives strokes are recommended. Also the use of more viscous oils or anti stick slip oils can help. The reciprocating speed reduces the stick slip phenomenon, as well as the breakout friction stage period, by encouraging the formation of a fluid film in contact. Stick slip phenomenon reduces hydraulic system service life by wearing the elastomeric seals, increasing system leakages. As a conclusion, in order to reduce stick slip the system lubrication regime must be improved. The formation of a fluid film in contact takes place faster at high speeds [1]. Pressure also encourages the formation of the fluid film [1] and the use of more viscous oils can improve system lubrication, when long standing time between strokes are encountered.

**Acknowledgments**

The work has been funded by the Sectoral Operational Programmed Human Resources Development 2007-2013 of the Romanian Ministry of Labor, Family and Social Protection through the Financial Agreement POSDRU/88/1.5/S/61178.
The authors wish to thank INOE 2000 IHP, Bucharest, Romania for the support and technical assistance in performing this work.

**REFERENCES**

[1] A.S.Rana and R.S.Sayles: "An experimental study on the friction behavior of aircraft hydraulic actuator elastomeric reciprocating seals", Elsevier B.V 2005.

[2] Pavelescu, D., Muşat, M., Tudor, A.. *Tribology*., Didactic and Pedagogic Publishing House, Bucharest, Romania, **1971**

[3] Cristescu, C., Drumea, P.**,** *Mathematical modelling and numerical simulation of the tribological behaviour of mobile translation sealing subjected at high pressures*, In: Hidraulica, Sept. 2008, no. 2, pp. 26-33, ISSN 1453-7303. Bucharest, Romania, 2008.

[4] Fătu A. et al., Development of an Experimental Device to Study Real Hydraulic Rod Seals During Fully Transient Operation, 8th EDF-LMS Poitiers Workshop, Futuroscope, France, October 5, 2009.

[5] Fatu A. et al.**,** Evaluation of the elastomeric hyper elastic behavior a U-cup hydraulic rod seal. In: Hidraulica, No. 3, 2010, p. 41-48, ISSN 1453-7303

**ISSN 1454 - 8003**
**Proceedings of 2011 International Salon of Hydraulics and Pneumatics - HERVEX**
*9 – 11 November, Calimanesti-Caciulata, Romania*

# DIGITAL CONTROL MODULE DEVELOPED FOR A SERVO-HYDRAULIC POSITIONING SYSTEM

**Iulian DUTU[1], Radu RADOI[1], Marian BLEJAN[1]**

[1] Hydraulics and Pneumatics Research Institute, Bucharest, Romania, dutu.ihp@fluidas.ro

***Abstract:***
***Keywords****: digital, microcontroller, servo-hydraulics, positioning*

## 1. Introduction

The concept of the digital control module developed by the authors is using a mechatronic approach of the electro-hydraulic driving area, integrating micro-mechanics, digital electronics, data acquisition and signal conditioning structures, informatics technologies, virtual instrumentation and digital control algorithms with or without “self-learning ability”. Again, the concept has an interdisciplinary approach using a strong knowledge base to solve a complex problem that is considered to be fundamental for modernization of electro-hydraulic machinery or fixed/mobile installations. Electro-hydraulic driving systems are used in a large number of industrial applications such as machinery tools, automated feeding and transport lines, industrial robots, power equipment, mining equipment, forging installations etc. The common feature of all these is the usage of a pressurized fluid for transmitting signals and energy in a controlled manner. All these are grouped together under the general concept of "fluid power".

## 2. Digital control basis

Large scale integration, miniaturization and the new developments in the SMT (Surface-Mount Technology) changed the way electronic modules are integrated into the structure of modern sensors or equipments. The usage of new materials and technologies allow to develop new hydraulic actuators with integrated sensors and digital electronic modules, all these leading to higher dynamic and static performances, also improving the system’s precision and response time. Modern hydraulic actuators are treated as a set of three main components: mechanics, digital electronic hardware and software application. In such a way, researchers have made the transition from classic hydraulic equipments to digital servo-hydraulics. Computer controlled systems allow the user to develop more flexible control solutions including advanced control algorithms, current control systems being based on applications that use digital hardware and software. In such a way, the design of monitoring and control solutions has changed by considering the software as a part of control loop. This new approach leads to new problems that are related to error management and time-delays generated by software execution. In the past few years, there is a trend in developing digital control modules which include the following main directions:

a. the development of control algorithms used to determine automatically the controller parameter values and provide to the hydraulic servo-actuator optimized electrical signals for achieving the desired work program. Thus, if the load and displacement to be achieved are considered as inputs / requirements, the program will generate a command signal so that it will increase servo-actuator’s positioning accuracy and lower response times, besides a better settling time. It should be emphasized that the basic performances of one controller are given by the proportional gain factor and when using the integrative gain factor in order to increase precision and the derivative gain factor to anticipate and attenuate oscillations it may result an improvement of dynamic performances;

b. the implementation of intelligence by adding an additional correction to the control signal. For example, such a correction takes into account the working fluid viscosity change that will cause higher

hysteresis and lower precision. The correction will be made in real-time by designing a secondary feedback loop that uses a temperature sensor;
c. expanding system's inter-connectivity by using intelligent communication routines, the equipment will be able to efficiently exchange data with other digital systems and components. When using digital systems with increased computing power it may involve learning and adapting capability of the system.

Servo-controllers or newer PCs with data acquisition boards drive regulation systems that automatically are adjusting functional parameters such as force, pressure, speed, flow rate or stroke, always try to cancel the difference between the output and the reference signals. The feedback loop is operating with a reference signal which can be considered as the overall effect of the necessary changes in functional parameters and the disturbances that occur in the system. A modern trend in the field of digital control modules for servo-hydraulic systems lies in their integration into hydraulic control devices. There are currently various types of hydraulic equipment with "on board electronics" (OBE) from the major manufacturers of devices and hydraulic equipment. Overall, there are two basic types of architectures of electronic drive and control determined by the way of implementing the regulation algorithm, namely analog architecture and digital architecture. Analog architecture is based on the use of analog electronic modules that implement various mathematical functions such as adders, integrated circuits, differentiators etc. As advantages there can be mentioned the low price and good dynamic performances but having as disadvantages low integration, low stability of parameters over time and lack of connection to microcontroller systems. Digital architectures are based on the conversion of analog signals from transducers into numeric values using analog to digital converters, followed by digital conditioning and processing of these values and generating analog output signals using a digital to analog convertor. Digital control architectures have as central element a 8/16/32/64 bit microprocessor or microcontroller. As advantages, there are: the possibility to connect and exchange information with other digital or computer systems and better opportunities for integration into complex systems. As disadvantages, there can be mentioned higher price and lower dynamic performances than the analog version. A first digital architecture is using a solution based on a PC and a data acquisition board, which means that the control algorithm can be developed using common software environments, making easy to interface with other digital or computer systems. As disadvantages there can be mentioned high price. The benefits arise from the use of a regular PC as a central processing element (high computing power, flexibility and ease of use). The second architecture is using microcontrollers - basically, most of the necessary hardware elements are concentrated in the microcontroller's structure with advantages in terms of physical size and price of the entire system; as disadvantages - system development requires more time - microcontroller programming is more difficult (it is always related to the limited available resources) and slightly lower flexibility. A third digital architecture is using Single Board Computer concept which is represented by a PC on a single circuit board. It has small dimensions and it combines the advantages of both digital architectures given above with the performances and flexibility of a PC at a small microcontroller based circuit board. In addition, it benefits from cutting edge technologies in terms of peripherals, such as memory cards, GSM modems or Ethernet network cards.

## 3. Digital control module for a servo-hydraulic positioning system

The digital control module was developed to meet the requirements of the servo-hydraulic positioning systems that allow making complex measurements of the functional parameters of linear hydraulic servo-actuators. In order to accomplish such purpose it is necessary that the digital control modules must have an easy integration into the working installation of the monitored servo-actuator. The monitoring structure is made of transducers and digital electronics that will be designed to be compact and reliable. It was obtained a punctual monitoring method of the working parameters and equipment that can be easily integrated into a servo-hydraulic installation or system. The digital control modules will be inserted on the paths of hydraulic lines, having a simple coupling mode by using

**ISSN 1454 - 8003**
**Proceedings of 2011 International Salon of Hydraulics and Pneumatics - HERVEX**
*9 – 11 November, Calimanesti-Caciulata, Romania*

hydraulic quick couplers. Regarding the electrical power source that will be designed and integrated into the structure of the digital control modules, it must have a large range of input voltages, using as much as possible the available power source of the installation or system where it will be integrated. A common power source used in modern servo-hydraulic systems has an output voltage between 9 …36 volts DC. The power consumption of the digital control module is estimated to be low therefore the main power source of the hydraulic installation/system will not be overloaded. In order to meet the European regulations on energy consumption, the digital electronic structure as well as the electrical power source will have a stand-by feature that will significantly reduce power consumption while waiting for an event. The digital electronic module has central processing equipment (microcontroller) that can deal with energy management procedures through specific methods. Regarding the communication features of the digital control modules it will be used a MODBUS protocol through RS485 serial lines. This is considered to be a standard in industrial automation area being present in the structure of almost 90% of automation equipments used in the servo-hydraulic area. In this way the integration of the digital control modules into working servo-hydraulic installations or systems will be natural thus reducing the hardware and software effort.

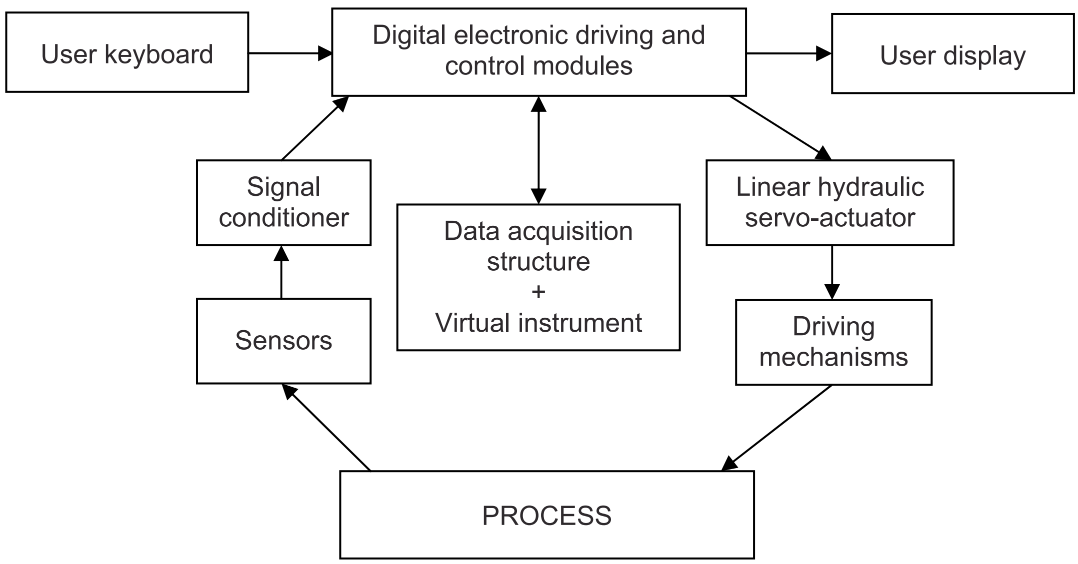


Figure 1 - Block diagram of a digital control module

The data acquisition structure of real-time mechatronic equipments will be designed using real-time concepts, regarding the: acquisition of measurement data, storage of acquired or processed data, processing of acquired data in order to take decisions and pass them to the servo-actuators of the system, sending of information to the operator or to a central processing unit. There will be used a multi-channel data acquisition structure with digital multiplexing, depending on the number and type of measuring parameters, their speed and way of variation, required acquisition speed and so on. Choosing a data acquisition structure imposes making a few technological and technical analysis and studies regarding the system's structure and nature and evolution of the process, as well as an economical analysis on efficiency, development-maintenance-running costs and so on. It is necessary to develop an objective function in which the parameters to be modified are the weights of the fundamental functions of data acquisition structure and as restrictions will have technical and economic conditions. It is necessary to define and analyze the following: fundamental functions of the data acquisition system; process technical conditions and parameters; economical conditions. Data conditioning and processing will be done according to the complexity of the data acquisition system and the type of acquired data.

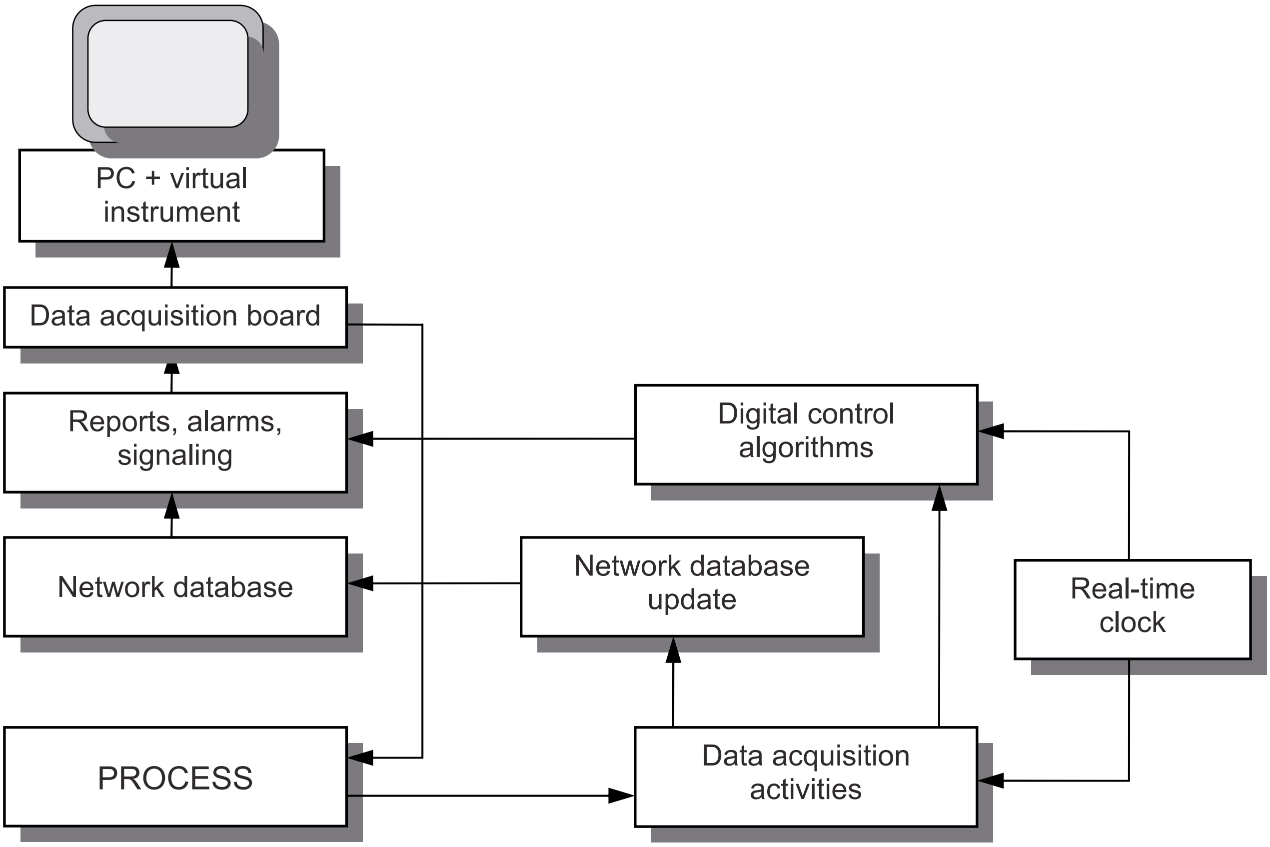


**Figure 2** - Schematic of the data acquisition structure

The technical conditions and restrictions imposed by the process are related to the type of the measured parameters, the way the parameters are varying, the number of monitored parameters and location on the sensors/transducers relative to the data acquisition structure. In figure 2 is given the preliminary schematic of the data acquisition structure that will be used at the development of digital control modules for linear hydraulic servo-actuators. Some important features of the structure given in figure 2 are: the flexibility to fit a wide variety of situations, increasing the integration of automation equipment in servo-hydraulic drives area; a higher accuracy when measuring process parameters, higher reliability through a reduced number of component equipments and auto-test/self-diagnosis features, miniaturization of components, ability to process complex data and simplifying electrical and technological design because of the usage of families of equipment with standard connections.

## 4. Conclusions

The need to develop intelligent hydraulic equipment by integrating digital electronic modules, sensors and computer technology was the starting point in developing modern hydraulic equipment. They have local intelligence and can be connected to computer systems or communicate on standard data buses with a significant improvement in accuracy and response times, all at reduced dimensions compared to conventional solutions. Command and control systems that use modern hydraulic equipment provides superior static and dynamic performances, providing optimal solutions for a certain range of applications and in some cases constituting itself as the only solution available to solve complex control issues. One of the current trends in the development of modern hydraulic equipment are:

- continuous improvement of static and dynamic performances;
- increasing operational precision;
- lower production and exploitation costs;
- increased reliability;
- reducing the overall size.

**REFERENCES**

[1] M. Blejan, I. Duțu, B. Lupu, C. Cristescu, Data acquisition and control unit for electro hydraulic applications, ISSE 2009 Abstracts Proceedings, ISBN 978-80-214-3874-3, pag.268-269.
[2] Marian Blejan, **Iulian Duțu**, Bogdan Lupu, Corneliu Cristescu, Data Acquisition and Control Unit for Electro-Hydraulic Applications, ABSTRACT PROCEEDINGS of the 32nd International Spring Seminar on Electronics Technology-ISSE 2009, May 13-17, 2009 Brno, Czech Republic, pag. 268-269, ISBN 978-80-214-3874-3, http://www.isse2009.org/. (ISI-Thomson).
[3] A.Drumea, P. Svasta, M. Comes, Module electronice în sistemele hidraulice, Salonul Natonal de Hidraulică şi Pneumatică HERVEX2003, Noiembrie 2000, Calimanesti-Caciulata, ISSN 1454-8003, pp. 147-152. [45] I. Dumitrache, Tehnica reglării automate, Editura Didactică şi Pedagogică, Bucureşti 1980.
[4] *** http://www.ni.com
[5] *** http://www.microchip.com

**ISSN 1454 - 8003**
**Proceedings of 2011 International Salon of Hydraulics and Pneumatics - HERVEX**
*9 – 11 November, Calimanesti-Caciulata, Romania*

# STAND FOR TESTING HIGH-PRESSURE HYDRAULIC EQUIPMENT

Catalin DUMITRESCU[1], Dragoş Daniel ION-GUȚĂ [2]
Radu SAUCIUC[3], Liliana DUMITRESCU[4]

[1, 3,4] National Research Development Institute for Optoelectronics
Subsidiary Research Institute for Hydraulic and Pneumatic, INOE 2000-IHP
[2] University POLITEHNICA Bucharest, Faculty of Energetics

**Abstract**: Increasing the working pressure in hydraulic drives is a method for increasing efficiency, for reducing material consumption and the weightof the equipment.

In our country, high pressure equipment are present in various areas: transportation, construction, energy, industry, etc. Maintaining their optimal parameters, checking and repairing them requires the existence of modern means of working in the field of high pressure hydraulic machines, work procedures and qualified personnel. The authors have developed a specialized test stand at high pressure (max. 630 bar) hydraulic equipment based on modern procedures.

**Keywords**: hydraulics, high pressure, testing

## 1. Introduction

Hydraulic systems have emerged and developed rapidly, especially due to the need to control and regulate the high and very high forces and moments with high precision, while they allow control of the position and velocity pregnancy involved. Hydraulic adjustment of the transmitted power offers possibilities of which it can not be benefited if used solely electrical or mechanical equipment.

In the current competitional context between different types of drives, especially between the hydraulic and electric, hydraulics have important advantages, being widespread in the construction equipment; the advantages directly related to the high level of pressure in the hydraulic system are:

- easy implementation of force and high power and easy control of such high energies with hydraulic apparatus and permanent control over the forces acting on system;
- maintaining or insignificant increasing with the increasing pressure equipment, with positive effects on economic efficiency and dynamic performance.

Besides these advantages, hydraulic drive presents a number of disadvantages, among which the most important concerns:

- wear of equipment, which increases with the working pressure, resulting in shortening the proper functioning of the equipment; the problem is more complex for basics elements, pumps and motors;
- with the increasing pressures of work, in some cases appears the problem of changing materials for some components, with negative implications on price.

Development trends of hydraulic equipment pressure increase occurs in the directions of work (concentration in time), ensuring multiple functions for a given building element module (working concentration), increased energy indicators (power concentration), increased reliability and durability etc. [1]

Of these trends, increasing pressure is the most visible in recent years; the tendency is to raise the maximum working pressures from the range 250 ... 320 in the domain 350 to 450 bar and over, depending on the application. [2]; many major companies in the industry (Bosch - Rexroth, Vickers, Parker, etc..) illustrate this by providing equipment operating at elevated pressure than those of previous generations. This equipment, implemented in various hydraulic assemblies, mainly in construction, energy, and industry, can be found in our country too. Maintenance, checking and repairing these equipment require the existence of appropriate means (specialized stands, consistent work procedures, qualified personnel, etc.).

ISSN 1454 - 8003
**Proceedings of 2011 International Salon of Hydraulics and Pneumatics - HERVEX**
*9 – 11 November, Calimanesti-Caciulata, Romania*

In this context, the authors have developed in the Research Institute for Hydraulics and Pneumatics INOE 2000 – IHP Bucharest a stand for checking the characteristics of hydraulic equipment working at pressures up to 630 bar. Unlike solutions that exist in this moment on national stage, which are using pressure amplifiers [3], it has chosen a more modern solution, the use of a pump that provides continuous flow. The stand has four lines of work:

- Carrying out checks on repaired equipment to determine the current characteristics;
- Test new equipment manufactured by different companies in the field, requesting it to determine the characteristics of their products;
- Carrying out research in high pressure;
- Carrying out checks on equipment functioning, to determine the safety of operation, this field can be made RENAR accredited testing after procedures developed for this purpose.

**2. Relevant aspects regarding the stand for high pressure testing equipment**

The main elements of a hydraulic installation are the flow generator (hydraulic pump) and the elements for control and adjustment of pressure and flow.

Taking into account future possibilities of working with stand, for the flow generation was chosen a radial piston pump type WEPUKO that allows a rated working pressure of 1000 bar (maximum 1200 bar). It was intended to increase pressure further work on stand up to pressure of 1000 bar. This pump requires a pressure of 2,5 bar at the suction port; the requirement has been met by mounting a hydraulic boost circuit (figure 1), having as main element a gear pump, shown in figure 2.

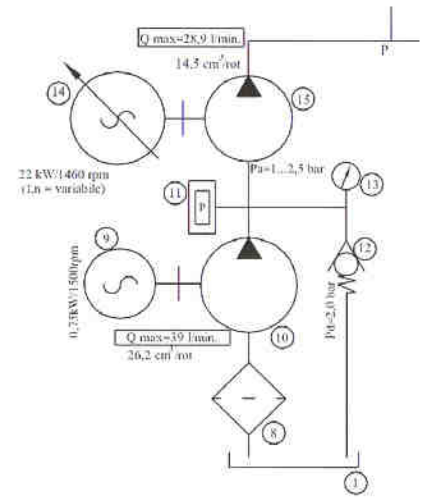


Figure 1: Hydraulic boost circuit

Figure 2: The gear pump electrically driven

The choice of drive schemes and distributors

In the domain of high pressure drives, a typical solution use direct actuated directional poppet valve, solenoid actuated; to obtain a scheme of distributor type 06 (H center), have studied various possible combinations of existing distributors and have used two types of directional control valve 3 / 2 electrically actuated: 1 directional control valve MSEW6U2x630LG24 type and 2 directional control valve MSEW6C2x630LG24 type.

Table 1. Connections made with block distribution

| **Electromagnets condition** | **Connections** |
|---|---|
| $S_1$, $S_2$, $S_3$ – non-supplied | P, A, B → T |
| $S_1$, $S_2$ – supplied<br>$S_3$ - non-supplied | P → A<br>B → T |

| | |
|---|---|
| $S_1$, $S_3$ – supplied<br>$S_2$ - non-supplied | P → B<br>A → T |

Schematic diagram of the stand is shown in figure 3.

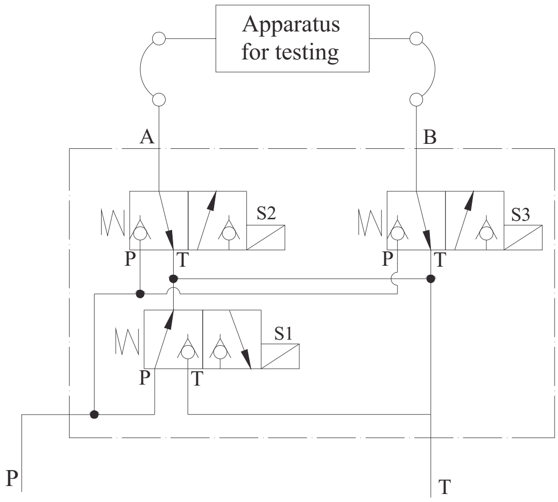

Figure 3: Hydraulic scheme of the obtained distributor

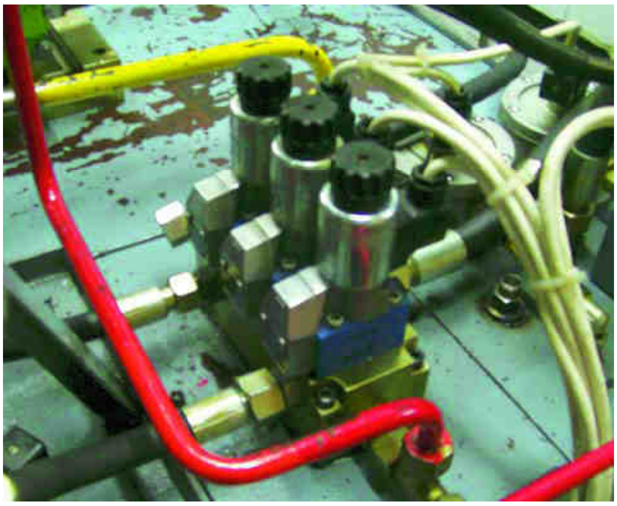
Figure 4: The block of distributors

The stand consists of three main subassemblies:
1 – The mechanical-hydraulic system;
2 – Electricity supply system;
3 – Information system.

Mechanical-hydraulic system is the main component of the stand and contains two main devices:

- Main circuit equipment, working pressure of 630 bar;
- Auxiliary / filtration circuit equipment that allows a maximum working pressure of 315 bar.

Hydraulic scheme of the stand containing the 2 circuits are shown below.

Main circuit working at maximum pressure of 630 bar contains, in addition to high pressure pump and distributors block, a 630 bar maximum pressure valve and connecting elements between components: rigid and flexible pipes, fittings, etc.. Information about the pressure and flow in the circuit are obtained from pressure and flow transducers, which display this information locally, but send these information too toward the computer system, where they are received, processed and stored; the link between sensors and the computer is done by using a data acquisition board National Intruments PCI-6259 model. The choice of transducers to take into account the specific use in high pressure circuit.[4]

Auxiliary / filtration circuit has a double role:

- To maintain the purity of the oil, being provided with 2 filters installed in series with finesse of 25 and 10 μm;
- To provide flow at low pressure (max. 315 bar) when working in this field pressure.

In this structure, the stand has the following characteristics:
1. Stand dimensions: L x W x H (mm): 2080 x 1330 x 1800;
2. Electrical connection: 0.75 + 11 + 22 = 33.75 kW (3 phase induction motors);
3. Oil tank volume (empty) = 765 $dm^3$;
4. Useful volume of oil = 650 ... .700 $dm^3$;
5. Voltage of the electromagnets: 24 VDC;
6. Working fluid: hydraulic mineral oil HLP with additives or equivalent with kinematics viscosity at 40°C = 44.4 ... 49 cSt ($mm^2$ / sec.);

7. The degree of filtration of hydraulic oil: 10 μm;
8. Maximal pressure = 630 bar;
9. Flow: max. 20 l / min at 1460 rpm;
10. Main pump type: radial piston, high pressure (1000 bar), manufacturer WEPUKO.

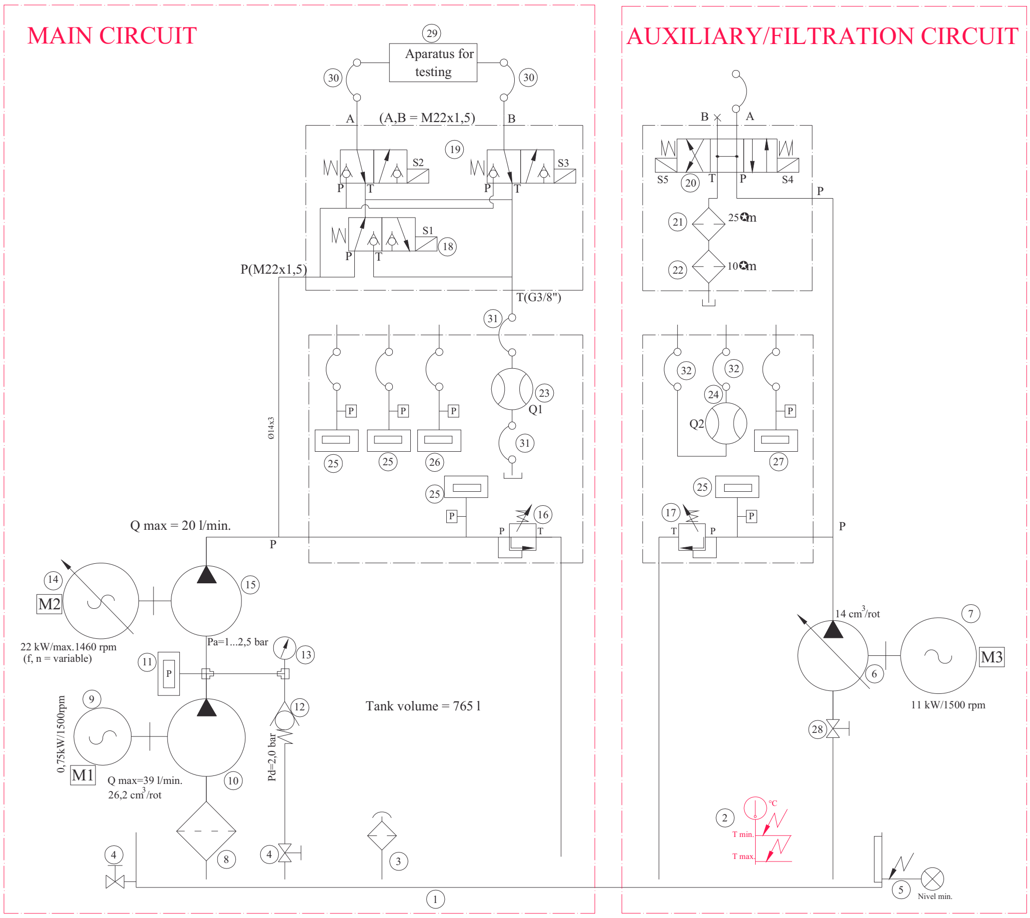


Fig. 5 – Hydraulic scheme of the stand

### 3. Tests performed on stand

***Test nr. 1***

One of the tests performed until now aimed to check the flow of the pump at different pressures in the circuit to determine the actual flow that the pump can provide at different loads and different driving speeds; for this, the hydraulic load was accomplished with a hydraulic pressure valve, set at a pressure of 100, 200, 300, 400, 500, 600 and 630 bar.

In parallel with the supplied pump flow were also recorded and the pressure variation in time and flow variation in time; computer with which you made the acquisition and processing has as operational system Windows XP program, and the work program LabView program was used, with an application made on-site.

Rotational speed for the pump was between 292 and 1460 rpm, speed being adjusted using a frequency converter in accordance with the power of the electric motor used for drive (22 kW). During the test, load pressure was kept constant. The resulted graphs are presented below.

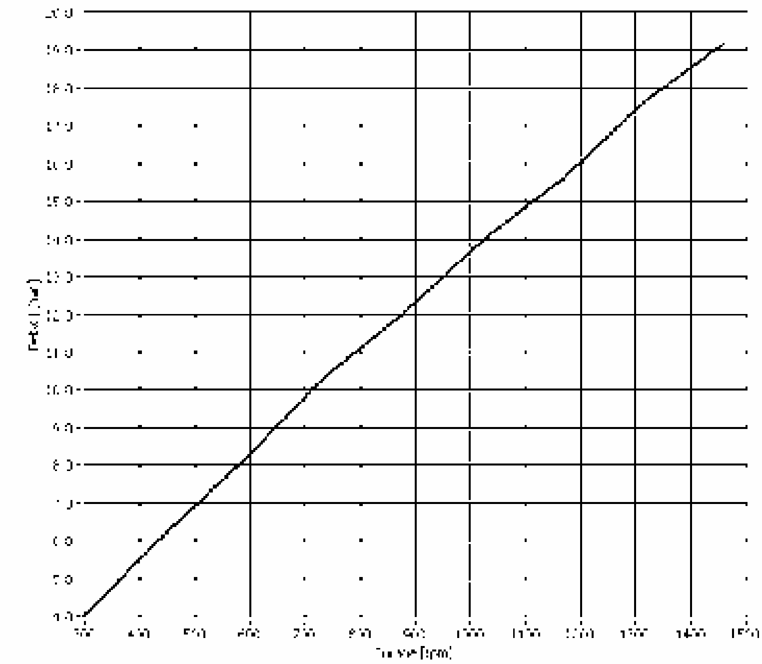

Figure 6: Flow depending on the rotational speed at pressure 300 bar

To better visualize the pump behavior at different levels of pressure, in the following chart are positioned three curves at pressures of 200, 400 and 630 bar respectively.

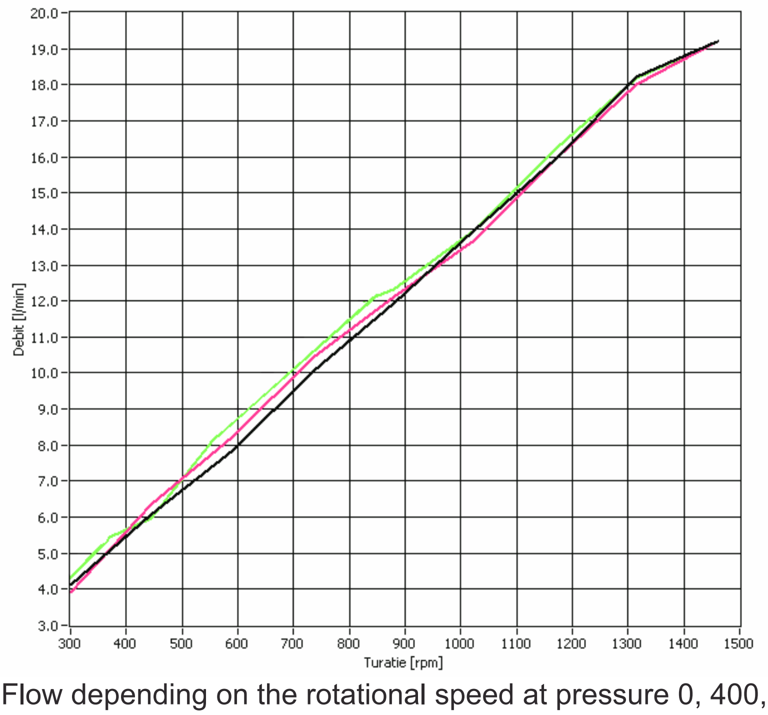


Figure 7: Flow depending on the rotational speed at pressure 0, 400, 630 bar
__________ - 0 bar __________ - 400 bar __________ - 630 bar

In parallel with experiments performed on the stand, was made a general application of hydrostatic simulation of a pump used to obtain high pressures. This was done by AmeSIM simulation program, and results were compared with the experimental.

To analyze the simulated volume pump were developed two simulation networks. A simplified model of the pump (fig. 8) was carried out using mathematical models of the driving element, the mechanical energy transmission system differentiated for pistons skate (cams shaped which drive the pairs of three pistons), piston models (with internal leaks dQ (dP)), inertial masses of the pistons and distribution elements (valves which separate suction and delivery of the pump).

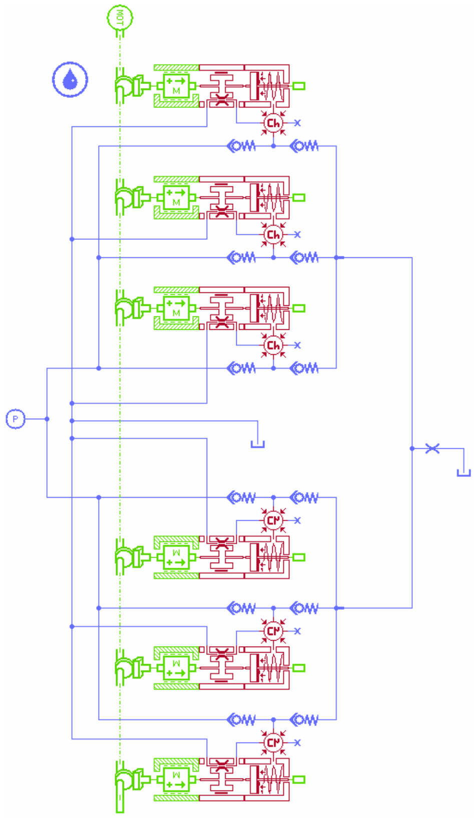

Figure 8: Simulation network – simplified model

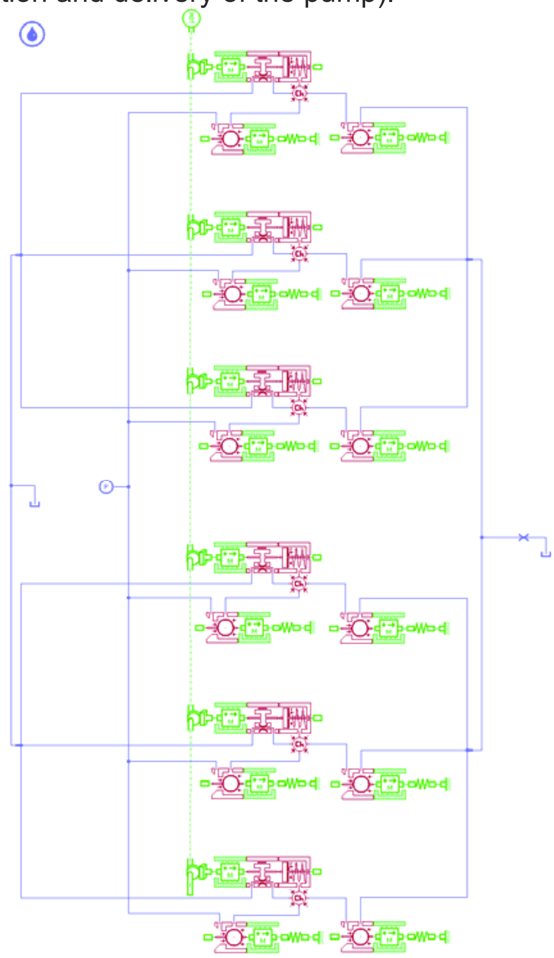

Figure 9: Simulation network for the WEPUKO pump

A dissipative element type throttle (whose area of flow can be changed dynamically during the simulation) was used as load. For comparative analysis with experimental results the throttle valve was replaced with a normally closed valve having similar characteristics with the valve fitted on the high pressure stand.

For further analysis of the phenomena occurring in the system, was developed a second network simulation in which the check valves used for oil distribution were analyzed with sub-components from the library of the AmeSIM program. [5] (Fig. 9).

The complete model of distribution elements comprises the model of inertial mass of the obturator element, the spring and the variable area section of the flow obturator element, according to the position. Both models have a power boost oil pressure source, with parameters corresponding to the experimental stand.

The comparison between the flow pump values experimentally obtained above and those obtained by simulation are shown in the graph in Figure 10.

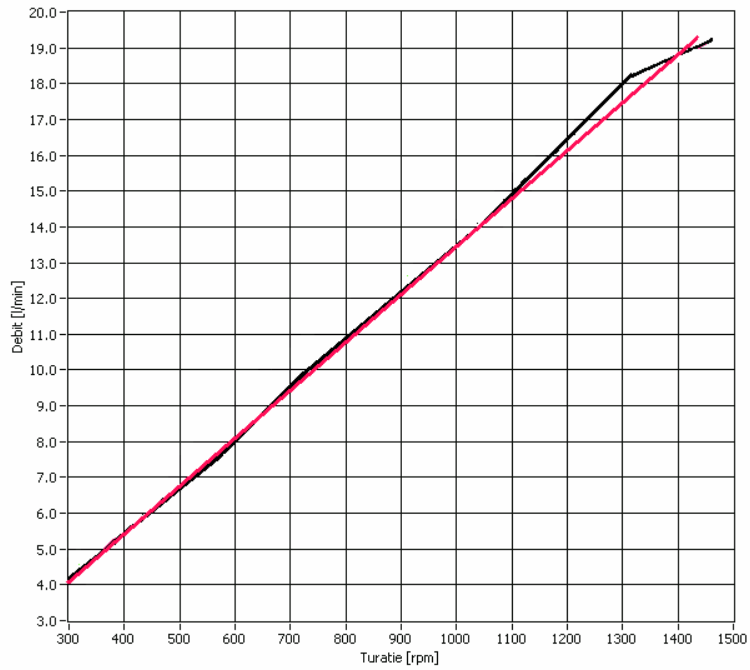


Figure 10: Flows depending on rotational speed at 630 bar, experimentally and simulated
_________ - 630 bar (experimentally) ; _________ - 630 bar (simulated)

To measure the technological parameters of the quantities of interest in the testing stand was performed a typical application of data acquisition and processing using LabVIEW program. Figure 11 shows operator interface application note, and fig. 12 is a section diagram of the application program source.

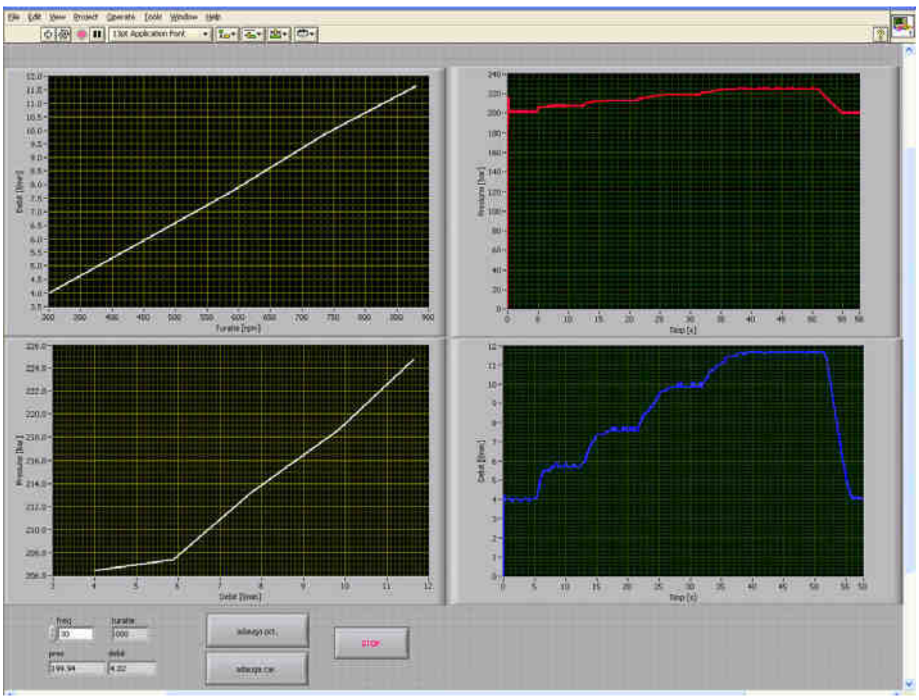

Figure 11: Application interface for experimental data acquisition and processing

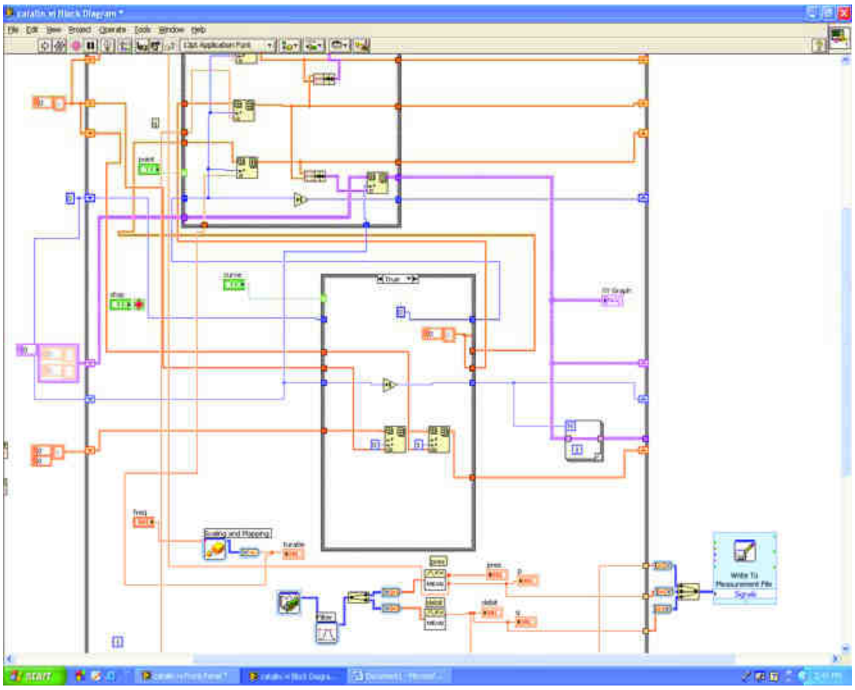

Figure 12: Block diagram of data acquisition program

Conclusions of the tests performed on the pump:

- Analyzing the flow characteristics at different pressures in the circuit show that the flow does not vary with increasing pump pressure circuit, which is normal for pressures up to 630 bar, taking into account the pump is designed for pressure 1000 bar (maximal working pressure 1200 bar);
- Experimentally obtained values are close to those obtained by simulation.

***Test nr. 2***

It was tested on the high pressure stand an adjustable pressure valve, with direct control, which was refurbished earlier in the engineering department. The test was aimed at determining the static characteristic of the valve after reconditioning. Valve type: HAWE MV 42A

Tests were made based on a procedure developed in INOE 2000-IHP Bucharest, in accordance with RENAR.

SP sample valve was mounted as shown in the figure below.

To achieve sampling pressure, open the way to SP high pressure valve, supplying the electromagnets of the S1 and S2 distributors.

Adjust the system working pressure at successive values of 4, 200, 400, 600, 630 bar and aims the influence of increasing the flow on the pressure regulated by valve. Since the maximum flow through the valve is 12 l / min, the tests were made up to this flow.

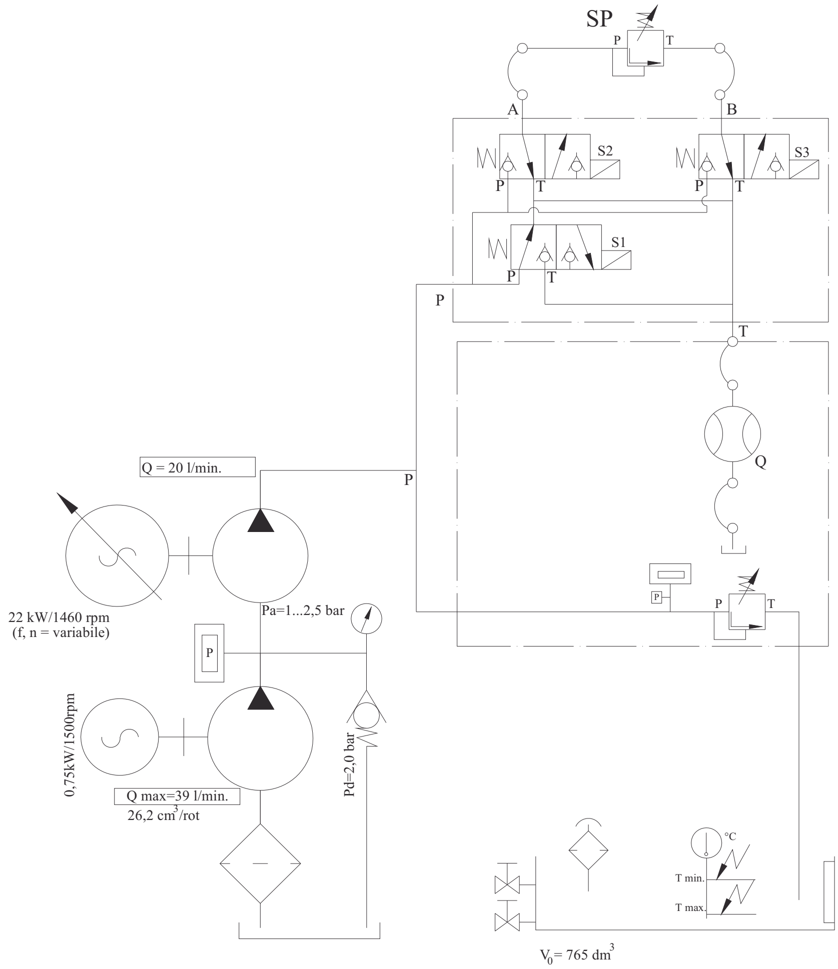


Figure 13 – Hydraulic scheme for pressure valve testing

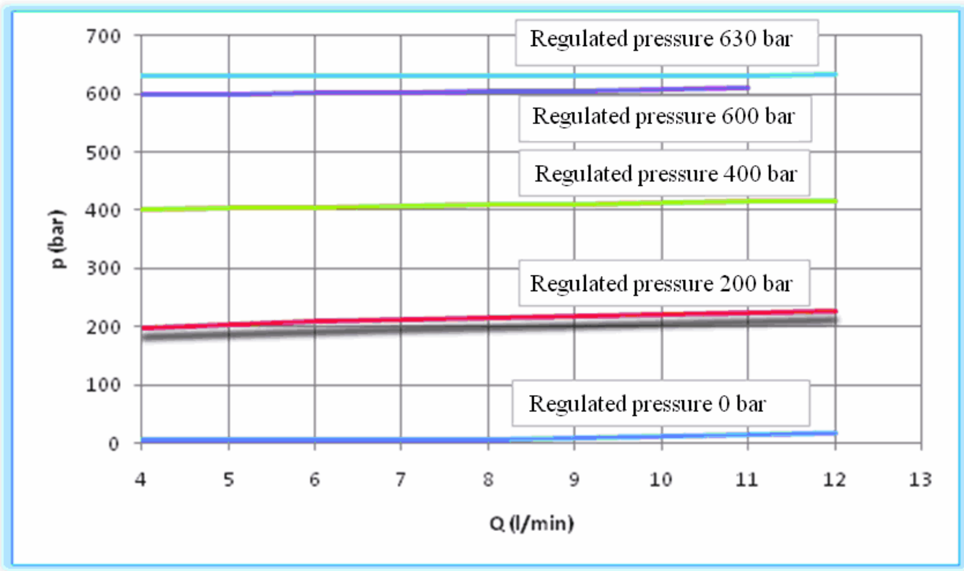


Figure 14: Result of testing for the pressure valve

Change in set pressure with flow at various pressure levels, is shown in the table below.

Table 2: Pressure deviation

| Set pressure (bar) | 0 | 200 | 400 | 600 | 630 |
|---|---|---|---|---|---|
| Deviation from set pressure $P_{max} – P_{min}$ (bar) | 14 | 25 | 17 | 12 | 3 |

These results are analyzed in comparison with the diagrams provided by the manufacturer for the product in new condition [6]; in terms of safety in operation, is very important maintaining the set pressure as small deviations, especially in the upper area of work pressures.

Comparative analysis of these results with the initial manufacturing data of the valve proved the following conclusions can be drawn:

- Fixed equipment characteristics are very similar to the one in new condition;
- Stand allows evidence of this type can provide the required flow and pressure parameters.

## 4. Conclusions

Experimental stand for studying the characteristics of hydraulic equipment with operating at high pressure (max. 630 bar), developed by the authors, allow performing tests for 630 bar maximum pressure equipment. Compared to existing solutions on a national means of high pressure testing, usually performed by hydraulic pressure amplifiers, stand shown has a continuous flow pump, which recommends a maximum working pressure for further developments.

The results of experiments can be compared with those obtained from simulations with specialized programs or given by manufacturers; where this has been done, the results were similar between the different types of results.

Procedures for performing tests was developed in parallel with experimental stand, allow the performing in good conditions of the tests; at present, the procedures for tests cover a wide range of high pressure devices, and some tests (for valves, distributors, throttles, etc.) are accredited by the national authority.

## Bibliography

[1] *Mihai Avram*, Acționari hidraulice şi pneumatice. Elemente şi sisteme clasice şi mecatronice, Editura Universitară, Bucureşti, 2005
[2] *Peter Dschida,* Statement Service*,* Bosch-Rexroth Catalogue, 2010
[3] *A.C. Hanganu, C.Chiriță, M. Frunză*, Consideration pour integrer les equipments hydrauliques modulaires de pressions éleveés – 70 [MPa] pour tester les installations technologiques, a VIII-a Conferință Ştiințifică nternațională, „Tehnologii Moderne, Calitate, Restructurare” – TMCR 2006 Iaşi, România, Mai 2006
[4] *Doru Dumitru Palade,* Traductoare şi senzori - curs, Tipografia UPB, 1995
[5] *** - AMESIM 4.0 User Manual, 2004
[6]*** - HAWE Catalogue – Hydraulics Components, 2008

ISSN 1454 - 8003
Proceedings of 2011 International Salon of Hydraulics and Pneumatics - HERVEX
9 – 11 November, Calimanesti-Caciulata, Romania

**HERVEX 2011**

- *CETOP*
- *CETOP EDUCATION COMMISSION*
- *NATIONAL FLUID POWER CENTRE (UK)*

  *Centre of Vocational Excellence*

***Presented by John R Savage- Vice President CETOP Education***
***Chairman BFPA Education & Training (UK)***
***Director National Fluid Power Centre (UK)***

## Introduction MESSAGE-

*The purpose of this presentation is to raise your Awareness of* ***"WHO IS CETOP"*** *together with that of the* ***CETOP Education Commission.*** *The 2nd part of the presentation will take you into the world of the* ***National Fluid Power Centre in the UK****, explaining to you how a successful centre of fluid power vocational excellence has been developed through the support of the National Fluid Power Trade Association, the BFPA, its member companies, distributors, manufacturers and end users.*
*It clearly identifies what can be achieved through COLLABORATION and EMPLOYER ENGAGEMENT*

## A Frequently asked question No 1.

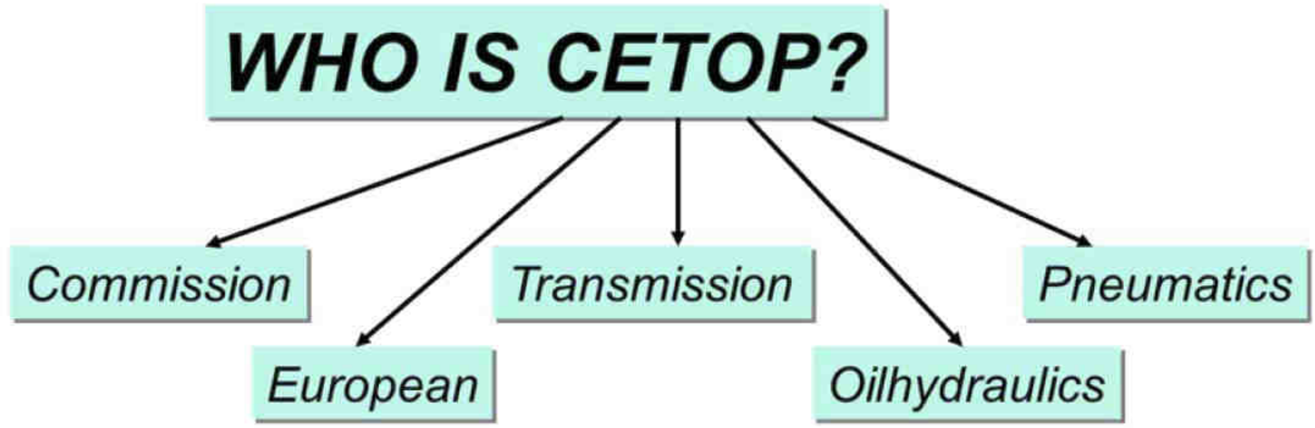



*The INTERNATIONAL UMBRELLA ORGANISATION*
*REPRESENTING*
*THE NATIONAL FLUID POWER ASSOCIATIONS*
*IN EUROPE and Beyond.*
*It is a vital FORUM for the FLUID POWER INDUSTRY*

## WHO IS REPRESENTED BY CETOP?


- Romania
- France
- Germany
- Italy
- Turkey
- United Kingdom
- Netherlands
- Poland
- Finland
- Switzerland (2)
- Norway
- Spain/Portugal
- Norway
- Sweden
- Slovenia
- Czech Republic
- Russia

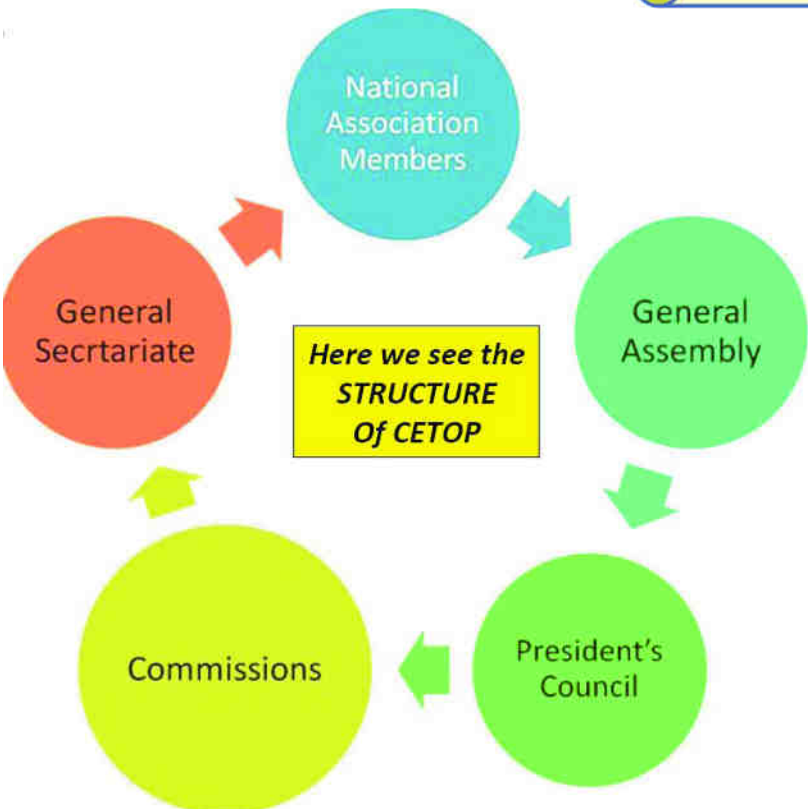

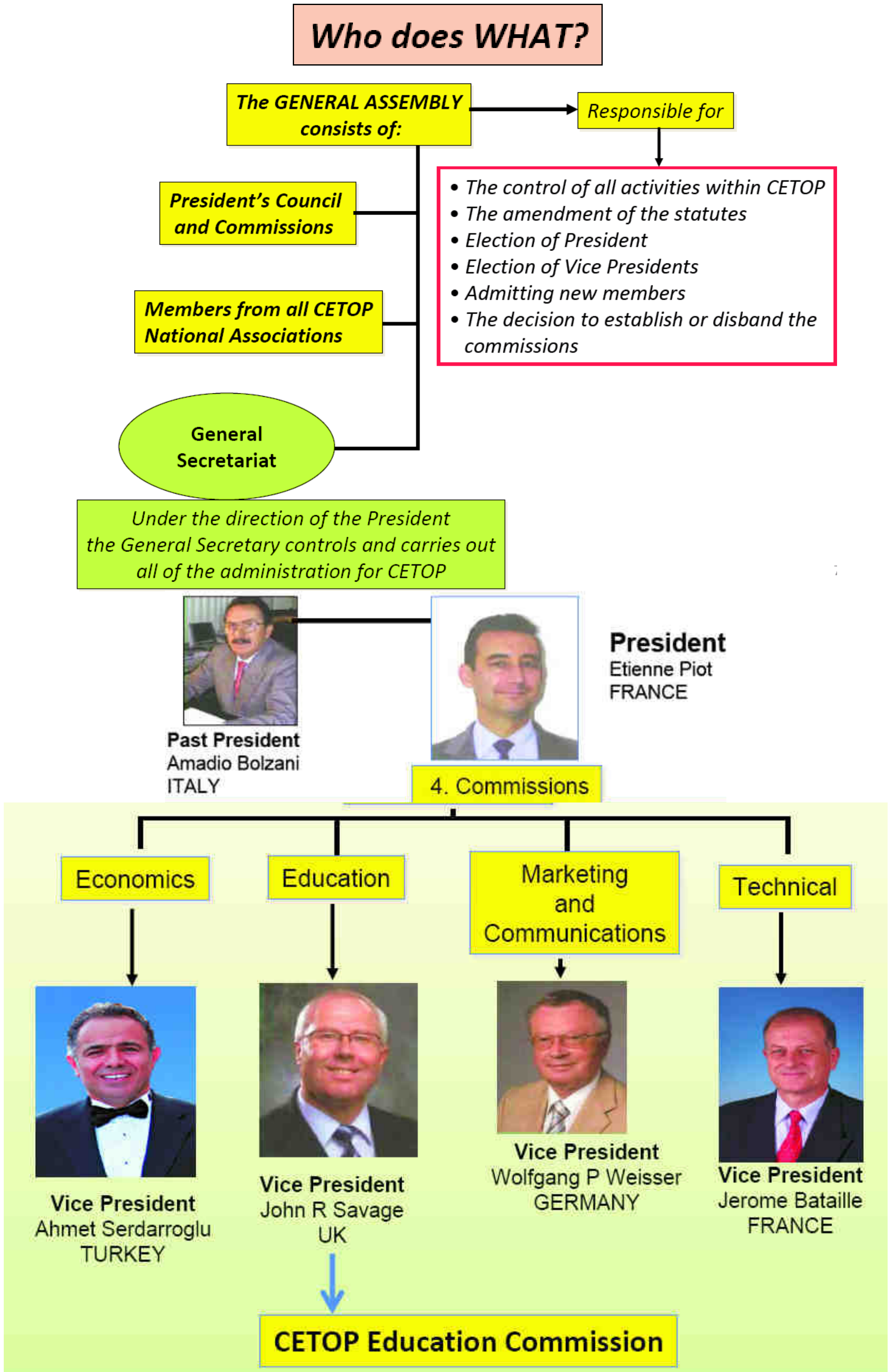
Who does WHAT?
The GENERAL ASSEMBLY consists of:
Responsible for
President's Council and Commissions
Members from all CETOP National Associations
General Secretariat
• The control of all activities within CETOP
• The amendment of the statutes
• Election of President
• Election of Vice Presidents
• Admitting new members
• The decision to establish or disband the commissions
Under the direction of the President the General Secretary controls and carries out all of the administration for CETOP
Past President
Amadio Bolzani
ITALY
President
Etienne Piot
FRANCE
4. Commissions
Economics
Education
Marketing and Communications
Technical
Vice President
Ahmet Serdarroglu
TURKEY
Vice President
John R Savage
UK
Vice President
Wolfgang P Weisser
GERMANY
Vice President
Jerome Bataille
FRANCE
CETOP Education Commission


## CETOP EDUCATION MISSION STATEMENT

*To provide the forum for National Associations to take up an active role in developing, driving and implementing standards, quality and content of "COMPETENCE BASED EDUCATION AND TRAINING" involving hydraulics, pneumatics and associated controls. This gives a recognised qualification structure throughout Europe*

***In respect to EDUCATION and TRAINING the role of the CETOP Education Commission is to:***

- ***set standards***
- ***put forwards recommendations***
- ***provide advice and guidance***

*Their role is not to get directly involved with processes*

***We have in place a STRATEGIC PLAN for the members of the EDUCATION COMMISSION to implement***

1. ***Raise awareness and greater understanding of CETOP competence based qualifications.***

2. ***Become a strong and active member of the EDUCATION COMMISSION and work together to address the common goals***

3. ***Ensure that your National Association takes a lead and have a clear vision of how to achieve a successful outcome***

4. ***Be part of a STRONG COMMUNICATION network.***

5. ***Share good practices and create improvements***

## *Our ULTIMATE GOAL*

***To develop a network of "CENTRES OF VOCATIONAL EXCELLENCE***
- ***Approved and qualified to manage, administer and deliver to a common recognised standard as laid down within the CETOP Education Recommendations.***

***Here we are at present***

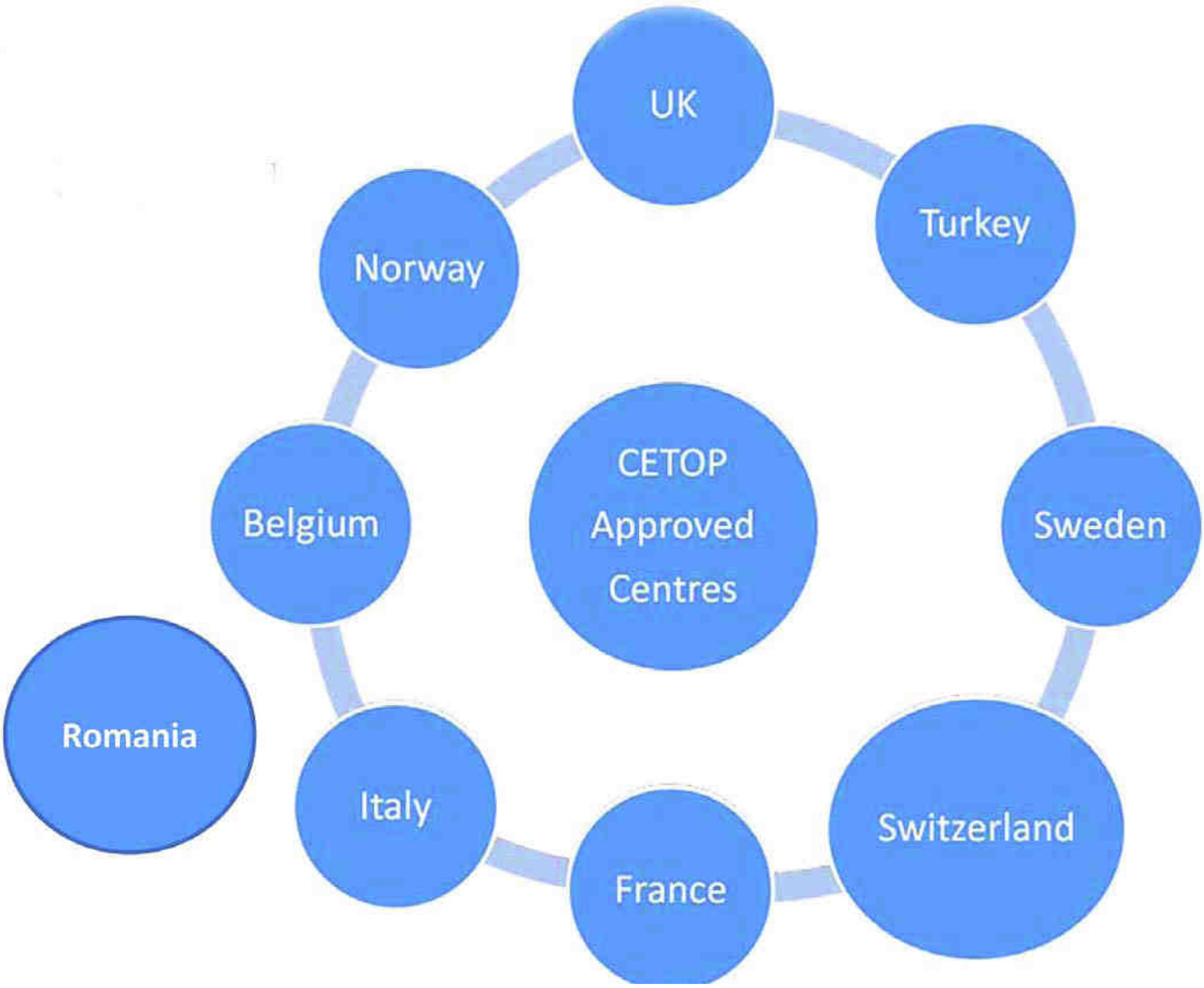

ISSN 1454 - 8003
Proceedings of 2011 International Salon of Hydraulics and Pneumatics - HERVEX
*9 – 11 November, Calimanesti-Caciulata, Romania*

NFPC National Fluid Power Centre (UK)
*for Fluid Power Motion Control*

# *In 1997 discussions began in the UK to consider the development of a NATIONAL FLUID POWER CENTRE*

*The THEME behind what is to follow*
*is what can be achieved through collaboration and employer engagement with:*
- *The Fluid Power National Association and its member companies*
- *End users of fluid power systems*
- *Major original equipment manufacturers*
- *Distributor networks*

*Supported by:*
- *Good leadership and direction*
- *An Industrial Advisory and Strategic Planning Committee*
- *The development of saleable products and marketing strategy*

*Combined with:*
- *The provision of an outstanding team of Systems Training Engineers at the Centre with extensive knowledge and real world experience*

NFPC National Fluid Power Centre
for Fluid Power Motion Control

In 2000 the UK opened its NATIONAL FLUID POWER CENTRE

It is a WORLD CLASS LEADER IN EDUCATION & TRAINING with emphasis upon SKILLS & COMPETENCE

NFPC National Fluid Power Centre
for Fluid Power Motion Control

Officially opened by AMADIO BOLZANI- President of CETOP and PAUL COOKE – President of the BFPA and MD (Bosch Rexroth UK)

***To establish and secure a NATIONAL CENTRE would require strong support from industry and the formation of strong and lasting partnerships***

***In 1987-***

***The decision was made to form an Advisory and Strategic Planning Committee, to support the FLUID POWER CENTRE established by a College of Further Education***

***1997-***

***This same committee decided to support project to build a NATIONAL CENTRE***

***These companies were:***

19

***2011- National Fluid Power Centre Advisory and Strategic Planning Committee***

20

ISSN 1454 - 8003
Proceedings of 2011 International Salon of Hydraulics and Pneumatics - HERVEX
*9 – 11 November, Calimanesti-Caciulata, Romania*

## *Officially APPROVED TRAINING PROVIDER for:*

*On entering the National Fluid Power Centre reception the CETOP Approval and Industry Approval Certification is on show.*

ISSN 1454 - 8003
Proceedings of 2011 International Salon of Hydraulics and Pneumatics - HERVEX
*9 – 11 November, Calimanesti-Caciulata, Romania*


Advisory member companies use the PRACTICAL WORKSHOP AREA

**ISSN 1454 - 8003**
**Proceedings of 2011 International Salon of Hydraulics and Pneumatics - HERVEX**
*9 – 11 November, Calimanesti-Caciulata, Romania*

# EDUCATION METHOD OF HYDRAULICS AT FACULTY OF MECHANICAL ENGINEERING SLOVAK UNIVERSITY OF TECHNOLOGY

**Karol PRIKKEL[1], Andrea HARINGOVÁ[2]**

[1] Institute of process and fluid engineering, Faculty of Mechanical Engineering, Slovak University of Technology, Nám. Slobody 17, 812 31 Bratislava1, [1]karol.prikkel@stuba.sk, [2]andrea.haringova@stuba.sk

***Abstract:*** *The research in Slovakia in the field of hydraulics is connected with the creation of Institute of Process and Fluid Engineering (recently known as Water engines) in the 1951, as the unique work place in the past ČSR. The education is secured in two fields: university and professional. This paper would deal with the detailed description of these education processes and possibilities in the Institute of Process and Fluid Engineering.*

***Keywords****: power engineering, KCOV, education*

## 1. Introduction

Alongside the 60 years history the Institute of Process and Fluid Engineering has developed own laboratories, and practical cooperation with industry and thanks to this has obtained significant place as not only educational but also important research centre.

The education is secured in 3 degrees, and is fully connected with industry. The final thesis are mostly fitted for needs of industry that also support the educational process. The very popular are excursions in the manufactures as Slovpump Zavadka, Sauer Danfoss and water power plants Gabčíkovo, Čierny Váh. The visible results of the education process are absolvents working for such a prestige companies as Siemens, Festo, Parker Hannifin, Eurofluid, Sauer Danfoss... The institute could be also proud that has educated such a young specialists as **Dušan Mikeska (LMS Germany)**, Juraj Guláš (Bergen Group, Norway), **Baláž** (DAIMLER AG Mercedes- Benz, Germany).

Since its establishment, the department has educated 950 absolvents of engineering degree and 55 graduates of doctorate studies. One of the first absolvent~~s~~ of doctorate studies were in 1956~~,~~ that times Ing. Jaromír Noskievič, under the patronage of Prof. Ing. Dr. Miroslav Nechleba, DrSc. with doctorate theme „Cavitation corrosion“ and that times Ing. Alexander Paciga, under the patronage of Prof. Ing. Dr. Alois Hebký, with doctorate theme „ Influence of viscosity on the work cycle of centrifugal pumps“.

Another view is on the professional education, secured by centre KCOV- Coordination centre of professional education. The centre was developed with the support of French ministry of education and French car manufacturer PSA. The centre KCOV provides the professional education for the following issues industrial maintenance and automation, electricity, safety of work. However, the equipment of the centre and lectors allow to educate in the courses for the positions according to the unique demand.

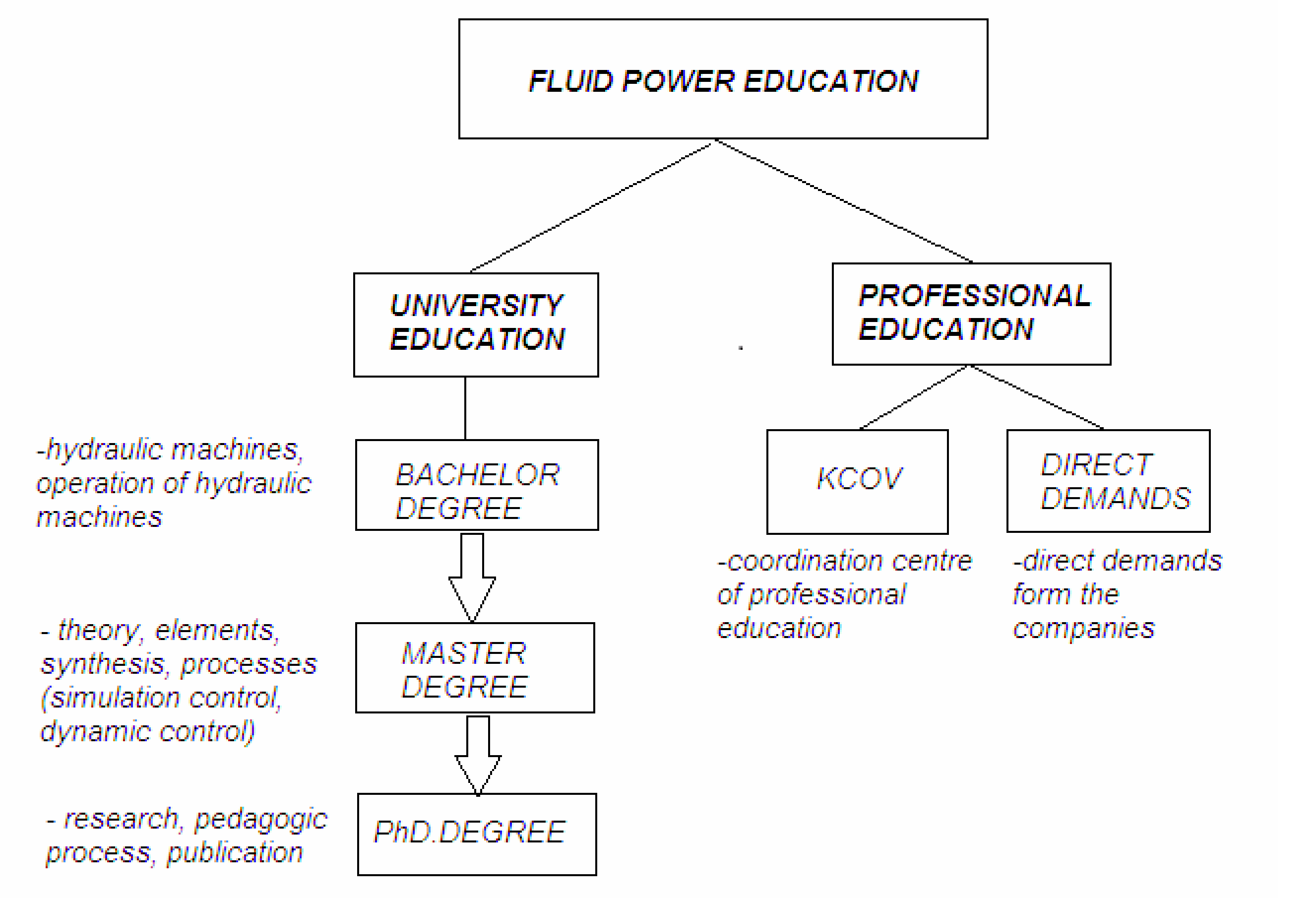


*Figure 1. Scheme of education at Faculty of mechanical engineering*

## 2. University education

The university education is divided into the 3 degrees: each of whom prepares graduates for desired specialisation, according to the CETOP recommendations. The garant of the university education is prof. Ing. Michal Varchola, CSc.

**The hydraulic bachelor degree** is secured in the programme Power machinery. The aim is to provide the graduates with basic knowledge in fluid engineering. The education is provided in three subjects. The first subject is Fluid mechanics- introduces basic knowledge about fluid, its types and character of flow, the forces acting during the flow and one part of subject is dedicated to the laboratory exercises. The laboratory exercises demonstrate the fluid flow-laminar/turbulent, the losses during the flow, the flow on the obstruction. The second subject: Hydraulic machines and equipment gives basic, but complex knowledge about the hydraulic machines and on the basis of its physical principle explains its working cycle. The subject provides also closer look on difference between fluid power and hydrodynamic machines . The subject operation of hydraulic equipment provides to students basic knowledge about the design of pump technique, water power plants, fluid power, vacuum and pneumatic systems, as well as the knowledge about the effective operation of hydraulic systems.

**The master degree** is provided in the specialisation Hydraulic and Pneumatic machinery. The profile of the absolvent is build up from the wider theoretical and practical knowledge obtained during the two years standard period. During the two years period students could fully concern on hydraulic problematic and questions in the provided subjects. The students also get in touch with various computational programs as MATLAB, ANSYS, FLUENT, EPANET. According to the selected optional subjects and the theme of the final thesis, the students are specialised to the selected directions: Hydraulic machines, Pump technique, Water turbines, and Pneumatic machines. The students have possibility to get professional experience after the second semester during the obligatory 6 week industrial practise.

**The PhD degree** in hydraulics is done under the specialisation Fluid machines and equipment. In the third-last degree of education student´s have wider access and possibilities to their own research activities during studies. They also get experience with pedagogical process and with active attendance in the conferences. The aim of this degree is to bring own solution to the selected problematic, demonstration of their solution and conclusion to the suggested idea.

## The laboratories at Institute of Process and Fluid Engineering

Although the institute has wide cooperation with industry, the institute itself comprises laboratories that hold since year 2003 the statute “Prestige laboratory of STU”.

The laboratories are divided into the 3 main groups: Hydroenergetics, Hydrodynamics and Hydrulic and pneumatic mechanisms.

The first laboratory is concerned on Hydroenergetics and serve as test station for water turbines. It could be used for measurement of universal characteristics of water turbines, measurement of cavitation characteristics of water turbines.

The second is group of laboratories concerned on hydrodynamic pumps. The whole laboratory is composed from 4 stations: station for testing radial and special hydrodynamic pumps, station for testing axial and diagonal hydrodynamic pumps, station for testing submerging hydrodynamic pumps and station for investigation of hydrodynamic forces in pump. All stations could be used for measurement of output and cavitation characteristics of hydrodynamic pumps and for specified investigations according to the type of station.

*Figure 2. Hydrodynamic laboratory*

The third group of laboratories is concerned on hydraulic and pneumatic mechanisms. This group of laboratories is divided into the 8 stations. Station for testing power fluid mechanism, station for testing hydraulic cylinders, station for testing rotation actuators, station for testing pneumatic mechanisms, station for testing circle-fluid vacuum pumps and compressors, station for investigation of cavitation in hydraulic mechanisms, station for experimental investigation of hydraulic resistance, station for records and processing of acoustic  emission of fluid systems.

*Figure 3. Hydraulic and pneumatic laboratory*

**Research at Institute of Process and Fluid Engineering**

The actual projects at the institute are dealing with antiflood barriers, problem of cavitation in the flow in narrow gap, problematic of floating chamber in water power plants, the effect of fluid on navigation of floating bodies, the effect of lubrication on lifetime of endoprosthesis.

## 3. Professional education

Professional education is secured by the centre KCOV- Coordination centre of Professional education. The beginning of this centre comes from the cooperation university-industry, Faculty of Mechanical Engineering- PSA group, in the year 2003. According to the experiences of PSA group with education projects around the world such as in Mexico, Brazil, China, Cuba, Algeria, Senegal, Egypt, Poland, it was created a tripartite partnership of the French Ministry of Education, the Slovak Ministry of Education and PSA Slovakia sro. On the basis of this tripartite, it was founded the project Carriers campus that resulted in a training centre "The Institute of education for PSA."

The French partner selected as a main administrative as well as training centre of the project Carrier campus Faculty of mechanical engineering STU in Bratislava and three secondary schools, Secondary School of Mechanical Engineering in Bratislava on Fajnors´quai, Secondary School of Mechanical Engineering in Trnava (at that time Associated secondary school) on Komenského street and Secondary School of Transport in Trnava on Študentská Street. By these steps it was created training centre, located at the four centres of learning and coordinated in the centre located in the site of the Faculty of Mechanical Engineering STU in Bratislava.

Training Centre at Faculty of mechanical engineering STU is concerned at a group of senior and middle management, with specialisation on issues of industrial maintenance, industrial automation , electric, safety at work and safety while working with electrical equipment.

The process of trainings is following: first of all, all participants have to undergo entrance tests (checking the knowledge, skills and competencies of perspective employees ). According to the results of the test, the lectors determine the concept of individual trainee on the selected issue. At the end of the training module, trainees again undergo the final test, to find out the instantaneous state of the acquired knowledge. Training modules are developed for the area - automation, maintenance, robotics, quality and control of manufacturing, electrical, safety at work by facing of electrical risks.

From the 1st January 2008, the project Carrier campus was transformed into the Coordination Centre of Vocational/Professional Training (KCOV). The organisational structure of the Coordinating Centre has remained in the original way, administrative and organisational centre remains located on the Faculty of Mechanical Engineering STU in Bratislava. The technical and laboratory equipment has passed under the administration of the Faculty of mechanical engineering.

*Figure 4. Automatic filling, line-ERM Training Centre*

The training centre consists of 3 classrooms.
**1, Industrial maintenance classroom**- serves for both theoretical education and practical training in the area of preventive and corrective maintenance on MOM and Ermaflex lines.

*Figure 5. Classroom of industrial maintenance, training centre*

**2, Industrial automation classroom-** is used for both theoretical education and practical training in the area of production device and lines control, programming of control automatic machines, sensor and pneumatic systems.

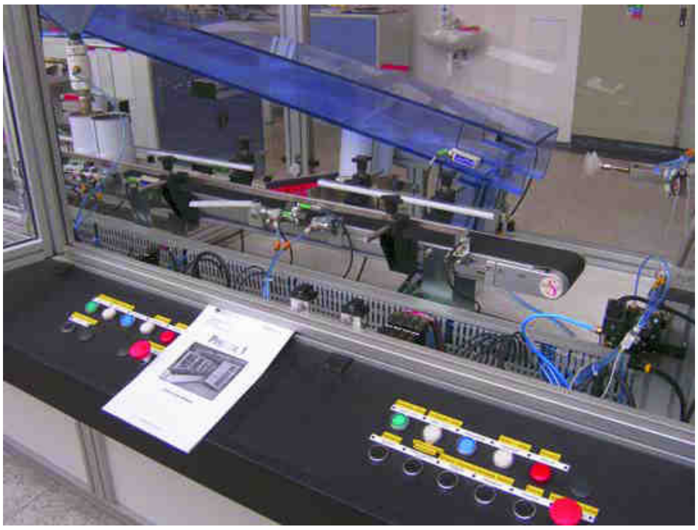

*Figure 6. Automatic line in the classroom of industrial automation-Training Centre*

**3, Electrotechnics classroom-** enables the students, thanks to its equipment, to study problems of electrical driving mechanisms as well as safety of electrical devices.

*Figure 7. Technical equipment of electrical classrooms- training centre*

**<u>The Centre covers the following modules:</u>**

- *Industrial maintenance*
- *Hydraulic systems*
- *Pneumatic systems*
- *Industrial robotics*
- *Mechanics*
- *Automatic systems*
- *Electrotechnics*
- *Electrical distribution and protection systems*
- *Electric power conversion and modulation*

- *Electrical risks prevention*
- *Component flows and production flows*
- *Production control*
- *Quality and logistics*
- *Geometry, metrology, 3D measurements*

KCOV cooperates with several external companies (as PSA Peugeot Citroen Slovakia, USS Steel, Slovnaft, SE Mochovce, SE Jaslovské Bohunice, VOP Trenčín, Swedwood Majcichov, Swedspan Malacky...) to provide required technical trainings according to the demands. The permanent KCOV course that provides training is "Master of maintenance“, that was prepared in cooperation with the Slovak Society of maintenance.

Other training provided to external companies are prepared according to the agreement with the client and are "tailored" to the customer by 29 lectors. The concept is developed according to client's exact requirements. The courses are accredited by The Slovak Ministry of Education, under the number of accreditation 2763/2008/393.

**Education of hydraulics in KCOV**

The hydraulics could be found in all modules of KCOVs´ education. However for better demonstration of the processes and the behaviour of hydraulic systems the centre contains special station- hydraulic didactic cabin, exclusively for education of hydraulics.

*Figure 8. Hydraulic didactic cabin*

The aim of the workshops on this station is to provide education in the field of TOR (all or nothing method) and proportional hydraulics. The practical exercises are based on the realisation of hydraulic schemes by connection between components of hydraulic cabin. The software enables realisation of electro-hydraulic circuits, the components and schemes control together with visualisation of theoretical values and circuits control. The whole station is constructed to work with fluids from 0 to 4000 bar.

Another specialised station for hydraulics is station for testing clearance of the fluid, mostly oil analysis.

*Figure 9. Oil analysis station*

## 4. Conclusions

Education of hydraulics is done at the Faculty of Mechanical Engineering under the Institute of process and fluid engineering. The whole process is divided into the two stages. The university education prepares the absolvent for all hydraulic issues. The professional education prepares absolvent in the desired issues. All in all the education system try to fulfil all demands from the industry, alongside with the tradition and experiences.

## REFERENCES

[1] Prikkel, Karol and Haringová, Andrea, "University and professional education in branch of fluid power systems at the Slovak Technical University in Bratislava". Ostrava: VŠB - TU Ostrava, 2011, Czech Republic, 1.-3. 6. 2011. Hydraulics and pneumatics : Proceedings of the 21th international conference, ISBN 978-80-248-2430-7, s. 197--202.

[2] http://www.sjf.stuba.sk/generate_page.php?page_id=3042

ISSN 1454 - 8003
Proceedings of 2011 International Salon of Hydraulics and Pneumatics - HERVEX
*9 – 11 November, Calimanesti-Caciulata, Romania*

# ADVANCED TECHNOLOGIES USED IN EDUCATION AND TRAINING FOR LUBRICATION PROCESSES

**Alexandru RĂDULESCU[1], Irina RĂDULESCU[2]**

[1] University POLITEHNICA Bucharest, e-mail: varrav2000@yahoo.com

[2] S.C. ICTCM S.A. Bucharest, e-mail: irena_sandu@yahoo.com

***Abstract:*** *The paper presents a wear degree and durability modeling and simulation tool for oils, by developing a fast diagnostic device for liquid lubricants, with minimum investment, with a high precision degree and easy to use. Significant benefits are made by the proposed procedure: the small amount of lubricant required for a determination, the short time measurement and the possibility of adapting the method according to concrete conditions. This is used as a method of educating and training students and specialists in the lubricating process.*

***Keywords***:*informatic integrated tool, wear, durability, lubricant*

## 1. Introduction

The paper aims to present an integrated tool for the lubricants wear degree and durability modeling and simulation, which was made during a CEEX partnership project. Several research units, institutes and excellence centers from universities worked for this idea: SC ICTCM Mechanical Engineering and Research Institute SA Bucharest, POLITEHNICA University of Bucharest - the Center for Excellence in Scientific and Engineering Tribology - UPB-CESIT, the Center for Advanced Technologies – UPB - CTANM, the Research Center for Energy and Environmental Protection - UPB -CCEPM, the National Research Institute of Materials Physics INCDFM Bucharest - Magurele, the Technical University of Civil Engineering from Bucharest.

Researches basic idea consider the current fabrication conditions by developing a fast diagnostic method for liquid lubricants, able to be used in automotive domain. The actual need for rapid and adaptive design in industry requires the use of advanced technologies, the namely tools for modeling, simulation and integrated products.

Based on current practice of exchanging oil from cars, the proposed idea was to make the change when the oil is completely worn out and not according to the manufacturer's theoretical recommendations. Using advanced technologies by making a modeling and simulation tool for lubricants behavior involved minimal investment, a high degree precision and an easy to use way. The procedure has as advantages a small amount of lubricant required for a determination, a short time measurement and the possibility of adapting the method according to specific conditions.

### 1.1. The current state of research in the field

At current stage, in Western Europe, USA or Japan - the oil from equipments is changed according to manufacturer's recommendations, considering the minimum number of operation hours or of miles traveled. In Romania these instructions are almost not followed, the oil is changed faster because the engine oil market was invaded by pirate products. The oil replacement timing is difficult to establish, there are many factors to control, that is why the oil changing is more frequently than necessary, being a unharmless technical process, but expensive.

The replacement of used oil can not be established by a common term for all engines, to define the vehicle distance covered or the timing. Oil degradation during service depends on the engine life, oxidation and contamination. The oil degrees of contamination and utilization time depend on

operating conditions, on oil quality, engine construction and technical condition. The assessment of degradation state and changing time are made considering a periodical analysis of its physical and chemical characteristics; there are established acceptable limit values for each type of engine, by the manufacturer.
At international level, the main directions and guidelines are channeled in predictive maintenance, which is applicable to any closed loop lubrication system. To be effective, it is necessary to adopt a modern program for oil analysis, monitoring the wear residues for the qualitative determination of the wear particles nature, which are carried by working lubricant and monitoring lubricant estate, which is based on physical-chemical tests, to determine if the lubricant is fit for exploitation [1], [2].

### 1.2. The proposed method for the achievement of the integrated instrument

The new method for the lubricants diagnosis is based on the expulsion process of lubricant film (squeeze-film). It is a fast one; determinations for lubricants behavior are made during 5-10 minutes on a small amount of lubricant (about 100 ml).
By collecting and comparative test of oil samples at different times and varying wear degrees, there are assigned viscometric curves for each lubricant. Using an appropriate mathematical apparatus, it can be determined the variation law of the wear degree according to time, which is required in order to establish the lubricant "reserve life" considered. It is an objective criterion for assessing the oil degradation and the optimal timing of replacement. The accuracy and precision of the method are provided by the determinations comparative character, by using two parallel measurement systems, one in original conception and the other – the viscometric reference one.
Lab VIEW software facilities were used among the advanced technologies to create the modeling and simulation tool for evaluating and quantifying the lubricant wear degree. It represents one of the most modern management tools, used for processing and data acquisition, also being a device for the education and training for lubrication processes, in this case [3].
The device has a multidisciplinary character, by combining its centralized type architecture, which manages a set of four main working modules: the theoretical module, the rheological experimental module, the validation viscometric module and the spectrometric analysis module.

## 2. Advanced technologies of integrated informatic device used for education and training in lubrication processes

For obtaining the integrated informatic device there were used advanced technologies, which are present in the four working component modules, in order to realize the lubricants behavior modeling and simulation. Their core functions are described here:
1. **The theoretical module** role is to analyze the phenomena which are based the lubricant film extrusion process. Also it generates theoretical curves specific to the interstitial fluid flow, which are necessary for the experimental results correlation and interpretation, [7].
2. **The rheological experimental module** is a modern one, containing an original measurement device, which is coupled with a data acquisition and data processing system. By using a small amount of lubricant for the diagnose (100 ml) and two semi - coupling, it is registered the time variation function lubricant pressure and thickness. It is important to work with qualified staff or to educate students and specialists to work with the three presure transducers and one proximity sensor, while the oil film is expelled under the wight of the upper coupling (figure 1). Squeeze-film curve is recorded as the „fingerprint" of the used lubricant, that depends on many factors, including the lubricant wear degree, [4].

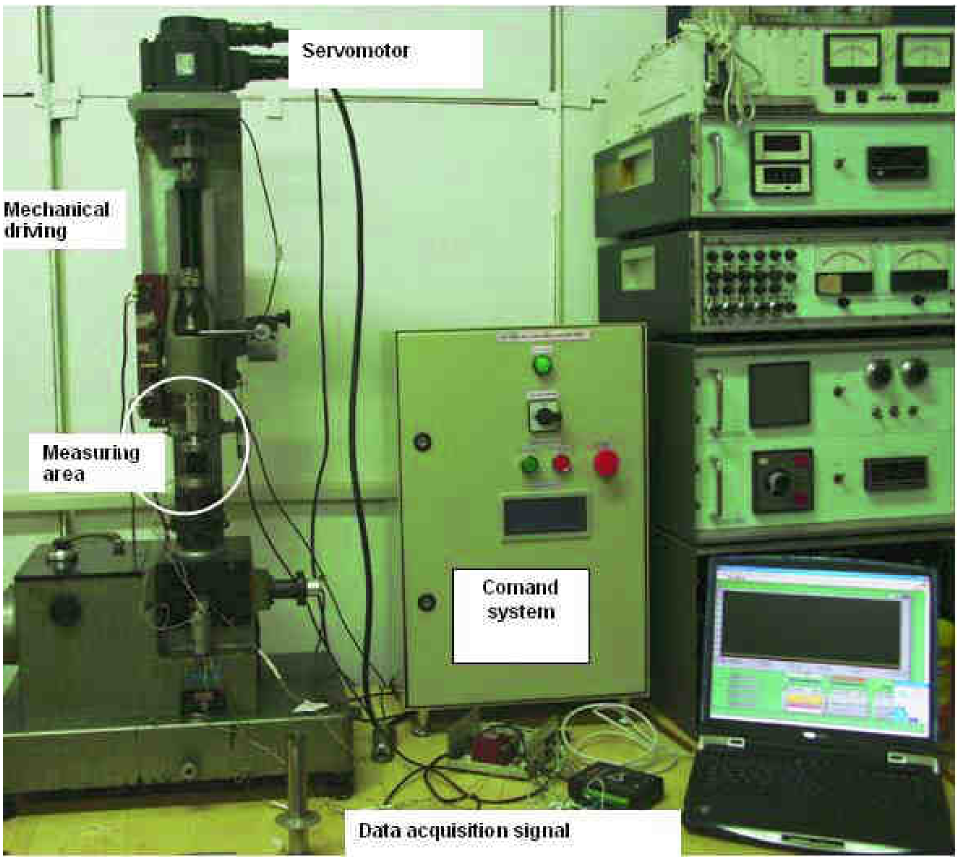


Figure 1. Experimental stand for lubricants testing in "squeezing" movement (the fluid extrusion between two parallel flat plates)

3. Considering **the viscometric validation module**, this one is based on a PHYSICA rheometer and it is composed of a mechanical unit and an electronic one. The components of mechanical unit are represented by the measurement system, thermostat installation, training system and additional installations. The electronic unit is composed of a transfer system for the measured parameters, the data processing system and the central control and command unit. The module role is to validate the experimental results which are supplied by the experimental rheological module and to establish the necessary correlations [5], [6].
4. **The spectrometric analysis module** is based on the use of transmission electron microscopy by obtaining information concerning the wear particles which can be identified in samples of worn off lubricants. By comparing two microscopic structures of the same lubricant (Figure 2), in various stages of use, it may reveal the wear particles, their shape and their size [8].
Among the advanced technologies used in education and training for lubrication processes a special one is represented by the Lab VIEW software - Laboratory Virtual Instrument Engineering Workbench, a graphical programming environment developed by National Instruments Corporation. The software is useful in data acquisition, processing and presentation, also for control and industrial process control, for the systems dynamic behavior analysis.

**ISSN 1454 - 8003**
**Proceedings of 2011 International Salon of Hydraulics and Pneumatics - HERVEX**
*9 – 11 November, Calimanesti-Caciulata, Romania*

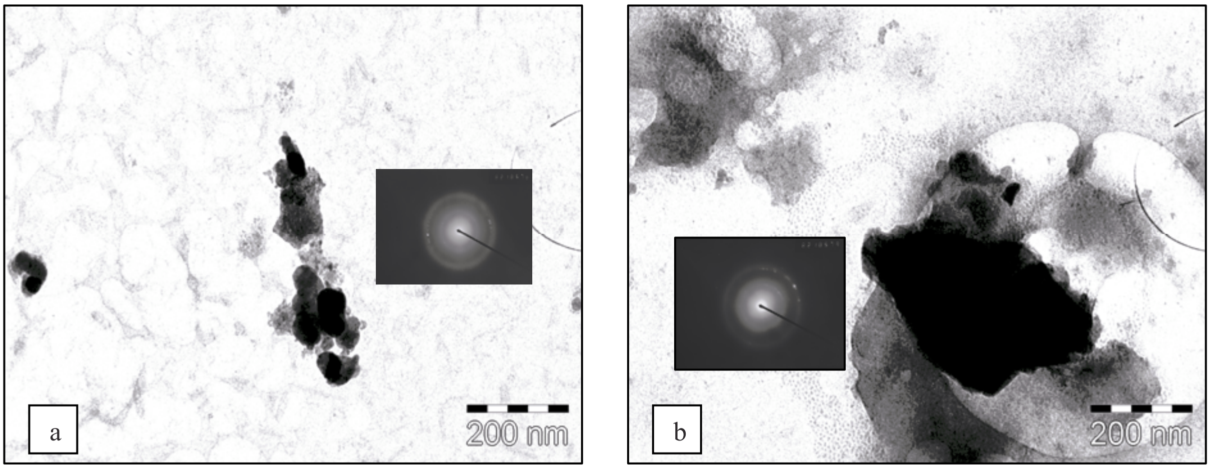


Figure 2. Unused M30 (a) and used M30 (b) Multigrade engine oil samples

The specialists are using a graphical programming language; in this environment they can run applications, which are called virtual instruments. There are used block diagrams (Figure 3), which are then compiled into machine code. Virtual instruments are made up of a front panel, which simulates the mask of the meter and a block diagram, which represents the executable software. The front panel contains icons representing various buttons, switches, screens and other elements that might enter into the meter composition, [3].

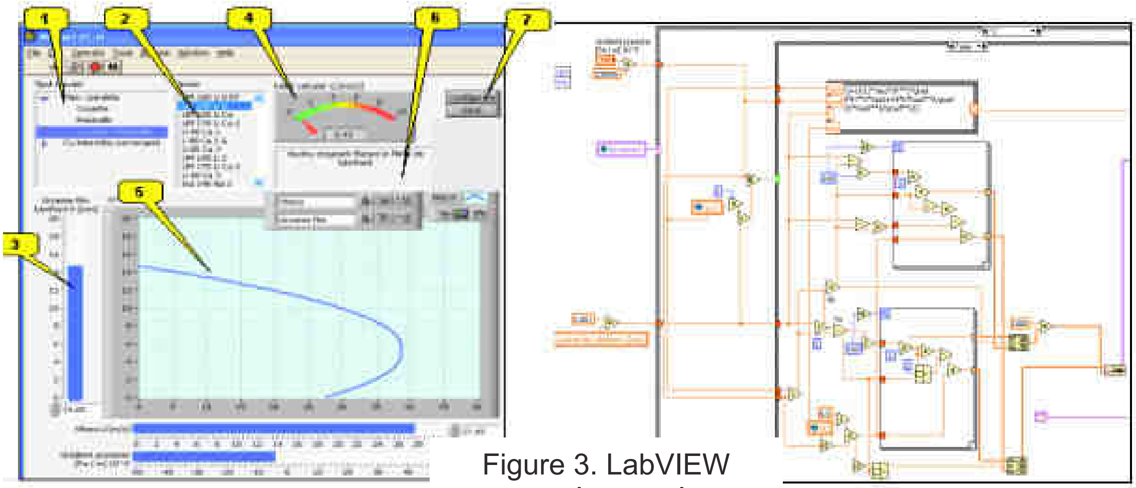


Figure 3. LabVIEW panel example

### 3. Results and conclusions

By using advanced technologies it was obtained a new, modern and efficient methodology; The assessment and the quantification of lubricant wear degree and durability and the lubricant diagnosis behavior are performant and environmentally friendly.  By developing research in this area it was asssured the modernization of existing laboratories and there were created premises for new ways for lubricants sustainability development.

Modern technologies used to achieve the integrated informatics instrument have contributed to obtain a "friendly" environment device, also friendly with its users. It can be used by a large number of beneficiaries, both in research, educational and training laboratories and in production units with small financial possibilities.

The high level of performance and quality parameters of developed system is outlined by the main characteristics and performance:

***The system is fully integrated.*** All modules are interlinked, the users can work simultaneously and they can process the same network data. It is a direct connection between modules, without imports and exports or data redundancy. Data flows are fast and well organized, which is an important support for information management.

***The system is flexible and scalable***. It is easy to adapt the system to each specific beneficiary potential, with a minimal cost. It is possible to achieve an optimal configuration for each user, by the selection of components and services required.

***The system uses top information technology***. It is well adapted for network work. There are achieved quality and performance, ensured by the processing system and Lab VIEW data acquisition use. Data access has safely conditions, according to each user access protocols.

***The system is open***. The access to inner system data is free, for the use in analysis program or other systems. It is capable of operate on multiple hardware platforms, with latest technologies (Web / Intranet / Internet). There are facilities which allow integration with existing applications and a smooth transition, with minimal efforts, from other applications to the developed software system.

This tool involves a fast and easy way over an oriented adapted design, by using advanced technologies. The implementation and the use of virtual modeling and simulation tool is equivalent with a highly customer oriented product.

## REFERENCES

[1] *** "The rheology of lubricating greases", ELGI, Amsterdam, 2000.
[2] Alliston-Greiner A.F., „Test methods in tribology", Proc.1 st World Tribology Congress, London, 1997
[3] Arsenoiu, L., Savu, T., Szuder, A., "Bazele programării în LabVIEW", Ed. Printech, Bucureşti, 1999.
[4] Briant, J. ş.a., „Propriétés rhéologiques des lubrifiants", Ed. Technique, Paris, 1985.
[5] Crocker, D.C., „How to use regression analysis in quality control", Vol. IX, American Society for Quality Control, 1983.
[6] Salvendy, G., „Handbook of Industrial Engineering," Sect.13.6, John Wiley &Sons, Inc., New York, 1982.
[7] Vodă, Gh.V., „Noi modele statistice în studiul durabilității produselor", Ed. Academiei R.S.R., Bucureşti, 1980.
[8] M. Born et al., "Relationship between Chemical Structure and Effectiveness of Some Dialkyl-Diaryldithiophosphates in Lubricated Mech.", Lubrication Science, 4-2, pp. 97-100.

**ISSN 1454 - 8003**
**Proceedings of 2011 International Salon of Hydraulics and Pneumatics - HERVEX**
*9 – 11 November, Calimanesti-Caciulata, Romania*

# FORMAREA COMUNICATORILOR DE ŞTIINȚĂ LA NIVELUL REȚELEI NAȚIONALE DE INOVARE ŞI TRANSFER TEHNOLOGIC PRIN COLABORAREA CU REȚEAUA COMUNICATORILOR DE ŞTIINȚĂ DIN ROMÂNIA

**Ing. Radu Jecu – Centrul de Informare Tehnologică CENTIREM,**
**Institutul de Cercetare – Dezvoltare pentru Metale şi Resurse Radioactive**
**ICPMRR Bucureşti**

**REZUMAT**

Prezenta comunicare constituie un avertisment succint în vederea demarării activităților de formare a comunicatorilor de ştiință in cadrul Rețelei Naționale de Inovare şi Transfer Tehnologic, prin sublinierea necesității şi utilității colaborării în această direcție cu membrii Rețelei Comunicatorilor de Ştiință din România.

**ABSTRACT**

This paper is a warning in order to start the training of the science communicators in the entities of the National Network for Innovation and Technological Transfer from Romania. In order to make this possible, we present the role that could be played in the process by the Network of The Science Communicators from Romania.

## 1. Introducere

Începând de la mijlocul secolului trecut, schimbarea configurației politice mondiale, apoi explozia mass-media şi procesul de globalizare în expansiune, precum şi unele efecte nedorite ale revoluției tehnico-ştiințifice ca: apariția şi utilizarea armelor nucleare, poluarea, creşterea fondurilor alocate cercetării etc. au condus la necesitatea ca:

1) oameni fără cunoştințe ştiințifice, dar cu posibilitatea de a influența activitățile de cercetare-dezvoltare (politicieni, oameni de afaceri, autorități etc.) să perceapă facil şi corect mesajele comunității ştiințifice. Înainte de al doilea război mondial, nu se punea problema contestării explicațiilor, soluțiilor şi realizărilor oferite de ştiința vremii, iar costurile şi consecințele nu alarmau societatea. Noile condiții au obligat comunitatea ştiințifică să-şi prezinte realizările, punctele de vedere, solicitările şi opțiunile sale din ce în ce mai mult *ad extra*, prin modalități care s-au diversificat odată cu evoluția mijloacelor de comunicare.

2) oamenii de ştiință să comunice între ei mult mai fluid, atât în cadrul aceluiaşi domeniu de activitate, cât şi între specialişti din zone diferite odată dezvoltarea treptată a cercetărilor indisciplinare..

## 2. Situația pe plan internațional

Interesul crescând pentru cunoaşterea ştiințifică, necesitățile mediului economic şi de afaceri, numeroşi alți factori au favorizat apariția de noi specializări interdisciplinare: comunicatorii şi jurnaliştii de ştiință. Comunicatorii ataşați comunității ştiințifice (în cadrul serviciilor pentru cercetare) încearcă să ofere o înțelegere corectă, coerentă şi punctuală a diverselor chestiuni legate de activitatea ştiințifică, în timp ce jurnaliştii preiau informațiile furnizate şi le transmit într-un format accesibil grupului-țintă căruia se adresează.

## 2. Situația din țara noastră

Totalitarismul comunist a menținut ideologia scientistă, ideologia sa favorizând poziția ştiinței de a oferi singurele adevăruri şi soluții viabile, permanent perfectibile, de rezolvare a problemelor societății. Viziunea politică internă şi amploarea tehnoştinței pe plan mondial au condus la dezvoltarea cu predilecție a ştiințelor inginereşti în scopul dezvoltării țării în direcțiile hotărâte de către factorul politic a fi prioritare. Comunicarea ştiinței era rudimentară, axată fiind pe popularizarea rezultatelor, de multe ori în mod propagandistic sau polemic, în încercarea de a prezenta într-o lumină favorabilă sistemul politic pe plan intern şi/sau extern.

Evenimentele din decembrie 1989 au determinat transformări radicale. Tranziția a condus la un nou evantai al ştiințelor. Economia şi celelalte ramuri de activitate nu au mai preluat în mod automat rezultatele cercetării româneşti, iar opțiuni politice diverse şi-au pus amprenta asupra modului de coordonare şi finanțare a cercetării-dezvoltării.

Inadecvarea inițială a cercetării-dezvoltării la necesitățile noului mediu economic precum şi decalajul tehnologic, determinate de izolarea şi dirijismul totalitar, au condus la preferința agenților economici de procurare din import a tehnologiilor, aparaturii, utilajelor necesare. Treptat, entitățile de cercetare-dezvoltare au început să se adapteze noilor cerințe ale societății. A fost necesar mai mult de un deceniu şi jumătate pentru actualizarea, pe cât posibil, a bazei materiale a organizațiilor de cercetare-dezvoltare, concomitent cu asimilarea viziunii mondiale şi apoi integrarea în spațiul european al cercetării.

Cercetarea-dezvoltarea românească luptă să-şi recâştige prestigiul național, concomitent făcând eforturi de a se face cunoscută şi apreciată pe plan internațional. Lipsa de abilități necesare comunicării rezultatelor şi problemelor la nivelul organizațiilor de cercetare-dezvoltare distorsionează puternic atât imaginea entităților cât şi a domeniului de activitate, îngreunând relațiile cu mediul economic şi de afaceri, precum şi cu societatea. Sunt favorizate astfel tendințele de subfinanțare a acestui domeniu de activitate, de minimalizare a rolului pe care ştiința îl poate avea în societatea şi economia românească etc.

La rândul lor, mass-media din țară (cu foarte puține excepții) nu dispun de jurnalişti specializați în ştiință pentru a prezenta realitățile existente, preferând uneori senzaționalul ieftin în locul unor anchete, reportaje şi interviuri profesioniste.

Evoluțiile din ultima perioadă au evidențiat, implicit sau explicit, necesitatea comunicatorilor şi jurnaliştilor de ştiință în spațiul serviciilor pentru cercetare din România, respectiv în mass-media.

## 3. Comunicarea ştiinței şi Rețeaua Națională de Inovare şi Transfer Tehnologic

Serviciile pentru cercetare sunt un domeniu de activitate complex şi relativ nou în țara noastră. Între acestea se regăsesc unele activități mai vechi (de exemplu, cele legate de proprietatea intelectuală) alături de altele generate de noul context de desfăşurare a activităților de cercetare-dezvoltare.

Infrastructura de inovare şi transfer tehnologic, care a a început să se dezvolte în ultimii ani în țara noastră, este cadrul organizatoric al acestui tip de servicii. Rețeaua Națională de Inovare şi Transfer Tehnologic integrează principalii actori din domeniul transferului de cunoştințe şi tehnologie la nivel național (20 centre de informare tehnologică, 14 centre de transfer tehnologic, 16 incubatoare tehnologice şi de afaceri, 4 parcuri ştiințifice şi tehnologice) fiind prezentă în toate regiunile de dezvoltare ale țării.

În general, serviciile depind, prin excelență, de comunicarea interumană. Activitățile de comunicare a ştiinței se numără printre serviciile pentru cercetare, iar entitățile enumerate mai sus au între obiectivele lor:

- creşterea vizibilității organizațiilor de cercetare – dezvoltare;
- creşterea gradului de valorificare a rezultatelor cercetării;

• îmbunătățirea relațiilor între unitățile de cercetare – dezvoltare şi agenții economici şi respectiv, între unitățile de cercetare – dezvoltare şi societate.

La realizarea lor, comunicatorii de ştiință se pot implica prin:

• promovarea imaginii organizațiilor de cercetare – dezvoltare oferind informații structurate conform solicitărilor mediilor interesate;
• prezentarea rezultatelor activităților de cercetare – dezvoltare potrivit momentului, locului, participanților şi celorlalți factori conjuncturali în cadrul unor manifestări şi evenimente interne şi externe, stimulând încheierea de noi contacte şi parteneriate;
• facilitarea comunicării şi a transferului de cunoştințe şi tehnologii cu agenții economici, informarea societății în probleme legate de activitatea de cercetare-dezvoltare.

Totodată, feed-back-ul activității comunicatorilor de ştiință poate constitui o sursă de informații extrem de utilă atât pentru unitățile de cercetare-dezvoltare, cât şi pentru entitățile de inovare şi transfer tehnologic în sensul unei mai juste şi rapide corelări a activității lor cu problemele concrete şi imediate ale economiei şi cu aşteptările societății.

Prin urmare, entitățile Rețelei Naționale de Inovare şi Transfer Tehnologic oferă un cadru optim de desfăşurare a activității pentru comunicatorii de ştiință spre folosul activității şi comunității ştiințifice, al economiei şi al societății în general.

## 4. Rețeaua Comunicatorilor de Ştiință din România

Este un grup de specialiți din mediul ştiințific, academic şi de afaceri preocupat de comunicarea ştiinței şi problemele conexe, pe linie profesională şi nu numai. Într-un cadru informal, membrii îşi transmit noutăți referitoare la comunicarea ştiinței din zona de activitate proprie, se consultă reciproc şi activează în sensul fluidizării şi eficientizării comunicării. Înființată de un grup de entuziaşti în frunte cu dl. Cătălin Mosoia, Rețeaua Comunicatorilor de Ştiință din România s-a consolidat în urma unor importante evenimente de profil din ultimii doi ani. Cu ocazia workshop-ului „Jurnalism ştiințific şi comunicare” din cadrul Conferinței ”Diaspora românească în cercetarea ştiințifică şi învățământul superior”, a simpozioanelor „Ştiința Comunicării pentru Comunicarea Ştiinței – SC4CS” (ambele din 2010) şi „Comunicarea de criză” (2011), participarea membrilor a fost consistentă atât cantitativ, prin numărul mare al celor prezenți, cât şi calitativ - prin comunicările şi luările de poziție ale membrilor.

## 5. Formarea comunicatorilor de ştiință

Pentru ca formarea comunicatorilor de ştiință să îşi atingă scopurile dorite, este necesară mai întâi inițierea unui dialog între membrii celor două rețele amintite pentru cunoaşterea reciprocă şi explorarea posibilităților concrete de colaborare.

La ora actuală, putem evidenția două forme de conlucrare, funcție de solicitările comunității ştiințifice:

1. pentru necesitățile imediate, considerăm că o colaborare între entitățile Rețelei Naționale Inovare şi Transfer Tehnologic şi unitățile de învățământ superior sau/şi cele de formare continuă acreditate în domeniul comunicării poate conduce la crearea de consorții interdisciplinare care pot demara proiecte de formare în domeniu, susținute de specialişti – parte din ei, membri ai Rețelei Comunicatorilor de Ştiință din România.
2. pentru necesitățile pe termen lung, la nivelul unităților de învățământ superior acreditate în domeniul comunicării se pot elabora programe de masterat, şcoli doctorale, forme de învățământ post-universitare, respectiv postdoctorale pentru viitorii specialişti în comunicarea ştiinței, la care pot participa de asemenea membri ai Rețelei Comunicatorilor de Ştiință din România.

În paralel, prin aceleaşi modalități se poate demara şi formarea jurnaliştilor de ştiință – specializare profesională, după cum am menționat deja, de asemenea deficitară în România şi care constituie o verigă deosebit de importantă în procesul de comunicare cu societatea.

Este important de menționat faptul că specialiştii străini şi cei români care activează în străinătate, prezenți la manifestările amintite în capitolul anterior, şi-au exprimat disponibilitatea de colaborare cu cei din țară în cadrul unor proiecte transnaționale de formare.

5. Concluzii

Prezenta comunicare este o continuare a campaniei în favoarea formării de comunicatori şi jurnalişti de ştiință profesionişti, începută cu ocazia workshop-ului „Jurnalism ştiințific şi comunicare” din cadrul Conferinței ”Diaspora românească în cercetarea ştiințifică şi învățământul superior”, continuată la simpozioanele "Interferențe socio-economice la frontiera inovării", editia a III-a, HERVEX editia a XI-a şi „Ştiința Comunicării pentru Comunicarea Ştiinței – SC4CS” (desfăşurate în 2010), precum şi „Comunicarea de criză” (2011). Prezenta constituie un avertisment succint în vederea demarării acestor activități (şi) în cadrul Rețelei Naționale de Inovare şi Transfer Tehnologic.

www.hervex.eu